DOCTOR OF PHILOSOPHY

The medical biomarker and oncogenic potential of the human cancer- and stem/germ cell-specific gene TDRD12

Oyouni, Atif

Award date:
2016

Awarding institution:
Bangor University

The medical biomarker and oncogenic potential of the human cancer- and stem/germ cell-specific gene *TDRD12*

A Thesis Submitted
For the Degree of Doctor of Philosophy
In Medical Molecular Biology with Genetics

Atif Abdulwahab A. Oyouni

North West Cancer Research Institute
Bangor University, United Kingdom

PRIFYSGOL
BANGOR
UNIVERSITY

May 2016

Declaration and Consent

Details of the Work

I hereby agree to deposit the following item in the digital repository maintained by Bangor University and/or in any other repository authorized for use by Bangor University.

Author Name: Atif Abdulwahab A. Oyouni

Title: The medical biomarker and oncogenic potential of the human cancer- and stem/germ cell-specific gene *TDRD12*.

Supervisor/Department: Dr Ramsay James McFarlane

Funding body (if any): Tabuk University, Kingdom of Saudi Arabia

Qualification/Degree obtained: PhD

This item is a product of my own research endeavours and is covered by the agreement below in which the item is referred to as "the Work". It is identical in content to that deposited in the Library, subject to point 4 below.

Non-exclusive Rights

Rights granted to the digital repository through this agreement are entirely non-exclusive. I am free to publish the Work in its present version or future versions elsewhere.

I agree that Bangor University may electronically store, copy or translate the Work to any approved medium or format for the purpose of future preservation and accessibility. Bangor University is not under any obligation to reproduce or display the Work in the same formats or resolutions in which it was originally deposited.

Bangor University Digital Repository

I understand that work deposited in the digital repository will be accessible to a wide variety of people and institutions, including automated agents and search engines via the World Wide Web. I understand that once the Work is deposited, the item and its metadata may be incorporated into public access catalogues or services, national databases of electronic theses and dissertations such as the British Library's EThOS or any service provided by the National Library of Wales.

I understand that the Work may be made available via the National Library of Wales Online Electronic Theses Service under the declared terms and conditions of use (http://www.llgc.org.uk/index.php?id=4676). I agree that as part of this service the National Library of Wales may electronically store, copy or convert the Work to any approved medium or format for the purpose of future preservation and accessibility. The National Library of Wales is not under any obligation to reproduce or display the Work in the same formats or resolutions in which it was originally deposited.

Statement 1:

This work has not previously been accepted in substance for any degree and is not being concurrently submitted in candidature for any degree unless as agreed by the University for approved dual awards.

Signed: …….. (candidate)

Date: ……..

Statement 2:

This thesis is the result of my own investigations, except where otherwise stated. Where correction services have been used, the extent and nature of the correction is clearly marked in a footnote(s).

Other sources are acknowledged by footnotes giving explicit references. A bibliography is appended.

Signed: ……. (candidate)

Date: …….

Statement 3:

I hereby give consent for my thesis, if accepted, to be available for photocopying, for inter-library loan and for electronic repositories, and for the title and summary to be made available to outside organisations.

Signed: ……. (candidate)

Date: …….

NB: Candidates on whose behalf a bar on access has been approved by the Academic Registry should use the following version of **Statement 3:**

Statement 3 (bar):

I hereby give consent for my thesis, if accepted, to be available for photocopying, for inter-library loans and for electronic repositories after expiry of a bar on access.

Signed: …… (candidate)

Date: ……

Statement 4:

Choose **one** of the following options

a) I agree to deposit an electronic copy of my thesis (the Work) in the Bangor University (BU) Institutional Digital Repository, the British Library ETHOS system, and/or in any other repository authorized for use by Bangor University and where necessary have gained the required permissions for the use of third party material.	
b) I agree to deposit an electronic copy of my thesis (the Work) in the Bangor University (BU) Institutional Digital Repository, the British Library ETHOS system, and/or in any other repository authorized for use by Bangor University when the approved **bar on access** has been lifted.	
c) I agree to submit my thesis (the Work) electronically via Bangor University's e-submission system, however I **opt-out** of the electronic deposit to the Bangor University (BU) Institutional Digital Repository, the British Library ETHOS system, and/or in any other repository authorized for use by Bangor University, due to lack of permissions for use of third party material.	

Options B should only be used if a bar on access has been approved by the University.

In addition to the above, I also agree to the following:

That I am the author or have the authority of the author(s) to make this agreement and do hereby give Bangor University the right to make available the Work in the way described above.

That the electronic copy of the Work deposited in the digital repository and covered by this agreement, is identical in content to the paper copy of the Work deposited in the Bangor University Library, subject to point 4 below.

That I have exercised reasonable care to ensure that the Work is original and, to the best of my knowledge, does not breach any laws – including those relating to defamation, libel and copyright.

That I have, in instances where the intellectual property of other authors or copyright holders is included in the Work, and where appropriate, gained explicit permission for the inclusion of that material in the Work, and in the electronic form of the Work as accessed through the open access digital repository, *or* that I have identified and removed that material for which adequate and appropriate permission has not been obtained and which will be inaccessible via the digital repository.

That Bangor University does not hold any obligation to take legal action on behalf of the Depositor, or other rights holders, in the event of a breach of intellectual property rights, or any other right, in the material deposited.

That I will indemnify and keep indemnified Bangor University and the National Library of Wales from and against any loss, liability, claim or damage, including without limitation any related legal fees and court costs (on a full indemnity bases), related to any breach by myself of any term of this agreement.

Signature: ……

Date: ……..

Abstract

Cancer is a common illness that affects many people across the world each year. Cancer mortality is often due not only to the limitations of existing therapies but also to its late diagnosis. In this light, efficient and effective tools to target and diagnose cancer in its early stages will make an enormous significant impact on improving the survival of cancer patients. Cancer/germ-line or cancer/testis antigen (CTA) genes are expressed in a tumour-specific fashion so can provide a powerful source of cancer biomarker/therapeutic target. Additionally, these genes may have oncogenic activity.

In this study, we identify a novel human cancer- and stem/germ cell-specific gene, *TDRD12*, which may serve as a biomarker, therapeutic target and may have oncogenic activity. The expression of *TDRD12* is found in human pluripotent embryonal carcinoma cells, human induced pluripotent stem cells, embryonic stem cells and colon adenocarcinoma cells. This indicates that *TDRD12* might have stem cell and cancer stem cell (CSC) specificity, so it might play a role in conferring stemness on cancer cells. *TDRD12* might also be required for the germ-line/stem cell regulation of retro elements (REs) and endogenous retro viruses (HERVs). Therefore, we establish that *TDRD12* controls the RE/HERV expression levels in human germ-line tumour cells. We demonstrate that human PIWIL2 protein becomes depleted upon siRNA reduction of TDRD12 in pluripotent embryonal carcinoma cells, suggesting a functional regulatory relationship. Human PIWIL1 and TDRD12-T17 antibodies have consistent co-localisation, and they appear to have similar sub-cellular localisation patterns; these two antibodies localise in the same cells in the testis, which suggests a co-function of these proteins. *TDRD12* was further validated and analysed to identify its medical molecular and biological functions, as well as its possible application in developing human cancer therapies. The protein encoded by this gene might also be promising targets for new cancer therapies and clinical uses.

Acknowledgements

The writing of this thesis would not have been possible without the help I received from Allah and the wonderful people around me.

First, I would like to thank Allah for the power and strength He has given me to start and complete this important step in my educational and professional life.

Second, I would like to offer special thanks to my supervisor, Dr Ramsay James McFarlane, for all his academic guidance and advice that assisted me during my PhD research and throughout the writing of my thesis. I am grateful for his continuous support and encouragement as well as the opportunity to work with him. In addition, I particularly want to thank him for his clear explanations and for training me to understand important information and tools in the field of medical molecular biology with genetics and cancer biomarkers as well as stem cells.

Third, I would like to express my gratitude to Dr David Warren Pryce, who was the medical molecular biology with genetics MSc course organiser at Bangor University in 2010/2011 when I was an MSc researcher. He was the internal examiner of my PhD project. I would also like to thank him for organising this essential, fundamental MSc course, necessary for any researcher in the field of molecular biology.

I wish to thank and extend my appreciation to all my colleagues at Bangor University, both past and present; I am deeply grateful for their assistance and support along the way as well as their sharing useful academic and research knowledge. They were always ready to offer friendly laboratory experimental discussions. I particularly wish to express my gratitude to Dr Jane Wakeman, Dr Natalia Gomez Escobar, Dr Ellen Vernon, Dr Stephen John Sammut, Dr Faisal Abdulrahman Alzahrani, Dr Jana Jezkova, Dr Mikhlid Hammad Almutairi, Dr Ahmed Mubrik Almatrafi, Vicente Planells Palop, Saad Ali Aljohani, Jason Saunders Williams, Fayez Alhumaidi Althobaiti, Ffion Jones Hutchings, Naif Alsiwiehri, Othman Rashed Alzahrani and Mishal Olayan Alsulami.

I would like to acknowledge that my MSc and PhD courses were funded by the government of Saudi Arabia. Therefore, I would like to express my gratitude and thanks to the Saudi Government, especially Tabuk University, for the scholarship and funds.

Finally, I am deeply grateful and thankful to my parents for always being there for me, encouraging, supporting and inspiring me to do the best I can. My thanks also goes to my daughters, brothers, sisters and all the people around me for their understanding and support during my journey to improve my education and career prospects.

Acronyms

3'	Three prime end of DNA
5'	Five prime end of DNA
A2780	Ovarian carcinoma
A-431	Epidermal carcinoma
ASCs	Adult stem cells
BJ	Fibroblast
BMP	Bone morphogenetic protein
BOLL	Boule-like RNA-binding protein
bp	Base pair (s)
BRCA1	Breast cancer susceptibility 1
BRCA2	Breast cancer susceptibility 2
BTB	Blood-testis barrier
Cat. No.	Catalogue number
C-BJ	Commercial fibroblast (control)
cDMEM	Completed Dulbecco's modified eagle's medium
cDNA	Complementary DNA
C-iPSCs	Induced pluripotent stem cells control
CNS	Central nervous system
COLO800	Melanoma
COLO857	Melanoma
Cq	Quantification cycle
CSCs	Cancer stem cells
CT41.1	Cancer/testis antigen 41.1
CT41.2	Cancer/testis antigen 41.2
CTAs	Cancer-testis antigens
DAZ1	Deleted in azoospermia 1
DAZL	Deleted in azoospermia-like
DEPC	Diethylpyrocarbonate
dH_2O	Distilled water
D-iPSCs	Differentiated induced pluripotent stem cells
DMEM	Dulbecco's modified eagle's medium

DMSO	Dimethyl sulphoxide
DNA	Deoxyribonucleic acid
DNMT	DNA methyltransferases
dNTPs	Deoxyribonucleotide triphosphates
DPBS	Dulbecco's phosphate buffered saline
e.g.,	For example
EB	Elution buffer
ECAT8	ES cell-associated transcript 8 protein
ECCs	Embryonic carcinoma cells
ECL	Enhanced chemiluminescence
ECM	Extra-cellular matrix
EDTA	Ethylenediaminetetraacetic acid
EGCs	Embryonic germ cells
ELDA	Extreme limiting dilution analysis
EpiSCs	Epiblast stem cells
ESCs	Embryonic stem cells
eTuds	Extended Tudor domains
EVEs	Endogenous viral elements
F	Forward primer
FBS	Foetal bovine serum
FGF	Fibroblast growth factor
g	Gram
G361	Caucasian malignant melanoma
GAPDH	Glyceraldehyde 3-phosphate dehydrogenase
GSCs	Germinal stem cells
h	Hours
H460	Large cell lung carcinoma
HAT	Histone acetyltransfers
HCT116	Colon carcinoma
HDAC	Histone deacetylases
hECCs	Human embryonic carcinoma cells
HeLa-S3	Cervical adenocarcinoma
HEP G2	Liver carcinoma

HERVs	Human endogenous retrovirus
HIG-1	Hypoxia-inducible HIG-1
HL-60	Promyelocytic leukaemia
HMBA	Hexamethylene bisacetamide
HMT	Histone methyltransferases
HSCs	Hematopoietic stem cells
HSP90AB1	Heat shock protein 90kDa alpha (cytosolic), class B member 1
HT29	Colon adenocarcinoma
IF	Immunofluorescence
IHC	Immunohistochemistry
iPSCs	Induced pluripotent stem cells
Jurkat	T-cell leukaemia
K-562	Leukaemia
kb	Kilobase
KDa	Kilodalton
L	Litre
LIF	Leukaemia inhibitor factor
LINE-1	Type transposase domain-containing protein 1
LoVo	Colon adenocarcinoma
mA	Milliamperes
MBP	Methyl-CPG-binding proteins
MCF-7	Breast adenocarcinoma
MDA-MB-453	Breast carcinoma
mg	Milligram
min	Minute
miRNAs	microRNAs
mL	Milliliter
mM	Millimolar
MM127	Malignant melanoma
MRC-5	Diploid lung
mRNA	Messenger RNA
MSCs	Mesenchymal stem cells
NCBI	National Centre for Biotechnology Information

ng	Nanogram
NI	Non-interference
nM	Nanomolar
NRT	No reverse transcriptase
NSCs	Neural stem cells
NT2	Pluripotent embryonal carcinoma
NTC	No template control
^{o}C	Degrees centigrade
Oct4	Octamer-binding transcription factor 4
oligo-dT	Oligodeoxythymidylic acid
p53	Cellular tumour antigen p35
PC-3	Prostate adenocarcinoma
PCR	Polymerase chain reaction
PCTAIRE2BP	PCTAIRE2-binding protein
PE014	Ovarian cancer; oestrogen receptor negative
piRNA	PIWI-interacting RNA
PIWI	P-element induced wimpy testis genes
PIWIL	PIWI-like RNA-mediated gene silencing
pmol	Picomole
POU5F1	POU class 5 homeobox 1
PSA	Prostate-specific antigen
PSCs	Pluripotent stem cells
PTM	Histone post-translation modification
R	Reverse primer
Raji	Burkitts lymphoma
Rb	Retinoblastoma-associated
Ref	Reference
REs	Retro elements
RNA	Ribonucleic acid
RNAi	RNA interference
RNF17	RING finger protein 17
rpm	Rotation per minute
rRNA	Ribosomal RNA

RT	Room temperature
RT-PCR	Reverse transcription-polymerase chain reaction
RT-qPCR	Quantitative, real time-polymerase chain reaction
SCs	Stem cells
sDMAs	Symmetrical dimethyl arginines
SDS-PAGE	Sodium dodecyl Sulphate-polyacrylamide gel electrophoresis
Sec	Seconds
siRNA	Small interfering RNA
SPATA23	Spermatogenesis associated 23
STAP	Stimulus-triggered acquisition of pluripotency
Std. Dev	Standard deviation
STK31	Serine/threonine kinase 31
SW480	Colon adenocarcinoma
T84	Colon carcinoma
TBE	Tris-borate-EDTA
TDR2	Tudor repeat 2
TDRD	Tudor domain containing protein
TDRKH	Tudor and KH domain-containing protein
TF	Transcription factors
TGF	Transforming growth factor
Tm	Melting temperature
TRAP	Tudor repeat associator with PCTAIRE 2
TRAs	Tumour-related antigens
Tris	Tris (hydroxymethyl) aminomethane
TSGs	Tumour suppressing genes
V	Voltage
WB	Western blot
µg	Microgram
µL	Microliter

Table of Contents

Table of Figures

List of Tables

1. Introduction

1.1. Cancer

Cancer is a common illness that leads to approximately 7 million deaths per year, and affects an estimated 25 million people worldwide per year (Butterfield, 2015; Popat *et al.,* 2013). Cancer or malignant tumours are all cell-growth disorders that result in the damage and invasion of surrounding normal tissue by abnormal cell proliferation. Cancerous cells originate due to the accumulation of epigenetic or genetic alterations, which allow the cells to proliferate in an un-regulated way (Bagci and Kurtgöz, 2015; Macheret and Halazonetis, 2015; Wodarz and Zauber, 2015).

Cells within malignant tumours can proliferate more quickly and aggressively than normal cells and do not appear to be subject to normal regulation by hormones and nerves (Jayashree *et al.,* 2015). These tumours may spread through the lymphatic system or bloodstream to other body organs, where they cause additional tissue damage (metastases; see Figure 1.1) (Fridman *et al.,* 2014). Cancer types can be grouped into different categories, such as cancer that begins in the epithelium (carcinoma), cancer that begins in connective or supportive tissue (sarcoma), cancer that begins in white blood cells (leukaemia), and cancer that begins in lymphoid tissue (lymphoma). In addition, cancer may also begin in the plasma cells of the bone marrow (myeloma). Table 1.1 illustrates the prevalence of the most common types of cancer (Siegel *et al.,* 2012). Cancer is characterised by the development of a subset of neoplasms and is therefore medically referred to as a malignant neoplasm.

1.1.1. Cancer risk factors

Cancer is caused by a number of complex pathways that are not fully understood; however, external factors such as smoking, radiation and environmental pollutants are known to affect cancer development. These factors can have a direct effect on genetic material and cause damage. It is estimated that 90-95% of cancer cases are caused by environmental factors, whereas only 5-10% are directly caused by hereditary genetic factors (see Figure 1.2 and Figure 1.3) (Anand *et al.,* 2008; Wodarz and Zauber, 2015).

Tomasetti and Vogelstein recently reported that the differences in malignant neoplasm risk between human tissues could be described by the number of stem cell (SC) (see Section 1.7) divisions. The most malignant neoplasms or cancer cases are due to cells that proliferate uncontrollably as a function of the number of cell divisions a tissue undergoes (Tomasetti and Vogelstein, 2015).

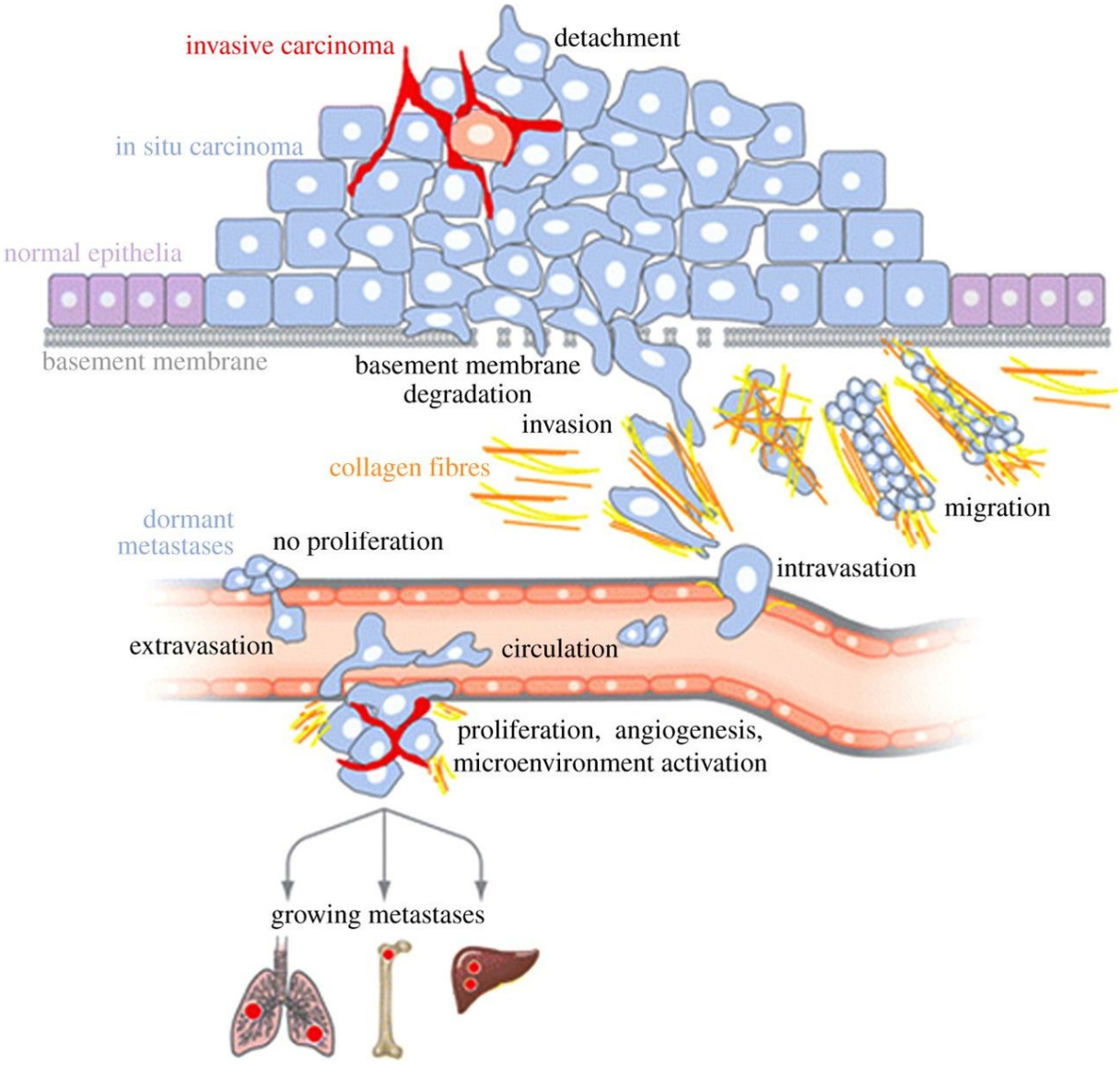

Figure 1.1 Phases in metastasis.
The primary tumour first causes breaks in the basement membrane within the epithelial tissues, leading to a loss of adherens junctions. The cells move into the bloodstream and enter the parenchyma, thereby creating a new cancer microenvironment.
Taken from (Bacac and Stamenkovic, 2008; Djamgoz *et al.,* 2014).

Table 1.1 The 10 leading cancer categories with estimated new cases and deaths in the USA in 2012. Adapted and modified from (Siegel *et al.,* 2012).

Estimated new cases					
Males			**Females**		
Prostate	241,740	29%	Breast	226,870	29%
Lung and bronchus	116,470	14%	Lung and bronchus	109,690	14%
Colon and rectum	73,420	9%	Colon and rectum	70,040	9%
Urinary bladder	55,600	7%	Uterine corpus	47,130	6%
Melanoma of the skin	44,250	5%	Thyroid	43,210	5%
Kidney and renal pelvis	40,250	5%	Melanoma of the skin	32,000	4%
Non-Hodgkin lymphoma	38,160	4%	Non-Hodgkin lymphoma	31,970	4%
Oral cavity and pharynx	28,540	3%	Kidney and renal pelvis	24,520	3%
Leukaemia	26,830	3%	Ovary	22,280	3%
Pancreas	22,090	3%	Pancreas	21,830	3%
All sites	848,170	100%	All sites	790,740	100%
Estimated deaths					
Males			**Females**		
Lung and bronchus	87,750	29%	Lung and bronchus	72,590	26%
Prostate	28,170	9%	Breast	39,510	14%
Colon and rectum	26,470	9%	Colon and rectum	25,220	9%
Pancreas	18,850	6%	Pancreas	18,540	7%
Liver and intrahepatic bile duct	13,980	5%	Ovary	15,500	6%
Leukaemia	13,500	4%	Leukaemia	10,040	4%
Oesophagus	12,040	4%	Non-Hodgkin lymphoma	8,620	3%
Urinary bladder	10,510	3%	Uterine corpus	8,010	3%
Non-Hodgkin lymphoma	10,320	3%	Liver and intrahepatic bile duct	6,570	2%
Kidney and renal pelvis	8,650	3%	Brain and other nervous system	5,980	2%
All sites	301,820	100%	All sites	275,370	100%

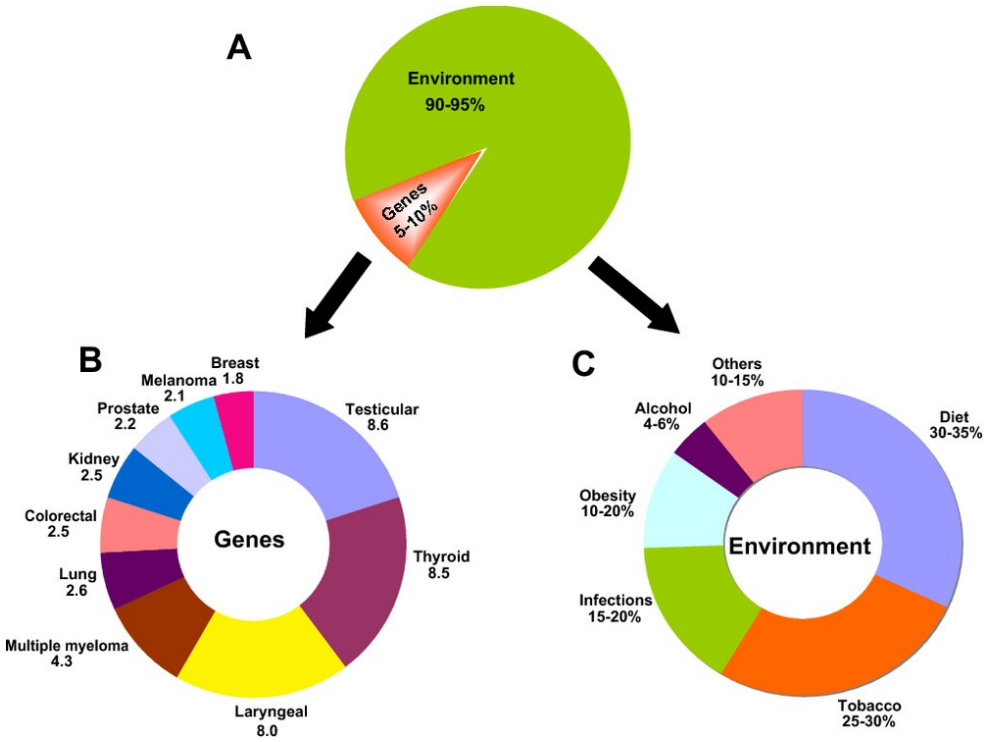

Figure 1.2 Roles of environmental factors and genetics in cancer development.
(A) Percentages of environmental factors and genetics in relation to cancer and tumours. (B) Risk ratios for a number of cancerous genes. (C) Percentages for environmental factors.
Taken from (Anand *et al.*, 2008).

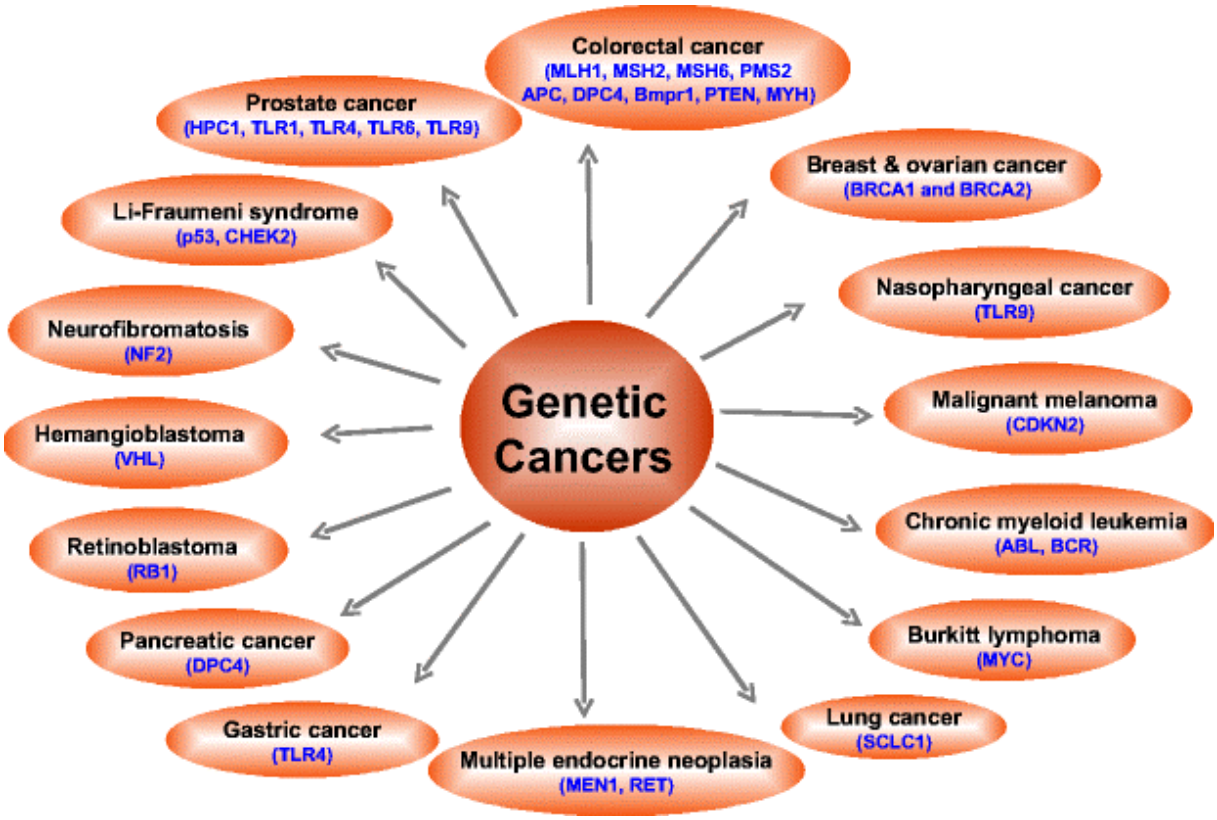

Figure 1.3 Examples of genes related to the risk of different malignant tumours.
Taken from (Anand *et al.*, 2008).

1.1.2. Cancer hallmarks and tumourigenesis development

In normal cells, the development of the neoplastic state is associated with the acquisition of one or more of the hallmarks of cancer, which determine neoplastic organisation. Cancer hallmarks include the following: sustained of proliferative signalling; evasion of growth suppressors; resistance of apoptosis or cell death; enabling of DNA replication, thus leading to immortality; induction of angiogenesis; activation of invasion and metastasis; genomic instability and mutation; tumour-initiating inflammation; and reprogramming energy metabolism. All of these hallmarks occur while evading immune destruction (Hanahan and Weinberg, 2011; Macheret and Halazonetis, 2015; Walenkamp *et al.,* 2014; Wang *et al.,* 2015). Therefore, insight into the hallmarks of cancer can assist in the design of clinically relevant therapeutic drugs, which target cancer (Figure 1.4).

Normal cell growth and proliferation is strictly controlled by the release and secretion of growth-stimulating signals such as maintenance signals, which regulate energy metabolism and cell survival processes. Two kinds of signals have been identified; one is related to cell surface binding factors and the other acts intra-cellularly (e.g., on kinase domains). In contrast, in cancerous cells, the same signals become de-controlled, resulting in the cells becoming ‘masters of their own destiny’ (Flippot *et al.,* 2015; Hanahan and Weinberg, 2000; Hanahan and Weinberg, 2011). Cancerous cells can begin to make their own growth factors or may even promote normal cells to become involved with the tumour via cell-to-cell signalling (Hembruff *et al.,* 2010).

Another hallmark of cancer is its ability to evade growth suppressors. Under normal conditions, tumour suppressor genes (TSGs), such as *p53* (cellular tumour antigen p53) and *Rb* (retinoblastoma-associated), suppress unusual cell growth and unlimited proliferation (Cairns *et al.,* 2011; Morris and Chan, 2015). Therefore, the mutation of these TSGs results in deregulated cell proliferation (e.g., a null *Rb* causing the progression of neoplasia, while a null of *p53* can cause leukaemia and other cancers). The apoptotic program targets cancer cells in the process of tumourigenesis and a malfunction in the apoptotic program is a hallmark of cancer (Hanahan and Weinberg, 2011; Morris and Chan, 2015).

The ability to carry out unlimited replication, thus resulting in immortality, is another cancer hallmark. Cancer cells have the unlimited ability to divide and replicate and thus reach the macroscopic tumour stage. Replicative immortality rarely occurs because of natural cell senescence or elimination, but it is aided due to disrupted apoptosis (Hanahan and Weinberg, 2011; Walenkamp *et al.,* 2014). Furthermore, the telomeres that protect the ends of the chromosomes are related to unlimited proliferation of cancer cells because pathways that maintain telomeres becomes activated (Blasco, 2005). Normal tissues and cancer tissues require angiogenesis because it allows movement of nutrients and oxygen and the expulsion of CO_2 and metabolic wastes. Thus, when a tumour grows, new blood vessels help expand neoplastic growths, which makes angiogenesis a hallmark of cancer (Bredholt *et al.,* 2015; Hou *et al.,* 2015; Hu *et al.,* 2015; Ilhan-Mutlu *et al.,* 2015; Raica *et al.,* 2009).

Other signs or hallmarks of cancer include the presence of activated invasion and metastasis. The presence of multiplying cells in the same organ as any primary tumour is called an "invasion." When cancer migrates from one organ to another, the dissemination process is not directly linked to the primary site. This is known as metastasis and it is mediated via a complex relationship between the cancer cells and other cells via the extra-cellular matrix (ECM) (Hanahan and Weinberg, 2011; Walenkamp *et al.,* 2014; Wang *et al.,* 2015).

Both genomic instability and mutation have been described as cancer hallmarks in recent studies. A majority of the identified hallmarks depend on alterations in the genomic structure of the neoplastic cells (Hanahan and Weinberg, 2011; Walenkamp *et al.,* 2014; Wang *et al.,* 2015). This can include so called epigenetic changes; for example, the reactions of DNA methylation and histone modification can result in the inactivation of TSGs (Cedar and Bergman, 2009).

When deregulation occurs in the energy metabolising process, it is also considered a cancer hallmark. An example of this is seen in the unusual glycolytic fuelling that can cause mutations in TSGs and the activation of different oncogenes, such as *Ras* (Hanahan and Weinberg, 2011; Hirschey *et al.,* 2015; Jones and Thompson, 2009; Ma and Vosseller, 2014; Wang *et al.,* 2015).

The immune system plays a vital role in resisting or mitigating the incidence of cancer. Nevertheless, cancerous tumours/cells have the ability to avoid the immune system. The mechanisms by which they do so are not clear. Thus, the evasion of immune destruction is a main hallmark of cancer (Hanahan and Weinberg, 2011; Walenkamp *et al.,* 2014; Wang *et al.,* 2015). For this reason, the combined use of immunotherapy and chemotherapy is a viable option that provides increased efficiency when immunotherapy is used as a cancer treatment (Mellman *et al.,* 2011).

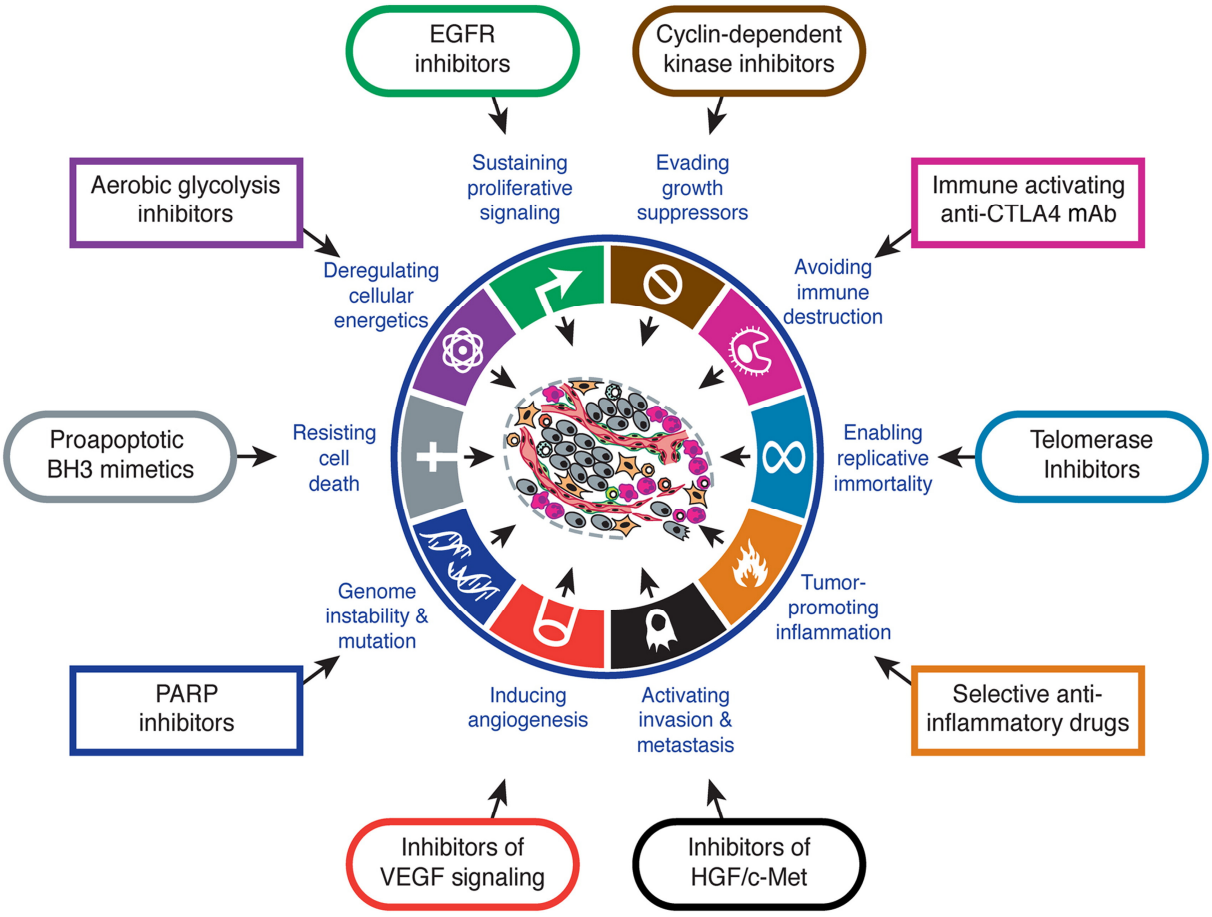

Figure 1.4 A schematic diagram showing the hallmarks of cancer.
Hanahan and Weinberg (2011) indicated that cancerous cells possess the capacity to achieve immortality via replication, developing resistance to cellular death or apoptosis, evading growth suppressors, promoting proliferative signalling, sustaining angiogenesis and using tissue invasion and metastasis. Furthermore, these cells also evade immune destruction and can cause the re-programming of energy metabolising processes such as mutation and genomic instability. They can also initiate inflammation.
Taken from (Hanahan and Weinberg, 2011; Walenkamp *et al.,* 2014).

1.2. The function played by TSGs and oncogene during tumourigenesis

The mutational changes that occur in three groups of genes have been implicated in the process of tumourigenesis. These gene groups include TSGs, oncogenes and genes responsible for maintaining genome stability (e.g., those associated with repairing damaged DNA) (Hanahan and Weinberg, 2011; Kim, 2015; Morris and Chan, 2015; Negrini *et al.,* 2010; Vogelstein and Kinzler, 2004).

1.2.1. Tumour suppressor genes (TSGs)

TSGs, which are also known as anti-oncogenes, are genes that encode that proteins required to inhibit cellular growth or induce cellular apoptosis or death. Many kinds of TSGs have been recognised based on their role in various kinds of cancer, such as *p53* (TP53), which is referred to as the keeper or guardian of the genome. A loss of function or inactivation occurs in genes through the process of genetic mutation and DNA methylation (Kim, 2015; Li and Wang, 2015; Thoma *et al.,* 2011). An important explanation or hypothesis for functional loss in TSGs is the "two-hit hypothesis" (Knudson, 1971), which stipulates that there must be a functional loss in two alleles resulting in cancer. A typical example is seen in the mutation of the *Rb1* gene, which manifests in different kinds of cancer including lung, breast and eye cancer (Chen *et al.,* 2009; Kim, 2015; Morris and Chan, 2015; Thoma *et al.,* 2011). Another example, TP53 is vital in activating both the senescence and apoptosis processes. Loss of the *TP53* gene or mutational changes in that gene are seen in over 50% of human cancers. It is associated with metastatic processes such as the migration of cells and invasive processes (Kim, 2015; Li and Wang, 2015; Meek, 2015; Muller *et al.,* 2011). p53 is involved in many functions that might overlap with the tumour-suppressing ability in cellular processes, which include metabolic cycles, DNA damage response, stem cell differentiation and cellular aging. p53 possesses the ability to regulate the expression of many genes; some of these genes are associated with cellular growth control, cell division, survival and apoptosis (Aloni-Grinstein *et al.,* 2014; Hu *et al.,* 2012; Meek, 2015). Some results suggest an association of p53 with the induction of neuronal death during Alzheimer's disease (Checler and da Costa, 2014; Meek, 2015). Mice that do not have p53 are vulnerable to spontaneous tumour formation; the deliberate removal of p53 in mice models for some particular cancers results in rapid tumour development and mortality (Chen *et al.,* 2005; Dankort *et al.,* 2007; Meek, 2015).

1.2.2. Oncogenes

The term "oncogene" includes all the families of genes with the ability to cause cancer by promoting unlimited cell proliferation. Proto-oncogenes refer to normal genes inside cells that code for protein-enhanced cellular development by stimulating cell division, mitigating cell differentiation and disrupting apoptosis processes. Genetic mutations, the translocation of chromosomes and overexpression can result in such genes being converted into oncogenes (Bagci and Kurtgöz, 2015; Croce, 2008; Kanda *et al.,* 2015; Li and Wang, 2015; Luo and Hahn, 2015; Saito *et al.,* 2015). Although these genes cannot cause cancer on their own, they act together with other oncogenes or in combination with a lack of cellular TSGs. Oncogenes code for particular cell proteins that play vital roles in a range of functions, including chromatin remodelling, transcriptional factor secretion, apoptosis, signal transduction or growth control (Bagci and Kurtgöz, 2015; Croce, 2008; Luo and Hahn, 2015; Saito *et al.,* 2015). Furthermore, viral oncogenes can also begin and support the development of many kinds of cancers that occur due to chronic viral infections. Viral oncogenes can also cause mutations in pro-oncogenes via the insertion of their promoters within the host chromosomal DNA (e.g., within the enhancer or promoter region), thus resulting in the activation of the transcription factor genes. When these genes are overexpressed, they usually cause expression changes in TSGs (Ajiro and Zheng, 2014; Bagci and Kurtgöz, 2015; Luo and Hahn, 2015; Ranzani *et al.,* 2013).

1.2.3. Genome stability genes

Genome stability genes (also known as caretaker genes) refer to a family of genes associated with the repair of mistakes in DNA during its replication or following induction after being exposed to mutagens (Langie *et al.,* 2015; Maluszek, 2015; Negrini *et al.,* 2010; Vogelstein and Kinzler, 2004). This family of genes includes genes such as Nijmegen breakage syndrome 1 (*NBS1*), ataxia telangiectasia protein (*ATM*) and breast cancer susceptibility 1 and 2 (*BRCA1* and *BRCA2*), all of which are mutations seen in different cancers such as ovarian cancer, breast cancer, lymphomas and leukaemia (Donepudi *et al.,* 2014; Kuo *et al.,* 2015; Mateo *et al.,* 2015; Negrini *et al.,* 2010). This gene family limits the level of genetic changes known to heighten the percentage of changes in other genes (Langie *et al.,* 2015; Maluszek, 2015; Negrini *et al.,* 2010; Vogelstein and Kinzler, 2004).

1.3. Methods of cancer treatment

The treatment of cancer during its late stages, when cancerous cells have invaded the body and changed to form metastatic cells, is difficult. Therapy generally takes the form of surgical interventions, radiotherapy, chemotherapy and combined therapy plans using one or more of these treatments (Aly, 2012; Brown *et al.,* 2015; Islam *et al.,* 2015; Suri, 2006). Treatments have certain benefits for patients, although they may be related to detrimental side effects and a failure to target all of the cancerous cells. Surgical interventions are the most effective option for the treatment of pre-metastatic solid tumours (Aly, 2012). Using radiotherapy as a therapeutic option is difficult because it has very severe side effects, such as fatigue, nausea, anorexia, alterations in taste and increased risk of microbial infection combined with skin inflammations. In addition, lengthy sessions of radiotherapy cause memory loss, endocrine malfunction, incontinence and unbalanced gaits (Aly, 2012; Brown *et al.,* 2015; Eichler and Plotkin, 2008).

Chemotherapeutic treatment options also have many side effects, such as emesis, anorexia, fatigue, hair loss, nausea, nosebleeds, stomach ache with oedema, chronic diarrhoea and weight gain or weight loss (Carelle *et al.,* 2002; Carr *et al.,* 2014; Kreamer, 2014). Because cancer cells divide more quickly than normal cells, they are much more vulnerable to chemotherapeutic medicines than are normal cells. Chemotherapy does not specifically target cancer cells but rather targets all the cells undergoing multiplication, including normal cells that are in various phases of cell division. Furthermore, resistance to chemotherapeutic agents may occur because of various underlying mechanisms, such as continuous mutations in cancer cells that lead to the failure of effective treatments (Rivera and Gomez, 2010).

Immunotherapy is a vital option for cancer treatments. For example, adoptive T-cell therapies and immune checkpoint blockade approaches (Sathyanarayanan and Neelapu, 2015). The immune system of patients battling cancer usually does not cope effectively with the quick growth rate of malignant tumours. This leads to the need for new immunotherapeutic options combining early recognition, diagnostics and appropriate treatment of cancerous growths. The development of these options is a vital aim of most cancer immunotherapeutic plans. Cancer immunotherapy plans possess more benefits than other traditional treatment options because they promote the proper functioning of a patient's immune system to fight malignant tumour cells. Furthermore, they have relatively fewer side effects and are more target-specific (a good example is tumour-related antigens [TRAs]; see Section 1.5) (Aly, 2012; Domingues *et al.,* 2014; Pardoll, 2003; Shah and Goldberg, 2015; Zavala and Kalergis, 2015).

The human immune system can recognise and distinguish between auto antigens and foreign antigens. The aim of immunotherapy is to improve the patient's immune system so it destroys cancerous cells with assistance from T-cells, B-cells and other natural killer cells (Aly, 2012; Domingues *et al.,* 2014; Harris and Drake, 2013; Mellman *et al.,* 2011; Pardoll, 2003; Shah and Goldberg, 2015).

There have been major recent advances in immunotherapy due to immune checkpoint inhibitors (e.g., ipilimumab and nivolumab). They are powerful and important new drugs and approved for the advanced melanoma treatment, as well as showing great promise to benefit other cancers; ipilimumab is a cytotoxic T-lymphocyte-associated antigen 4 (CTLA-4) checkpoint inhibitor; nivolumab is a programmed death 1 (PD-1) checkpoint inhibitor (Domingues *et al.,* 2014; Larkin *et al.,* 2015; Postow *et al.,* 2015; Topalian *et al.,* 2015). The process of T-cell activation is an extreme controller event. This event is initiated by T-cell activation, anti-tumour impacts and proliferation. In addition, the T cell is required to receive two diverse signals. First, a presented tumour antigen must recognise the T cell. Second, a co-stimulatory signal makes the activation response strong (Hoos *et al.,* 2010; Kreamer, 2014). When a T cell recognises any tumour antigens, this is followed by signalling via the CTLA-4 pathway; these result in the prevention of the co-stimulatory signal. This cellular process is known to be a natural inhibitory mechanism that affects the immune response. Ipilimumab refers to a human anti–CTLA-4 antibody that performs the function of blocking CTLA-4 signalling. As such, it provides for co-stimulatory signalling and the initiation of anti-tumour T-cell responses. PD-1 refers to a separate inhibitory receptor, which is expressed within T cells. However, this receptor possesses a non-overlapping functionality that is different from the one seen in CTLA-4. In the cancer progression scenario, the ligands for PD-1, PD-L1 (indicated to be the predominant ligand) and PD-L2 have been documented to be expressed within the tumour's microenvironment (Kreamer, 2014; Nirschl and Drake, 2013; Pardoll, 2012; Zou and Chen, 2008).

Several monoclonal antibodies of anti-PD-1 and anti-PD-L1 are present in the highly developed phase of clinical research. These include nivolumab (anti-PD-1), pidilizumab (CT-011; anti-PD-1), pembrolizumab (Keytruda, MK-3475; anti-PD-1), MEDI4736 (anti-PD-L1) and MPDL3280A (anti-PD-L1). It has been indicated that the functions are carrying out the inhibition of PD-1/PD-L1 binding and restoring the anti-tumour immune responses (Kreamer, 2014; Langer, 2014).

The main goals remain the utilisation of immunotherapy in targeting cancer cells while not affecting normal healthy cells (Domingues *et al.,* 2014; Iclozan and Gabrilovich, 2012). Based on this view, one significant goal is the identification of cancer-specific biomarkers or antigens for use in clinical immunotherapy strategies. The cancer testis antigens (CTAs) (see Section 1.6) are a perfect immunological target that can be used by all forms of clinical approaches, similar to adoptive cell therapies (see Section 1.6.4.1). Therefore, cancer immunotherapy may become an optimal treatment, replacing traditional therapies for cancerous tumours in the future (Emens and Romero, 2015).

1.4. Antigen markers for defining cancer

Cancer markers are factors present in the human body that indicate the presence of a tumour (Yalak and Vogel, 2015). Certain cancer markers are known to exist on/within the solid tumour itself, within the lymph nodes, inside the bone marrow or in other bodily fluids, such as blood and urine. These markers are created by the body's responsive mechanisms to cancer or the cancerous cells themselves. Certain markers found in various kinds of cancers are proteins, but many of the latest markers identified are genes or include some levels of genetic materials (either DNA or RNA) (Mäbert *et al.,* 2014). Two separate kinds of cancer markers have been identified: specific markers, which are related to a single type of cancer, and non-specific markers, which can be seen in many kinds of cancer (Freidlin and Korn, 2014; Lindblom and Liljegren, 2000).

Cancer markers are useful in many ways. First, they can be used for cancer screening and the early identification of malignant tumours. The main aim of a cancer marker is to help diagnose cancer in people who do not have any clinical indications or symptoms of the disease. The quick and early diagnosis of malignant tumours is vital to patient survival (Duffy, 2001; Duffy *et al.,* 2014; Lech *et al.,* 2014; Thomas and Sweep, 2001; Yalak and Vogel, 2015). One commonly utilised malignant tumour diagnostic marker is the prostate-specific antigen (PSA). The PSA blood-testing procedure is utilised to screen for prostate cancer in men because men who have prostate cancer generally exhibit heightened PSA levels (Duffy, 2014; Schröder *et al.,* 2009; Young *et al.,* 2015). Second, markers are used to diagnose particular kinds of cancer. In many patients, cancer markers themselves do not provide a definitive diagnosis for any specific type of cancer; however, they can be complemented with a biopsy for a clear diagnosis. Third, markers are used to determine the prognosis for some kinds of cancer. Fourth, the markers can be used to evaluate the

effectiveness of any administered cancer therapy. If a particular kind of cancer has a definitive marker, alterations in its levels (i.e. decreases or increases) this can indicate the efficiency of the treatment being used (Duffy, 2001; Molinari *et al.,* 2015; Thomas and Sweep, 2001).

Several known cancer biomarkers can be utilised in targeted therapies and in forming a diagnosis. A good example of this is the use of the ErbB2 receptor tyrosine kinase 2 (ErbB2) and carcinoembryonic antigen (CEA) biomarkers for human breast cancer and colon, respectively. In addition, the two biomarkers can be utilised in active and passive therapeutic plans (Baulande *et al.,* 2014; Butterfield, 2015; Even-Desrumeaux *et al.,* 2011; Jr and Partridge, 2014).

Many research studies have indicated that cancer cells can alter gene expression by changing them from up-regulated to down-regulated or vice versa. Up-regulated genes are used as cancer biomarkers for various tumours (Caballero and Chen, 2009; Costa *et al.,* 2007; Du *et al.,* 2015b; Paoletti and Hayes, 2014).

1.5. Classifying tumour-related antigens (TRAs)

Changes in gene expression and sequence, such as mutational changes in proto-oncogenes, TSGs and instability genes as well as epigenetic alterations, all cause the unusual production of proteins. Such proteins are called TRAs. TRAs can induce the human immune system to produce a single epitope (peptide) identifiable to the immune system. To be used in cancer immunotherapy, TRAs must be limited within malignant tumours and not be present in normal cells, located in stable and homogenous forms within identified detected malignant tumours and targeted using cytotoxic T lymphocytes (Krishnadas *et al.,* 2013). The characterisation and recognition of TRAs is now one of the main fields of cancer research that focuses on immunotherapy (Butterfield, 2015; Zavala and Kalergis, 2015). TRAs can be grouped into various types based on their expression patterns.

1.5.1. Viral antigens

Many kinds of tumours result from viral infections that initiate the cellular production of viral proteins, which can be identified by the human immune system. For instance, the human papillomavirus antigen (HPV) is related to incidents of cervical cancer (Mirkovic *et al.,* 2015; Reyes *et al.,* 2015; Roberts *et al.,* 2014; Tertipis *et al.,* 2015; Vogt, 2012).

1.5.2. Differentiation antigens

These antigens are expressed in malignant tumours and normal cells with the same kinds of lines. For instance, tyrosine, MART1/MelanA and gp100 glycoprotein are involved in the development of melanoma cancer. This protein may serve as a target for the human immune system, which can then destroy the tumour (Barrio *et al.,* 2012; de Araújo Farias *et al.,* 2015; Gupta *et al.,* 2015; Kozłowska *et al.,* 2013; Roy *et al.,* 2015).

1.5.3. Overexpressed antigens

Many genes have been documented as being up-regulated or down-regulated inside cancerous tissues. Peptides obtained due to overexpressed proteins are also involved in T-cell responses. The decreased rate of expression within normal cells should not lead the human immune system to identify such proteins. For instance, overexpressed antigens, such as the transmembranemucin MUC1, are related to several carcinomas (Apostolopoulos *et al.,* 2015; Kaur *et al.,* 2014; Singh *et al.,* 2006).

1.5.4. Cancer testis antigens (CTAs)

This family of genes codes for the expression of proteins only from human germ-lines and malignant tumours. Because of their specific expression pattern, CTAs can be utilised for immunotherapy, cancer diagnosis, biomarkers and the creation of cancer drugs; in addition, they may be oncogenic (Gjerstorff *et al.,* 2015; Krishnadas *et al.,* 2013; Whitehurst, 2014).

1.6. CTAs biology: Regulation, therapeutic potential, clinical uses and putative function

CTA genes belong to a large family of genes that have been expressed in many different types of tumours in humans (Butterfield, 2015; Marcar *et al.,* 2015; Yang *et al.,* 2015). However, CTA genes are not normally expressed in noncancerous tissues other than the testis and the placenta. These antigens are particularly useful for the study and development of immunotherapeutic approaches, including CTA-based vaccine therapy (see Section 1.6.3.2) and adoptive therapies (see Section 1.6.4.1) (Feichtinger *et al.,* 2012; Taguchi *et al.,* 2014). A better understanding of the biology of CTAs is required to further develop these tumour-specific immunological approaches. More than 70 families of CTA have been identified, and research is being conducted to further investigate their biology. How these antigens function in noncancerous tissues is still not understood, but it is clear that many CTA genes are

expressed in spermatogenesis (Fratta *et al.,* 2011; Whitehurst, 2014). According to Gjerstorff *et al.,* (2015) and Simpson *et al.,* (2005). CTAs can be organised into two categories. The first type of CTAs are called X-CTA genes because the CTA genes are located on the X chromosome (see Figure 1.5). The second category contains CTA genes, which are not encoded on the X chromosome; therefore, these are known as non-X-CTA genes. According to several reports, X-CTA families account for 10% of all genes on the X chromosome. In addition, the X-CTA family includes over 50% of all CTAs, which frequently represent multigene families. These families are structured in clearly defined groups along the X chromosome, where the different components are positioned into complex inverted and direct repeats (Domae *et al.,* 2014; Gjerstorff *et al.,* 2015; Simpson *et al.,* 2005; Zendman *et al.,* 2003). However, as shown in Table 1.2, the genes corresponding to the non-X CTA are dispersed throughout the genome and are frequently single-copy genes (Simpson *et al.,* 2005).

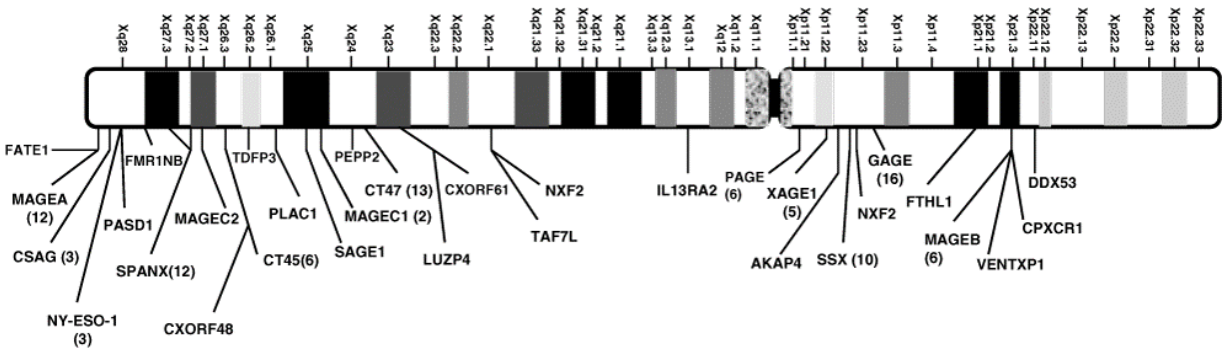

Figure 1.5 Placement of X-CT genes on the X-chromosome.
Various groups of CTAs are seen location-wise on the X-chromosome. The number of single gene groups is given between brackets.
Taken from (Caballero and Chen, 2009).

Table 1.2 Some identified families of X-CTA genes and non-X CTA genes[a].
Adapted from (Fratta *et al.,* 2011).

	CT antigen gene family	Number of genes in family	Chromosome location	Identification method
	MAGE family			
X-CTA	MAGE-A	12	Xq28	T-cell epitope cloning/ molecular methods[b]
	MAGE-B	6	Xp21.3	Molecular methods/RDA[c]
	MAGE-C	3	Xp26-27	SEREX[d]/RDA
	GAGE/PAGE/XAGE super-family			
	GAGE-A	8	Xp11.23	T-cell epitope cloning/ molecular methods
	GAGE-B	8	Xp11.23	RDA/database mining
	PAGE	5	Xp11.23	RDA/database mining
	XAGE	5	Xp11.21-11.22	Database mining
	SSX family			
	SSX	5	Xp11.2	SEREX
	NY-ESO family			
	CTAG	3	Xq28	RDA/SEREX
	Non-familial			
	CAGE	1	Xp22.11	SEREX
	HOM-TES-85	1	Xq23	SEREX
	SAGE	1	Xq26	RDA
Non-X CTA	BAGE	5	21p11.1	CTL epitope cloning
	BORIS	1	20q13.2	Molecular methods
	CT9/3BRDT	1	1p22.1	Database mining
	HAGE	1	6q12-13	RDA
	OY-TES-1	1	12p12-13	SEREX
	SCP-1	1	1p12-p13	SEREX
	SPO11	1	20q13.2-q13.3	Database mining

a) Their wide characterisation is at the base of CTA selection.
b) Screening recombinant libraries with probes, exon trapping and electrophoretic mobility shift assays are included in molecular methods.
c) Representative differential examination.
d) Serological examination of complementary DNA (cDNA) expression libraries.

1.6.1. CTA gene expression in healthy and malignant tumour tissues

X-CTA genes in normal testis are expressed mostly on the spermatogonia due to meiotic X inactivation, which are reproducing germ cells (Domae *et al.,* 2014; Gjerstorff *et al.,* 2015; Lim *et al.,* 2012; Turner, 2007), in contrast to non-X CTA genes, which are also expressed in later phases of germ-cell differentiation (e.g., spermatocytes) (Domae *et al.,* 2014; Lim *et al.,* 2012; Simpson *et al.,* 2005). The messenger RNA of numerous CTA genes has been found to be present in a number of somatic tissues, such as the liver, pancreas or spleen. Nevertheless, as it results from the quantitative reverse transcription-polymerase chain reaction (RT-qPCR) data, the mRNA levels of CTA genes in somatic tissues generally represent less than 1% of their expression in testis (Caballero and Chen, 2009; Scanlan *et al.,* 2004).

The distribution of CTAs is wide and variable among tumours of diverse histotypes. The examination of their transcripts forms the base of current information, which can be interpreted as a high variation of CTA gene expression among tumour kinds. According to reverse transcription-polymerase chain reaction (RT-PCR) investigation, the diverse family and super-family members of CTA genes are moderately expressed in malignant prostate and breast tumours and are strongly expressed in bladder, melanoma and non-small cell lung malignant tumours. According to the same analysis, the CTA genes are weakly expressed in colon and kidney cancers (Domae *et al.,* 2014; Sammut *et al.,* 2014; Scanlan *et al.,* 2002; Scanlan *et al.,* 2004). Similar low amounts of CTA genes have been reported in hematologic cancers, such as non-Hodgkin's lymphomas and primary effusion lymphoma and Hodgkin's (Calabro *et al.,* 2005; Gattei *et al.,* 2005; Lim *et al.,* 2012; Lin *et al.,* 2014).

1.6.2. Regulation of CTA gene expression

To date, epigenetic processes seem to embody the exclusive mechanism equally controlling CTA gene expression in neoplastic cells and normal cells (Karpf and Jones, 2002; Videtic Paska and Hudler, 2015). "Epigenetic" is defined as modifications in gene expression that do not originate in variations of the genomic DNA nucleotide sequence (Antequera and Bird, 1999; Ke *et al.,* 2014; Klose and Bird, 2006; Saleem *et al.,* 2015; Sigalotti *et al.,* 2007). Histone post-translational modifications and DNA methylation modifications are important epigenetic factors involved in the regulation of several CTA gene expression profiles, as shown in Figure 1.6 (Fratta *et al.,* 2011; Saleem *et al.,* 2015; Wang and Chim, 2015; Whitehurst, 2014).

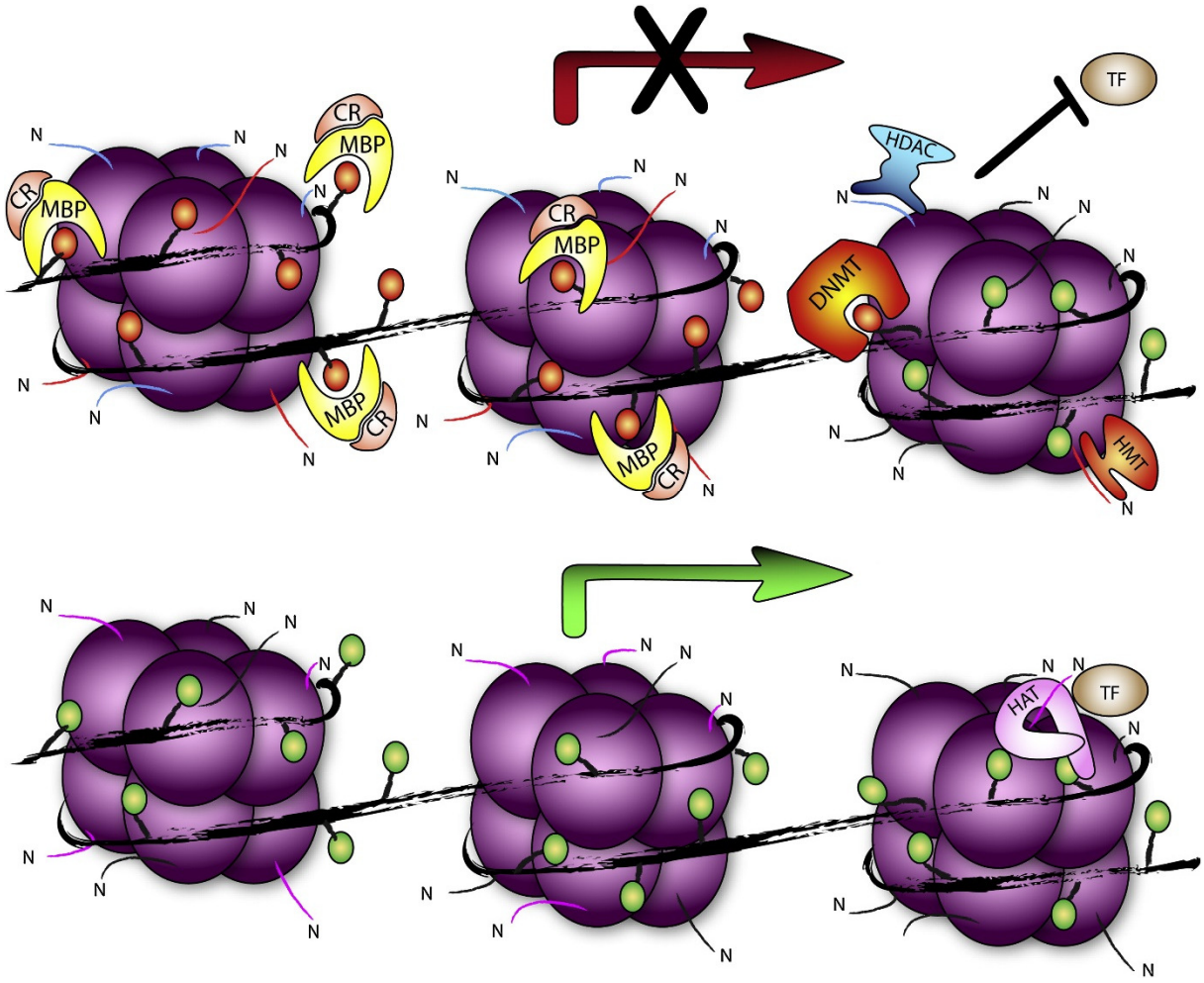

Figure 1.6 Epigenetic control of CTA gene expression.
The presence of methylated cytosines characterises the transcriptionally inactive CTA genes (upper panel) surrounded by the promoter region (small orange circles) that is carried out and supported by DNA methyltransferases (DNMT). The reticence of CTA gene transcription might arise from the methylated recognition sequence, which stops the binding of transcription factors (TF), or it could be an outcome of the binding of methyl-CpG-binding proteins (MBP). The compression of chromatin is a result of the existence within CR of histone deacetylases (HDAC), which are represented by blue N-terminal tails (these mediate the histones' deacetylation), and histone methyltransferas (HMT), which are represented by red N-terminal tails (these catalyse the histones' methylation). The result becomes unreachable to TF, even though it represents a very important part of DNA methylation in inhibiting CTA expression (see red arrow). At the same time, the demethylated CTA promoters (represented by small green circles) also play a very important role; they can prevent the binding of CR and MBP. TF and histone acetyltransfers (HAT) mediate the acetylation of histones (represented by pink N-terminal tails). The outcome of the process is transcriptionally active CTA genes (see green arrow).
Taken from (Fratta *et al.,* 2011).

1.6.2.1. Methylation of DNA

DNA methylation is a common process through which DNA is modified; this process often results in the silencing of gene expression (Ramachandran *et al.,* 2015; Wang and Chim, 2015). The gene silencing can be caused by DNA methylation through a straight interference with the binding of particular transcription factors (TFs) to the DNA (Ramachandran *et al.,* 2015; Saleem *et al.,* 2015; Watt, 1998). Demethylation activates CTA genes during spermatogenesis (Fratta *et al.,* 2011). Recent reports have confirmed the association between CTA gene expression and the DNA hypomethylation of CTA gene promoters. Such an association has been observed in groups of supposed melanoma SCs, which suggests that CTA gene regulation in cancer stem cells (CSCs) (see Section 1.7) might manifest epigenetic regulation as a vital process. DNA methylation, histone acetylation and histone methylation are also involved in the development of carcinogenesis and tumour (Sigalotti *et al.,* 2008; Sowa and Sakai, 2015).

1.6.2.2. Modification of histones

An important role in the epigenetic regulation of CTA gene expression seems to be played by histone modifications (Karpf, 2006; Ke *et al.,* 2014; Sigalotti *et al.,* 2007; Wischnewski *et al.,* 2006). Histones are fundamental proteins with elastic N-terminal tails that extended from the nucleosomes. Post-translational modifications, such as methylation and acetylation, alter the functional role of these proteins (Du *et al.,* 2015a; Iizuka and Smith, 2003). Gene expression is also controlled by histone methylation. During this process, methyl groups are added to the N-terminal arginine and lysine residues, and, in contrast with histone acetylation, histone methylation is linked to both transcriptional activation and repression depending on which histone residues is methylated (Du *et al.,* 2015a; Ramachandran *et al.,* 2015; Santos-Rosa and Caldas, 2005). Shinkai and co-workers provided early evidence for a possible function of histone methylation in CTA gene regulation. It was shown that the knockout of the HMT G9a and/or GLP, which target euchromatic loci as well as catalyse H3K9 dimethylation (H3K9me2), was adequate by itself to stimulate the *MAGE-A* gene expression in embryonic stem cells (ESCs) (see Section 1.7.1.1) (Tachibana *et al.,* 2002; Tachibana *et al.,* 2005). Nonetheless, the genetic knockdown of G9a and/or GLP in colon cancer cells of humans did not stimulate CTA gene expression, despite the fact that it decreased H3K9 methylation at a general level and at CTA gene promoters (Link *et al.,* 2009). Cell Survival pathways are also controlled by histone-modifying proteins (Füllgrabe *et al.,* 2014).

1.6.3. Therapeutic potential of CTA

1.6.3.1. CTA immunogenicity

From an immunological perspective, CTAs could be considered fundamentally tumour-specific targets. The main reasons for this are that CTA genes are generally expressed in malignant tumours and not in healthy tissue, with the exception of the testis, which reside in immune-privilege (Gjerstorff *et al.,* 2015; Whitehurst, 2014). The blood-testis barrier (BTB) along with the lack of HLA class I expression on the surface of germ cells block the immune system from the interface with CTA proteins producing what are known as non-self-structures (Bart *et al.,* 2002; Fiszer and Kurpisz, 1998; Gjerstorff *et al.,* 2015; Kalejs and Erenpreisa, 2005; Modarressi *et al.,* 2011). Cell-mediated and spontaneous humoral immune reactions have been shown against numerous CTAs. One of the most immunogenic CTAs identified is NY-ESO-1, which is responsible for inducing coordinated and spontaneous humoral and cell-mediated immunoreactions in a very large proportion in the patients with NY-ESO-1 positive malignant tumours. The anti-NY-ESO-1 antibody is present in 4-12.5% of lung cancers, 36% of thyroid cancers, 10% of melanomas and approximately 8-16% of breast cancers (Fratta *et al.,* 2011; Gjerstorff *et al.,* 2015; Srivastava *et al.,* 2014).

1.6.3.2. CTA vaccine therapy

Ideal cancer treatments target the CTA molecules for specific immunotherapeutic intervention. There are numerous clinical trials that have been finalised or are currently ongoing which use CTAs, in particular NY-ESO-1 and MAGE-A3, as vaccinating agents in patients with melanoma, prostate, ovarian as well as lung cancers (Fratta *et al.,* 2011; Gjerstorff *et al.,* 2015; Srivastava *et al.,* 2014; Whitehurst, 2014).

The basis for the early approaches of CTA-based immunotherapy for cancer patients was comprised of the classification of immunogenic peptides from chosen CTAs, along with the detection of the corresponding HLA class I antigen limitations. This immunotherapy was based on using CTA peptides like vaccinating agents. For example, peptides derived from MAGE-A3 have been part of vaccines used to treat tumours producing this specific antigen. When treated with MAGE-A3 peptides in a pivotal clinical trial, more than 30% of the treated patients with melanoma (7 patients out of 25) presented substantial tumour regressions, and three patients saw full responses (Gjerstorff *et al.,* 2015; Marchand *et al.,* 1999). In addition, NY-ESO-1 and MAGE-A3 proteins are being analysed as anticancer vaccines in several clinical tests (Gjerstorff *et al.,* 2015; Marchand *et al.,* 2003; Yang *et al.,* 2015).

1.6.4. Clinical uses of CTA genes

Vaccines have been extremely efficient in creating defensive immunity against infectious agents; nevertheless, their use against cancerous disease has been generally disappointing (Mellman *et al.,* 2011; Tagliamonte *et al.,* 2014). Two types of cancer vaccines have been developed: prophylactic vaccines, which help prevent viral origin cancers (e.g., hepatitis B and human papilloma virus vaccines to help treat cervical cancer); and therapeutic vaccines, which help treat existing cancers. These vaccines usually attempt to work by strengthening the body's natural defence system against foreign invaders (Mellman *et al.,* 2011; Palucka *et al.,* 2010; Tagliamonte *et al.,* 2014). Immunotherapy for cancer is utilised in two main ways: passive immunotherapy that is inclusive of adoptive cell therapy (see Section 1.6.4.1) and the use of monoclonal antibodies (see Section 1.6.4.2) as well as active immunotherapy (see Section 1.6.4.3) that is dependent on using vaccines.

1.6.4.1. Adoptive cell therapy

Adoptive immunotherapy works on the basis of being able to isolate the lymphocyte T-cells of a patient, then carrying out a culture with an enrichment process *in vitro* to promote the expression of desired tumour antigens and then re-infusion into the patient's body (Fujiwara, 2014; Restifo *et al.,* 2012; Rosenberg and Restifo, 2015). An example was shown by Hunder *et al.,* (2008) who carried out treatment of a patient suffering from melanoma metastasis use autologous CD4+ T cells to target the CTA NY-ESO-1. They did isolation and subsequent expansion of CD4+ T cells from a patient *in vitro* isolating CD4+ T cell that react against the CTA NY-ESO-1 and then carried out an infusion of these cells back into the patient. After 60 days, following the infusion of these cells into the patient, no incidence of either nodal or pulmonary tumours was seen, and the patient was cancer-free for at least two years post-treatment (Hunder *et al.,* 2008).

1.6.4.2. Use of monoclonal antibodies

Monoclonal antibodies are currently utilised to treat cancer. Many commercially branded monoclonal antibodies are manufactured to target cancer cells, including Cetuximab that is utilised to treat colorectal cancer (Van Cutsem *et al.,* 2009; Weiner, 2015). Monoclonal antibodies specifically target TRAs, and they have demonstrated a certain degree of therapeutic efficiency. For instance, antibodies conjugated with radioactive isotopes or chemotherapeutic medications are utilised to treat haematological malignancies and have

demonstrated their benefit in significant results. In stark contrast, non-leukaemia cancers are normally treated using unconjugated antibodies, which generally block growth factor receptors such as epidermal growth factor receptors 1 and 2 (ERBB1 and ERBB2), both of which are expressed in 10–39% of human breast cancers (Cohen and Sznol, 2015; Omenn *et al.,* 2014; Patanè, 2014; Weiner *et al.,* 2010).

1.6.4.3. Active immunotherapy

Many studies have shown that humoral immune responses to CTAs are seen in various kinds of malignant tumours. For instance, many of the antibodies against CTSP-1, NY-ESO-1, SCP-1 and SSX-2 in breast cancer work because of this response. Antibodies against NY-ESO-1, SSX2 and MAGE-A3 in numerous myelomas are also due to such responses. Furthermore, trials of a cancer vaccine for melanoma patients (utilising NY-ESO-1 or MAGE-A3) have documented a regression in the numbers of tumour nodules. For NY-ESO-1, 34 trials have been conducted using NY-ESO-1 peptide, protein and pox-NY-ESO-1. A significantly effective vaccine that gives positive results in treating cancer is NY-ESO-1 protein/ISCOMATRIX®. As such, CTAs could be a potentially effective target for decreasing the risk of melanomas and may assist in immune system adaptations (Caballero and Chen, 2009; Fujiwara, 2014; Hinrichs and Rosenberg, 2014).

1.6.5. Genome-wide examination of CT gene expression

Certain CT genes that are usually expressed in human germ-line cells or are activated in numerous cancer categories are likely to encode antigens with an immune response in cancer patients. These CT genes have the prospect of becoming biomarkers and targets in immunotherapy. Hofmann *et al.,* (2008) conducted an extensive genome-wide survey of expression for a group of 153 CT genes that were present in cancer and normal tissue expression libraries. This survey was performed utilising several *in silico* investigation tools for gene expression protein, including double the expressed sequence tag numbers used before. The results showed that the gene expression profiles of these genes are heterogeneous, despite the fact that such genes are expressed in synchrony in the testis. This fact permits classification of CT genes into three groups that present supplementary expression in somatic tissues: testis/brain restricted, testis restricted and testis selective (Hofmann *et al.,* 2008; Whitehurst, 2014).

It has been observed that the expression of certain CTA genes occurs within immunologically privileged regions such as the central nervous system (CNS) (genes from this group are called cancer testis/CNS genes). Usually, CTA genes have been further divided on the basis of their expression inside cancer and normal tissues as shown below:

(A) Testis and/or CNS restricted genes: The expression of genes in this family is limited to the testis or to the testis, certain central nervous tissues and cancerous tissues.

(B) Testis and/or CNS selective genes: The expression of genes in this family is observed within the testis and/or the CNS, a few normal tissues and cancerous tissues (Feichtinger *et al.,* 2012; Sammut *et al.,* 2014).

1.6.6. CTAs, spermatogenesis and carcinogenesis

According to investigations conducted over the latest 15 years, developing germ cells express an enormous number of genes. Such genes have been found to be proto-oncogenes and/or oncogenes that were expressed or not expressed in low levels in normal mammalian cells. However, an exception to the above statement appears when cells are transformed and /or induced to go through carcinogenesis. Utilising the sera of cancer patients to monitor the cDNA library or recombinant proteins of the human testis, numerous CTAs were discovered to be extremely antigenic. Other CTAs that have been used are biomarkers of different tumours, for instance, those found in cervical, ovarian, lung and breast cancer (Cheng *et al.,* 2011; Whitehurst, 2014).

1.6.6.1. Functional roles of human CTAs in the gamete

The functional role of many CTAs in human gametogenesis is still unclear. However, knockout and gene expression analysis of several CTA genes to identify their functional roles have detected that the expression of *MAGEA1* and *NY-ESO-1* X-linked CTA genes are expressed during early spermatogenesis, suggesting that during the early stages of spermatogenesis these CTA proteins are important as the X chromosome is inactivated during later spermatogenesis (see Figure 1.7) (Jungbluth *et al.,* 2000; Whitehurst, 2014).

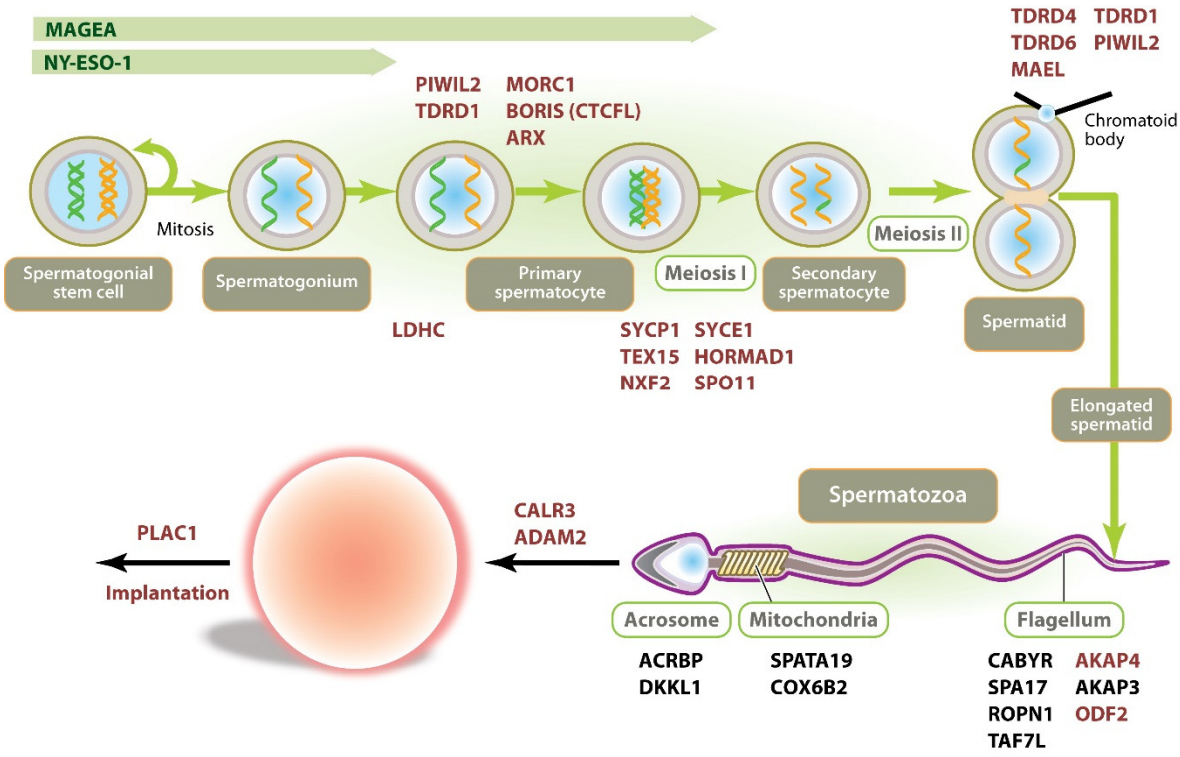

Figure 1.7 Examples of CTA gene expression timing during spermatogenesis.
Taken from (Whitehurst, 2014).

Numerous CTAs are associated and involved in controlling the energy production in human sperm. Furthermore, many CTAs contain functional roles in controlling mRNA expression and maintaining genomic integrity in sperm. TDRD1 (see Section 1.8), PIWIL2 (see Section 1.8.1) and piRNAs (see Section 1.8.2) associate together in silencing transposons throughout spermatogenesis. PIWIL2 might control the levels of p53 (Aravin *et al.,* 2007; Hüttemann *et al.,* 2003; Kuramochi-Miyagawa *et al.,* 2004; Lu *et al.,* 2012; Whitehurst, 2014). Figure 1.8 illustrates the CTAs oncogenic functions (Gjerstorff *et al.,* 2015).

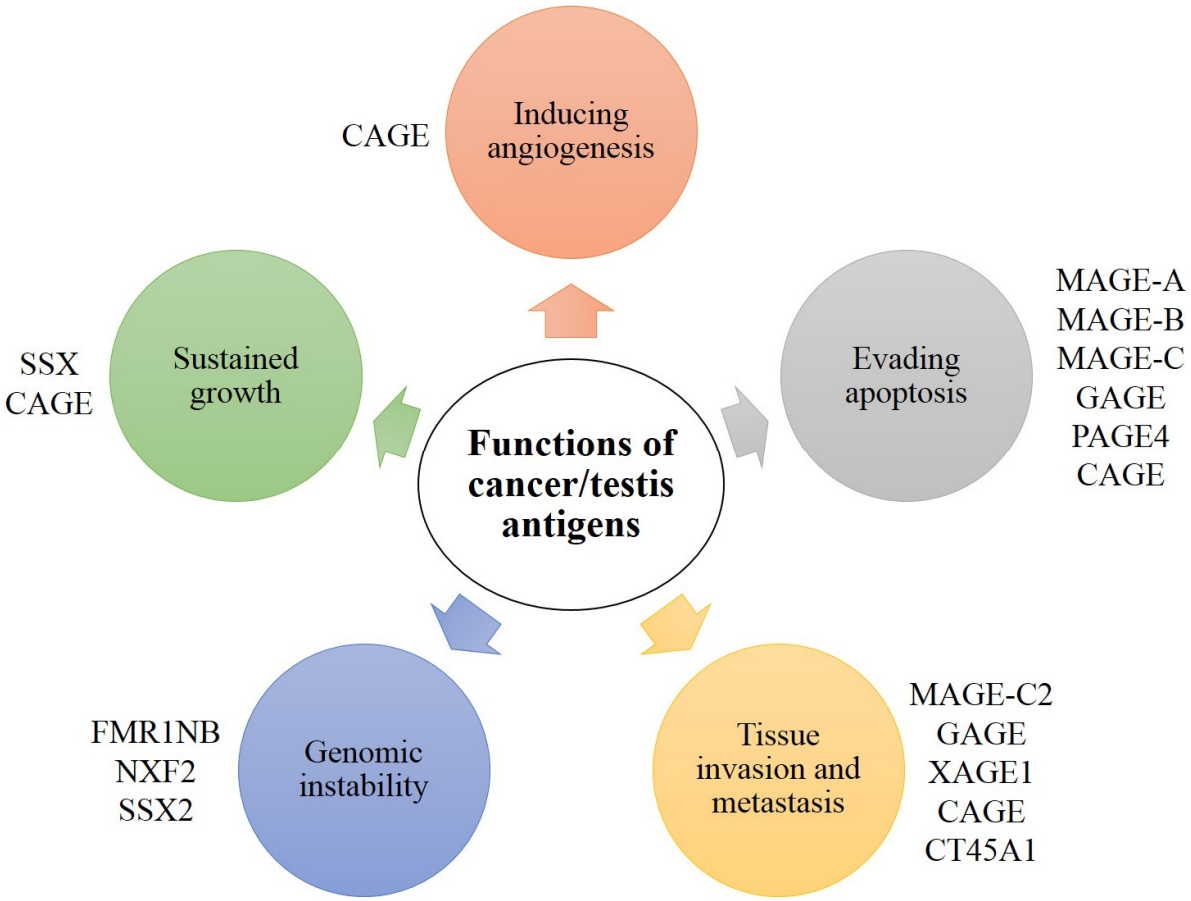

Figure 1.8 Examples of CTA oncogenic functions.
Adapted and modified from (Gjerstorff *et al.,* 2015).

1.7. Stem cells (SCs) and cancer stem cells (CSCs)

CTAs have been linked to stemness (Yang *et al.,* 2015). SCs are characterised by their ability to self-renew and their capacity to differentiate and divide into various specialised cell categories (Goodell *et al.,* 2015; Simara *et al.,* 2013; Wong *et al.,* 2013) To date, five types of SCs have been identified: induced pluripotent stem cells (iPSCs); germinal stem cells (GSCs); embryonic stem cells (ESCs); those originated from somatic stem cells, called adult stem cells (ASCs) and cells originated from embryonic carcinomas cells (ECCs). ASCs currently the most promising participants in regenerative medicine. Such cells perform the functions of renewing tissues and regenerating them following injury (Devine *et al.,* 2011; Gong *et al.,* 2015; Gonzalez and Bernad, 2012; Huang *et al.,* 2015; Mae and Osafune, 2015; Matsa *et al.,* 2014; Wagers, 2012; Yu *et al.,* 2012).

ESCs are also of particular interest as they are able to differentiate into all cell kinds through the development of an embryonic process. In recent years, researchers have been able to re-programme somatic cells into SC-like cells, which have the characteristics of ESCs and are referred to as iPSCs (Huang *et al.,* 2015; Takahashi and Yamanaka, 2013; Zhou *et al.,* 2013). All these cells types have the potential to be used in a number of therapeutic applications, particularly in the field of tissue regeneration and engineering (Diekman *et al.,* 2012; Fox and Duncan, 2013; Matsa *et al.,* 2014; Wong *et al.,* 2013). In addition to the development of iPSCs, a subpopulation of SC-like cells have recently been located in tumours; these cells are known as CSCs (Ajani *et al.,* 2015; Dashyan *et al.,* 2015; Gong *et al.,* 2015; Kesanakurti *et al.,* 2013; Qiu *et al.,* 2015).

Observations of the correspondence between normal organ self-renewal mechanisms and the successive proliferation of cancers led to a theory regarding the creation of CSCs (Ajani *et al.,* 2015; Plaks *et al.,* 2015; Reya *et al.,* 2001). CSCs have been described and recognised in instances of brain, lung, breast and myeloid leukaemia cancers (Jordan, 2004; Osaki *et al.,* 2015). The CSC theory proposes that not all tumour cells contain the capacity to maintain and proliferate tumour progression and further suggests that only a small subpopulation of tumour cells, i.e. CSCs, are primed to self-renew and proliferate (Ajani *et al.,* 2015; Bonnet and Dick, 1997). Furthermore, CSCs might arise from differentiated cells or even from committed progenitors (see Figure 1.9) (Friedmann-Morvinski and Verma, 2014; Joseph *et al.,* 2008; Zheng *et al.,* 2008). CSCs have yet to be recognised in certain cancers, and ongoing research aims to associate SC markers with malignant cancer cells (Islam *et al.,* 2015; Ye *et al.,* 2008). The discovery of CSCs has had a major impact on modern medicine and research. The evolution of the CSC is illustrated in Figure 1.9 and Figure 1.10.

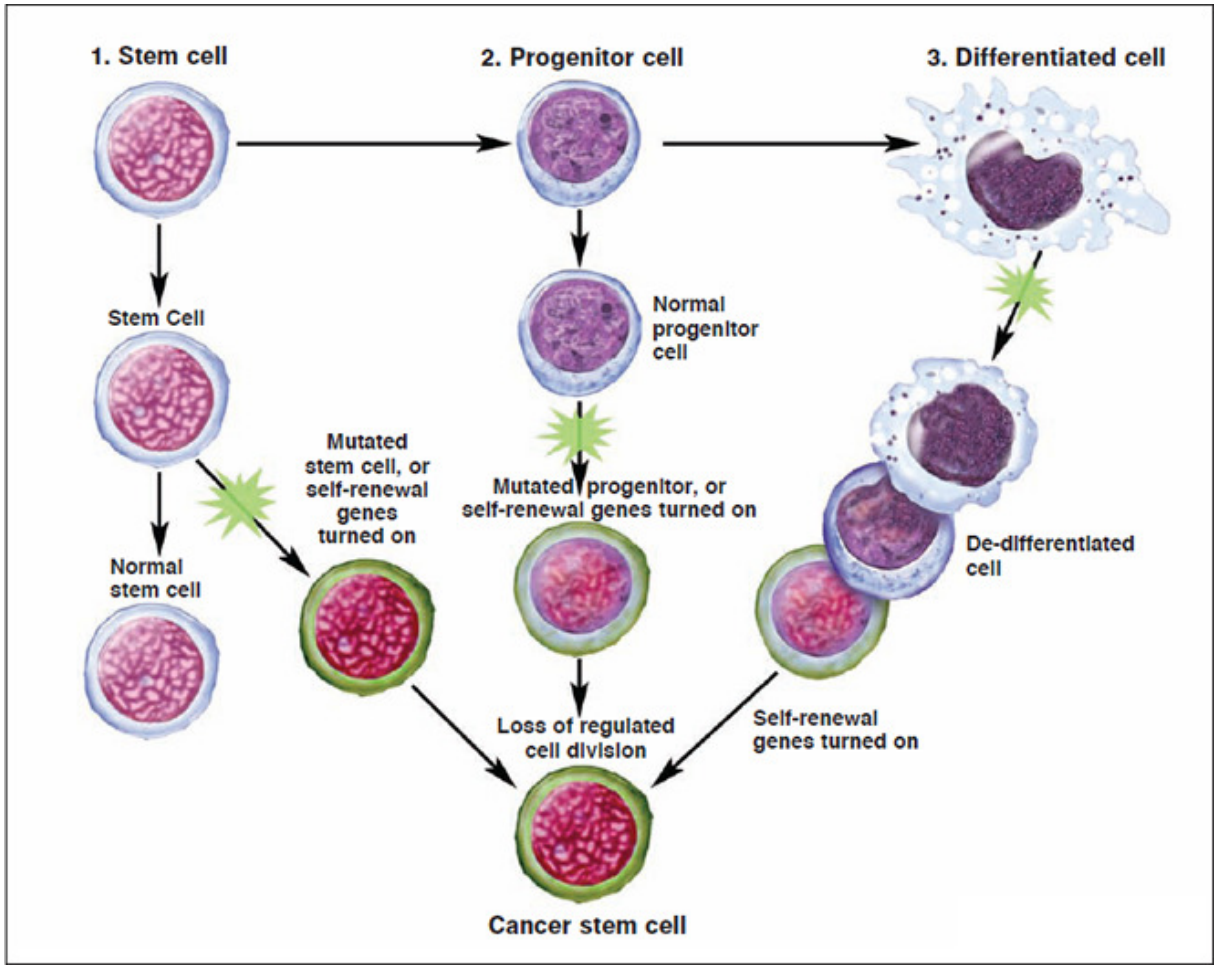

Figure 1.9 How do CSCs originate?
This figure demonstrates three hypotheses of how a CSC might be created. First, a SC sustains a mutation. Second, a progenitor cell sustains two, three or more mutations. Finally, a completely differentiated cell sustains numerous mutations, which move it back to a stem-like state. In all three situations, the resulting CSC has lost the capacity to regulate its particular cell division.
Taken from (the National Institutes of Health (NIH) resource for SC research, 2015).

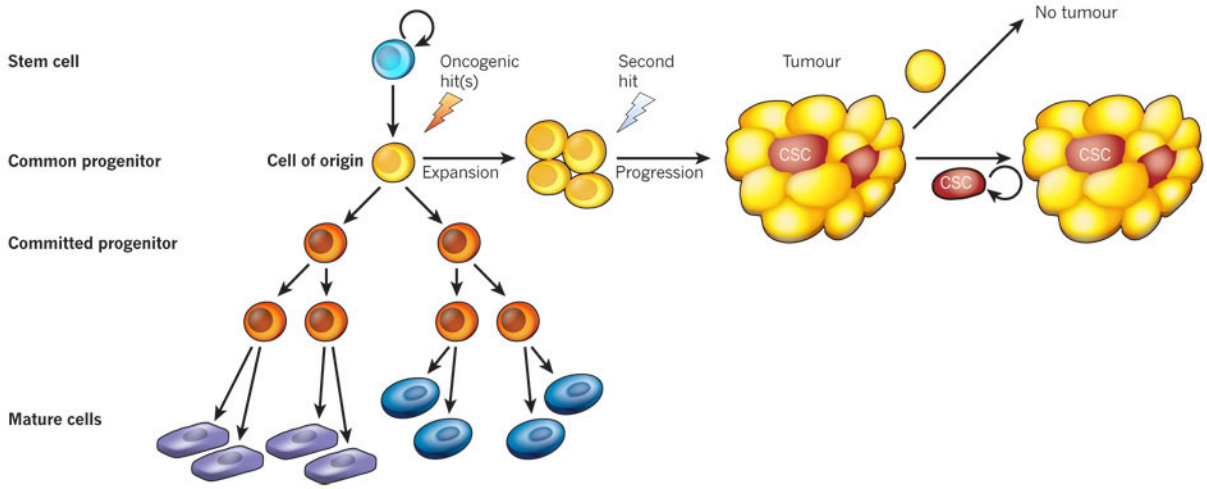

Figure 1.10 The evolution of a CSC.
The original progenitor cell can become mutated during proliferation. During neoplastic progression, CSCs can emerge and the presence of the cells can then go on to initiate tumourigenesis.
Taken from (Visvader, 2011).

1.7.1. Pluripotent stem cells (PSCs)

The research carried out on SCs during the last ten years has broadened because of their importance in providing insights into the early stages of embryo development, their use as a tool in drug screening and their significance in the cancer research field. Moreover, the potential possibilities SCs applications provide in regenerative medicine required a proper understanding of the methods SCs use to maintain their genomic integrity (De Los Angeles *et al.,* 2015; Islam *et al.,* 2015; Noggle *et al.,* 2005; Wu and Hochedlinger, 2011; Zhu and Huangfu, 2013).

SCs are grouped into four categories according to their potency:
(A) Totipotent cells, which can give rise to every other cell type in an organism together with extra-embryonic tissue, such as the placenta.
(B) Pluripotent cells that can give rise to every cell in an embryo ESCs are pluripotent.
(C) Multipotent cells, which can give rise to numerous lineages. These include a majority of ASCs, such as neural stem cells (NSCs), hematopoietic stem cells (HSCs), as well as mesenchymal stem cells (MSCs).
(D) Unipotent cells, which can differentiate and develop to form just one kind of cell. For example, spermatogonial SCs which are able to differentiate and develop to form sperm cells (Dang-Nguyen and Torres-Padilla, 2015; De Los Angeles *et al.,* 2015; Do and Schöler, 2009; Hochedlinger and Plath, 2009; Kar *et al.,* 2014).

1.7.1.1. Embryonic stem cells (ESCs)

ESCs can maintain their property of pluripotency using a network of transcription factors, POU domain class 5 transcription factor 1 (Pou5f1 or Oct4), the SRY (sex determining region Y) -box 2 (Sox2) and Nanog homeobox. This network is combined with external signals originating in their microenvironment [e.g., fibroblast growth factor [FGF], leukaemia inhibitor factor [LIF] and bone morphogenetic protein [BMP]) (Boyer *et al.,* 2005; Chambers *et al.,* 2003; Chambers and Smith, 2004; Dang-Nguyen and Torres-Padilla, 2015; Gong *et al.,* 2015; Menasche *et al.,* 2015; Mitsui *et al.,* 2003; Niwa *et al.,* 2000).

1.7.1.1.1. Transcription factors that regulate pluripotency in human ESCs

(Okamoto *et al.,* 1990; Rosner *et al.,* 1990; Scholer *et al.,* 1989) Oct4 was formerly characterised independently by a number of groups. The name is derived from Oct4's ability bind octamer DNA sequences for the activation or suppression of transcriptional processes (Martello and Smith, 2014; Pesce and Schöler, 2001). Oct4, Sox2 and Nanog are involved in maintaining ESC pluripotency through the suppression of differentiation genes and the activation of genes involved in renewal as well as the non-differentiated form by binding to their promoters (Boyer *et al.,* 2005; Chew *et al.,* 2005; Guo *et al.,* 2002; Jeter *et al.,* 2015; Menasche *et al.,* 2015; Pan *et al.,* 2002; Pan *et al.,* 2006; Pesce and Schöler, 2001).

Oct4 also matters quantitatively because critical levels of *OCT4* expression should be kept constant to preserve the pluripotent form of ESCs and any down- or up-regulation of amounts might result in differentiation (Martello and Smith, 2014; Niwa *et al.,* 2000). In contrast, *NANOG* overexpression causes a rise in SC self-renewal abilities in a scenario involving a lack of LIF (Chambers *et al.,* 2003; Martello and Smith, 2014; Mitsui *et al.,* 2003), whilst a decrease in their abilities leads to a loss of self-renewal and differentiation (Martello and Smith, 2014; Mitsui *et al.,* 2003).

An association has been observed consisting of a feedback loop mechanism between Nanog and Oct4, during which Oct4 causes the activation of Nanog with normal levels of expression, i.e. when Oct4 levels are maintained within reasonable limits of stemness, and the supersession of Nanog occurs when Oct4 is overexpressed. Still, Nanog is known to activate Oct4. Thus, in this fashion, Oct4 acts as its own suppressor (Niwa *et al.,* 2000; Pan *et al.,* 2006; Wu and Schöler, 2014).

Although the levels of Sox2 and Oct4 are uniform in ESCs, high and low Nanog-expressing ESCs have been found to differentiate or stay pluripotent, respectively. Navarro *et al.,* (2012) found that such fluctuations can be accounted for by auto-repressing action of Nanog. This study proposed that Oct4/Sox2-independent activity of Nanog is possible, but a new study showed interactions among Sox2 and Nanog and the involvement of Oct4 and Nanog in controlling ESCs' self-renewal (Gagliardi *et al.,* 2013; Jeter *et al.,* 2015; Muñoz Descalzo *et al.,* 2012). The contradicting data from these studies demonstrate the need for further research on the factors governing the ESCs' self-renewal process.

The first isolation and maintenance procedure for ESCs included plating the inner cell mass (ICM) in a media with mitotically inactivated embryonic fibroblasts serving as the feeder serum and cells. The feeder cells have factors that are vital for maintaining the pluripotency of the ESCs. At present, many of the pathways involved in maintaining the pluripotency have been characterised as ESCs (Evans and Kaufman, 1981; Martello and Smith, 2014; Martin, 1981; Seymour *et al.,* 2015; Thomson *et al.,* 1998).

1.7.1.1.2. Signalling process of human ESCs

Bone morphogenetic protein (BMP) and Leukaemia inhibitor factor (LIF) are not involved in the signalling pathways that maintain ESC pluripotency. Instead, BMP promotes a differentiation pathway in ESCs (Xu *et al.,* 2002). It has been documented that ESCs need transforming growth factor (TGF) and fibroblast growth factor (FGF) or Activin/Nodal pathways to maintain their pluripotency when no serum and feeder cells are present (Beattie *et al.,* 2005; James *et al.,* 2005; Romito and Cobellis, 2015; Vallier *et al.,* 2005).

The target of the TGF/Activin pathway is usually the activation of the transcription factor Nanog. The role of FGF is the suppression of the BMP pathway, which results in ESC differentiation (Greber *et al.,* 2011; Romito and Cobellis, 2015; Sakaki-Yumoto *et al.,* 2013; Xu *et al.,* 2008). Furthermore, the WNT pathway is involved in maintaining ESC pluripotency, and the underlying mechanism is not understood (Davidson *et al.,* 2012; Fernandez *et al.,* 2014; Sato *et al.,* 2004).

1.7.1.2. Embryonic carcinoma cells (ECCs)

ECCs refer to malignant SCs in teratocarcinomas, which is a type of malignant tumour from germ cells (Lin *et al.,* 2012). ECCs have the ability for self-renewal and can differentiate in cultured forms (Andrews *et al.,* 2005). ECCs show expression of the same core transcription factors, which maintain pluripotency in ESCs, namely Sox2, Nanog and Oct4 (Boer *et al.,* 2009; Jeter *et al.,* 2015; Jung *et al.,* 2010; Lin *et al.,* 2012). Similar to ESC counterparts, ECCs have different surface marker expressions in human cells. For example, ECCs show expression in stage specific embryonic antigens 4 and 3 (SSEA4 and SSEA3) but do not express SSEA1 (Andrews, 1984; Andrews *et al.,* 1996; Simerman *et al.,* 2014; Sivasubramaniyan *et al.,* 2015). The Oct4 knockdown in ECCs results in their differentiation (Matin *et al.,* 2004; Niwa *et al.,* 2000; Wu and Schöler, 2014).

1.8. Human TDRD protein (TDRD1-TDRD12) family

TDRD proteins refer to a class of mammalian functionally associated methyl arginine binding proteins, which take part in small RNA silencing pathways (Iwasaki *et al.,* 2015; Ying and Chen, 2012; Zhou *et al.,* 2014). Most of the proteins in this class contain several tandem Tudor domain sections, which are repeated. A few of them have domains associated with RNA, such as the RNA helicase domain or the K homology (KH) domain (Figure 1.11) (Chen *et al.,* 2011; Iwasaki *et al.,* 2015; Lu and Wang, 2013; Zhou *et al.,* 2014).

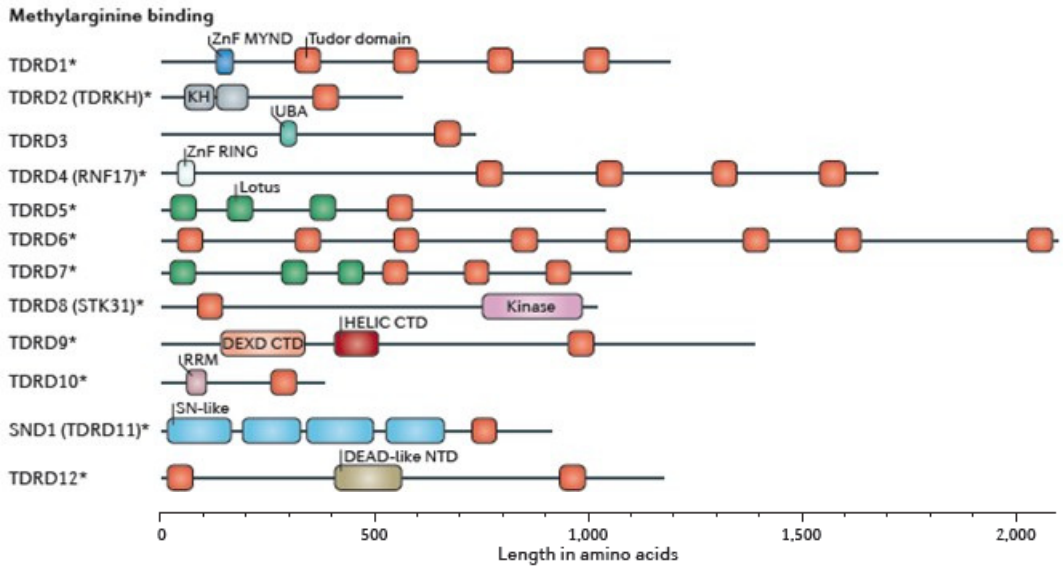

Figure 1.11 Domains of the human TDRD proteins family.
ZnF MYND: MYND-type zinc-finger domain; KH: K homology domain; UBA: ubiquitin-associated domain; ZnF RING: RING-type zinc-finger domain; DEXD: DEAD-like helicase domain; CTD: carboxy-terminal domain; HELIC: helicase super-family; RRM: RNA recognition motif; SN-like: staphylococcal nuclease-like domain; NTD: amino-terminal domain; SND1: SN-like domain containing protein 1.
Adapted from (Chen *et al.,* 2011).

Numerous *TDRD* genes show high levels of expression in the germ-line as well, as they are functionally related to p-element induced wimpy testis genes (PIWI)-interacting RNA (piRNA) pathway and the process of gametogenesis. Almost all the Tudor domains found in many of the TDRD proteins possess extra lengths of conserved structural elements found on the basic canonical 60-amino-acid Tudor core. These extra domains consist of approximately 180 residues and show structural similarities to the initial predicted repeated Tudor domain units found in *Drosophila melanogaster* (TUD; also known as extended Tudor domains or eTuds). The TDRD types of eTuds are also referred to as maternal Tudor domains in the Pfam database (Chen *et al.,* 2011; Hirakata and Siomi, 2015; Irie *et al.,* 2014; Iwasaki *et al.,* 2015; Lu and Wang, 2013; Zhou *et al.,* 2014).

The TDRD proteins engage with PIWI proteins via symmetrical dimethyl arginines (sDMAs) in different but specific patterns. Although Tud domains from the Tud family of proteins have been confirmed to perform as sDMA-binding modules, the association of the Tudor family in molecular-level functions along the piRNA pathway has been of interest to researchers (Gayatri and Bedford, 2014; Iwasaki *et al.,* 2015; Siomi *et al.,* 2010). Tudor domains have been identified as methyl arginine binders, yet not much is known regarding how they attain maximum specificity for natural ligands. Further research is necessary to ascertain if the multiple tandem domains of proteins in the TDRD family possess any methyl arginine-binding ability. Not much is known about their preferences in methylation motifs amongst PIWI proteins and other targets or their function in multivalent interactions (Chen *et al.,* 2011; Gayatri and Bedford, 2014; Iwasaki *et al.,* 2015).

1.8.1. P-element-induced wimpy testis genes (PIWI)

P-element-induced wimpy testis genes (PIWI) are essential in gametogenesis, SC self-renewal development and RNA interference of various multi-cellular organisms (Hadziselimovic *et al.,* 2015; Xiang *et al.,* 2014).

1.8.2. PIWI-interacting RNA (piRNA)

piRNA are a newly identified faction of small non-coding RNA molecules that contain 26–33 nucleotides and are mostly expressed in the cells of the germ-line (Hirakata and Siomi, 2015; Huang *et al.,* 2014; Itou *et al.,* 2015; Lim *et al.,* 2014; Sato and Siomi, 2013). These types of RNA create complexes with the PIWI proteins (Huang *et al.,* 2014; Itou *et al.,* 2015).

The germinal cells of both genders in many organisms contain these piRNA complexes. Although the mechanisms of piRNA biogenesis are unknown, it has been widely accepted that they originate in long single-stranded RNA precursors, which are determined by repetitive sequences that occur in the genome (Kowalczykiewic and Wrzesinski, 2011; Rizzo *et al.,* 2014; Saito, 2014).

1.8.3. PIWI family members, piRNA and Tudor proteins

Proteins can be altered using techniques that can carry out post-translational alterations such as methylation, ubiquitylation, phosphorylation and acetylation to create unique functional sites: they only bind specialised protein domains. Methylation is an important protein-modification process for creating complexes; it is vital to cellular regulation and small RNAs creation. The arginine methylation process was identified over five decades ago; yet the capacity of methyl arginine sites for binding the Tudor protein family members motifs is well known, and the functional importance of protein–protein associations, which are controlled by Tudor domains was only recently discovered. Tudor proteins have been identified in PIWI complexes, where they perform the function of interaction with methylated PIWI proteins and regulate the germ line's piRNA pathway (Chen *et al.,* 2011; Gayatri and Bedford, 2014; Iwasaki *et al.,* 2015; Pek *et al.,* 2012).

The association of PIWI family members with the Tudor protein family indicates that they contain regulatory functions in the pathway of piRNA (Iwasaki *et al.,* 2015; Sato and Siomi, 2013). In the case of animal gonads, the piRNA silencing pathway plays an important role in protecting the genome against attacks by harmful mobile genetic elements (e.g., transposons) (Rajan and Ramasamy, 2014).

At the same time, the piRNA silencing pathway must permit the accurate transmission of the genetic material to the subsequent generation. Moreover, the mechanism of piRNA regulates the establishment of germ cell destinies and directs the differentiation of germ cells along the meiotic pathway to create efficient haploid gametes (Hirakata and Siomi, 2015; Lim *et al.,* 2014; Yadav and Kotaja, 2014). The PIWI protein family, the germ-line Tudor protein family and other piRNA pathway elements collaborate to guarantee the efficient process of the germ-line function and the piRNA pathway (Chen *et al.,* 2011; Gayatri and Bedford, 2014; Iwasaki *et al.,* 2015).

1.8.4. Targeting Tudor-histone binding interfaces as possible treatments

Tudor-containing proteins are associated with several types of human diseases (e.g., cancer). A large family of protein domains, including Tudor, have been documented to be able to recognise the post-translation modifications (PTMs) of histones and interact with the tails of methylated histones (Chi *et al.,* 2010; Hirakata and Siomi, 2015; Kim *et al.,* 2014; Lu and Wang, 2013; Musselman *et al.,* 2012; Taverna *et al.,* 2007; Wang *et al.,* 2007; Wang *et al.,* 2009; Zhou *et al.,* 2014).

Of the approximately 30 mammalian Tudor-containing proteins that were identified as harbours for the histone methylation-binding ability through Tudor, the first family is the JMJD2 protein family. This family of proteins contain three members: JMJD2A, JMJD2B and JMJD2C (Berry and Janknecht, 2013; Kim *et al.,* 2014; Liu *et al.,* 2015; Lu and Wang, 2013; Shi and Whetstine, 2007). Several human disorders, including cancers, have been found to contain many mutations, which deregulate chromatin PTM-specific readers (Baker *et al.,* 2008; Chi *et al.,* 2010; Liu *et al.,* 2015; Lu and Wang, 2013). Numerous Tudor-containing readers are established to be deregulated in human cancerous cells; all JMJD2 proteins family members are identified that they have high levels of expression in different types of cancers (Berry and Janknecht, 2013; Kim *et al.,* 2014; Liu *et al.,* 2015; Lu and Wang, 2013).

Therefore, focusing on discovering and designing inhibitors, which have the ability to target the Tudor-histone binding interactions, might deliver new tools that allow researchers to investigate and analysis the functional role of these interfaces in standard biological methods and techniques. Moreover, these inhibitors would allow researchers to study and explore these interactions and their significance in pathogenesis in humans (Baylin, 2005; Kim *et al.,* 2014; Lu and Wang, 2013). The first inhibitors for the histone methylation readers are being established, and were recently developed by a group of scientists (James *et al.,* 2013; Lu and Wang, 2013).

1.9. Project aims

The aims of this project are to elucidate the functional role of the recently identified human *TDRD12* gene. This gene has been identified as a possible cancer marker that may contain CSC-specific activity (Feichtinger *et al.,* 2012). The *TDRD12* gene is of interest because in a primary study its expression appeared to be restricted to pluripotent embryonal carcinoma cells (NT2), a germ-line tumour cell line. This leads the hypothesis that *TDRD12* might have a role in conferring stemness on cancer cells, as NT2 cells have many features in common with ESCs. Moreover, it is hypothesised the *TDRD12* gene is required for the human germ-line/SC regulation of retro elements (REs) and endogenous viruses (HERV) elements as it might be linked to piRNA activity in cancer cells/stem cells (Almatrafi *et al.,* 2014; Feichtinger *et al.,* 2012; Pandey *et al.,* 2013).

The specific aims of the project are:

(A) To determine whether *TDRD* and *PIWIL* genes (*TDRD1–TDRD12* and *PIWIL1–PIWIL4*) have testis-restricted expression and can serve as human cancer-specific markers.

(B) To determine if the *TDRD12* gene regulates HERV and RE gene expression levels in human germ-line tumour cells.

(C) To address whether the *TDRD12* gene function is linked to the function of human SC marker genes (*OCT4* and/or *SOX2*).

(D) To determine if the *TDRD12* gene plays a functional role in human SCs and CSCs specificity.

(E) To analyse the sub-cellular localisation of TDRD12, TDRD1, PIWIL1, and PIWIL2 proteins in normal human tissues and cancerous cells, to determine their cancer marker potential and provide insight into their normal function.

2. Methods and Materials

2.1. Sourcing and origin of human cells

The NTERA2 (NT2) human pluripotent embryonal carcinoma cells used in this study were donated by Professor Peter W. Andrews (University of Sheffield). The SW480 human colon adenocarcinoma cells were purchased from the European Collection of Cell Cultures (ECACC). The human embryonic stem cells (ESCs) were obtained from the Centre for Stem Cell Biology at the University of Sheffield. The BJ human fibroblast cells were obtained from the foreskin of a newborn child (ATTC #CRL-2522). The BJ cells can be distinguished from other types of fibroblasts due to their ability to divide through more than 85 doubling population sets before the onset of apoptosis. The NT2 and SW480 cells were authenticated prior to use using LGC Standards Cell Line Authentication Service (Tracking number 710418378).

2.2. Culturing of human cells

The cells used in this research were cultured at a temperature of 37˚C using a humidified incubator and ambient environment with CO_2 enrichment. The media utilised for culturing cells was supplemented with foetal bovine serum (FBS) (Gibco by invitrogen; Ref: 10270-089; Lot: 41Q6208K). The cells used in this study, as well as the conditions used for proliferation, are outlined in Table 2.1; each human cell was regularly monitored for mycoplasma contamination utilising the LookOut® Mycoplasma PCR Detection Kit (Sigma Aldrich; MP0035) in accordance with the manufacturer's instructions.

2.3. Thawing of human cells

In order to thaw cells, a 10 mL volume of complete media was added to a 15 mL conical tube. Cells were then removed from liquid nitrogen storage (appropriate protective equipment was worn). The cells were carefully thawed in a water bath at 37°C for approximately 90 minutes. The cells were added to a 15 mL conical tube containing the 10 mL of complete media and gently mixed. The tube was centrifuged for 3 minutes at 400x*g*. The supernatant was carefully removed by aspiration. Another 10 mL of fresh complete media was added to the cells and mixed gently by pipetting in an up-and-down method. The tube was centrifuged for 3 minutes at 400x*g*. The supernatant was again carefully removed by aspiration.

Another 10 mL of complete media was added to the cells and gently mixed using the up-and-down pipetting method. A 5 mL volume of the prepared mixture was added to two T25 flasks containing 5 mL of complete media. The two flasks were incubated at 37°C in a humidified incubator and ambient environment with an appropriate percentage of CO_2 enrichment (see Table 2.1). The cultures were removed from the incubator and the cells were examined microscopically. The medium was discarded and the cells were washed with 5 mL of sterile 1x Dulbecco's phosphate buffered saline (1x DPBS) buffer (Gibco® by life technologies; Ref: 14190-094, 500 mL; Lot: 1163250). The DPBS buffer was discarded and 0.5 mL of Trypsin-EDTA solution (1x) (Sigma; Ref: SLBD0804) was added to each flask. The flasks were incubated at 37°C with the appropriate percentage of CO_2 (see Table 2.1) for 5 minutes, mixed by hard agitation and examined microscopically. A 10 mL volume of fresh media was added to each flask to inhibit the Trypsin-EDTA solution. Each sample was transferred to a 15 mL conical tube and centrifuged for 3 minutes at 400x*g*. The supernatants were discarded from each sample by aspiration. The cells were re-suspended in 14 mL of the media. The cells and the medium were transferred into two new T75 flasks and incubated at 37°C with an appropriate percentage of CO_2.

2.4. Routine passaging of human cells

After transference, the cultures were removed from the incubator and the cells were examined microscopically to verify confluence. The medium was discarded from each flask and the cells were washed with 5 mL of a 1x DPBS buffer. The DPBS buffer was removed from each flask and 1 mL of Trypsin-EDTA solution (1x) was then added to each flask. The flasks were incubated at 37°C with appropriate percentage of CO_2 (see Table 2.1) for 5 minutes, mixed by hard agitation and examined microscopically. A 10 mL volume of fresh complete media was added to each flask to inhibit the Trypsin-EDTA solution. Each sample was transferred to a 15 mL conical tube and centrifuged for 3 minutes at 400x*g*. The supernatants were discarded from each tube by aspiration. Each tube of cells was re-suspended in 8 mL of the complete media. A 2 mL volume from each tube mixture was transferred into four T75 flasks (each containing 12 mL of the complete media) and then incubated at 37°C with appropriate percentage of CO_2 (see Table 2.1).

Table 2.1 Description of human cells and the conditions used for proliferate.

Cell line	Description	CO_2	Media
NT2	Pluripotent embryonal carcinoma	10%	Dulbecco's modified Eagle's medium (DMEM 1x). With GlutaMAX-1™ (Invitrogen; Ref: 61965-026, 500 mL; Lot: 1116527) + 10% FBS.
SW480	Colon adenocarcinoma	5%	
BJ	Fibroblasts	5%	These cells were cultured using a modified MEM (ATCC® 30-2003™) that had additions of non-essential amino acids, sodium pyruvate, sodium bicarbonate and glutamine. This medium was further supplemented using a 10% FBS (Atlas Biologicals F-0500-A) and Penicillin/streptomycin (Gibco®, #15070-063).
Colonospheres	Colonosphere formation from human colon adenocarcinoma (SW480) cells	5%	These cells were cultured using a 49 mL volume of DMEM:F12 1:1 with Glutamax (Life technologies; Ref: 31331-028; Lot: 1453118) + 1 mL volume of B27 serum free supplement (50x) + 10 µL of EGF (final concentration 20 ng/mL) (Life technologies; Ref: PHG0314; Lot: 1380077C) + 5 µL of FGF (final concentration 10 ng/mL) (Life technologies; Ref: PHG0264; Lot: 383774A) + 0.5 mL of penicillin/streptomycin (100X) (Gibco®, #15070-063).

2.5. Counting of human cells

(A) Counting of cells using a haemocytometer (Sigma-Aldrich; Ref: Z169021-1EA): After inhibiting the Trypsin-EDTA solution in the cells (see splitting in Section 2.4), cells in a 10 µL aliquot from each culture were counted to determine the total number of cells in each culture. Cells were counted by placing 10 µL of culture onto the square metal grid of a microscope counting chamber (haemocytometer) and viewing under a light microscope using a 10x magnification lens. Cell viability was verified by observation and the number of cells in the large grid squares was counted. The total number of cells counted in the large grid squares was multiplied by 10 to determine the cell count in the 10 µL of culture on the square metal grid. This number was again multiplied by 10,000 to calculate the cell count in the original culture flask (e.g., 32.5 x 10 x 10,000 = 4 x 10^6 cells).

(B) Counting of cells using a Trypan Blue dye (Gibco® #15250-061): Cells were counted by mixing 10 µL of culture with 10 µL of Trypan blue dye. After that, a 10 µL volume of this mixture was taken to fill the counting slide chamber (BIO-RAD; Cat: 145-0011). Finally, an automated cell counter (BIO-RAD; TC20™) was used to count the cells.

2.6. Freezing (banking) of human cells

(A) Preparation of 90% FBS, 10% Dimethyl sulfoxide (DMSO) (1:9 DMSO: FBS) solution: A 1 mL volume of DMSO was added to 9 mL of FBS and the solution was thoroughly mixed; 1 mL of this solution was used and the remaining 9 mL was stored at - 20°C.

(B) Methods of freezing: The cells were prepared as described in Section 2.4. However, each culture of cells was re-suspended in 1 mL of the prepared 10% DMSO solution. Then, 1 mL of each mixture was transferred to a separate 1 mL cryotube. The cells were stored at - 80°C for roughly 48 hours. Finally, the cells were transferred to liquid nitrogen storage with the appropriate protective equipment for long-term storage.

2.7. Isolation of total RNA from human cells

The culture of cells was removed from the incubator and the cells were examined microscopically to verify confluence. The media was discarded from the culture flask. A 1 mL volume of TRIzoL reagent (Life technologies; Ref: 15596-026; Lot: 11846302) was added directly to the cells and the cells were lysed by pipetting up and down. This was followed by incubation at room temperature (RT) for approximately 4–5 minutes. Then, the lysed cells were transferred to 1.5 mL Eppendorf draft tubes.

The cell suspension was then treated with the addition of 0.2 mL of chloroform, after which the entire solution was shaken for 15 seconds and then incubated for a period of 5 minutes at RT. This aqueous phase was moved to a new tube after being centrifuged at a speed of 12,000x*g* for a 15-minute period at a temperature of 4°C. The collected RNA underwent precipitation from the solution by the addition of 0.5 mL of isopropanol and then incubation at RT for a period of 10 minutes. All samples were again subjected to centrifugation at a speed of 12,000x*g* for 20 minutes at 4°C and the pellet was washed using 70% ethanol and centrifuged at 7,500x*g* for a period of 5 minutes with a temperature of 4°C. The resulting supernatant was taken out and the pellet was then left to air dry. All of the RNA preparations made in this way were then re-suspended using approximately 50 µL of DEPC-treated water together with an addition of 1 µL of DNase I (Sigma-Aldrich; D5319) for each sample. This was followed by incubation at 37˚C for 10 minutes and then at a temperature of 75˚C for a 10-minute time-frame. The quality as well as concentration of each extracted RNA was evaluated by use of a NanoDrop (ND_1000) spectrophotometer.

2.8. Synthesising of complementary DNA (cDNA)

(A) All of the RNA preparations originating from normal human cells (Clontech; 636643) as well as a selection of tumour cells were bought from Clontech and Ambion; European Collection of Cell Cultures (ECACC); American Type Culture Collection (ATCC); and Cancer Research Technology Ltd. In addition, some RNAs were extracted from cell culture (see Table 2.1). The reverse transcription of 1 µg of total RNA was carried out to form cDNA by utilising the SuperScript III First Strand synthesis system kit (Invitrogen; Cat: 18080-051; Lot: 1005890) in accordance with the manufacturer's instructions (see Section B). The cDNA was then diluted eight-fold for further use. The human *β-actin* gene was used as a quality control for the generated cDNAs.

(B) The components were thawed and then mixed. After mixing, they were briefly centrifuged. Next, 1 µg of RNA was added into different PCR tubes (Alpha Laboratories; Cat: LW2170) followed by a master mix of oligo-dT primer (it was utilised for transcribing the RNA to develop a single-strand cDNA that binds with the poly-A tail of the mRNAs); 10 mM dNTPs mix and dH_2O was made and divided into PCR tubes containing RNAs. Subsequently, the prepared reactions were incubated in the PCR machine for 5 minutes at 65ºC and then placed on ice for about 1 minute.

While the reactions were incubating in the PCR machine, the cDNA mixture was prepared as indicated in Table 2.2 and each component was added in an exact order.

Table 2.2 Preparation of cDNA synthesis mixture using SuperScript III First Strand synthesis system.

Component	1x
10x RT buffer	2 µL
25 mM $MgCl_2$	4 µL
0.1 M DTT	2 µL
RNase OUT	1 µL
Superscript III RT	1 µL

10 µL of the cDNA synthesis master mix was added to each RNA mixture tube and the tubes were then mixed gently up and down by pipette. Next, the PCR tubes were incubated in the PCR machine as follows: 50 minutes at 50ºC, 5 minutes at 85ºC and then chilled on ice. Afterwards, 1 µL of RNaseH was added to each PCR tube and the tubes were incubated at 37ºC for 20 minutes. Later, 140 µL of dH_2O was added to each cDNA reaction tube (final volume now for each cDNA reaction is 160 µL). Finally, the cDNA synthesis reactions were stored at - 20ºC.

2.9. Reverse transcription-polymerase chain reaction (RT-PCR) analysis

(A) Obtaining the sequences of human genes: Genes were found using the National Centre for Biotechnology Information (NCBI) nucleotide database at www.ncbi.nlm.nih.gov and the Ensembl Genome Browser at http://www.ensembl.org/index.html. The corresponding primers of each gene were created to span introns wherever possible.

(B) Exactly 2 µL of diluted cDNA was utilised for the PCR process with an overall or final volume of 50 µL. BioMix™ Red (Bioline; BIO-25006) was utilised in the PCR amplification methodology and this was done in accordance with the provided manufacturer's instructions (see Section C).

(C) The RT-PCR components were thawed. After that, they were mixed and centrifuged at 7,500x*g* for a period of 30 seconds. A master mix was then made, as demonstrated in Table 2.3.

Table 2.3 Preparation of RT-PCR mixture using BioMix™ Red.

Component	1x
BioMix™ Red	25 µL
Forward primer	1 µL
Reverse primer	1 µL
dH_2O	21 µL

Next, 48 µL of the master mix was added into each PCR tube and then 2 µL of cDNA reaction was added into appropriate tubes. The PCR reactions were incubated in the PCR, which was carried out using a Techne TC-312 thermal cycler at 96°C for 5 minutes; 40 cycles at 96°C for 30 seconds; 55°C for 30 seconds; 72°C for 40 seconds; a final extension of 72°C for 5 minutes; and then holding at 4°C. Finally, 10 µL of each PCR reaction was loaded onto a 1% agarose gel stained with ethidium bromide (see Section 2.9.2). The gel was electrophoresed at 400 mA and 100 V for 75 minutes.

2.9.1. Preparation of RT-PCR primers

The primers were designed as illustrated in the general guidelines recommended by Rozen and Skaletsky (2000) (see Table 2.4) using the following websites:

- Oligo Calc: Oligonucleotide Properties Calculator (http://www.basic.northwestern.edu/biotools/oligocalc.html).
- Primer3 Input (Version 0.4.0) (http://frodo.wi.mit.edu/).
- Primer3 Plus (http://www.bioinformatics.nl/cgi-bin/primer3plus/primer3plus.cgi).

The initial concentrations of the prepared stock solutions must be 100 pmol/µL. Thus, once the forward primers and reverse primers for all used human genes were received from the manufacturer (Eurofins MWG / Operon) they were prepared as concentrations, after which time the stock solutions were vortexed and then centrifuged for 10 seconds at 14,000x*g*.

In order to make 100 µL of working solution at 10 pmol/µL for each stock solution, each stock was diluted 1:10 with dH_2O (10 µL of stock + 90 µL of dH_2O).

The primer sequences and the predicted PCR product sizes used to analyse genes by RT-PCR are detailed in Table 2.5.

Table 2.4 General guidelines for designing of primers (adapted from Rozen and Skaletsky, 2000)

Length	18-30 nucleotides
GC content	40-60%
T_m	For best results, use commercially available oligo-design software, such as OLIGO 6 or Web-based tools, such as Primer3* to determine primer T_ms. Simplified formula for estimating melting temperature (T_m): T_m = 2°C x (number of [A+T]) + 4°C x (number of [G+C]) Whenever possible, design primer pairs with similar T_m values. **QuantiTect SYBR Green Kits:** Optimal annealing temperatures may be above or below the estimated T_m. As a starting point, use an annealing temperature 5°C below T_m.
Sequence	• Always check the specificity of primers by performing a BLAST search. Ensure that primer sequences are unique for your template sequence. • Ideally, the length of the PCR product should be 100-150 bp when using QuantiTect SYBR Green Kits. When using QuantiFast SYBR Green Kits, ensure the length of the PCR product is less than 200 bp. • Avoid complementarity of 2 or more bases at the 3' ends of primer pairs to minimise primer-dimer formation. • Avoid mismatches between the 3' end of primers and the template sequence. • Avoid runs of 3 or more Gs or Cs at the 3' end. • Avoid a 3'-end T. Primers with a T at the 3' end have a greater tolerance of mismatch. • Avoid complementary sequences within a primer sequence and between the primer pair. • Commercially available computer software (e.g., OLIGO 6) or Web-based tools (e.g., Primer3) can be used for primer design. Use the software to minimise the likelihood of formation of stable primer-dimers.
Special considerations for design of RT-PCR primers	• Design primers so that one half hybridises to the 3' end of one exon and the other half to the 5' end of the adjacent exon (see figure "Primer design"). The primers will therefore anneal to cDNA synthesised from spliced mRNAs, but not to genomic DNA, eliminating detection of contaminated DNA. • Alternatively, RT-PCR primers should be designed to flank a region that contains at least one intron. Products amplified from cDNA (no introns) will be smaller than those amplified from genomic DNA (containing introns). Size differences in products allow for detection of contaminated DNA by melting curve analysis. If possible, select a target with very long introns: the RNA target may then be preferentially amplified because of the higher PCR efficiency of this shorter PCR product without introns. If genomic DNA is detected (i.e., presence of amplification product in the no RT control), treat the template RNA with RNase-free DNase, or synthesise cDNA using the QuantiTect Reverse Transcription Kit (which includes integrated genomic DNA removal). Alternatively, redesign primers to avoid amplification of genomic DNA.

Table 2.5 Designed primer sequences and the predicted PCR product sizes used to analyse of human genes by RT-PCR.

Gene	Primer	Sequence	Length	CG	Tm	Region	Product size
β-actin	Forward	5'AGAAAATCTGGCACCACACC3'	20 bp	50%	58.4ºC	332	553 bp
β-actin	Reverse	5'AGGAAGGAAGGCTGGAAGAG3'	20 bp	55%	60.5ºC	884	
OCT4	Forward	5'AGCCCTCATTTCACCAGGCC3'	20 bp	60%	62.5ºC	-	872 bp
OCT4	Reverse	5'CTCGGACCACATCCTTCTCG3'	20 bp	60%	62.5ºC	-	
SOX2	Forward	5'GCAACCAGAAAAACAGCCCG3'	20 bp	55%	60.5ºC	95	590 bp
SOX2	Reverse	5'CGAGTAGGACATGCTGTAGG3'	20 bp	55%	60.5ºC	114	
TDRD1	Forward	5'GCTCTACCAAAAGGGATGCC3'	20 bp	55%	60.5ºC	2869	523 bp
TDRD1	Reverse	5'CACTCTGCCTTTGAGGTGTG3'	20 bp	55%	60.5ºC	3391	
TDRD2	Forward	5'GGAGACATTGTAGCAGCACC3'	20 bp	55%	60.5ºC	1068	488 bp
TDRD2	Reverse	5'GAGGCATCTGTTTCTGTGGC3'	20 bp	55%	60.5ºC	1556	
TDRD3	Forward	5'GATCAGGAAAAGGTCCCTCC3'	20 bp	55%	60.5ºC	1516	624 bp
TDRD3	Reverse	5'GATCGTAGGTGCCTTCTTCC3'	20 bp	55%	60.5ºC	2140	
TDRD4	Forward	5'CCCAGGAGAACTCTATGCTG3'	20 bp	55%	60.5ºC	4226	490 bp
TDRD4	Reverse	5'CTCCATGCTCCATTTGGGAC3'	20 bp	55%	60.5ºC	4716	
TDRD5	Forward	5'CAGATTCTTCCACACTGCCC3'	20 bp	55%	60.5ºC	2671	425 bp
TDRD5	Reverse	5'CCTTTTCACACTGGGGTACC3'	20 bp	55%	60.5ºC	3096	
TDRD6	Forward	5'GGCGCCATGGAGCTATTTAC3'	20 bp	55%	60.5ºC	5655	559 bp
TDRD6	Reverse	5'CAGGGTTCACTATCTCCTCC3'	20 bp	55%	60.5ºC	6214	
TDRD7	Forward	5'CGCTTTCTCCACAGAGGAAC3'	20 bp	55%	60.5ºC	2681	433 bp
TDRD7	Reverse	5'CATAGAAGCCTCCTCAGACC3'	20 bp	55%	60.5ºC	3114	
TDRD8	Forward	5'GCCAAGGTGATTGAGAGAGC3'	20 bp	55%	60.5ºC	2301	429 bp
TDRD8	Reverse	5'GTCTGAACCTGGAGAAGCAG3'	20 bp	55%	60.5ºC	2730	
TDRD9	Forward	5'CGATGCTGCTGAGAGAAACC3'	20 bp	55%	60.5ºC	3625	449 bp
TDRD9	Reverse	5'CTGCTCCATGACCAGCTTTG3'	20 bp	55%	60.5ºC	4074	
TDRD10	Forward	5'CTTCTTTGCAGTCCCGTTGG3'	20 bp	55%	60.5ºC	476	545 bp
TDRD10	Reverse	5'CCGAGTTCAAAGCACCAGTG3'	20 bp	55%	60.5ºC	1021	
TDRD11	Forward	5'GGCCGCAAAGCAGAAGAAAG3'	20 bp	55%	60.5ºC	1943	319 bp
TDRD11	Reverse	5'CTCGACTTTCTCTACTCGGG3'	20 bp	55%	60.5ºC	2262	
TDRD12	Forward	5'GGTATTGTCGGTGACCTCAG3'	20 bp	55%	60.5ºC	825	355 bp
TDRD12	Reverse	5'GCTGGAGATCAGAGATTCCG3'	20 bp	55%	60.5ºC	1180	
TDRD1-201	Set 1 (F)	5'GCTCTACCAAAAGGGATGCC3'	20 bp	55%	60.5ºC	2869	523 bp
TDRD1-201	Set 1 (R)	5'CACTCTGCCTTTGAGGTGTG3'	20 bp	55%	60.5ºC	3391	
TDRD1-201	Set 2 (F)	5'CAGAACACTGCCAGCAGAAG3'	20 bp	55%	60.5ºC	2249	551 bp
TDRD1-201	Set 2 (R)	5'CGTCTTCCATTGCTCAGCTG3'	20 bp	55%	60.5ºC	2799	
TDRD1-201	Set 3 (F)	5'CTCCTTGTGCCATAAAGTGC3'	20 bp	50%	58.4ºC	1118	727 bp
TDRD1-201	Set 3 (R)	5'GATGGCTTTACTCCTGCTAG3'	20 bp	50%	58.4ºC	1844	
RNF17-003	Set 1 (F)	5'GACACTCCTCTTTTACCACC3'	20 bp	50%	58.4ºC	4183	557 bp
RNF17-003	Set 1 (R)	5'CAGTCTATCATAGCCCACAG3'	20 bp	50%	58.4ºC	44739	
RNF17-003	Set 2 (F)	5'GGAGAGCGTGTTGATGTTTC3'	20 bp	50%	58.4ºC	3259	635 bp
RNF17-003	Set 2 (R)	5'GGTGTGGTATTATGGAGCTG3'	20 bp	50%	58.4ºC	3893	
RNF17-003	Set 3 (F)	5'CGATTCTCTTGGTGCTCCTG3'	20 bp	55%	60.5ºC	2520	660 bp
RNF17-003	Set 3 (R)	5'GTTGCTACAGCTCCAGTCAG3'	20 bp	55%	60.5ºC	3179	
TDRD5-201	Set 1 (F)	5'CCTCTACAGGCTAAGATGGG3'	20 bp	55%	60.5ºC	2398	699 bp
TDRD5-201	Set 1 (R)	5'CCTTTTCACACTGGGGTACC3'	20 bp	55%	60.5ºC	3096	
TDRD5-201	Set 2 (F)	5'CCCTTGTTCTTTGGCTTGGG3'	20 bp	55%	60.5ºC	1767	925 bp
TDRD5-201	Set 2 (R)	5'GGGCAGTGTGGAAGAATCTG3'	20 bp	55%	60.5ºC	2691	

TDRD5-201	Set 3 (F)	5'GATCCAAAGTGGTCCAACCC3'	20 bp	55%	60.5ºC	2272	610 bp
TDRD5-201	Set 3 (R)	5'GGATCTCTGGTGAGCTTTCC3'	20 bp	55%	60.5ºC	2881	
TDRD5-001	Set 1 (F)	5'GTTATCCTTCCCAGCAGCAC3'	20 bp	55%	60.5ºC	2081	639 bp
TDRD5-001	Set 1 (R)	5'GGATCTCTGGTGAGCTTTCC3'	20 bp	55%	60.5ºC	2719	
TDRD5-001	Set 2 (F)	5'GCAGTTCCAGAAGTTGTGCG3'	20 bp	55%	60.5ºC	1827	628 bp
TDRD5-001	Set 2 (R)	5'CTGAGCACCCAGTACTTCTG3'	20 bp	55%	60.5ºC	2454	
TDRD5-001	Set 3 (F)	5'GTGGTATCGGGTCATTATCC3'	20 bp	50%	58.4ºC	1623	647 bp
TDRD5-001	Set 3 (R)	5'CATCACCTCCTTTTCCCATC3'	20 bp	50%	58.4ºC	2269	
TDRD6-001	Set 1 (F)	5'GTGCCATCTGGTTGACAAAG3'	20 bp	50%	58.4ºC	5394	880 bp
TDRD6-001	Set 1 (R)	5'CAAACCCCTTTTCTCAGGTG3'	20 bp	50%	58.4ºC	6273	
TDRD6-001	Set 2 (F)	5'GGATGAAGAAAAAGGGGAGC3'	20 bp	50%	58.4ºC	5586	586 bp
TDRD6-001	Set 2 (R)	5'CCTTGTTCCTTCTTCAGCTG3'	20 bp	50%	58.4ºC	6171	
TDRD6-001	Set 3 (F)	5'GGCGCCATGGAGCTATTTAC3'	20 bp	55%	60.5ºC	5656	559 bp
TDRD6-001	Set 3 (R)	5'CAGGGTTCACTATCTCCTCC3'	20 bp	55%	60.5ºC	6214	
TDRD12-001	Set 1 (F)	5'GCTTTTTCACAGGGTTCAGG3'	20 bp	50%	58.4ºC	3146	682 bp
TDRD12-001	Set 1 (R)	5'GAATACCAAGTACCCACCAG3'	20 bp	50%	58.4ºC	3827	
TDRD12-001	Set 2 (F)	5'GAAATGGACCTCTCGCAGTC3'	20 bp	55%	60.5ºC	1786	459 bp
TDRD12-001	Set 2 (R)	5'CCTCTTCCATGGCTGTGATC3'	20 bp	55%	60.5ºC	2244	
TDRD12-001	Set 3 (F)	5'GCTTAACCATTGACTCGTCG3'	20 bp	50%	58.4ºC	1564	409 bp
TDRD12-001	Set 3 (R)	5'GGGGTCGTAACAATCACATC3'	20 bp	50%	58.4ºC	1972	
TDRD12-003	Set 1 (F)	5'GAGCTAAAGTGCTGGTGCAG3'	20 bp	55%	60.5ºC	205	641 bp
TDRD12-003	Set 1 (R)	5'CTGAGGTCACCGACAATACC3'	20 bp	55%	60.5ºC	845	
TDRD12-003	Set 2 (F)	5'CCGAGACAGTACTGACATTG3'	20 bp	50%	58.4ºC	420	403 bp
TDRD12-003	Set 2 (R)	5'GCACCATGTATGTTGCAGAG3'	20 bp	50%	58.4ºC	822	
TDRD12-003	Set 3 (F)	5'GGAAGCCAGATTATGTGCTG3'	20 bp	50%	58.4ºC	510	531 bp
TDRD12-003	Set 3 (R)	5'CTTGCTTCTGGTACATCTGG3'	20 bp	50%	58.4ºC	1040	
TDRD12-002	Set 1 (F)	5'AAGAAAGCCTAAGCCAGACC3'	20 bp	50%	58.4ºC	37	285 bp
TDRD12-002	Set 1 (R)	5'GTTCTGCTAATGAAGGCACC3'	20 bp	50%	58.4ºC	321	
TDRD12-002	Set 2 (F)	5'GATCATCCATCCGAGGAGC3'	19 bp	58%	59.5ºC	96	485 bp
TDRD12-002	Set 2 (R)	5'AGCTCCAGATCAGCCAGGTA3'	20 bp	55%	60.5ºC	580	
TDRD12-002	Set 3 (F)	5'CTCAGAAAACCAGAAGCCTG3'	20 bp	50%	58.4ºC	259	534 bp
TDRD12-002	Set 3 (R)	5'TCACTGTGTACGGCAGGTTT3'	20 bp	50%	58.4ºC	792	
PIWIL1-001	Set 1 (F)	5'CGAAGTGCCACAGTTTTTGG3'	20 bp	50%	58.4ºC	2145	439 bp
PIWIL1-001	Set 1 (R)	5'GAGGTAGTAAAGGCGGTTTG3'	20 bp	50%	58.4ºC	5583	
PIWIL1-001	Set 2 (F)	5'GAACTGCAAGATGGGAGGAG3'	20 bp	55%	60.5ºC	1824	542 bp
PIWIL1-001	Set 2 (R)	5'CACTACCACTTCTCACAGCC3'	20 bp	55%	60.5ºC	2365	
PIWIL1-001	Set 3 (F)	5'GACCAGAATCCCAAGAGCAC3'	20 bp	55%	60.5ºC	973	350 bp
PIWIL1-001	Set 3 (R)	5'CAGTCTCGAAGCTCCCTTTG3'	20 bp	55%	60.5ºC	1322	
PIWIL2-001	Set 1 (F)	5'CACAAAATGGTATTCCCGGG3'	20 bp	50%	58.4ºC	2304	482 bp
PIWIL2-001	Set 1 (R)	5'GGCACAGTTTGAAAGTCAGC3'	20 bp	50%	58.4ºC	2785	
PIWIL2-001	Set 2 (F)	5'CTATCCCCATGCATTTCTGG3'	20 bp	50%	58.4ºC	1801	435 bp
PIWIL2-001	Set 2 (R)	5'CCATCCCGATCACCATTAAC3'	20 bp	50%	58.4ºC	2233	
PIWIL2-001	Set 3 (F)	5'GCTTCACGATGTCTGATGGG3'	20 bp	55%	60.5ºC	1322	476 bp
PIWIL2-001	Set 3 (R)	5'CAAGATGGAAGGGTCTCTGG3'	20 bp	55%	60.5ºC	1797	
PIWIL3-001	Set 1 (F)	5'CAGAGGGTACAGTGGTACAG3'	20 bp	55%	60.5ºC	359	579 bp
PIWIL3-001	Set 1 (R)	5'CCTCTCGGATGTTTCCTGTC3'	20 bp	55%	60.5ºC	937	
PIWIL3-001	Set 3 (F)	5'GAATTGCAAGATGGGAGGAG3'	20 bp	50%	58.4ºC	1890	593 bp
PIWIL3-001	Set 3 (R)	5'TATCTGGGCTCAAGCCAATC3'	20 bp	50%	58.4ºC	2482	
PIWIL4-001	Set 1 (F)	5'GCAGGATCTCAACCAACGAT3'	20 bp	50%	58.4ºC	149	472 bp
PIWIL4-001	Set 1 (R)	5'TTGAAGACCTGGATGCACAC3'	20 bp	50%	58.4ºC	620	

PIWIL4-001	Set 2 (F)	5'GAGCTGCCATCAAGTTCTCC3'	20 bp	55%	60.5ºC	580	400 bp
PIWIL4-001	Set 2 (R)	5'GAAAGGTGTGTGTGGGCTTC3'	20 bp	55%	60.5ºC	979	
PIWIL4-001	Set 3 (F)	5'AAGAGTTGCAGGTTCCATGG3'	20 bp	50%	58.4ºC	1521	448 bp
PIWIL4-001	Set 3 (R)	5'CTGAAGGATACAGCGGGAAA3'	20 bp	50%	58.4ºC	1968	

2.9.2. Preparation of 1% agarose gel

Preparation began with 100 mL of 10x TBE buffer (Alpha Laboratories; Cat: EL0080; Lot: 041413) that was added to 900 mL of distilled H_2O (dH_2O). Then, 1.5 g of electrophoresis-grade agarose (MELFORD; CAS NO: 9012-36-6; Batch No: F24755) was added to 150 mL of 1x TBE. The solution was heated in a microwave for 3 minutes. Then, 1.5 µL of ethidium bromide was added and the solution was quickly poured into a gel former (which contained a well former) and was left to set; 1x TBE buffer (30 mL) and 570 mL of dH_2O were mixed and placed in an electrophoresis tank. The well former was gently removed. Some marker lanes contain 10 µL of HyperLadder II (Bioline; BIO-33039) and some contain 10 µL of HyperLadder I (Bioline; BIO-33025). The samples were exposed to electrophoresis in the agarose gels for 75 minutes at 100 V and 400 mA.

2.9.3. Purification of RT-PCR products from agarose gel using the Roche High Pure PCR Product Purification Kit

The purification of PCR products was carried out using the Roche's High Pure PCR Product Purification Kit (Roche Applied Science; Cat: 11732668001). To begin, 40 µL of the PCR products were loaded onto a 1% agarose gel. Next, the desired bands were cut from the gel and then gel slices were placed into micro centrifuge tubes (1.5 mL). Next, 300 µL of a Binding Buffer was added for every 100 mg gel slice. Subsequently, the tubes were vortexed for 30 seconds to re-suspend the gel slices in the Binding Buffer. Subsequently, the samples were incubated at 56°C for 10 minutes and the tubes were vortexed briefly every 3 minutes during the incubation process. Once the slices of agarose gel had dissolved completely, 150 µL of isopropanol was added for every 100 mg gel slice.

High pure filter tubes were inserted into collection tubes. Afterwards, the samples were transferred from the micro centrifuge tubes to the upper reservoir of the filter tubes and the tubes were centrifuged for 60 seconds at 16,000x*g*; the flow-through solutions were then discarded. Next, 500 µL of washing buffer was added and the tubes were centrifuged for 60 seconds at 16,000x*g*; the flow-through solutions were discarded. 200 µL of washing buffer was added back to each tube and then both the flow-through solutions and the collection tubes

were discarded. The filter tubes were recombined with clean 1.5 mL micro centrifuge tubes and 50 µL of elution buffer was added. Finally, the tubes were centrifuged for 1 minute at 16,000x*g*.

2.9.4. Sequencing of the RT-PCR products for selected human gene

A 5 ng/µL quantity of DNA was transferred to a clean Eppendorf tube and then sent at RT to Eurofins MWG Operon Company for sequencing to confirm that the right sequences were amplified. In addition to 15 pmol of the matching forward primer as needed. The obtained results of sequencing were blasted to the BLAST search and then aligned with the sequences of predicted PCR product by making use of the Global Sequence Alignment Tool at http://blast.ncbi.nlm.nih.gov/Blast.cgi?PAGE_TYPE=BlastSearch&PROG_DEF=blastn&BLAST_PROG_DEF=blastn&BLAST_SPEC=GlobalAln&LINK_LOC=BlastHomeLink.

2.10. Quantitative, real time-polymerase chain reaction (RT-qPCR) analysis

The total RNAs were previously isolated from confluent cell cultures through the use of the TRIzoL reagent in accordance with the instructions provided in Section 2.7. The quality as well as concentrations of these RNAs were evaluated through the use of the NanoDrop (ND_1000) spectrophotometer. A 1 µg quantity of total RNA was subjected to reverse transcription to form cDNA by utilising the SuperScript III First Strand synthesis system kit in accordance with the provided instructions in Section 2.8. The resulting cDNA was then diluted eight-fold.

Commercially available RT-qPCR primer sequences and their predicted PCR product sizes (from Qiagen) were utilised to perform SYBR® Green-Based RT-qPCR processes for several human genes (detailed in Table 2.6). Moreover, designed primer sequences and their predicted PCR product sizes are detailed in Table 2.7.

The GoTaq® RT-qPCR Master Kit (Promega; Ref: A6002; Lot: 0000144571) was utilised to set up the RT-qPCR reactions in accordance with the provided manufacturer's instructions. Specifically, 1.5 µL of cDNA was utilised for every 25 µL reaction inside a 96 well plate and each reaction was done three times. The samples were then amplified using a pre-cycling hold at a temperature of 95°C for 10 minutes, then for another 40 cycles at a temperature of 95°C for 15 seconds, 60°C for 1 minute and then at a temperature of 60°C for 5 seconds; finally, 95°C for 5 seconds. A melt curve analysis was done after completing 40 cycles. The Bio-Rad CFX machine was utilised for RT-qPCR and the obtained results were analysed with the Bio-Rad CFX Manager Software (version 2.0).

Table 2.6 Commercial primer sequences and the predicted PCR product sizes used to perform SYBR® Green-Based RT-qPCR for several human genes.

Gene	Primer	Source	Product size
PIWIL1	Hs_PIWIL1_1_SG QuantiTect Primer Assay	Qiagen; QT00064638	80 bp
PIWIL2	Hs_PIWIL2_va.1_SG QuantiTect Primer Assay	Qiagen; QT01326990	134 bp
PIWIL3	Hs_PIWIL3_1_SG QuantiTect Primer Assay	Qiagen; QT00071526	112 bp
PIWIL4	Hs_PIWIL4_1_SG QuantiTect Primer Assay	Qiagen; QT00011074	118 bp
TDRD12	Hs_TDRD12_2_SG QuantiTect Primer Assay	Qiagen; QT1157184	85 bp
OCT4	Hs_POU5F1_1_SG QuantiTect Primer Assay	Qiagen; QT00210840	77 bp
GAPDH	Hs_GAPDH_1_SG QuantiTect Primer Assay	Qiagen; QT00079247	95 bp
HSP90AB1	Hs_HSP90AB1_2_SG QuantiTect Primer Assay	Qiagen; QT01679790	81 bp
Tubulin	Hs_TUBA1C_1_SG QuantiTect Primer Assay	Qiagen; QT00062720	116 bp
Lamin	Hs_LMNA_1_SG QuantiTect Primer Assay	Qiagen; QT00083349	73 bp
SOX2	Hs_SOX2_1_SG QuantiTect Primer Assay	Qiagen; QT00237601	64 bp

Table 2.7 Designed primer sequences and the predicted PCR product sizes used to perform SYBR® Green-Based RT-qPCR for several human genes.

Gene	Primer	Sequence	Length	CG	Tm	Product size
HERV-K-Gag	Forward	5'GAGAGCCTCCCACAGTTGAG3'	20 bp	60%	60.0ºC	172 bp
HERV-K-Gag	Reverse	5'TTTGCCAGAATCTCCCAATC3'	20 bp	45%	60.0ºC	
HERV-Gag-Domain1	Forward	5'CCCGACATTTGTCTTGGTCT3'	20 bp	50%	60.0ºC	178 bp
HERV-Gag-Domain1	Reverse	5'CCTGGGGAATCCTTCTCTTC3'	20 bp	55%	60.0ºC	
HERV-K-Pro	Forward	5'TGTTCCTCAGGGTTTTCAGG3'	20 bp	50%	60.1ºC	153 bp
HERV-K-Pro	Reverse	5'CCCTGGAAGCAGAGAGACTG3'	20 bp	60%	60.1ºC	
HERV-K-10	Forward	5'GATAACGTGGGGGAGAGGTT3'	20 bp	55%	60.1ºC	156 bp
HERV-K-10	Reverse	5'TCCATCCATGTGACTGGTGT3'	20 bp	50%	60.0ºC	
HERV-K-107	Forward	5'GAGAGCCTCCCACAGTTGAG3'	20 bp	60%	60.0ºC	172 bp
HERV-K-107	Reverse	5'TTTGCCAGAATCTCCCAATC3'	20 bp	45%	60.0ºC	
HERV-K-Env	Forward	5'AAATTTGGTGCCAGGAACTG3'	20 bp	45%	60.0ºC	245 bp
HERV-K-Env	Reverse	5'CCACATTTCCCCCTTTTCTT3'	20 bp	45%	60.1ºC	
HERV-KHML2-Rec	Forward	5'ATGAACCCATCGGAGATGCA3'	20 bp	50%	58.0ºC	471 bp
HERV-KHML2-Rec	Reverse	5'AACAGAATCTCAAGGCAGAAGA3'	22 bp	41%	58.0ºC	
HERV-K-Pol	Forward	5'TTGAGCCTTCGTTCTCACCT3'	20 bp	50%	60.0ºC	216 bp
HERV-K-Pol	Reverse	5'CTGCCAGAGGGATGGTAAAA3'	20 bp	50%	60.1ºC	
LINE-1	Forward	5'AAATGGTGCTGGGAAAACTG3'	20 bp	45%	60.0ºC	209 bp
LINE-1	Reverse	5'GCCATTGCTTTTGGTGTTTT3'	20 bp	40%	60.0ºC	
SINE-ALU-Domain	Forward	5'ACGAGGTCAGGAGATCGAGA3'	20 bp	55%	59.9ºC	290 bp
SINE-ALU-Domain	Reverse	5'GATCTCGGCTCACTGCAAG3'	19 bp	57%	59.7ºC	
DAZL-001	Forward	5'AATGACGTGGATGTGCAGAA3'	20 bp	45%	60.1ºC	178 bp
DAZL-001	Reverse	5'AACTGTGGTGGAGGAGGATG3'	20 bp	55%	60.0ºC	
DAZ1	Forward	5'TCCATGTATACAATTACCAGATGC3'	20 bp	37.5%	58.0ºC	153 bp
DAZ1	Reverse	5'AAACAGACAAGATACCACCATTTG3'	20 bp	37.5%	59.3ºC	
DAZ2/3/4	Forward	5'GCTGCAAATCCTGAGACTCC3'	20 bp	55%	60.0ºC	156 bp
DAZ2/3/4	Reverse	5'CCAAAGCAGCTTCCAATCTC3'	20 bp	50%	60.0ºC	
BOLL-001	Forward	5'TACCAGGCCACCACACAGTA3'	20 bp	55%	60.0ºC	172 bp
BOLL-001	Reverse	5'TGATGGCACTTGGAGCATAA3'	20 bp	45%	60.2ºC	
TDRD1-201	Forward	5'GCTCCACAGCATGTCAAAGA3'	20 bp	50%	60.0ºC	173 bp
TDRD1-201	Reverse	5'AGCCCAAATGGCTATTTCCT3'	20 bp	45%	59.9ºC	
TDRD12-001	Forward	5'TCTTCCGCAGACCAGTACCT3'	20 bp	55%	60.5ºC	187 bp
TDRD12-001	Reverse	5'CAGTACTGTCTCGGCAGAAG3'	20 bp	55%	60.5ºC	

2.11. Western blot (WB) analysis

2.11.1. Preparation of whole cell extracts from cell cultures

The RIPA buffer (Radio Immuno Precipitation Assay buffer) (SIGMA; Cat: R 0278) was initially utilised in the extraction of full cell proteins, which included cell proteins from the cytoplasm and nucleus as well as the cell membranes. The RIPA buffer was prepared using the following method, as indicated below:

- 150 mM of NaCl
- 1.0% of Triton X-100
- 0.5% of sodium deoxycholate
- 0.1% of SDS (sodium dodecyl sulphate)
- 50 mM of Tris at a pH of 8.0

One culture flask was removed from the incubator and the cells were examined microscopically to verify confluence. The media was then discarded from the culture flask. The cells were washed with 5 mL of cold 1x DPBS buffer. The DPBS buffer was removed from the flask and 1 mL of Trypsin-EDTA solution (1x) was added. The flask was incubated at 37°C in a humidified incubator and ambient environment with an appropriated percentage of CO_2 enrichment (see Table 2.1) for 5 minutes, mixed by hard agitation and examined microscopically. The cells were re-suspended with 10 mL of complete media and then the cell suspension was transferred into a new 15 conical tube and centrifuged for 3 minutes at 400x*g*. The supernatant was discarded following aspiration.

The cells were re-suspended with 10 mL of 1x DPBS. A small portion of the cell suspension was taken (10 µL) and placed onto the haemocytometer to determine the total number of cells in the suspension. A suitable volume of the RIPA buffer was used. A commercially available cocktail of inhibitors was mixed into the RIPA buffer (which included the complete Mini, EDTA-free from Roche; Cat: 1183617000; Lot: 14738900 together with some 4-(2-Aminoethyl) along with benzenesulfonyl fluoride hydrochloride from Sigma-Aldrich; Cat: #A8456. After the cell count, the cells were pelleted by centrifugation for 5 minutes at 400x*g*. The supernatant was discarded. Based on the cell count, the cells were re-suspended with 7 mL of fresh 1x DPBS in order to make in each 1 mL 1 million cells. After that, 4 mL were transferred to four 1.5 mL Eppendorf draft tubes, each 1 mL in a separate tube, and then centrifuged at 17,000x*g* for 5 minutes at 4^{o}C.

The supernatants were discarded, 166 µL of lysis buffer was added to each sample (1,000,000 cells were divided by 6,000 = 166 in order to load 60,000 cells in the WB well (10 µL). The cells were heated in the heat block (98°C) for 10 minutes to lyse the cells, which resulted in the pellet completely dissolving. Finally, the cells were stored at – 80°C freezer.

2.11.2. SDS-Polyacrylamide gel electrophoresis (SDS-PAGE) analysis

The lysate samples were taken from the – 80°C freezer. After that, the samples were vortexed and incubated in the heat block (98°C) for 5 minutes and then re-vortexed. A 1x MOPS SDS running buffer (Invitrogen; Ref: NP0001; Lot: 1179544) was made and added to the electrophoresis tank (45 mL of 20x MOPS SDS running buffer was added to 855 mL of dH_2O to make a total volume of 900 mL). The SDS-PAGE (NuPAGE 4-12% Bis-Tris gel 1.0 mm x 12 well (Invitrogen; Cat: NP03 22) was prepared in order to separate the proteins; it was flashed with the 1x MOPS SDS running buffer in the electrophoresis tank by pipetting up and down. A 10 µL of Precision Plus Protein™ Dual Colour Standards (Bio-Rad; Cat: 161-0374) and 10 µL of each sample were loaded onto the gel. Finally, the gel was run for roughly 90 minutes at 120 V and 400 mA (it was switched off before the dye ran out of the gel).

2.11.3. Transferring of the separated proteins

While the gel was running, 6 pieces of the flitter paper sheets and one piece of a PVDF membrane (Millipore, Immozilon; Cat: IPVH00010; Lot: K2DA2698HK) were cut (6 cm x 8 cm). The membrane was then soaked in methanol in order to activate. After the running on the SDS page gel was completed, the proteins that separated on the gel were transferred onto the membrane in a 1x transfer buffer. The transfer stack or "sandwich" was compiled in the following order: 3 filter paper sheets, gel, membrane and another 3 filter sheets (between the two sponges in the transfer cassette). The transfer stack was run at 120 V for about 2 hours and 1,000 mA.

2.11.4. Blocking of non-specific binding

The membrane was placed into 0.5% non-fat dry milk buffer in 1x PBS + 0.05 Tween® 20 (Sigma Aldrich; Cat: P1379-500L; Lot: SZBC1240V) (see Table 2.12) and incubated on the shaker at RT for 1 hour.

2.11.5. Incubation with the primary antibody

The membrane was incubated on the shaker overnight with the primary antibody (see Table 2.8) diluted in milk buffer. The primary antibody was discarded and the membrane was washed with milk buffer three times for 10 minutes and then for 10 minutes with tween buffer (see Table 2.11).

2.11.6. Incubation with the secondary antibody

The membrane was immediately incubated for 2 hours at RT with the secondary antibody (see Table 2.9) diluted in milk buffer. The secondary antibody was discarded and the membrane was washed with the tween buffer on the shaker three times for 10 minutes.

2.11.7. Development methods

The tween buffer was discarded and the membrane was incubated for 5 minutes with several types of ECL detection, such as SuperSignal® West Pico Chemiluminescent Substrate (Thermo Scientific; Prod: # 34080; Lot: PJ210045), Pierce® ECL Plus Western Blotting Substrate (Thermo Scientific; Prod: # 32132; Lot: # NE171297) and Chemiluminescent Peroxidase Substrate-3 (SIGMA; Cat: CPS3100-1KT; Lot: SLBB5823). The signal of chemiluminescence was detected by exposure with X-ray films using CL-X Posure™ Film (Thermo Scientific; Cat: 34091; Lot: NC14728216).

2.11.8. Primary antibodies used to analyse human proteins by WB

A variety of primary antibodies were utilised for the WB analysis. The antibodies and the dilutions at which they were utilised are stated in Table 2.8.

Table 2.8 Primary antibodies and the dilution used to analyse human proteins by WB.

Primary antibody	Source	Dilution
TDRD12 Antibody (T-17)-Goat IgG	Santa Crus Biotechnology; sc-248802	1:200
Anti-TDRD12-Rabbit IgG	ATLAS ANTIBODIES; HPA-042684	1:200
TDRD12-Guinea pig	Eurogentec; PEP-1310598	1:50
TDRD12-Guinea pig	Eurogentec; PEP-1310599	1:50
Anti-TDRD1 antibody-Rabbit IgG	Abcam; ab107665	1:100
Monoclonal Anti-PIWIL1 antibody-Mouse IgG	SIGMA-ALDRICH; SAB-4200365	1:400
PIWIL2 monoclonal antibody-Mouse IgG	Abnova; MAB0843	1:400
Monoclonal mouse anti-α-Tubulin	Sigma; T6074	1:5000

2.11.9. Secondary antibodies used to analyse human proteins by WB

The matching IgG secondary antibodies for each of the primary antibodies mentioned in Table 2.8 are detailed in Table 2.9.

Table 2.9 Secondary antibodies and the dilution used to analyse human proteins by WB.

Secondary antibody	Source	Dilution
Peroxidase-conjugated AffiniPure Donkey Anti-Rabbit IgG (H+L)	Jackson ImmunoResearch Laboratories Inc.; 711-035-152	1:50,000
Peroxidase-conjugated AffiniPure Donkey Anti-Mouse IgG (H+L)	Jackson ImmunoResearch Laboratories Inc.; 715-035-150	1:25,000
Rabbit Anti-Goat IgG H&L (HRP)	Abcam; ab97100	1:25,000
Goat Anti-Guinea pig IgG H&L (HRP)	Abcam; ab97155	1:25,000

2.11.10. Preparation of WB solutions

Table 2.10 Preparation of 10x transfer buffer.

Component	Amount
Trizma® base, Primary Standard and Buffer ≥ 99.9% (titration) (SIGMA; Cat: T1503-1KG; Lot: SLBH5708V)	30.3 g
Glycine (MELFORD; CAS no: 56-40-6; Batch no: E24409)	144 g
Add to 1 L of dH_2O. After that, the transfer buffer was diluted to 1x in order to use.	

Table 2.11 Preparation of 1x DPBS + 0.5% Tween 20®.

Component	Amount
1x DPBS (Gibco® by life technologies; Ref: 14190-094, 500 mL; Lot: 1163250)	200 mL
Tween® 20 (Sigma Aldrich; Cat: P1379-500 mL; Lot: SZBC1240V)	1 mL

Table 2.12 Preparation of 0.5% non-fat dry milk buffer.

Component	Amount
1x DPBS	400 mL
Tween® 20	2 mL
non-fat dry milk	20 g

Table 2.13 Preparation of 1x MOPS SDS running buffer.

Component	Amount
MOPS SDS running buffer (20x) (Novex by life technologies; Ref: NP0001; Lot: 1179544)	45 mL
dH_2O	855 mL

2.12. Human *TDRD12-001* siRNAs (small interfering RNA) knockdown

A three "hit" strategy was utilised for the *TDRD12-001* siRNA knockdown, in which the first siRNA treatment was added at 24 hours, the second treatment was added at 48 hours and the third treatment was added at 72 hours after seeding of the cells.

The transfection complex was created by adding 6 µL of the HiPerFect transfection reagent (Qiagen; Cat: 301707; Lot: 142353341) and 0.6 µL siRNA to 100 µL of the serum-free medium that had been incubated at RT for a period of 25 minutes. The untreated cells were seeded at a rate 75,000 cells/well inside a 6 Well Cell Culture Cluster Plate (Costar®; Cat: 3516) while the treated cells were seeded at a rate of 200,000 cells/well and then the transfection mixture was put into the cells via dropper whilst slowly shaking the plate.

The cells were separated and extracted using TRIzoL reagent and then were prepared as RNAs and proteins, as previously described in sections 2.7 and 2.11.1.

2.12.1. Human *TDRD12-001* siRNA sequences utilised for knockdown

(A) Numerous siRNAs were utilised to carry out the knockdown within cultured cells and their specifications are given in Table 2.14.

(B) Preparation of siRNA solution: 100 µL of sterile, RNase-free water was added to each tube containing 1 nmol lyophilised siRNA to obtain a 10 uM solution; the tubes were then stored at -20°C freezer.

(C): Identifying the target siRNA sequences in the *TDRD12-001* transcript was as follows: The sequences were accurately identified, as seen in Figure 2.1.

Table 2.14 Human *TDRD12* and Non-Interference siRNA sequences utilised for knockdown.

Qiagen name	Tube ID	Sequence	Region	Source
Hs_TDRD12_3	siRNA1	5'ATGGAAGATTCACATGGTGTA3'	1086-1106	Qiagen; S104713877
Hs_TDRD12_1	siRNA3	5'ACCCAGGTGGAAGCCAGATTA3'	822-842	Qiagen; S104713863
Hs_TDRD12_2	siRNA4	5'ATCCAGGTTGCTTCTGGGTTA3'	352-372	Qiagen; S104713870
Non-Interference	NI*	-	-	Qiagen; 1027280

* AllStars Negative Control siRNA

A.

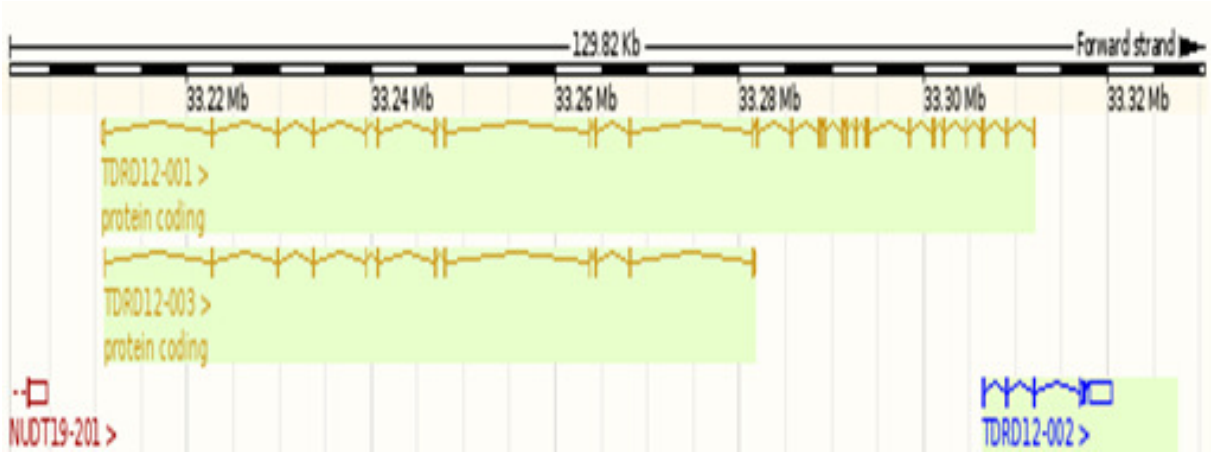

B.

CGACGCCTCAAGGCCTGCTCAGCGTGCGCGGGCATCCGGTGGGTGCGGGAGGCCCGAGGCCA
GGCAGGCAGGGATCCCGCAGCGAGGGGCTGGTTACTGCCAGGACGGAGCGCATTGCCTCGAG
CCGACCCCGGGGTCCGCGAGGGCTCCTGGGGACGAGGAGTGTGGGGCACCTGCCGCGGGGGG
CCCAGGCGCTAAAGGTGGAGGGAAGGAACGCACTCGCGGCGGGGGCCTGGCCGGGGCGGACG
CAGCCAGCCTCACCCGCGACGGTAGGGGACTTCCAGGGCGAGGGGGCCCATCTGCCCTCGGG
CGCCAGGAGGATGCTCCAGCTCCTGGTGCTGAAGATTGAAGATCCAGGTTGCTTCTGGGTTA
TTATAAAAGGGTGTAGTCCCTTTTTAGATCATGATGTCGATTATCAAAAATTAAATAGTGCC
ATGAATGACTTCTACAACAGCACGTGTCAAGATATAGAAATAAAACCCTTAACATTGGAAGA
AGGACAGGTGTGTGTGGTCTATTGTGAGGAGCTAAAGTGCTGGTGCAGGGCCATTGTCAAAT
CAATTACGTCTTCCGCAGACCAGTACCTGGCAGAATGTTTCCTTGTGGACTTTGCCAAGAAC
ATTCCAGTCAAATCTAAAAACATCCGAGTTGTAGTAGAATCGTTTATGCAGCTTCCCTATAG
AGCAAAAAAATTCAGCCTGTACTGCACAAAGCCTGTCACATTACACATTGACTTCTGCCGAG
ACAGTACTGACATTGTACCTGCCAAGAAGTGGGACAATGCAGCTATTCAGTACTTTCAGAAC
CTTCTGAAAGCAACTACCCAGGTGGAAGCCAGATTATGTGCTGTGGAAGAAGATACATTTGA
GGTTTACCTTTATGTAACTATAAAAGATGAAAAAGTTTGTGTTAATGATGATCTTGTTGCAA
AGAACTATGCTTGTTATATGTCACCTACAAAGAATAAAAACCTTGATTATTTAGAAAAACCA
AGATTGAATATAAAATCAGCACCCTCCTTCAATAAACTCAATCCAGCACTTACACTCTGGCC
AATGTTTTTGCAAGGAAAAGATGTTCAAGGAATGGAAGATTCACATGGTGTAAATTTTCCGG
CACAATCTCTGCAACATACATGGTGCAAGGGTATTGTCGGTGACCTCAGGCCAACAGCCACA
GCACAGG

Figure 2.1 Map of human *TDRD12* splice variants and *TDRD12-001* transcript sequence.
Panel (A): map of *TDRD12* splice variants; Panel (B): *TDRD12-001* transcript sequence. Blue and black nucleotide sequences indicate alternating exons and the grey highlighted areas are the target siRNA sequences used (adapted from the Ensembl Genome Browser, 2012).

2.12.2. Counting of human cell viability

Cell viability counts were done at pre-specified time intervals following the *TDRD12-001* siRNA knockdown. Cell viability was assessed by mixing in 10 µL of the cell suspension with an equal amount of 0.4% Trypan Blue (Invitrogen; 15250-061). The counting was done with a haemocytometer using the automated cell counter (BIO-RAD; TC20^{TM}). Cell viability values were calculated in the form of a percentage of the non-stained cells out of the overall number of cells.

2.12.3. Extreme limiting dilution analysis (ELDA)

(A) Preparation of the working solution stock: 10 µL of siRNA (see Table 2.14) was added to 1 mL of free serum media.

(B) The impact of the *TDRD12-001* knockdown was explored in NT2 cell growth by first seeding the cells inside 96 Well Cell Culture Plates (COSTAR; Cat: 3595) at concentrations of 1, 10, 100 and 1,000 cells using 100 µL of the completed medium. Twelve more well repeats were utilised for untreated cells (positive control), cells treated with Non-Interfering siRNA (negative control), cells treated with HiPerFect transfection and cells treated with *TDRD12-001* siRNA. The transfection complex was compiled through the addition of 5 µL siRNA (from the working solution stock) + 0.3 µL of the HiPerFect reagent + 4.7 µL of a serum-free medium followed by incubation for a period of 25 minutes at RT. The negative control Non-Interfering siRNA was made in the same manner.

The *TDRD12-001* siRNA transfection mix and the negative control siRNA or HiPerFect only were put drop by drop into the medium (12 well repeats were used per condition) together with the untreated cells. The cells were subjected to incubation for 8 days inside a humidified incubator at a temperature of 37°C with a 10% CO_2 atmosphere. The cells used 50 µL of a serum-free medium and a transfection mixture was further applied at intervals of two and six days during incubation.

After being incubated for a period of 8 days, the well numbers that exhibited cell growth were pictured using a light microscopy (AMG; AMEX-1200; G2211-1712-017).

The frequency of cell growth was calculated with the ELDA web tool (http://bioinf.wehi.edu.au/software/elda/).

2.13. Chemically induced differentiation of human NT2 cells

The cells were differentiated by the use of two separate inducer agents, namely retinoic acid (RA) (Sigma; R2625) and hexamethylene bisacetamide (HMBA) (Sigma).

2.13.1. Preparation of differentiation inducer agents

(A) Preparation of DMSO media: 0.5 mL of DMSO was added to 500 mL of complete media.
(B) Preparation of RA media (3 mg/mL): 167 µL of RA was mixed with 333 µL of DMSO and then added to 500 mL of complete media.
(C): Preparation of HMBA media (3 mM): 3 gm of HMBA (powder) was added to 50 mL of dH_2O and then 5 mL of this mixture was added to 500 mL of complete media.

2.14. Immunohistochemistry (IHC) staining of human tissues

2.14.1. Deparaffinsation and hydration

The normal tissue section slides were dewaxed in xylene (SIGMA-ALDRICH; Cat: 534056-4L; Lot: BCBH4113V) three times for 5 minutes each at RT in the hood to remove the paraffin. To hydrate the tissues, the slides were rinsed for approximately 2 minutes each using the following concentrations of ethanol: 100%, 95%, 80%, 70% and 50%. The slides were then washed twice in dH2O for 5 minutes each.

2.14.2. Antigen retrieval

The slides were placed in a large glass jar with 1x pre-treatment buffer [DakoCytomation target Retrieval Solution Citrate pH 6 (x 10)] (Dako; Cat: S2369; Lot: 20016175) at 80°C for 60 minutes. After that, the slides were incubated at RT for about 25 minutes to cool the tissue samples. The slides were washed twice with 1x Dako Wash Buffer (Dako; Ref: S3006; Lot: 20016228) for 5 minutes each.

2.14.3. Blocking of endogenous peroxidase

The tissue section slides were incubated with the blocking solution [1.5 mL of Dako Antibody Diluent with Background Reducing Components (Dako; Ref: S3022) + 7.5 µL of normal rabbit serum (Dako; Ref: X0902) or normal mouse serum (Dako; X0910)] at RT for roughly 60 minutes in the dark.

2.14.4. Incubation with the primary antibody

The excess fluid was carefully removed from around the tissues and the back of each slide with tissue paper without touching the tissue samples and the tissues were kept wet at all times. After that, markings were drawn around the tissues using a Dako pen (Dako; Ref; S2002: Lot: 00094840). The slides were placed into a wet chamber and 250 µL of the primary antibodies (see Table 2.15) were added to the slides before incubating them overnight at 4°C in the dark.

2.14.5. Quenching endogenous peroxidase

The primary antibodies were removed by tapping the slides on the tissue paper and then they were washed twice with 1x Dako Wash Buffer for 5 minutes each. Next, every two slides were placed back-to-back in a glass staining dish and washed with a methanol/hydrogen peroxide mix (100 mL of methanol + 10 mL of hydrogen peroxide solution were purchased from Sigma; Cat: 21673-500ML; Lot: SZBE2530V) for about 7 minutes to remove the carryover water.

2.14.6. Incubation with the secondary antibody

The slides were placed into the wet chamber and 250 µL of the secondary antibodies (see Table 2.16) were added to the slides, which were then incubated for 2 hours at RT in the dark.

2.14.7. Chromogenic reaction

The secondary antibodies were removed by tapping the slides on the tissue paper and then washing them twice with 1x Dako Wash Buffer for 5 minutes each. Each tissue slide was covered with 150 µL of liquid DAB + substrate chromogen (Dako; K3468) solution for approximately 5 minutes at RT. After that, the slides were rinsed three times in running tap water and then incubated in haematoxylin (Mayer's Haematoxylin, Lillie's Modification, Histological Staining Reagent) (Dako; Ref: S3309; Lot: 10081632) solution for 15 seconds at RT. The slides were then rinsed with running tap water for about 5 minutes.

2.14.8. Dehydration, cleaning and mounting

The slides were first dehydrated in 80% ethanol, then in 95% ethanol and then in 100% ethanol for approximately 2 minutes each. After that, they were rinsed in the xylene for about 5 minutes at RT in the hood. Finally, two drops of DPX Mountant for histology (Sigma; Cat: 06522-100ML; Lot: BCBH4393V) were added and a coverslip (Scientific Laboratory Supplies Ltd; 22 x 50 mm No. 1) was placed on each slide ensuring that all of the air bubbles were removed. The slides were then left to dry. The images are captured by ZEISS-ZEN 2 LITE (blue edition) AXIO scan software.

2.14.9. Primary antibodies used to analyse human proteins by IHC staining in normal tissues

A variety of primary antibodies were utilised for the IHC staining analysis. The antibodies and the dilutions at which they were utilised are presented in Table 2.15.

Table 2.15 Primary antibodies and the dilution used to analyse human proteins by IHC staining in normal tissues.

Primary antibody	Source	Dilution
TDRD12-Guinea pig	Eurogentec; PEP-1310599	1:20
Anti-TDRD1 antibody-Rabbit IgG	Abcam; ab107665	1:100
Monoclonal Anti-PIWIL1 antibody-Mouse IgG	SIGMA-ALDRICH; SAB-4200365	1:100
PIWIL2 monoclonal antibody-Mouse IgG	Abnova; MAB0843	1:100
TDRD12 Antibody (T-17)-Goat IgG	Santa Crus Biotechnology; sc-248802	1:100
Anti-TDRD12-Rabbit IgG	ATLAS ANTIBODIES; HPA-042684	1:100

2.14.10. Secondary antibodies used to analyse human proteins by IHC staining in normal tissues

The matching IgG secondary antibodies for each of the primary antibodies mentioned in Table 2.15 are detailed in Table 2.16.

Table 2.16 Secondary antibodies and the dilution used to analyse human proteins by IHC staining in normal tissues.

Secondary antibody	Source	Dilution
Goat Anti-Guinea pig IgG H&L (HRP)	Abcam; ab97155	1:500
Goat Anti-Rabbit IgG H&L (HRP)	Abcam; ab6721	1:1000
Goat Anti-Mouse IgG + IgM H&L (HRP)	Abcam; ab47827	1:1000
Rabbit Anti-Goat IgG H&L (HRP)	Abcam; ab97100	1:250

2.15. Immunofluorescence (IF) staining of normal human tissues

2.15.1. Deparaffinsation/rehydration

The normal tissue section slides were washed four times in xylene for 5 minutes each at RT in the hood to remove the paraffin. To hydrate the tissues, the slides were washed for approximately 2 minutes each using the following concentrations of ethanol: 100%, 95%, 80%, 70% and 50%. The slides were then rinsed twice in dH_2O for 5 minutes each.

2.15.2. Antigen retrieval

The slides were placed in a large glass jar with 1x pre-treatment buffer [DakoCytomation target Retrieval Solution Citrate pH 6 (x 10)] (Dako; Cat: S2369; Lot: 20016175) at 80°C for 60 minutes. After that, the slides were incubated at RT for about 25 minutes to cool the tissue samples.

2.15.3. Blocking

The tissue section slides were incubated with the blocking buffer (1x PBS/5% FBS/0.3% Triton X-100) (see Table 2.19) at RT for roughly 60 minutes in the dark.

2.15.4. Incubation with the primary antibody

The excessed fluid was carefully removed from around the tissues and the back of each slide with tissue paper without touching the tissues and the tissues were kept wet at all times. After that, markings were drawn around the tissues using a Dako pen. The slides were placed into a wet chamber and the primary antibodies (see Table 2.17) were diluted in an antibody dilution buffer (see Table 2.20) and then 250 µL of the diluted primary antibodies was added to the slides, which were then incubated overnight at 4°C in the dark.

2.15.5. Incubation with the secondary antibody

The primary antibodies were removed by tapping the slides on the tissue paper and then the slides were washed three times with 1x PBS for 5 minutes each. The slides were placed into the wet chamber and the secondary antibodies (see Table 2.18) were diluted in the antibody dilution buffer (see Table 2.20) and then 250 µL of the diluted secondary antibodies was added to the slides, which were then incubated for 2 hours at RT in the dark. The slides were washed three times with 1x PBS for 5 minutes each.

2.15.6. Coverslips for the slides

The slides were cover slipped with ProLong® Gold antifade reagent with DAPI (molecular probes by Life Technologies; Ref: P36935; Lot: 1626789) and then they were incubated overnight at RT to allow the Mountant to cure. Staining was viewed using a ZEISS LSM 710 confocal microscope.

2.15.7. Primary antibodies used to analyse human proteins by IF staining in normal tissues

A variety of primary antibodies were utilised for the IF staining analysis. The antibodies and the dilutions at which they were utilised are presented in Table 2.17.

Table 2.17 Primary antibodies and the dilution used to analyse human proteins by IF staining in normal tissues.

Primary antibody	Source	Dilution
TDRD12-Guinea pig	Eurogentec; PEP-1310599	1:20
Anti-TDRD1 antibody-Rabbit IgG	Abcam; ab107665	1:20
Monoclonal Anti-PIWIL1 antibody-Mouse IgG	SIGMA-ALDRICH; SAB-4200365	1:100
PIWIL2 monoclonal antibody-Mouse IgG	Abnova; MAB0843	1:20
Anti-MAGEA1 Antibody (clone 6C1)-Mouse IgG	LSBio; LS-C87868	1:15
TDRD12 Antibody (T-17)-Goat IgG	Santa Crus Biotechnology; sc-248802	1:500
Anti-TDRD12-Rabbit IgG	ATLAS ANTIBODIES; HPA-042684	1:20

2.15.8. Secondary antibodies used to analyse human proteins by IF staining in normal tissues

The matching IgG secondary antibodies for each of the primary antibodies mentioned in Table 2.17 are detailed in Table 2.18.

Table 2.18 Secondary antibodies and the dilution used to analyse human proteins by IF staining in normal tissues.

Secondary antibody	Source	Dilution
Goat anti-Guinea Pig IgG (H + L), Alexa Fluor 647 conjugate	Life technologies; A-21450	1:400
Goat anti-Mouse IgG (H + L), Alexa Fluor 488 conjugate	Life technologies; A-11029	1:250
Goat anti-Rabbit IgG (H + L), Alexa Fluor 568 conjugate	Life technologies; A-11011	1:250
Donkey anti-Mouse IgG (H + L), Alexa Fluor 647 conjugate	Life technologies; A-31571	1:250
Donkey anti-Goat IgG (H + L), Alexa Fluor 568 conjugate	Life technologies; A-11057	1:400
Goat anti-Rabbit IgG (H + L), Alexa Fluor 488 conjugate	Life technologies; A-11034	1:250

2.15.9. Preparation of IF solutions for staining of normal human tissues

Table 2.19 Preparation of 10 mL blocking buffer for IF staining in normal human tissues.

Component	Amount
Foetal bovine serum (FBS) (Gibco by invitrogen; Ref: 10270-089; Lot: 41Q6208K).	0.5 mL
1x phosphate buffered saline (1x PBS) buffer (Lonza; Cat: BE17-516F; Lot: 4MB127).	9.5 mL
Triton X-100 (Sigma; Cat: T8787-50ML; Lot: MKBQ0896V	30 µL

Table 2.20 Preparation of 10 mL antibody dilution buffer for IF staining in normal human tissues.

Component	Amount
Triton X-100	30 µL
1x PBS	10 mL
Albumin from bovine serum (BSA) (Sigma; Cat: A7638-5G; Lot: 110M7400V)	0.1 g

2.16. Immunofluorescence (IF) staining of human cells

2.16.1. Seeding of cells

Approximately 50,000 cells were seeded in a 24 well plate (Costar; 3524) on circle glass coverslips (Chemglass Life Sciences; 12 mm; Cat: CLS-1760-012) (1 mL of media and cells per well) and left to grow for 24 hours at a temperature of 37˚C using a humidified incubator and ambient environment with CO_2 enrichment. The media utilised for culturing the cells was supplemented with foetal bovine serum (FBS).

2.16.2. Fixing of human cells

The media was discarded and the cells were washed once with 1 mL of warm sterile 1x PBS buffer. The 1x PBS buffer was discarded and then 1 mL of 4% paraformaldehyde fixing solution [10 mL of 16% paraformaldehyde (Thermo Scientific; Cat: 28908; Lot: PL19466510) + 30 mL of 1x PBS] was add and incubated in the hood for 10 minutes. The paraformaldehyde fixing solution was discarded and the cells were washed three times with 1 mL of warm sterile 1x PBS buffer on the shaker at RT for 5 minutes each. After that, 1 mL of 0.2% (v/v) Triton X-100 (permeabilisation) buffer (50 mL of 1x PBS + 100 µL of 100x Triton) was added and incubated in the hood for 10 minutes. The permeabilisation buffer was discarded and the cells were washed three times with 1 mL of warm sterile 1x PBS buffer on the shaker at RT for 10 minutes each.

2.16.3. Blocking

The 1x PBS was discarded and then the cells were incubated with 1 mL of the blocking buffer (2.5 mL of FBS + 47.5 mL of 1x PBS) on the shaker at RT for 60 minutes.

2.16.4. Incubation with the primary antibody

The blocking buffer was discarded and then the cells were incubated with the primary antibodies (see Table 2.21) were diluted in the blocking buffer and then 200 µL of the diluted primary antibodies was added to the cells, which were then incubated on the shaker overnight at 4°C in the dark.

2.16.5. Incubation with the secondary antibody

The primary antibodies were discarded and then the cells were washed three times with warm 1 mL of 1x PBS for 10 minutes each. The cells were incubated with the secondary antibodies (see Table 2.22) were diluted in the blocking buffer and then 300 µL of the diluted secondary antibodies was added to the cells, which were then incubated on the shaker for 2 hours at RT in the dark. The secondary antibodies were discarded and then the cells were washed three times with warm 1 mL of 1x PBS for 10 minutes each.

2.16.6. Mounting of the slides

One drop of Mounting medium with DAPI (VECTOR LABORATORIES; Cat: H-1500; Lot: ZA0509) were added to each of the places on the slides where the coverslip cells are eventually fixed. The coverslip cells were levered up carefully from the 24 well plate using a tip and tweezers to grab them gently. The excessed fluid was carefully removed with tissue paper without touching the cells and the cells were kept wet at all times. After that, the coverslip cells were inverted and placed onto the drops on each slide ensuring that all of the air bubbles were removed. Finally, the slides were incubated overnight at 4°C in the dark to allow the Mountant to cure. Staining was viewed using a ZEISS LSM 710 confocal microscope.

2.16.7. Primary antibodies used to analyse human proteins by IF staining in cells

A variety of primary antibodies were utilised for the IF staining analysis. The antibodies and the dilutions at which they were utilised are presented in Table 2.21.

Table 2.21 Primary antibodies and the dilution used to analyse human proteins by IF staining in cells.

Primary antibody	Source	Dilution
TDRD12-Guinea pig	Eurogentec; PEP-1310599	1:20
Anti-TDRD1 antibody-Rabbit IgG	Abcam; ab107665	1:20
Monoclonal Anti-PIWIL1 antibody-Mouse IgG	SIGMA-ALDRICH; SAB-4200365	1:20
PIWIL2 monoclonal antibody-Mouse IgG	Abnova; MAB0843	1:20
Anti-beta Actin antibody-Mouse IgG	Abcam; ab6277	1:100
TDRD12 Antibody (T-17)-Goat IgG	Santa Crus Biotechnology; sc-248802	1:500
Anti-TDRD12-Rabbit IgG	ATLAS ANTIBODIES; HPA-042684	1:20

2.16.8. Secondary antibodies used to analyse human proteins by IF staining in cells

The matching IgG secondary antibodies for each of the primary antibodies mentioned in Table 2.21 are detailed in Table 2.22.

Table 2.22 Secondary antibodies and the dilution used to analyse human proteins by IF staining in cells.

Secondary antibody	Source	Dilution
Goat anti-Guinea Pig IgG (H + L), Alexa Fluor 647 conjugate	Life technologies; A-21450	1:400
Goat anti-Mouse IgG (H + L), Alexa Fluor 488 conjugate	Life technologies; A-11029	1:250
Goat anti-Rabbit IgG (H + L), Alexa Fluor 568 conjugate	Life technologies; A-11011	1:250
Donkey anti-Goat IgG (H + L), Alexa Fluor 568 conjugate	Life technologies; A-11057	1:400

3. Gene expression analysis for the human *TDRD* and *PIWIL* gene family

3.1. Introduction

A number of human meiosis-specific genes are expressed in various kinds of human cancerous cells (e.g., *SPO11* gene) (Koslowski *et al.,* 2002; Lam and Keeney, 2014). The presence of meiotic or germ-line proteins inside cancerous cells presents antigens, which can be used in immunotherapy tools and potential cancer diagnostics markers (Grizzi *et al.,* 2015). Meiosis-specific genes can be a group of genes that are considered a rich source of CTA genes (see Section 1.9.4). If the germ-line genes that are controlling the processes of meiotic cell division are activated in human somatic cells, they might participate and contribute to human oncogenesis (McFarlane *et al.,* 2015). Several human CTA genes show correlations in their cancer expression profiles with poorer prognosis (Choi and Chang, 2012; Luo *et al.,* 2013; Rousseaux *et al.,* 2013; Yakirevich *et al.,* 2003). Nevertheless, the functional meaning of this correlation remains unclear. It has been postulated that CTA gene activation drives genetic instability in certain cancerous cells. Hence, there are strong direct links between cancer formation and the activation of such genes (Cho *et al.,* 2014a; Janic *et al.,* 2010; Watkins *et al.,* 2015).

Germ-line factors are identified as oncogenic drivers in a *Drosophila* brain tumour model (Janic *et al.,* 2010). Orthologues of these genes are activated in human cancers. This suggested that a soma-to-germ-line transition might be a main oncogenic driver (McFarlane *et al.,* 2014). Moreover, these studies and findings increased the evidence that solid tumours produce a gametogenic programme for stimulating and promoting cancerous hallmarks (McFarlane *et al.,* 2015; Simpson *et al.,* 2005). Consequently, meiosis-specific genes might play fundamental roles in driving and inducing such a transition. For, example, it has recently been demonstrated that the meiotic factors Mnd1 and Hop2 are required for telomere maintenance in some cancers (Cho *et al.,* 2014b). For that important reason, studying the functional roles of meiotic and germ-line genes might assist in understanding the mechanisms of oncogenesis. Additionally, these gene products might be vital targets for immunotherapeutics and/or might be clinically useful biomarkers in oncology. As a result, this study is aiming to identify novel human genes (*TDRD1-TDRD12* and *PIWIL1-PIWIL4*) that might encode CTAs or might be used for human patient stratification based on their expression profiles.

Therefore, in this study, two different strategies are used for the identification of new or novel CTA genes. These include the following:

(A) Manual literature analysis for finding meiosis-specific genes.

(B) Use of a systematic method through a bioinformatics pipeline.

It has been observed that a manual search of the literature to find extremely restricted CTA genes was not just time consuming, but it was able to classify only a low number of meiosis-specific genes. Consequently, a bioinformatics pipeline using EST and microarray data sets was developed for identifying novel CTA candidate genes (Feichtinger *et al.,* 2012a; Feichtinger *et al.,* 2012b; Feichtinger *et al.,* 2014). Briefly, the pipeline made use of a prior microarray analysis that recognised 744 genes with extremely restricted expression within meiotic spermatocytes in mice (Chalmel *et al.,* 2007). This group of genes helped to identify 408 orthologues human genes (Figure 3.1). A MitoCheck filter was applied using the following tool (http://www.mitocheck.org) to eliminate non-germ-line-specific (mitotically active) genes, and this yielded 375 genes in total. These candidate genes were then examined using a previously formulated bioinformatics pipeline, which was based on two techniques: the utilisation of the microarray examination from ArrayExpress and GEO (http://www.cancerma.org.uk/) or an EST (expressed sequence tag) examination done using the Unigene tool (http://www.cancerest.org.uk/) (Feichtinger *et al.,* 2012a; Feichtinger *et al.,* 2012b; Feichtinger *et al.,* 2014).

The approach taken involved mining EST data set. ESTs are composed of around 200–500 nucleotide sequences; one can generate an EST by carrying out single pass sequencing of a 5′ or 3′ cDNA sequence, which is later clustered and counted (Feichtinger *et al.,* 2014; Nagle, 1992). Many studies and analyses have utilised this method for classifying potential and possible CTA genes (for example, see Hofmann *et al.,* 2008; Kim *et al.,* 2007). The 375 human genes were subjected to investigation using the EST pipeline (Feichtinger *et al.,* 2014). In brief, the genes were used to screen tissue/cancer EST databases to identify testis-specific genes that are also expressed in cancers. 177 human candidate genes were identified. The identified genes were given classification per their expression within the EST pipeline into various sub-classes. The first class consisted of 21 genes, which were cancer-testis/CNS-restricted; the second class consisted of 75 genes, which were testis-restricted; the third class consisted of 72 genes that were testis/CNS-restricted and the fourth class was made up of nine genes, which were cancer/testis-restricted (Feichtinger *et al.,* 2012a; Feichtinger *et al.,* 2012b; Feichtinger *et al.,* 2014). Validation of expression profiles of some of these genes identified *TDRD12* as a candidate CTA gene (Feichtinger *et al.,* 2012b). *TDRD12* interacts with PIWI/piRNA regulatory pathways and so this study aims to explore the potential of *TDRD12* and related genes as CTA genes.

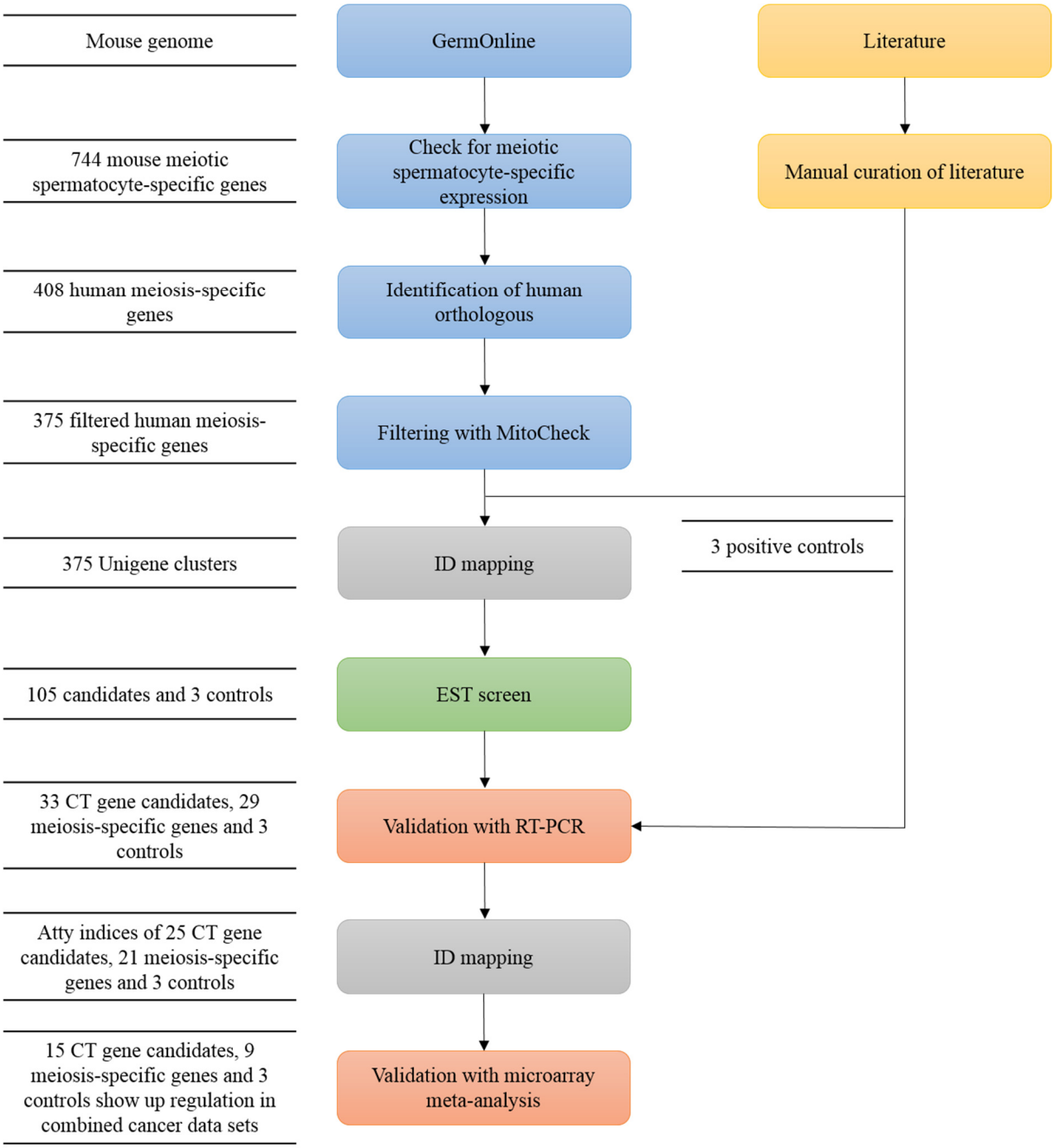

Figure 3.1 Schematic flow diagram that demonstrates the pipeline used for the characterisation and identification of novel and new possible CTA genes utilising the tools of bioinformatics.
Based on an important large-scale microarray analysis, about 744 mouse meiosis-specific genes were chosen to be the preliminary point. In total, nearly 408 human genes were recognised, and around 375 human meiosis-specific genes were left over after filtration was done to eliminate non-testis-specific genes. All the 375 human candidate genes, including the three control genes *MAGE-C1*, *SSX2* and *GAGE1*, were fed into the EST investigation pipeline, and this returned about 105 candidates that were then further validated using the RT-PCR validation/microarray meta-analysis.
Adapted from (Feichtinger *et al.,* 2012b).

3.2. Aims

The aim of the work described in this Chapter was to determine whether *TDRD* genes (*TDRD1–TDRD12*) and *PIWIL* genes (*PIWIL1–PIWIL4*) have testis-restricted expression and can serve as human cancer-specific markers.

The *TDRD* genes are analysed in this study because the *TDRD12* gene has been identified as a possible cancer marker that may encode CSC-specific activity (Almatrafi *et al.,* 2014; Feichtinger *et al.,* 2012b). The *TDRD12* gene is of interest because in a primary study, its expression appeared to be restricted to the human pluripotent germ-line carcinoma cells (NT2). This lead the belief that it might play a role in conferring stemness on cancer cells, as NT2 cells have many features in common with ESCs (Feichtinger *et al.,* 2012b).

The *PIWIL* family of related genes are analysed because they are thought to be involved in the process of gametogenesis (Chen *et al.,* 2011; Zhou *et al.,* 2014). Moreover, the *TDRD12* gene has been recognised as a unique piRNA biogenesis factor. The TDRD12 protein is also present in complexes with PIWIL2 protein and TDRD1 protein, a complex linked to primary piRNA processing. In addition, the *TDRD12* gene is also necessary for the process of spermatogenesis and is required during the biogenesis of *PIWIL4* piRNA (Lim *et al.,* 2014; Pandey *et al.,* 2013; Zhou *et al.,* 2014).

3.3. Results

To analyse and validate the expression profiles of *TDRD* and *PIWIL* genes, several cDNAs were generated from 21 normal and 33 cancerous human cells/tissues, and then the expression was analysed by RT-PCR. A schematic of how these genes were classified is provided in Figure 3.2. The *β-actin* gene was used as a quality control for the generated cDNAs. The *β-actin* RT-PCR products migrated close to the expected size (533 bp) for all cell/tissue types, indicating that the cDNA is of reasonable quality (see Figure 3.3).

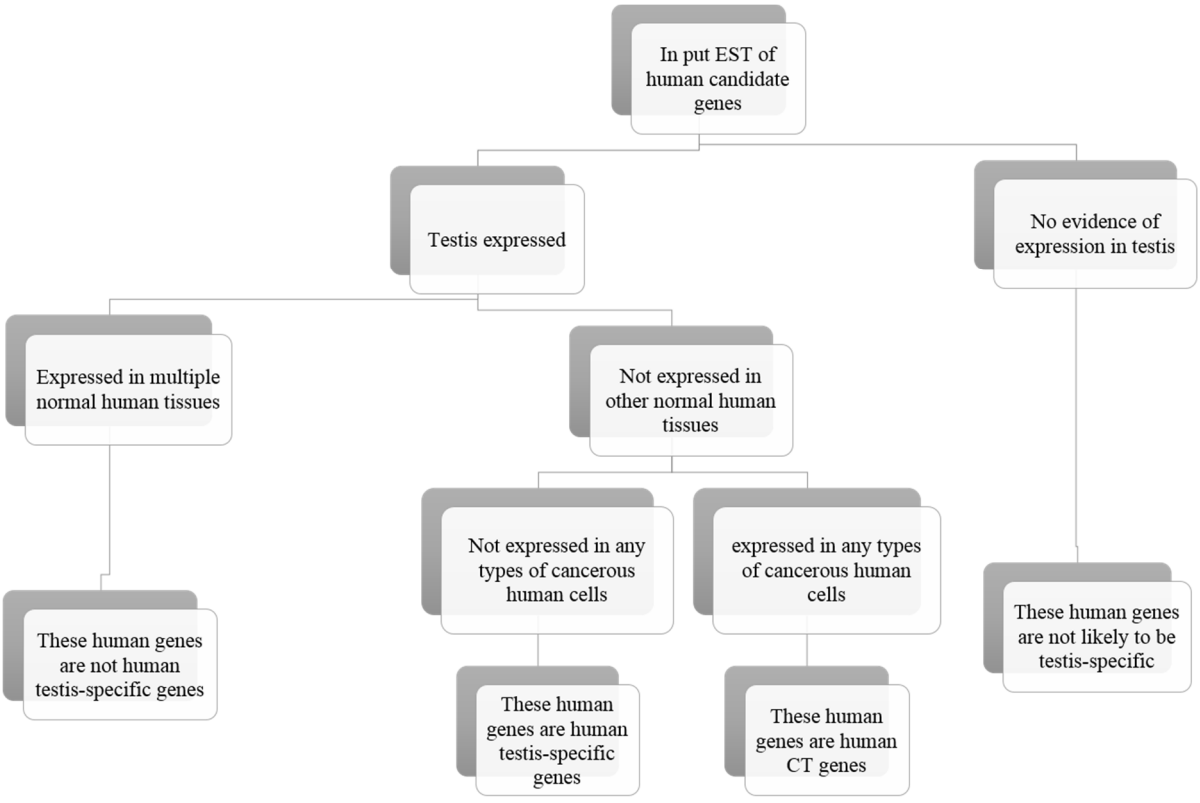

Figure 3.2 Schematic showing expression classification for candidate CT genes.
This figure provides an overview of how to classify the expression profiles of testis-specific genes and CT genes.

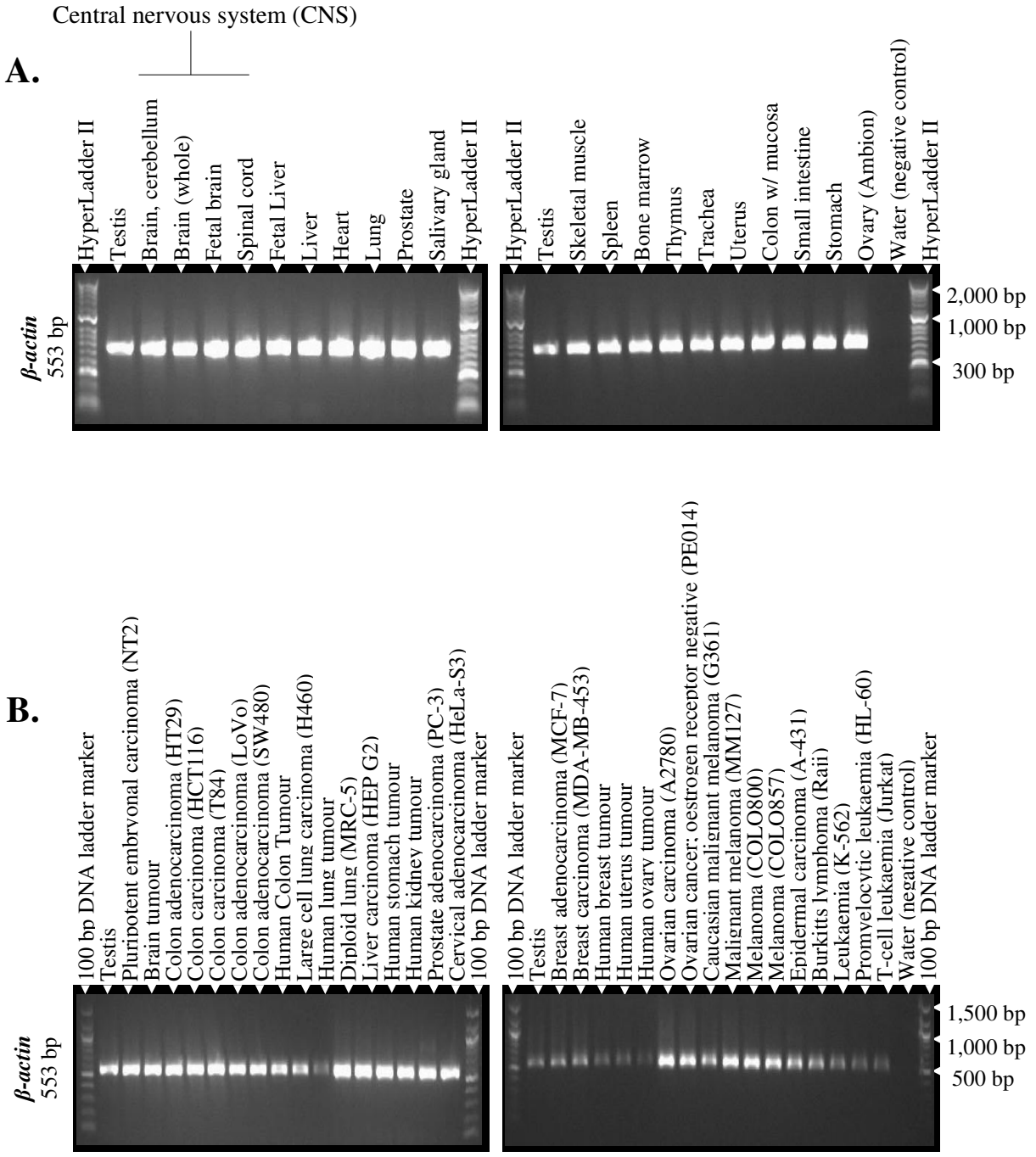

Figure 3.3 RT-PCR analysis of *β-actin* gene expression in normal and cancerous cells.
The expression of the *β-actin* gene was used as a quality control for the cDNA generated from normal and cancerous cells. Panel (A): expression of the *β-actin* gene in normal cells. Panel (B): expression of the *β-actin* gene in cancerous cells. The *β-actin* PCR products migrated close to the expected size (553 bp).

3.3.1. Analysis of *TDRD* gene family expression profiles in normal human tissues

Because the *TDRD12* gene was identified as a possible cancer marker and it was shown to have a germ-line association, an analysis of the expression profiles of all *TDRD* genes (*TDRD1–TDRD12*) in 21 normal tissues was carried out using RT-PCR. One set of forward and reverse primer sequences was designed for each *TDRD* gene (see Table 2.5 in Chapter 2), and RT-PCR analysis was performed (see Figure 3.4 and Figure 3.5).

All the *TDRD* RT-PCR products migrated close to the expected sizes. The outcomes of the analysis show that seven out of 12 *TDRD* genes appear to display expression in all types of normal tissues used in this study, including testis tissue. These are *TDRD2*, *TDRD3*, *TDRD7*, *TDRD8*, *TDRD9*, *TDRD10* and *TDRD11* genes. This indicates that these seven genes might not be good CT gene candidates and that they are not testis-specific (see Figure 3.2). As a result, these *TDRD* genes were removed from the list of potential CTA genes, and their expression profiles were not analysed in cancerous cells.

Furthermore, as can be seen in Figure 3.4 and Figure 3.5, the initial analysis of the *TDRD1* and *TDRD12* genes suggests they are not CT genes (show expression in most types of normal tissues), which for *TDRD12* is in direct conflict with previously published data (Akiyama *et al.,* 2014; Almatrafi *et al.,* 2014; Feichtinger *et al.,* 2012a; Loriot *et al.,* 2003). To validate the RT-PCR, selected PCR products were purified and subjected to DNA sequencing (sequence outcomes shown in Table 3.1). The *TDRD1* gene-sequencing was only confirmed (100%) in normal testis and (97%) in brain/cerebellum tissues. The *TDRD12* gene-sequencing was only confirmed (100%) in normal testis tissue; other sequences were not *TDRD12,* which suggests a lack of primer specificity. Consequently, the *TDRD1* and *TDRD12* genes are demonstrated to possibly be CT genes. Additionally, these analyses suggest that *TDRD4*, *TDRD5* and *TDRD6* are candidate CT genes.

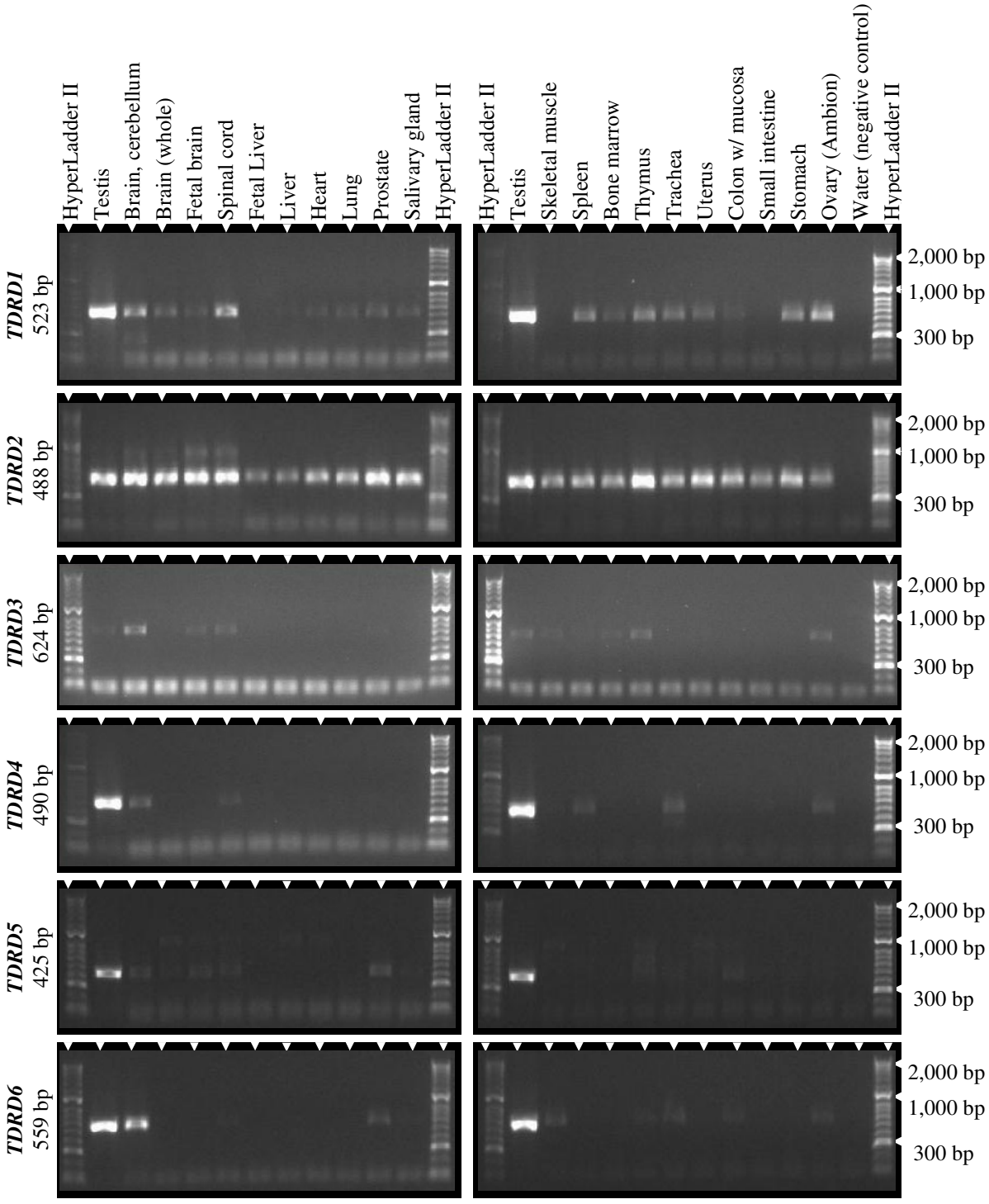

Figure 3.4 RT-PCR analysis of *TDRD1–TDRD6* gene expression in normal human tissues.
Agarose gels presenting the RT-PCR profiles created from normal cells. Note: the sizes in the left margin adjacent to the gene names are the predicted PCR product sizes.

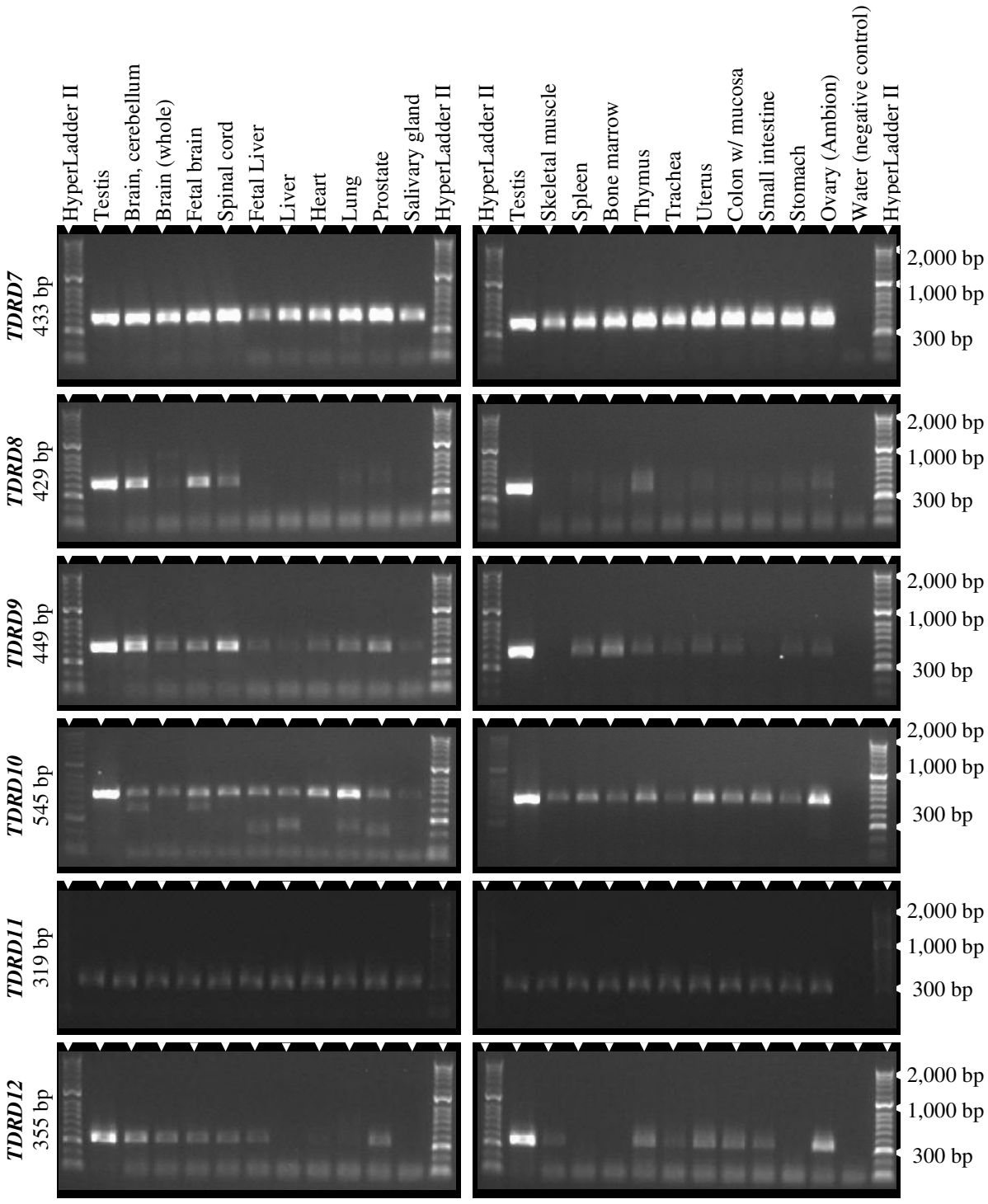

Figure 3.5 RT-PCR analysis of *TDRD7–TDRD12* gene expression in normal human tissues.
Agarose gels presenting the RT-PCR profiles created from normal cells. Note: the sizes in the left margin adjacent to the gene names are the predicted PCR product sizes.

3.3.2. RT-PCR analysis of the gene expression profiles of *TDRD* and *PIWIL* CT genes in normal tissues

To further explore/verify the finding that a sub-set of *TDRD* genes (*TDRD1, TDRD4, TDRD5, TDRD6* and *TDRD12*) and *PIWIL* genes (*PIWIL1–PIWIL4*) could be CT genes, three sets of forward and reverse primer sequences were designed for each of the above-mentioned genes and for their different isoforms to detect specific transcripts. These primers were used to analyse the expression profiles of these *TDRD* and *PIWIL* genes in 21 types of normal tissues and 33 types of cancerous cells using RT-PCR. The expected sizes of the RT-PCR products in base pairs (bp) were included in the maps for each gene (see Figure 3.6, Figure 3.7, Figure 3.10, Figure 3.12, Figure 3.15, Figure 3.16, Figure 3.19, Figure 3.22, Figure 3.25, Figure 3.28, Figure 3.31 and Figure 3.34).

The RT-PCR validation process identified six genes (*TDRD4*, *TDRD5*, *TDRD12*, *PIWIL1*, *PIWIL2* and *PIWIL3*) that appear to be testis-restricted, as they display expression only in testis tissue (see Figure 3.8, Figure 3.13, Figure 3.17, Figure 3.26, Figure 3.29 and Figure 3.32). Consequently, this group of genes could be classified as testis-restricted genes, and based on these results, it can be concluded that they might be good candidates for CT genes or testis-specific genes. However, the *TDRD1* and *TDRD6* genes (see Figure 3.20 and Figure 3.23) displayed expression in some types of non-testis normal tissues. This group of genes might be CTA gene candidates. Given that they showed expression in some limited non-testis normal tissues, these genes could be classified as testis-selective.

The *TDRD* and *PIWIL* RT-PCR products migrated close to the expected sizes. Additionally, the RT-PCR products for selected *TDRD* and *PIWIL* candidate genes in normal tissues were subjected to purification and sequencing to verify the DNA sequences (a summary of the sequencing results is shown in Table 3.1). Therefore, their expression profiles were analysed in cancerous cells (see Section 3.3.3).

3.3.3. RT-PCR analysis of the gene expression profiles of predicted *TDRD* and *PIWIL* CT genes in cancerous cells

Based on the RT-PCR analysis outcomes of the predicted *TDRD* and *PIWIL* CT genes within normal tissues (refer to Section 3.3.2), eight of the 16 *TDRD* and *PIWIL* genes in total were identified as candidate CT genes (*TDRD1, TDRD4*, *TDRD5*, *TDRD6, TDRD12*, *PIWIL1*, *PIWIL2* and *PIWIL3*), while the remaining eight *TDRD* and *PIWIL* genes were dismissed (*TDRD2*, *TDRD3*, *TDRD7*, *TDRD8*, *TDRD9*, *TDRD10*, *TDRD11* and *PIWIL4*). The eight candidate *TDRD* and *PIWIL* genes were categorised as follows: six genes (*TDRD4*, *TDRD5*, *TDRD12*, *PIWIL1*, *PIWIL2* and *PIWIL3*) could be classified as testis-restricted and two genes (*TDRD1* and *TDRD6*) could be classified as testis-selective. Therefore, to determine whether these candidate *TDRD* and *PIWIL* genes can serve as cancer-specific markers and whether they might be potential and possible CTA genes, their expression profiles were evaluated in 33 types of cancerous cells using RT-PCR.

It was shown that five genes (*TDRD4*, *TDRD5*, *TDRD12*, *PIWIL1* and *PIWIL2*) not only showed expression in normal testis tissue, but they also showed expression within some of the 33 types of cancerous cells (see Figure 3.9, Figure 3.14, Figure 3.18, Figure 3.27 and Figure 3.30). Thus, this group of genes was classified as cancer testis-restricted. Additionally, two genes (*TDRD1* and *TDRD6*) showed expression in some types of normal tissues, including testis, and they were expressed within some of the 33 types of cancerous cells (see Figure 3.21 and Figure 3.24). Therefore, these genes were classified as cancer testis-selective. One gene, *PIWIL3*, appeared to be expressed only in normal testis tissue and did not show any expression within the 33 types of cancerous cell (see Figure 3.33). As a result, this gene was classified as non-cancer testis-restricted.

The *TDRD12* gene is found to be expressed in normal testis tissue (an intense band), pluripotent embryonal carcinoma (NT2) (an intense band), colon carcinoma (HCT116) (a faint band) and colon carcinoma (T84) (a faint band) (see Figure 3.9; see also Feichtinger *et al.,* 2012b). The expression in NT2 cells leads us to believe that it may play a role in conferring stemness in cancer cells because the NT2 cells have many features in common with embryonic stem cells (ESCs). Hence, the *TDRD12* gene and NT2 cells are of particular interest to this analysis and project. The *TDRD4* gene was expressed in normal testis tissue (an intense band), brain tumour (an intense band) and leukaemia (K-562) (a faint band) (see Figure 3.14). The *TDRD5* gene was expressed in normal testis tissue (an intense band), breast adenocarcinoma (MCF-7) (a faint band) and breast carcinoma (MDA-MB-453) (a faint band) (see Figure 3.18).

The *TDRD6* gene was expressed in normal testis tissue (an intense band), brain cerebellum (a faint band), prostate adenocarcinoma (PC-3) (a faint band) and cervical adenocarcinoma (HeLa-S3) (a faint band) (see Figure 3.21). The *TDRD1* gene was expressed in several normal tissues (mix between faint and strong bands), including normal testis tissue (an intense band) and MCF-7 (an intense band) (see Figure 3.24). The *PIWIL1* gene was expressed in normal testis tissue (an intense band), T48 (a faint band), colon adenocarcinoma (LoVo) (a faint band), colon adenocarcinoma (SW480) (a faint band), colon tumour (a faint band) and uterus tumour (a faint band) (see Figure 3.27). The *PIWIL2* gene was expressed in normal testis tissue (an intense band), NT2 (an intense band) and liver carcinoma (HEP-G2) (a faint band) (see Figure 3.30).

The *TDRD* and *PIWIL* RT-PCR products migrated close to the expected sizes. In addition, the RT-PCR products for selected *TDRD* and *PIWIL* genes in cancerous cells were subjected to purification and sequencing to verify the DNA sequences (a summary of the sequencing results is shown in Table 3.1).

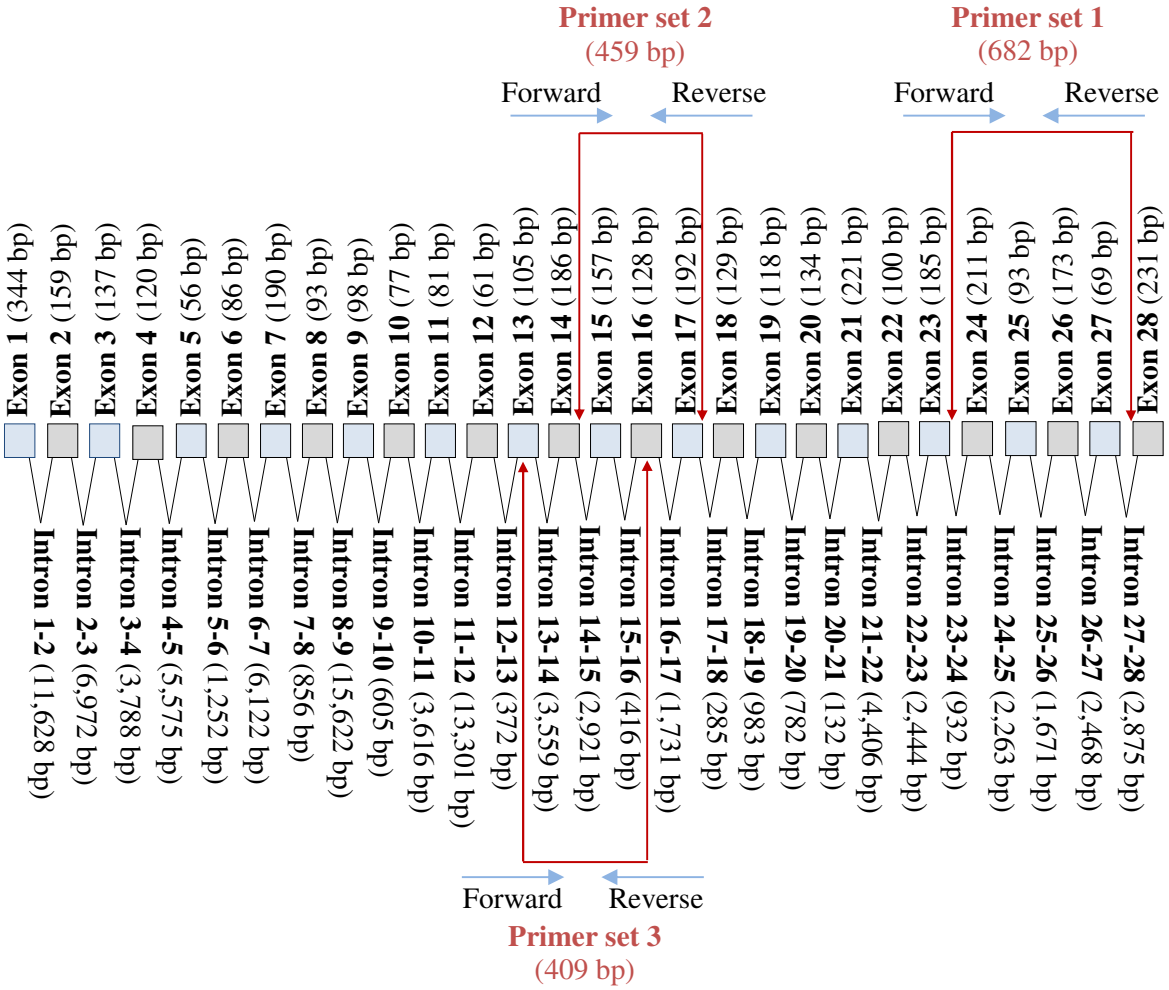

Figure 3.6 Map showing the design of three sets of forward and reverse primer sequences for the analysis of human *TDRD12-001* transcript.
The spliced transcript contains 3934 nucleotides and predicted 28 exons. The primers were used to analyse the expression of the *TDRD12-001* transcript in 21 types of normal human tissues and 33 types of cancerous human cells using RT-PCR. Moreover, the expected size of the PCR products in base pairs (bp) is included in the map. Note: exon and intron sizes are not to scale.

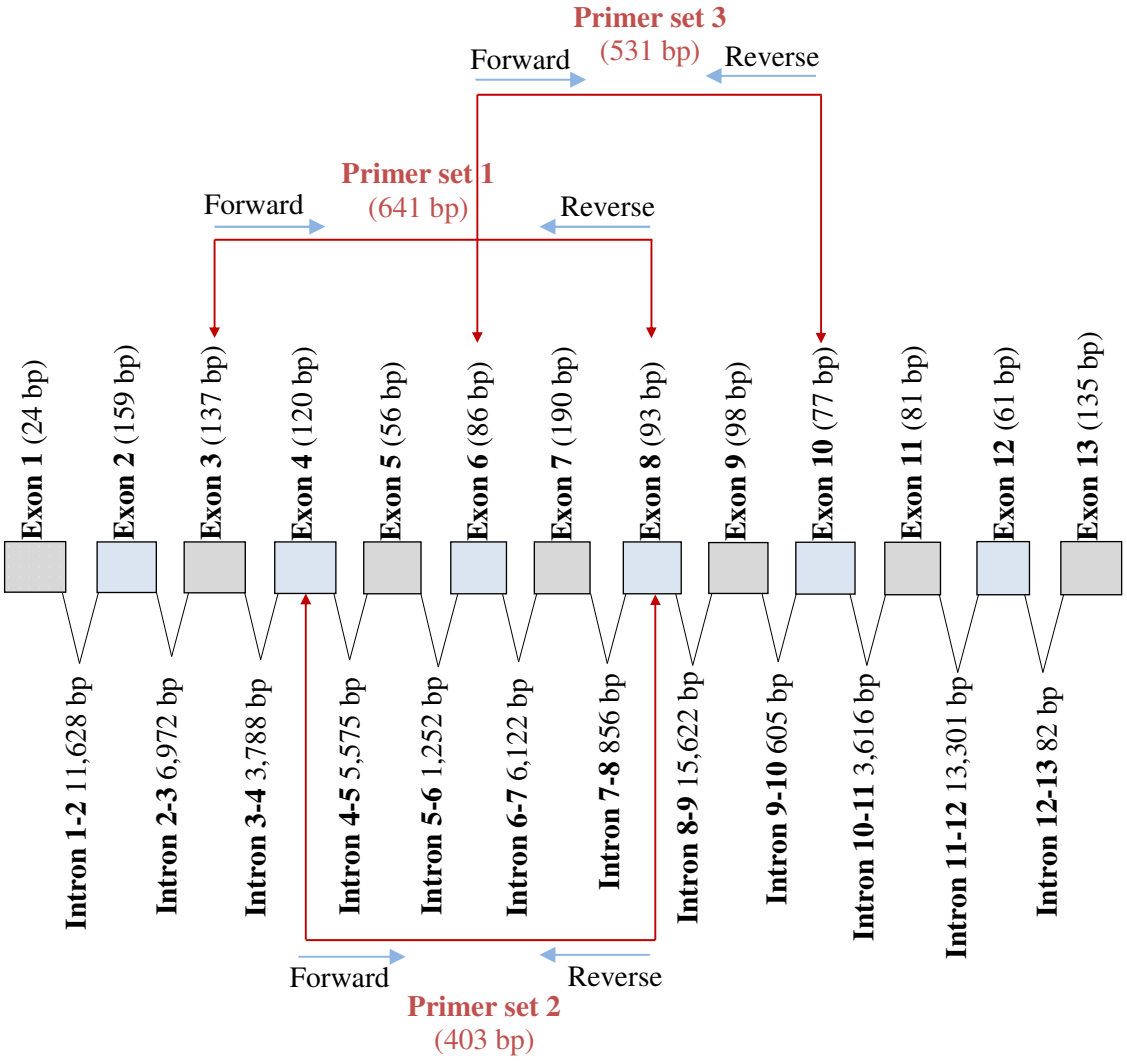

Figure 3.7 Map showing the design of three sets of forward and reverse primer sequences for the analysis of human *TDRD12-003* transcript.
The spliced transcript contains 1188 nucleotides and predicted 13 exons. The primers were used to analyse the expression of the *TDRD12-003* transcript in 21 types of normal human tissues and 33 types of cancerous human cells using RT-PCR. Moreover, the expected size of the PCR products in base pairs (bp) is included in the map. Note: exon and intron sizes are not to scale.

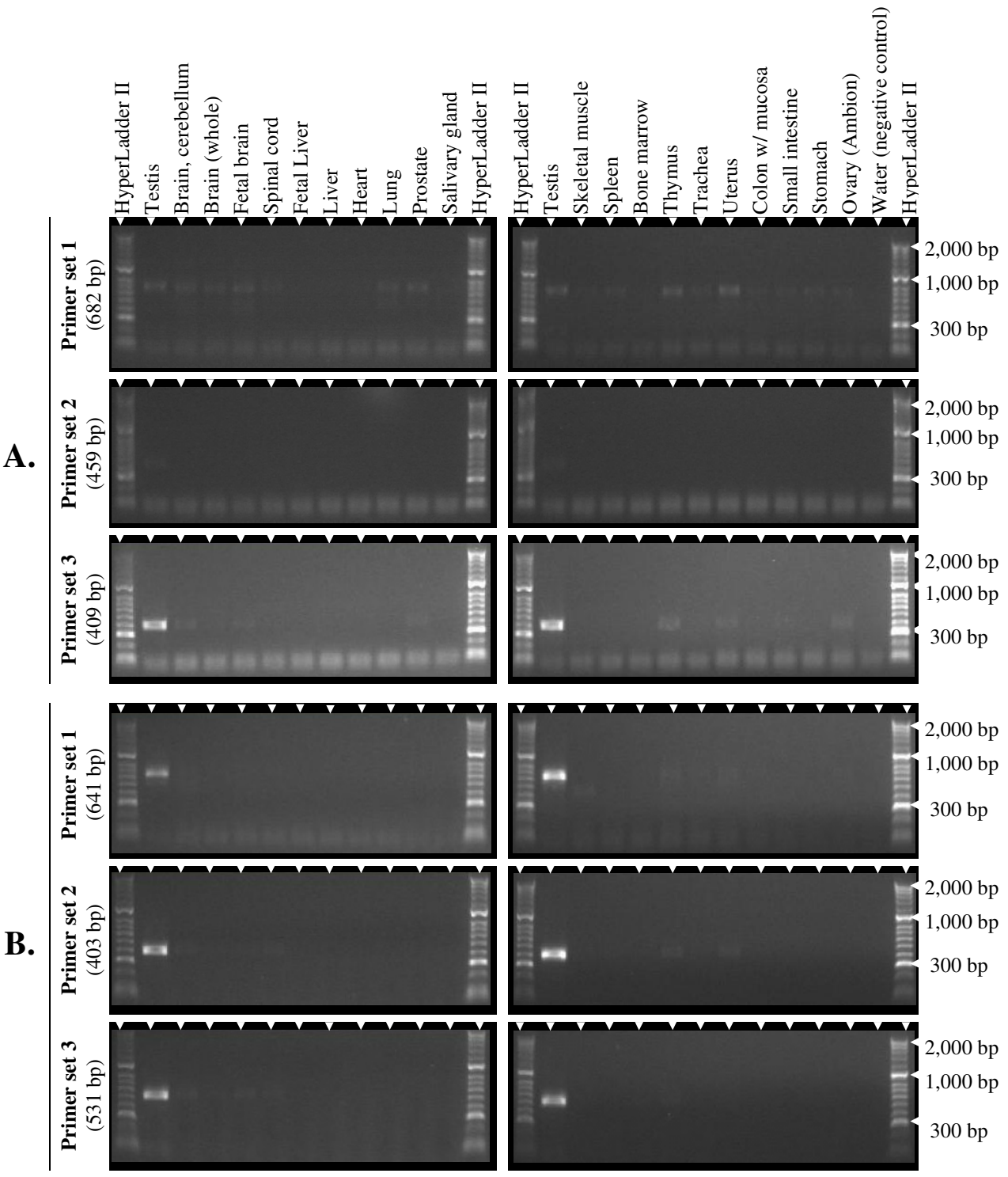

Figure 3.8 RT-PCR analysis of *TDRD12-001* and *TDRD12-003* transcripts in normal tissues. Agarose gels presenting the RT-PCR profiles created from normal cells. Panel (A): expression of the *TDRD12-001* transcript. Panel (B): expression of the *TDRD12-003* transcript. The PCR products migrated close to the expected sizes (shown in parenthesis on the left).

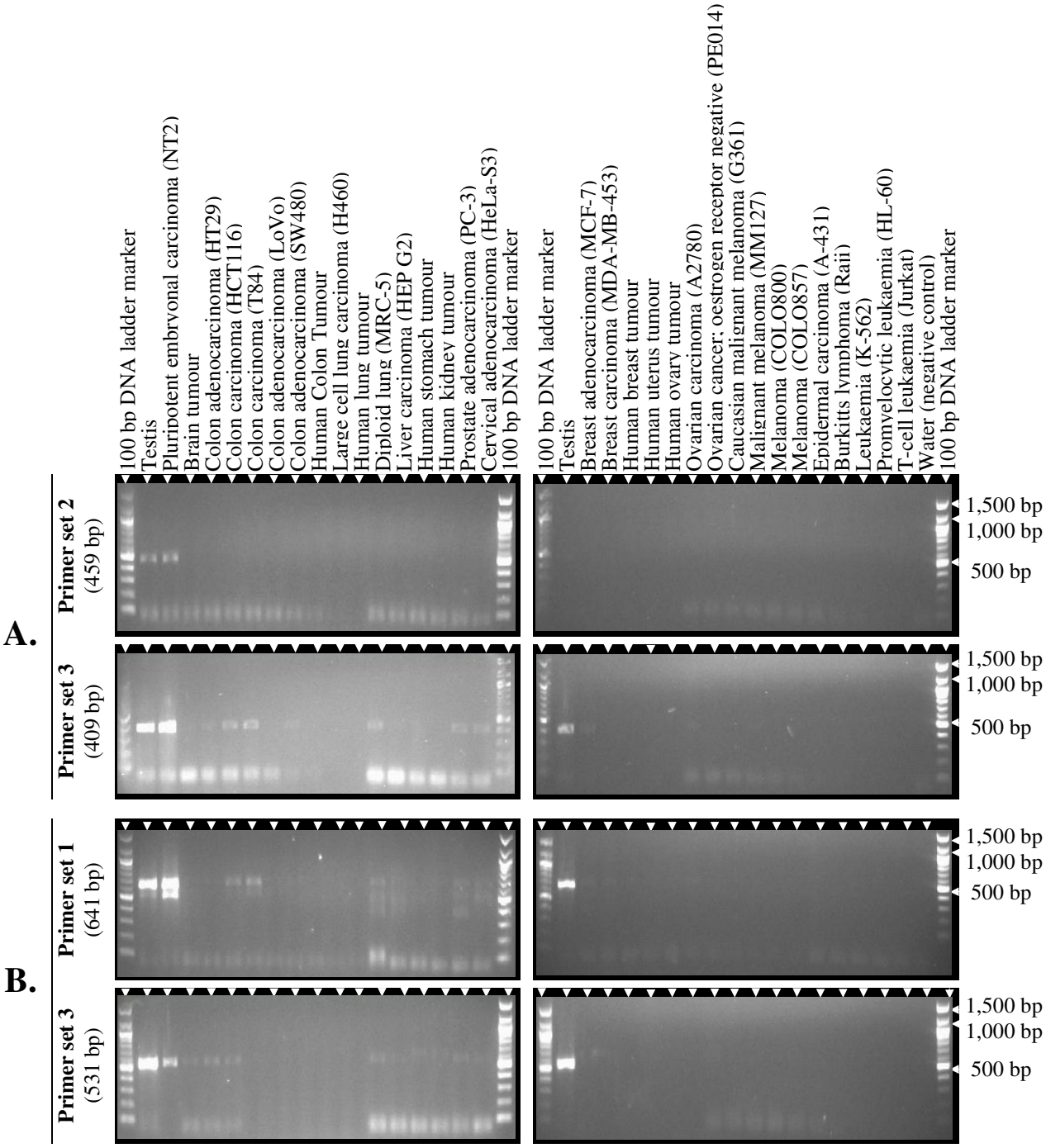

Figure 3.9 RT-PCR analysis of *TDRD12-001* and *TDRD12-003* transcripts in cancerous cells. Agarose gels presenting the RT-PCR profiles created from cancerous cells. Panel (A): expression of the *TDRD12-001* transcript. Panel (B): expression of the *TDRD12-003* transcript. The PCR products migrated close to the expected sizes (shown in parenthesis on the left).

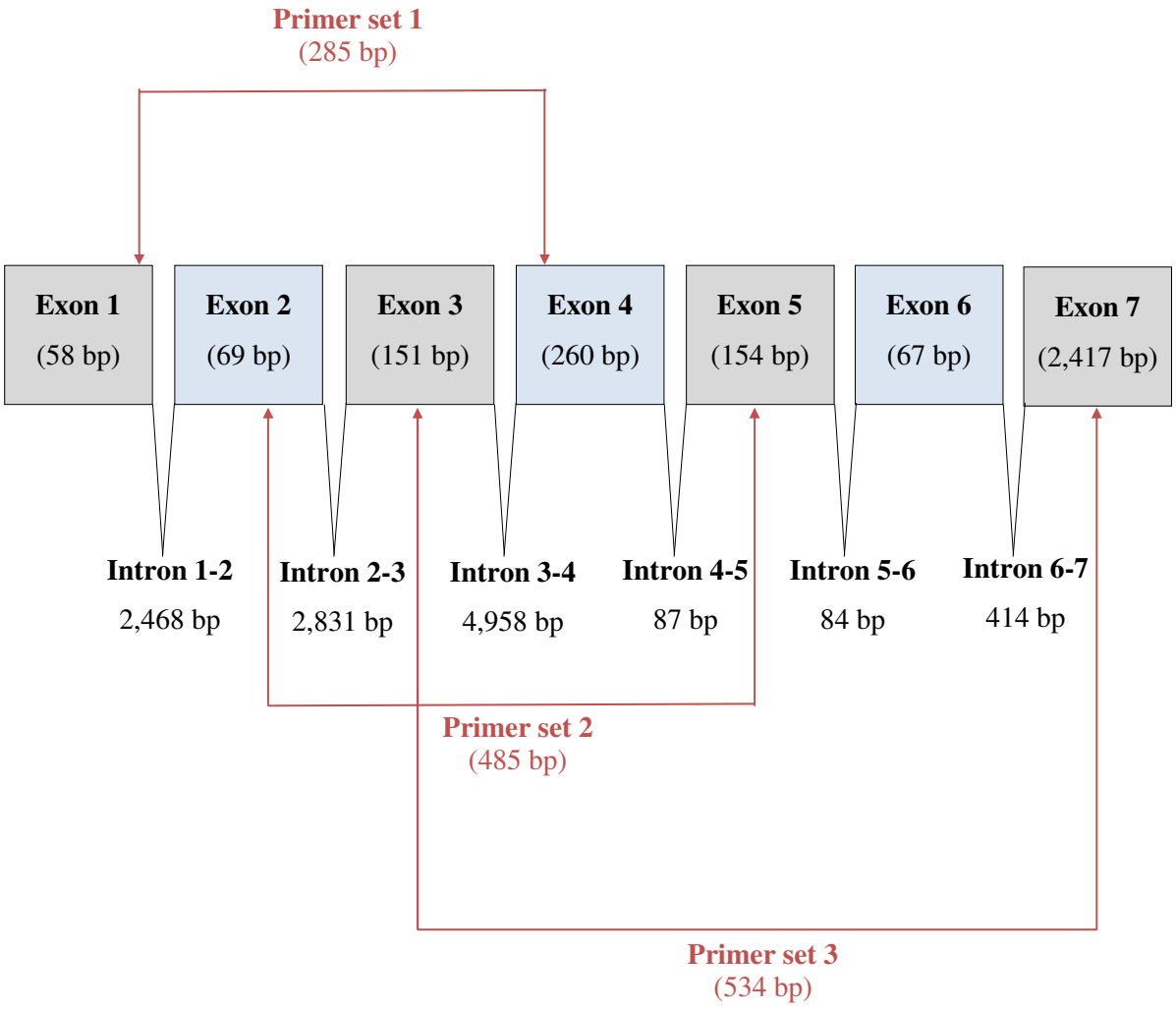

Figure 3.10 Map showing the design of three sets of forward and reverse primer sequences for the analysis of human *TDRD12-002* transcript.
The spliced transcript contains 3176 nucleotides and predicted 7 exons. The primers were used to analyse the expression of the *TDRD12-002* transcript in human testis tissues using RT-PCR. Moreover, the expected size of the PCR products in base pairs (bp) is included in the map. Note: exon and intron sizes are not to scale.

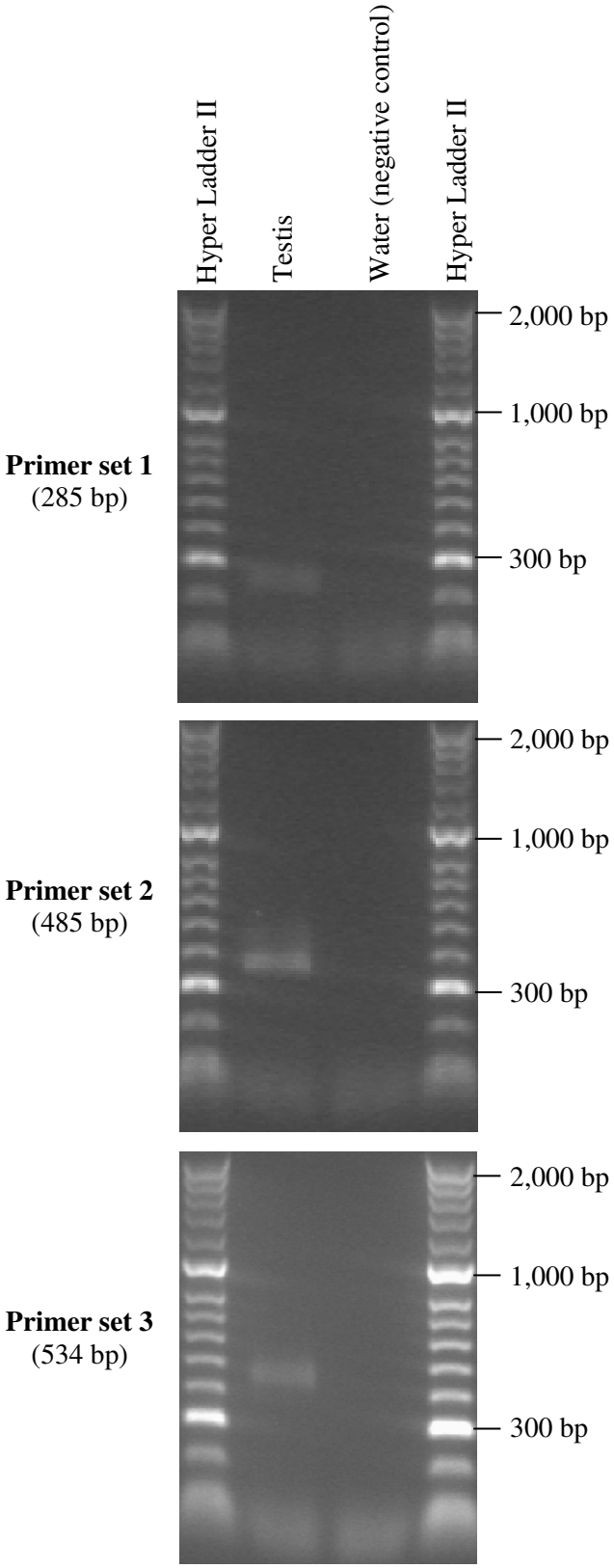

Figure 3.11 RT-PCR analysis of *TDRD12-002* transcript in testis tissues.
Agarose gels presenting the RT-PCR profiles created from testis tissue. The PCR products migrated close to the expected sizes (shown in parenthesis on the left).

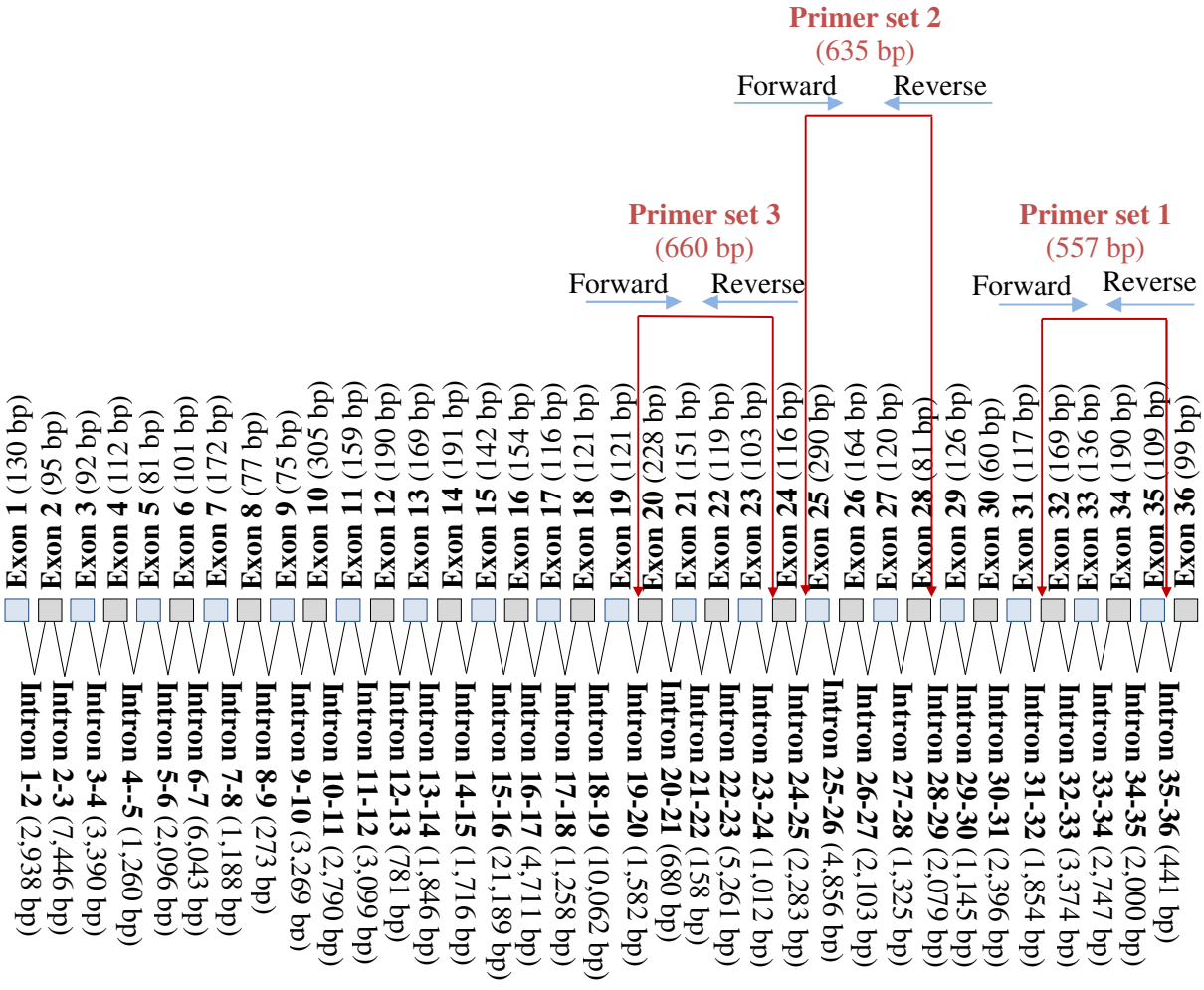

Figure 3.12 Map showing the design of three sets of forward and reverse primer sequences for the analysis of human *RNF17-003* transcript.
This gene is also known as *TDRD4*; the spliced transcript contains 4872 nucleotides and predicted 36 exons. The primers were used to analyse the expression of the *RNF17-003* transcript in 21 types of normal human tissues and 33 types of cancerous human cells using RT-PCR. Moreover, the expected size of the PCR products in base pairs (bp) is included in the map. Note: exon and intron sizes are not to scale.

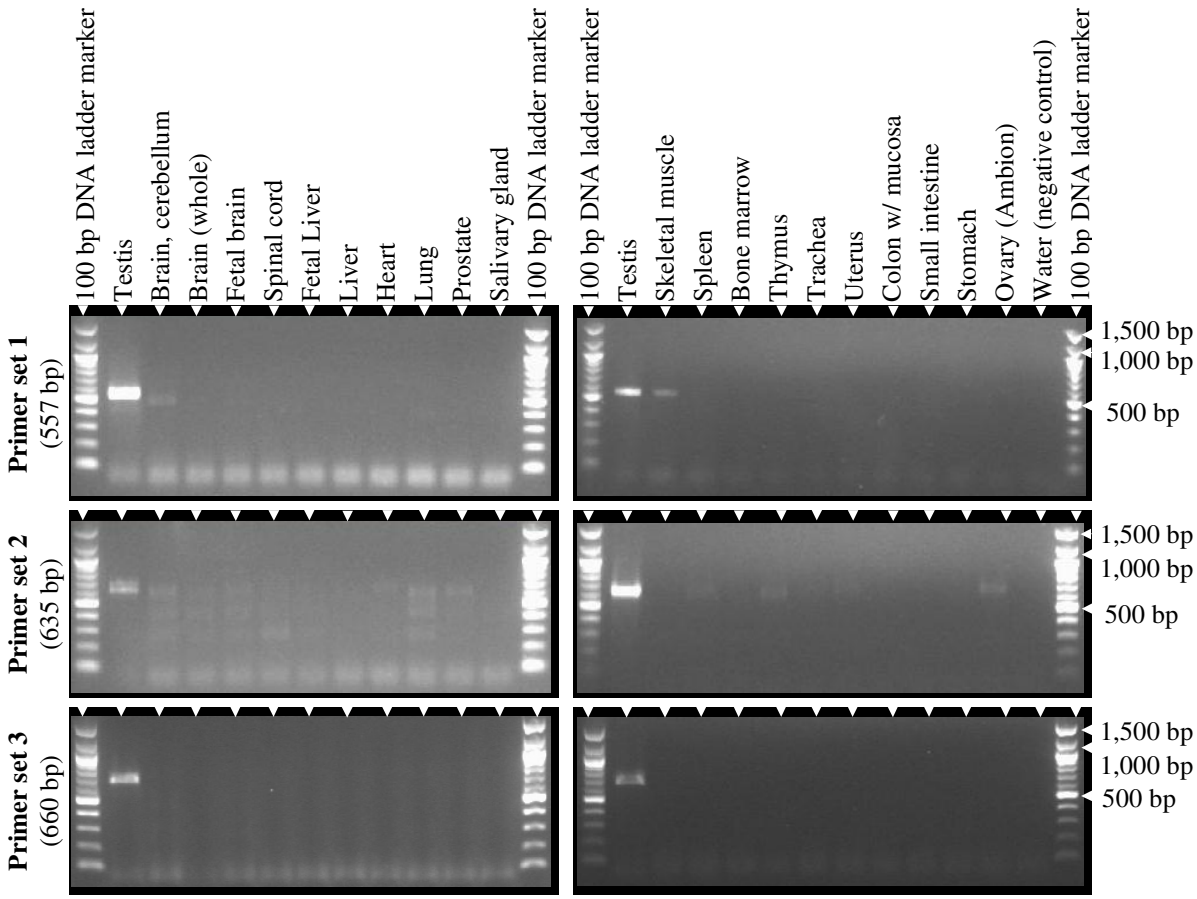

Figure 3.13 RT-PCR analysis of *RNF17-003* transcript in normal tissues.
Agarose gels presenting the RT-PCR profiles created from normal cells. The PCR products migrated close to the expected sizes (shown in parenthesis on the left).

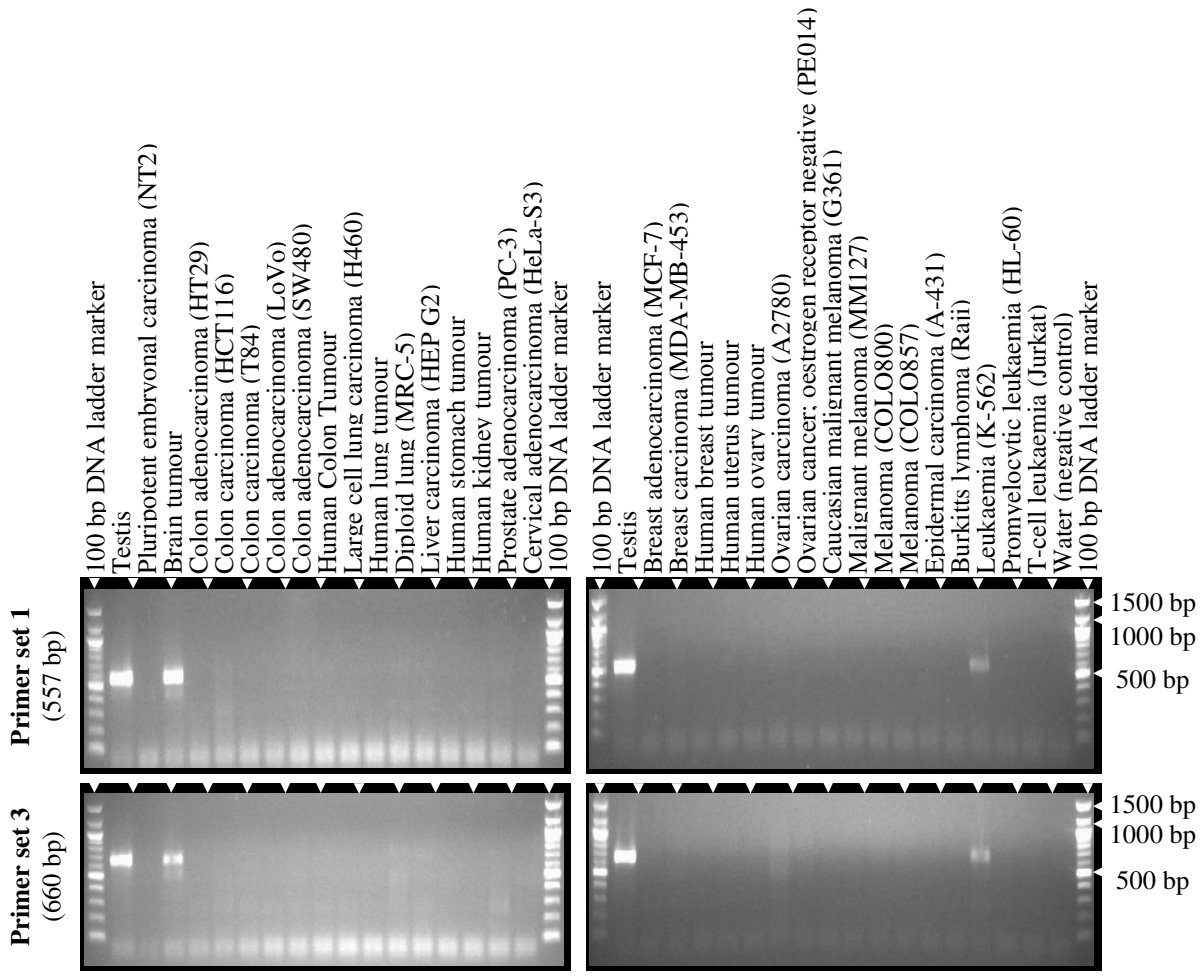

Figure 3.14 RT-PCR analysis of *RNF17-003* transcript in cancerous cells.
Agarose gels presenting the RT-PCR profiles created from cancerous cells. The PCR products migrated close to the expected sizes (shown in parenthesis on the left).

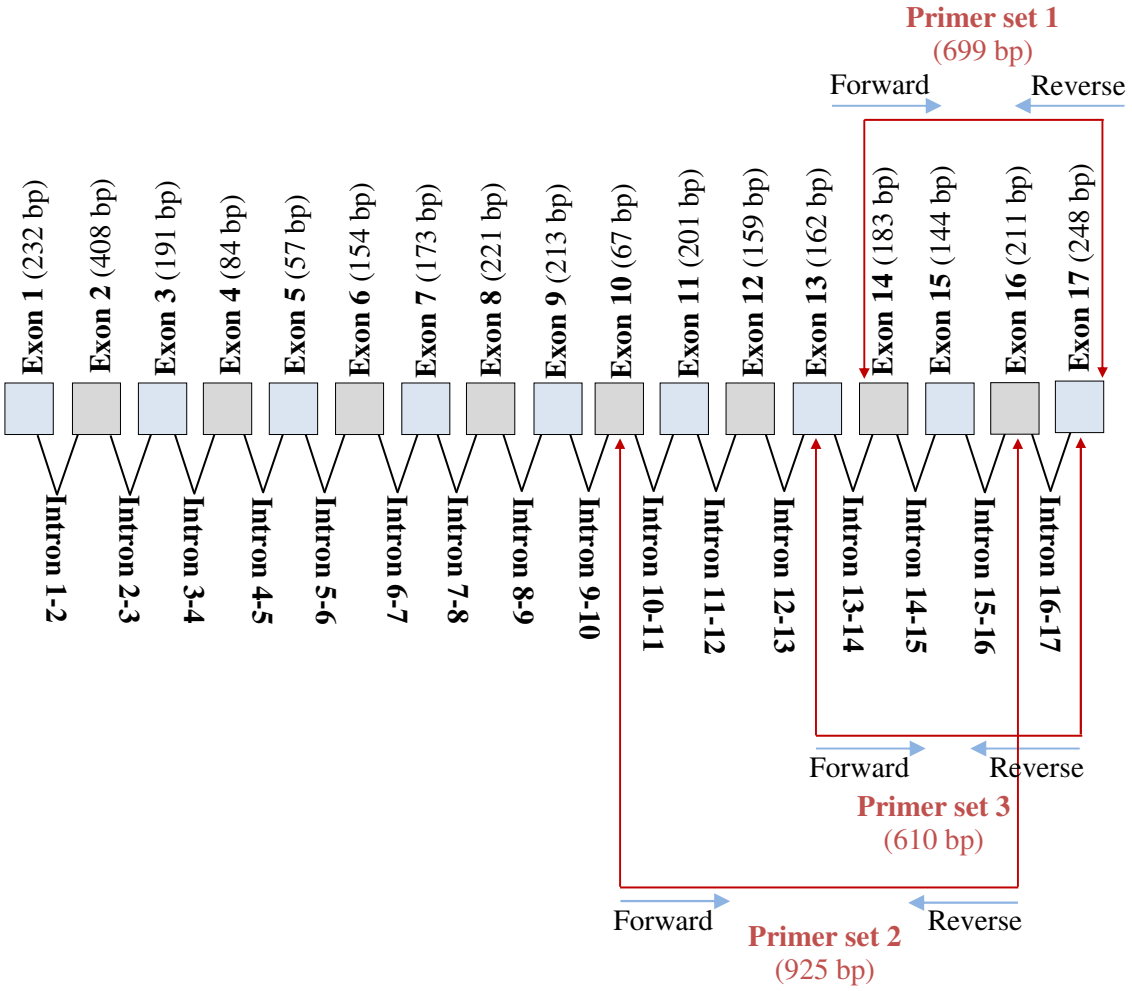

Figure 3.15 Map showing the design of three sets of forward and reverse primer sequences for the analysis of human *TDRD5-201* transcript.
The spliced transcript contains 3108 nucleotides and predicted 17 exons. The primers were used to analyse the expression of the *TDRD5-201* transcript in 21 types of normal human tissues and 33 types of cancerous human cells using RT-PCR. Moreover, the expected size of the PCR products in base pairs (bp) is included in the map. Note: exon and intron sizes are not to scale.

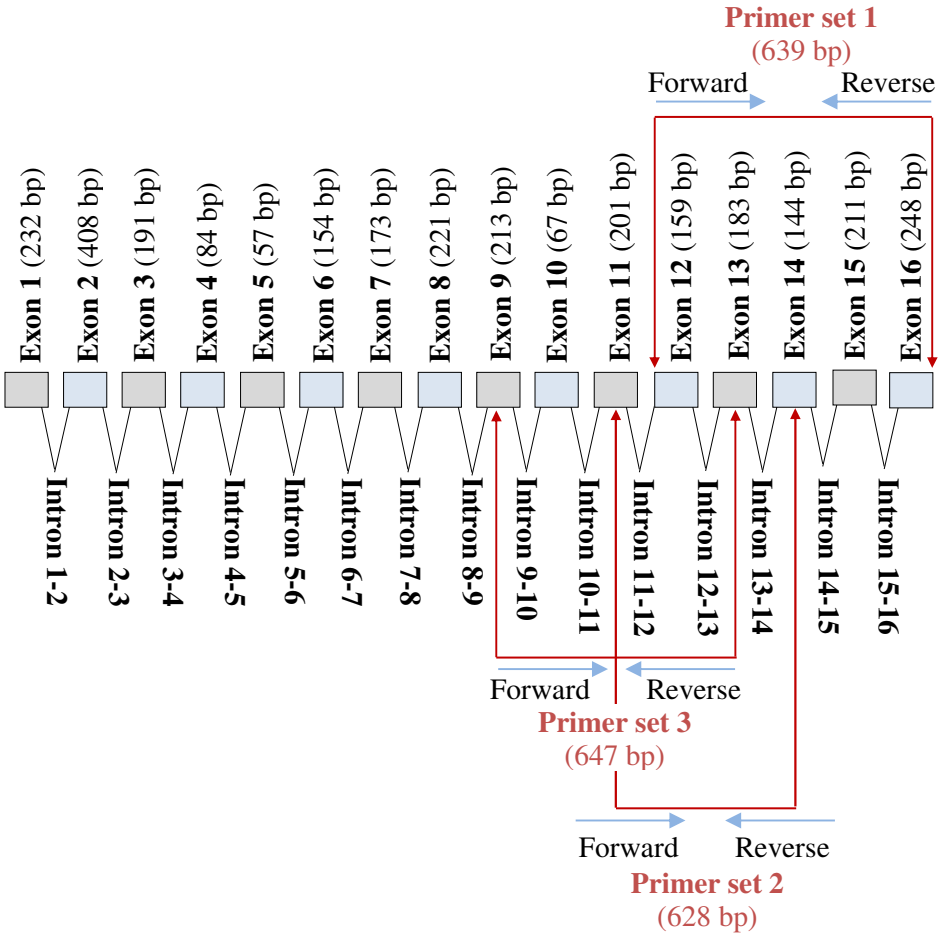

Figure 3.16 Map showing the design of three sets of forward and reverse primer sequences for the analysis of human *TDRD5-001* transcript.
The spliced transcript contains 2946 nucleotides and predicted 16 exons. The primers were used to analyse the expression of the *TDRD5-001* transcript in 21 types of normal human tissues and 33 types of cancerous human cells using RT-PCR. Moreover, the expected size of the PCR products in base pairs (bp) is included in the map. Note: exon and intron sizes are not to scale.

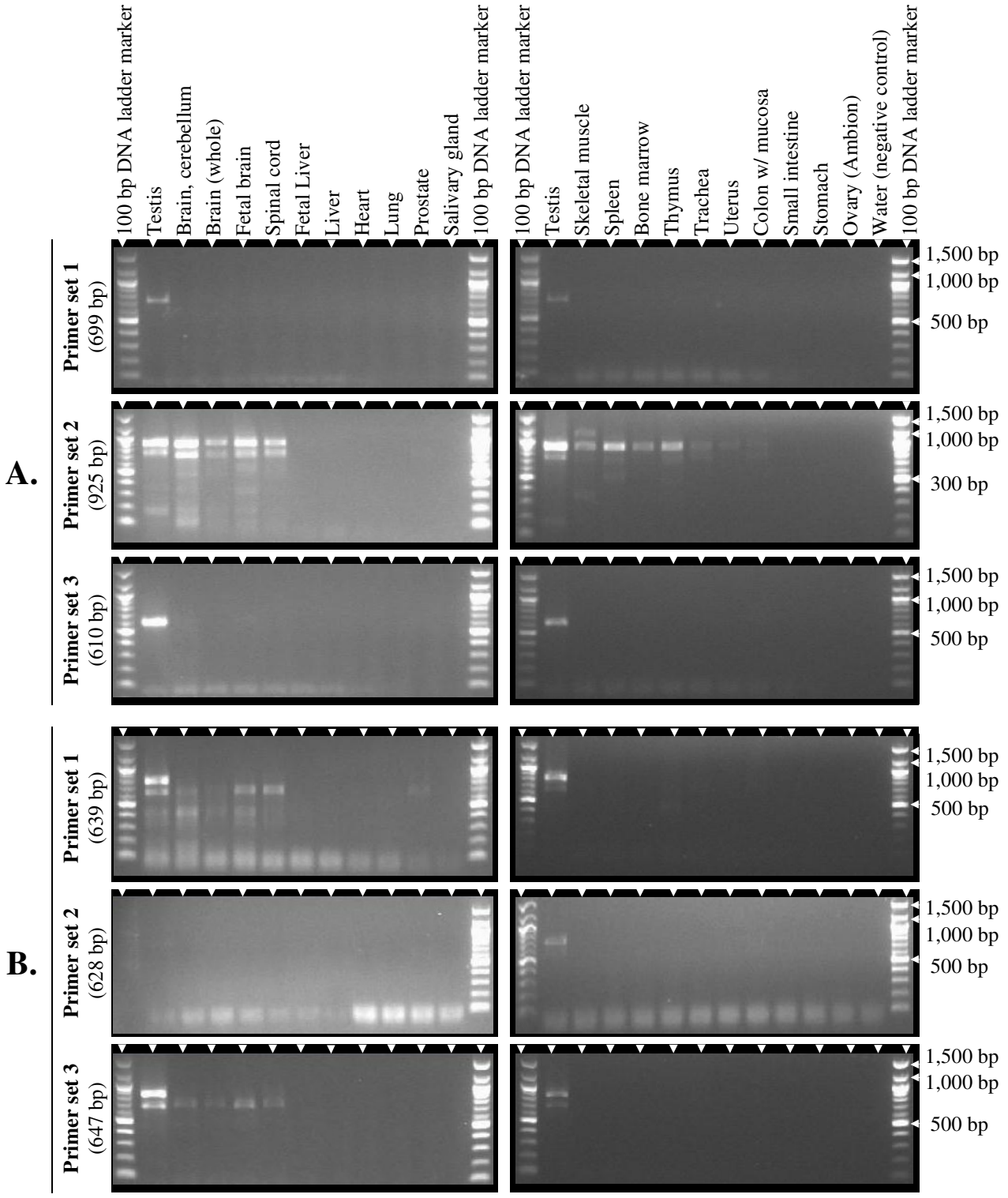

Figure 3.17 RT-PCR analysis of *TDRD5-201* and *TDRD5-001* transcripts in normal tissues.
Agarose gels presenting the RT-PCR profiles created from normal cells. Panel (A): expression of the *TDRD5-201* transcript. Panel (B): expression of the *TDRD5-001* transcript. The PCR products migrated close to the expected sizes (shown in parenthesis on the left).

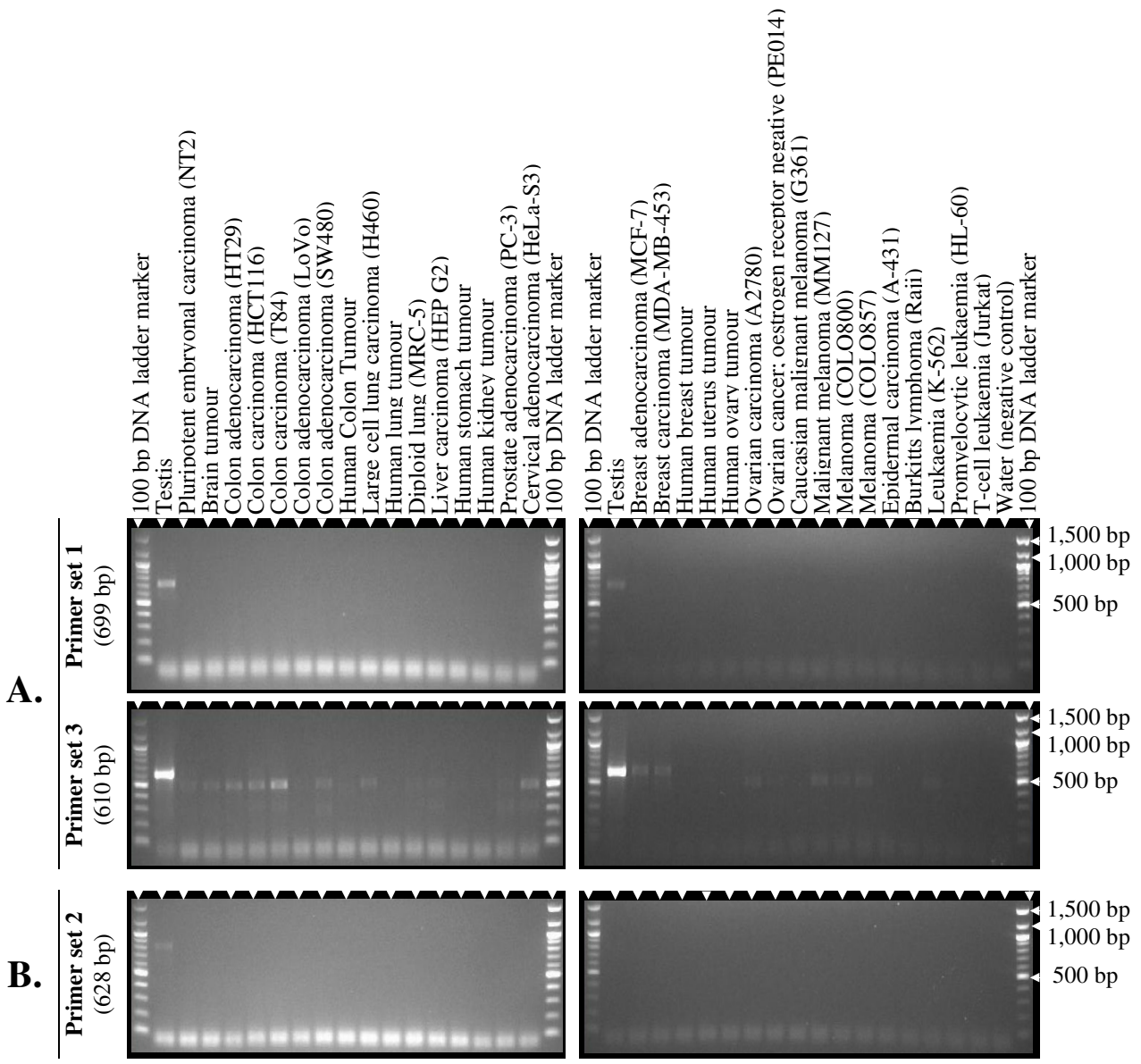

Figure 3.18 RT-PCR analysis of *TDRD5-201* and *TDRD5-001* transcripts in cancerous cells.
Agarose gels presenting the RT-PCR profiles created from cancerous cells. Panel (A): expression of the *TDRD5-201* transcript. Panel (B): expression of the *TDRD5-001* transcript. The PCR products migrated close to the expected sizes (shown in parenthesis on the left).

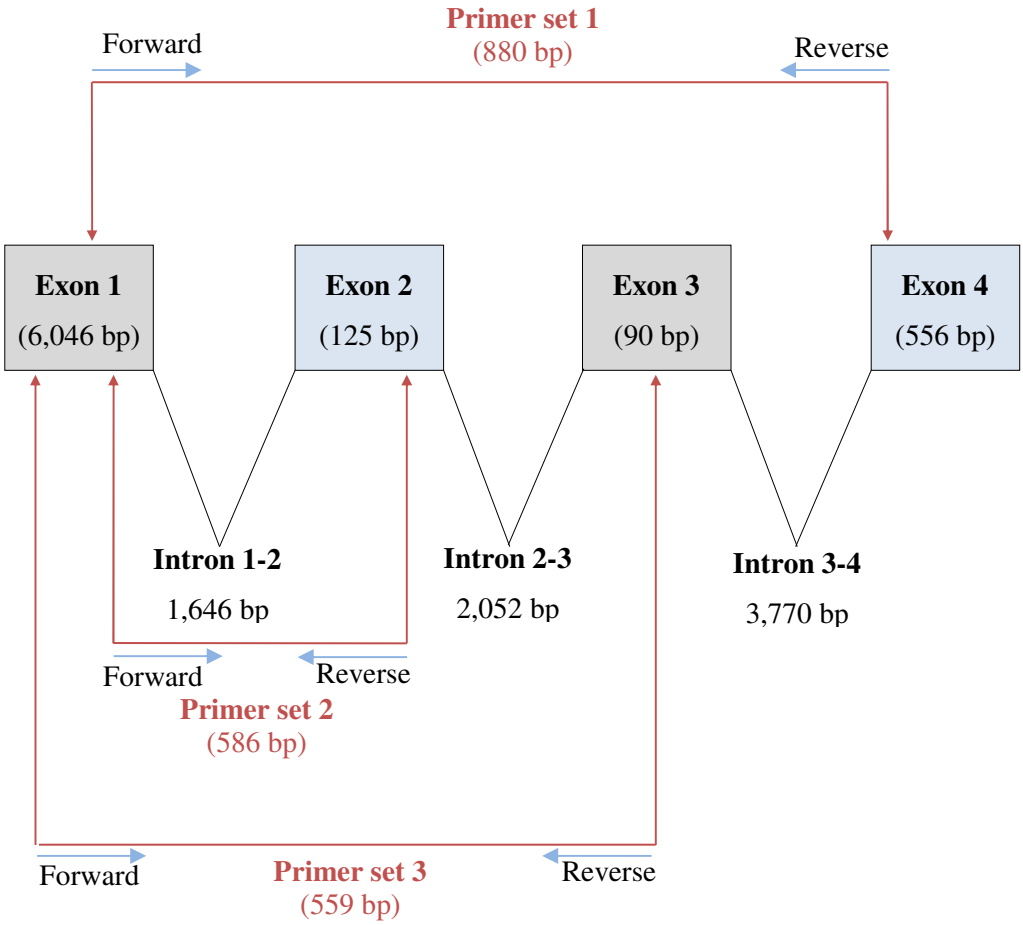

Figure 3.19 Map showing the design of three sets of forward and reverse primer sequences for the analysis of human *TDRD6-001* transcript.
The spliced transcript contains 6291 nucleotides and predicted 4 exons. The primers were used to analyse the expression of the *TDRD6-001* transcript in 21 types of normal human tissues and 33 types of cancerous human cells using RT-PCR. Moreover, the expected size of the PCR products in base pairs (bp) is included in the map. Note: exon and intron sizes are not to scale.

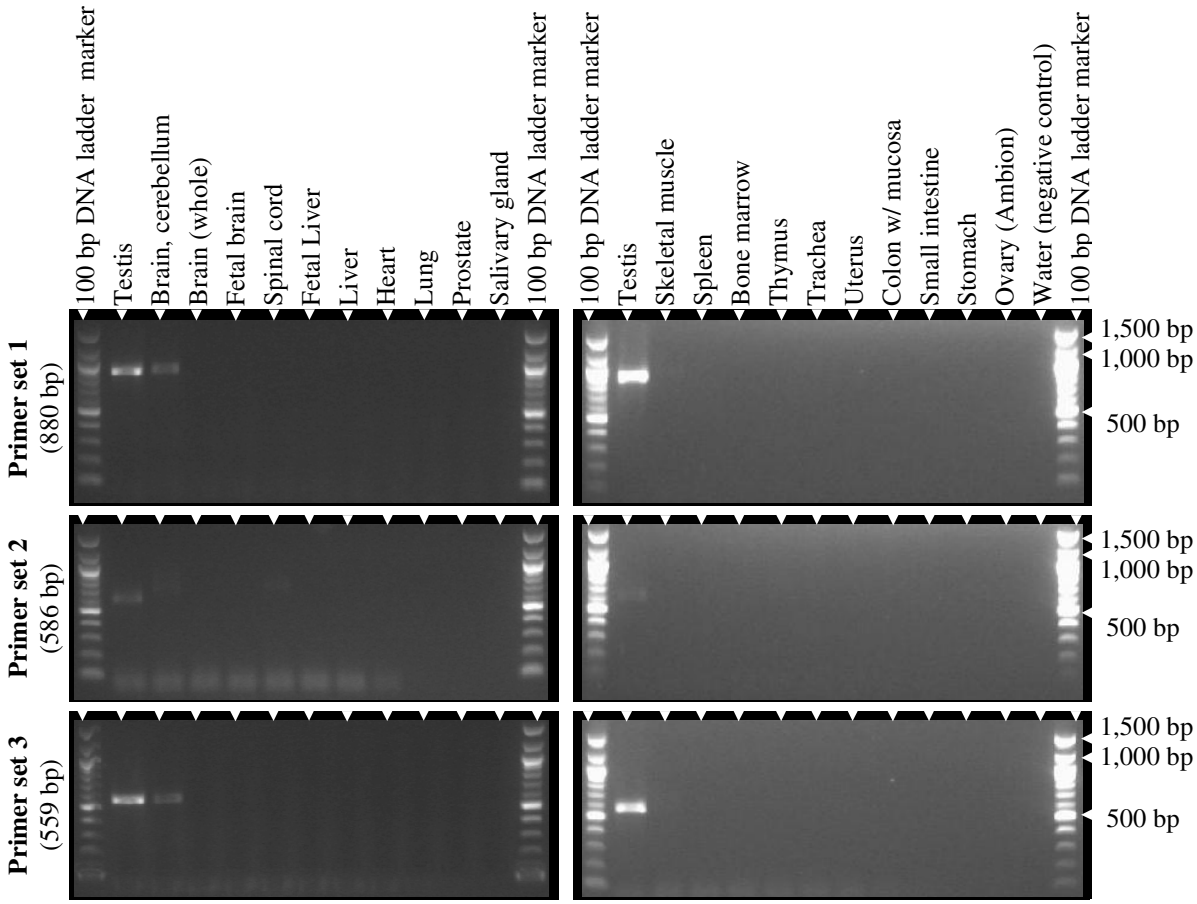

Figure 3.20 RT-PCR analysis of *TDRD6-001* transcript in normal tissues.
Agarose gels presenting the RT-PCR profiles created from normal cells. The PCR products migrated close to the expected sizes (shown in parenthesis on the left).

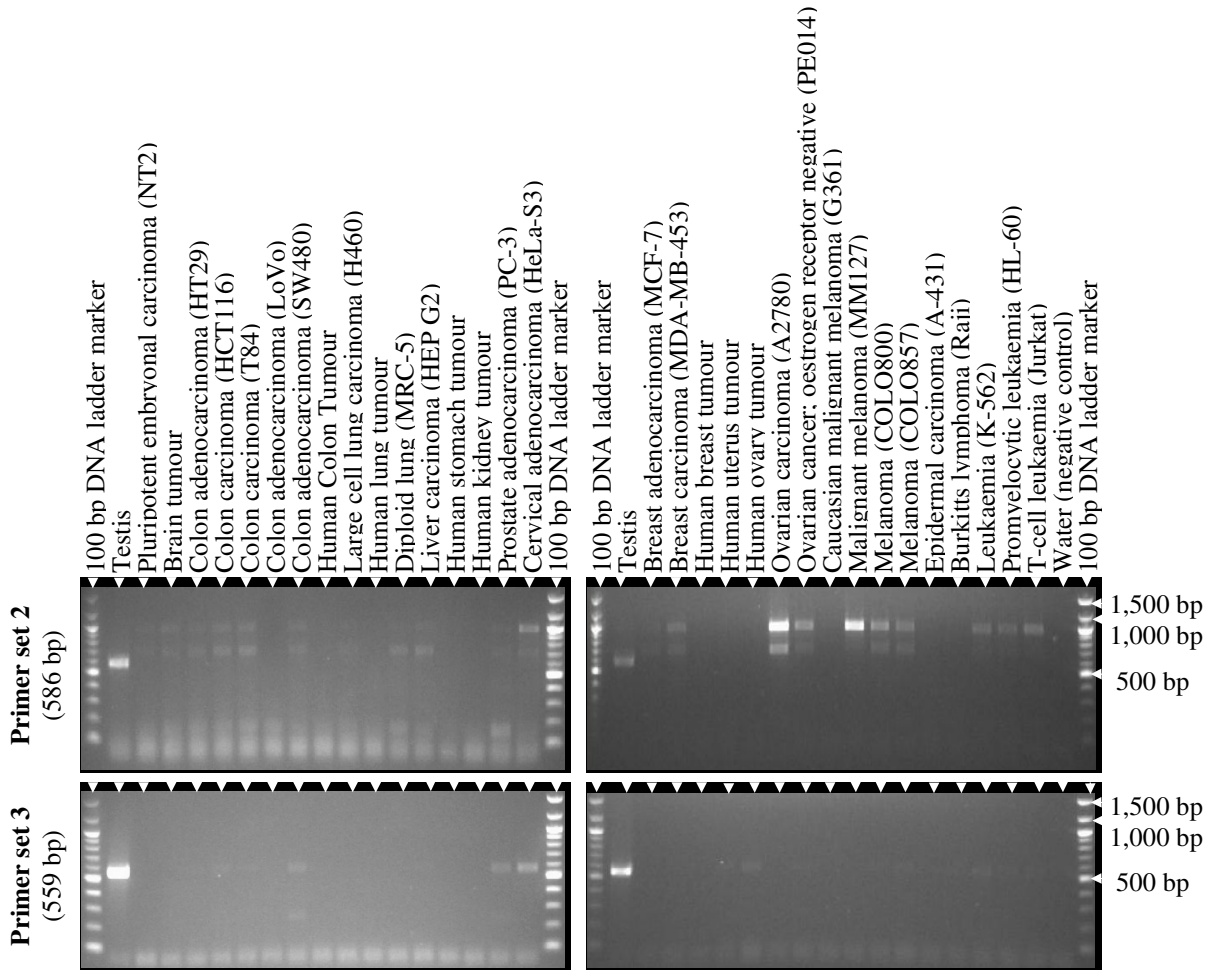

Figure 3.21 RT-PCR analysis of *TDRD6-001* transcript in cancerous cells.
Agarose gels presenting the RT-PCR profiles created from cancerous cells. The PCR products migrated close to the expected sizes (shown in parenthesis on the left).

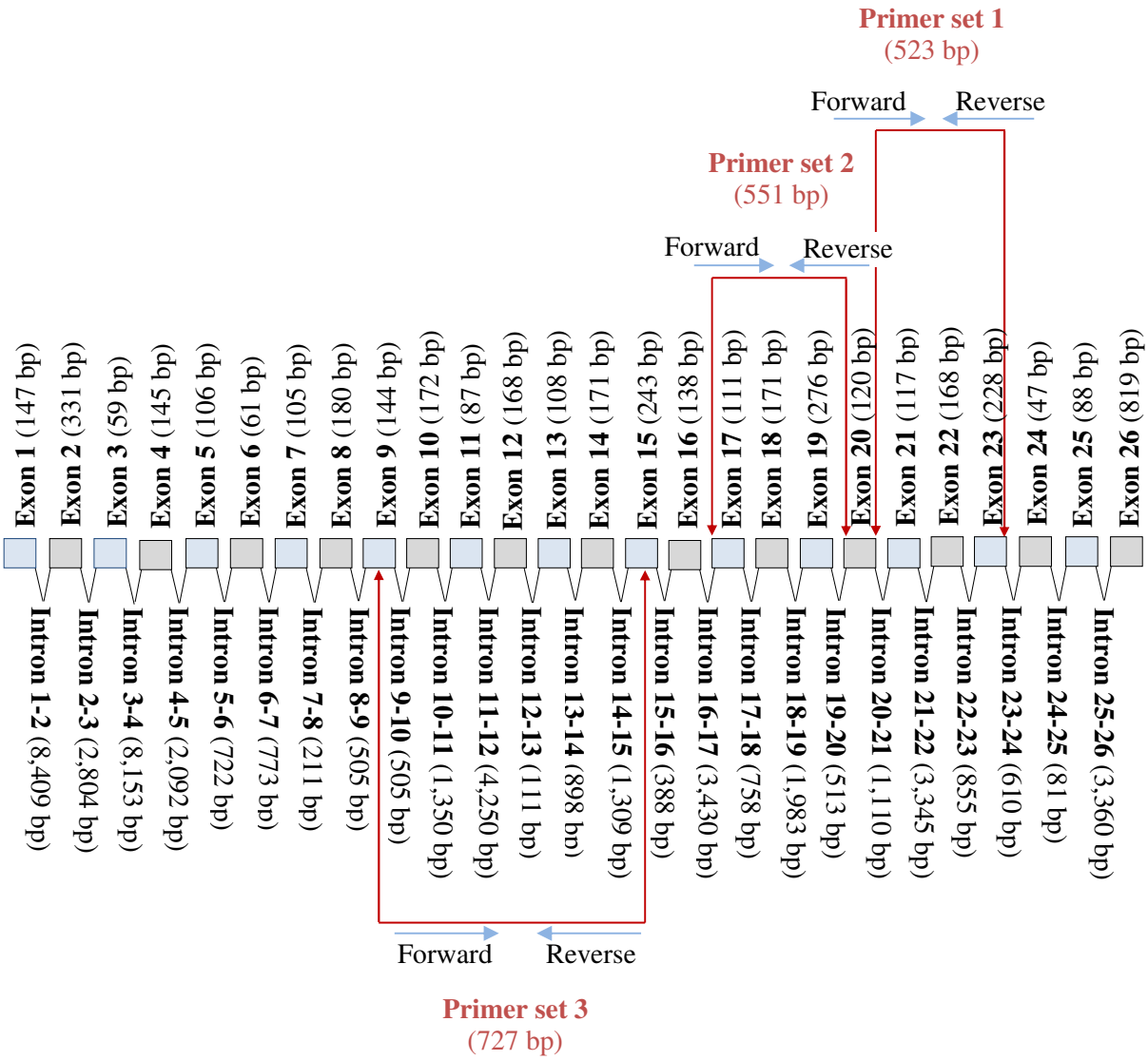

Figure 3.22 Map showing the design of three sets of forward and reverse primer sequences for the analysis of human *TDRD1-201* transcript.
This gene is also known as *CT41.1;* the spliced transcript contains 3570 nucleotides and predicted 26 exons. The primers were used to analyse the expression of the *TDRD1-201* transcript in 21 types of normal human tissues and 33 types of cancerous human cells using RT-PCR. Moreover, the expected size of the PCR products in base pairs (bp) is included in the map. Note: exon and intron sizes are not to scale.

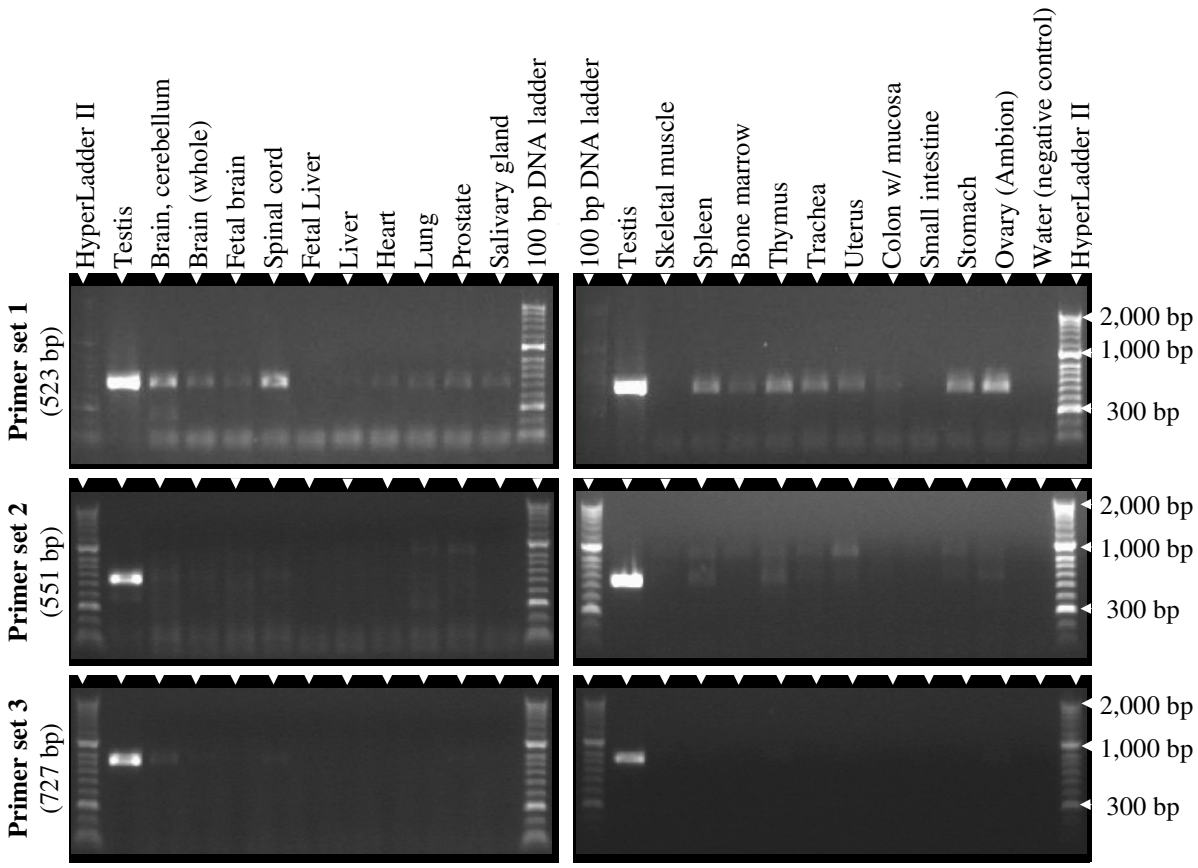

Figure 3.23 RT-PCR analysis of *TDRD1-201* transcript in normal tissues.
Agarose gels presenting the RT-PCR profiles created from normal cells. The PCR products migrated close to the expected sizes (shown in parenthesis on the left).

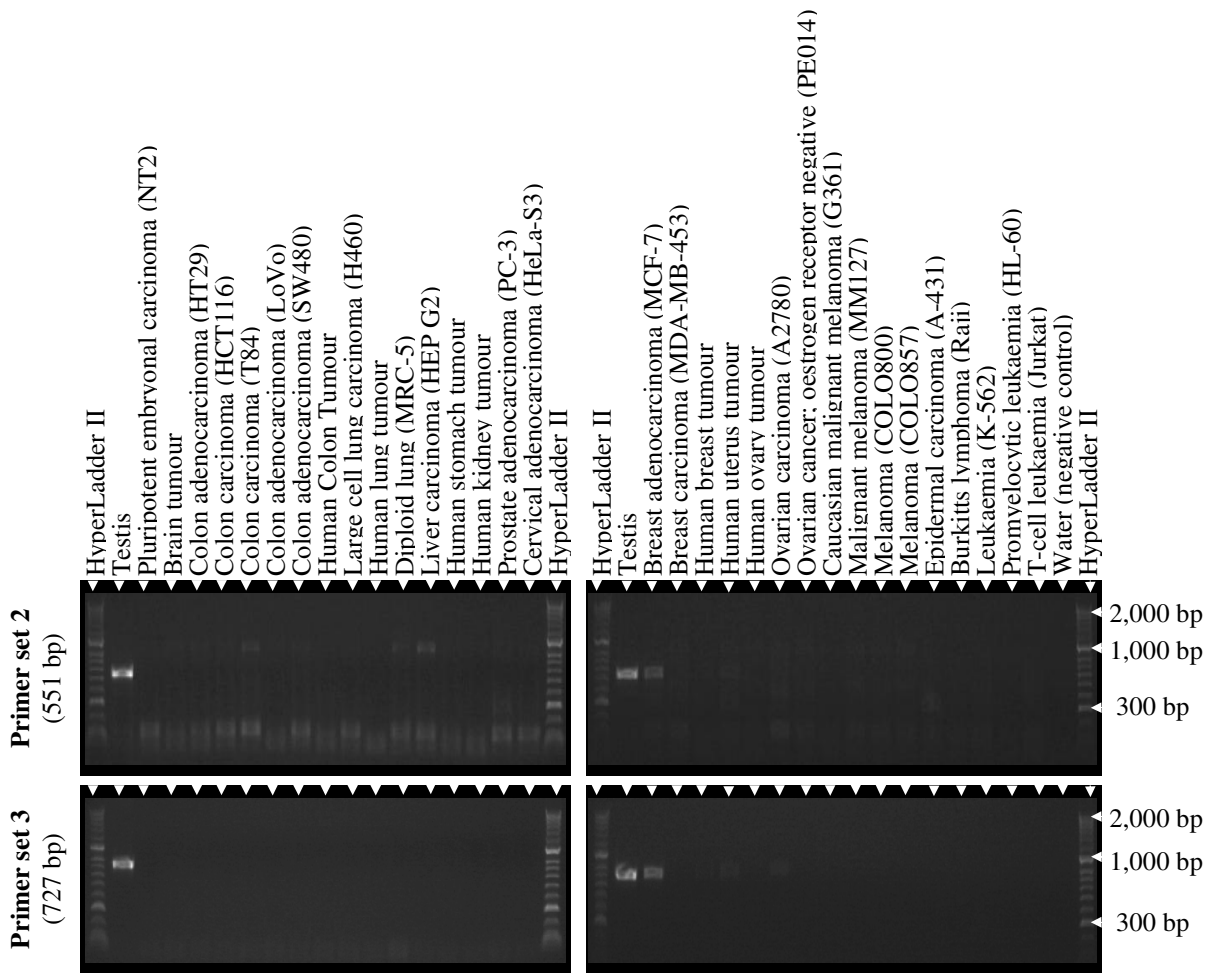

Figure 3.24 RT-PCR analysis of *TDRD1-201* transcript in cancerous cells.
Agarose gels presenting the RT-PCR profiles created from cancerous cells. The PCR products migrated close to the expected sizes (shown in parenthesis on the left).

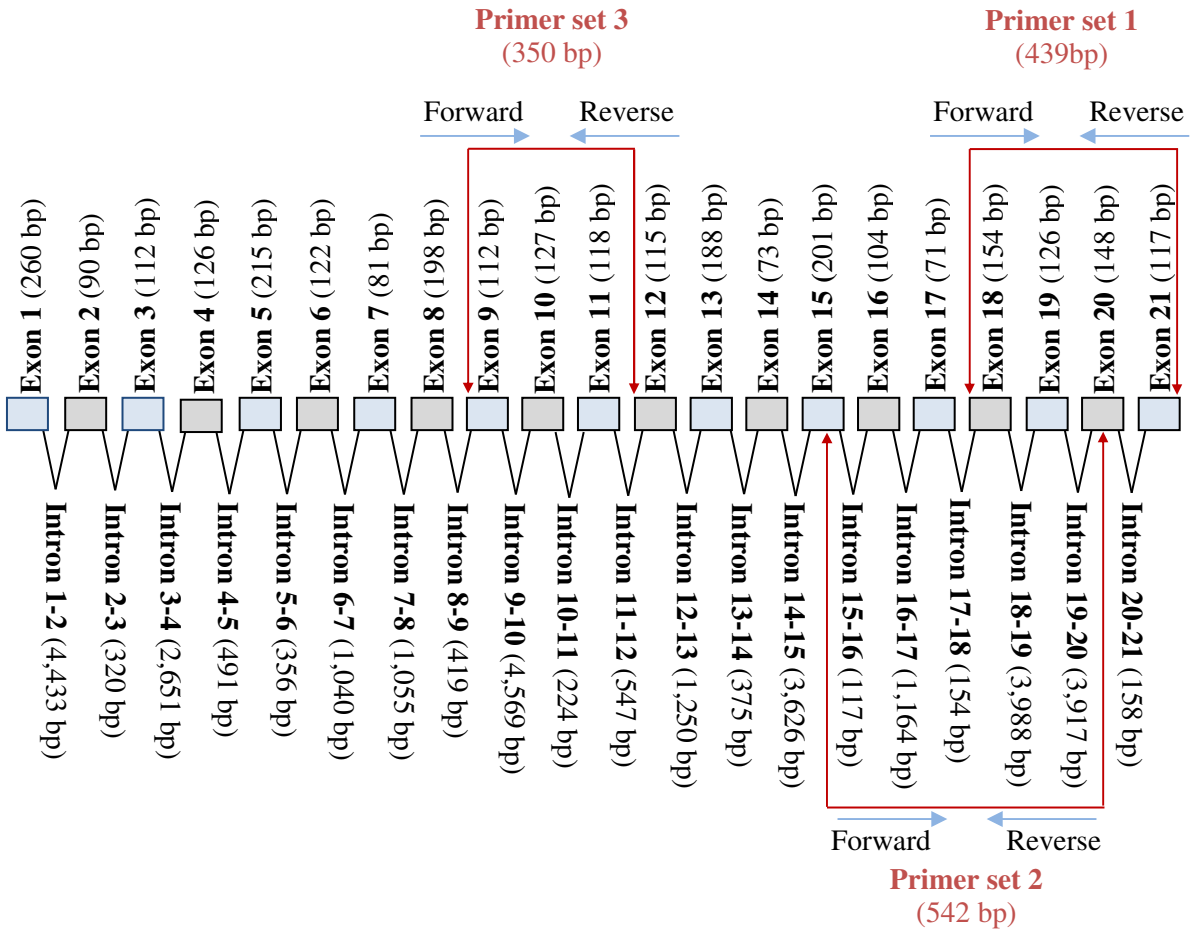

Figure 3.25 Map showing the design of three sets of forward and reverse primer sequences for the analysis of human *PIWIL1-001* transcript.
This gene is also known as *HIWI; MIWI*; the spliced transcript contains 2586 nucleotides and predicted 21 exons. The primers were used to analyse the expression of the *PIWIL1-001* transcript in 21 types of normal human tissues and 33 types of cancerous human cells using RT-PCR. Moreover, the expected size of the PCR products in base pairs (bp) is included in the map. Note: exon and intron sizes are not to scale.

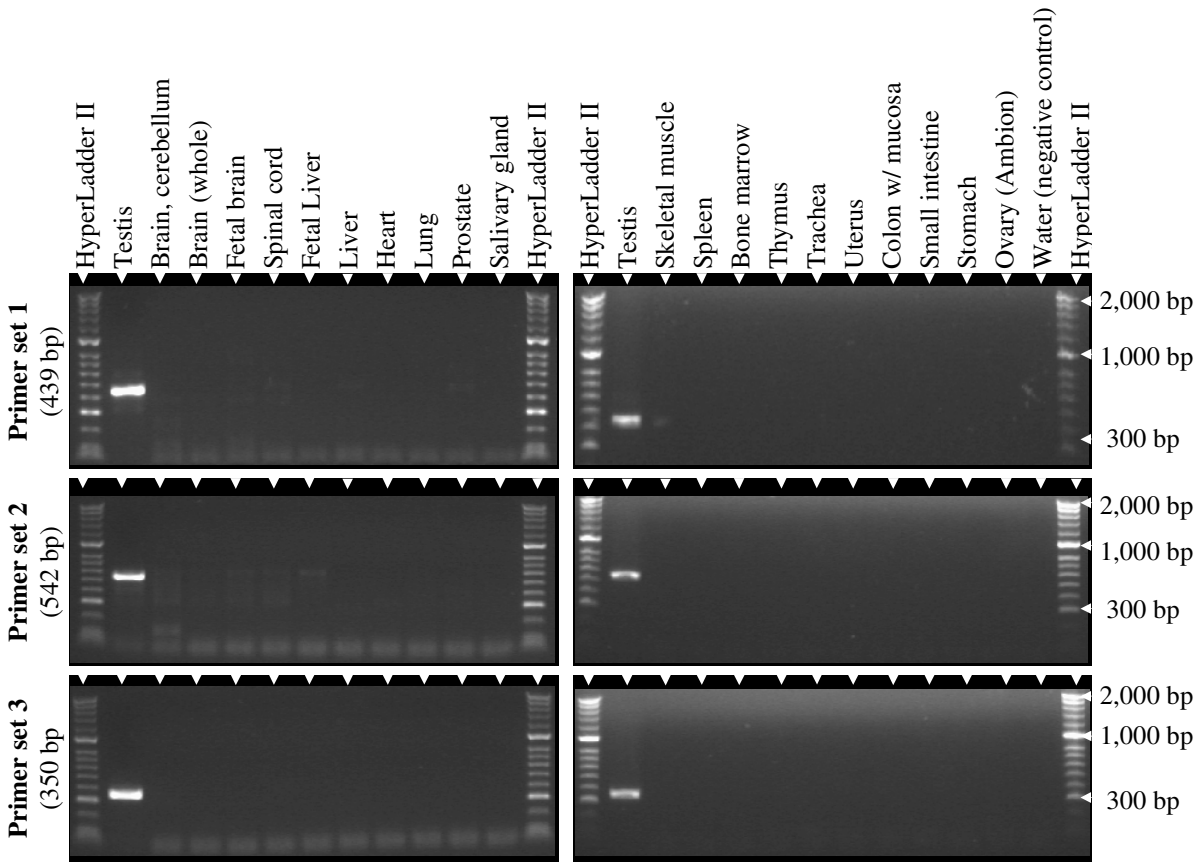

Figure 3.26 RT-PCR analysis of *PIWIL1-001* transcript in normal tissues.
Agarose gels presenting the RT-PCR profiles created from normal cells. The PCR products migrated close to the expected sizes (shown in parenthesis on the left).

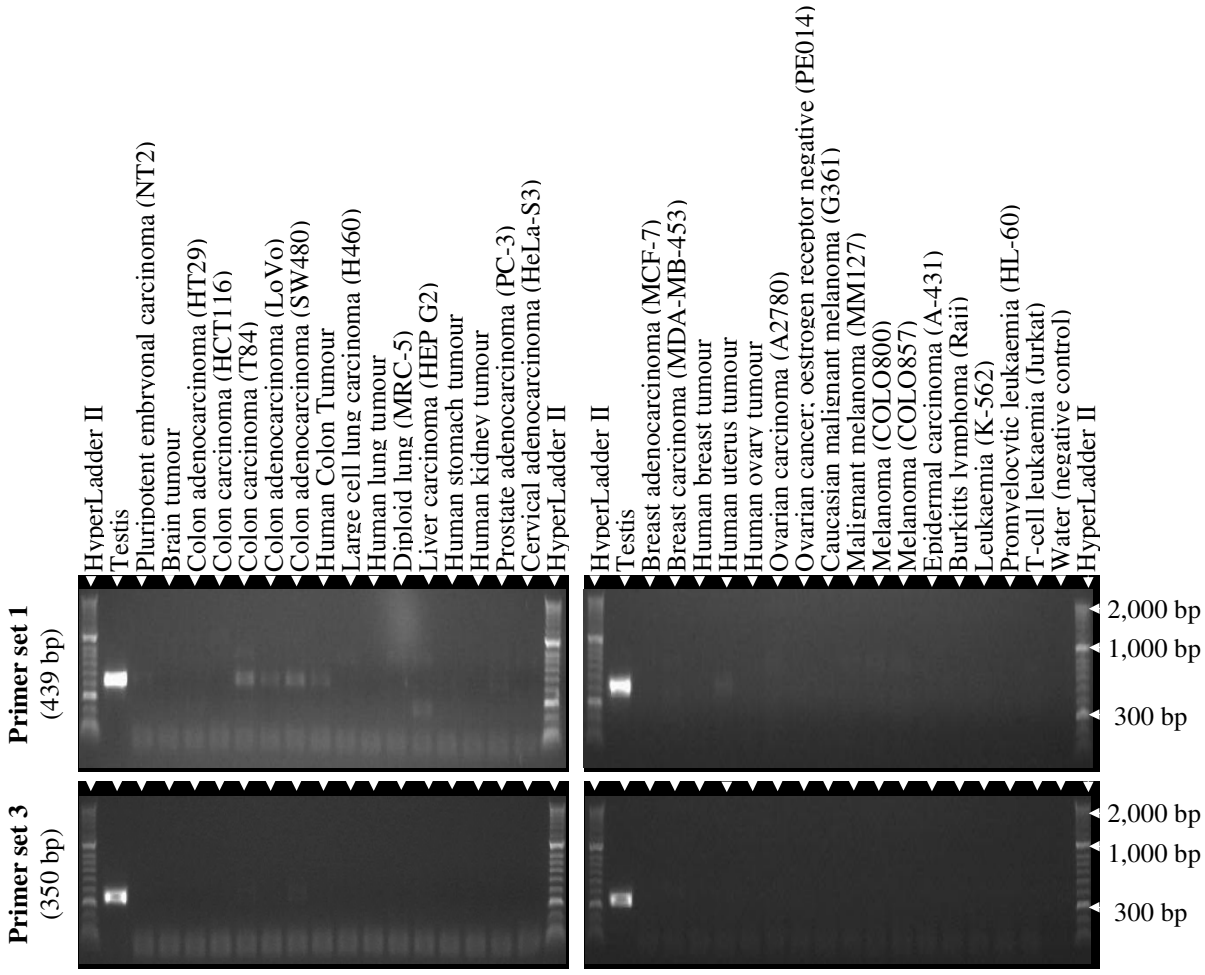

Figure 3.27 RT-PCR analysis of *PIWIL1-001* transcript in cancerous cells.
Agarose gels presenting the RT-PCR profiles created from cancerous cells. The PCR products migrated close to the expected sizes (shown in parenthesis on the left).

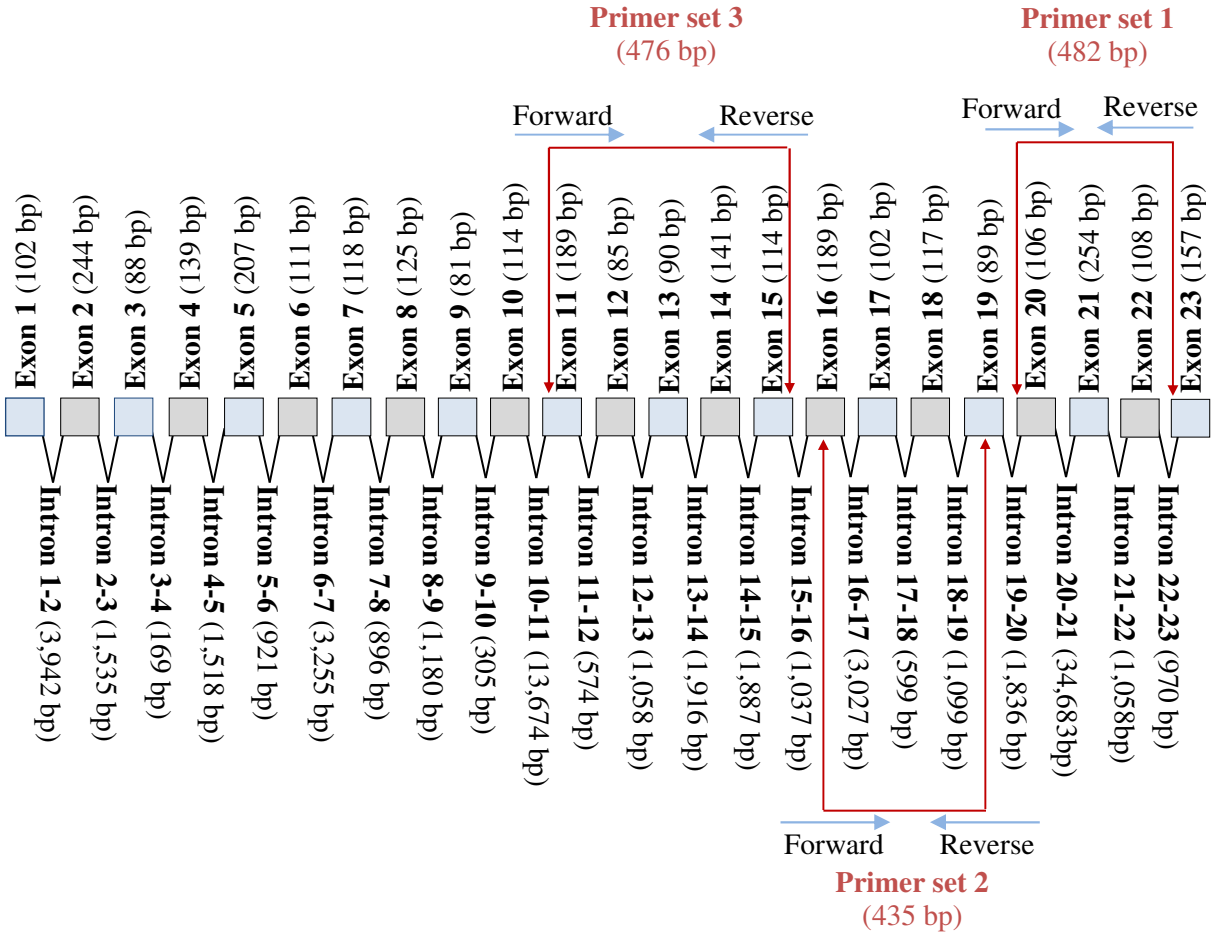

Figure 3.28 Map showing the design of three sets of forward and reverse primer sequences for the analysis of human *PIWIL2-001* transcript.
This gene is also known as *HILI; MILI; PIWIL1L; CT80*; the spliced transcript contains 2922 nucleotides and predicted 23 exons. The primers were used to analyse the expression of the *PIWIL2-001* transcript in 21 types of normal human tissues and 33 types of cancerous human cells using RT-PCR. Moreover, the expected size of the PCR products in base pairs (bp) is included in the map. Note: exon and intron sizes are not to scale.

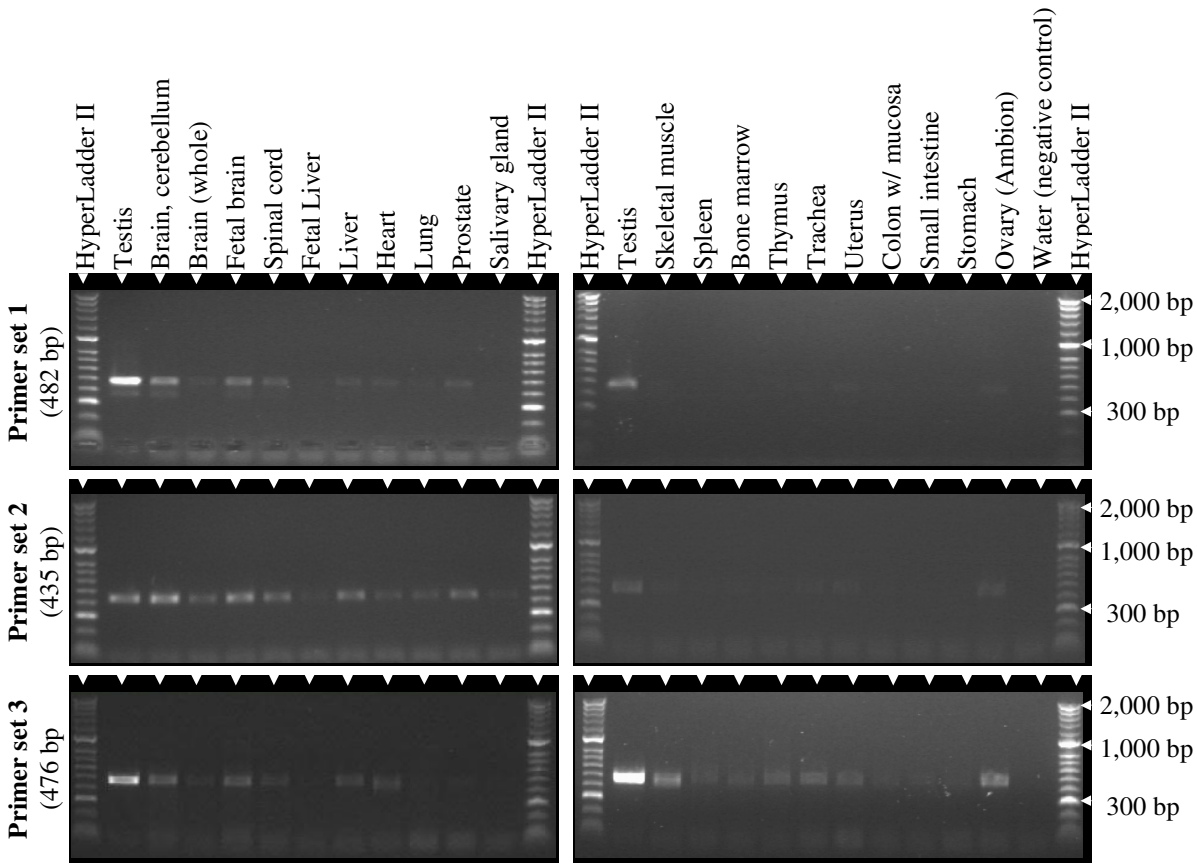

Figure 3.29 RT-PCR analysis of *PIWIL2-001* transcript in normal tissues.
Agarose gels presenting the RT-PCR profiles created from normal cells. The PCR products migrated close to the expected sizes (shown in parenthesis on the left).

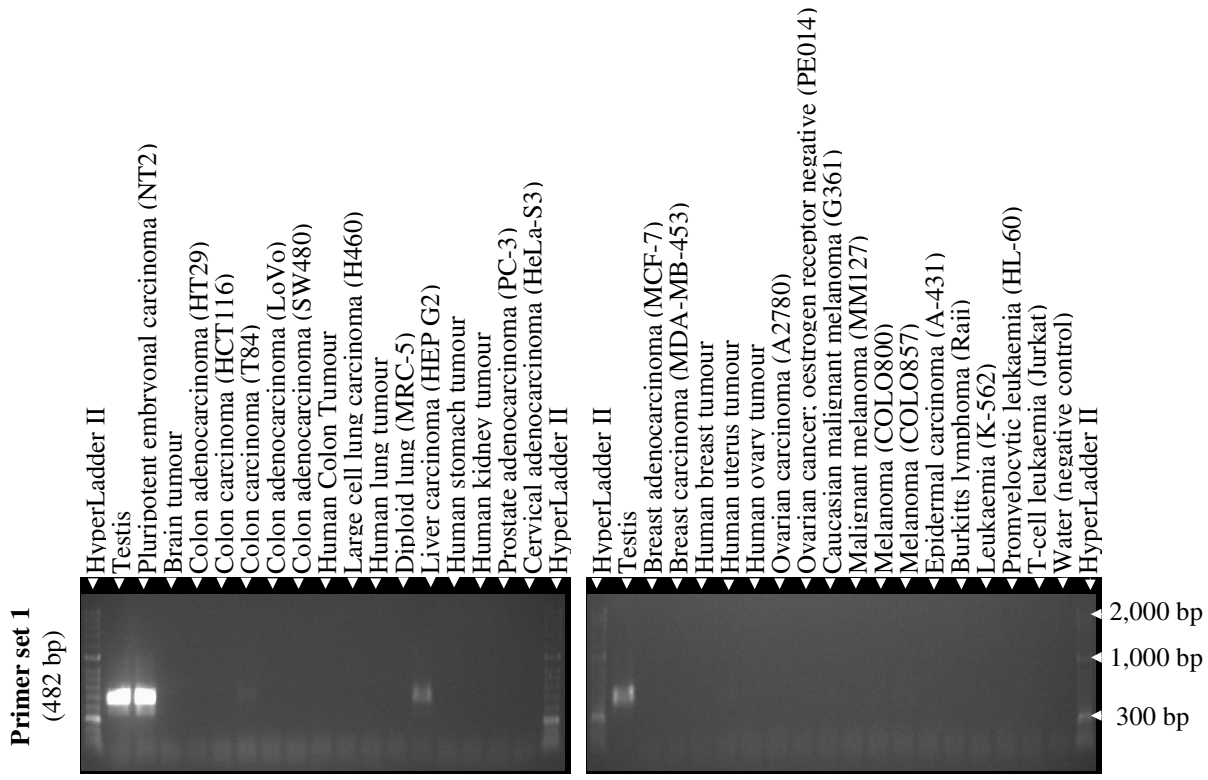

Figure 3.30 RT-PCR analysis of *PIWIL2-001* transcript in cancerous cells.
Agarose gels presenting the RT-PCR profiles created from cancerous cells. The PCR products migrated close to the expected sizes (shown in parenthesis on the left).

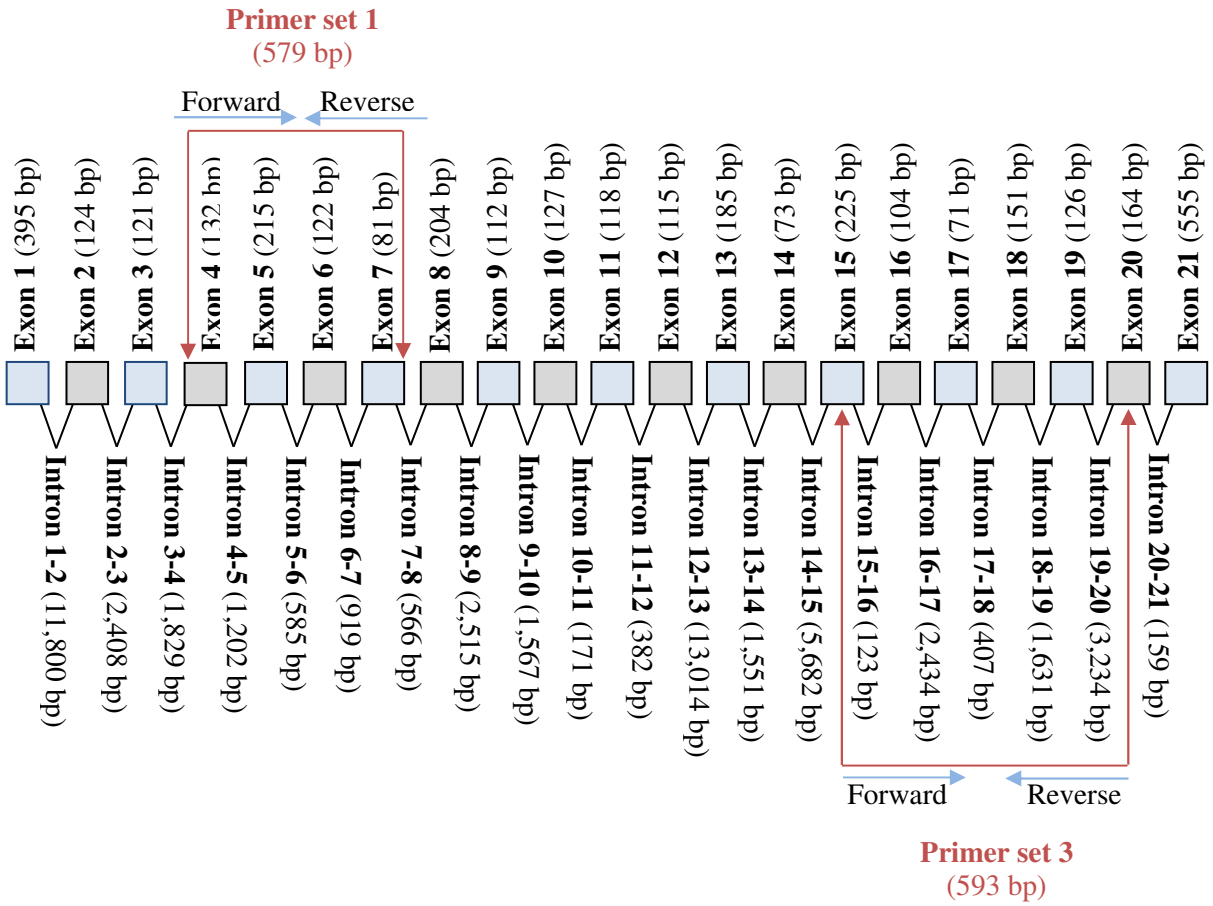

Figure 3.31 Map showing the design of two sets of forward and reverse primer sequences for the analysis of human *PIWIL3-001* transcript.
This gene is also known as *HIWI3*; the spliced transcript contains 2649 nucleotides and predicted 21 exons. The primers were used to analyse the expression of the *PIWIL3-001* transcript in 21 types of normal human tissues and 33 types of cancerous human cells using RT-PCR. Moreover, the expected size of the PCR products in base pairs (bp) is included in the map. Note: exon and intron sizes are not to scale.

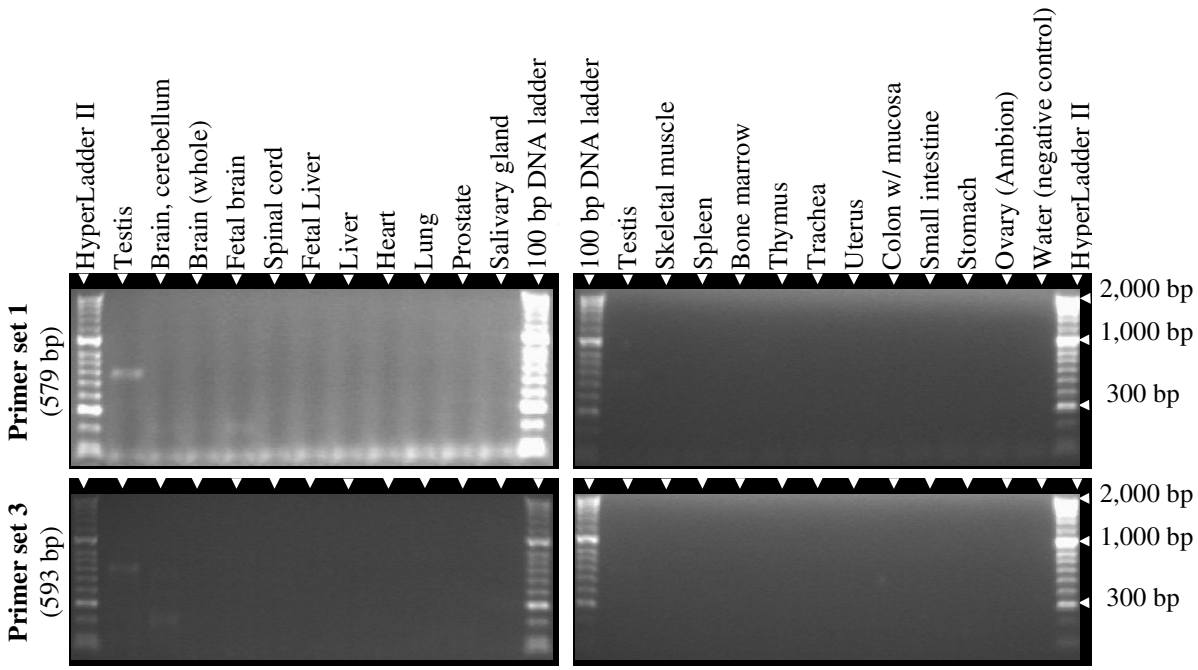

Figure 3.32 RT-PCR analysis of *PIWIL3-001* transcript in normal tissues.
Agarose gels presenting the RT-PCR profiles created from normal cells. The PCR products migrated close to the expected sizes (shown in parenthesis on the left).

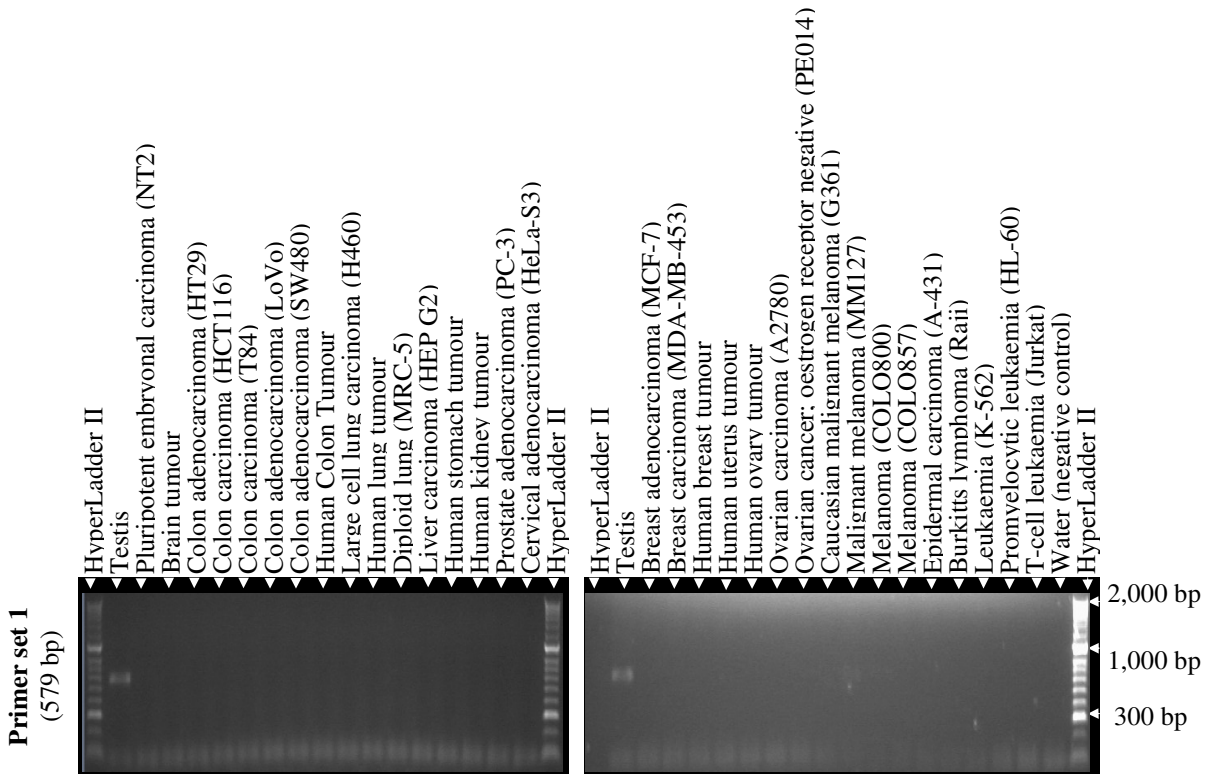

Figure 3.33 RT-PCR analysis of *PIWIL3-001* transcript in cancerous cells.
Agarose gels presenting the RT-PCR profiles created from cancerous cells. The PCR products migrated close to the expected sizes (shown in parenthesis on the left).

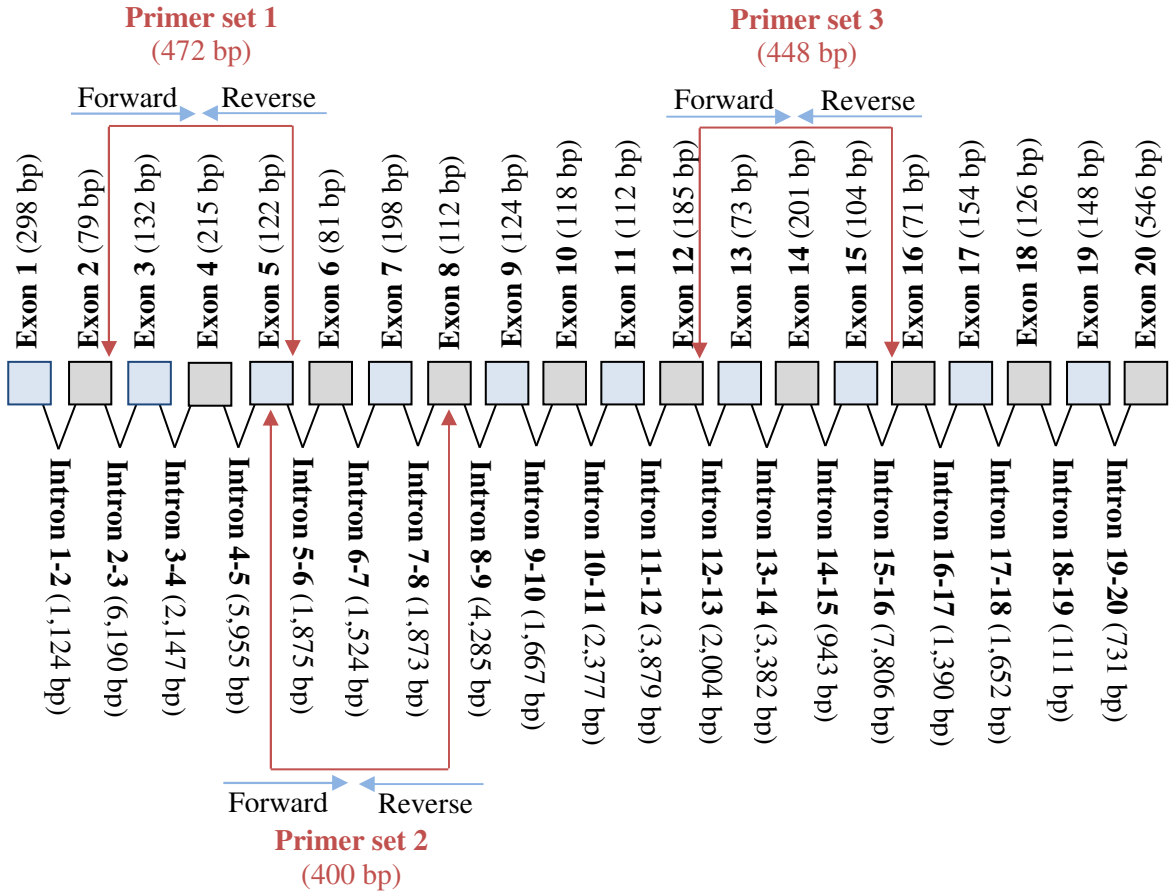

Figure 3.34 Map showing the design of three sets of forward and reverse primer sequences for the analysis of human *PIWIL4-001* transcript.
This gene is also known as *HIWI2; MIWI2*; the spliced transcript contains 2559 nucleotides and predicted 20 exons. The primers were used to analyse the expression of the *PIWIL4-001* transcript in 21 types of normal human tissues and 33 types of cancerous human cells using RT-PCR. Moreover, the expected size of the PCR products in base pairs (bp) is included in the map. Note: exon and intron sizes are not to scale.

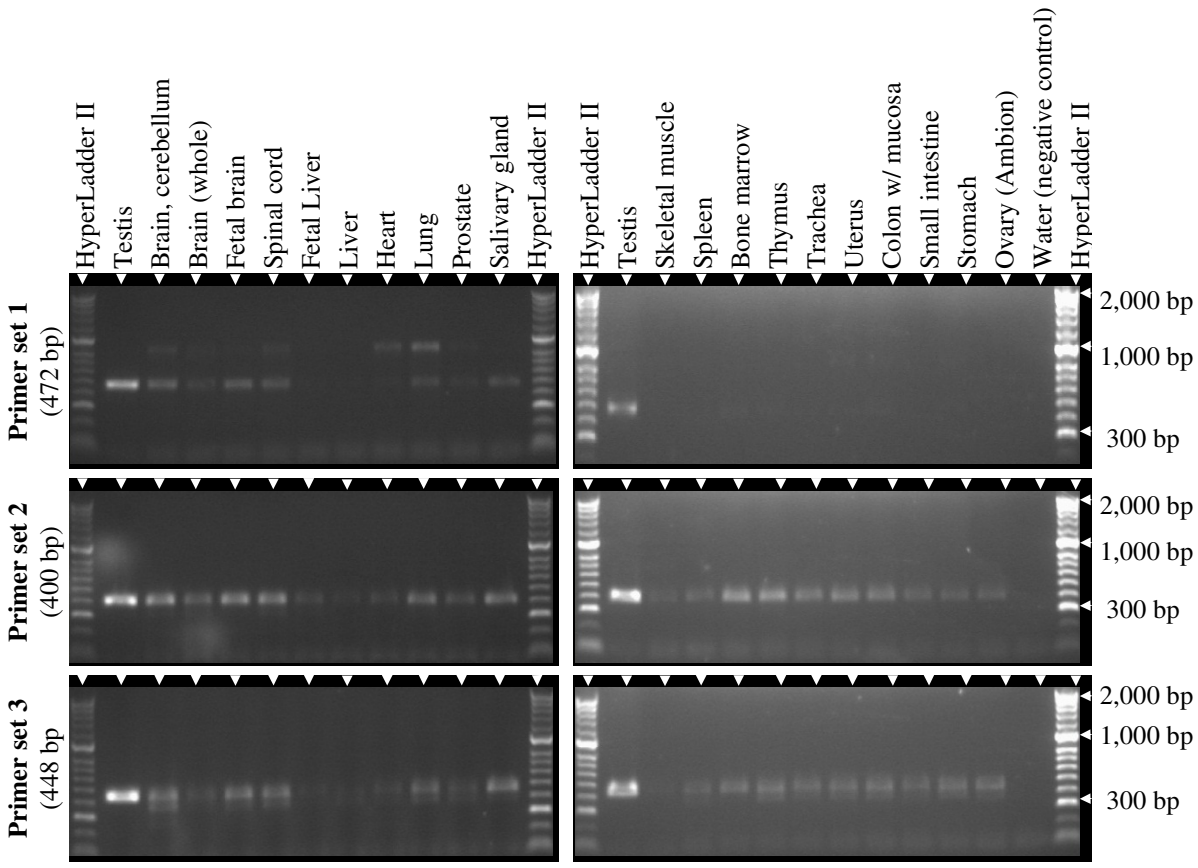

Figure 3.35 RT-PCR analysis of *PIWIL4-001* transcript in normal tissues.
Agarose gels presenting the RT-PCR profiles created from normal cells. The PCR products migrated close to the expected sizes (shown in parenthesis on the left).

Table 3.1 Sequencing results of RT-PCR screening for selected *TDRD* and *PIWIL* gene transcripts in normal tissues and cancerous cells.
This table provides a summary of the PCR products sequencing results; these products were first purified and then sent to Eurofins MWG Operon Company for sequencing to confirm that the right sequences were being amplified.

Gene	Primer	Sequence identity (%) in normal tissue	Sequence identity (%) in cancerous cells
TDRD12-001	Primer set 1 (forward)	Testis (100 %) Uterus (0 %)	-
TDRD12-003	Primer set 2 (forward)	Testis (100 %) Uterus (0 %)	-
TDRD12-001	Primer set 3 (forward)	Testis (100 %)	NT2 (100 %) HCT116 (95 %) T84 (100 %)
RNF17-003 (TDRD4)	Primer set 2 (forward)	Prostate (0 %)	-
RNF17-003 (TDRD4)	Primer set 3 (forward)	Testis (100 %)	-
RNF17-003 (TDRD4)	Primer set 1 (forward)	-	Brain tumour (100 %) Leukaemia (k-562) (100 %)
TDRD5-201	Primer set 2 (forward)	Brain, cerebellum (bottom band) (0 %) Testis (top band) (97 %) Spleen (0 %)	-
TDRD1-201	Primer set 3 (forward)	Brain, cerebellum (97 %)	-
TDRD1-201	Primer set 3 (forward)	-	Breast adenocarcinoma (MCF-7) (100 %)
TDRD1-201	Primer set 3 (forward)	Testis (100 %)	-
PIWIL1-001	Primer set 3 (forward)	Testis (100 %)	-
PIWIL1-001	Primer set 1 (forward)	-	Colon carcinoma (T84) (100 %)
PIWIL2-001	Primer set 2 (forward)	Testis (100 %)	-
PIWIL2-001	Primer set 1 (forward)	-	-
PIWIL2-001	Primer set 1 (forward)	-	NT2 (100 %)
TDRD12-002	Primer set 1 (Forward)	Testis (100 %)	-
TDRD12-002	Primer set 2 (Forward)	Testis (100 %)	-

3.4. Discussion

Human cancers are complex genetic diseases, which result in uncontrolled cell division, invasion, reduction of cell death, destruction of nearby tissues and migration to other organs in the human body (Michor *et al.,* 2005; Stratton *et al.,* 2009; Tomasetti *et al.,* 2013; Wodarz and Zauber, 2015). Cancers are frequently diagnosed and treated during the late phases, when cancers have migrated (Aly, 2012; Suri, 2006). Changes in gene expression profiles and mutations can often lead to the production of abnormal proteins known as TRAs (refer to Section 1.9). The recognition, characterisation and identification of novel TRAs as potential cancer biomarkers and/or targets is major challenge in developing strategies that target human tumours, such as immuno-therapeutics (Butterfield, 2015; Krishnadas *et al.,* 2013; Zavala and Kalergis, 2015). CTA genes are attractive targets for human cancer therapies because of their restricted expression patterns in testis tissue and cancerous cells. (Gjerstorff *et al.,* 2015; Krishnadas *et al.,* 2013; Whitehurst, 2014).

Figure 3.36, Figure 3.37 and Table 3.2 (below) provide an overview of the expression profiles of the genes analysed in this study. As can be seen, the expression profiles of the *TDRD* and *PIWIL* genes were analysed in about 21 types of normal human tissues and 33 types of cancerous human cells. The analysis outcomes of the RT-PCR expression profiles show that eight out of 16 *TDRD* and *PIWIL* genes in total (*TDRD2*, *TDRD3*, *TDRD7*, *TDRD8*, *TDRD9*, *TDRD10, TDRD11* and *PIWIL4*) might not be good candidates for CTA genes. One out of 16 *TDRD* and *PIWIL* genes (*PIWIL3*) might not be a good candidate for CTA genes but appears to be testis-specific. Five out of 16 *TDRD* and *PIWIL* genes (*TDRD4*, *TDRD5*, *TDRD12*, *PIWIL1* and *PIWIL2*) might be good candidates for CTA genes and might classify as cancer testis-restricted. Two out of 16 *TDRD* and *PIWIL* genes (*TDRD1* and *TDRD6*) might be good candidates for CTA genes and might classify as cancer testis-selective.

Figure 3.38 and Figure 3.39 (below) show Circos plots of meta upregulated genes (*PIWIL1*, *PIWIL2*, *TDRD1* and *TDRD5*). Figure 3.38 Circos plots show the meta-change in gene expression in relation to corresponding cancer types. Figure 3.39 Circos plots show the proportion of genes expressed in the various cancer types for upregulated genes. Figure 3.40 shows Single-Circos plots of upregulated genes (*PIWIL1*, *PIWIL2*, *TDRD1*, *TDRD5*, *TDRD6* and *TDRD12*). The Circos plots show single array data set gene expression analysis in relation to corresponding cancer types.

In 2003, the findings of Loriot *et al.,* indicated that the *TDRD1* gene is activated in malignant tumours of several histological kinds. In 2011, Yoon *et al.,* however, stated that the *TDRD1* and *TDRD5* genes are not good candidates for CTA genes, based on expression profiling in liver cancers. Moreover, they reported that the *TDRD4* gene is a good candidate CTA gene for liver malignant tumours (Loriot *et al.,* 2003; Yoon *et al.,* 2011). In 2014, Akiyama *et al.,* developed novel therapeutic approaches, including immunotherapy, against glioblastoma multiforme (GBM) that is one of the most aggressive malignant cancers; these tumours express about 54 CTA genes, including *TDRD1*. (Akiyama *et al.,* 2014).

In 2002, Scanlan *et al.,* found that the *TDRD6* gene is over-expressed in colon malignant tumour cells, while in 2008 Goulet *et al.,* suggested that the *TDRD3* gene might contribute to breast malignant tumour progression. In 2009, Kuruma *et al.,* confirmed that the *TDRD11* gene is highly expressed in prostate cancer tissue and it is expressed negatively or weakly in normal epithelium. In addition, this gene was reported in 2007 by Tsuchiya *et al.,* to be one of the more highly expressed genes in colon cancer (Goulet *et al.,* 2008; Kuruma *et al.,* 2009; Scanlan *et al.,* 2002; Tsuchiya *et al.,* 2007). In 2014, Zhou *et al.,* indicated that the *TDRD8* gene is a germ cell-specific factor and stated that the *TDRD1*, *TDRD2*, *TDRD9* and *TDRD12* genes play important roles in piRNA biogenesis and silencing of retrotransposons. While, the *TDRD4*, *TDRD5*, *TDRD6* and *TDRD7* genes play significant roles in spermatogenesis (Zhou *et al.,* 2014). In 2015, Panjarian *et al.,* found that the *TDRD10* gene has the ability to increase DNA methylation in breast cancers (Panjarian *et al.,* 2015).

In 2015, Chen *et al.,* reported that the *PIWIL1* gene is found to be over-expressed in the majority and most kinds of solid tumours and cancerous cells (e.g., endometrial cancer). In addition, the abnormal expression of *PIWIL1* and *PIWIL2* genes may have significant functions in the development process of colon cancerous cell growth (Chen *et al.,* 2015; Wang and Mu, 2015). In 2014, Lim *et al.,* specified that piRNA pathway-related genes and the *PIWIL1*, *PIWIL2*, *PIWIL3* and *PIWIL4* genes were established previously at numerous phases of germ cell development (particularly in testis tissues) (Lim *et al.,* 2014).

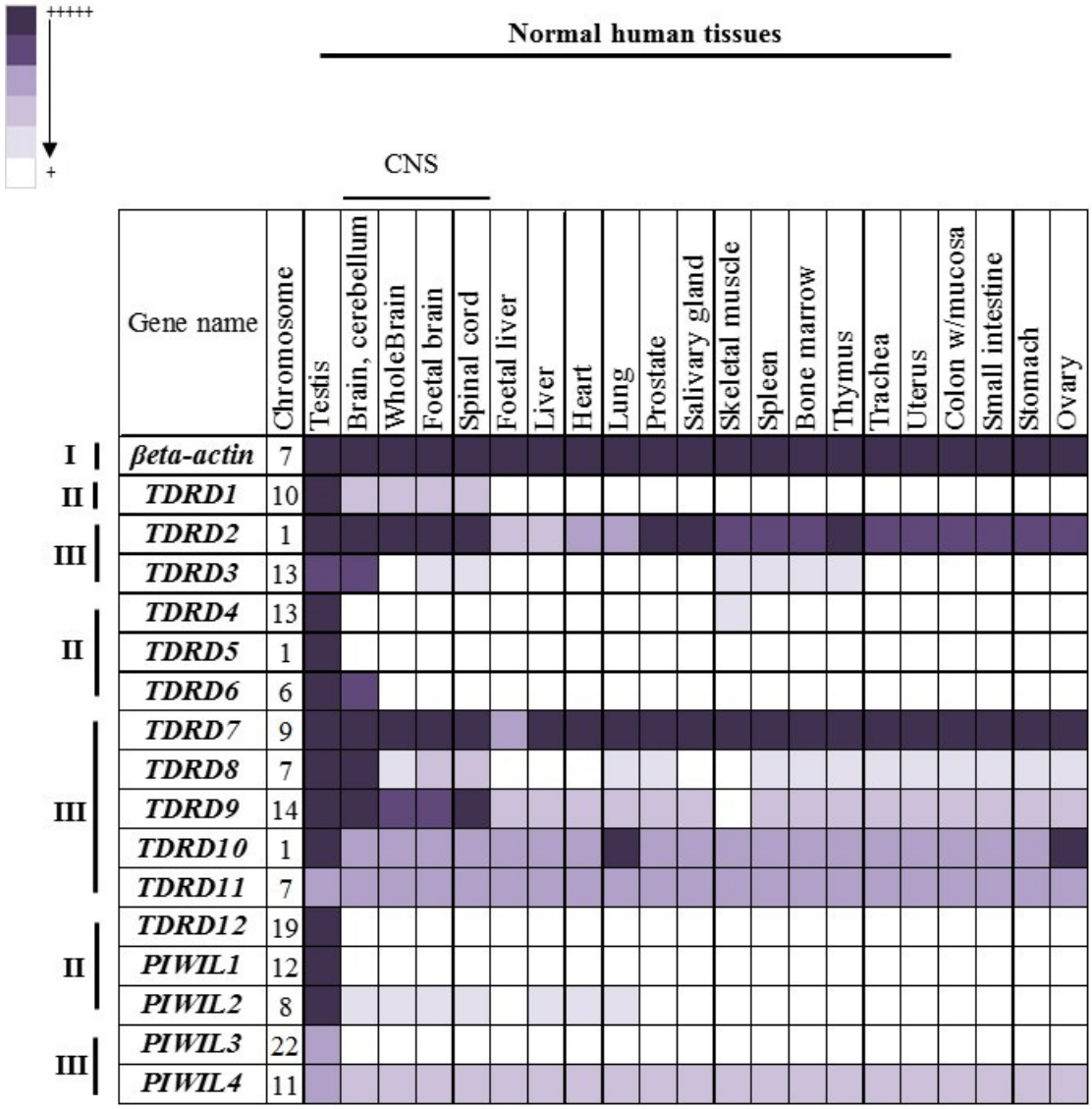

Figure 3.36 Summary of RT-PCR analysis of expression profiles for several *TDRD* and *PIWIL* genes in normal human tissues.

The expression profile of genes is shown in the form of one row of the grid, while each column shows the relevant normal tissue. The degree of intensity exhibited by every PCR product, as seen by using ethidium bromide stained agarose gel, has been given a qualitative rank using different shades of the colour purple relative to the degree of intensity of each PCR product from the testis. The chromosomal location of the genes is specified next to the name of each gene.

(I); The expression of *β-actin* gene as a positive control for analysing the quality of the normal tissue cDNAs. **(II);** The expression of *TDRD1*, *TDRD4*, *TDRD5*, *TDRD6*, *TDRD12*, *PIWIL1* and *PIWIL2* genes in normal tissues. The analysis of this genes group indicated that they might be good candidates for CTA genes. **(III);** The expression of *TDRD2*, *TDRD3*, *TDRD7*, *TDRD8*, *TDRD9*, *TDRD10*, *TDRD11*, *PIWIL3* and *PIWIL4* genes in normal tissues. The analysis of this group of genes indicated that they might not be good candidates for CTA genes because all of these genes were found to be expressed in multiple normal tissues.

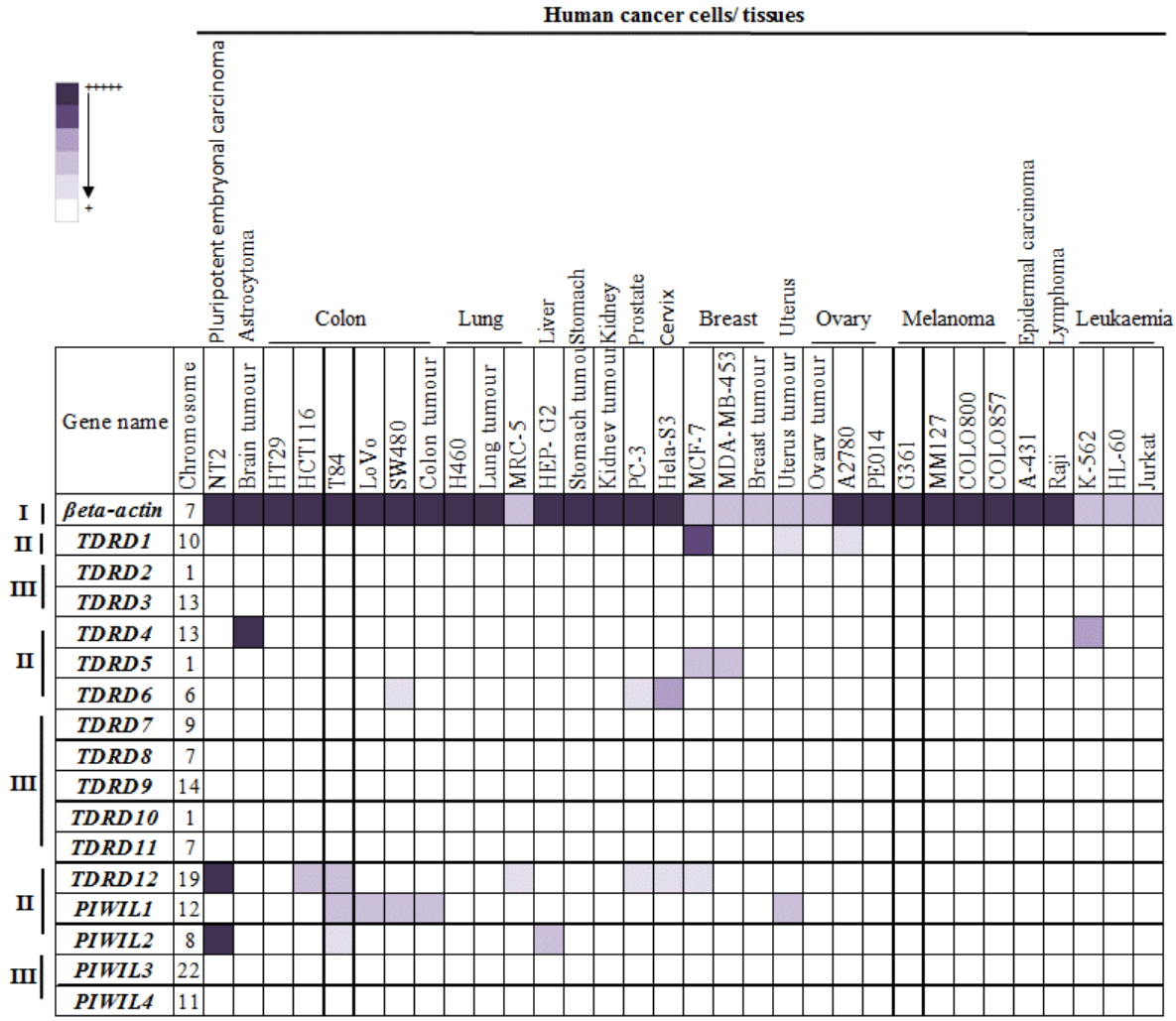

Figure 3.37 Summary of RT-PCR analysis of expression profiles for several *TDRD* and *PIWIL* genes in cancerous human cells.

The expression profile of genes is shown in the form of one row of the grid, while each column shows the relevant cancerous cells. The degree of intensity exhibited by every PCR product, as seen by using ethidium bromide stained agarose gel, has been given a qualitative rank using different shades of the colour purple (see the key at the top left). The chromosomal location of the genes is specified next to the name of each gene.

(I); The expression of *β-actin* gene as a positive control for analysing the quality of the cancerous cell cDNAs. **(II);** The expression of *TDRD1*, *TDRD4*, *TDRD5*, *TDRD6*, *TDRD12*, *PIWIL1* and *PIWIL2* genes in cancerous cells. It can be clearly seen from the chart that the analysis of this genes group indicated that they might be good candidates for CTA genes. **(III);** The expression of *TDRD2*, *TDRD3*, *TDRD7*, *TDRD8*, *TDRD9*, *TDRD10*, *TDRD11*, *PIWIL3* and *PIWIL4* genes in cancerous cells. The analysis of this genes group indicated that they might not be good candidates for CTA genes; these genes are testis-restricted genes. Moreover, it was previously found that all of these genes were expressed in multiple normal tissues.

Table 3.2 Synonym names and symbols of TDRD and PIWIL proteins and their potentials as CT antigens.

Symbols	Full Names	References	Are they potential CT genes? (Yes or No)
- TDRD1 - CT41.1	- Tudor domain containing protein 1 - Cancer/testis antigen 41.1 - Tudor domain-containing protein 1	National Centre for Biotechnology Information. (2015). TDRD1 tudor domain containing 1 [*Homo sapiens*]. http://www.ncbi.nlm.nih.gov/gene/56165. Accessed 4/4/15.	Yes
- TDRD2 - TDRKH	- Tudor domain containing 2 - Tudor and KH domain containing protein - Tudor and KH domain-containing protein - Putative RNA binding protein - Tudor domain-containing protein 2	National Centre for Biotechnology Information. (2015). TDRKH tudor and KH domain containing [*Homo sapiens*]. http://www.ncbi.nlm.nih.gov/gene/11022. Accessed 4/4/15.	No
- TDRD3 - RP11-459E2.1	- Tudor domain containing 3	National Centre for Biotechnology Information. (2015). TDRD3 tudor domain containing 3 [*Homo sapiens*]. http://www.ncbi.nlm.nih.gov/gene/81550. Accessed 4/4/15.	No
- TDRD4 - RNF17 - SPATA23 - Mmip-2	- Tudor domain containing 4 - RING finger protein 17 - Spermatogenesis associated 23 - Tudor domain-containing protein 4	National Centre for Biotechnology Information. (2015). RNF17 ring finger protein 17 [*Homo sapiens*]. http://www.ncbi.nlm.nih.gov/gene/56163. Accessed 4/4/15.	Yes
- TDRD5 - TUDOR3 - RP11-427G13.1	- Tudor domain containing 5 - Tudor domain-containing protein 5	National Centre for Biotechnology Information. (2015). TDRD5 tudor domain containing 5 [*Homo sapiens*]. http://www.ncbi.nlm.nih.gov/gene/163589. Accessed 4/4/15.	Yes
- TDRD6 - BA446F17.4 - TDR2 - NY-CO-45 - CT41.2	- Tudor domain containing 6 - Tudor domain-containing protein 6 - Tudor repeat 2 - Antigen NY-CO-45 - Cancer/testis antigen 41.2	National Centre for Biotechnology Information. (2015). TDRD6 tudor domain containing 6 [*Homo sapiens*]. http://www.ncbi.nlm.nih.gov/gene/221400. Accessed 4/4/15.	Yes
- TDRD7 -PCTAIRE2BP - TRAP - RP11-508D10.1 - CATC4	- Tudor domain containing 7 - PCTAIRE2-binding protein - Tudor repeat associator with PCTAIRE 2 - Tudor domain-containing protein 7	National Centre for Biotechnology Information. (2015). TDRD7 tudor domain containing 7 [*Homo sapiens*]. http://www.ncbi.nlm.nih.gov/gene/23424. Accessed 4/4/15.	No
- TDRD8 - STK31 - SGK396	- Tudor domain containing 8 - Serine/threonine kinase 31 - Sugen kinase 396 - Serine/threonine-protein kinase 31 - Serine/threonine-protein kinase NYD-SPK	National Centre for Biotechnology Information. (2015). STK31 serine/threonine kinase 31 [*Homo sapiens*]. http://www.ncbi.nlm.nih.gov/gene?term=TDRD8. Accessed 4/4/15.	No
- TDRD9 - HIG-1 - C14orf75 - NET54	- Tudor domain containing 9 - Hypoxia-inducible HIG-1 - Tudor domain-containing protein 9 - Putative ATP-dependent RNA helicase TDRD9	National Centre for Biotechnology Information. (2015). TDRD9 tudor domain containing 9 [*Homo sapiens*]. http://www.ncbi.nlm.nih.gov/gene/122402. Accessed 4/4/15.	No
- TDRD10 - RP11-61L14.3	- Tudor domain containing 10 - Tudor domain-containing protein 10	National Centre for Biotechnology Information. (2015). TDRD10 tudor domain containing 10 [*Homo sapiens*]. http://www.ncbi.nlm.nih.gov/gene/126668. Accessed 4/4/15.	No
- TDRD11 - SND1 - P100	- Tudor domain-containing protein 11 - Staphylococcal nuclease and tudor domain containing 1 - P100 co-activator - 100 kDa coactivator - EBNA2 coactivator p100 - P100 EBNA2 co-activator - EBNA-2 co-activator (100kD) - Staphylococcal nuclease domain containing 1	National Centre for Biotechnology Information. (2015). SND1 staphylococcal nuclease and tudor domain containing 1 [*Homo sapiens*]. http://www.ncbi.nlm.nih.gov/gene/27044. Accessed 4/4/15.	No
- TDRD12 - ECAT8	- Tudor domain containing 12 - ES cell associated transcript 8 - ES cell-associated transcript 8 protein - Tudor domain-containing protein 12	National Centre for Biotechnology Information. (2015). TDRD12 tudor domain containing 12 [*Homo sapiens*]. http://www.ncbi.nlm.nih.gov/gene/91646. Accessed 4/4/15.	Yes

- PIWIL1 - HIWI - MIWI - PIWI - CT80.1	- Piwi-like RNA-mediated gene silencing 1 - Piwi-like protein 1 - Piwi	National Centre for Biotechnology Information. (2015). Piwi-like RNA-mediated gene silencing 1 [*Homo sapiens*]. http://www.ncbi.nlm.nih.gov/gene/9271. Accessed 4/4/15.	Yes
- PIWIL2 - CT80 - HILI - MILI - PIWIL1L	- Piwi-like RNA-mediated gene silencing 2 - Piwi-like protein 2 - Miwi like - cancer/testis antigen 80 - piwi-like 2 - piwil2-like protein	National Centre for Biotechnology Information. (2015). Piwi-like RNA-mediated gene silencing 2 [*Homo sapiens*]. http://www.ncbi.nlm.nih.gov/gene/55124. Accessed 4/4/15.	Yes
- PIWIL3 - HIWI3	- Piwi-like RNA-mediated gene silencing 3 - Piwi-like protein 3 - Piwi-like 3	National Centre for Biotechnology Information. (2015). Piwi-like RNA-mediated gene silencing 3 [*Homo sapiens*]. http://www.ncbi.nlm.nih.gov/gene/440822. Accessed 4/4/15.	No
- PIWIL4 - HIWI2 - MIWI2	- Piwi-like RNA-mediated gene silencing 4 - Piwi-like protein 4 - Piwi-like 4	National Centre for Biotechnology Information. (2015). Piwi-like RNA-mediated gene silencing 4 [*Homo sapiens*]. http://www.ncbi.nlm.nih.gov/gene/143689. Accessed 4/4/15.	No

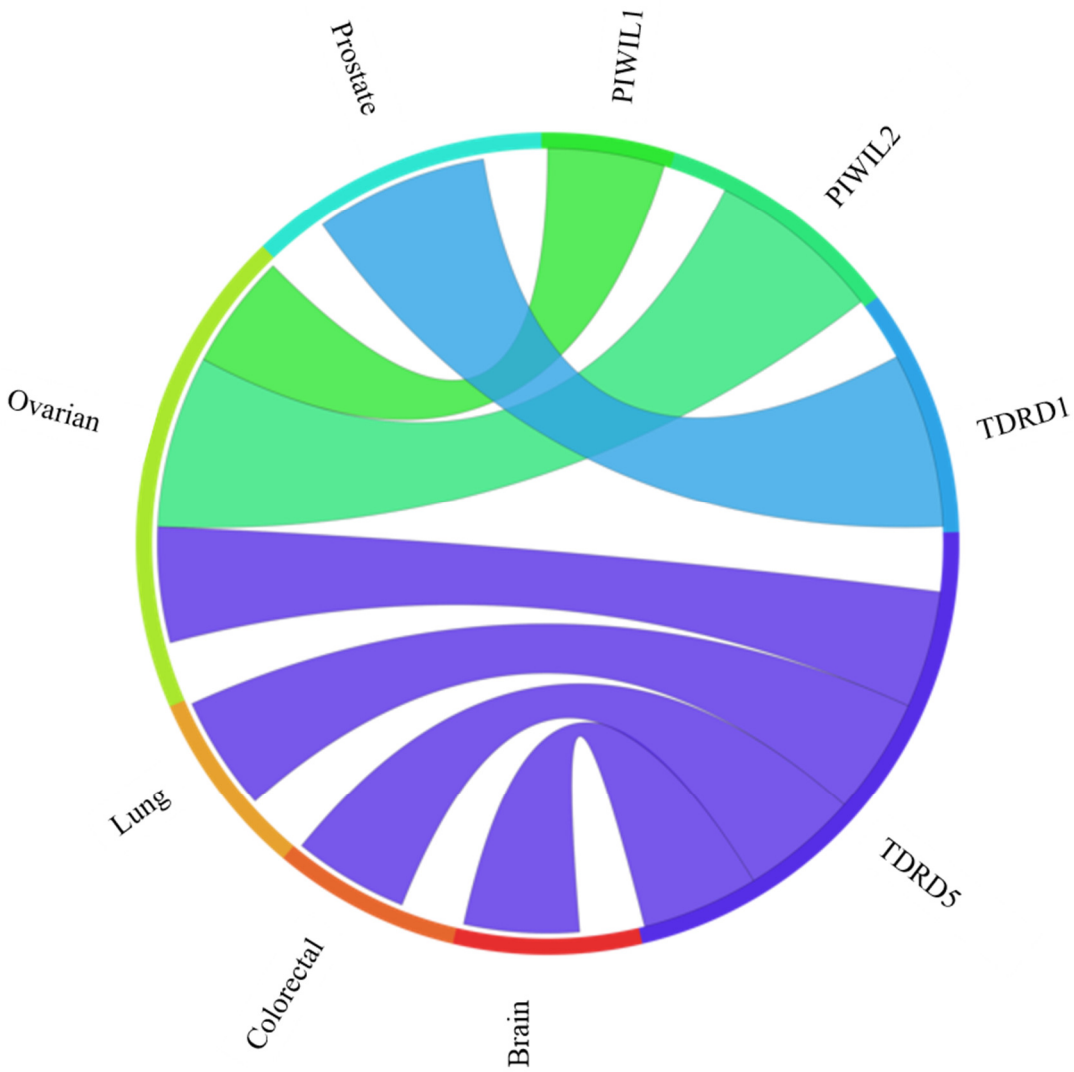

Figure 3.38 Circos plots of meta upregulated genes.
The Circos plots show the meta-change in gene expression in relation to corresponding cancer types for the four candidate genes. These genes were analysed utilising the CancerMA (http://www.cancerma.org.uk/index.html; Feichtinger *et al.,* 2012b) online tool; *PIWIL1*, *PIWIL2*, *TDRD1* and *TDRD5*. Each connection between a gene and a cancer type indicates a statically significant mean upregulation for that cancer type derived from a number of combined array studies for cancer tissue VS. normal tissue.

Figure 3.39 Circos plots of meta upregulated genes.
The Circos plots show the proportion of genes expressed in the various cancer types for upregulated genes.

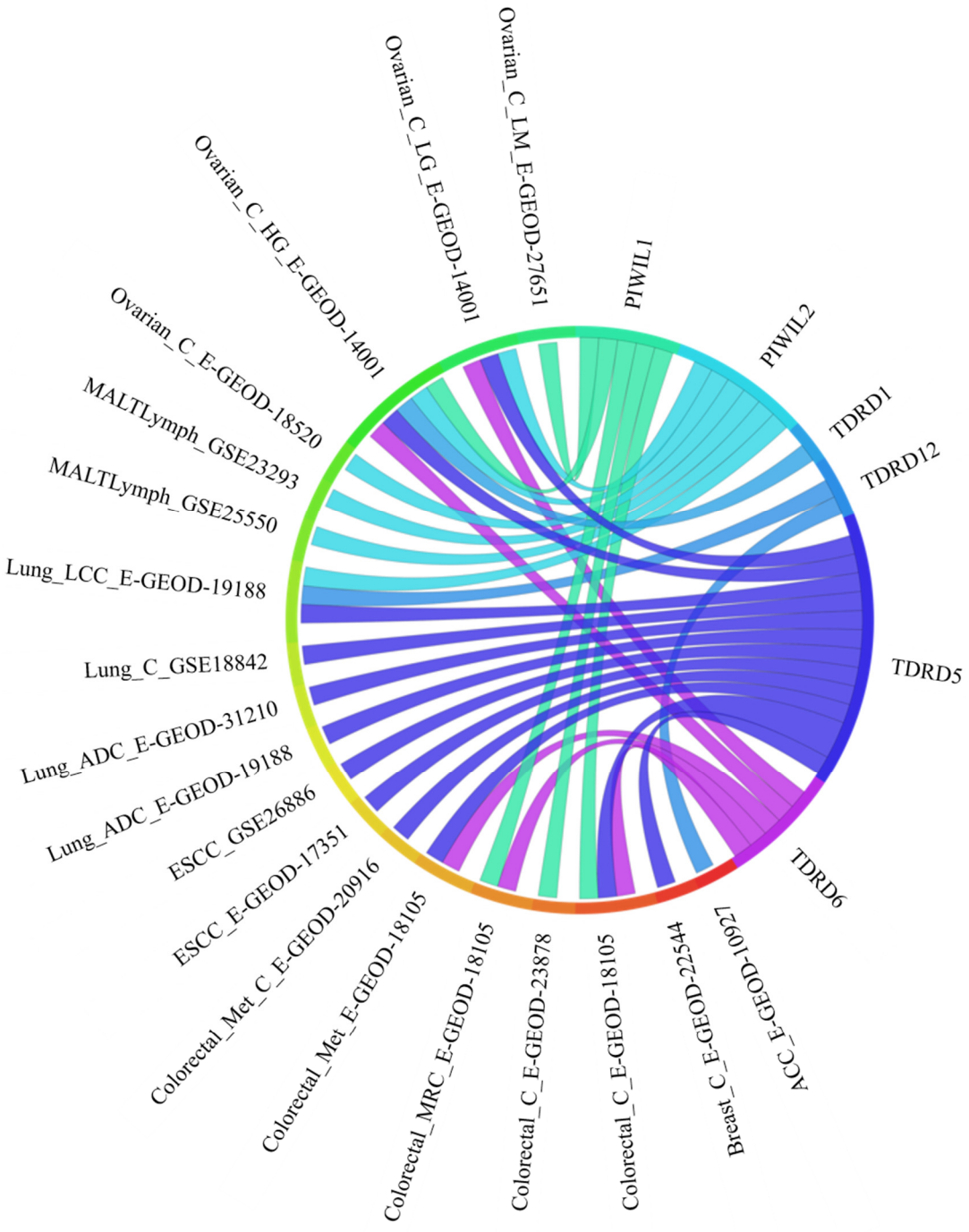

Figure 3.40 Single-Circos plots of upregulated genes.
The Circos plots show single array data set gene expression analysis in relation to corresponding cancer types for the six candidate genes. These genes were analysed utilising the CancerMA (http://www.cancerma.org.uk/index.html; Feichtinger *et al.,* 2012b) online tool; *PIWIL1*, *PIWIL2*, *TDRD1*, *TDRD5*, *TDRD6* and *TDRD12*. Each connection between a gene and a cancer type indicates a statically significant upregulation for that cancer type derived from a single array study for cancer tissue VS. normal tissue.

3.5. Concluding remarks

This chapter focused on the human Tudor protein family genes (*TDRD1-TDRD12*) and PIWIL protein family genes (*PIWIL1-PIWIL4*), with particular emphasis on their potentials as CT antigen genes. The associated antigens could be utilised for immunotherapy, cancer diagnosis, biomarkers and the creation of cancer drugs; in addition, they may be oncogenic. (Gjerstorff *et al.,* 2015; Krishnadas *et al.,* 2013; Whitehurst, 2014). Therefore, the main aim was to explore the potential of these genes as CT biomarkers.

The expression profiles of the *TDRD* and *PIWIL* genes were analysed in about 21 types of normal human tissues and 33 types of cancerous human cells. The analysis outcomes of the RT-PCR expression profiles show that eight out of 16 *TDRD* and *PIWIL* genes in total (*TDRD2*, *TDRD3*, *TDRD7*, *TDRD8*, *TDRD9*, *TDRD10, TDRD11* and *PIWIL4*) might not be good candidates for CTA genes. One out of 16 *TDRD* and *PIWIL* genes (*PIWIL3*) might not be a good candidate for CTA genes but appears to be testis-specific. Five out of 16 *TDRD* and *PIWIL* genes (*TDRD4*, *TDRD5*, *TDRD12*, *PIWIL1* and *PIWIL2*) might be good candidates for CTA genes and might classify as cancer testis-restricted. Two out of 16 *TDRD* and *PIWIL* genes (*TDRD1* and *TDRD6*) might be good candidates for CTA genes and might classify as cancer testis-selective.

These *TDRD* and *PIWIL* genes further validation and analysed to identify their molecular and biological functions and their possible application in developing human cancer therapies. Moreover, proteins encoded by these genes requires more study to determine if they might be oncogenic. In the following chapters, one of the identified *TDRD* and *PIWIL* CT genes, *TDRD12*, is analysed in further detail.

4. Analysis of the stem cell association of *TDRD12*

4.1. Introduction

One of the major aims of this study is to identify whether the human *TDRD12* gene function is linked to human stem cell functions. Moreover, it aims to determine whether the *TDRD12* gene plays a functional role in stem cell (SC) and cancer stem cell (CSC) specificity. SCs are characterised by their ability to self-renew and their capacity to differentiate and divide into various specialised cell categories (Goodell *et al.,* 2015; Simara *et al.,* 2013; Wong *et al.,* 2013). Embryonic stem cells (ESCs) are also of particular interest, as they are able to differentiate into all types of cells during embryogenesis. In recent years, researchers have been able to re-programme somatic cells into SC-like cells, which have characteristics of ESCs and are referred to as induced pluripotent stem cells (iPSCs) (Huang *et al.,* 2015; Takahashi and Yamanaka, 2013; Zhou *et al.,* 2013). In addition to the development of iPSCs, a subpopulation of SC-like cells has recently been identified in tumours; these cells are known as cancer stem cells (CSCs) (Ajani *et al.,* 2015; Dashyan *et al.,* 2015; Kesanakurti *et al.,* 2013).

Epigenetic and genetic alterations are responsible for CSC formation from normal adult SCs; the accumulation of these alterations can direct some CSC markers to switch on or off (Chanmee *et al.,* 2015; Vincent and Van Seuningen, 2012). The discovery of CSCs has had major implications for modern medicine and cancer research. More markers of CSCs are needed, as the discovery of the CSC markers will help to improve, develop and expand the design of oncology treatments and drugs (see Figure 4.1). The heterogeneities of malignant tumour cells might be generated from de-differentiated and/or differentiated CSCs. Therefore, further identification of CSCs is needed for the development of better and faster therapies in the near future. The combination of therapies, which target all tumour cells including CSCs, will drive new clinical strategies (Chanmee *et al.,* 2015; Frank *et al.,* 2010).

4.1.1. Human NTERA2 (NT2) cells

NT2 cells are pluripotent embryonal carcinoma cells; they are germ-line tumour cells, which have many features in common with ESCs. Moreover, they have the ability to rapidly generate unlimited numbers of cells. They can be differentiated into neurons using retinoic acid (RA) and under so less defined differentiation in response to hexamethylene bisacetamide (HMBA). The NT2 cells share gene expression profiles with ESCs, with specific gene markers, for example, the *OCT4* gene being active (Andrews, 2002; Ceci *et al.,* 2015; Serra *et al.,* 2009; Terrasso *et al.,* 2015). RAs are derivative of vitamin A, which is vital for embryogenesis, particularly for neural development (Rhinn and Dolle, 2012). RAs are utilised as major inducers of neural differentiation in NT2 cells (Elizalde *et al.,* 2011; Honecker *et al.,* 2014; Tonge and Andrews, 2010). HMBAs are known to produce proliferation–inhibitions and terminal differentiations in leukaemia cells, cancerous cells and pluripotent SCs (Ding *et al.,* 2013; Ren *et al.,* 2013). HMBAs induce the activity of proliferation–inhibitions via complex and poorly characterised mechanisms. Cultures of NT2 cells, which are exposed to HMBAs lack neural markers and HMBA treated cells are thought to go more down the epidermal lineage (Ding *et al.,* 2013; Öz *et al.,* 2013).

4.1.2. Human colon CSCs

Human colorectal malignant solid tumours represent one of the main causes of cancer-associated death. Most patients who suffer from this type of cancer are diagnosed at the age of 50 years or older; this support the theory that human colorectal carcinogenesis is linked to human genetic mutations, which accumulate with age. Intestinal epithelial cells take an extremely long time to develop into malignant phenotypes (Fanali *et al.,* 2014; Lin *et al.,* 2011; Zhang *et al.,* 2015). Hence, SCs, which are normally present in the colon, represent possible targets for tumourigenic mutations. As a result, their self-renewal and longevity and comparable to those of their cellular progeny. In addition, they might result in an increase of CSCs due to their ability to survive in the human body and initiate tumours (Chen *et al.,* 2011a; Chung *et al.,* 2015; Fanali *et al.,* 2014).

Recent data and research studies have reported that tumour initiating mutations might also have the ability to originate in SCs either in human crypt cells or after differentiation, as differentiated cells can de-differentiate and re-express the markers of pluripotency. Consequently, the complexity of CSCs needs to be understood to optimise novel anti–human cancer therapies and treatments (Puglisi *et al.,* 2013).

4.1.2.1. Human SW480 cells

SW480 cells are colon adenocarcinoma cells/colorectal cancer cells. These are epithelial cells extracted from colorectal adenocarcinomas. These cells were initially derived from a combination of human bipolar and epithelial cells. However, at a later stage, most of the bipolar cells disappear (Courtaut *et al.,* 2015; Dong *et al.,* 2015; Fanali *et al.,* 2014; Holzapfel *et al.,* 2015; Leyssens *et al.,* 2015; Min *et al.,* 2015; Valadez-Vega *et al.,* 2011; Wang *et al.,* 2015).

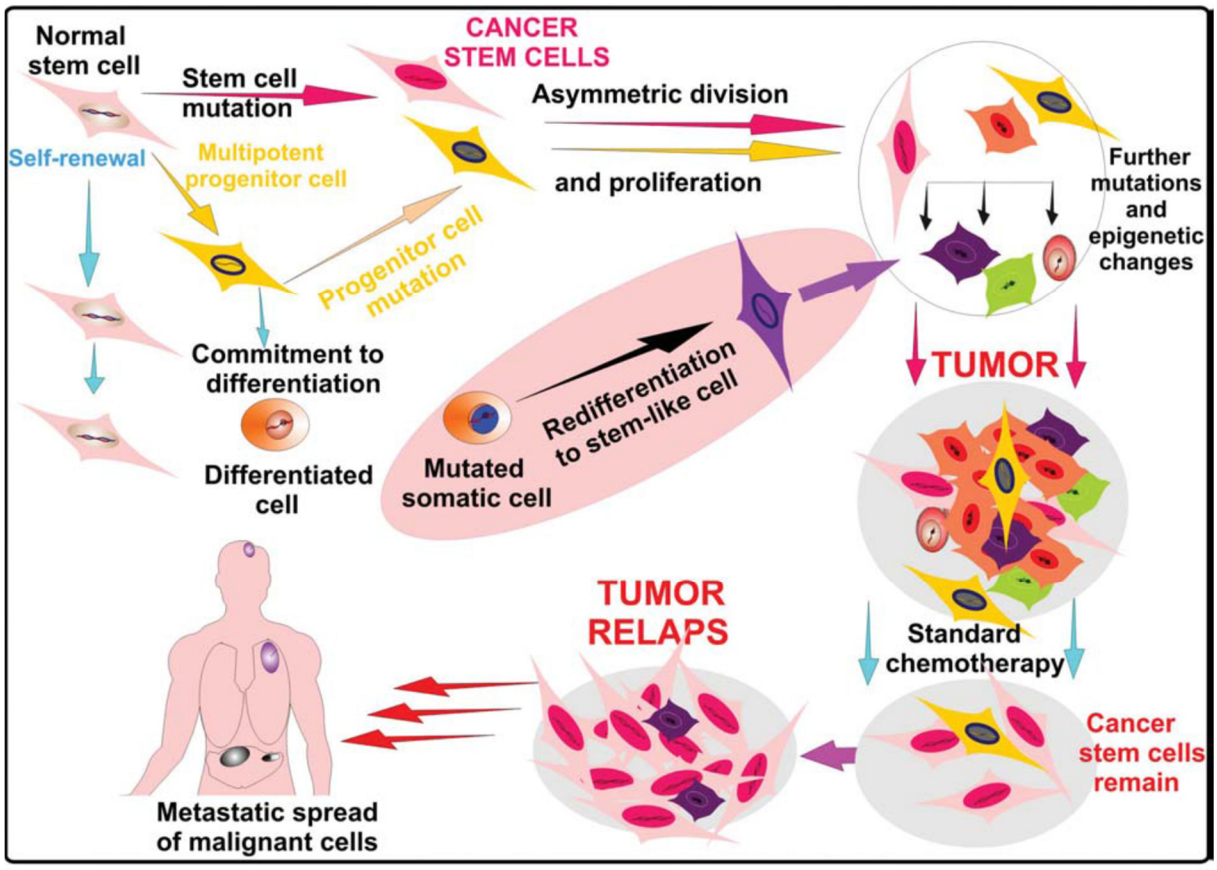

Figure 4.1 How do CSCs originate in the human body?
SCs are usually present naturally in the body of both genders; these cells divide asymmetrically by themselves to produce cells, which have a multipotent progenitor. The diagram shows how CSCs generate from progenitor cells and/or mutated SCs by genetic changes. The cancerous cells might generate after initial treatments using radiotherapy or chemotherapy. These therapies may be responsible for spreading the metastatic malignant cancerous and tumour cells in the human body.
Taken from (Soltysova *et al.,* 2005).

4.2. Aims

(A) This study aims to address whether human *TDRD12* gene function is linked to the function of human SC marker genes (*OCT4* and/or *SOX2*).

(B) This study aims to determine if the *TDRD12* gene plays a functional role in SCs and CSCs specificity.

The *TDRD12* gene has been identified as a possible cancer marker that may contain CSC-specific activity (Feichtinger *et al.,* 2012). The *TDRD12* gene is of interest because in a previous study its expression is activated in the human NT2 cells (see Chapter 3). This leads to the hypothesis that it might play a role in conferring stemness on cancer cells, as NT2 cells have many features in common with ESCs (see above).

4.3. Results

Here, NT2 cells were differentiated via RA (to form neuron cells) and HMBA (to generate other cells) (DMSO treatment was used as a negative control) treatment for six days. To analyse the *TDRD12* and *OCT4* gene expression profiles, total RNA was extracted from the differentiated NT2 cells. Following this, cDNA was generated from the extracted RNAs. Quality assessments and controls were carried out for the extracted RNA and generated cDNA (see Figure 4.2 and Figure 4.3).

Figure 4.2 shows the quality assessment of the RNA extracted from differentiated NT2 cells. The expected sizes of 28S and 18S RNA fragments were 1,800 bp and 900 bp, respectively and the RNA bands were detected at approximately the expected sizes. Figure 4.3 shows the RT-PCR analysis of the *β-actin* gene expression in the differentiated NT2 cells. The expression of the *β-actin* gene was used as a quality control for the cDNA generated from NT2 cells; the *β-actin* PCR products were detected at approximately the expected sizes (553 bp).

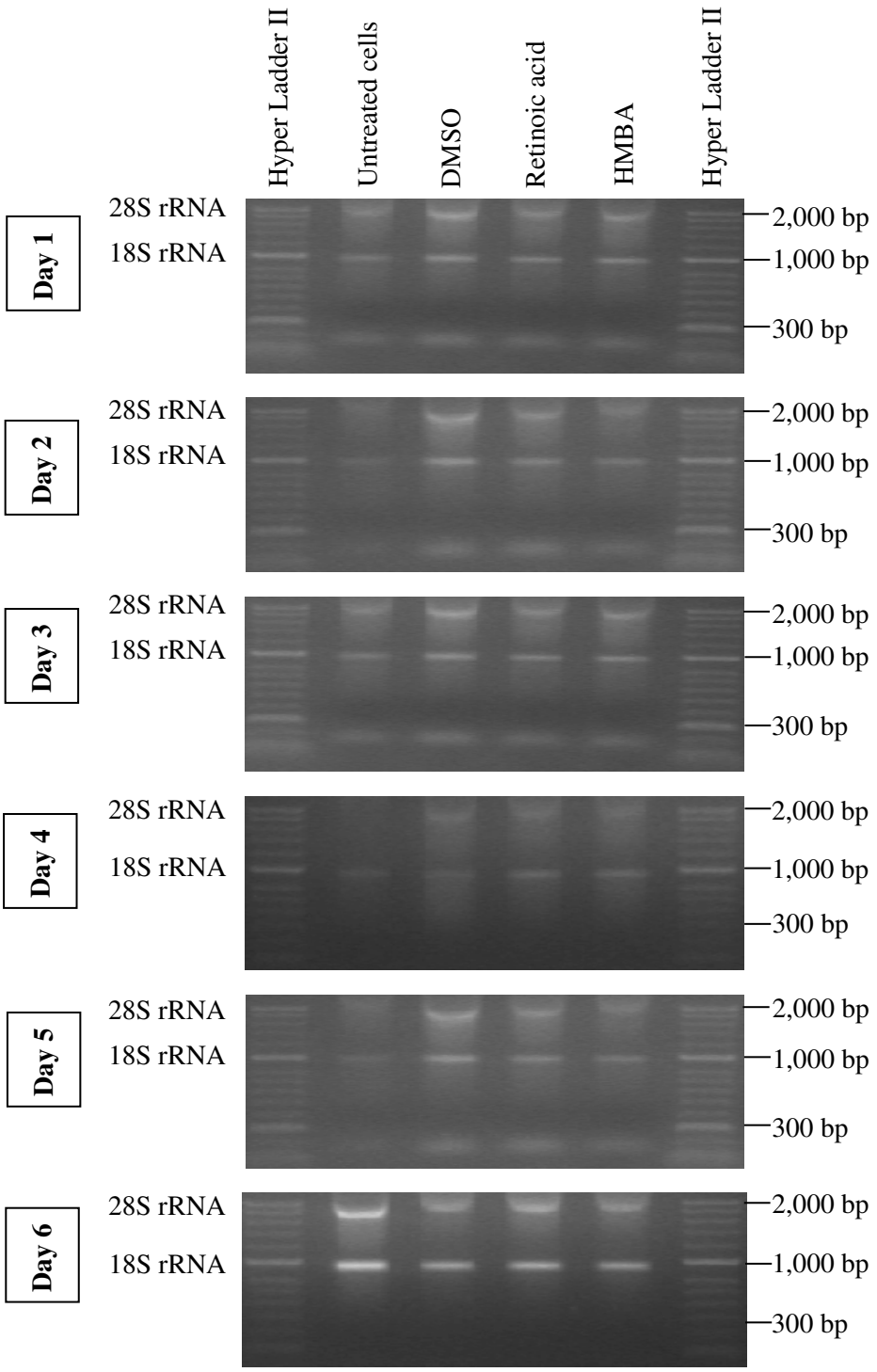

Figure 4.2 Quality assessment of the RNA extracted from human differentiating NT2 cells.
The expected sizes of 28S and 18S RNA fragments are 1,800 bp and 900 bp respectively.

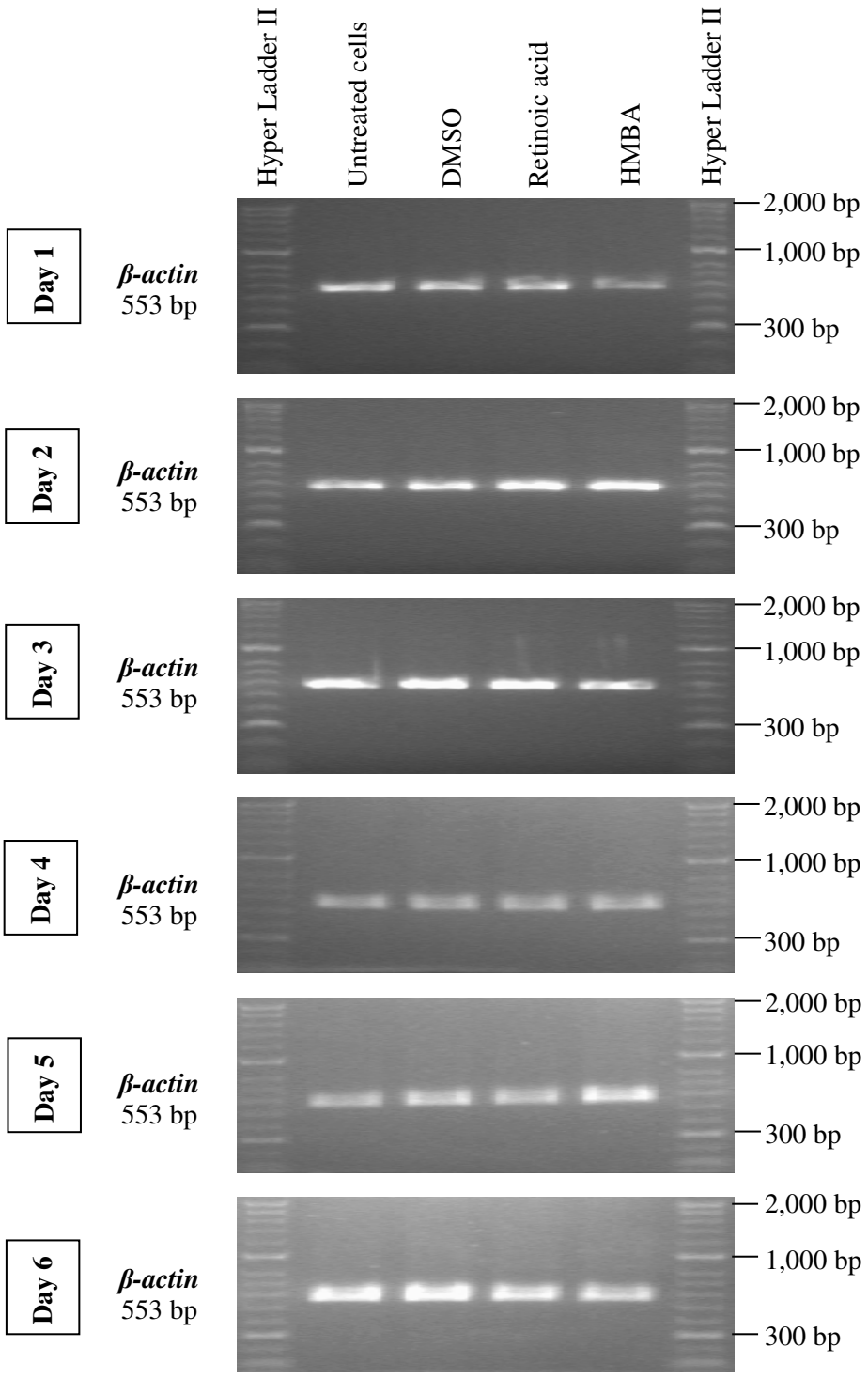

Figure 4.3 RT-PCR analysis of *β-actin* gene expression in human differentiating NT2 cells.
Agarose gels presenting the RT-PCR profiles created from the NT2 cells. The expression of *β-actin* gene was used as a quality control for the cDNA generated from NT2 cells. The *β-actin* PCR products were detected at approximately the expected sizes (553 bp).

4.3.1. Analysis of *OCT4* and *TDRD12* gene expression during NT2 differentiation

As can be seen from the results (Figure 4.4, Figure 4.5, Figure 4.6, Figure 4.7, Figure 4.8, Figure 4.9, Figure 4.10 and Figure 4.11), the treatments successfully differentiated NT2 cells, as the expression of the *OCT4* gene started to decline and cease from day five. However, the expression of *TDRD12* remained constant throughout the six days of treatment. RT-qPCR primer sequences were designed in exon three and four of the *TDRD12-001* transcript. The results suggested that the *TDRD12* gene does not behave in the same way at the transcription level as the *OCT4* gene does. Furthermore, the analysis was repeated using the same set of primers because the DMSO (negative control) treatment in the analysis of the *TDRD12* gene was not completely convincing; the same results were obtained. For confirmation, the analysis was repeated once more using Qiagen primer sequences (commercially designed in exon 24 and 25 of the *TDRD12-001* transcript); again, the same results were obtained.

Figure 4.4 shows the RT-PCR analysis of the *OCT4* gene expression in the differentiated NT2 cells. The expression of the *OCT4* gene was used as an SC marker. The *OCT4* PCR products were detected at approximately the expected size (872 bp). Figure 4.5 shows the RT-PCR analysis of the *TDRD12* gene expression in the differentiated NT2 cells. Untreated cells were used as positive controls. Cells treated with DMSO were used as negative controls. The *TDRD12* PCR products were detected at approximately the expected sizes (409 bp). Figure 4.6, Figure 4.7, Figure 4.8, Figure 4.9, Figure 4.10 and Figure 4.11 show the RT-qPCR analysis of *OCT4* and *TDRD12* gene expression in the differentiating NT2 cells from day one to day six of treatments. Normalising of the *OCT4* and *TDRD12* expression was relative to the *GAPDH* and *HSP90AB1* genes.

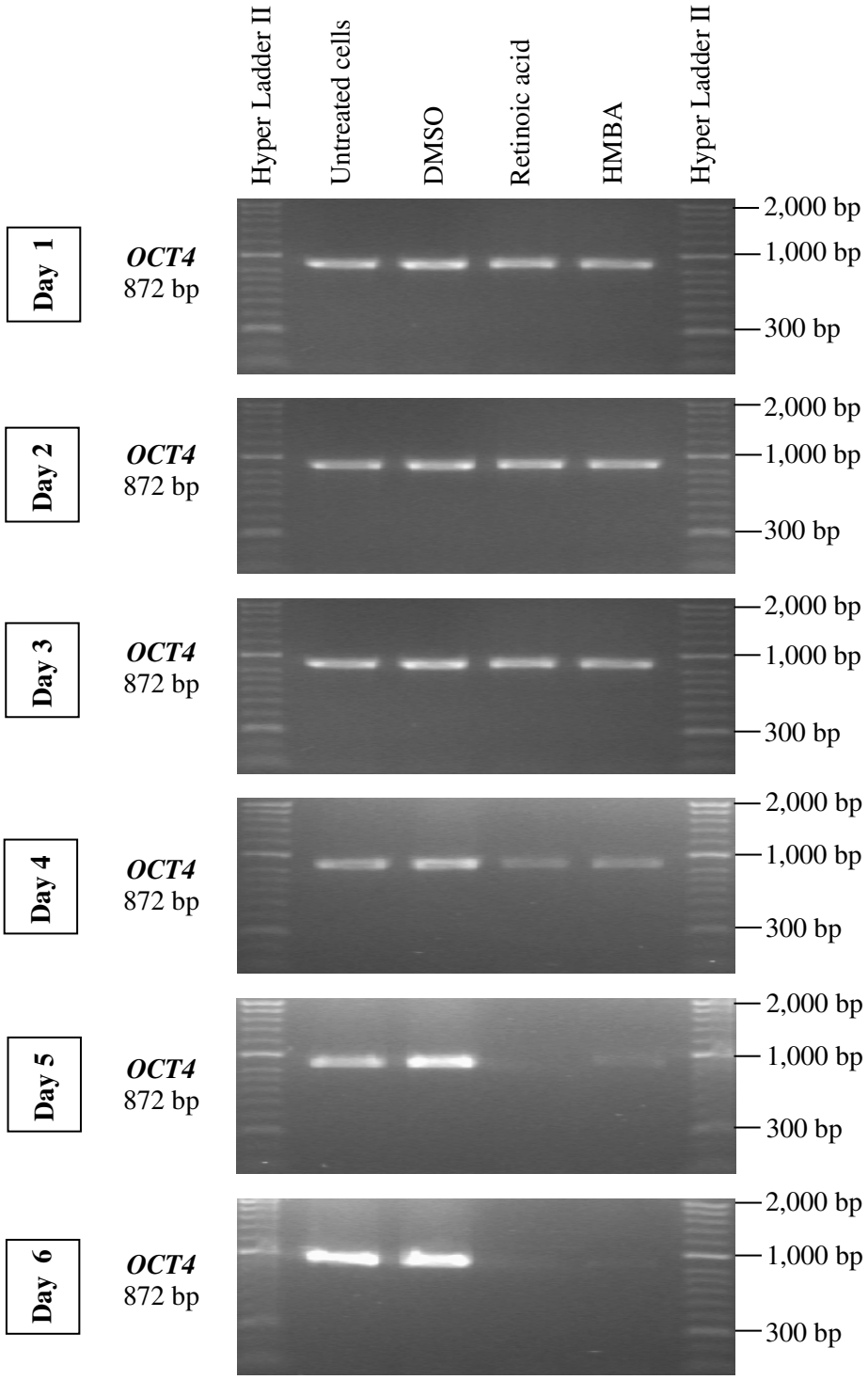

Figure 4.4 RT-PCR analysis of *OCT4* gene expression in human differentiating NT2 cells.
Agarose gels presenting the RT-PCR profiles created from the NT2 cells. The expression of *OCT4* gene was used as an SC marker. Untreated were used as positive controls. Cells treated with DMSO were used as negative controls. The *OCT4* PCR products were detected at approximately the expected sizes (872 bp).

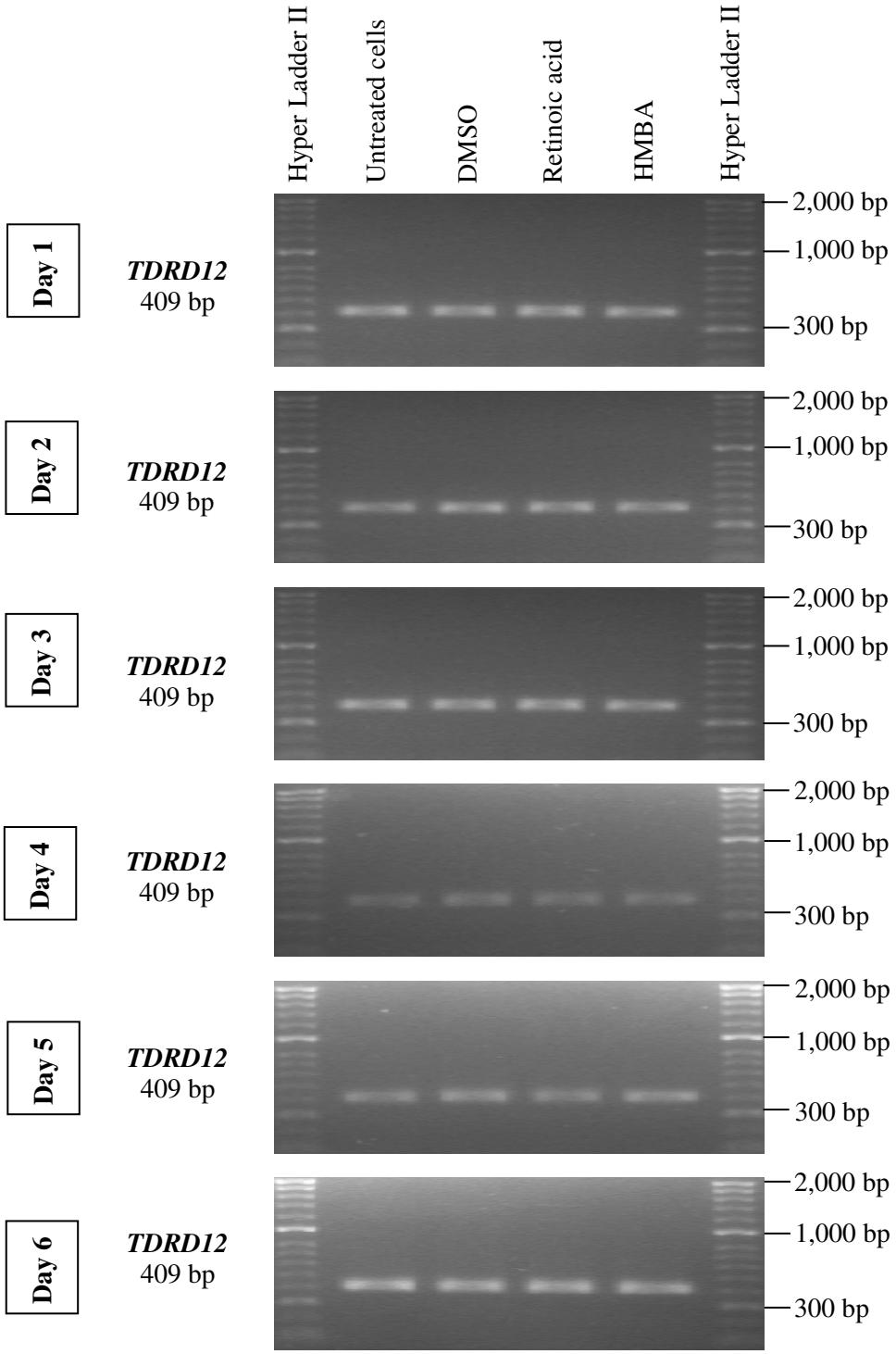

Figure 4.5 RT-PCR analysis of *TDRD12* gene expression in human differentiating NT2 cells.
Agarose gels presenting the RT-PCR profiles created from the NT2 cells. Untreated cells were used as positive controls. Cells treated with DMSO were used as negative controls. The *TDRD12* PCR products were detected at approximately the expected sizes (409 bp).

A.

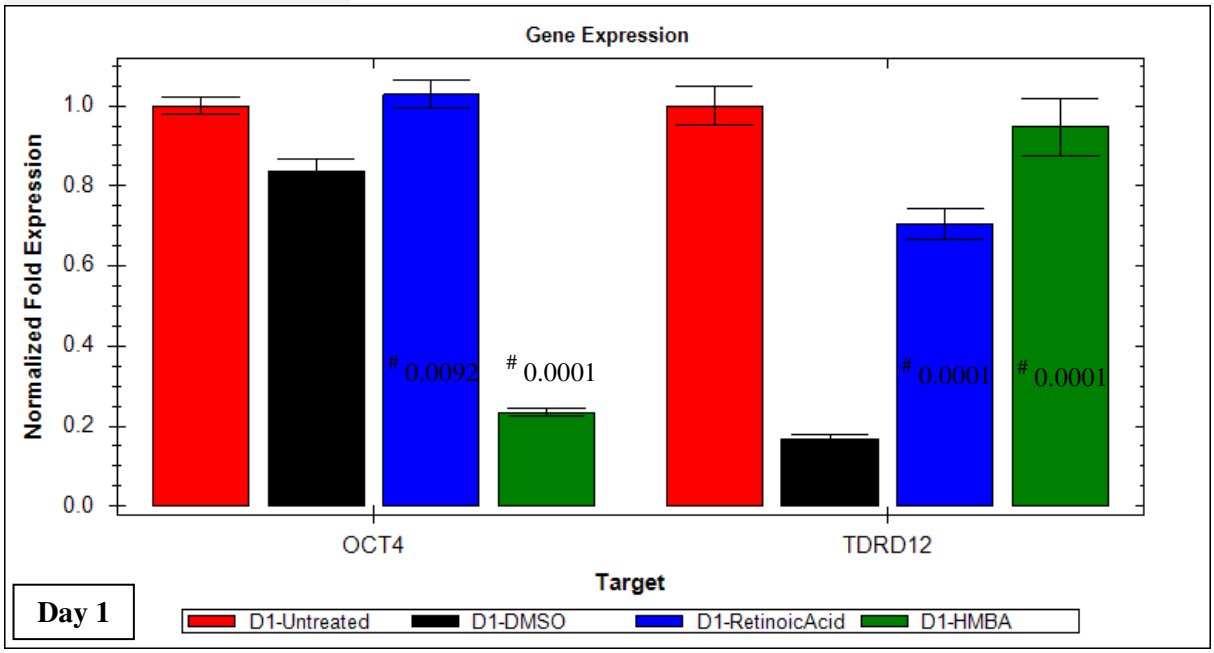

B.

Target	Sample	Wells	Cq Reading 1	Cq Reading 2	Cq Reading 3	Cq Mean	Cq Std. Dev
GAPDH	D1-Untreated	3	16.57	16.50	16.46	16.51	0.057
GAPDH	D1-DMSO	3	16.88	16.92	16.70	16.84	0.118
GAPDH	D1-RetinoicAcid	3	17.34	17.37	17.40	17.37	0.030
GAPDH	D1-HMBA	3	22.16	22.09	22.29	22.18	0.099
HSP90AB1	D1-Untreated	3	20.30	20.25	20.28	20.27	0.024
HSP90AB1	D1-DMSO	3	20.56	20.47	20.48	20.50	0.052
HSP90AB1	D1-RetinoicAcid	3	21.06	21.12	21.17	21.12	0.052
HSP90AB1	D1-HMBA	3	25.18	25.29	25.26	25.24	0.055
OCT4	D1-Untreated	3	21.33	21.25	21.30	21.30	0.043
OCT4	D1-DMSO	3	21.77	21.82	21.89	21.83	0.060
OCT4	D1-RetinoicAcid	3	22.20	22.06	22.06	22.10	0.079
OCT4	D1-HMBA	3	28.80	28.62	28.71	28.71	0.092
TDRD12	D1-Untreated	3	25.19	25.41	25.26	25.29	0.115
TDRD12	D1-DMSO	3	28.23	27.96	28.21	28.13	0.149
TDRD12	D1-RetinoicAcid	2	26.72	26.57	N/A	26.64	0.107
TDRD12	D1-HMBA	3	30.51	30.66	30.87	30.68	0.182

Figure 4.6 RT-qPCR analysis of *OCT4* and *TDRD12* gene expression in human NT2 cells after day 1 following initiation of differentiation.
Panel (A): bar chart demonstrating the normalisation of the *OCT4* and *TDRD12* gene expression analysed by RT-qPCR. The Bio-Rad CFX Manager was used to analyse the data. The error bars show the standard error for three replicates. Panel (B): table illustrating the number of replications (wells) and the Cq (quantification cycle) mean, standard deviation and Cq readings for the *GAPDH* and *HSP90AB1* genes, to which the *OCT4* and *TDRD12* genes reading was normalised. # P-Value.

A.

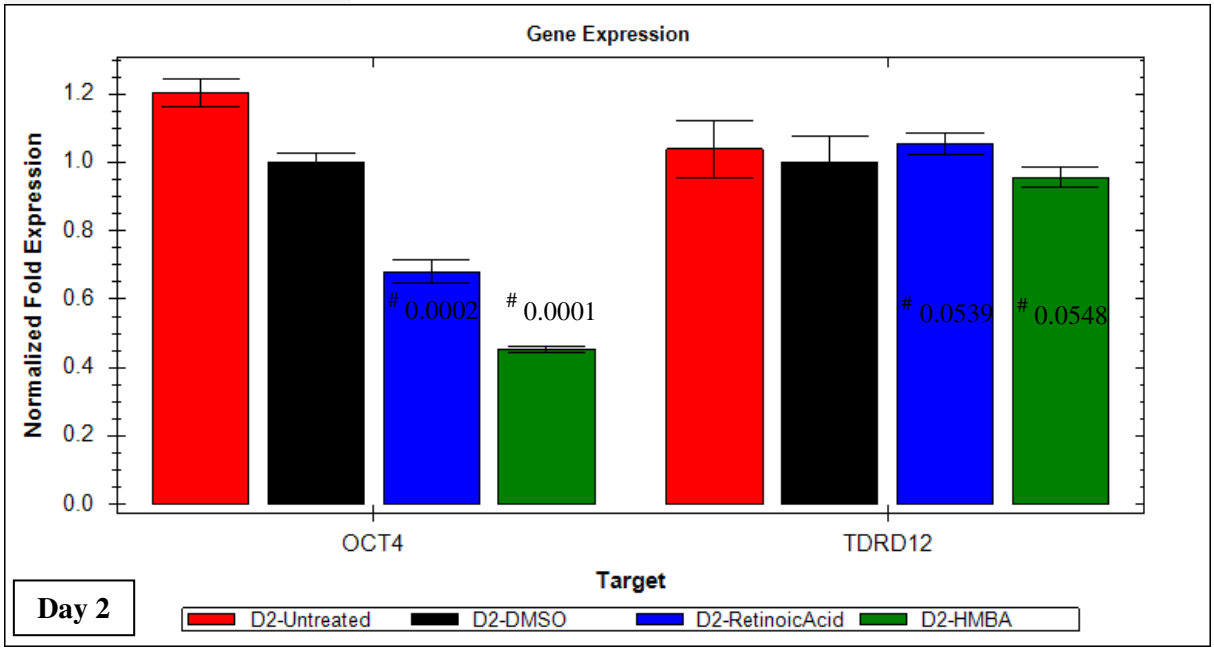

B.

Target	Sample	Wells	Cq Reading 1	Cq Reading 2	Cq Reading 3	Cq Mean	Cq Std. Dev
GAPDH	D2-Untreated	3	17.14	17.02	17.09	17.08	0.059
GAPDH	D2-DMSO	3	16.08	16.09	16.00	16.06	0.049
GAPDH	D2-RetinoicAcid	3	16.34	16.34	16.34	16.34	0.003
GAPDH	D2-HMBA	3	16.23	16.16	16.20	16.19	0.036
HSP90AB1	D2-Untreated	3	20.99	20.97	21.06	21.01	0.046
HSP90AB1	D2-DMSO	3	19.68	19.66	19.47	19.60	0.115
HSP90AB1	D2-RetinoicAcid	3	20.03	20.08	20.13	20.08	0.050
HSP90AB1	D2-HMBA	3	19.90	19.98	19.90	19.93	0.046
OCT4	D2-Untreated	3	21.66	21.72	21.81	21.73	0.075
OCT4	D2-DMSO	3	20.81	20.76	20.78	20.78	0.022
OCT4	D2-RetinoicAcid	3	21.85	21.61	21.69	21.72	0.124
OCT4	D2-HMBA	3	22.18	22.12	22.16	22.15	0.029
TDRD12	D2-Untreated	3	25.97	26.36	26.21	26.18	0.197
TDRD12	D2-DMSO	3	25.19	24.83	25.04	25.02	0.179
TDRD12	D2-RetinoicAcid	3	25.25	25.33	25.39	25.32	0.070
TDRD12	D2-HMBA	3	25.23	25.37	25.34	25.32	0.073

Figure 4.7 RT-qPCR analysis of *OCT4* and *TDRD12* gene expression in human NT2 cells after day 2 following initiation of differentiation.
Panel (A): bar chart demonstrating the normalisation of the *OCT4* and *TDRD12* gene expression analysed by RT-qPCR. The Bio-Rad CFX Manager was used to analyse the data. The error bars show the standard error for three replicates. Panel (B): table illustrating the number of replications (wells) and the Cq (quantification cycle) mean, standard deviation and Cq readings for the *GAPDH* and *HSP90AB1* genes, to which the *OCT4* and *TDRD12* genes reading was normalised. # P-Value.

A.

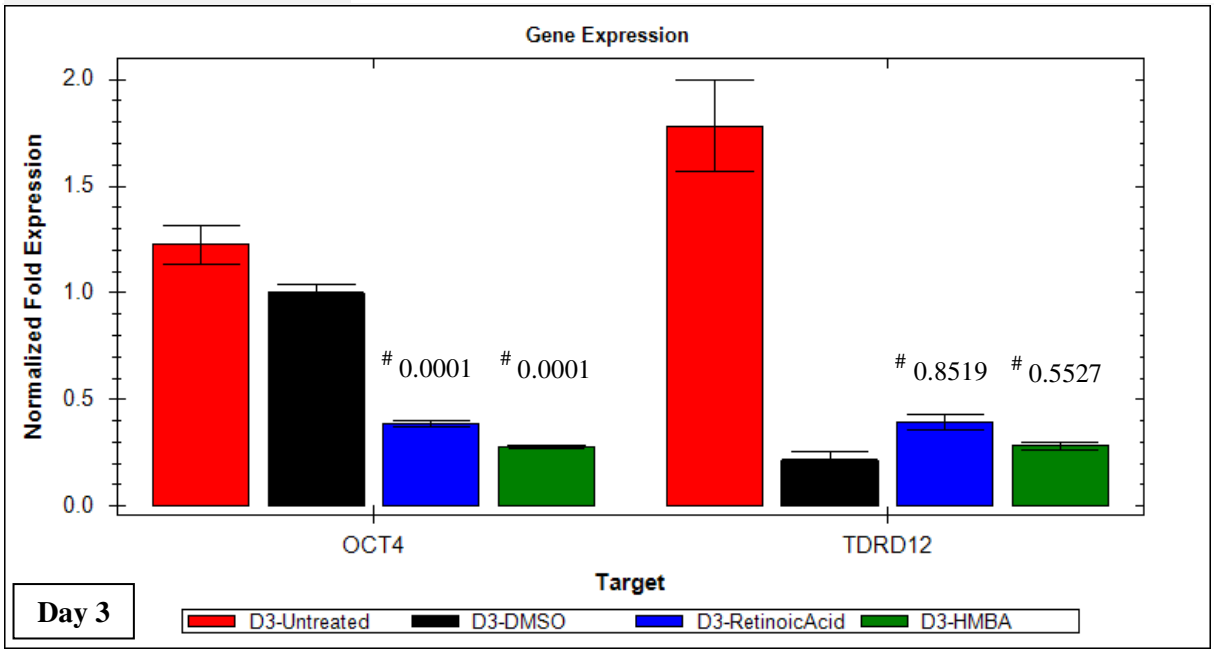

B.

Target	Sample	Wells	Cq Reading 1	Cq Reading 2	Cq Reading 3	Cq Mean	Cq Std. Dev
GAPDH	D3-Untreated	3	16.42	16.99	17.01	16.81	0.334
GAPDH	D3-DMSO	3	16.35	16.27	16.34	16.32	0.046
GAPDH	D3-RetinoicAcid	3	16.99	17.24	17.11	17.12	0.123
GAPDH	D3-HMBA	3	16.36	16.42	16.57	16.45	0.106
HSP90AB1	D3-Untreated	3	21.46	21.36	21.36	21.39	0.058
HSP90AB1	D3-DMSO	3	20.38	20.11	20.16	20.22	0.146
HSP90AB1	D3-RetinoicAcid	3	21.28	21.07	21.29	21.21	0.123
HSP90AB1	D3-HMBA	3	20.48	20.59	20.53	20.53	0.056
OCT4	D3-Untreated	3	21.67	21.56	21.65	21.63	0.057
OCT4	D3-DMSO	3	21.09	21.01	21.14	21.08	0.064
OCT4	D3-RetinoicAcid	3	23.38	23.32	23.32	23.34	0.037
OCT4	D3-HMBA	3	23.19	23.11	23.21	23.17	0.053
TDRD12	D3-Untreated	2	26.93	26.68	N/A	26.81	0.175
TDRD12	D3-DMSO	2	29.27	28.74	N/A	29.00	0.371
TDRD12	D3-RetinoicAcid	3	28.96	28.88	29.31	29.05	0.227
TDRD12	D3-HMBA	3	29.02	28.79	28.74	28.85	0.153

Figure 4.8 RT-qPCR analysis of *OCT4* and *TDRD12* gene expression in human NT2 cells after day 3 following initiation of differentiation.
Panel (A): bar chart demonstrating the normalisation of the *OCT4* and *TDRD12* gene expression analysed by RT-qPCR results to the *GAPDH* and *HSP90AB1* genes. The Bio-Rad CFX Manager was used to analyse the data. The error bars show the standard error for three replicates. Panel (B): table illustrating the number of replications (wells) and the Cq (quantification cycle) mean, standard deviation and Cq readings for the *GAPDH* and *HSP90AB1* genes, to which the *OCT4* and *TDRD12* genes reading was normalised. # P-Value.

A.

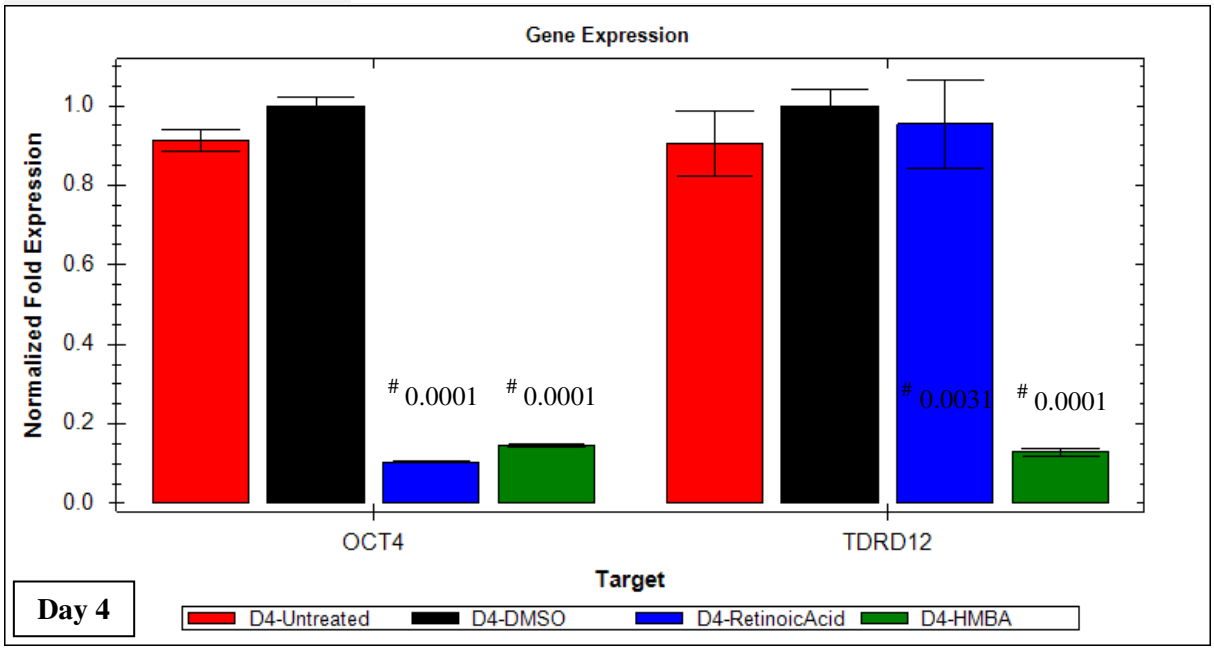

B.

Target	Sample	Wells	Cq Reading 1	Cq Reading 2	Cq Reading 3	Cq Mean	Cq Std. Dev
GAPDH	D4-Untreated	3	17.43	17.33	17.30	17.35	0.071
GAPDH	D4-DMSO	3	16.19	16.21	16.23	16.21	0.022
GAPDH	D4-RetinoicAcid	3	16.96	17.01	17.04	17.00	0.039
GAPDH	D4-HMBA	3	16.73	16.72	16.82	16.76	0.055
HSP90AB1	D4-Untreated	3	21.52	21.36	21.39	21.42	0.085
HSP90AB1	D4-DMSO	3	20.21	20.09	20.26	20.19	0.085
HSP90AB1	D4-RetinoicAcid	3	21.08	21.01	21.07	21.06	0.036
HSP90AB1	D4-HMBA	3	20.66	20.69	20.65	20.67	0.024
OCT4	D4-Untreated	3	22.11	22.15	22.21	22.16	0.050
OCT4	D4-DMSO	3	20.88	20.81	20.82	20.84	0.039
OCT4	D4-RetinoicAcid	3	24.91	24.95	24.97	24.94	0.032
OCT4	D4-HMBA	3	24.19	24.09	24.13	24.14	0.051
TDRD12	D4-Untreated	2	26.65	26.90	N/A	26.77	0.177
TDRD12	D4-DMSO	2	25.49	25.39	N/A	25.44	0.072
TDRD12	D4-RetinoicAcid	2	26.17	26.50	N/A	26.34	0.234
TDRD12	D4-HMBA	3	29.04	28.96	28.73	28.91	0.159

Figure 4.9 RT-qPCR analysis of *OCT4* and *TDRD12* gene expression in human NT2 cells after day 4 following initiation of differentiation.
Panel (A): bar chart demonstrating the normalisation of the *OCT4* and *TDRD12* gene expression analysed by RT-qPCR. The Bio-Rad CFX Manager was used to analyse the data. The error bars show the standard error for three replicates. Panel (B): table illustrating the number of replications (wells) and the Cq (quantification cycle) mean, standard deviation and Cq readings for the *GAPDH* and *HSP90AB1* genes, to which the *OCT4* and *TDRD12* genes reading was normalised. # P-Value.

A.

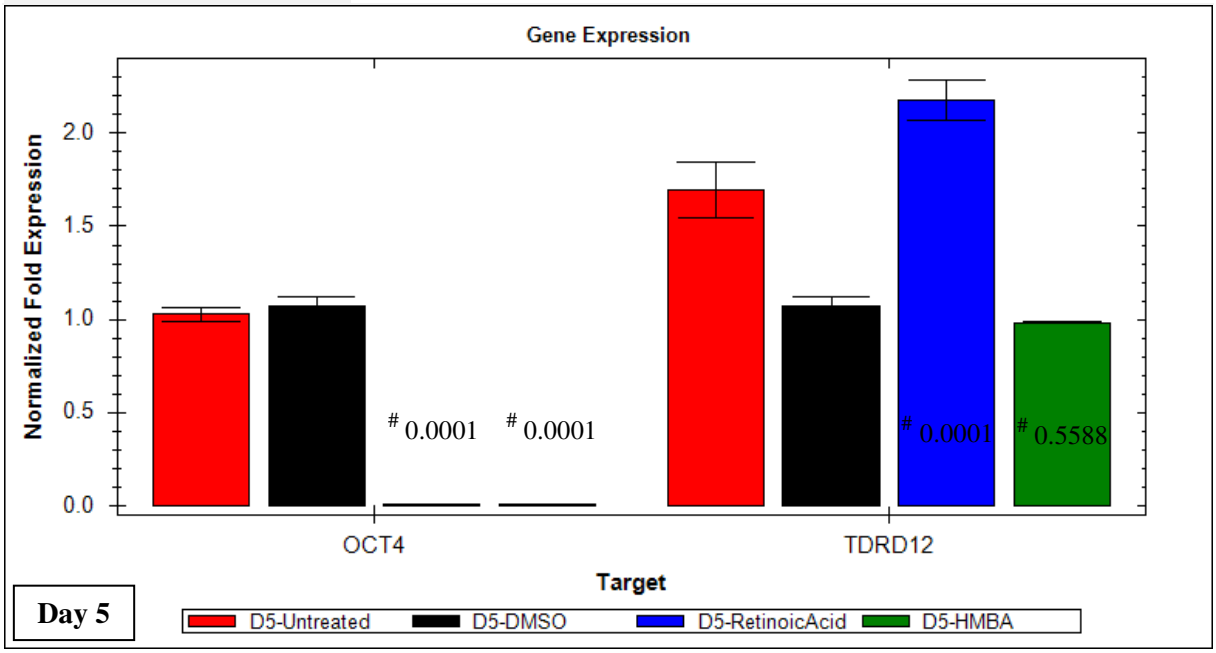

B.

Target	Sample	Wells	Cq Reading 1	Cq Reading 2	Cq Reading 3	Cq Mean	Cq Std. Dev
GAPDH	D5-Untreated	3	17.87	17.89	17.85	17.87	0.017
GAPDH	D5-DMSO	3	16.01	15.91	15.80	15.91	0.104
GAPDH	D5-RetinoicAcid	3	18.92	19.02	18.87	18.94	0.075
GAPDH	D5-HMBA	3	15.78	15.78	15.80	15.79	0.011
HSP90AB1	D5-Untreated	3	20.91	20.92	20.92	20.92	0.007
HSP90AB1	D5-DMSO	3	19.22	19.06	19.07	19.12	0.090
HSP90AB1	D5-RetinoicAcid	3	21.73	21.71	21.77	21.74	0.028
HSP90AB1	D5-HMBA	3	19.02	19.03	19.02	19.02	0.005
OCT4	D5-Untreated	3	21.88	21.84	22.01	21.91	0.090
OCT4	D5-DMSO	3	19.92	19.91	20.04	19.96	0.071
OCT4	D5-RetinoicAcid	3	29.31	29.35	29.34	29.33	0.023
OCT4	D5-HMBA	3	26.42	26.19	26.53	26.38	0.175
TDRD12	D5-Untreated	3	25.16	25.34	24.91	25.14	0.217
TDRD12	D5-DMSO	3	23.99	23.83	23.91	23.91	0.080
TDRD12	D5-RetinoicAcid	2	25.66	25.79	N/A	25.72	0.092
TDRD12	D5-HMBA	3	23.93	23.95	23.92	23.94	0.016

Figure 4.10 RT-qPCR analysis of *OCT4* and *TDRD12* gene expression in human NT2 cells after day 5 following initiation of differentiation.
Panel (A): bar chart demonstrating the normalisation of the *OCT4* and *TDRD12* gene expression analysed by RT-qPCR. The Bio-Rad CFX Manager was used to analyse the data. The error bars show the standard error for three replicates. Panel (B): table illustrating the number of replications (wells) and the Cq (quantification cycle) mean, standard deviation and Cq readings for the *GAPDH* and *HSP90AB1* genes, to which the *OCT4* and *TDRD12* genes reading was normalised. # P-Value.

A.

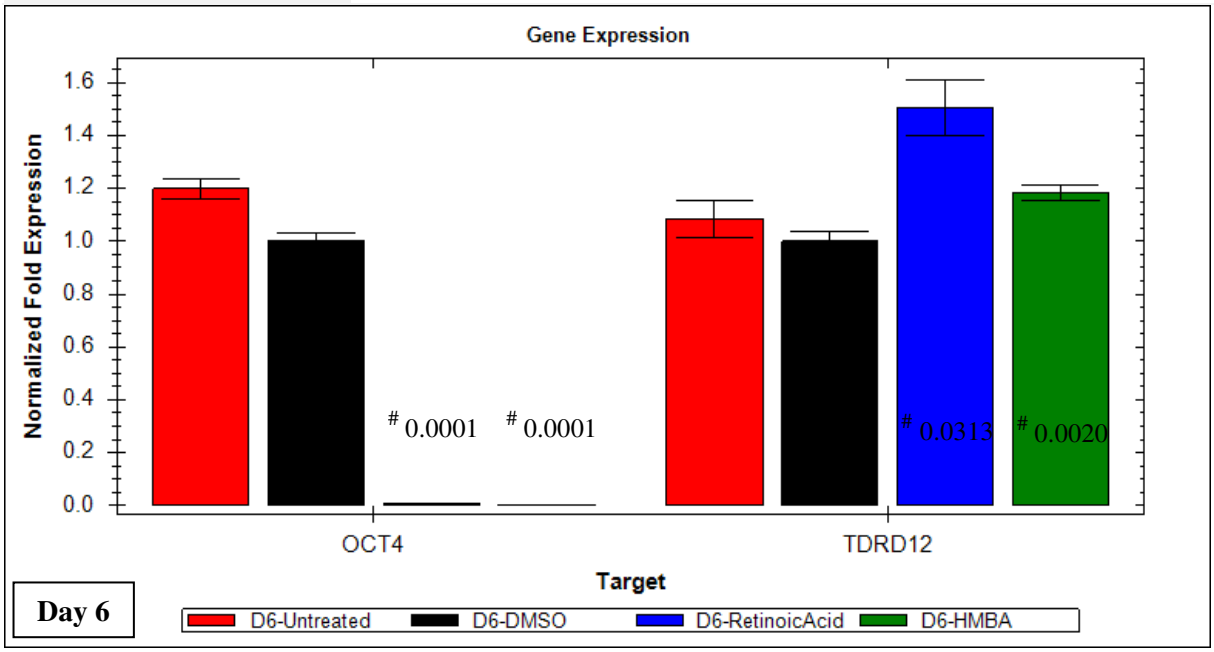

B.

Target	Sample	Wells	Cq Reading 1	Cq Reading 2	Cq Reading 3	Cq Mean	Cq Std. Dev
GAPDH	D6-Untreated	3	15.62	15.50	15.61	15.58	0.066
GAPDH	D6-DMSO	3	15.36	15.33	15.32	15.34	0.025
GAPDH	D6-RetinoicAcid	3	16.16	16.21	16.24	16.20	0.044
GAPDH	D6-HMBA	3	15.96	15.97	16.08	16.00	0.070
HSP90AB1	D6-Untreated	3	19.03	18.80	18.91	18.91	0.116
HSP90AB1	D6-DMSO	3	18.70	18.43	18.60	18.58	0.134
HSP90AB1	D6-RetinoicAcid	3	19.19	19.68	19.26	19.38	0.266
HSP90AB1	D6-HMBA	3	19.05	19.10	19.04	19.07	0.034
OCT4	D6-Untreated	3	19.48	19.46	19.55	19.50	0.048
OCT4	D6-DMSO	3	19.48	19.43	19.49	19.47	0.032
OCT4	D6-RetinoicAcid	3	27.59	27.51	27.60	27.56	0.047
OCT4	D6-HMBA	3	28.27	28.06	28.12	28.15	0.104
TDRD12	D6-Untreated	3	23.90	23.96	23.69	23.85	0.142
TDRD12	D6-DMSO	3	23.75	23.66	23.63	23.68	0.065
TDRD12	D6-RetinoicAcid	3	23.81	24.03	23.92	23.92	0.110
TDRD12	D6-HMBA	3	24.07	23.98	23.99	24.01	0.046

Figure 4.11 RT-qPCR analysis of *OCT4* and *TDRD12* gene expression in human NT2 cells after day 6 following initiation of differentiation.
Panel (A): bar chart demonstrating the normalisation of the *OCT4* and *TDRD12* gene expression analysed by RT-qPCR. The Bio-Rad CFX Manager was used to analyse the data. The error bars show the standard error for three replicates. Panel (B): table illustrating the number of replications (wells) and the Cq (quantification cycle) mean, standard deviation and Cq readings for the *GAPDH* and *HSP90AB1* genes, to which the *OCT4* and *TDRD12* genes reading was normalised. # P-Value.

4.3.2. Analysis of *TDRD12* expression in human SCs

The original finding that *TDRD12* was expressed in NT2 cells inferred that it could be associated with stemness. However, differentiation of NT2 with RA and HMBA did not cause silencing of *TDRD12*. To explore this further, the expression profiles of *TDRD12* and *OCT4* genes were analysed in iPSCs, ESCs and differentiated iPSCs (D-iPSCs) (see Figure 4.12, Figure 4.13, Figure 4.14, Figure 4.15 and Figure 4.16). As a result, the *TDRD12* gene was found to be expressed in iPSCs and ESCs. In contrast, *TDRD12* was not expressed in differentiated iPSCs (D-iPSCs) or precursor fibro blasts. These results suggest that the *TDRD12* gene behaves in a similar way at the transcription level as the *OCT4* gene does. This could implicate *TDRD12* as a stem cell marker gene.

The RT-PCR products for the *TDRD12* gene in iPSCs and ESCs were subjected to purification and sequencing to ensure that the correct DNA sequences were amplified (a summary of the results is given in Table 4.1). Quality assessments and controls were also carried out for the cDNA made from iPSCs, ESCs and D-iPSCs (see Figure 4.12, Figure 4.13 and Figure 4.15).

Figure 4.12 shows the RT-PCR analysis of *OCT4* and *TDRD12* gene expression in iPSCs. Figure 4.13 shows the RT-PCR analysis of *OCT4* and *TDRD12* gene expression in iPSCs and D-iPSCs. Figure 4.14 shows the RT-qPCR analysis of *OCT4* and *TDRD12* gene expression in iPSCs and D-iPSCs. Figure 4.15 shows the RT-PCR analysis of *OCT4* and *TDRD12* gene expression in ESCs. Finally, Figure 4.16 shows the RT-qPCR analysis of *OCT4* and *TDRD12* gene expression in ESCs. The normalising of *OCT4* and *TDRD12* gene expression was relative to the *GAPDH* and *HSP90AB1* genes. The expression of the *OCT4* gene was used as an SC marker. The expression of the *β-actin* gene was used as a quality control for the cDNA generated from SCs and differentiated SCs. As can be seen from the obtained RT-PCR results, the *β-actin*, *OCT4* and *TDRD12* PCR products were detected at approximately the expected sizes (553 bp, 872 bp and 409 bp, respectively).

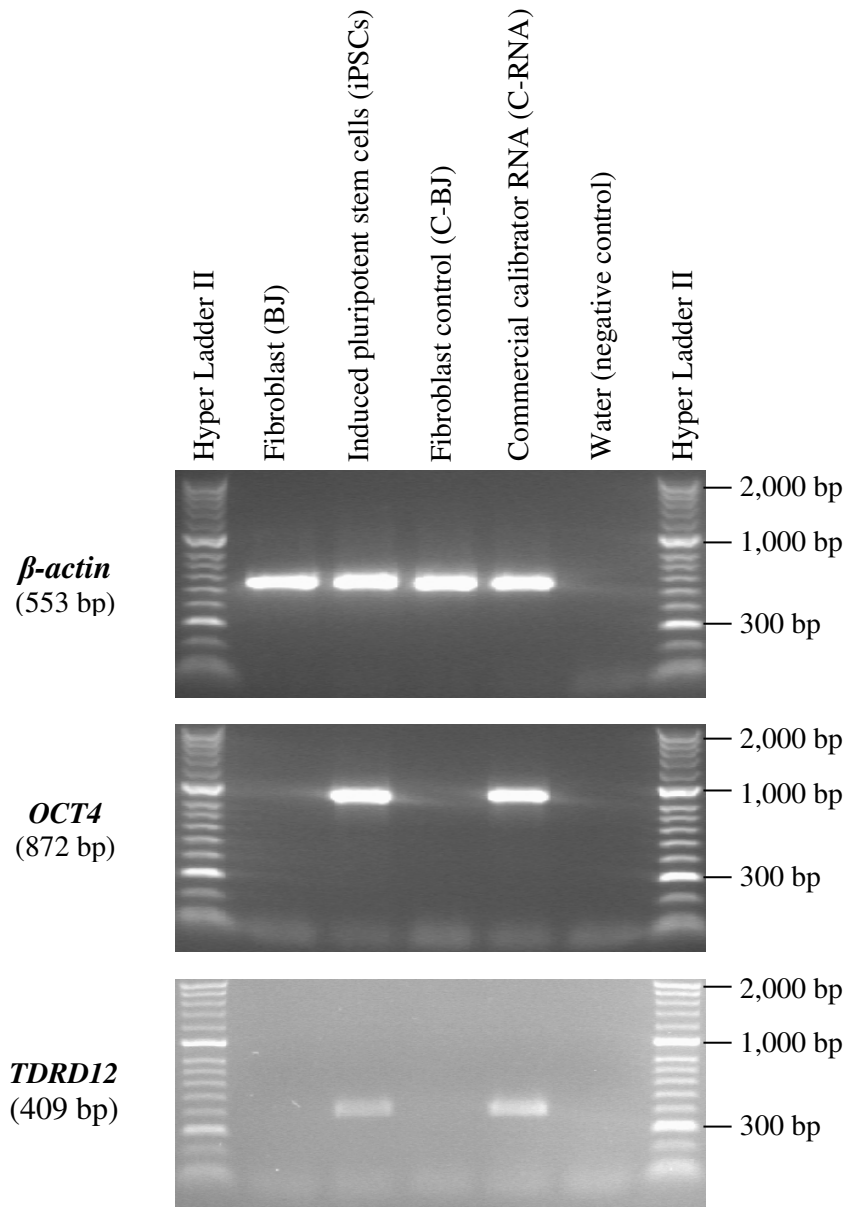

Figure 4.12 RT-PCR analysis of *OCT4* and *TDRD12* gene expression in human iPSCs.
The expression of the *β-actin* gene was used as a quality control for the generated cDNA; The expression of the *OCT4* gene was used as an SC marker. The BJ cells were used as negative controls for the iPSCs. The C-BJ cells were used as positive controls for the BJ cells. The C-RNA was used as a positive control for the iPSCs. The PCR products were detected at approximately the expected sizes (shown in parenthesis on the left).

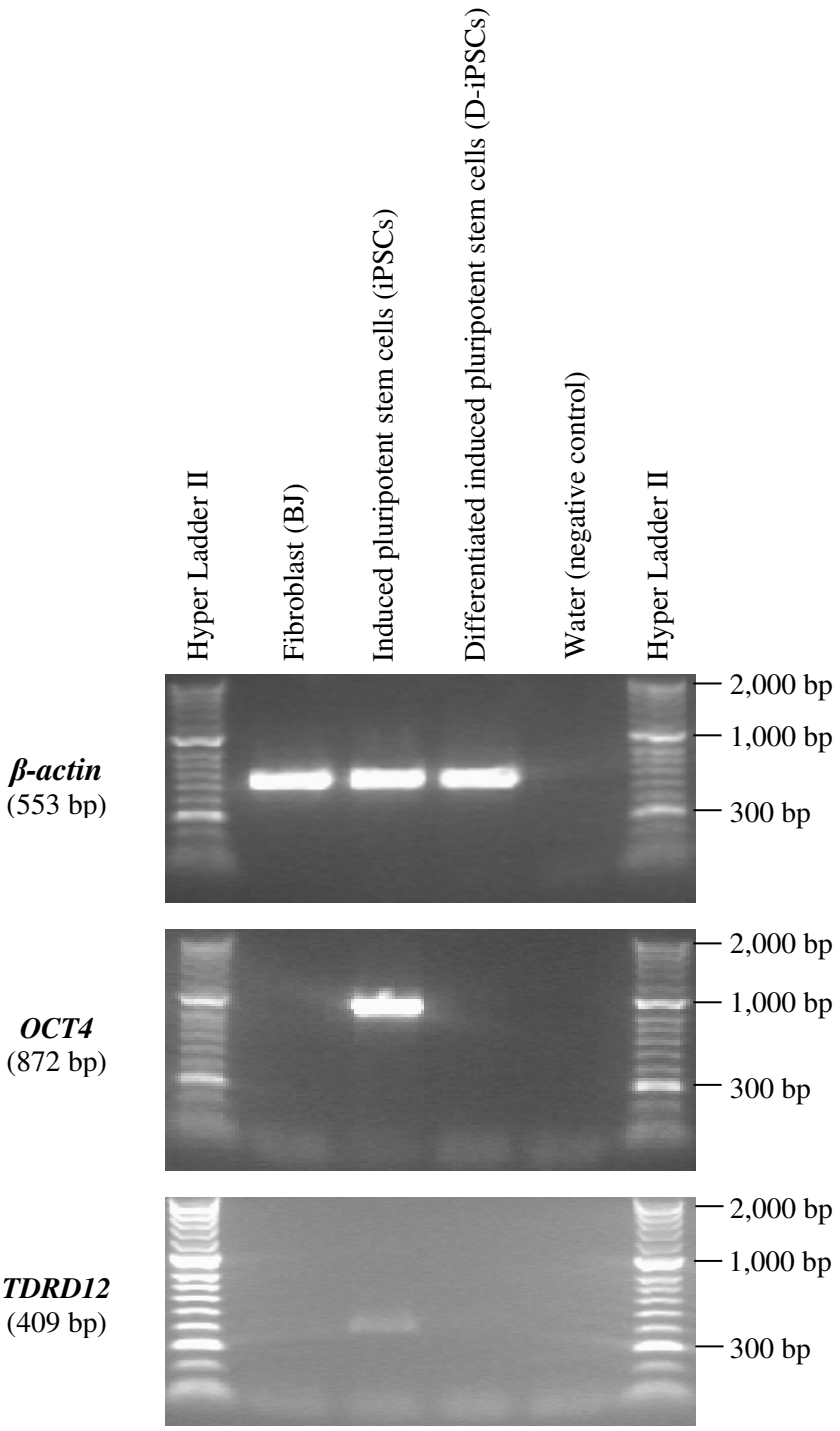

Figure 4.13 RT-PCR analysis of *OCT4* and *TDRD12* gene expression in human iPSCs and D-iPSCs.

The expression of the *β-actin* gene was used as a quality control for the generated cDNA. The expression of the *OCT4* gene was used as an SC marker. The BJ cells were used as negative controls for the iPSCs. The iPSCs were used as controls for the D-iPSCs. The PCR products were detected at approximately the expected sizes (shown in parenthesis on the left).

A.

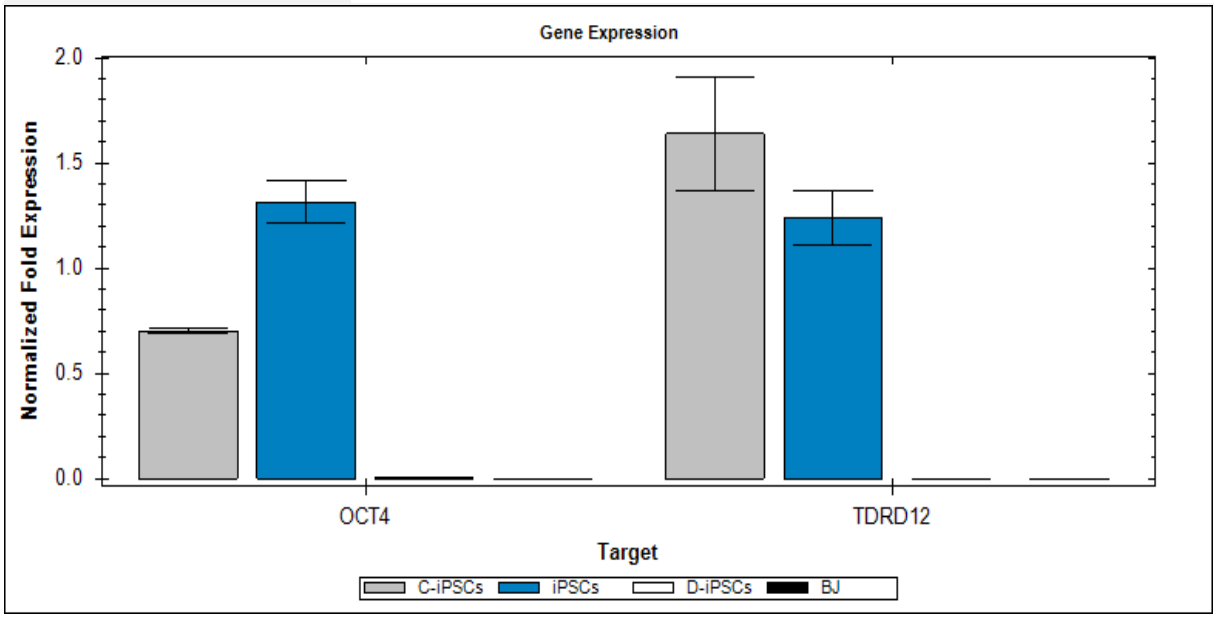

B.

Target	Sample	Wells	Cq Reading 1	Cq Reading 2	Cq Reading 3	Cq Mean	Cq Std. Dev
GAPDH	Fibroblast (BJ)	3	19.31	19.25	19.16	19.24	0.075
GAPDH	Induced pluripotent stem cells (iPSCs)	3	20.06	20.12	19.92	20.03	0.103
GAPDH	Induced pluripotent stem cells control (C-iPSCs)	3	19.20	19.27	19.31	19.26	0.056
GAPDH	Differentiated induced pluripotent stem cells (D-iPSCs)	3	20.46	20.46	20.36	20.43	0.058
HSP90AB1	Fibroblast (BJ)	3	23.25	23.34	23.23	23.27	0.054
HSP90AB1	Induced pluripotent stem cells (iPSCs)	3	21.16	20.95	21.15	21.09	0.115
HSP90AB1	Induced pluripotent stem cells control (C-iPSCs)	3	22.52	22.51	22.46	22.50	0.036
HSP90AB1	Differentiated induced pluripotent stem cells (D-iPSCs)	3	23.27	23.15	23.18	23.20	0.059
OCT4	Fibroblast (BJ)	3	38.04	37.23	38.48	37.91	0.635
OCT4	Induced pluripotent stem cells (iPSCs)	3	22.33	22.05	22.38	22.26	0.179
OCT4	Induced pluripotent stem cells control (C-iPSCs)	3	23.46	23.50	23.49	23.48	0.018
OCT4	Differentiated induced pluripotent stem cells (D-iPSCs)	3	33.61	33.69	33.67	33.66	0.041
TDRD12	Fibroblast (BJ)	0	N/A	N/A	N/A	N/A	0.000
TDRD12	Induced pluripotent stem cells (iPSCs)	3	34.35	34.33	34.77	34.48	0.250
TDRD12	Induced pluripotent stem cells control (C-iPSCs)	2	34.15	34.63	N/A	34.39	0.337
TDRD12	Differentiated induced pluripotent stem cells (D-iPSCs)	0	N/A	N/A	N/A	N/A	0.000

Figure 4.14 RT-qPCR analysis of *OCT4* and *TDRD12* gene expression in human iPSCs and D-iPSCs.
Panel (A): bar chart demonstrating the normalisation of the *OCT4* and *TDRD12* gene expression analysed by RT-qPCR. The Bio-Rad CFX Manager was used to analyse the data. The error bars show the standard error for three replicates. Panel (B): table illustrating the number of replications (wells) and the Cq (quantification cycle) mean, standard deviation and Cq readings for the *GAPDH* and *HSP90AB1* genes, to which the *OCT4* and *TDRD12* genes reading was normalised. The BJ cells were used as negative controls. The C-iPSCs (commercial calibrator RNA) were used as positive controls.

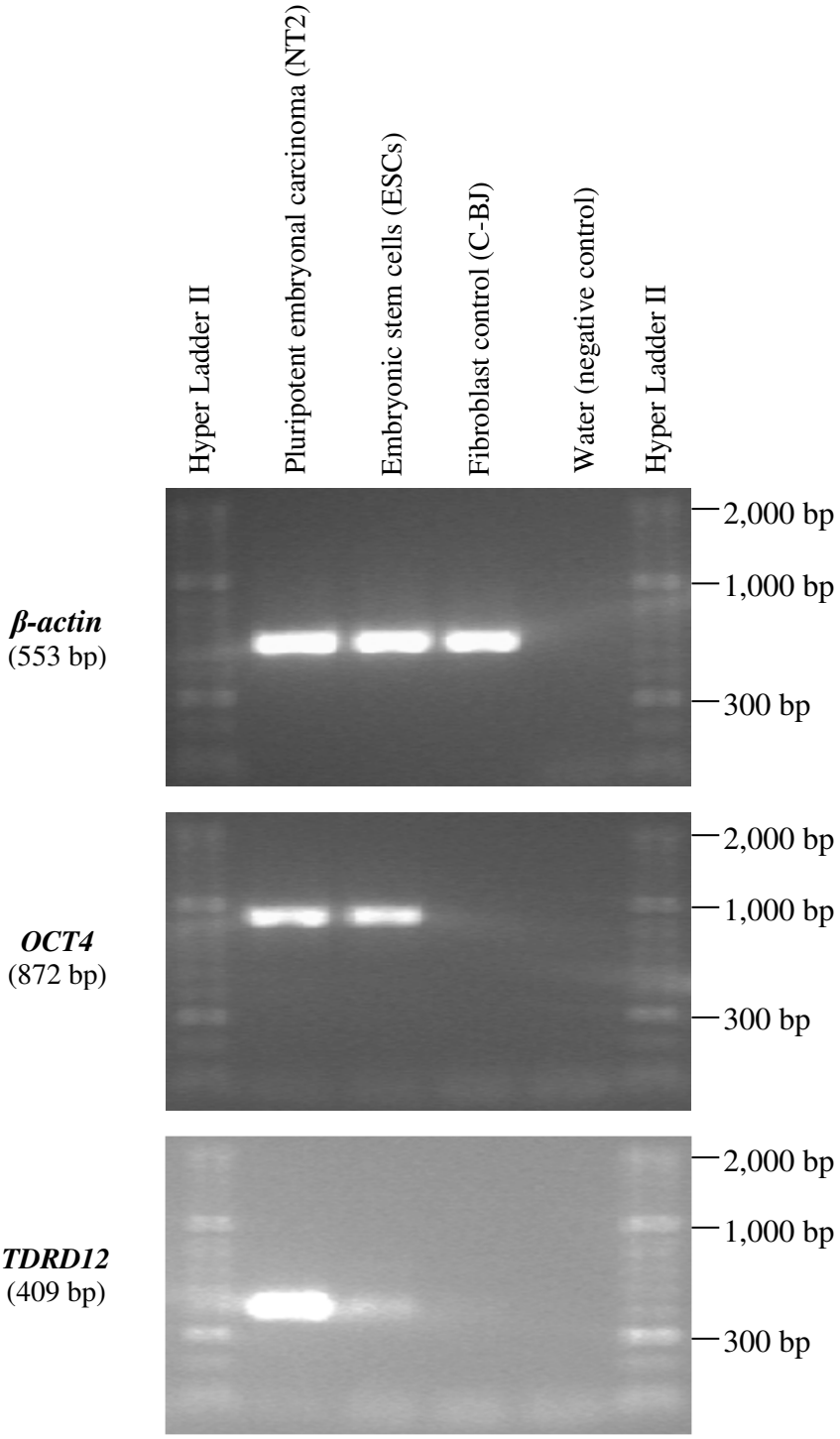

Figure 4.15 RT-PCR analysis of *OCT4* and *TDRD12* gene expression in human ESCs.
The expression of the *β-actin* gene was used as a quality control for the generated cDNA. The expression of the *OCT4* gene was used as an SC marker. The C-BJ cells were used as negative controls for the ESCs. The NT2 cells were used as positive controls for the expression of the *TDRD12* gene. The PCR products were detected at approximately the expected sizes (shown in parenthesis on the left).

A.

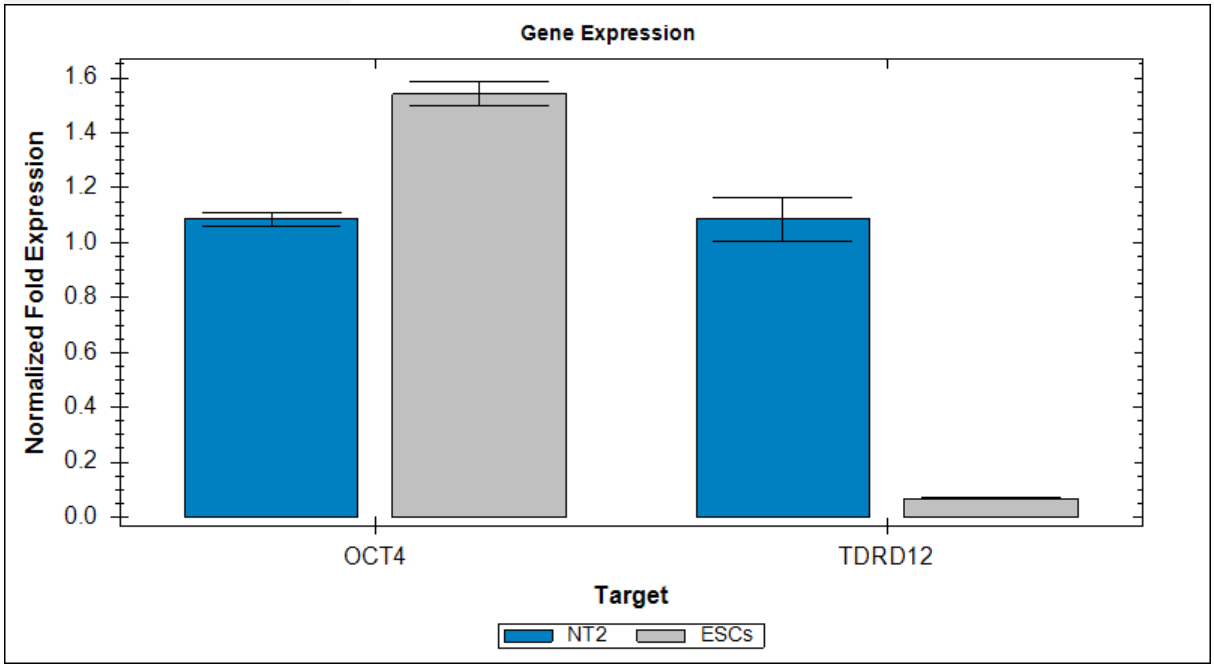

B.

Target	Sample	Wells	Cq Reading 1	Cq Reading 2	Cq Reading 3	Cq Mean	Cq Std. Dev
GAPDH	Embryonic stem cells (ESCs)	3	18.61	18.72	18.72	18.69	0.068
GAPDH	Pluripotent embryonal carcinoma cells (NT2)	3	16.49	16.41	16.49	16.46	0.048
HSP90AB1	Embryonic stem cells (ESCs)	3	20.27	20.09	20.25	20.20	0.096
HSP90AB1	Pluripotent embryonal carcinoma cells (NT2)	3	20.43	20.40	20.48	20.44	0.042
OCT4	Embryonic stem cells (ESCs)	3	21.88	21.91	21.97	21.92	0.044
OCT4	Pluripotent embryonal carcinoma cells (NT2)	3	21.49	21.40	21.42	21.44	0.046
TDRD12	Embryonic stem cells (ESCs)	3	30.50	30.16	30.26	30.31	0.173
TDRD12	Pluripotent embryonal carcinoma cells (NT2)	3	25.29	25.53	25.18	25.33	0.179

Figure 4.16 RT-qPCR analysis of *OCT4* and *TDRD12* gene expression in human ESCs.
Panel (A): bar chart demonstrating the normalisation of the *OCT4* and *TDRD12* gene expression analysed by RT-qPCR. The Bio-Rad CFX Manager was used to analyse the data. The error bars show the standard error for three replicates. Panel (B): table illustrating the number of replications (wells) and the Cq (quantification cycle) mean, standard deviation and Cq readings for the *GAPDH* and *HSP90AB1* genes, to which the *OCT4* and *TDRD12* genes reading was normalised. The NT2 cells were used as positive controls for the expression of the *TDRD12* gene.

4.3.3. Colonosphere formation and generation from human SW480

Other workers within our group have demonstrated that the colorectal cell line SW480 contains *OCT4* expressing cells that are thought to be a model for CSCs. These *OCT4* expressing cells are more enriched when SW480 is cultured as colonospheres. Spheres were generated to explore *TDRD12* expression in a CSC model. *SOX2* expression was assessed in SW480 spheres because *SOX2* is also a SC marker. To generate these CSC-enriched spheres, SW480 cells (parental cells) in the attached condition (pre-sphere) were suspended in serum-free media (SFM) mixed with DMEM/F12. Following this, the medium was supplemented within FGF, B27 and epidermal growth factors (EGF). The cells were cultured in ultra-low-attachment dishes for about five to seven days. This culturing of the SW480 cells resulted in a cell sphere (unattached individual parental SW480 cells forming a free-floating sphere colony) known as a human colonosphere/spheroid. The colonosphere was cultured back again in media with serum to re-attach the floating sphere and return the cell to the original epithelial morphology (post-sphere). Thus, three different conditions of SW480 cells were obtained, namely SW480 pre-sphere, SW480 sphere and SW480 post-sphere (see Figure 4.17).

cDNA was generated for every condition and then RT-PCR analysis was performed. The expression of the *β-actin* gene was used as a quality control for the cDNA generated (see Figure 4.17). The expression of the *SOX2* gene was used as an SC marker. As can be seen from the obtained RT-PCR results, the *β-actin*, *SOX2* and *TDRD12* PCR products were detected at approximately the expected sizes (553 bp, 590 bp and 409 bp, respectively). The RT-PCR products for the *TDRD12* gene in SW480 pre-sphere, SW480 sphere and SW480 post-sphere cells were subjected to purification and sequencing to ensure that the correct DNA sequences were being amplified (a summary of the sequencing results is given in Table 4.1).

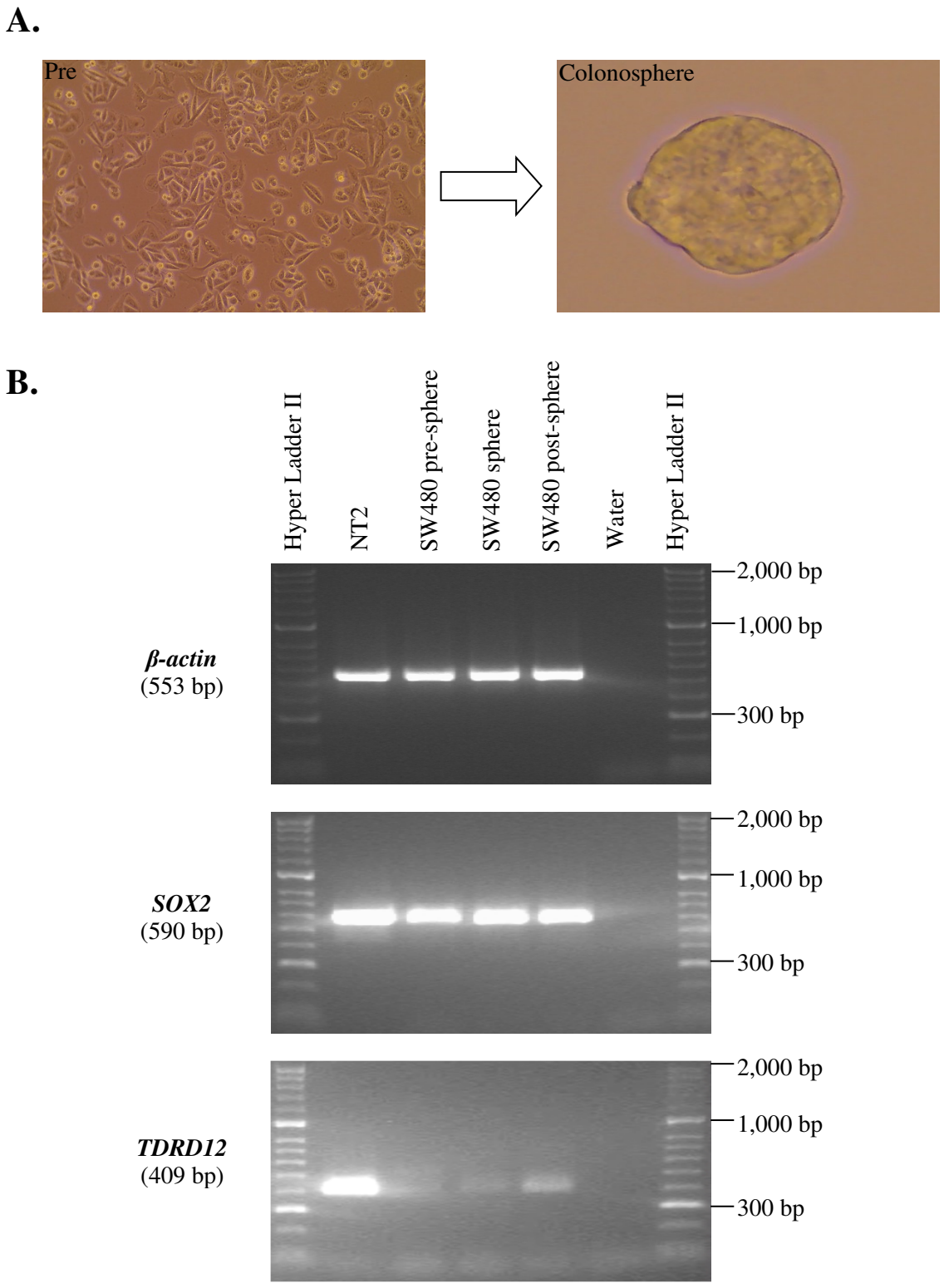

Figure 4.17 Colonosphere formation from human SW480.
(A) The left panel shows a characteristic image of SW480 cells (parental cells) in the attached condition (pre); the right panel shows a characteristic image of individual parental SW480 cells are to shape free-floating colonospheres/spheroids under specific conditions. The images were captured by Evos™ XL Core utilising a 20x objective lens. (B) RT-PCR analysis of *β-actin* (quality control), *SOX2* (SC marker) and *TDRD12* gene expression in NT2 cells as positive controls for the expression of the *TDRD12* gene in SW480 pre-sphere, SW480 sphere, SW480 post-sphere (re-attached condition) and water (negative control). The PCR products were detected at approximately the expected sizes (shown in parenthesis on the left).

4.3.4. RT-PCR analysis of the gene expression profiles of *TDRD12* and *SOX2* genes in several cancerous human cells, SCs and CSCs

The expression of the *TDRD12* and *SOX2* genes were analysed in NT2 cells (as positive controls for the expression of the *TDRD12* gene), SW480 pre-sphere, SW480 sphere, SW480 post-sphere, BJ, ESC, iPSC and D-iPSC cells (see Figure 4.18 and Figure 4.19). As a result, the *TDRD12* and *SOX2* genes were found to be expressed in NT2, SW480 pre-sphere, SW480 sphere, SW480 post-sphere, ESC and iPSC cells, but they did not show any expression in BJ or D-iPSCs (as previously shown; see Sections 4.3.2 and 4.3.3). The *SOX2* gene showed expression (intense band) in all the mentioned cells (NT2, SW480 pre-sphere, SW480 sphere, SW480 post-sphere, ESC and iPSC). However, the *TDRD12* gene showed an intense RT-PCR band only in NT2 cells while exhibiting a faint band in SW480 pre-sphere, SW480 sphere, SW480 post-sphere, ESC and iPSC cells.

Quality assessments and controls were also carried out for the cDNA made from NT2, SW480 pre-sphere, SW480 sphere, SW480 post-sphere, BJ, ESC, iPSC and D-iPSC cells (see Figure 4.18 and Figure 4.19). The expression of the *SOX2* gene was used as an SC marker. The expression of the *β-actin* gene was used as a quality control for the cDNA generated. As can be seen from the obtained RT-PCR results, the *β-actin*, *SOX2* and *TDRD12* PCR products were detected at approximately the expected sizes (553 bp, 590 bp and 409 bp, respectively).

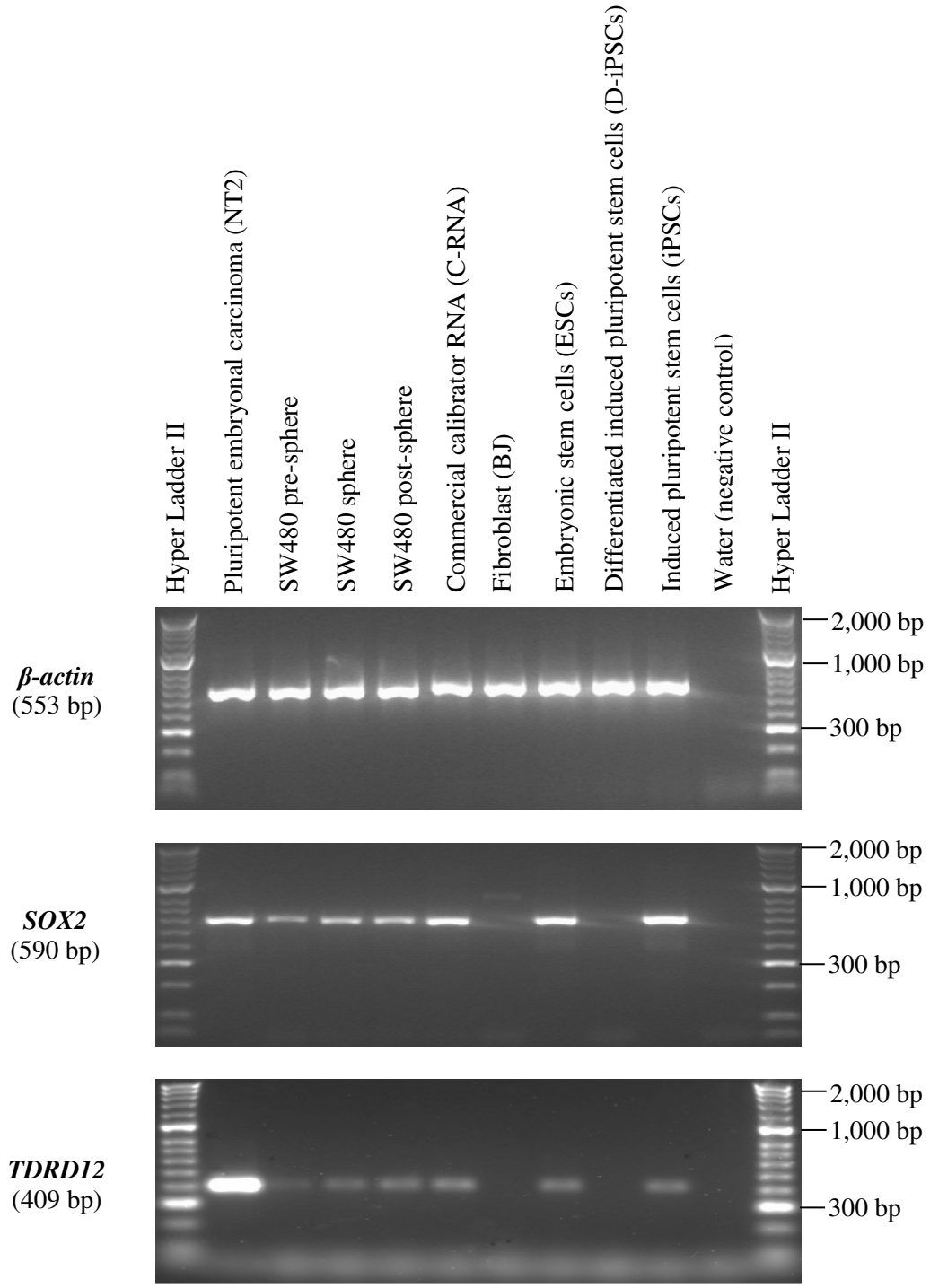

Figure 4.18 RT-PCR analysis of *SOX2* and *TDRD12* gene expression in several human cancerous cells, SCs and CSCs.
The expression of the *β-actin* gene was used as a quality control for the generated cDNA. The expression of the *SOX2* gene was used as an SC marker. The NT2 cells were used as positive controls for the expression of the *TDRD12* gene. The BJ cells were used as negative controls for the SCs. The C-RNA was used as a positive control for the SCs. The PCR products were detected at approximately the expected sizes (shown in parenthesis on the left).

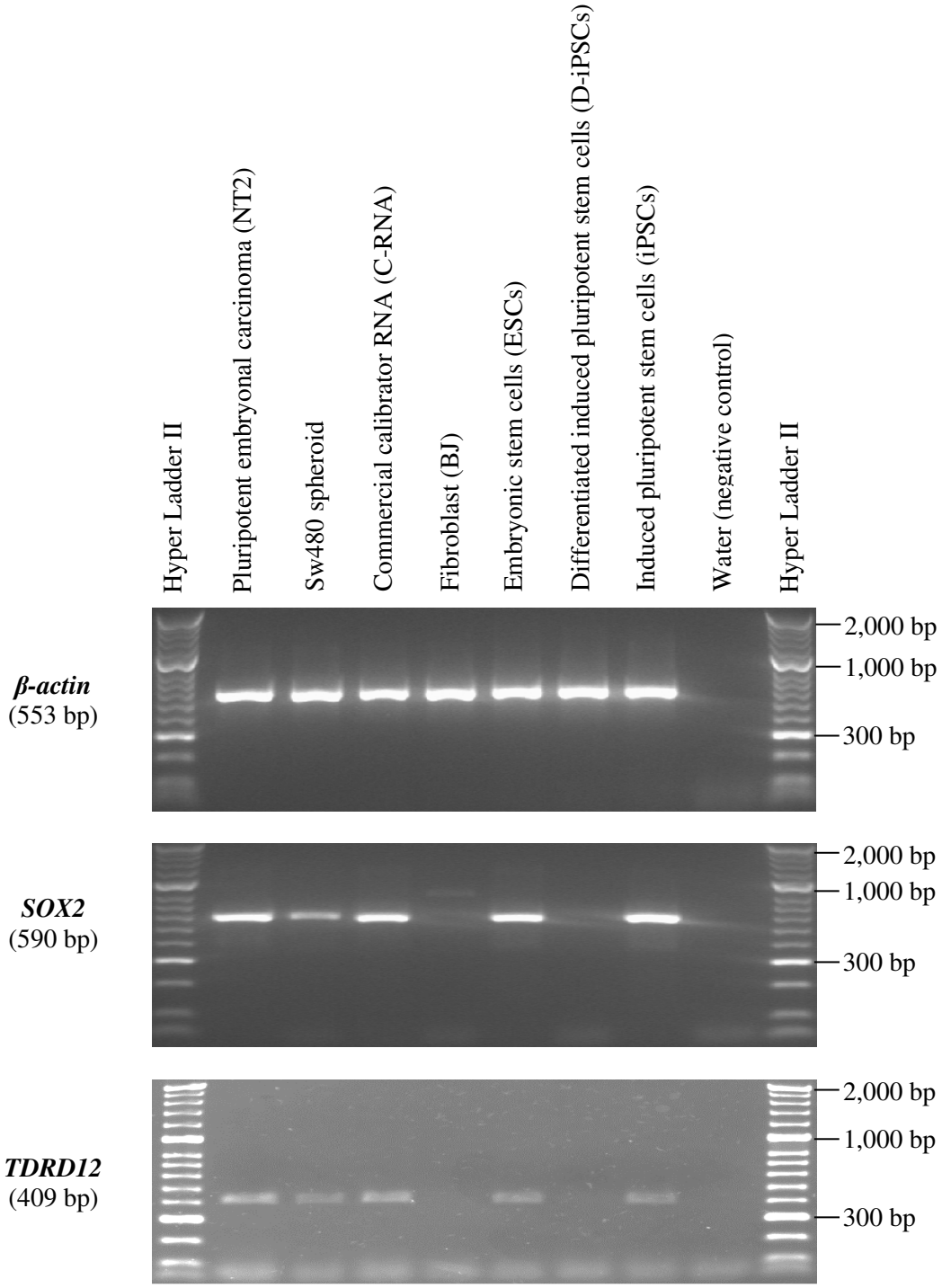

Figure 4.19 RT-PCR analysis of *SOX2* and *TDRD12* gene expression in several human cancerous cells, SCs and CSCs.
The expression of the *β-actin* gene was used as a quality control for the generated cDNA. The expression of the *SOX2* gene was used as an SC marker. The NT2 cells were used as positive controls for the expression of the *TDRD12* gene. The BJ cells were used as negative controls for the SCs. The C-RNA was used as a positive control for the SCs. The PCR products were detected at approximately the expected sizes (shown in parenthesis on the left).

4.3.5. *OCT4* expression in *TDRD12* depleted cells

Given that *TDRD12* might be linked to stem-like function, we explored possible relationship with stem-like factors. NT2 is pluripotent and expresses the SC marker gene *OCT4*. We analysed *OCT4* expression in *TDRD12* depleted NT2 cells to assess any regulatory link. *TDRD12* expression was reduced in NT2 cells using three different *TDRD12-001* siRNAs (siRNA1, siRNA3 and siRNA4), and a combination of the three siRNAs was also utilised (siRNA1+3+4). The *TDRD12-001* siRNA treatments were used for three days (3 "hits"). The three types of *TDRD12-001* siRNAs and the combination of these siRNAs were sufficient for reducing the levels of *TDRD12* transcripts (siRNA1 [96.26%], siRNA3 [93.69%], siRNA4 [89.35%] and siRNA1+3+4 [92.39%]) (data for RT-qPCR showing levels of *TDRD12* transcript depletion are shown in Section 5.3.1; RNA from these cells was used to analyse *OCT4* transcript levels). Figure 4.20 (below) shows the RT-PCR analysis results of *OCT4* gene expression in *TDRD12-001*-depleted NT2 cells; it can be seen that the *OCT4* gene remained active (intense band). Figure 4.21 shows the analysis of *OCT4* gene expression was normalised relative to the expression of *Tubulin* and *Lamin* genes; it was observed that *OCT4* expression is down-regulated slightly by about 8.07%. The biological significance of this is unclear.

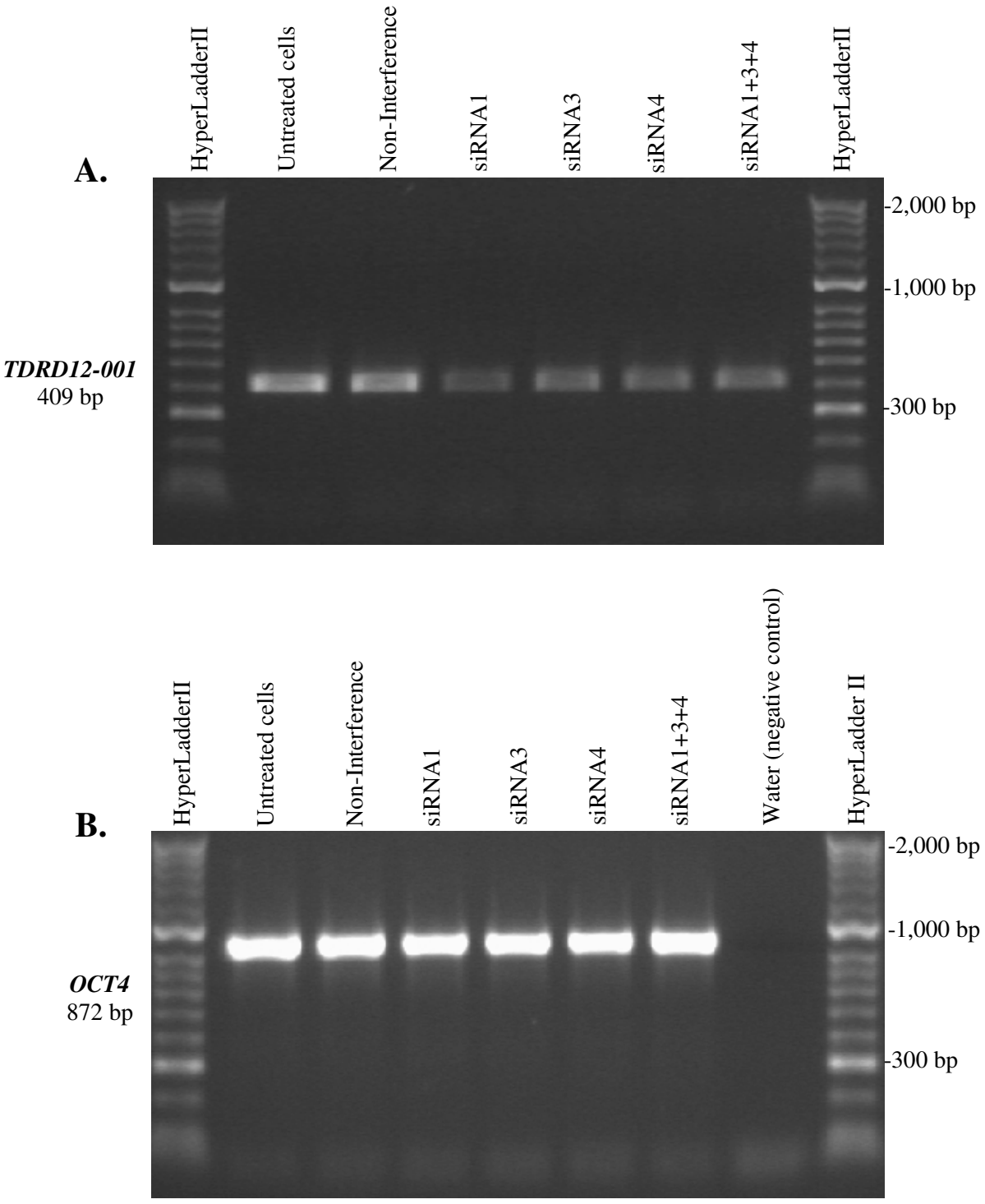

Figure 4.20 RT-PCR analysis of *OCT4* gene expression in human *TDRD12-001*-depleted NT2 cells.

Agarose gels presenting the RT-PCR profile created from the NT2 cells. Panel (A): RT-PCR analysis of *TDRD12-001* expression in siRNA-treated NT2 cells indicates downregulation of *TDRD12-001* (see Figure 5.3 for RT-qPCR data). Panel (B): RT-PCR analysis of *OCT4* gene expression in *TDRD12-001*-depleted NT2 cells. The RT-PCR products for the *OCT4* and *TDRD12-001* migrated close to the expected sizes.

A.

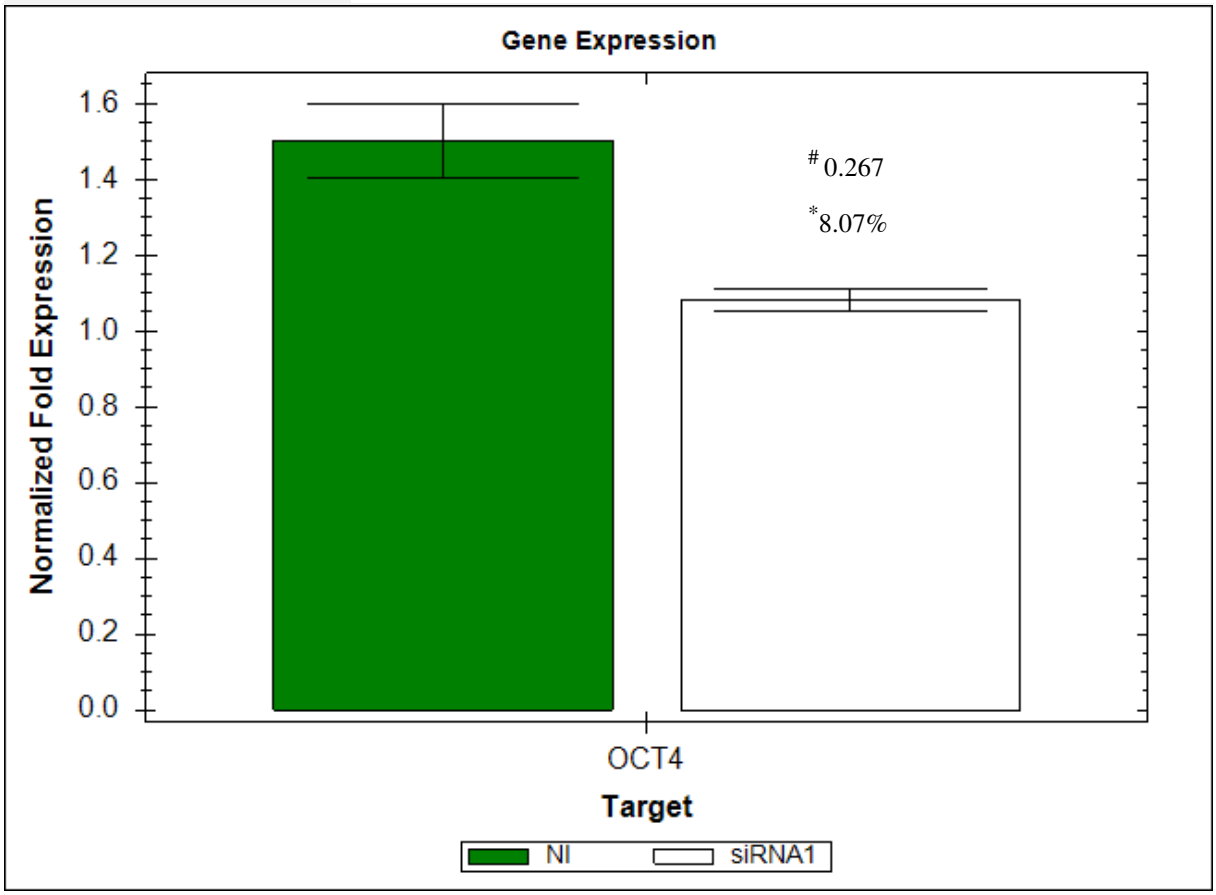

B.

Target	Sample	Relative Quantity	Wells	Cq Reading 1	Cq Reading 2	Cq Reading 3	Cq Mean	Cq Std. Dev
Lamin	Non-Interference	0.37529	3	25.10	25.13	25.08	25.10	0.028
Lamin	siRNA1	1.00000	3	23.75	23.64	23.68	23.69	0.055
Tubulin	Non-Interference	1.00000	3	19.40	19.34	19.24	19.33	0.084
Tubulin	siRNA1	0.85492	3	19.62	19.56	19.47	19.55	0.075
OCT4	Non-Interference	0.91934	3	21.24	21.53	21.27	21.35	0.159
OCT4	siRNA1	1.00000	3	21.18	21.22	21.27	21.22	0.045

Figure 4.21 RT-qPCR analysis of *OCT4* gene expression in human *TDRD12-001*-depleted NT2 cells.
Panel (A): bar chart demonstrating the normalisation of the *OCT4* gene expression analysed by qRT-PCR. The Bio-Rad CFX Manager was used to analyse the data. The error bars show the standard error for three replicates. Panel (B): table illustrating the number of replications (wells) and the Cq (quantification cycle) mean, standard deviation and Cq readings for the *Tubulin* and *Lamin* genes, to which the *OCT4* reading was normalised. * Expression percentage differences between control (NI) and different samples; # P-Value; (NI) cells treated with non-interfering siRNA.

Table 4.1 Sequencing results of RT-PCR screening for *TDRD12* gene expression in selected cancerous human cells, SCs and CSCs.
This table offers a summary of the PCR product sequencing results; these products were first purified and then sent to Eurofins MWG Operon Company for sequencing to confirm that the right sequences were being amplified.

Gene	Primer	Cell type	Sequence identity (%) in SCs
TDRD12	Primer set 3 (forward)	SW480 pre-sphere	100%
TDRD12	Primer set 3 (forward)	SW480 sphere	100%
TDRD12	Primer set 3 (forward)	SW480 post-sphere	99%
TDRD12	Primer set 3 (forward)	ESCs	99%
TDRD12	Primer set 3 (forward)	iPSCs	99%

4.4. Discussion

4.4.1. Human cancers, CSCs and ESCs share some similarities

CSCs share some features and regulatory mechanisms within ESCs (e.g., differentiation, migration and self-renewal). They both have the ability to undergo rapid clonal growth and proliferation. Furthermore, they contribute to some signalling pathways involved in the development of human embryonic and malignant tumours and cancer. Thus, understanding the processes involved CSC self-renewal and resistance to treatments is essential to enhance the efficiency of anti-cancer medications by targeting these CSCs (Dreesen and Brivanlou, 2007; Ebben *et al.,* 2010; Vishnoi *et al.,* 2015; Weissman, 2015).

NT2 cells represent an excellent *in vitro* cellular system for studying SC differentiation, as these cells have been utilised as models for analysing neuronal differentiation, CSCs and ESCs (Ceci *et al.,* 2015; Lin *et al.,* 2012; Pal and Ravindran, 2006; Serra *et al.,* 2009; Terrasso *et al.,* 2015; Yang *et al.,* 2012). Moreover, the *TDRD12* gene is expressed in NT2 cells (Chapter 3; Feichtinger *et al.,* 2012). Furthermore, colonospheres/spheroids, which are enriched for CSCs, have been reported to be successfully created with high efficiency from several cancerous tumours, including SW480 cells (Chen *et al.,* 2011b; Fanali *et al.,* 2014; Kanwar *et al.,* 2010). Therefore, SW480 cells were used in this analysis to form spheres to analyse the expression of *TDRD12* and SC marker genes.

4.4.2. The formation of human CSCs

Malignant and solid tumours exhibit a heterogeneous mixture of diverse cell types, which have functional differences (Meacham and Morrison, 2013). Malignant and solid tumours are composed of SC-like cells, which have the ability to differentiate and proliferate into heterogeneous human cancer cell lineages (Clevers, 2011; Magee *et al.,* 2012). CSCs are found in several kinds of solid tumours (e.g., colorectal tumours) (Jones *et al.,* 2015).

One of the key advances in CSC studies is the ability to form colonospheres/spheroids and raise them in specific media (SFM) containing cell growth factors (under unattached conditions). Colonosphere generation was first identified in normal SCs. After that, it was reported in several cancerous cells when tumours (including tumours of the colon, ovary, pancreas, prostate and breast) were found to have the ability to form spheroids. The approach of non-adherent sphere culturing has many advantages; most important is that it has the ability to isolate and enrich cell populations, which are isolated with CSC-like traits. Moreover, more

tumourigenicity in the spheroid state is apparent (Mathews *et al.,* 2013; Sukach and Ivanov, 2007). These types of cells have the capacity to self-renew and differentiate, as well as to express many kinds of SC markers. Furthermore, they show elevated resistance in the face of irradiation and chemotherapy treatments (Dotse and Bian, 2014; Zhong *et al.,* 2010).

4.4.3. Differentiation of human NT2 cells

SCs are significant cellular resources with potential roles in cell therapies. One of the fundamental tasks is to develop systems for *in vitro* differentiation and/or SC expression (Goodell *et al.,* 2015; Serra *et al.,* 2009). NT2 cells are good models for *in vitro* analysis of the mechanisms which regulate differentiation in the early embryogenic stage. NT2 cells represent highly malignant tumours, which are able to differentiate into several kinds of cells. The undifferentiated elements of the tumour cells contain either malignant pluripotent SCs or embryonal carcinoma cells, which are usually observed in the cultures as embryoid body–like structures. These differentiated cells could be histologically positive and helpful for numerous kinds of somatic tissues (e.g., nerves, muscles and bones), thereby shaping the elements of differentiation for these tumour cells (Ceci *et al.,* 2015; Goh *et al.,* 2013; Simoes and Ramos, 2007). NT2 cells express pluripotency markers of ESCs (e.g., *SOX2*, *NANOG* and *OCT4*). Due to the similarities between both cell types (ESCs and NT2), in the expression profiles of genes, growth and potency, NT2 cells are believed to be the malignant equivalent of ESCs. Hence, these cells are good models for analysing tumourigenesis. Moreover, they can be used to analyse particular parts of pluripotency and cellular differentiation (Andrews *et al.,* 1985; Coyle *et al.,* 2011; Pal and Ravindran, 2006; Schwartz *et al.,* 2005; Yang *et al.,* 2012).

4.4.4. The association between *TDRD12* and SC marker genes

The original finding that *TDRD12* was expressed in NT2 cells inferred that it could be associated with stemness. However, the results obtained in this Chapter suggested that differentiation of NT2 with RA and HMBA did not cause silencing of *TDRD12*. The results also suggested that the *TDRD12* gene does not behave in the same way at the transcriptional level as the SC marker genes do. To explore this further, the expression profiles of *TDRD12* and SC marker genes were analysed in iPSCs, ESCs and D-iPSCs. As a result, the *TDRD12* gene was found to be expressed in iPSCs and ESCs. In contrast, *TDRD12* was not expressed in D-iPSCs or precursor fibroblasts. These results suggest that the *TDRD12* gene behaves in a similar way at the transcription level as the SC marker genes do in that it is expressed in stem

cell. This could implicate *TDRD12* as a stem cell marker gene and the failure to inactivate *TDRD12* upon differentiation of NT2 would be specific to this cell model and may not be a normal feature of *TDRD12*. SW480 cells were also cultured as colonospheres and these cells were generated to explore *TDRD12* expression in a CSC model. The results suggested that the *TDRD12* gene also behaves in a similar way at the transcription level as the SC marker genes. The aim of Figure 4.22 below is to help determine whether the *TDRD12* gene could be functionally linked to SC marker gene functions.

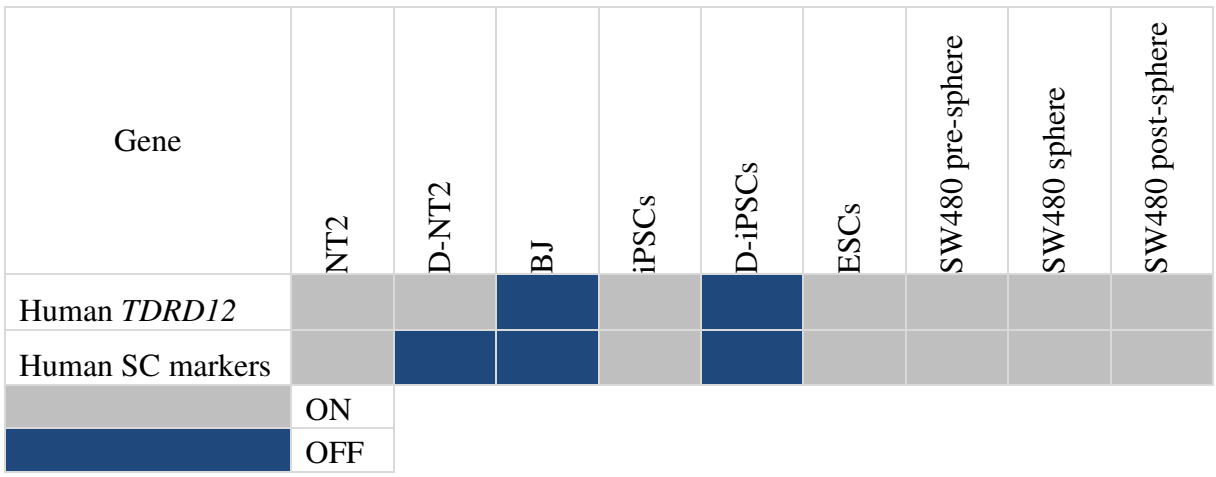

Figure 4.22 Summary of RT-PCR analysis of expression for *TDRD12* and SC marker genes in several human SC, CSC and cancerous cells.
The expression of *TDRD12* and SC marker genes are shown in grey and dark blue. Grey denotes the switching on of genes in the cells, while dark blue denotes the switching off of genes. It can be clearly observed that there might be an association between the *TDRD12* and SC marker genes.

4.5. Concluding remarks

Human CSCs are promising targets for new human cancer therapies; they are also important tools in molecular cancer research. The discovery of specific novel biomarkers of CSCs has shown that they are promising targets for the development of drugs and the early diagnosis of cancers. Therefore, more research is required in to the molecular biology of CSCs (García Martinez and Nogués, 2014; Rajendran and Dalerba, 2014). Consequently, this Chapter focussed on the *TDRD12* gene function linked to SC markers. Moreover, it highlighted a potential function of the *TDRD12* gene in the specificity of SCs and CSCs (Feichtinger *et al.,* 2012).

The RT-PCR and RT-qPCR analysis techniques were used to address the hypothesis. The results suggested that there might be an association between the *TDRD12* and SC marker genes. Furthermore, the expression of the *TDRD12* gene is elucidated in NT2, iPSC, ESC, SW480 pre-sphere, SW480 sphere and SW480 post-sphere cells. The results also suggested that the *TDRD12* gene might have SC and CSC specificity; thus, it is inferred that it might play a role in conferring stemness on cancer cells. In Chapter 5, *TDRD12* is analysed to determine if this gene is required for the human germ-line/SC regulation of retro elements (REs) in germ-line tumour cells.

5. *TDRD12* is required for the regulation of retro element (RE) expression in human germ-line tumour cells

5.1. Introduction

PIWI proteins refer to a particular subclade belonging to the proteins of the Argonaute family (Iwasaki *et al.,* 2015). This family has four kinds of PIWI proteins, which are produced in humans, namely PIWIL1/HIWI, PIWIL2/HILI, PIWIL3 and PIWIL4/HIWI2 (Hashim *et al.,* 2014). The human PIWI/piRNA cellular pathway is an epigenetic and genetic regulatory mechanism that carries out a vital function in developing human germ-line cells through the regulation of transposons, as well as other targets involved in the maintenance of human genomic integrity (Hirakata and Siomi, 2015; Iwasaki *et al.,* 2015). The functional aspects of PIWI proteins in germ-line development have been examined and analysed in detail, but recent studies suggest that *PIWIL1* and *PIWIL2* show aberrant expression in several types of cancers and solid tumours (Hirakata and Siomi, 2015; Iwasaki *et al.,* 2015; Sasaki *et al.,* 2003; Suzuki *et al.,* 2012).

5.1.1. Argonaute proteins family and small regulatory types of human RNA

In the last decade, it has been documented that several non-protein-coding sections of the genome are transcribed, and that such non-coding RNA sections are vital for the proper biological functioning and subsequent development of diseases in human hosts (Esteller, 2011; Hashim *et al.,* 2014). The biological importance of non-coding RNAs in humans is most obvious in the functions of the smaller types of RNAs that regulate protein production via complementary association with the specific RNA targets.

Currently, three main categories of smaller regulatory RNA have been characterised and recognised: microRNA (miRNA), short-interfering RNA (siRNA), and PIWI-interacting RNA (piRNA) (Dyawanapelly *et al.,* 2015; Farazi *et al.,* 2008; Ghildiyal and Zamore, 2009; Kim *et al.,* 2009; Suzuki *et al.,* 2012). The defining characteristics of smaller regulatory RNA include their short length, consisting of about 20–33 nucleotides, and the interactions carried out with the Argonaute family of proteins (Huang *et al.,* 2014).

The proteins of the Argonaute family consist of conserved proteins with an approximate size of 95 kDa, and are recognised by the presence of two main protein motifs: the human PAZ domain, which consists of a motif that binds nucleic acid, and the human PIWI domain, which has an RNase H fold (Swarts *et al.,* 2014). On the basis of the similar amino acid sequences, the proteins of the Argonaute family may be further sub-divided into two subclades: the human AGO proteins, which are named after the species in which they first identified, *Arabidopsis thaliana*, and the human PIWI proteins, which were named after the *Drosophila* protein PIWI (see Table 5.1) (Carmell *et al.,* 2002; Huang and Li, 2014; Parker and Barford, 2006; Suzuki *et al.,* 2012; Swarts *et al.,* 2014).

Table 5.1 Proteins of the human Argonaute family.
Adapted and modified from (Suzuki *et al.,* 2012).

	AGO		PIWI
Expression	All tissues		Germ-line and cancer
Human	AGO1, AGO2, AGO3 and AGO4		PIWIL1, PIWIL2, PIWIL3 and PIWIL4
Bound small RNA	miRNA	siRNA	piRNA
Nucleotide length	20-23	20-23	25-31
Function	Regulation of mRNA stability and translation	Regulation of transposon, protection from viral infection	Regulation of transposon

A number of proteins that have TUDOR domains have recently been examined and analysed in detail, due to the PIWI interactions they participate in, as well as their functional association with piRNAs (Hirakata and Siomi, 2015). Recent studies have demonstrated that *PIWIL1* expression is related to DNA methylation in cases of sarcoma, since down-regulation of *PIWIL1* decreases the total DNA methylation and places limitations on malignant tumour growth (Suzuki *et al.,* 2012). PIWI proteins might also be implicated in post-transcriptional regulatory control of oncogenes. PIWI proteins are altered after translation at their N termini through symmetrical dimethyl arginine (sDMA) marks that function as ligands for the TUDOR domains located on TDRD proteins (Grivna *et al.,* 2006a; Grivna *et al.,* 2006b; Hirakata and Siomi, 2015; Siomi *et al.,* 2010; Suzuki *et al.,* 2012).

5.1.2. Human REs associate with human disorders

REs refer to a large group of non-coding DNA that is found in approximately 50% of the genomes of both genders (Chénais, 2015; Guidez, 2014). These REs are known to "jump" via a process of retro-transposition, rearranging the genome through 5′ and 3′ transduction. They also encourage or inhibit the process of gene transcription by providing alternative promoters, or through the generation of antisense and/or controlling non-coding RNA. The latest evidence implies that the REs insert themselves into the introns and exons of human genes, resulting in diverse kinds of human genetic diseases and the development of various genetically inherited disorders, such as cancerous growths and solid tumour development (Guidez, 2014; Kaer and Speek, 2013). Approximately 0.27% of human genetically inherited disorders are due to REs (Callinan and Batzer, 2006). REs have an impact on the function of human gene expression in the following ways:

- Silencing by human RNA interference (RNAi) pathways.
- Provision of alternative promoters.

The RNAi pathways silence the expression of REs, resulting in a significant human genome regulation mechanism (Kaer and Speek, 2013).

5.1.3. Human endogenous retro viruses (HERVs)

Around 8% of the genomes of both genders is comprised of HERV families. The HERVs are derivatives of REs with insufficient genetic information to form active viral particles. Nevertheless, a number of HERVs are expressed in a range of cancerous cells and malignant tumours; the significance of this is poorly understood (Chénais, 2015; Knisbacher and Levanon, 2015; Suntsova *et al.,* 2015). Sequences located on the long terminal repeat (LTR) elements of HERVs can modify the neighbouring genes by changing their expression patterns (Kim, 2012; Suntsova *et al.,* 2015). Moreover, HERVs have the ability to effect human germ-line cells. There are four types of HERVs: HERV-W, HERV-R, HERV-H, and HERV-K. Each has four types of basic genes, which are *gag*, *pro*, *pol*, and *env*. The *gag* gene encodes for the expression of the human structural matrix (MA), the *env* gene encodes for the production of both envelope surface (SU) and trans-membrane (TM) proteins, the *pol* gene encodes for the secretion of enzymes that participate in reverse transcriptase (RT) and integrase (IN), and the *pro* gene encodes for the expression of human protease (PR) protein (see Figure 5.1) (Kim, 2012; Malfavon-Borja and Feschotte, 2015; Suntsova *et al.,* 2015; Tselis and Booss, 2014).

It has been documented that the genomes of both genders have approximately 30 to 50 distinct HERV-K proviruses. Some of these [HERV-K101, K102, K103, K104, K106, K107 (K10), K108 (HLM-2), K109] have already been proven to be specific to humans, and they have complete or full-length open reading frames for retroviral protein precursors (Contreras-Galindo *et al.,* 2015; Gonzalez-Hernandez *et al.,* 2014; Kim, 2012).

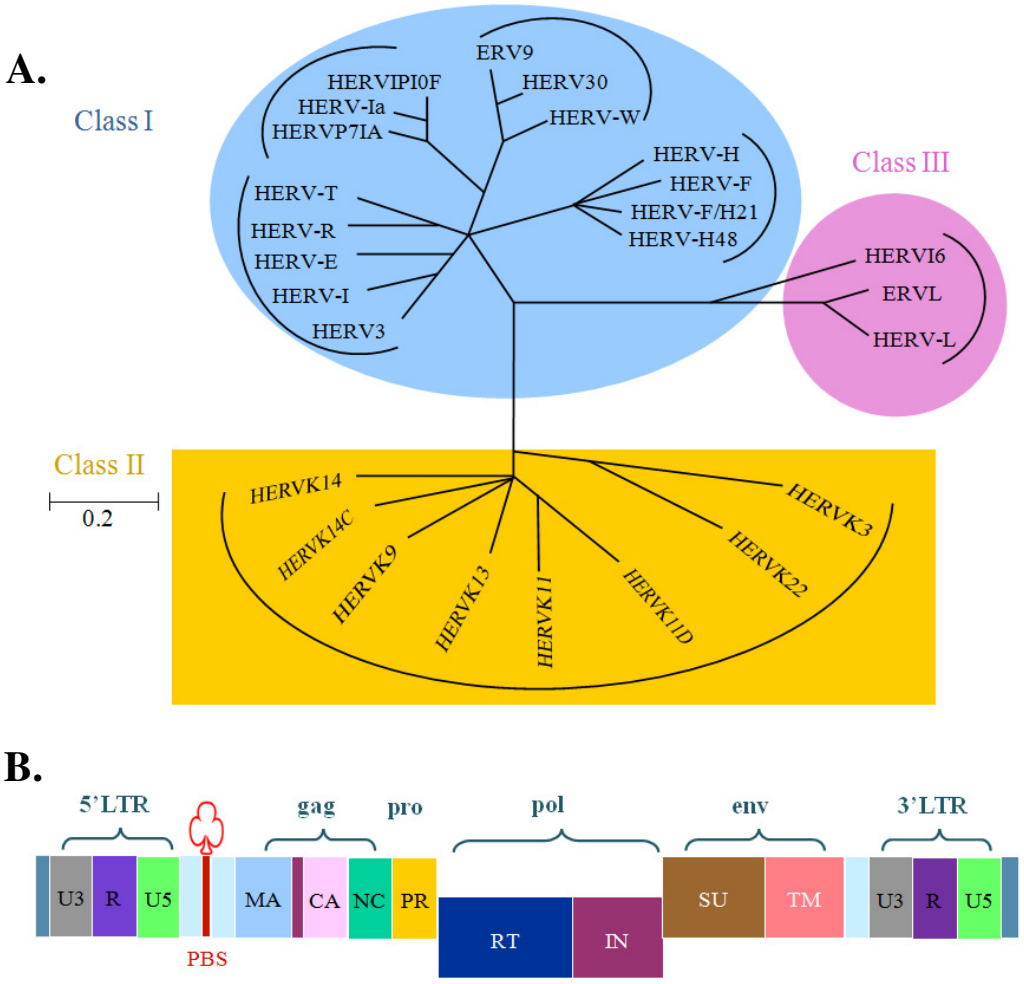

Figure 5.1 Schematic diagram showing the phylogenetic tree of the *pol* sequence homology.
Panel (A): The human genome and structural details of the HERVs that have the following genes: *env*, *gag*, *pol*, and *pro* (B). The LTR is made up of the U3, R and U5 elements, while PBS represents the primer binding sites.
Adapted from (Kim, 2012).

5.2. Aims

The work described in this Chapter aims to determine if the *TDRD12* gene regulates HERV and RE gene expression levels in human germ-line tumour cells.

The *TDRD* genes have high rates of expression in the germ-line. They are highly related and are involved in the piRNA pathway during gametogenesis (Chen *et al.,* 2011; Zhou *et al.,* 2014). The piRNA pathway is responsible for providing protection against REs. Moreover, the *TDRD12* gene has been recognised as a unique piRNA biogenesis factor in mice (Pandey *et al.,* 2013). *TDRD12* is also present in complexes with the PIWIL2 protein, which is linked to primary piRNA, as well as the TDRD1 protein in mice (Pandey *et al.,* 2013). In addition, the *TDRD12* gene is also necessary for the process of spermatogenesis and is required during the biogenesis of *PIWIL4* piRNA (Lim *et al.,* 2014; Pandey *et al.,* 2013; Zhou *et al.,* 2014).

5.3. Results

5.3.1. Analysis of the expression of the *TDRD12-001* transcript in siRNA-treated NT2 cells

To determine if RE and HERV expression levels in germ-line tumour cells are controlled by *TDRD12*, *TDRD12* expression was reduced in NT2 cells using siRNA (*TDRD12* is expressed in these cells; Chapter 3). The knockdown procedure was carried out using three different *TDRD12-001* siRNAs (siRNA1, siRNA3 and siRNA4), and a combination of the three siRNAs was also utilised (siRNA1+3+4). The *TDRD12-001* siRNA treatments were given on three days (3 "hits"). The total RNA was extracted from the siRNA *TDRD12-001*-depleted NT2 cells and cDNA was generated. Quality assessments and controls were carried out for the RNA extracted and cDNA generated. The expected sizes of 28S and 18S RNA fragments were 1,800 bp and 900 bp, respectively, and the RNA bands were detected at approximately the expected sizes. The expression of the *β-actin* gene was used as a quality control for the cDNA generated. The *β-actin* PCR products were detected at approximately the expected sizes (553 bp) (see Figure 5.2).

As can be seen from the results (Figure 5.2 and Figure 5.3), the three types of *TDRD12-001* siRNAs and the combination of these siRNAs were sufficient for reducing the levels of *TDRD12* transcripts (siRNA1 [96.26%], siRNA3 [93.69%], siRNA4 [89.35%] and siRNA1+3+4 [92.39%]). Based on these results, *TDRD12-001* siRNA1 was used in performing the analysis of RE/HERV expression, as it showed the highest percentage of gene knockdown. After that, the *TDRD12-001* transcript was knocked down again three times using *TDRD12-001* siRNA1 for further confirmation of the result; again, good depletion was obtained (94.59%, 95.57% and 98.21%). Quality assessments and controls were also conducted for the RNA extracted and the cDNA made from the siRNA1 knockdown of *TDRD12-001*-depleted in NT2 cells. The expected sizes of 28S and 18S RNA fragments were observed. The expression of the *β-actin* gene was used as a quality control for the cDNA (see Figure 5.4 and Figure 5.5).

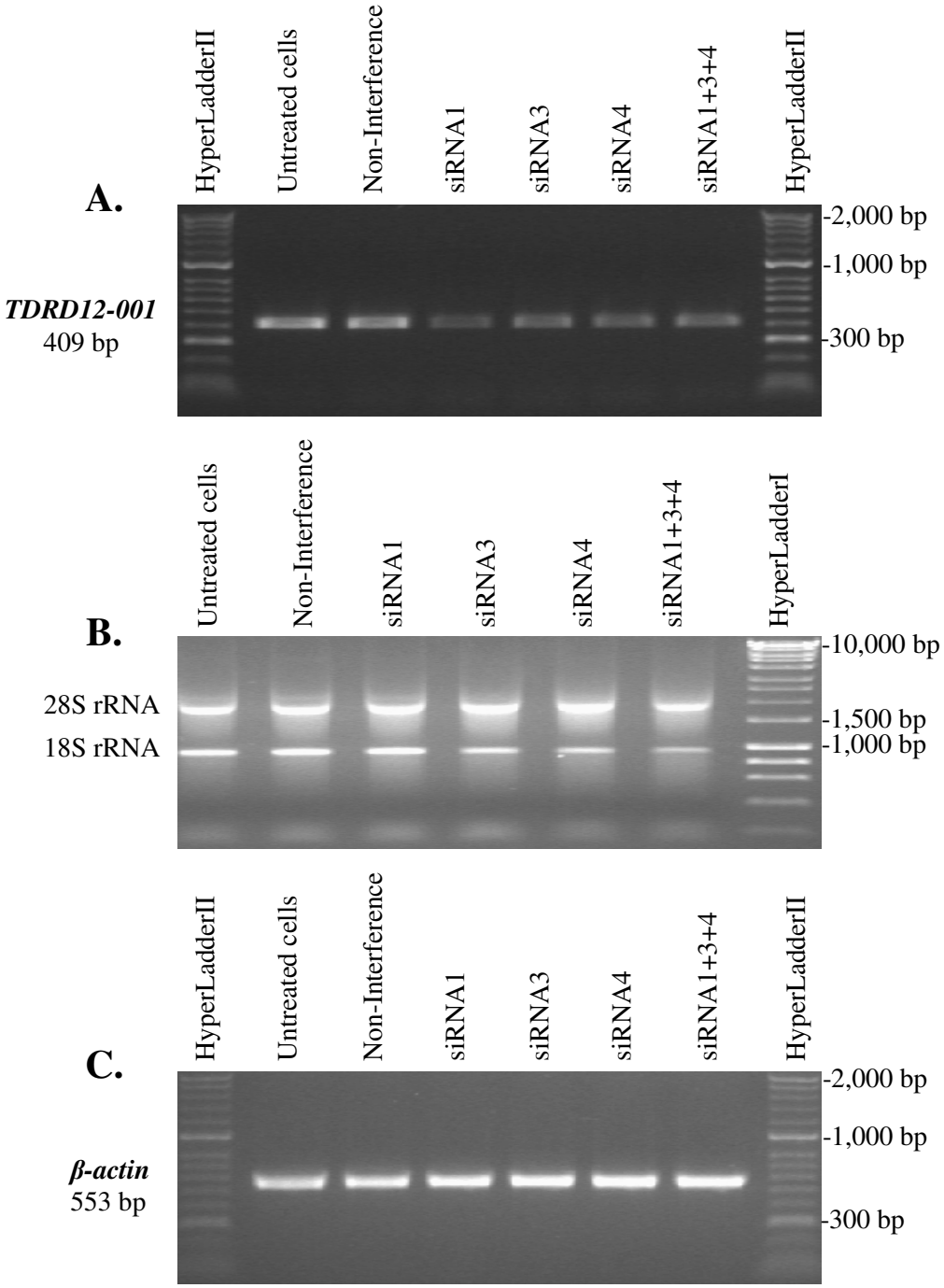

Figure 5.2 RT-PCR analysis of *TDRD12-001* expression in siRNA-treated NT2 cells.
Panel (A): Agarose gel presenting the RT-PCR profile created from the NT2 cells. Untreated cells were used as positive controls. Cells treated with non-interfering siRNA were used as negative controls for the *TDRD12-001* knockdown. Three different *TDRD12-001* siRNAs were analysed (siRNA1, siRNA3 and siRNA4), and a combination of the three siRNAs was also utilised (siRNA1+3+4). Panel (B): quality assessment of the RNA extracted from the NT2 cells. The expected sizes of 28S and 18S RNA fragments were 1,800 bp and 900 bp, respectively. Panel (C): RT-PCR analysis of *β-actin* gene expression in *TDRD12-001*-depleted NT2 cells. The expression of the *β-actin* gene was used as a quality control for the cDNA generated from the NT2 cells. The PCR products for the *β-actin* and *TDRD12-001* migrated close to the expected sizes.

A.

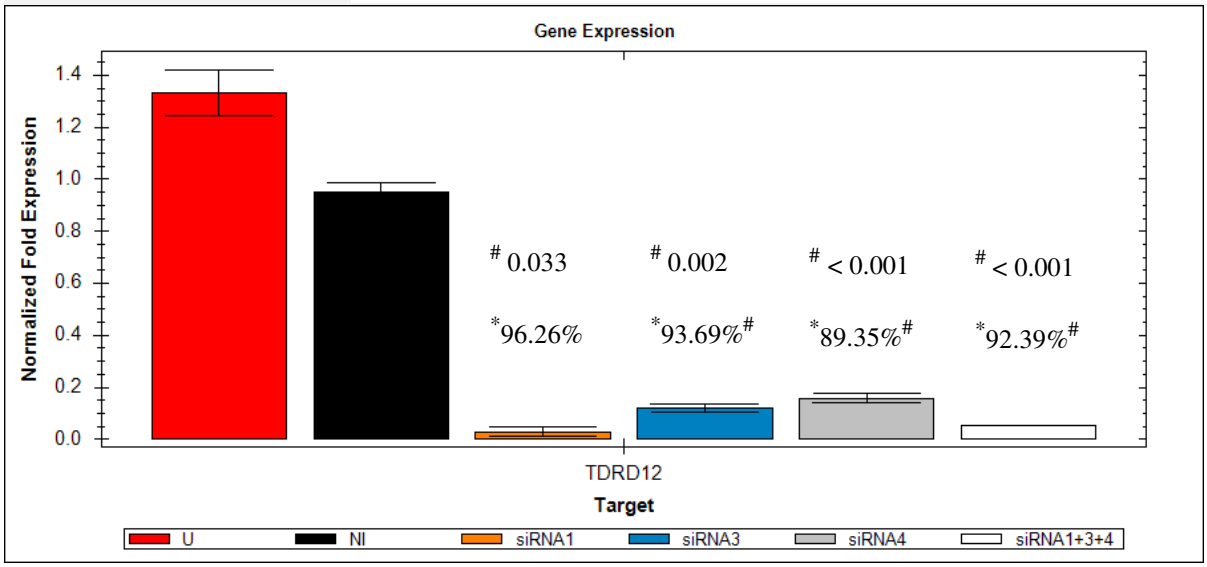

* Expression percentage differences between control (NI) and different samples; # P-Value.

B.

Target	Sample	Relative Quantity	Wells	Cq Reading 1	Cq Reading 2	Cq Mean	Cq Std. Dev
Lamin	Untreated cells	0.56254	2	25.65	25.38	25.52	0.191
Lamin	Non-Interference	0.57118	2	25.49	25.50	25.50	0.006
Lamin	siRNA1	0.97606	2	24.79	24.65	24.72	0.097
Lamin	siRNA3	0.36093	2	26.16	26.16	26.16	0.002
Lamin	siRNA4	0.49528	2	25.57	25.65	25.70	0.067
Lamin	siRNA1+3+4	1.00000	2	24.63	24.74	24.69	0.080
Tubulin	Untreated cells	1.00000	2	20.90	20.66	20.78	0.174
Tubulin	Non-Interference	0.85040	2	21.00	21.03	21.02	0.016
Tubulin	siRNA1	0.79551	2	21.06	21.16	21.11	0.074
Tubulin	siRNA3	0.33197	2	22.29	22.45	22.37	0.115
Tubulin	siRNA4	0.40260	2	22.38	21.81	22.09	0.406
Tubulin	siRNA1+3+4	0.90298	2	20.89	20.97	20.93	0.054
TDRD12-001	Untreated cells	1.00000	2	26.60	26.56	26.58	0.025
TDRD12-001	Non-Interference	0.66383	2	27.12	27.22	27.17	0.072
TDRD12-001	siRNA1	0.02483	2	32.80	31.03	31.91	1.247
TDRD12-001	siRNA3	0.04192	2	31.32	31.00	31.16	0.230
TDRD12-001	siRNA4	0.07070	2	30.39	30.42	30.40	0.018
TDRD12-001	siRNA1+3+4	0.05054	2	30.84	30.94	30.89	0.070

Figure 5.3 RT-qPCR analysis of *TDRD12-001* transcript in NT2 cells following knockdown. Panel (A): bar chart demonstrating the normalisation of the *TDRD12-001* expression analysed by RT-qPCR. The Bio-Rad CFX Manager was used to analysis the data. The error bars show the standard error for two replicates. Panel (B): table illustrating the number of replications (wells) and the Cq (quantification cycle) mean, standard deviation and Cq readings for the *Tubulin* and *Lamin* genes, to which the *TDRD12-001* reading was normalised. Note: (NI) cells treated with non-interfering siRNA; (U) untreated cells.

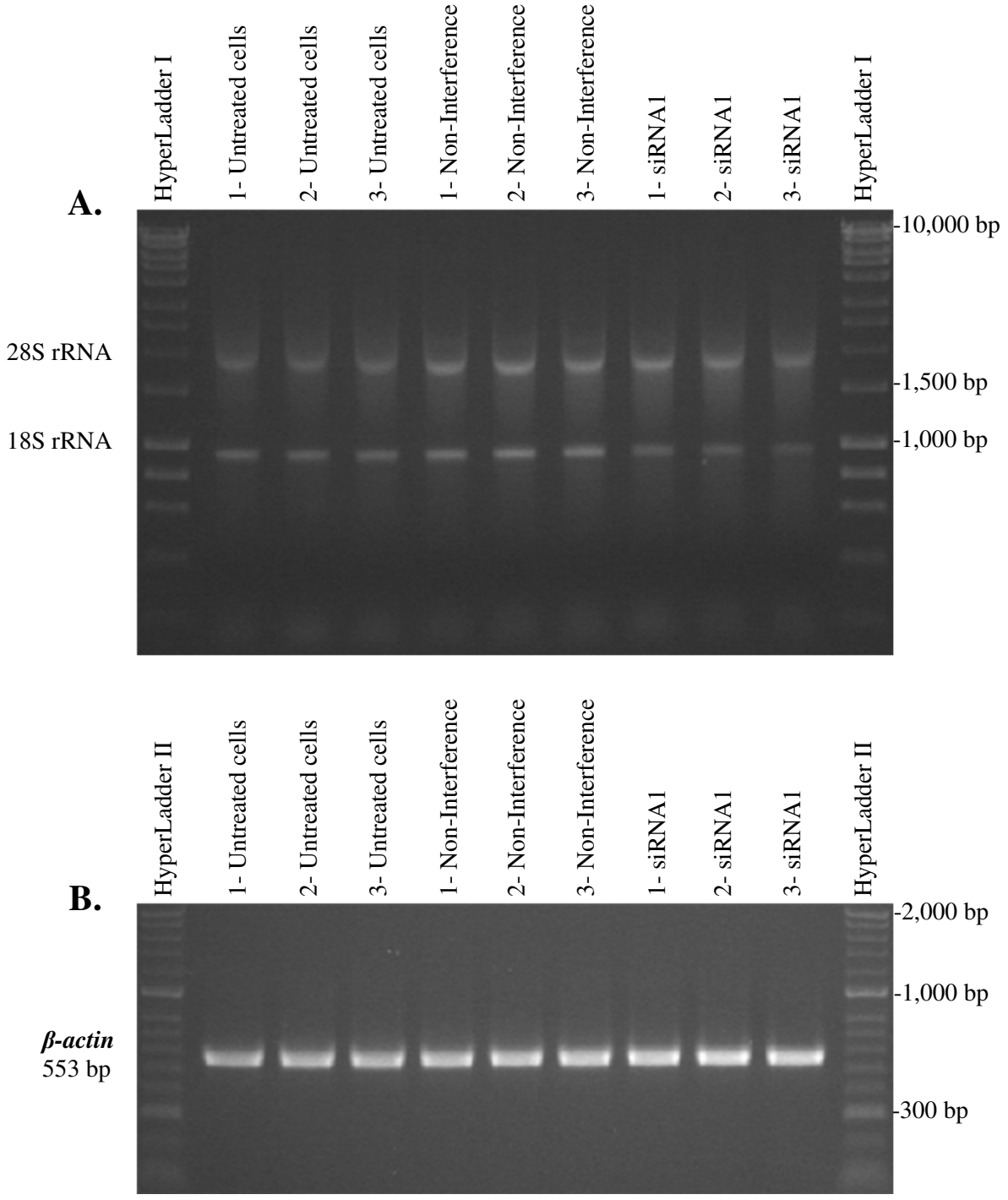

Figure 5.4 Quality assessment and control of the RNA extracted and cDNA made from three repeats siRNA knockdown of *TDRD12-001* in NT2 cells.
Panel (A): quality assessment of the RNA extracted from the NT2 cells. The expected sizes of the 28S and 18S RNA fragments were 1,800 bp and 900 bp, respectively. Panel (B): RT-PCR analysis of *β-actin* gene expression in *TDRD12-001*-depleted NT2 cells. The expression of the *β-actin* gene was used as a quality control for the cDNA generated from the NT2 cells. The PCR products for the *β-actin* migrated close to the expected size (553 bp).

A.

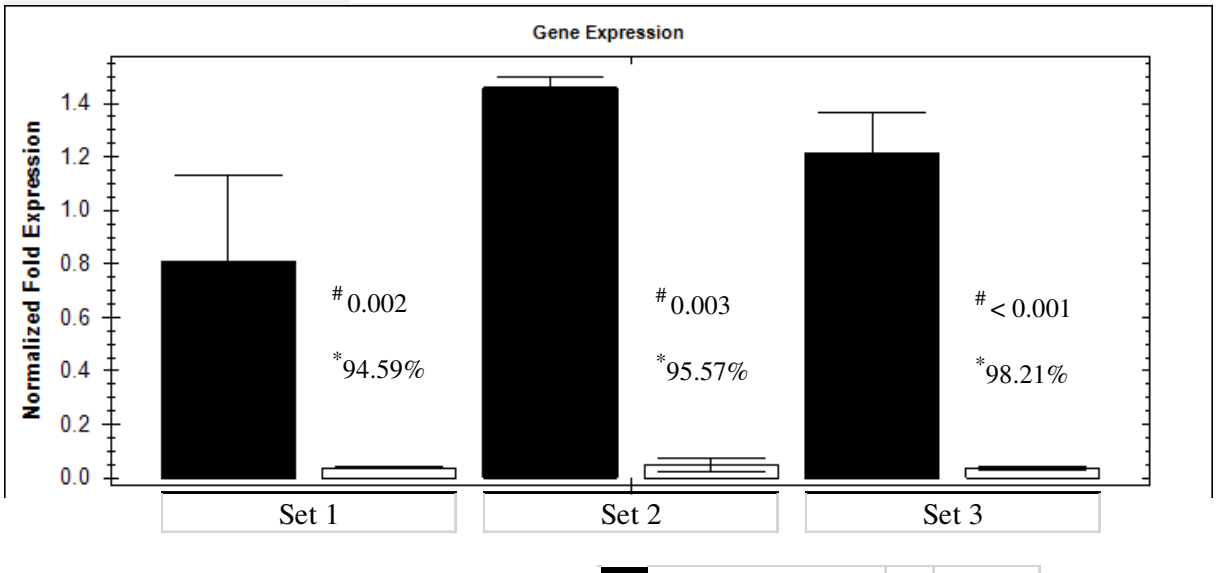

B.

Target	Sample	Relative Quantity	Wells	Cq Reading 1	Cq Reading 2	Cq Reading 3	Cq Mean	Cq Std. Dev
Lamin	1- Non-Interference	0.37238	3	24.7	24.58	24.54	24.60	0.085
Lamin	1- siRNA1	0.75214	3	23.56	23.72	23.5	23.59	0.114
Lamin	2- Non-Interference	0.40094	3	24.54	24.59	24.37	24.50	0.116
Lamin	2- siRNA1	1.00000	3	23.28	23.08	23.18	23.18	0.100
Lamin	3- Non-Interference	0.94433	3	23.43	23.67	24.13	23.74	0.352
Lamin	3- siRNA1	1.00000	3	23.86	24.05	23.08	23.66	0.513
Tubulin	1- Non-Interference	0.83034	3	18.85	18.72	18.71	18.76	0.080
Tubulin	1- siRNA1	0.5658	3	19.28	19.38	19.28	19.31	0.056
Tubulin	2- Non-Interference	1.00000	3	18.48	18.55	18.45	18.49	0.055
Tubulin	2- siRNA1	0.7178	3	19.03	18.92	18.96	18.97	0.056
Tubulin	3- Non-Interference	1.00000	3	17.56	17.7	17.74	17.67	0.098
Tubulin	3- siRNA1	0.36511	3	19.05	19.23	19.09	19.12	0.095
TDRD12-001	1- Non-Interference	0.48533	3	25.88	27.56	25.78	26.41	1.000
TDRD12-001	1- siRNA1	0.02628	3	30.74	30.54	30.57	30.61	0.111
TDRD12-001	2- Non-Interference	1.00000	3	25.34	25.35	25.4	25.36	0.033
TDRD12-001	2- siRNA1	0.04435	3	30.37	30.7	28.51	29.86	1.180
TDRD12-001	3- Non-Interference	1.00000	3	24.73	25.12	24.66	24.84	0.250
TDRD12-001	3- siRNA1	0.01788	3	30.83	30.34	30.75	30.64	0.262

Figure 5.5 RT-qPCR analysis of three repeats of *TDRD12-001* expression in NT2 cells following knockdown.
Panel (A): bar chart demonstrating the normalisation of three repeats of the *TDRD12-001* expression analysed by RT-qPCR. The Bio-Rad CFX Manager was used to analyse the data. The error bars show the standard error for three replicates. Panel (B): table illustrating the number of replications (wells) and the Cq (quantification cycle) mean, standard deviation and Cq readings for the *Tubulin* and *Lamin* genes, to which the *TDRD12-001* reading was normalised. * Expression percentage differences between control (NI) and different samples; # P-Value.

5.3.2. Analysis of RE, HERV and germ-line gene expression in *TDRD12-001*-depleted NT2 cells

The RT-qPCR analysis technique was performed to analyse the expression of RE, HERV and germ-line genes in a transcript of *TDRD12-001*-depleted NT2 cells. Figure 5.6 and Figure 5.7 show the normalising of the RE, HERV and germ-line gene expression profiles in *TDRD12-001*-depleted and non-depleted cells, calculated relative to the *GAPDH* and *HSP90AB1* genes. Figure 5.8 and Figure 5.9 show the normalising of the RE, HERV and germ-line gene expression profiles calculated relative to the *Tubulin* and *Lamin* genes. Four standardisation genes (*GAPDH*, *HSP90AB1*, *Tubulin* and *Lamin*) were used to ensure valid analysis.

In accordance with the RT-qPCR validation process of 20 RE, HERV and germ-line genes that were normalised to the expression of *GAPDH* and *HSP90AB1* genes, it was observed that the expression profiles of 16 genes were up-regulated (*HERV-K-Gag* [47.82%], *HERV-Gag-Domain1* [55.50%], *HERV-K-Pro* [42.31%], *HERV-K-10* [47.32%], *HERV-K-107* [44.10%], *HERV-K-Env* [17.62%], *HERV-KHML2-Rec* [2.99%], *HERV-K-Pol* [12.88%], *DAZL-001* [26.12%], *DAZ1* [75.71%], *BOLL-001* [27.46%], *TDRD1-201* [20.40%], *PIWIL2* [17.09%], *PIWIL3* [7.99%], *HERV-W-Env* [22.73%] and *PIWIL4* [2.06%]). Meanwhile, the expression profiles of four genes were down-regulated (*LINE-1* [39.93%], *SINE-ALU-Domain* [29.07%], *PIWIL1* [50.41%] and *DAZ2/3/4* [83.26%]).

Additionally, in accordance with the RT-qPCR validation process of 20 RE, HERV and germ-line genes that were normalised to the expression of *Tubulin* and *Lamin* genes, it was observed that the expression profiles of 10 genes were up-regulated (*HERV-K-Gag* [43.76%], *HERV-Gag-Domain1* [46.41%], *HERV-K-Pro* [41.38%], *HERV-K-10* [44.27%], *HERV-K-107* [44.31%], *HERV-K-Env* [47.03%], *HERV-KHML2-Rec* [43.51%], *HERV-K-Pol* [51.19%], *PIWIL4* [7.34%] and *DAZ2/3/4* [75.96%]). Meanwhile, the expression profiles of 10 genes were down-regulated (*LINE-1* [9.25%], *SINE-ALU-Domain* [12.60%], *PIWIL1* [47.70%], *PIWIL2* [37.51%], *PIWIL3* [47.64%], *HERV-W-Env* [100%], *DAZL* [36.88%], *DAZ1* [3.8%], *BOLL-001* [5.21%] and *TDRD1-201* [77.36%]) (see summary of the obtained results in Figure 5.10).

A.

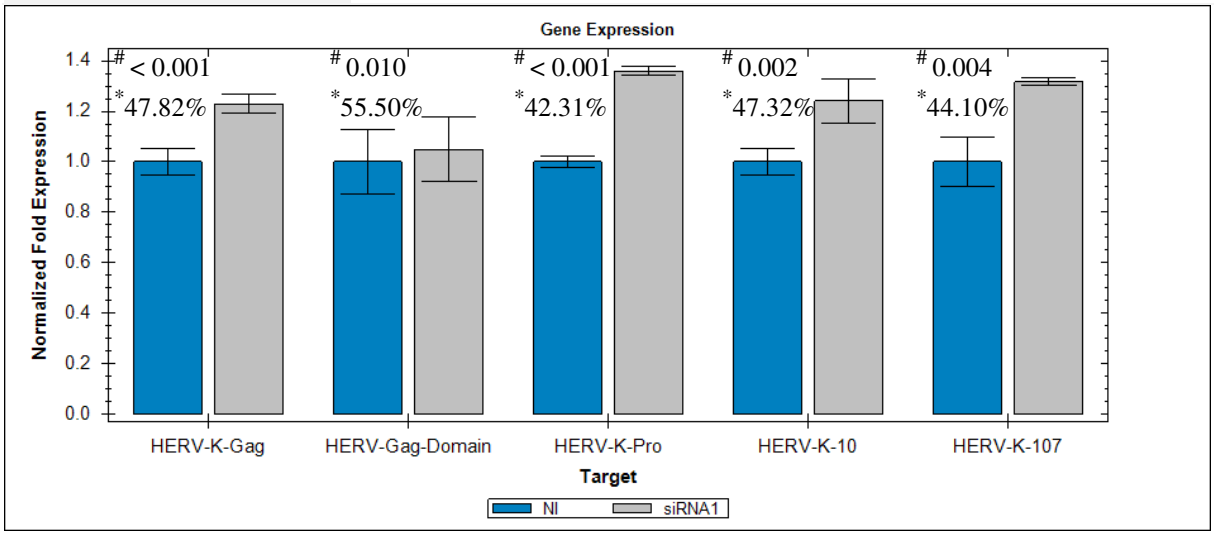
Gene Expression
Normalized Fold Expression
1.4
1.2
1.0
0.8
0.6
0.4
0.2
0.0
< 0.001
* 47.82%
# 0.010
* 55.50%
# < 0.001
* 42.31%
# 0.002
* 47.32%
# 0.004
* 44.10%
HERV-K-Gag
HERV-Gag-Domain
HERV-K-Pro
HERV-K-10
HERV-K-107
Target
NI
siRNA1

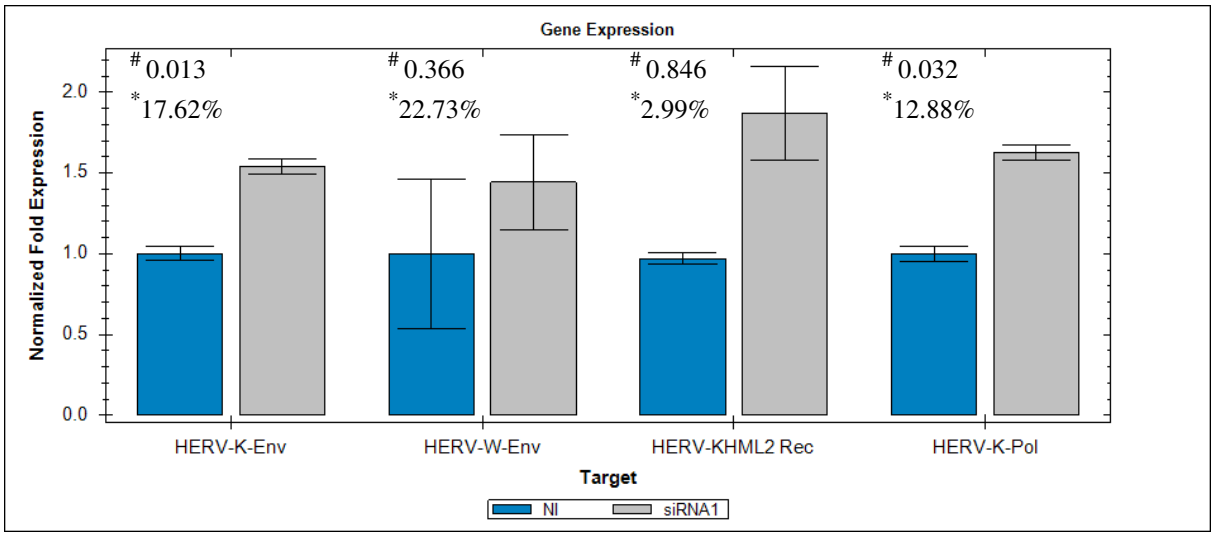
Gene Expression
Normalized Fold Expression
2.0
1.5
1.0
0.5
0.0
0.013
* 17.62%
# 0.366
* 22.73%
# 0.846
* 2.99%
# 0.032
* 12.88%
HERV-K-Env
HERV-W-Env
HERV-KHML2 Rec
HERV-K-Pol
Target
NI
siRNA1

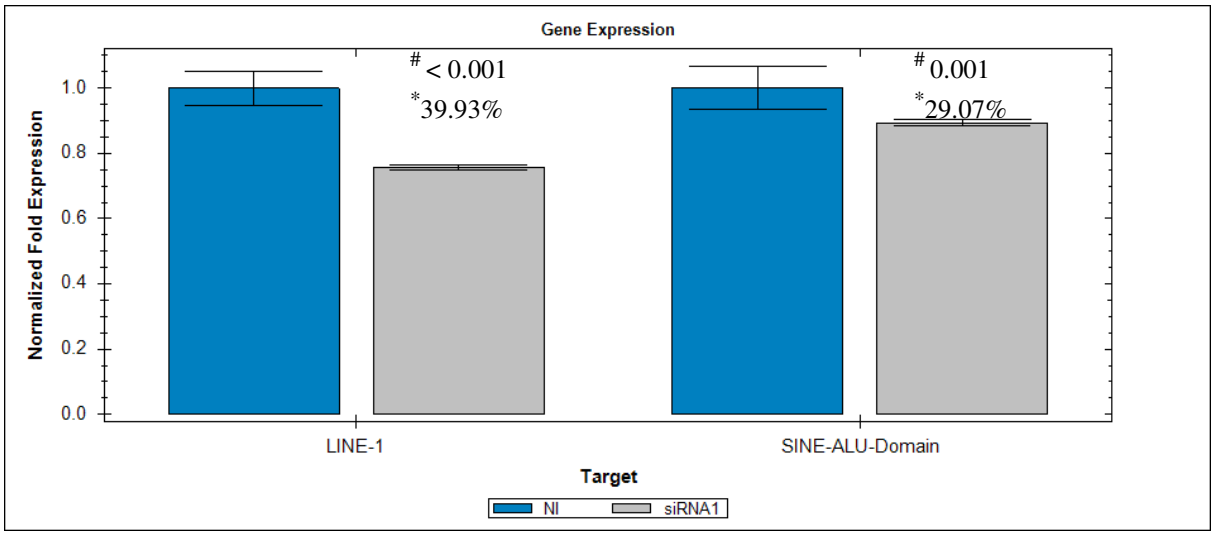
Gene Expression
Normalized Fold Expression
1.0
0.8
0.6
0.4
0.2
0.0
< 0.001
* 39.93%
# 0.001
* 29.07%
LINE-1
SINE-ALU-Domain
Target
NI
siRNA1

B.

Target	Sample	Relative Quantity	Wells	Cq Reading 1	Cq Reading 2	Cq Reading 3	Cq Mean	Cq Std. Dev
GAPDH	Non-Interference	1.00000	3	16.48	16.64	16.54	16.55	0.081
GAPDH	siRNA1	0.52892	3	17.51	17.44	17.46	17.47	0.035
HSP90AB1	Non-Interference	1.00000	3	20.21	20.08	20.17	20.15	0.066
HSP90AB1	siRNA1	0.34048	3	21.72	21.66	21.74	21.70	0.038
HERV-K-Gag	Non-Interference	1.00000	3	24.68	24.53	24.78	24.66	0.126
HERV-K-Gag	siRNA1	0.52185	2	N/A	25.64	25.56	25.60	0.056
HERV-Gag-Domain 1	Non-Interference	1.00000	3	32.11	31.53	31.61	31.75	0.312
HERV-Gag-Domain 1	siRNA1	0.44503	3	32.57	33.05	33.13	32.92	0.300
HERV-K-Pro	Non-Interference	1.00000	3	23.4	23.41	23.35	23.38	0.032
HERV-K-Pro	siRNA1	0.57691	3	24.2	24.18	24.16	24.18	0.018
HERV-K-10	Non-Interference	1.00000	3	24.66	24.67	24.46	24.60	0.119
HERV-K-10	siRNA1	0.52679	3	25.67	25.56	25.33	25.52	0.174
HERV-K-107	Non-Interference	1.00000	3	24.52	24.54	24.94	24.67	0.237
HERV-K-107	siRNA1	0.55898	3	25.52	25.50	25.51	25.51	0.010
GAPDH	Non-Interference	1.00000	3	16.55	16.64	16.38	16.52	0.131
GAPDH	siRNA1	0.64006	3	17.12	17.19	17.19	17.17	0.042
HSP90AB1	Non-Interference	1.00000	3	20.24	20.12	20.17	20.18	0.063
HSP90AB1	siRNA1	0.44826	3	21.27	21.35	21.38	21.33	0.058
HERV-K-Env	Non-Interference	1.00000	3	22.94	22.99	23.11	23.01	0.084
HERV-K-Env	siRNA1	0.82381	3	23.37	23.28	23.23	23.29	0.069
HERV-W-Env	Non-Interference	1.00000	3	N/A	38.60	39.92	39.26	0.938
HERV-W-Env	siRNA1	0.77269	2	39.33	N/A	39.93	39.63	0.418
HERV-KHML2 Rec	Non-Interference	0.97008	3	24.21	24.15	24.12	24.16	0.046
HERV-KHML2 Rec	siRNA1	1.00000	3	24.56	23.92	23.86	24.11	0.388
HERV-K-Pol	Non-Interference	1.00000	3	22.86	22.93	22.75	22.85	0.089
HERV-K-Pol	siRNA1	0.87117	3	23.02	23.12	23.01	23.05	0.064
GAPDH	Non-Interference	1.00000	3	17.19	16.85	16.73	16.92	0.240
GAPDH	siRNA1	0.90110	3	17.05	17.09	17.08	17.07	0.018
HSP90AB1	Non-Interference	1.00000	3	20.45	20.28	20.36	20.36	0.087
HSP90AB1	siRNA1	0.69930	3	20.89	20.86	20.89	20.88	0.020
LINE-1	Non-Interference	1.00000	3	17.42	17.36	17.38	17.39	0.031
LINE-1	siRNA1	0.60071	3	18.14	18.13	18.10	18.12	0.021
SINE-ALU-Domain	Non-Interference	1.00000	3	14.78	14.63	14.58	14.66	0.103
SINE-ALU-Domain	siRNA1	0.70930	3	15.13	15.17	15.18	15.16	0.026

Figure 5.6 RT-qPCR analysis of transposable element gene expression in *TDRD12-001*-depleted NT2 cells.
Panel (A): bar chart demonstrating the normalisation of the *HERV* gene expression analysed by RT-qPCR. The Bio-Rad CFX Manager was used to analysis the data. The error bars show the standard error for three replicates. Panel (B): table illustrating the number of replications (wells) and the Cq (quantification cycle) mean, standard deviation and Cq readings for the *GAPDH* and *HSP90AB1* genes, to which the *HERVs* reading was normalised. * Expression percentage differences between control (NI) and different samples; # P-Value; (NI) cells treated with non-interfering siRNA.

A.

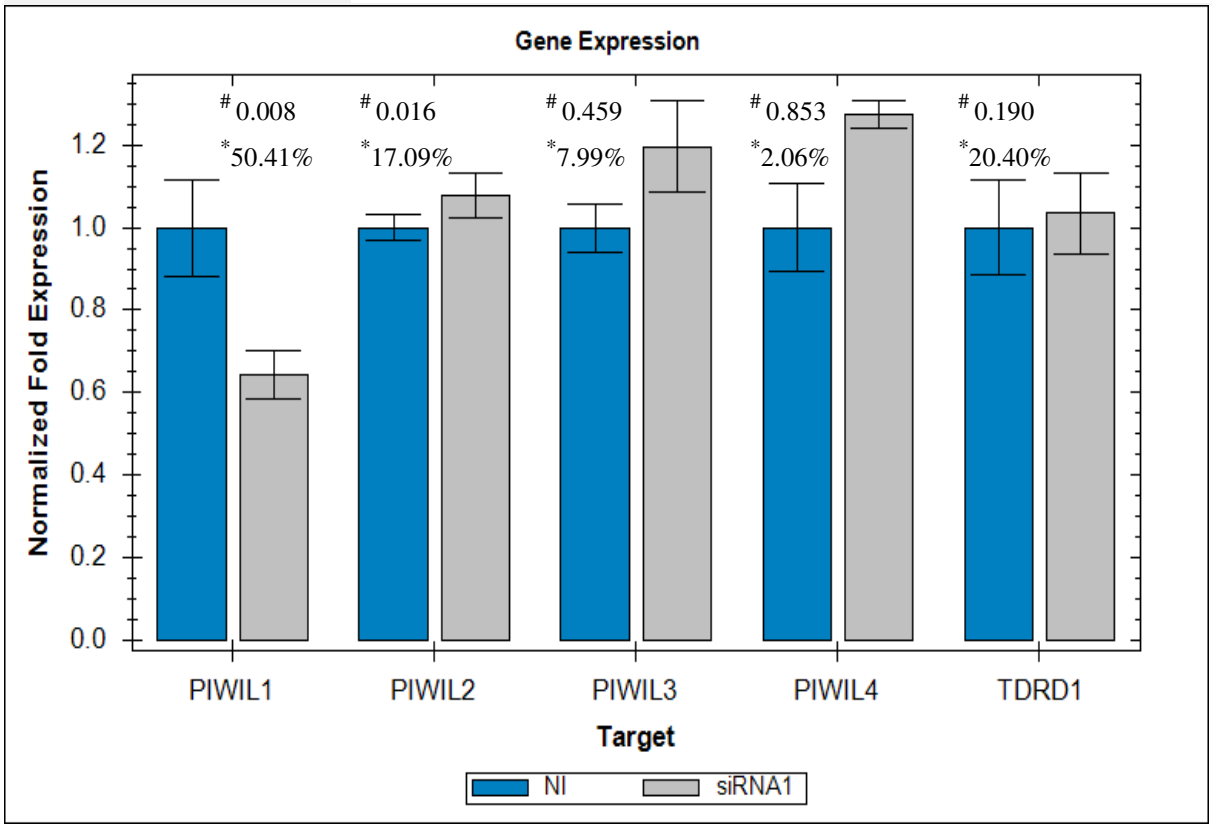
Gene Expression
Normalized Fold Expression
0.0
0.2
0.4
0.6
0.8
1.0
1.2
0.008
* 50.41%
# 0.016
* 17.09%
# 0.459
* 7.99%
# 0.853
* 2.06%
# 0.190
* 20.40%
PIWIL1
PIWIL2
PIWIL3
PIWIL4
TDRD1
Target
NI
siRNA1

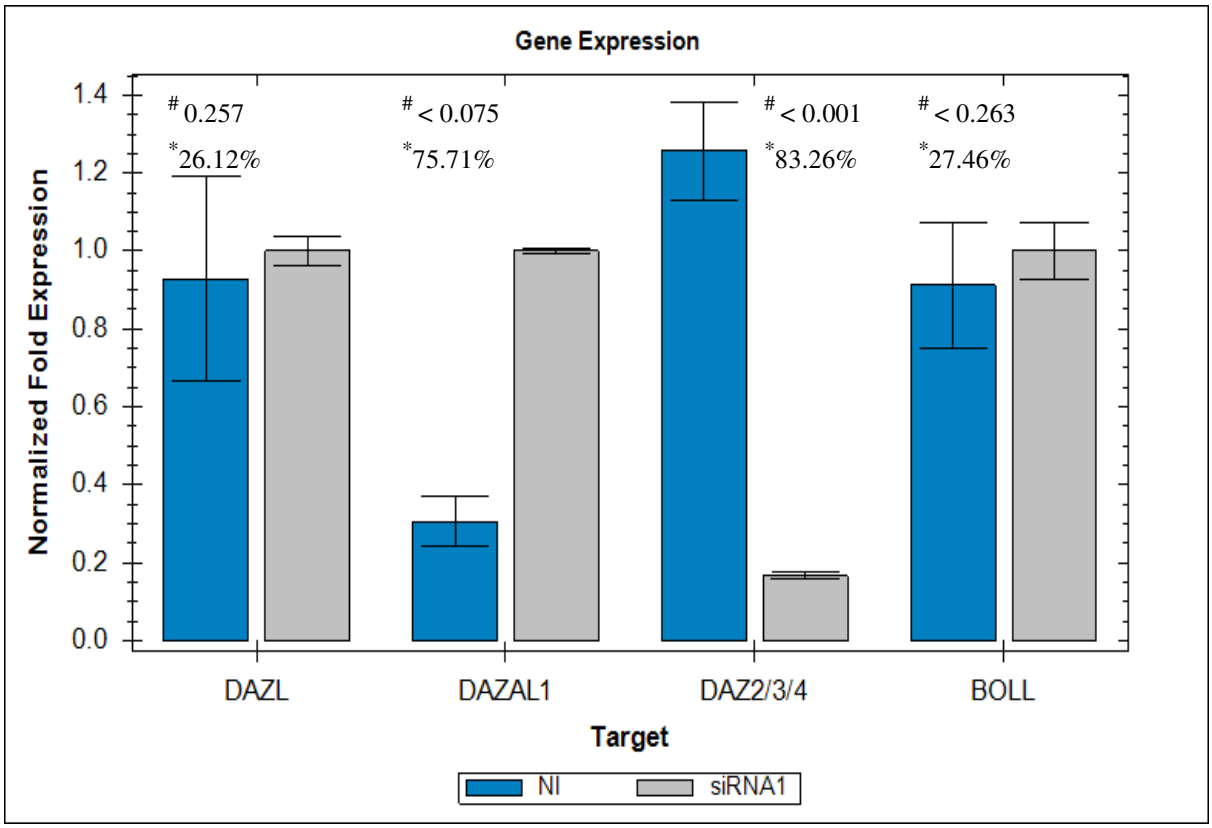
Gene Expression
Normalized Fold Expression
0.0
0.2
0.4
0.6
0.8
1.0
1.2
1.4
0.257
* 26.12%
# < 0.075
* 75.71%
# < 0.001
* 83.26%
# < 0.263
* 27.46%
DAZL
DAZAL1
DAZ2/3/4
BOLL
Target
NI
siRNA1

B.

Target	Sample	Relative Quantity	Wells	Cq Reading 1	Cq Reading 2	Cq Reading 3	Cq Mean	Cq Std. Dev
GAPDH	Non-Interference	1.00000	3	16.71	16.67	16.80	16.73	0.070
GAPDH	siRNA1	0.80004	3	17.17	16.94	17.03	17.05	0.119
HSP90AB1	Non-Interference	1.00000	3	20.21	20.02	20.18	20.14	0.104
HSP90AB1	siRNA1	0.73995	3	20.59	20.55	20.57	20.57	0.022
PIWIL1	Non-Interference	1.00000	3	31.74	32.30	31.92	31.99	0.286
PIWIL1	siRNA1	0.49590	3	32.82	32.93	33.24	33.00	0.219
PIWIL2	Non-Interference	1.00000	3	24.39	24.30	24.33	24.34	0.046
PIWIL2	siRNA1	0.82915	3	24.50	24.61	24.71	24.61	0.106
PIWIL3	Non-Interference	1.00000	3	35.52	35.47	35.27	35.42	0.132
PIWIL3	siRNA1	0.92011	3	35.79	35.41	35.42	35.54	0.220
PIWIL4	Non-Interference	1.00000	3	31.36	31.04	30.84	31.08	0.262
PIWIL4	siRNA1	0.97936	3	31.13	31.11	31.09	31.11	0.019
TDRD1	Non-Interference	1.00000	3	33.97	33.72	34.27	33.98	0.277
TDRD1	siRNA1	0.79597	3	34.41	34.05	34.48	34.31	0.228
GAPDH	Non-Interference	0.72823	3	17.96	18.08	17.96	18.00	0.070
GAPDH	siRNA1	1.00000	3	17.53	17.55	17.54	17.54	0.012
HSP90AB1	Non-Interference	0.86877	3	21.62	21.45	21.69	21.59	0.121
HSP90AB1	siRNA1	1.00000	3	21.37	21.39	21.39	21.38	0.008
DAZL	Non-Interference	0.73884	2	29.95	30.76	N/A	30.36	0.572
DAZL	siRNA1	1.00000	3	29.83	29.90	30.03	29.92	0.097
DAZAL1	Non-Interference	0.24291	3	38.29	37.38	38.24	37.97	0.514
DAZAL1	siRNA1	1.00000	1	35.93	N/A	N/A	35.93	0.000
DAZ2/3/4	Non-Interference	1.00000	3	33.66	34.14	33.84	33.88	0.242
DAZ2/3/4	siRNA1	0.16738	2	36.4	36.52	N/A	36.46	0.091
BOLL	Non-Interference	0.72543	3	35.23	35.27	36.01	35.50	0.440
BOLL	siRNA1	1.00000	2	35.15	34.93	N/A	35.04	0.151

Figure 5.7 RT-qPCR analysis of tumour germ-line gene expression in *TDRD12-001*-depleted NT2 cells.
Panel (A): bar chart demonstrating the normalisation of the tumour germ-line gene expression analysed by RT-qPCR. The Bio-Rad CFX Manager was used to analyse the data. The error bars show the standard error for three replicates. Panel (B): table illustrating the number of replications (wells) and the Cq (quantification cycle) mean, standard deviation and Cq readings for the *GAPDH* and *HSP90AB1* genes, to which the tumour germ-line genes reading was normalised. * Expression percentage differences between control (NI) and different samples; # P-Value; (NI) cells treated with non-interfering siRNA.

A.

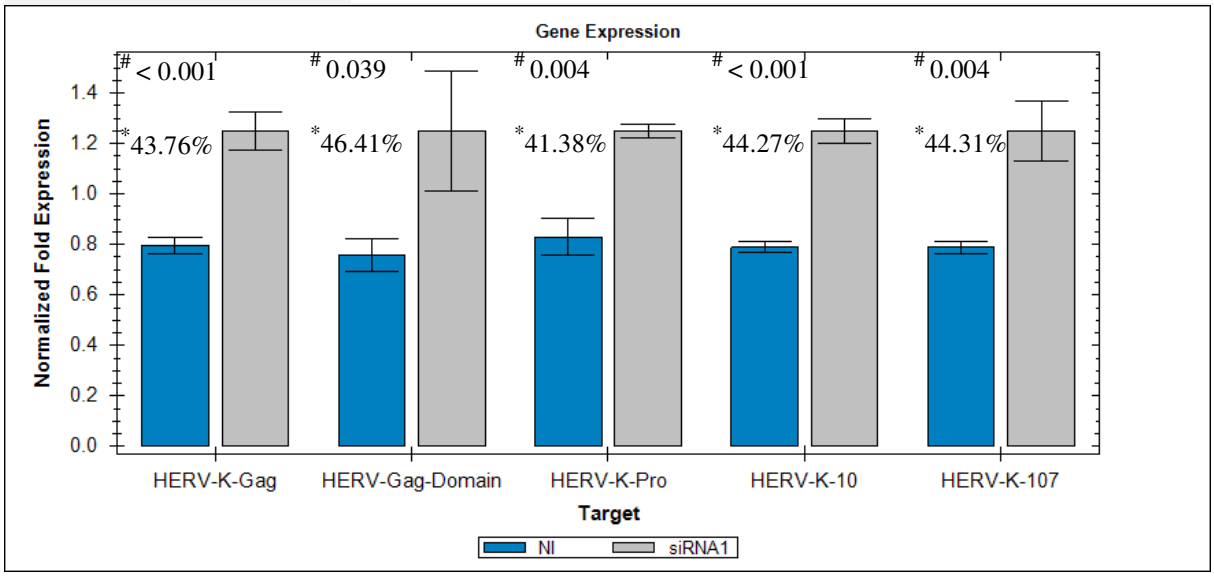
Gene Expression
Normalized Fold Expression
< 0.001
0.039
0.004
< 0.001
0.004
*43.76%
*46.41%
*41.38%
*44.27%
*44.31%
HERV-K-Gag
HERV-Gag-Domain
HERV-K-Pro
HERV-K-10
HERV-K-107
Target
NI
siRNA1

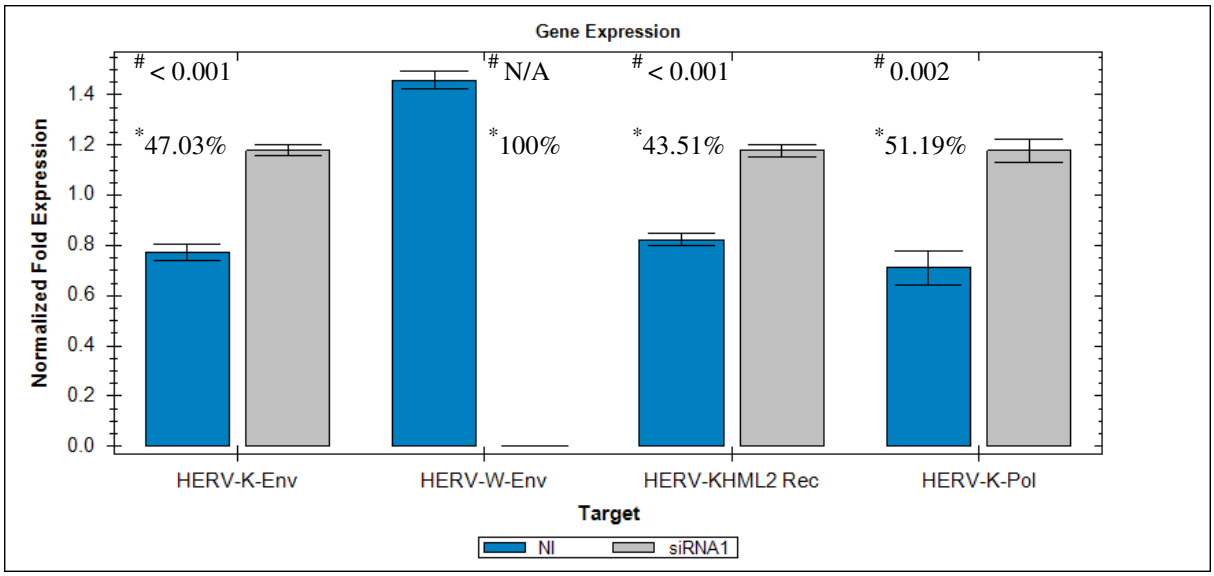
Gene Expression
Normalized Fold Expression
< 0.001
N/A
< 0.001
0.002
*47.03%
*100%
*43.51%
*51.19%
HERV-K-Env
HERV-W-Env
HERV-KHML2 Rec
HERV-K-Pol
Target
NI
siRNA1

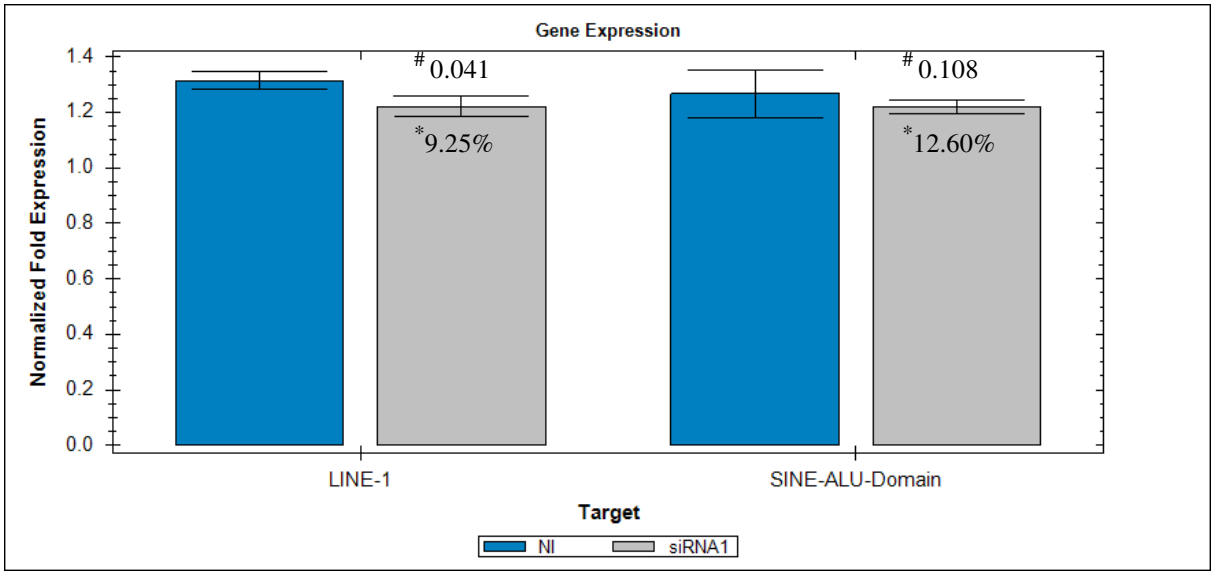
Gene Expression
Normalized Fold Expression
0.041
0.108
*9.25%
*12.60%
LINE-1
SINE-ALU-Domain
Target
NI
siRNA1

B.

Target	Sample	Relative Quantity	Wells	Cq Reading 1	Cq Reading 2	Cq Reading 3	Cq Mean	Cq Std. Dev
Lamin	Non-Interference	0.49962	3	24.05	23.89	24.00	23.98	0.079
Lamin	siRNA1	1.00000	3	23.02	22.94	22.98	22.98	0.036
Tubulin	Non-Interference	1.00000	3	18.07	18.10	18.05	18.08	0.023
Tubulin	siRNA1	0.63949	3	18.72	18.71	18.73	18.72	0.010
HERV-K-Gag	Non-Interference	0.56240	3	24.82	24.84	25.00	24.88	0.098
HERV-K-Gag	siRNA1	1.00000	3	24.22	23.95	23.98	24.05	0.147
HERV-Gag-Domain 1	Non-Interference	0.53588	3	33.55	33.19	33.15	33.30	0.218
HERV-Gag-Domain 1	siRNA1	1.00000	3	32.80	32.50	31.88	32.40	0.471
HERV-K-Pro	Non-Interference	0.58622	3	24.05	23.73	23.64	23.81	0.216
HERV-K-Pro	siRNA1	1.00000	3	23.07	22.98	23.06	23.04	0.050
HERV-K-10	Non-Interference	0.55731	3	25.14	25.10	25.03	25.09	0.056
HERV-K-10	siRNA1	1.00000	3	24.32	24.27	24.14	24.24	0.095
HERV-K-107	Non-Interference	0.55693	3	25.03	25.07	24.96	25.02	0.056
HERV-K-107	siRNA1	1.00000	3	24.45	24.06	24.01	24.17	0.240
Lamin	Non-Interference	0.47055	3	24.49	24.39	24.44	24.44	0.048
Lamin	siRNA1	1.00000	3	23.35	23.39	23.31	23.35	0.036
Tubulin	Non-Interference	1.00000	3	18.69	18.78	18.77	18.74	0.051
Tubulin	siRNA1	0.72103	3	19.14	19.31	19.20	19.22	0.084
HERV-K-Env	Non-Interference	0.52966	3	24.12	23.95	24.10	24.06	0.093
HERV-K-Env	siRNA1	1.00000	3	23.13	23.14	23.15	23.14	0.011
HERV-W-Env	Non-Interference	1.00000	0	N/A	37.51	N/A	37.51	0.000
HERV-W-Env	siRNA1	0.00000	1	N/A	N/A	N/A	N/A	0.000
HERV-KHML2 Rec	Non-Interference	0.56488	3	24.64	24.65	24.54	24.61	0.059
HERV-KHML2 Rec	siRNA1	1.00000	3	23.79	23.76	23.81	23.79	0.028
HERV-K-Pol	Non-Interference	0.48807	3	24.06	23.85	23.60	23.84	0.233
HERV-K-Pol	siRNA1	1.00000	3	22.90	22.78	22.73	22.80	0.086
Lamin	Non-Interference	0.47608	3	24.89	24.82	24.80	24.84	0.043
Lamin	siRNA1	1.00000	3	23.85	23.74	23.70	23.77	0.076
Tubulin	Non-Interference	1.00000	3	18.90	18.90	18.83	18.88	0.041
Tubulin	siRNA1	0.67037	3	19.44	19.48	19.45	19.45	0.017
LINE-1	Non-Interference	0.90748	3	18.25	18.27	18.35	18.29	0.054
LINE-1	siRNA1	1.00000	3	18.12	18.10	18.22	18.15	0.066
SINE-ALU-Domain	Non-Interference	0.87397	3	15.88	15.60	15.60	15.69	0.165
SINE-ALU-Domain	siRNA1	1.00000	3	15.46	15.51	15.52	15.50	0.033

Figure 5.8 RT-qPCR analysis of transposable element gene expression in *TDRD12-001*-depleted NT2 cells.
Panel (A): bar chart demonstrating the normalisation of the *HERV* gene expression analysed by RT-qPCR. The Bio-Rad CFX Manager was used to analyse the data. The error bars show the standard error for three replicates. Panel (B): table illustrating the number of replications (wells) and the Cq (quantification cycle) mean, standard deviation and Cq readings for the *Tubulin* and *Lamin* genes, to which the *HERVs* reading was normalised. * Expression percentage differences between control (NI) and different samples; # P-Value; (NI) cells treated with non-interfering siRNA.

A.

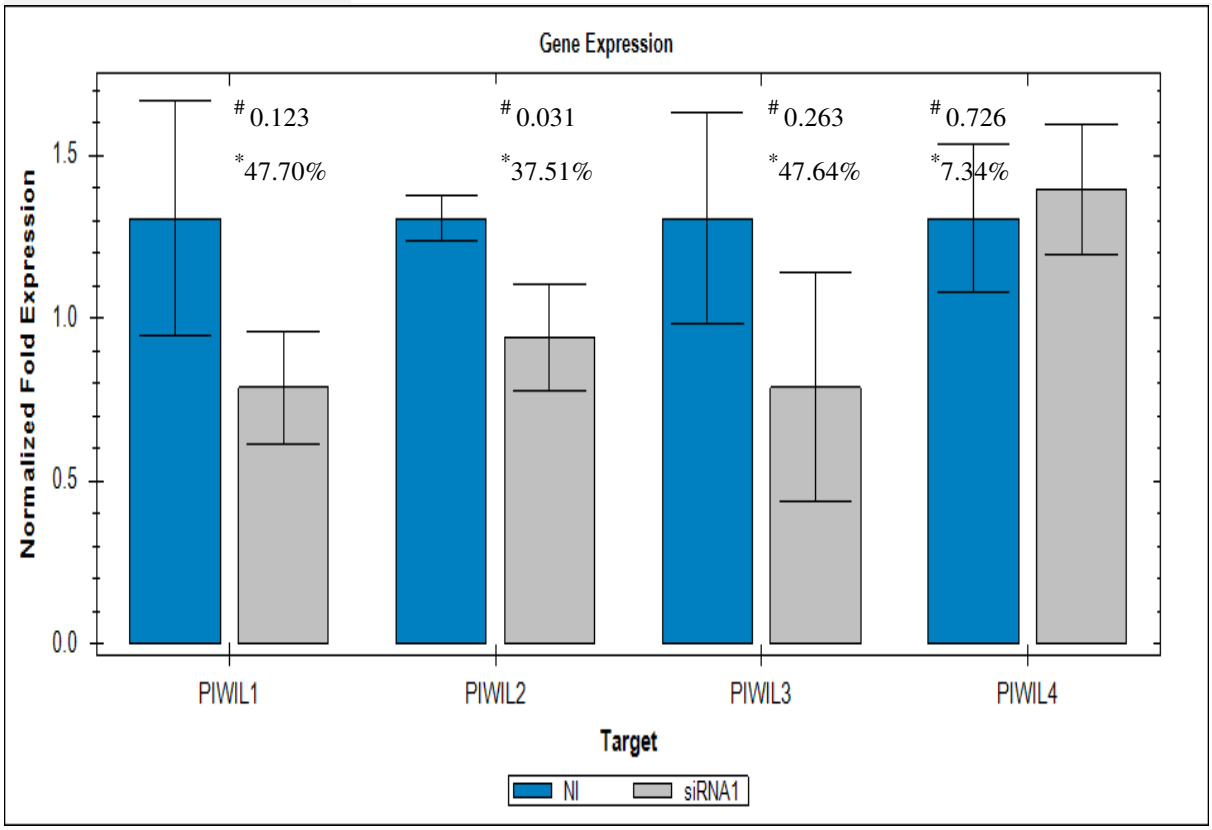
Gene Expression
0.123
*47.70%
0.031
*37.51%
0.263
*47.64%
0.726
*7.34%
Normalized Fold Expression
1.5
1.0
0.5
0.0
PIWIL1
PIWIL2
PIWIL3
PIWIL4
Target
NI
siRNA1

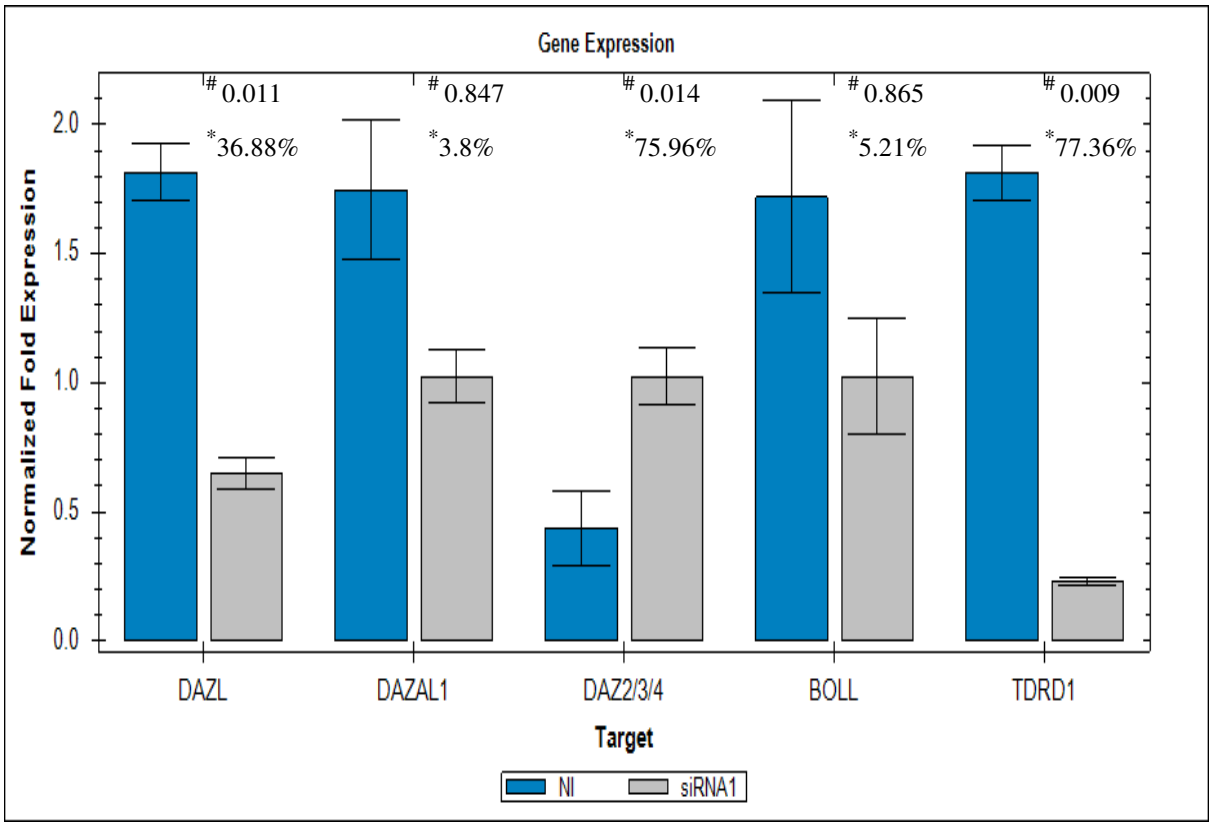
Gene Expression
0.011
*36.88%
0.847
*3.8%
0.014
*75.96%
0.865
*5.21%
0.009
*77.36%
Normalized Fold Expression
2.0
1.5
1.0
0.5
0.0
DAZL
DAZAL1
DAZ2/3/4
BOLL
TDRD1
Target
NI
siRNA1

B.

Target	Sample	Relative Quantity	Wells	Cq Reading 1	Cq Reading 2	Cq Reading 3	Cq Mean	Cq Std. Dev
Lamin	Non-Interference	0.29017	3	25.11	25.13	25.17	25.12	0.029
Lamin	siRNA1	1.00000	3	23.29	23.36	23.40	23.33	0.054
Tubulin	Non-Interference	0.97899	3	19.20	19.19	19.13	19.15	0.037
Tubulin	siRNA1	1.00000	3	19.24	19.07	19.12	19.12	0.083
TDRD1	Non-Interference	1.00000	1	37.63	N/A	N/A	37.61	0.000
TDRD1	siRNA1	0.22637	3	39.83	39.93	39.58	39.75	0.174
Lamin	Non-Interference	0.31776	3	24.82	24.61	25.08	24.84	0.233
Lamin	siRNA1	1.00000	3	23.20	23.20	23.16	23.18	0.021
Tubulin	Non-Interference	1.00000	3	18.86	18.98	18.82	18.89	0.081
Tubulin	siRNA1	0.88734	3	19.06	19.17	18.95	19.06	0.109
DAZL	Non-Interference	1.00000	3	32.51	32.57	32.75	32.61	0.126
DAZL	siRNA1	0.63120	3	33.14	33.53	33.15	33.27	0.224
DAZAL1	Non-Interference	0.96200	3	33.41	34.15	33.69	33.75	0.375
DAZAL1	siRNA1	1.00000	3	33.52	33.59	33.98	33.69	0.250
DAZ2/3/4	Non-Interference	0.24042	3	36.10	35.92	37.42	36.48	0.819
DAZ2/3/4	siRNA1	1.00000	3	34.42	34.68	34.17	34.42	0.255
BOLL	Non-Interference	0.94788	3	34.08	34.57	35.15	34.60	0.534
BOLL	siRNA1	1.00000	3	34.22	34.19	35.15	34.52	0.546
Lamin	Non-Interference	0.58482	3	24.36	24.24	24.29	24.30	0.059
Lamin	siRNA1	1.00000	3	23.20	23.55	23.83	23.53	0.317
Tubulin	Non-Interference	1.00000	3	18.52	18.50	18.25	18.42	0.149
Tubulin	siRNA1	0.44157	3	19.16	19.95	19.69	19.60	0.406
PIWIL1	Non-Interference	1.00000	3	31.97	33.27	32.27	32.51	0.682
PIWIL1	siRNA1	0.52298	3	33.12	34.00	33.21	33.44	0.487
PIWIL2	Non-Interference	1.00000	3	25.77	25.75	25.59	25.70	0.100
PIWIL2	siRNA1	0.62486	3	26.16	26.20	26.78	26.38	0.347
PIWIL3	Non-Interference	1.00000	3	34.91	35.66	36.12	35.56	0.610
PIWIL3	siRNA1	0.52364	3	36.05	35.71	37.73	36.50	1.083
PIWIL4	Non-Interference	1.00000	3	31.53	31.97	31.12	31.54	0.424
PIWIL4	siRNA1	0.92664	3	31.93	31.47	31.54	31.65	0.249

Figure 5.9 RT-qPCR analysis of tumour germ-line gene expression in *TDRD12-001*-depleted NT2 cells.
Panel (A): bar chart demonstrating the normalisation of the tumour germ-line gene expression analysed by RT-qPCR. The Bio-Rad CFX Manager was used to analyse the data. The error bars show the standard error for three replicates. Panel (B): table illustrating the number of replications (wells) and the Cq (quantification cycle) mean, standard deviation and Cq readings for the *Tubulin* and *Lamin* genes, to which the tumour germ-line genes reading was normalised. * Expression percentage differences between control (NI) and different samples; # P-Value; (NI) cells treated with non-interfering siRNA.

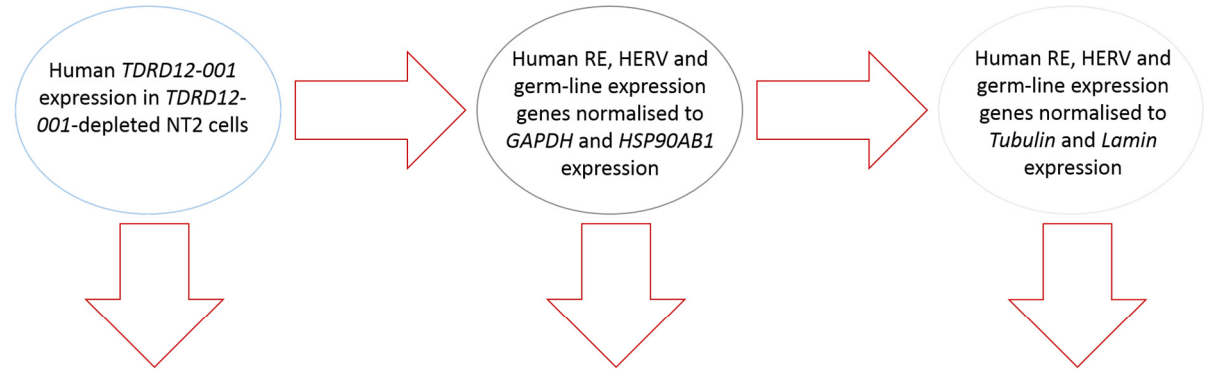

TDRD12	↓	*HERV-K-Gag*	↑	*HERV-K-Gag*	↑
TDRD12	↓	*HERV-Gag-Domain1*	↑	*HERV-Gag-Domain1*	↑
TDRD12	↓	*HERV-K-Pro*	↑	*HERV-K-Pro*	↑
TDRD12	↓	*HERV-K-10*	↑	*HERV-K-10*	↑
TDRD12	↓	*HERV-K-107*	↑	*HERV-K-107*	↑
TDRD12	↓	*HERV-K-Env*	↑	*HERV-K-Env*	↑
TDRD12	↓	*HERV-KHML2-Rec*	↑	*HERV-KHML2-Rec*	↑
TDRD12	↓	*HERV-K-Pol*	↑	*HERV-K-Pol*	↑
TDRD12	↓	*HERV-W-Env*	↑	*HERV-W-Env*	↓
TDRD12	↓	*DAZL-001*	↑	*DAZL-001*	↓
TDRD12	↓	*DAZ1*	↑	*DAZ1*	↓
TDRD12	↓	*BOLL-001*	↑	*BOLL-001*	↓
TDRD12	↓	*TDRD1-201*	↑	*TDRD1-201*	↓
TDRD12	↓	*PIWIL2*	↑	*PIWIL2*	↓
TDRD12	↓	*PIWIL3*	↑	*PIWIL3*	↓
TDRD12	↓	*PIWIL4*	↑	*PIWIL4*	↑
TDRD12	↓	*LINE-1*	↓	*LINE-1*	↓
TDRD12	↓	*SINE-ALU-Domain*	↓	*SINE-ALU-Domain*	↓
TDRD12	↓	*PIWIL1*	↓	*PIWIL1*	↓
TDRD12	↓	*DAZ2/3/4*	↓	*DAZ2/3/4*	↑

Figure 5.10 Summary of RT-qPCR analysis of expression profiles for several RE, HERV and germ-line genes in *TDRD12-001*-depleted NT2 cells.
The up regulation or down regulation of RE, HERV and germ-line gene expression profiles are shown in the form of arrows.

5.3.3. Analysis of TDRD12-associated proteins in NT2 cells

The analysis of TDRD12 was done in order to validate and test the specificity of the antibodies used for further analysis of localisation within normal tissues and cancerous cells using IHC and IF analysis techniques (see Chapter 6). Several dilutions were used in analysing and testing the antibodies' specificity and also in attempting to optimise the *TDRD12-001* siRNA knockdown at the protein levels, including increasing the number of siRNA "hits", as well as the number of cells per well. In addition, a variety of commercial TDRD12 primary antibodies were utilised for the WB analysis. Some antibodies were specifically generated by Eurogentec for use (see Table 2.8 in Chapter 2).

Therefore, as can be seen from the results (Figure 5.11 and Figure 5.12), the WB TDRD12 products were not detected at the expected sizes. Hence, these commercial antibodies were unlikely to be good antibodies to use. Figure 5.13 and Figure 5.14 show some WB TDRD12 products that were detected indicating that these might have been good antibodies (specifically designed antibodies). Nevertheless, the predicted molecular weight size was 133 kDa and the bands were found to be around 180 kDa. Thus, this observation was carefully questioned and analysed by looking at the *TDRD12* full transcript in Chapter 3 that actually corresponds to a product of 180 kDa. As a result, it can be concluded that significant levels of TDRD12 knockdown were found in NT2 cells. The α-tubulin antibody (used as a loading quality control) seems to be relatively equal.

TDRD12, TDRD1, PIWIL1 and PIWIL2 form a functional complex in mice (Pandey *et al.,* 2013). Given this, we set out to determine if any association/interdependence exists in human cells. WB analysis of human TDRD1, PIWIL1 and PIWIL2 proteins in *TDRD12-001*-depleted NT2 cells was performed. Figure 5.15 shows the WB analysis of the TDRD1 protein levels. The WB TDRD1 products were detected at approximately the expected sizes (132 kDa). Figure 5.16 shows the WB analysis of the PIWIL1 protein levels. Some of the WB PIWIL1 products were detected at approximately the expected sizes (95 kDa). These bands were not depleted or changed. However, it can be seen that there are a number of other higher molecular weight bands that disappeared. Figure 5.17 shows the WB analysis of the PIWIL2 protein levels. The WB PIWIL2 products were detected at approximately the expected sizes (105 kDa). These bands were depleted upon siRNA reduction of TDRD12, suggesting a functional regulatory relationship, whether this is at the transcriptional level or post-transcriptional level is unknown. Untreated cells were used as positive controls. Cells treated with non-interfering siRNA were used as negative controls for the *TDRD12-001* knockdown.

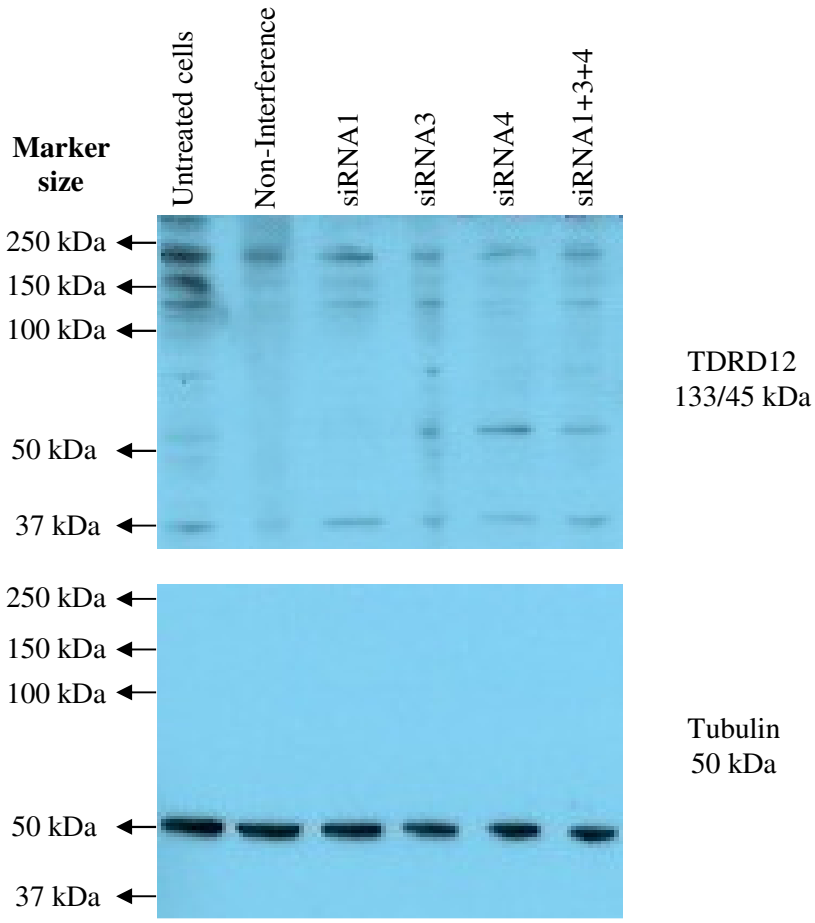

Figure 5.11 WB analysis of TDRD12 protein (Santa Cruz Biotechnology antibody; T-17: SC-248802) in NT2 cells following knockdown.
WB analysis presenting the WB profile created from the NT2 cells. Untreated cells were used as positive controls. Cells treated with non-interfering siRNA were used as negative controls for the *TDRD12-001* knockdown. Three different *TDRD12-001* siRNAs were analysed (siRNA1, siRNA3 and siRNA4), and a combination of the three siRNAs was also utilised (siRNA1+3+4). 10 µL of protein lysates was loaded on the SDS-PAGE gel, which contains around 60,000 cells/well. Anti-α-tubulin was utilised as a loading control. The primary and secondary antibodies and the dilutions at which they were utilised are shown in Table 2.8 and Table 2.9. The WB TDRD12 products were not detected at the expected sizes. It is clear that this was not a good antibody to use.

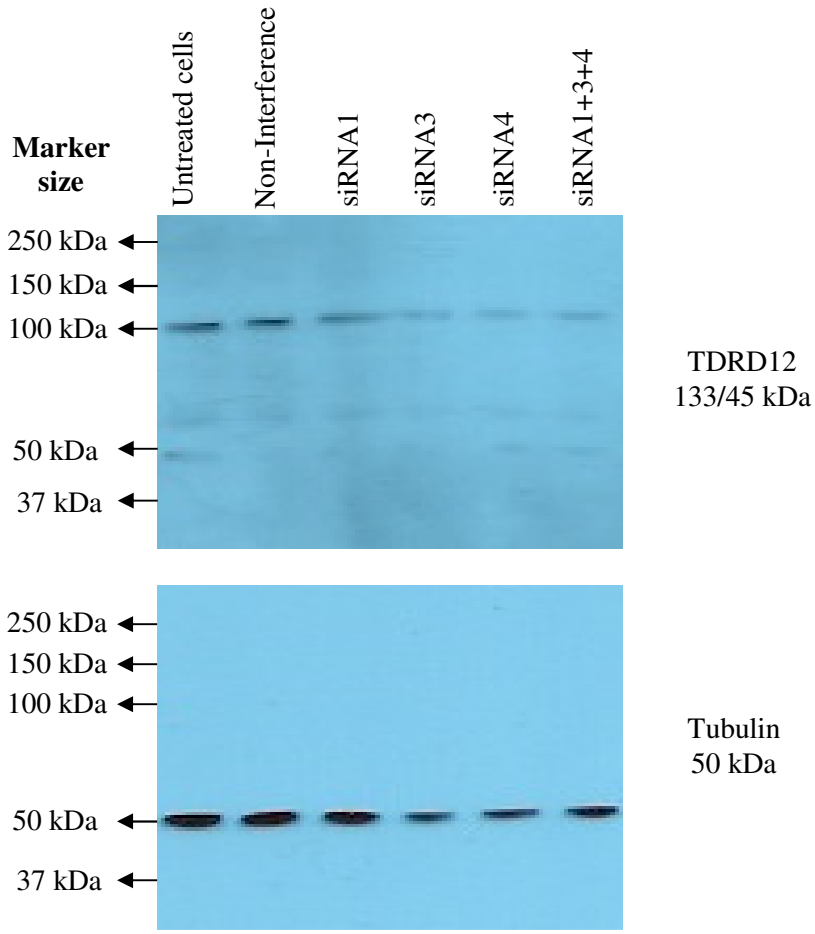

Figure 5.12 WB analysis of TDRD12 protein (ATLAS ANTIBODIES; Anti-TDRD12: HPA-042684) in NT2 cells following knockdown.
WB analysis presenting the WB profile created from the NT2 cells. Untreated cells were used as positive controls. Cells treated with non-interfering siRNA were used as negative controls for the *TDRD12-001* knockdown. Three different *TDRD12-001* siRNAs were analysed (siRNA1, siRNA3 and siRNA4), and a combination of the three siRNAs was also utilised (siRNA1+3+4). 10 µL of protein lysates was loaded on the SDS-PAGE gel, which contains around 60,000 cells/well. Anti-α-tubulin was utilised as a loading control. The primary and secondary antibodies and the dilutions at which they were utilised are shown in Table 2.8 and Table 2.9. The WB TDRD12 products were not detected at the expected sizes. It is clear that this was not a good antibody to use.

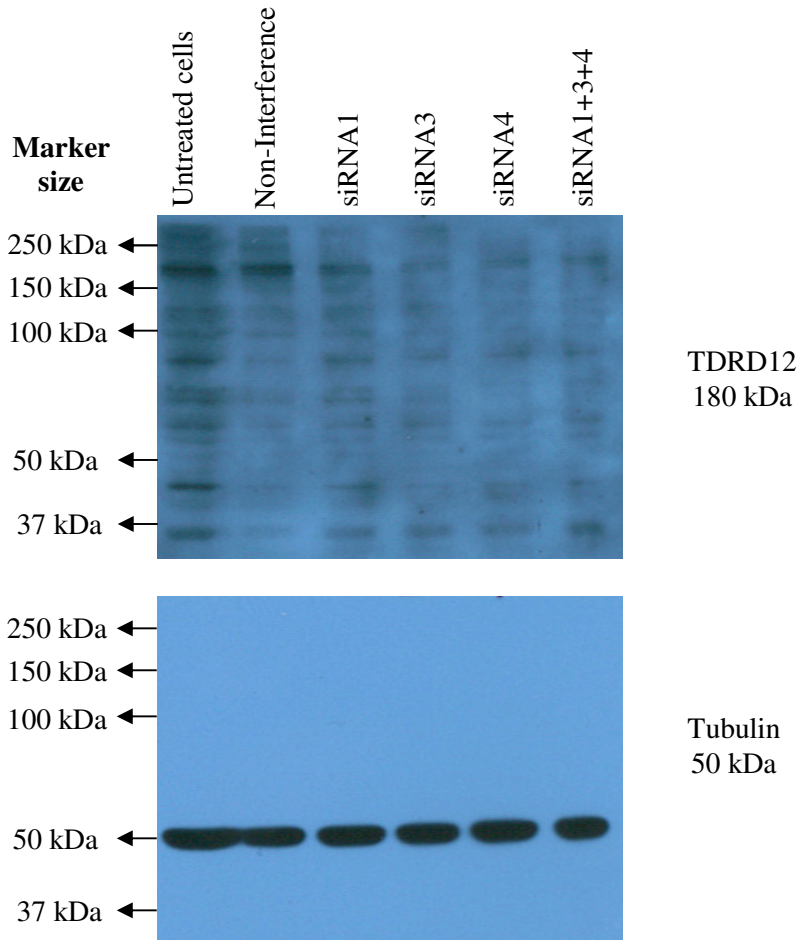

Figure 5.13 WB analysis of TDRD12 protein (TDRD12-Guinea pig antibody; PEP-1310598) in NT2 cells following knockdown.
WB analysis presenting the WB profile created from the NT2 cells. Untreated cells were used as positive controls. Cells treated with non-interfering siRNA were used as negative controls for the *TDRD12-001* knockdown. Three different *TDRD12-001* siRNAs were analysed (siRNA1, siRNA3 and siRNA4), and a combination of the three siRNAs was also utilised (siRNA1+3+4). 15 µL of protein lysates was loaded on the SDS-PAGE gel, which contains around 90,000 cells/well. Anti-α-tubulin was utilised as a loading control. The primary and secondary antibodies and the dilutions at which they were utilised are shown in Table 2.8 and Table 2.9. Some WB TDRD12 products that were detected that might has been good antibody. Nevertheless, the predicted molecular weight size was 133 kDa; the bands were found to be around 180 kDa. Thus, this observation was carefully questioned and analysed by looking at the fusion gene in Chapter 3 that corresponds to 180 kDa. Thus, this was a good antibody to use. However, it showed unspecific reactions and it seemed not a clear antibody.

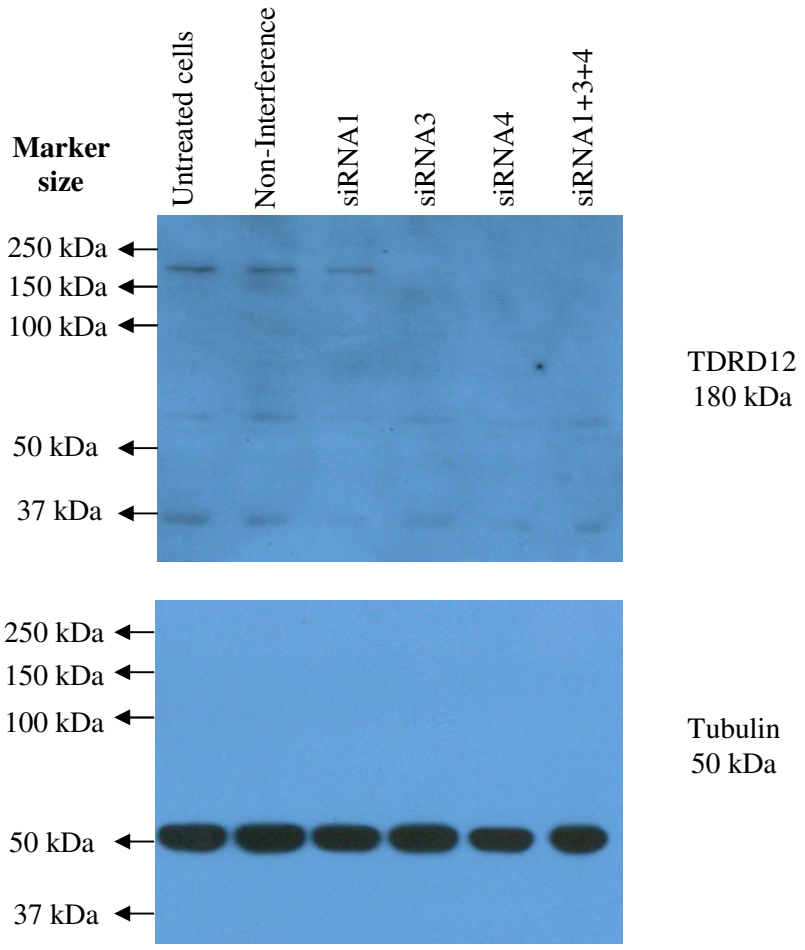

Figure 5.14 WB analysis of TDRD12 protein (TDRD12-Guinea pig antibody; PEP-1310599) in NT2 cells following knockdown.
WB analysis presenting the WB profile created from the NT2 cells. Untreated cells were used as positive controls. Cells treated with non-interfering siRNA were used as negative controls for the *TDRD12-001* knockdown. Three different *TDRD12-001* siRNAs were analysed (siRNA1, siRNA3 and siRNA4), and a combination of the three siRNAs was also utilised (siRNA1+3+4). 15 µL of protein lysates was loaded on the SDS-PAGE gel, which contains around 90,000 cells/well. Anti-α-tubulin was utilised as a loading control. The primary and secondary antibodies and the dilutions at which they were utilised are shown in Table 2.8 and Table 2.9. The WB TDRD12 products were detected that might has been good antibody. Nevertheless, the predicted molecular weight size was 133 kDa; the bands were found to be around 180 kDa. Thus, this observation was carefully questioned and analysed by looking at the fusion gene in Chapter 3 that corresponds to 180 kDa. Thus, this was a good antibody to use. Moreover, it seemed a clear antibody.

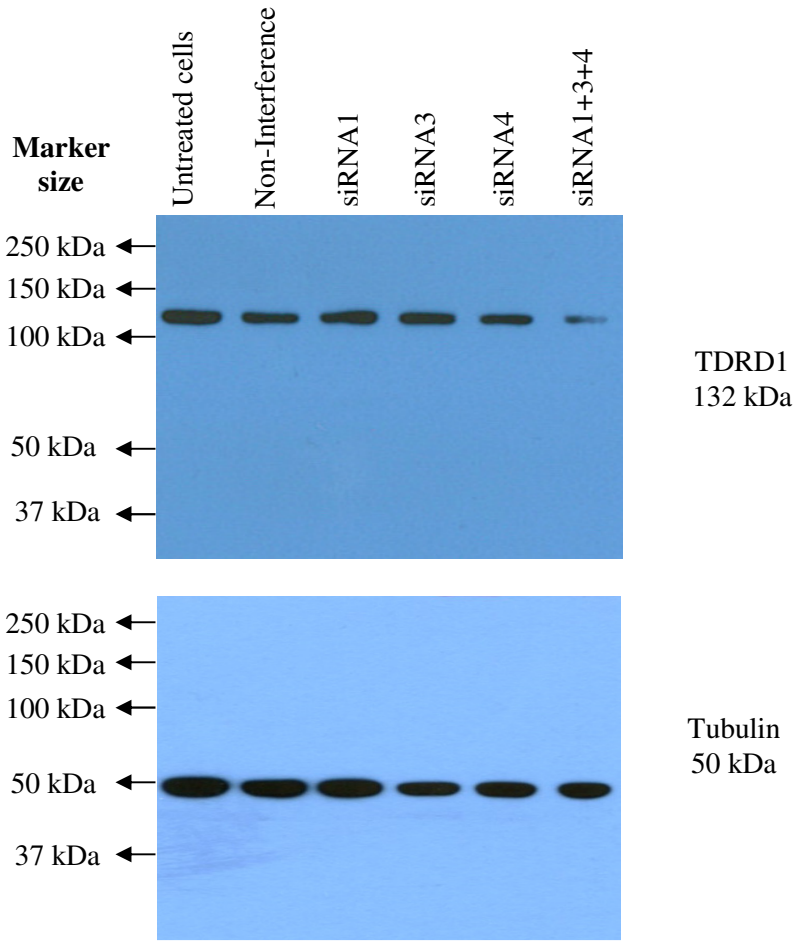

Figure 5.15 WB analysis of TDRD1 protein (Abcam; Anti-TDRD1 polyclonal: ab-107665) in *TDRD12-001*-depleted NT2 cells.
WB analysis presenting the WB profile created from the NT2 cells. Untreated cells were used as positive controls. Cells treated with non-interfering siRNA were used as negative controls for the *TDRD12-001* knockdown. Three different *TDRD12-001* siRNAs were analysed (siRNA1, siRNA3 and siRNA4), and a combination of the three siRNAs was also utilised (siRNA1+3+4). 15 µL of protein lysates was loaded on the SDS-PAGE gel, which contains around 90,000 cells/well. Anti-α-tubulin was utilised as a loading control. The primary and secondary antibodies and the dilutions at which they were utilised are shown in Table 2.8 and Table 2.9. The WB TDRD1 products were detected at approximately the expected sizes (132 kDa).

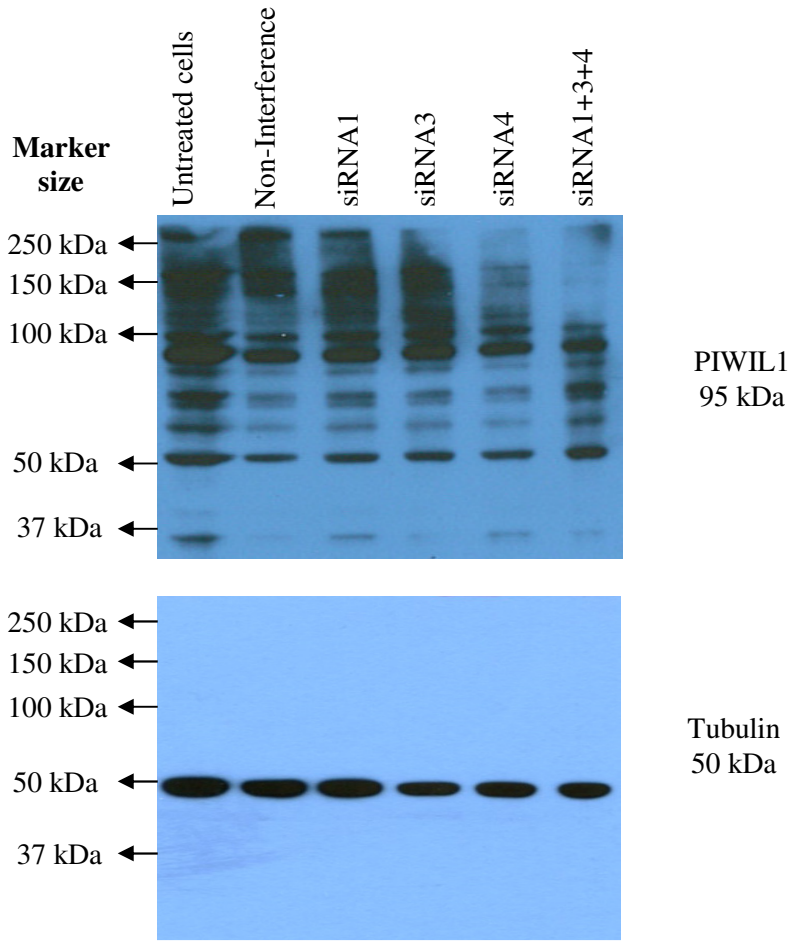

Figure 5.16 WB analysis of PIWIL1 protein (SIGMA-ALDRICH; Monoclonal Anti-PIWIL1: SAB-4200365) in *TDRD12-001*-depleted NT2 cells.
WB analysis presenting the WB profile created from the NT2 cells. Untreated cells were used as positive controls. Cells treated with non-interfering siRNA were used as negative controls for the *TDRD12-001* knockdown. Three different *TDRD12-001* siRNAs were analysed (siRNA1, siRNA3 and siRNA4), and a combination of the three siRNAs was also utilised (siRNA1+3+4). 15 µL of protein lysates was loaded on the SDS-PAGE gel, which contains around 90,000 cells/well. Anti-α-tubulin was utilised as a loading control. The primary and secondary antibodies and the dilutions at which they were utilised are shown in Table 2.8 and Table 2.9. Some WB PIWIL1 products were detected at approximately the expected sizes (95 kDa).

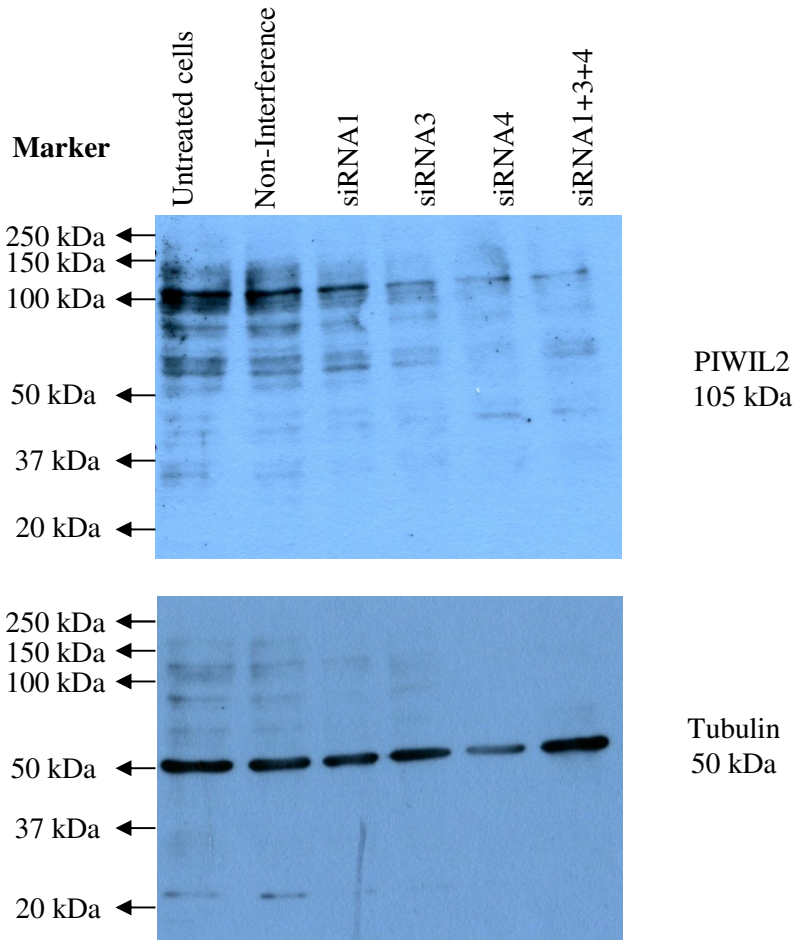

Figure 5.17 WB analysis of PIWIL2 protein (Abnova; PIWIL2 monoclonal: MAB-0843) in *TDRD12-001*-depleted NT2 cells.
WB analysis presenting the WB profile created from the NT2 cells. Untreated cells were used as positive controls. Cells treated with non-interfering siRNA were used as negative controls for the *TDRD12-001* knockdown. Three different *TDRD12-001* siRNAs were analysed (siRNA1, siRNA3 and siRNA4), and a combination of the three siRNAs was also utilised (siRNA1+3+4). 15 µL of protein lysates was loaded on the SDS-PAGE gel, which contains around 90,000 cells/well. Anti-α-tubulin was utilised as a loading control. The primary and secondary antibodies and the dilutions at which they were utilised are shown in Table 2.8 and Table 2.9. The WB PIWIL2 products were detected at approximately the expected sizes (105 kDa).

5.3.4. Analysis of self-renewal capacity following NT2 depletion

To evaluate NT2 proliferation after treatment with different *TDRD12-001* siRNAs, an extreme limiting dilution analysis was used. A series of cellular dilutions were applied during the seeding and growing of NT2 cells to analyse the proliferation capacity of NT2 cells in each condition of treatment, together with the positive controls (untreated cells), in order to compare the growth of the treated cells and the negative controls (cells treated with non-interfering siRNA and cells treated with HiPerFect transfection). Then, the NT2 cells were pictured over a period of 8 days using light microscopy (see Figure 5.18).

Moreover, the cell viability count analysis technique was used to evaluate the effect of *TDRD12-001* siRNA knockdown on cellular growth and proliferation (see Figure 5.19). The survival of NT2 cells is clearly affected when they are treated with HiPerFect transfection reagent in comparison with untreated NT2 cells. These results indicate that the HiPerFect transfection reagent has a toxic effect on NT2 cells, so no meaningful data can be acquired.

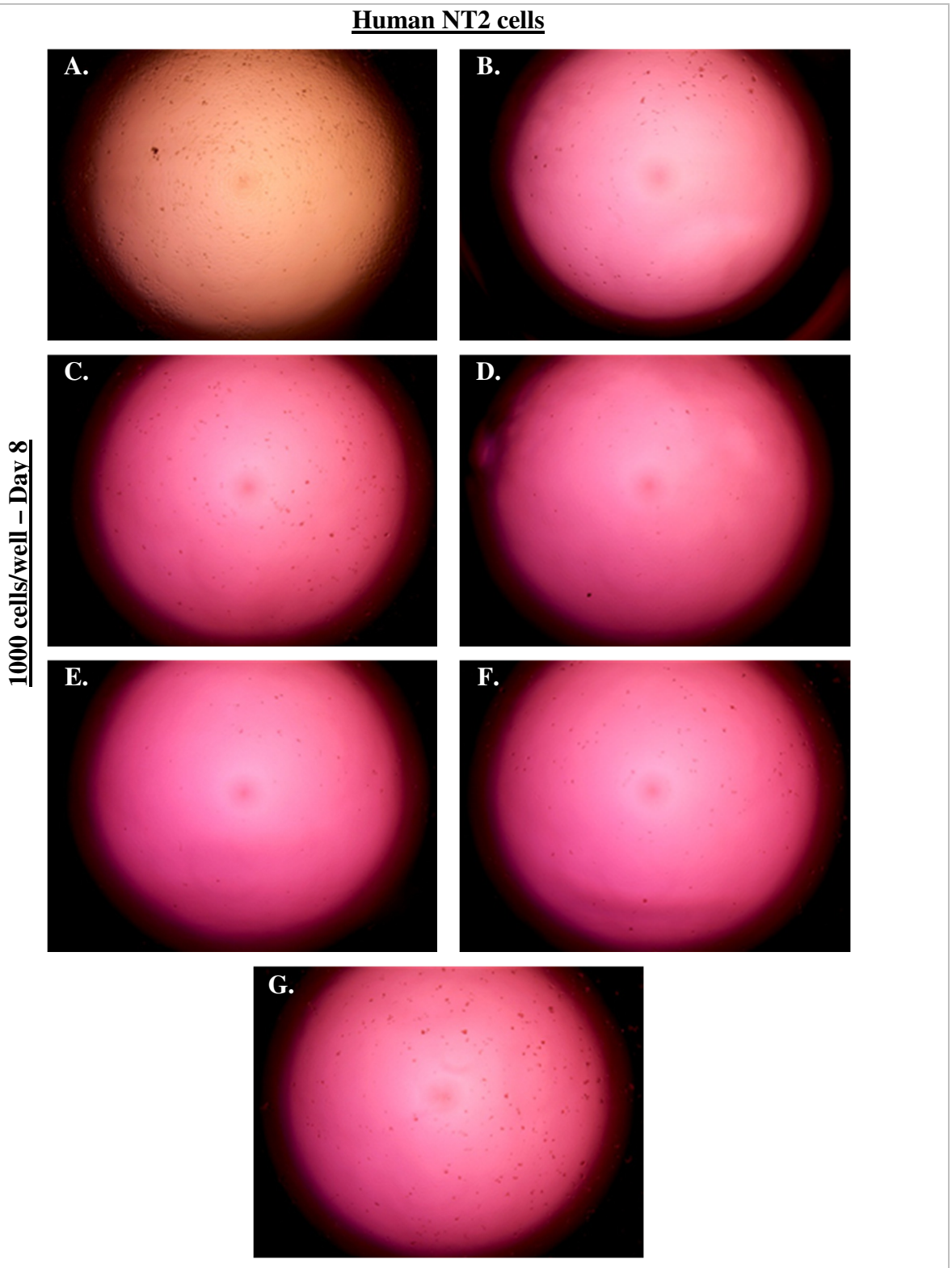

Figure 5.18 ELDA analysis of NT2 cell growth after treatment with different *TDRD12-001* siRNA for eight days (1000 cells are seeded/well).
Panel (A): untreated NT2 cells were utilised as positive controls to compare the growth of the treated cells. Panel (B): cells treated with non-interfering siRNA. Panel (C): cells treated with HiPerFect transfection. Panel (B+C): were used as negative controls for the *TDRD12-001* knockdown. Panel (D): cells treated with *TDRD12-001* siRNA1. Panel (E): cells treated with *TDRD12-001* siRNA3. Panel (F): cells treated with *TDRD12-001* siRNA4. Panel (G): cells treated with *TDRD12-001* siRNA1+3+4.

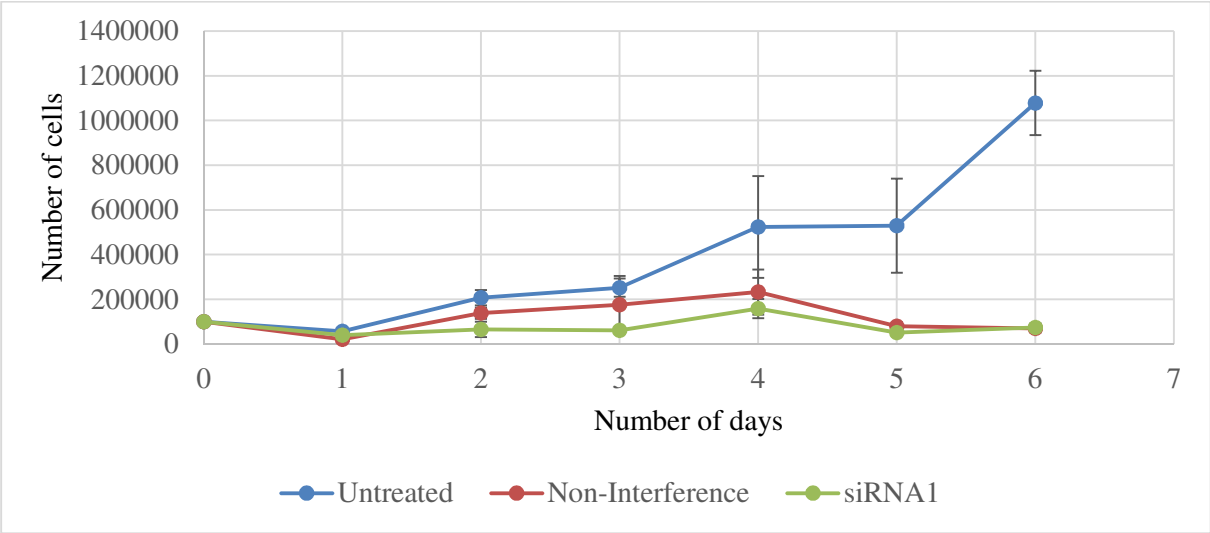

Figure 5.19 *TDRD12-001*-depleted NT2 cells growth curve.
Untreated NT2 cells were utilised as positive controls to compare the growth of treated cells. Cells treated with non-interfering siRNA were used as negative controls for the *TDRD12-001* knockdown. Cells treated with *TDRD12-001* siRNA1. A six "hit" method was utilised: the treatments were added after day 1, 2, 3, 4, 5, and 6 from seeding the NT2 cells. Trypan blue staining was utilised to analyse cell growth by counting the number of live cells after 1, 2, 3, 4, 5, and 6 siRNA and non-interference "hits". The error bars demonstrate the average error calculated from the six replications "hits" per condition of treatment.

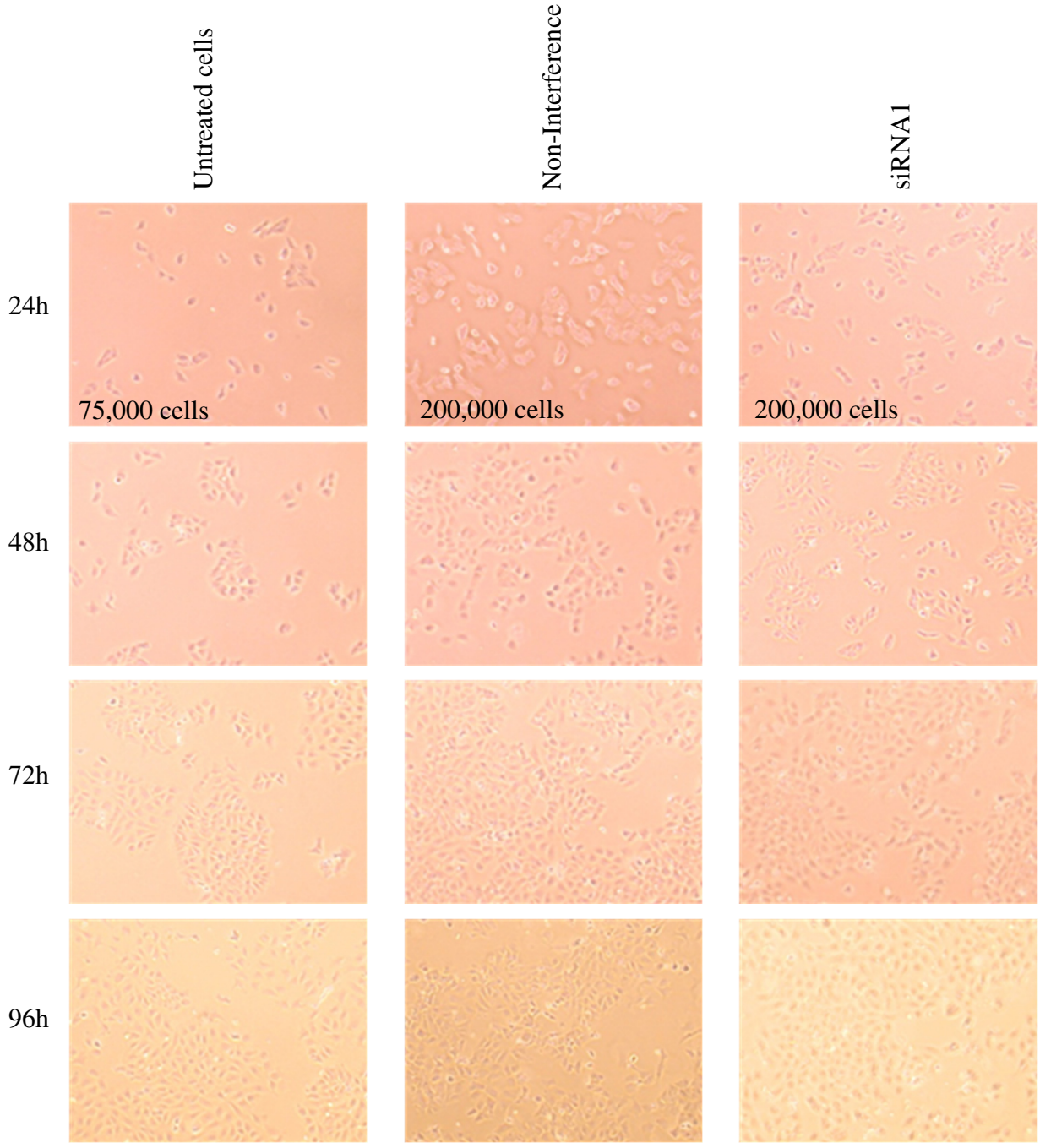

Figure 5.20 A three "hit" method utilised for the *TDRD12-001*-depleted NT2 cells siRNA knockdown.
Untreated NT2 cells were utilised as positive controls to compare the growth of the treated cells. Cells treated with non-interfering siRNA were used as negative controls for the *TDRD12-001* knockdown. The siRNA1 treatment was first added at 24 hours, and then the treatment was added at 48 hours. Finally, it was added at 72 hours after seeding the NT2 cells.

5.4. Discussion

Transposable elements (TEs) refer to a group of mobile DNA nucleotide sequences embodying and representing significant and vital roles in a majority of human genomes (Chénais, 2015; Guidez, 2014). TEs are critical factors in genome evolution. The insertion of TEs into genomes might have the ability to affect gene expression to drive oncogenesis. Furthermore, the insertion of TEs might cause genetic structural changes (Chénais, 2015). The Tudor family protein members have the capacity to play vital functions in a majority of processes and developments through human gametogenesis, cell division and genome stability. Additionally, these proteins are involved in numerous RNA metabolism processes, including piRNA, siRNA/miRNA pathways and RNA splicing processes. The piRNA pathways refer to germ-line-specific RNAs (26-31-nt), which are bound to the PIWI subfamily members of the Argonaute family in both human genders. The piRNA pathway roles are associated with protecting the genome by silencing the TEs during the development processes of the germ cells (Malone and Hannon, 2009; Pek *et al.,* 2012; Thomson and Lin, 2009; Zhou *et al.,* 2014).

The processes of controlling the PIWI-piRNA complex have functional roles in human somatic cells and germ cells. In addition, the function of PIWI proteins might be involved in the development and growth of cancerous cells and solid tumours—for example, the overexpression of the *PIWIL1* orthologue in a male germ-cell tumour (seminoma) as well as overproduction of PIWI proteins in different types of cancerous cells (e.g., cervical, breast, liver and gastric malignant tumours) (Ishizu *et al.,* 2012; Iwasaki *et al.,* 2015; Qiao *et al.,* 2002; Ross *et al.,* 2014; Suzuki *et al.,* 2012).

TDRD proteins are functionally linked to piRNA control. The TDRD8 protein is recognised as having the ability to play an important role in spermatogenesis in association with the PIWIL1 protein orthologue (Bao *et al.,* 2012). The TDRD1 protein is identified as interacting with the PIWIL2 protein orthologue as well as contributing to and taking part in the primary piRNA biogenesis (Reuter *et al.,* 2009; Wang *et al.,* 2009). The TDRD5 protein is specified as being required for the inhibition, repression and suppression of LINE1 transposons (Yabuta *et al.,* 2011). The TDRD9 protein is documented as interacting with the PIWIL4 protein orthologue to play a functional role in secondary piRNA biogenesis (Shoji *et al.,* 2009). The TDRD2 protein is known as interacting with the PIWIL1 and PIWIL4 protein orthologues and as participating in primary piRNA (Saxe *et al.,* 2013).

The TDRD4, TDRD6 and TDRD7 proteins are acknowledged as interacting with PIWIL1 protein orthologues, and this compensation of proteins is important and necessary for spermiogenesis (Pan *et al.,* 2005; Tanaka *et al.,* 2011; Vasileva *et al.,* 2009). The TDRD12 protein is identified as playing a vital role in interacting with the PIWIL2 protein orthologue, and this protein is important and required for the process of secondary piRNA biogenesis (Pandey *et al.,* 2013; Zhou *et al.,* 2014). TDRD protein family members play functional roles in controlling the primary and secondary piRNA pathways, and they usually cooperate with other proteins with sDMA modifications. Hence, understanding and analysing the functional role of each human *TDRD* gene and detecting clear links and pictures between these important family protein members and their interaction with piRNA biogenesis pathways is vital (Chen *et al.,* 2011; Iwasaki *et al.,* 2015).

Research has barely started to clarify the process of biogenesis in piRNA, but two biochemically separate pathways have already been identified. The primary biogenesis process involves converting long, single-stranded transcripts that arise from genomic loci, called piRNA clusters, to simple piRNA of about 24-30-nuclurides, which interact with PIWIL2 and PIWIL1 orthologues (Li *et al.,* 2013). However, the process of biogenesis in PIWIL4 orthologue-bound piRNA is not direct, and is done through the PIWIL2 orthologue-mediated slicer splitting the cleavage of any target. This is supposed to start the production of the new secondary piRNA (Aravin *et al.,* 2008; De Fazio *et al.,* 2011; Kuramochi-Miyagawa *et al.,* 2008). This procedure allows for monitoring the activities of TEs by germ cells, as well as showing an adaptive response to them by providing guidance for the movement of PIWIL4 orthologue to the genomic loci. The cellular processes that occur after this initial PIWIL2 orthologue cleaving of a target are as yet unclear, mainly due to lack of insight and full knowledge regarding the distinct functional units that participate in them (Pandey *et al.,* 2013).

The *TDRD12* gene shows high rates of expression in the germ-line and may be involved in the piRNA pathway during gametogenesis (Chen *et al.,* 2011; Zhou *et al.,* 2014). This piRNA pathway is a gonad-specific small non-coding RNA regulatory pathway, which is responsible for providing protection against REs. The TDRD12 protein has been recognised to be a unique piRNA biogenesis factor. It is also present in complexes, which have the PIWIL2 protein that is related and linked to primary piRNA, as well as the TDRD1 protein (Pandey *et al.,* 2013). In addition, the TDRD12 protein is also necessary for the process of spermatogenesis, and is required during the biogenesis of PIWIL4 piRNA (Lim *et al.,* 2014; Pandey *et al.,* 2013; Zhou *et al.,* 2014).

TDRD12, PIWIL1 and PIWIL2 form a functional complex in mice (Pandey *et al.,* 2013). Given this, the human PIWIL1 and PIWIL2 proteins in *TDRD12-001*-depleted NT2 cells was analysed using WB analysis technique. The results showing evidence that the WB PIWIL1 product bands were not depleted or changed. However, it can be seen that there are a number of other higher molecular weight bands that disappeared. The WB PIWIL2 product bands were depleted upon siRNA reduction of TDRD12, suggesting a functional regulatory relationship, whether this is at the transcriptional level or post-transcriptional level is unknown.

The results obtained in this Chapter suggested that we obtained significant levels of *TDRD12-001* transcript knockdown in NT2 cells using three different types of *TDRD12-001* siRNAs. It can be also seen from the results that the survival of NT2 cells, which were treated with non-interfering siRNA (used as negative controls for the *TDRD12-001* knockdown) was clearly affected when they treated with HiPerFect transfection reagent in comparison with untreated NT2 cells. These results indicated that the concentration of HiPerFect might have a toxic effect on NT2 cells (the cells might not die but they might stop proliferating). Therefore, it is suggested that the siRNA treatments be repeated with different HiPerFect concentrations or different transfection reagents (e.g., VIROMER or Lipofectamine).

The results also showing strong evidence that a large number of the RE, HERV and germ-line genes were up-regulated and a small number of them were down-regulated during the knockdown of the *TDRD12* gene. Consequently, the group of up-regulated genes shows that *TDRD12* might be repressing the REs.

5.5. Concluding remarks

This chapter focussed on the *TDRD12* gene in regulating the HERV and RE gene expression levels in human germ-line tumour cells. Many germ-line-specific genes show high levels of expression profiles in cancerous cells and malignant tumours. These genes are known as CT genes, which potential encode targets for human cancer immunotherapy, cancer diagnosis, biomarkers and the creation of cancer drugs (Gjerstorff *et al.,* 2015; Krishnadas *et al.,* 2013; Whitehurst, 2014; Zhou *et al.,* 2014). The *TDRD12* gene is identified as a CT gene (see Chapter 3). The results obtained in this chapter suggested that the *TDRD12* gene might play a role in conferring stemness to cancerous cells, and this gene might also requires for the germ-line/stem cell regulation of REs and HERVs in human germ-line tumour cells. Therefore, further analysis of genome wide transcription upon *TDRD12-001* depletion should reveal how extensive the role of *TDRD12* is in controlling stem-line gene and REs expression. Additionally, the specificity of TDRD12 antibodies was validated in this chapter for further analysis of localisation within normal tissues and cancerous human cells using IHC and IF analysis techniques (see Chapter 6).

6. Sub-cellular localisation of TDRD12

6.1. Introduction

6.1.1. The process of spermatogenesis

Spermatogenesis refers to the cellular process required for production of the male gametes, sperm. Spermatogenesis occurs when spermatogonial germ cells differentiate and produce spermatozoa (Dong *et al.,* 2015; Durairajanayagam *et al.,* 2015; Lie *et al.,* 2013; Meccariello *et al.,* 2014a). This process begins during puberty and slowly decreases following the early peaking stage. In contrast to oogenesis in females, wherein gametogenesis stops in menopause, spermatogenesis continues until old age in men (Eskenazi *et al.,* 2003). The gametogenic tissues of the testis are the seminiferous tubules, convoluted tube-shaped structures. At the seminiferous tubule basal membrane, the spermatogonial germ cells self-renew and migrate to the centre of the tube and differentiate to form primary spermatocytes, which subsequently differentiate further to make sperm cells (Dong *et al.,* 2015; Durairajanayagam *et al.,* 2015; Meccariello *et al.,* 2014a; Sadri-Ardekani and Atala, 2014).

6.1.1.1. Spermatozoa maturation

The spermatogonia cells located within the basal compartment of the seminiferous tubules serve as the progenitor cells that initiate the process of spermatogenesis. The non-differentiated spermatogonia make up the spermatogonial SCs. These spermatogonial SCs have been indicated to undergo division to form a new spermatogonial SC. Thus, they result in the self-renewing process of the SC compartment or end up forming an A1 type of spermatogonial cell. Retinoic acid is considered vital for triggering spermatogenesis, also suggesting that it could be needed in initial cellular differentiation. It also has a role in the later phases of germ cell development (Hogarth and Griswold, 2013; Zhang and Wu, 2015). After this process, the A1 spermatogonia produce the primary spermatocytes through a process of meiotic division. After undergoing the initial meiotic cell division, the primary spermatocytes change into secondary spermatocytes. After carrying out the second meiotic division, four haploid cells are produced and are the round spermatid cells. These spermatid cells elongate to form mature spermatids, which are released into the lumen of the tubules in the form of sperm or spermatozoa. This process of releasing the spermatozoa from the adluminal compartment to the lumen is known as ‘spermiation’ (Chen and Liu, 2015; Lui and Cheng, 2012; Zhang and Wu, 2015).

6.1.1.2. The blood-testis barrier (BTB)

The BTB divides the sectional parts of the seminiferous tubules inside which spermatogenesis takes place in order to form the basal and adluminal compartments. The BTB is created due to the formation of a tight junction between nearby Sertoli cells (see Figure 6.1), and it provides the developing germ cells a site with immune privileges (Gerber *et al.,* 2015; Kaur *et al.,* 2014; Lie *et al.,* 2013). The spermatogonia as well as the spermatogonial SCs are located within the basal compartment. Meanwhile, meiosis and subsequent development of the spermatocytes takes place in the adluminal compartment. The Sertoli cells create a physical barrier that prevents movement of larger molecules like proteins across the tubules to the adjoining blood vessels. Nevertheless, even spermatogonial cells found within the basal compartment 'beyond' the BTB cannot cause self-antigen production. This process happens due to the fact that germ-line cells lack the major histocompatibility complex (MHC) molecules needed to present peptides for identification by the immune system (Gerber *et al.,* 2015; Guillaudeux *et al.,* 1996; Kaur *et al.,* 2014).

The BTB is known to be a dynamic structural detail, continuously being reformed and dismantled. This characteristic exists partially for germ cells progressing towards the lumen between the supportive Sertoli cells (Kaur *et al.,* 2014; Lie *et al.,* 2013). Testosterone, together with cytokines like the transforming growth factor-β (TGF-β), controls the kinetics involved in protein endocytosis. They also regulate the recycling process of the Sertoli cells, which is essential in carrying out this dynamic cellular process (Gerber *et al.,* 2015; Kaur *et al.,* 2014; Yan *et al.,* 2008). Thus, the BTB is attained not only due to the tight junctions between nearby Sertoli cells creating an anatomical physical barrier but also because of physiology and immunology-based means (Gerber *et al.,* 2015; Kaur *et al.,* 2014; Mital *et al.,* 2011).

In previous Chapters, I report that *TDRD12* is a CT gene, which was expressed in cancer cell lines. One of the major aims of this study is to analyse the cellular and sub-cellular localisation of TDRD12 protein in normal testis tissues. This study also investigates the sub-cellular localisation of TDRD12 in NT2 and SW480 cancer cells.

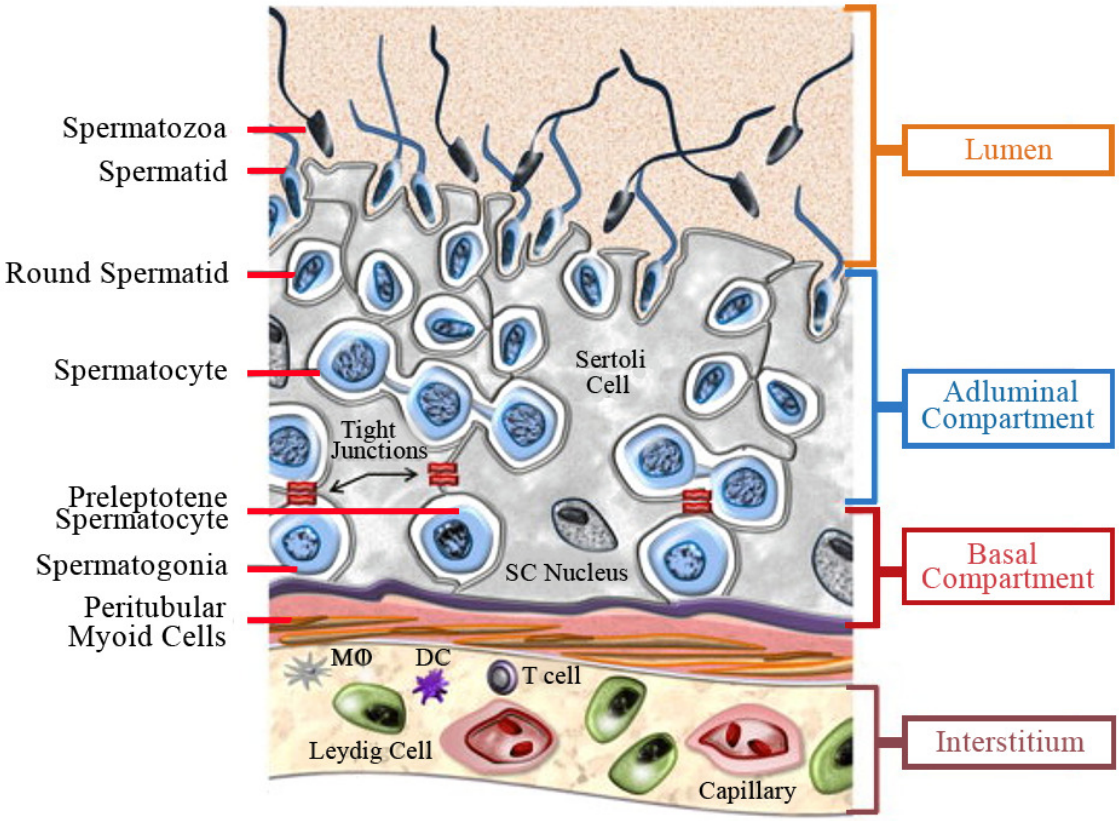

Figure 6.1 localisation of BTB barrier and testis cellular components.
Taken from (Kaur *et al.,* 2014).

6.2. Aims

This study aims to analyse the sub-cellular localisation of human TDRD12, TDRD1, PIWIL1 and PIWIL2 proteins in normal tissues and cancerous cells in order to determine their cancer marker potential and provide insight into their normal function.

This study analyses TDRD1, PIWIL1 and PIWIL2 proteins because the TDRD12 protein is required for the secondary PIWI interacting RNA biogenesis (Zhou *et al.,* 2014). Moreover, the TDRD12 protein presents in complexes with the PIWIL2 and TDRD1 proteins, a complex linked to primary piRNA processing in mice (Pandey *et al.,* 2013). In addition, the *TDRD12* gene is necessary for the process of spermatogenesis in mice (Pandey *et al.,* 2013). Furthermore, the PIWIL2 becomes depleted upon siRNA reduction of TDRD12, suggesting a functional regulatory relationship (refer to Chapter 5).

6.3. Results

6.3.1. IHC staining analysis of TDRD12, TDRD1, PIWIL1 and PIWIL2 in normal tissues.

Because the TDRD12 protein forms a functional complex with TDRD1 and PIWIL2 proteins, and plays a role in the secondary PIWI interacting RNA biogenesis in mice (Pandey *et al.,* 2013), this study analysed the presence of TDRD12, TDRD1, PIWIL1 and PIWIL2 in normal human tissues and cancerous cells using immunohistochemistry (IHC) and immunofluorescence (IF). Several commercial antibodies of TDRD12 protein were used for the IHC and IF analyses. Some antibodies were specifically raised by Eurogentec for use (see Table 2.15 in Chapter 2 for the antibodies; also see Sections 6.3.2 and 6.3.3 for the IF analysis results).

This study employed normal testis tissues because the *TDRD12*, *TDRD1*, *PIWIL1* and *PIWIL2* genes were identified as CTAs (they have testis-restricted expression; see Chapter 3). In addition, studies indicate that the *TDRD12* gene is necessary for spermatogenesis in mice (Pandey *et al.,* 2013). Normal colon tissues were used as negative controls, after the results were shown from RT-PCR (see Chapter 3; also see Feichtinger *et al.,* 2012) and haematoxylin was used for tissue staining.

The IHC results suggested that PIWIL1 localisation was detected in the adluminal compartment of the seminiferous tubules and appeared cytoplasmic (see Figure 6.2). TDRD12-PEP99 antibody was unlikely to be a good antibody to use for IHC as no positive signal could be detected (see Figure 6.3). TDRD1 localisation was detected in the spermatogonial layer of the seminiferous tubules and appeared nuclear (see Figure 6.4). PIWIL2 localisation was detected in the spermatogonial layer of the seminiferous tubules and appeared cytoplasmic (see Figure 6.5). TDRD12 (ATLAS antibody) localisation was detected in both the spermatogonial layer and adluminal compartment of the seminiferous tubules and appeared nuclear (see Figure 6.6). TDRD12 (T17 antibody) localisation was detected in both the spermatogonial layer and adluminal compartment of the seminiferous tubules and appeared cytoplasmic (see Figure 6.7). The images were captured by ZEISS-ZEN 2 LITE (blue edition) AXIO scan software.

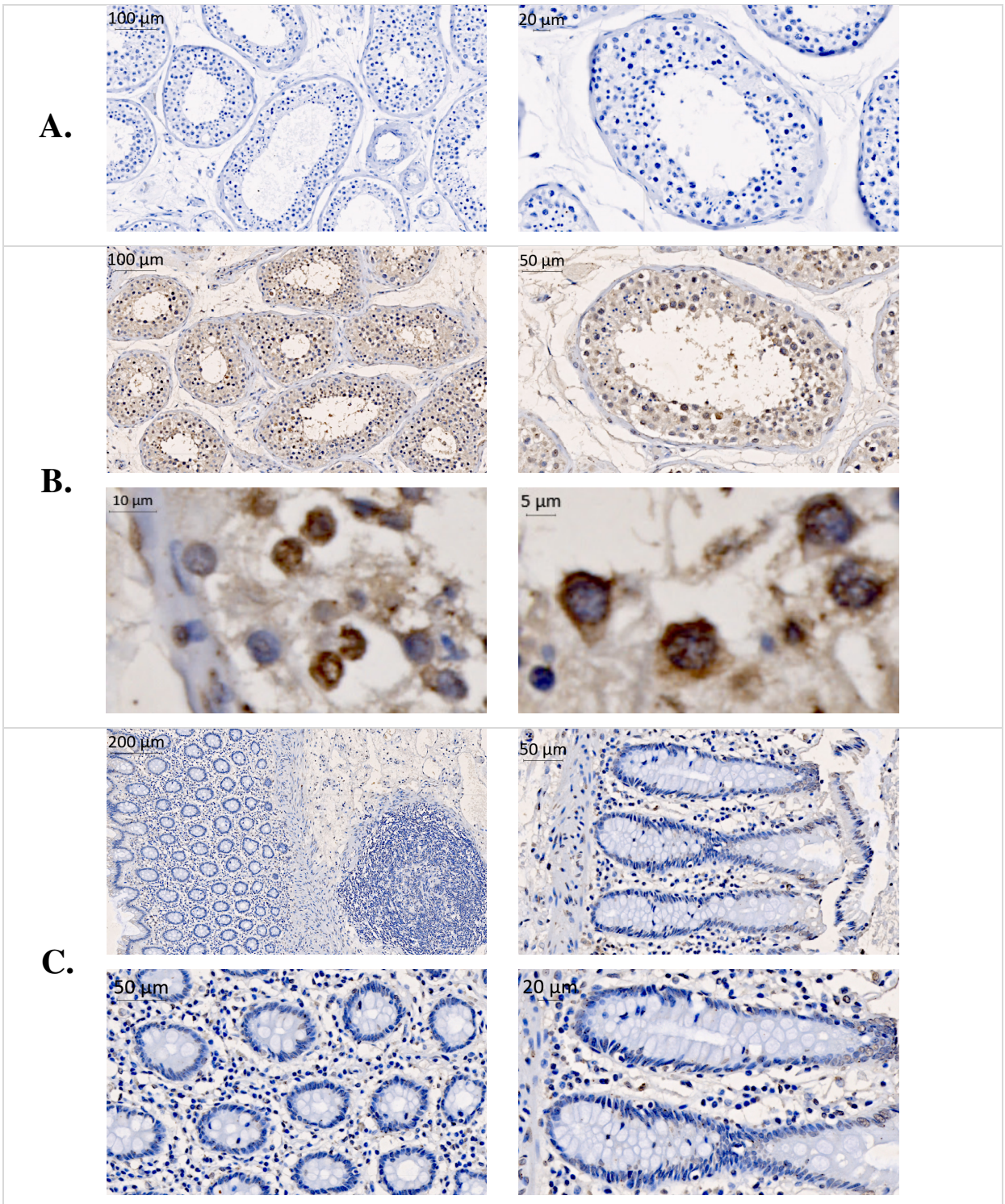

Figure 6.2 IHC staining analysis of PIWIL1 protein in normal testis and colon (B22 C22) tissues. Panel (A): shows the staining of the PIWIL1 protein negative control (overnight normal mouse serum (Dako; X0910) blocking and then 40 minutes 1:1000 of goat anti-mouse secondary antibody; Abcam; ab47827) in normal testis tissues. Panel (B): shows the staining of the PIWIL1 protein (overnight 1:100 of PIWIL1 primary antibody; SIGMA-ALDRICH; SAB-4200365 and then 40 minutes 1:1000 of goat anti-mouse secondary antibody) in normal testis tissues. Panel (C): shows the staining of the PIWIL1 protein (overnight 1:100 of PIWIL1 primary antibody and then 40 minutes 1:1000 of goat anti-mouse secondary antibody) in normal colon tissues as a negative control. Haematoxylin was used for the staining. The images were captured by ZEISS-ZEN 2 LITE (blue edition) AXIO scan software.

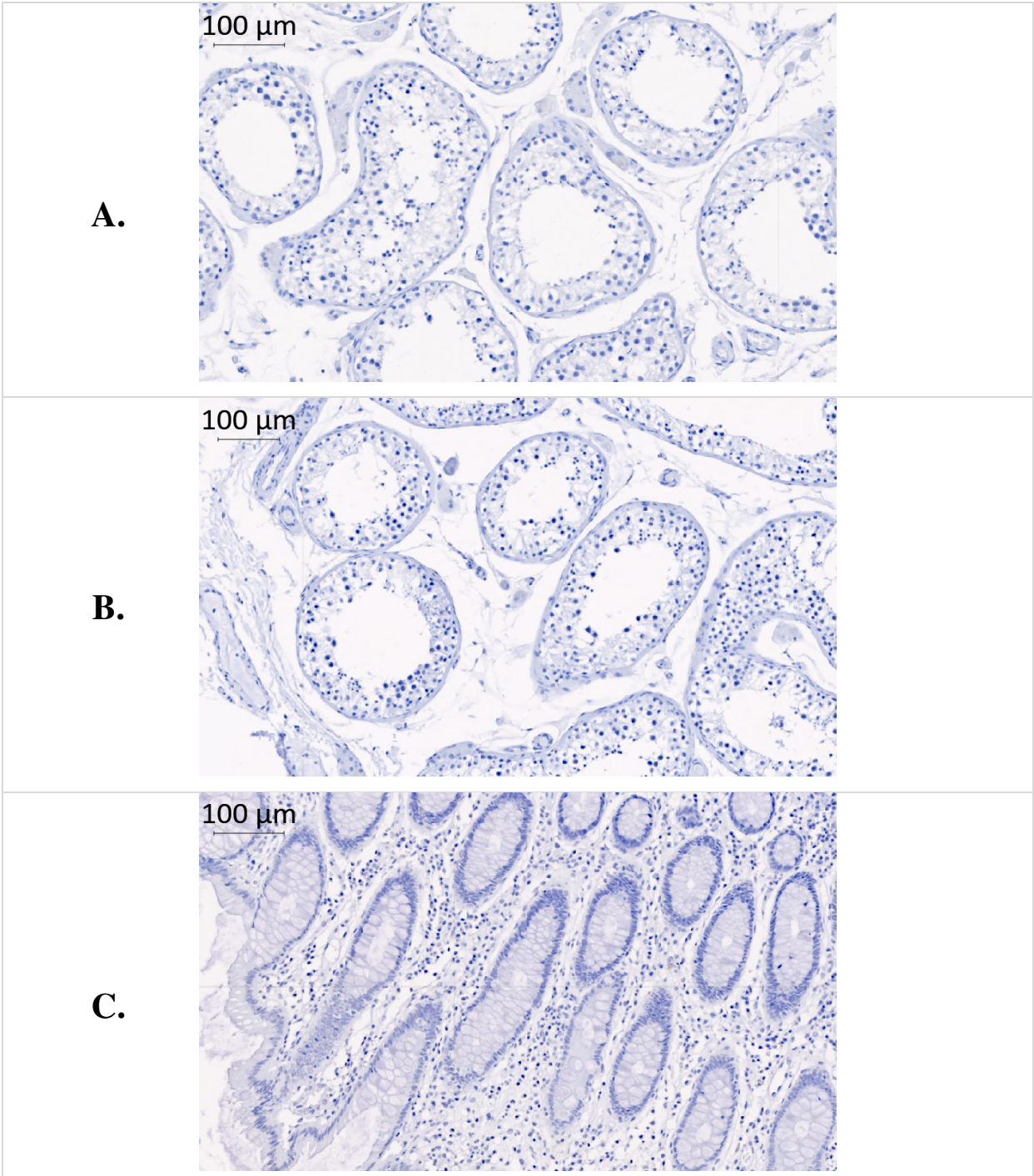

Figure 6.3 IHC staining analysis of TDRD12 protein using TDRD12-PEP99 antibody in normal testis and colon (B22 C22) tissues.
Panel (A): shows the staining of the TDRD12 protein negative control (overnight normal rabbit serum (Dako; X0902) blocking and then 40 minutes 1:500 of goat anti-guinea pig secondary antibody; Abcam; ab97155) in normal testis tissues. Panel (B): shows the staining of the TDRD12 protein (overnight 1:20 of TDRD12 primary antibody; Eurogentec; PEP-1310599 and then 40 minutes 1:500 of goat anti-guinea pig secondary antibody) in normal testis tissues. Panel (C): shows the staining of the TDRD12 protein (overnight 1:100 of TDRD12 primary antibody and then 40 minutes 1:1000 of goat anti-guinea pig secondary antibody) in normal colon tissues as a negative control. Haematoxylin was used for the staining. The images were captured by ZEISS-ZEN 2 LITE (blue edition) AXIO scan software.

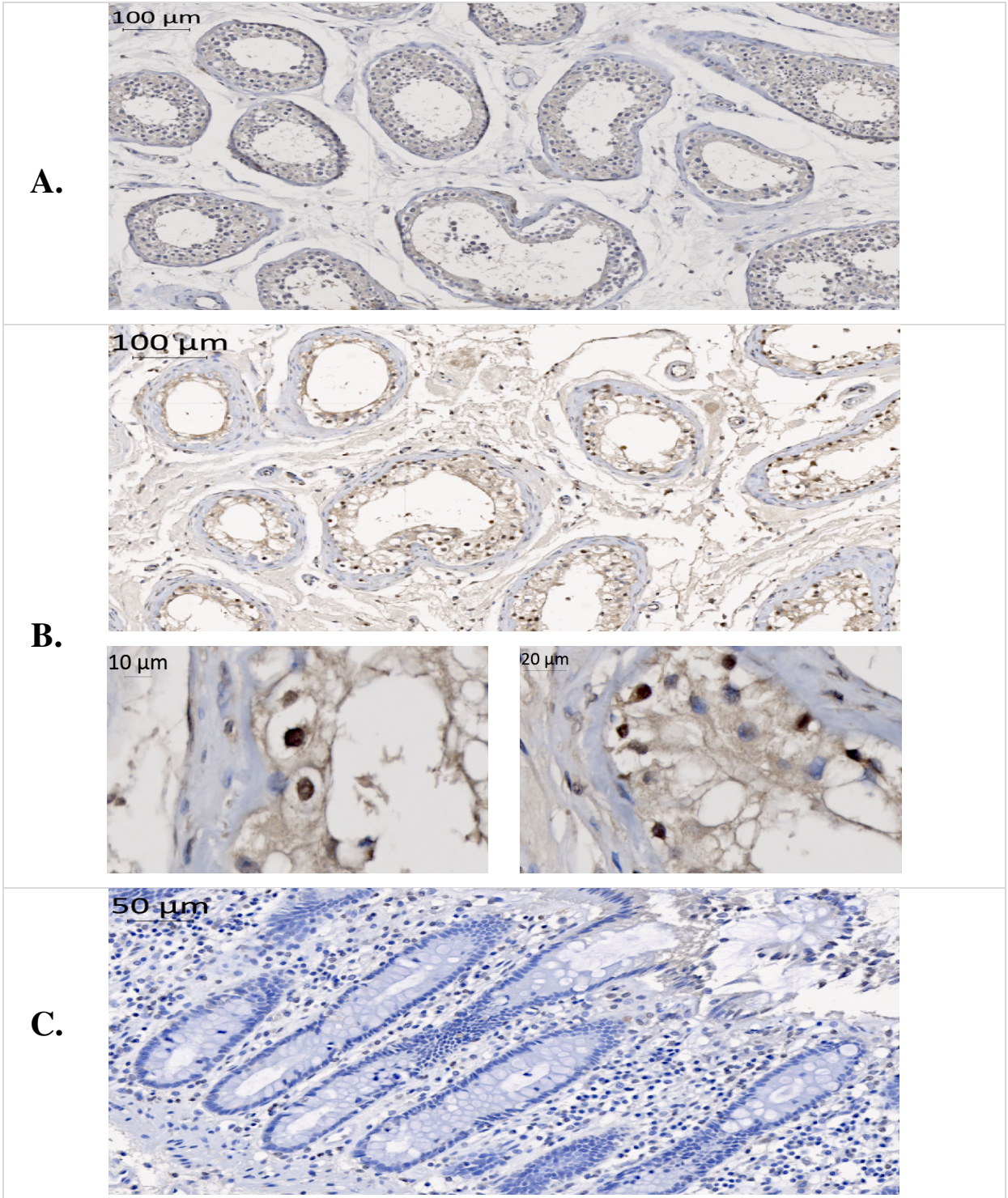

Figure 6.4 IHC staining analysis of TDRD1 protein in normal testis and colon (B22 C22) tissues. Panel (A): shows the staining of the TDRD1 protein negative control (overnight normal rabbit serum (Dako; X0902) blocking and then 40 minutes 1:1000 of goat anti-rabbit secondary antibody; Abcam; ab6721) in normal testis tissues. Panel (B): shows the staining of the TDRD1 protein (overnight 1:100 of TDRD1 primary antibody; Abcam; ab107665 and then 40 minutes 1:1000 of goat anti-rabbit secondary antibody) in normal testis tissues. Panel (C): shows the staining of the TDRD1 protein (overnight 1:100 of TDRD1 primary antibody and then 40 minutes 1:1000 of goat anti-rabbit secondary antibody) in normal colon tissues as a negative control. Haematoxylin was used for the staining. The images were captured by ZEISS-ZEN 2 LITE (blue edition) AXIO scan software.

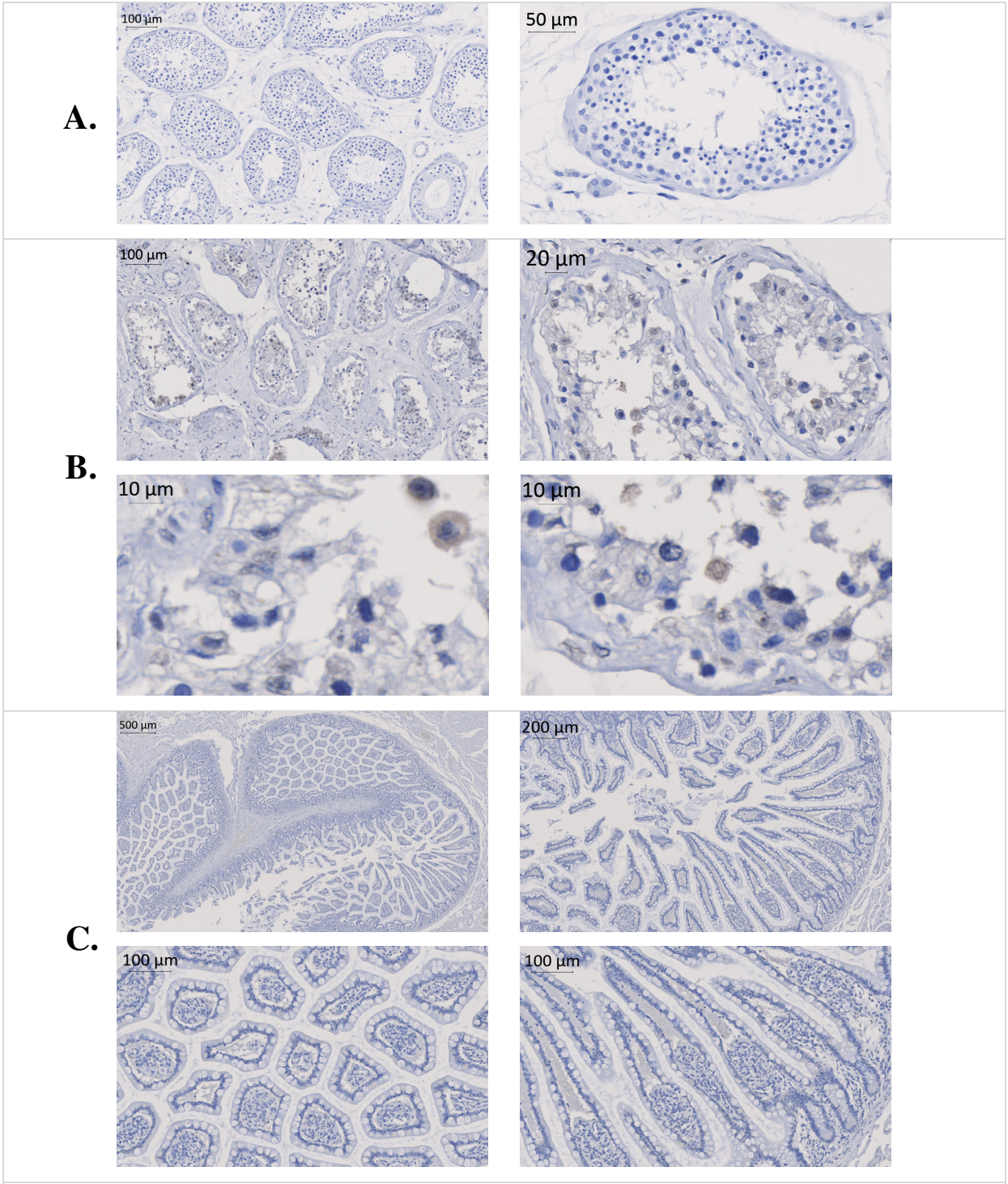

Figure 6.5 IHC staining analysis of PIWIL2 protein in normal testis and small intestine (THA2) tissues.
Panel (A): shows the staining of the PIWIL2 protein negative control (overnight normal mouse serum (Dako; X0910) blocking and then 45 minutes 1:1000 of goat anti-mouse secondary antibody; Abcam; ab47827) in normal testis tissues. Panel (B): shows the staining of the PIWIL2 protein (overnight 1:100 of PIWIL2 primary antibody; Abnova; MAB0843 and then 45 minutes 1:1000 of goat anti-mouse secondary antibody) in normal testis tissues. Panel (C): shows the staining of the PIWIL2 protein (overnight 1:100 of PIWIL2 primary antibody and then 45 minutes 1:1000 of goat anti-mouse secondary antibody) in normal small intestine tissues as a negative control. Haematoxylin was used for the staining. The images were captured by ZEISS-ZEN 2 LITE (blue edition) AXIO scan software.

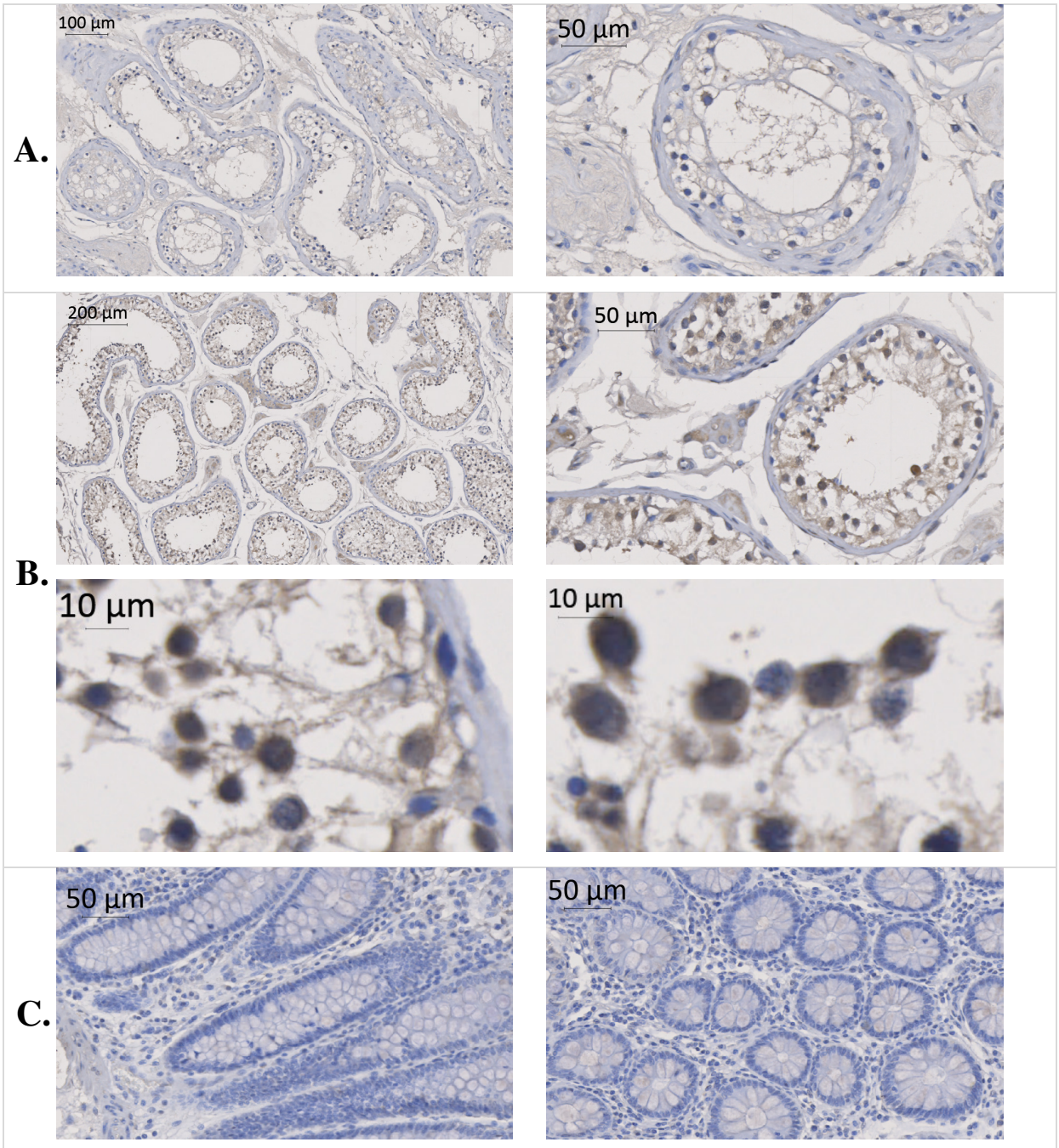

Figure 6.6 IHC staining analysis of TDRD12 protein using TDRD12-ATLAS antibody in normal testis and colon (NCA2) tissues.
Panel (A): shows the staining of the TDRD12 protein negative control (overnight normal rabbit serum (Dako; X0902) blocking and then 45 minutes 1:1000 of goat anti-rabbit secondary antibody; Abcam; ab6721) in normal testis tissues. Panel (B): shows the staining of the TDRD12 protein (overnight 1:100 of TDRD12 primary antibody; ATLAS ANTIBODIES; HPA-042684 and then 45 minutes 1:1000 of goat anti-rabbit secondary antibody) in normal testis tissues. Panel (C): shows the staining of the TDRD12 protein (overnight 1:100 of TDRD12 primary antibody and then 45 minutes 1:1000 of goat anti-rabbit secondary antibody) in normal colon tissues as a negative control. Haematoxylin was used for the staining. The images were captured by ZEISS-ZEN 2 LITE (blue edition) AXIO scan software.

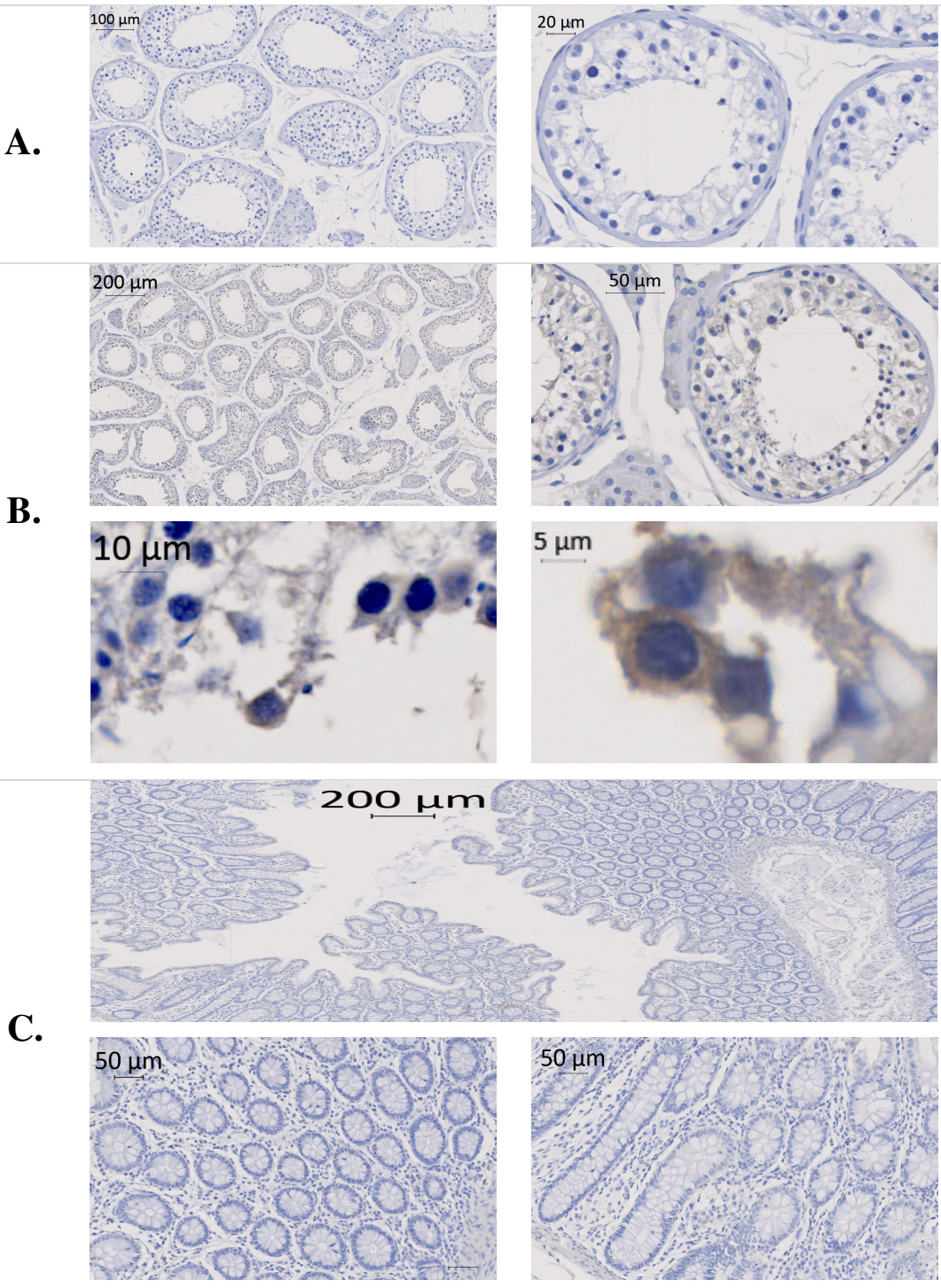

Figure 6.7 IHC staining analysis of TDRD12 protein using TDRD12-T17 antibody in normal testis and colon (NCA2) tissues.
Panel (A): shows the staining of the TDRD12 protein negative control (overnight 1x PBS/5% FBS/0.3% Triton X-100) blocking and then 45 minutes 1:250 of rabbit anti-goat secondary antibody; Abcam; ab97100) in normal testis tissues. Panel (B): shows the staining of the TDRD12 protein (overnight 1:100 of TDRD12 primary antibody; Santa Crus Biotechnology; sc-248802 and then 45 minutes 1:250 of rabbit anti-goat secondary antibody) in normal testis tissues. Panel (C): shows the staining of the TDRD12 protein (overnight 1:100 of TDRD12 primary antibody and then 45 minutes 1:250 of rabbit anti-goat secondary antibody) in normal colon tissues as a negative control. Haematoxylin was used for the staining. The images were captured by ZEISS-ZEN 2 LITE (blue edition) AXIO scan software.

6.3.2. IF staining analysis of TDRD12, TDRD1, PIWIL1 and PIWIL2 in normal tissues

To further exploring/verifying the localisation patterns observed by IHC (Section 6.3.1), an analysis of the presence of TDRD12, TDRD1, PIWIL1 and PIWIL2 in normal testis tissues was carried out using IF. As can be seen, the IF images of TDRD12, TDRD1, PIWIL1 and PIWIL2 were fixed and stained with DAPI (shown in blue). The IF results suggested that the TDRD12 (T17 antibody) localisation was detected in both the spermatogonial layer and adluminal compartment of the seminiferous tubules, but it seemed to be located mostly in the spermatogonial layer and appeared cytoplasmic (see Figure 6.9). TDRD12-ATLAS and TDRD12-PEP99 antibodies were unlikely to be good antibodies to use for IF as no fluorescence was detected (see Figure 6.11 and Figure 6.13). PIWIL1 localisation was detected in the adluminal compartment of the seminiferous tubules and appeared cytoplasmic (see Figure 6.14). PIWIL2 localisation was detected in the spermatogonial layer of the seminiferous tubules and appeared cytoplasmic. TDRD1 antibody was also unlikely to be a good antibody to use for IF because no fluorescence was detected (see Figure 6.18).

Figure 6.8 IF staining with only secondary antibodies in normal testis tissues (negative controls for Figure 6.9). Figure 6.9 IF staining for the TDRD12 (using TDRD12-T17 antibody) and MAGEA1 proteins in normal testis tissues. Figure 6.10 IF staining with only secondary antibodies in normal testis tissues (negative controls for Figure 6.11). Figure 6.11 IF staining for the TDRD12 (using TDRD12-ATLAS antibody) and MAGEA1 proteins in normal testis tissues. Figure 6.12 IF staining with only secondary antibodies in normal testis tissues (negative controls for Figure 6.13 and Figure 6.14). Figure 6.13 IF staining for the MAGEA1 and TDRD12 (using TDRD12-PEP99 antibody) proteins in normal testis tissues. Figure 6.14 IF staining for the PIWIL1 protein in normal testis tissues. Figure 6.15 IF staining with only secondary antibodies in normal testis tissues (negative controls for Figure 6.16). Figure 6.16 IF staining for the TDRD12 (using TDRD12-T17 antibody) and PIWIL1 proteins in normal testis tissues. Figure 6.17 IF staining with only secondary antibodies in normal testis tissues (negative controls for Figure 6.18). Figure 6.18 IF staining for the PIWIL2 and TDRD1 in normal testis tissues. The images were viewed using a ZEISS LSM 710 confocal microscope.

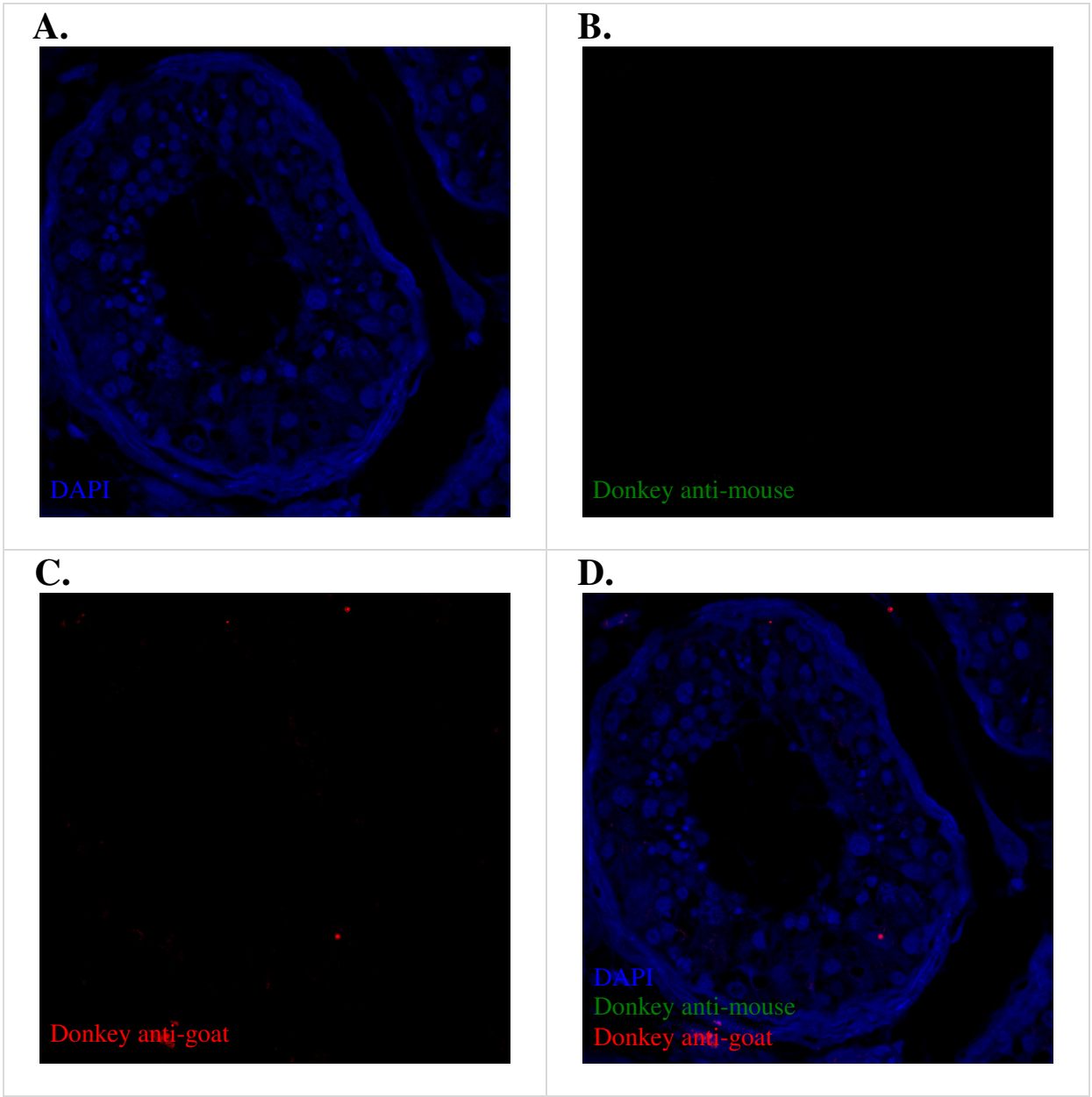

Figure 6.8 IF staining with only secondary antibodies in normal testis tissues (negative controls for Figure 6.9).
Images for the IF staining with only secondary antibodies used as negative controls, viewed using a ZEISS LSM 710 confocal microscope. Panel (A): shows the staining of DAPI (blue). Panel (B): shows donkey anti-mouse secondary antibody (Invitrogen; A31571; green) for the anti-MAGEA1-staining. Panel (C): shows donkey anti-goat secondary antibody (Invitrogen; A11057; red) for the anti-TDRD12-T17-staining. Panel (D): shows the staining of the DAPI, donkey anti-mouse and donkey anti-goat (blue, green and red). Note: Z-Position 4.

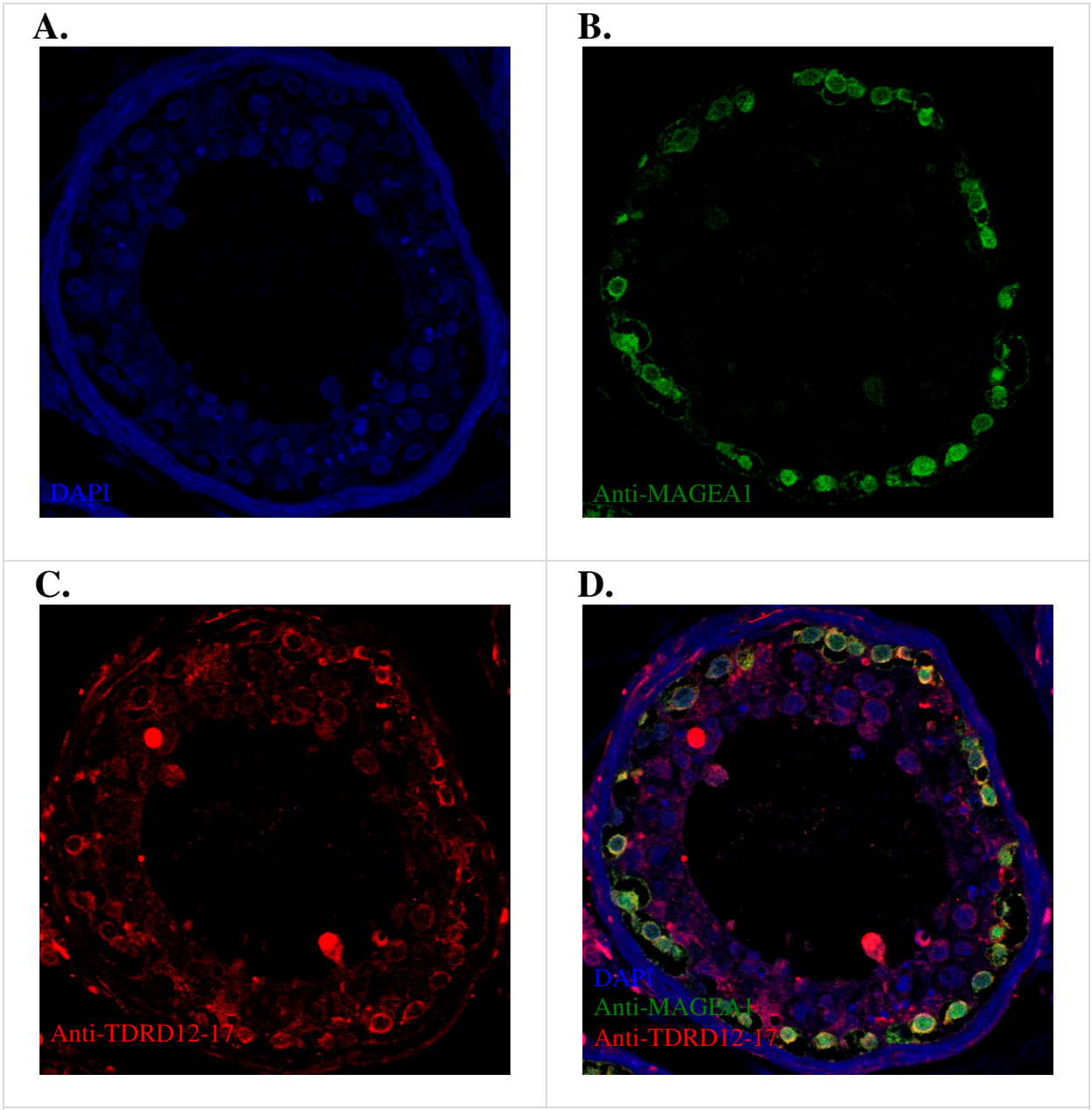

Figure 6.9 IF staining for the TDRD12 (using TDRD12-T17 antibody) and MAGEA1 proteins in normal testis tissues.
Images for the IF staining for anti-MAGEA1 (LSBio; LS-C87868; 1:15) and anti-TDRD12-T17 (Santa Crus Biotechnology; sc-248802; 1:500) in normal testis tissues, viewed using a ZEISS LSM 710 confocal microscope. Panel (A): shows the staining of DAPI (blue). Panel (B): shows the staining of the anti-MAGEA1 (green). Panel (C): shows the staining of the anti-TDRD12-T17 (red). Panel (D): shows the staining of the DAPI, anti-MAGEA1 and anti-TDRD12-T17 (blue, green and red). Note: Z-Position 4.

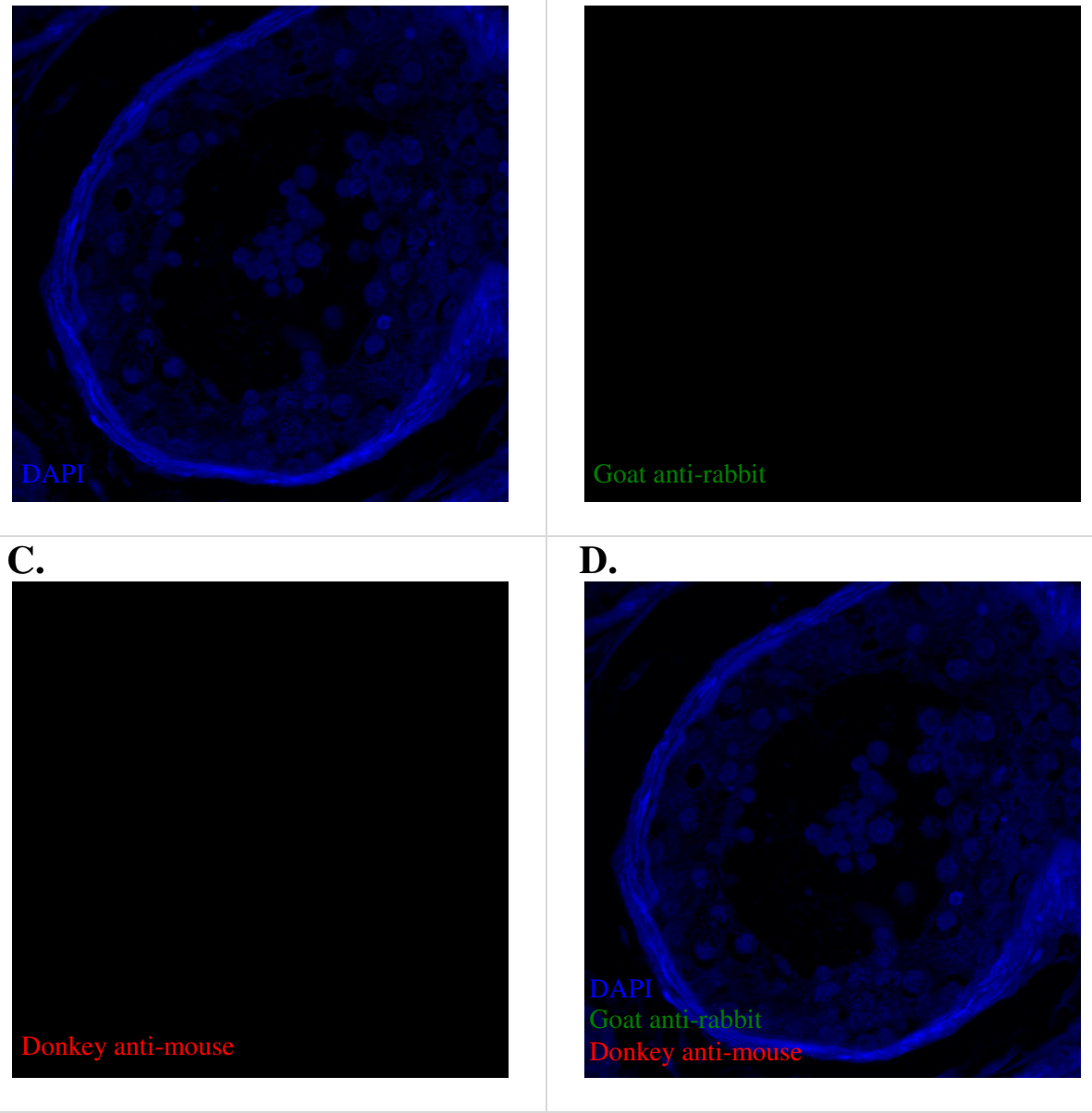

Figure 6.10 IF staining with only secondary antibodies in normal testis tissues (negative controls for Figure 6.11).
Images for the IF staining with only secondary antibodies used as negative controls, viewed using a ZEISS LSM 710 confocal microscope. Panel (A): shows the staining of DAPI (blue). Panel (B): shows goat anti-rabbit secondary antibody (Invitrogen; A11034; green) for the anti-TDRD12-ATLAS-staining. Panel (C): shows donkey anti-mouse secondary antibody (Invitrogen; A31571; red) for the anti-MAGEA1-staining. Panel (D): shows the staining of the DAPI, goat anti-rabbit and donkey anti-mouse. Note: maximum intensity projection.

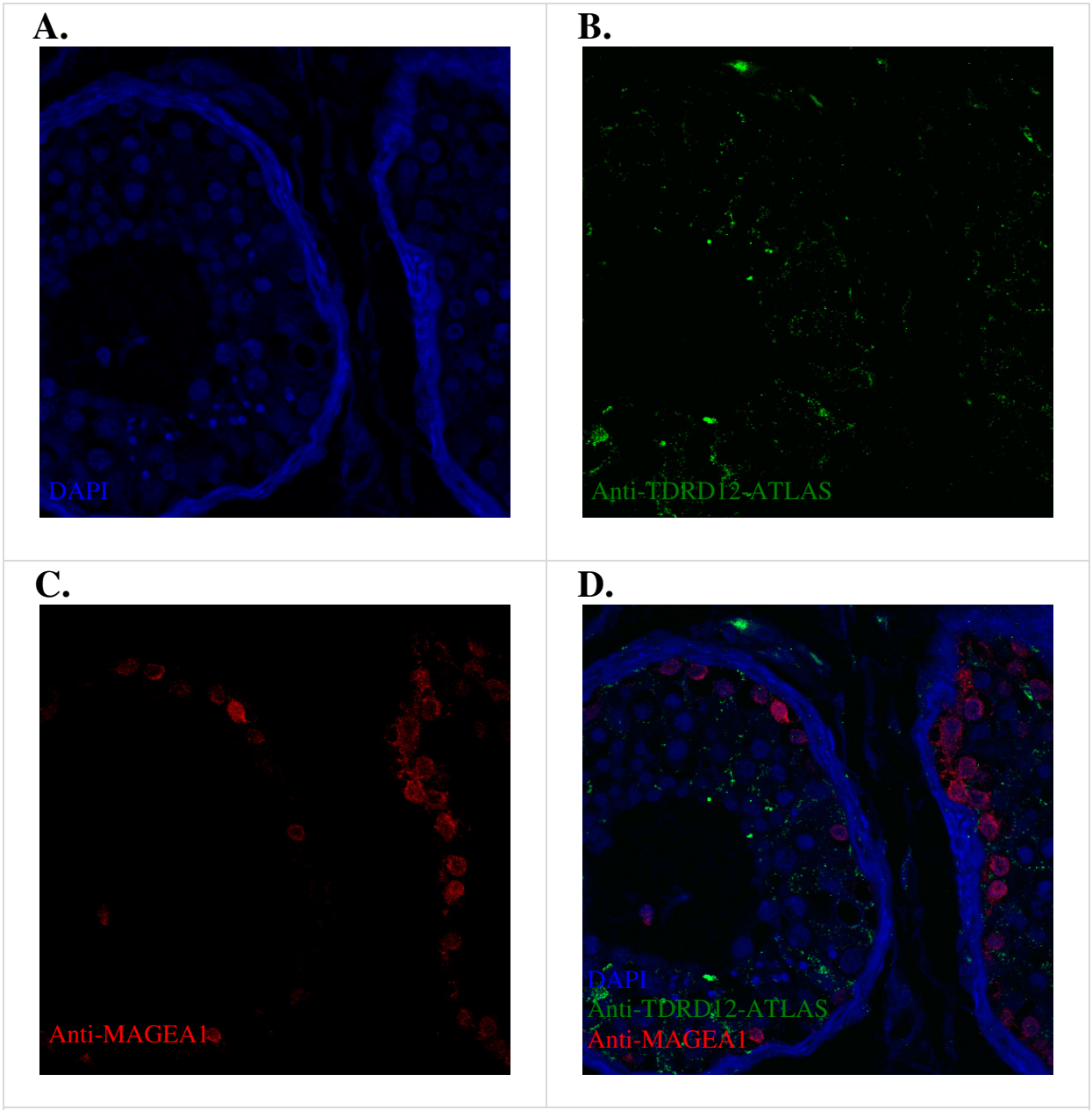

Figure 6.11 IF staining for the TDRD12 (using TDRD12-ATLAS antibody) and MAGEA1 proteins in normal testis tissues.
Images for the IF staining for anti-MAGEA1 (LSBio; LS-C87868; 1:20) and anti-TDRD12 (ATLAS ANTIBODIES; HPA-042684; 1:20) in normal testis tissues, viewed using a ZEISS LSM 710 confocal microscope. Panel (A): shows the staining of DAPI (blue). Panel (B): shows the staining of the anti-TDRD12 (green). Panel (C): shows the staining of the anti-MAGEA1 (red). Panel (D): shows the staining of the DAPI, anti-MAGEA1 and anti-TDRD12 (blue, green and red). Not: increased green and red contrast; maximum intensity projection.

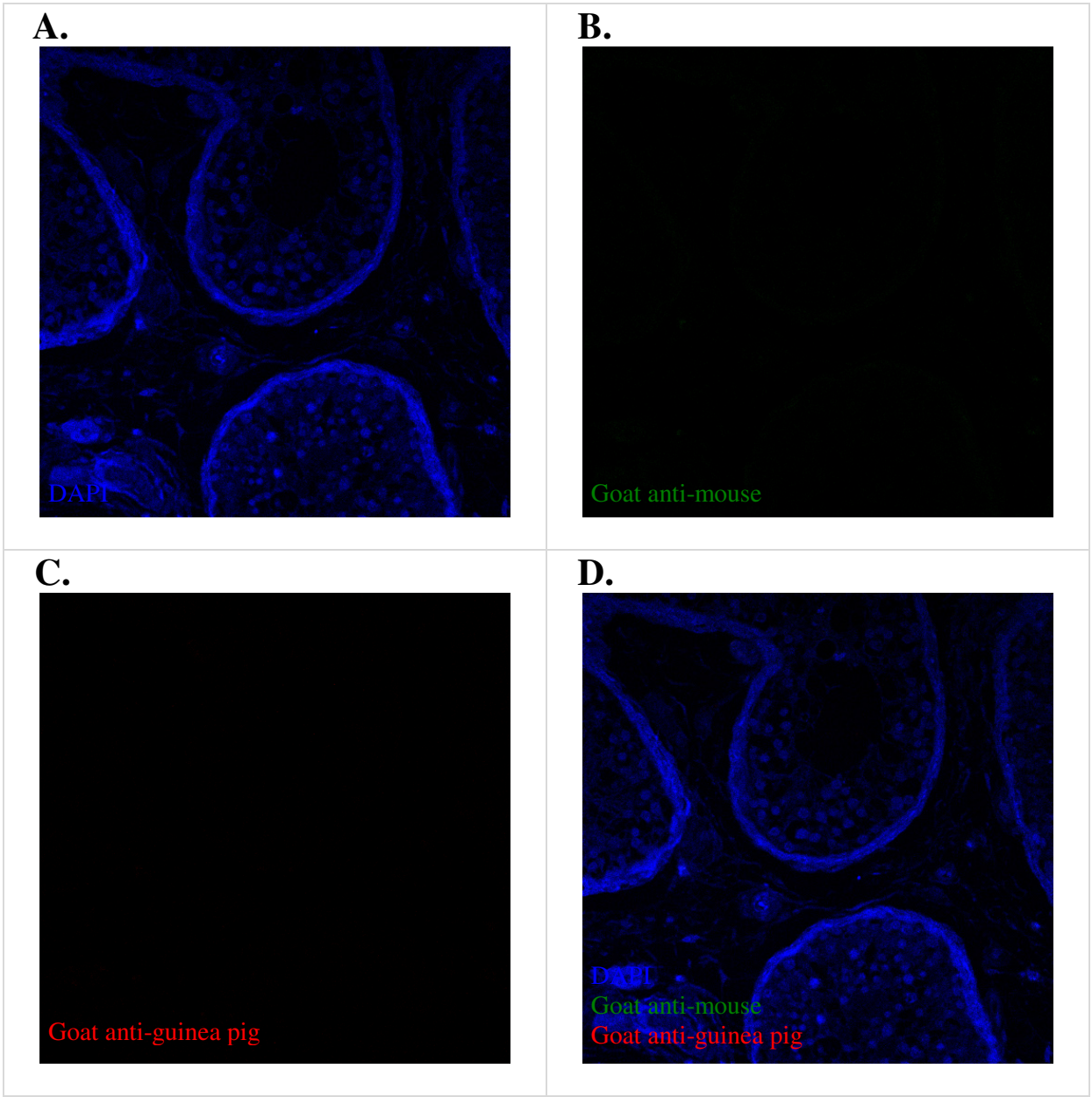

Figure 6.12 IF staining with only secondary antibodies in normal testis tissues (negative controls for Figure 6.13 and Figure 6.14).
Images for the IF staining with only secondary antibodies used as negative controls, viewed using a ZEISS LSM 710 confocal microscope. Panel (A): shows the staining of DAPI (blue). Panel (B): shows goat anti-mouse secondary antibody (Invitrogen; A11029; green) for the anti-PIWIL1 and anti-MAGEA1-staining. Panel (C): shows goat anti-guinea pig secondary antibody (life technologies; A21450; red) for the anti-TDRD12-PEP99-staining. Panel (D): shows the staining of the DAPI, goat anti-mouse and goat anti-guinea pig (blue, green and red).

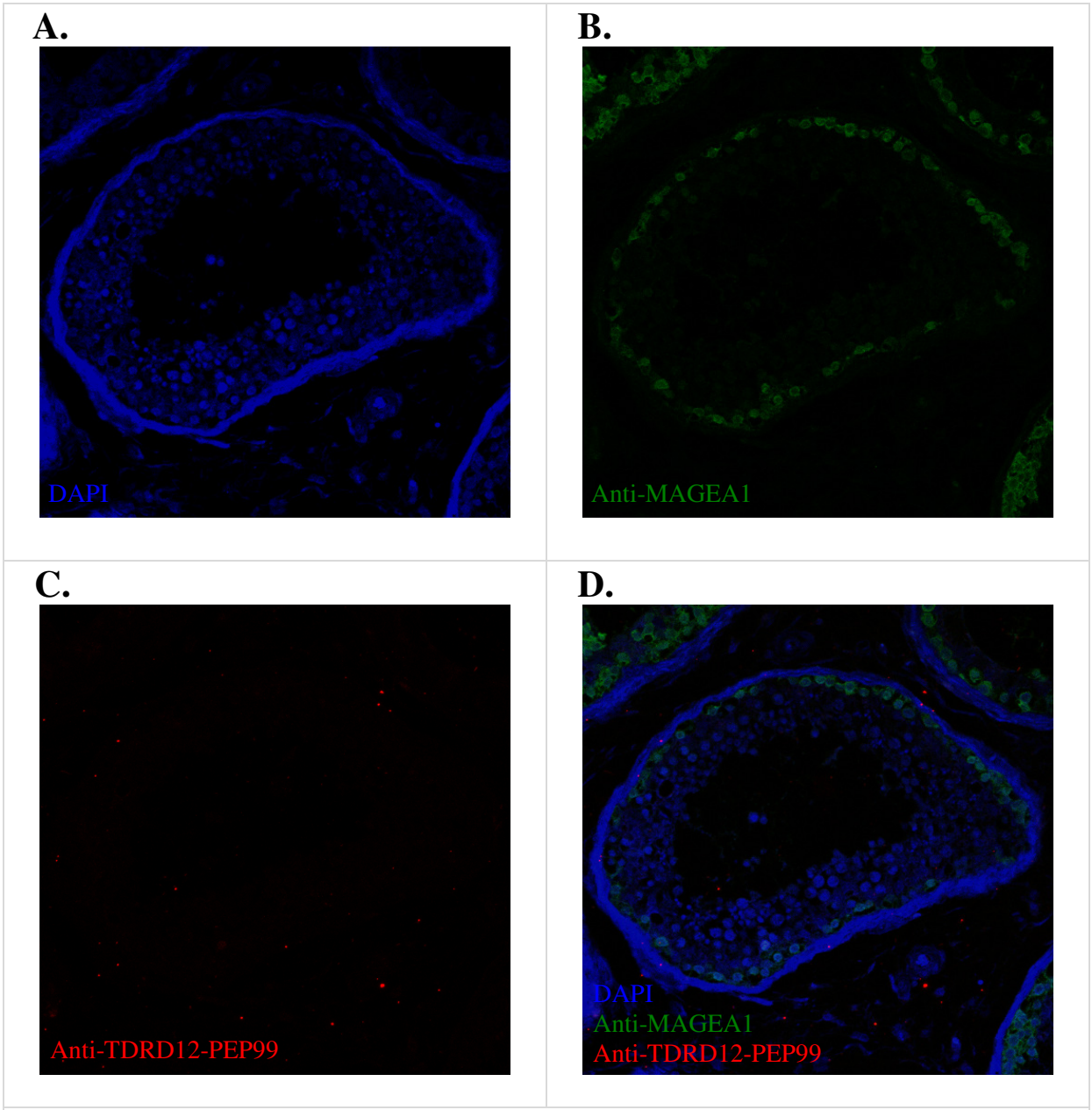

Figure 6.13 IF staining for the MAGEA1 and TDRD12 (using TDRD12-PEP99 antibody) proteins in normal testis tissues.
Images for the IF staining for anti-MAGEA1 (LSBio; LS-C87868; 1:20) and anti-TDRD12 (Eurogentec; PEP-1310599; 1:20) in normal testis tissues, viewed using a ZEISS LSM 710 confocal microscope. Panel (A): shows the staining of DAPI (blue). Panel (B): shows the staining of the anti-MAGEA1 (green). Panel (C): shows the staining of the anti-TDRD12 (red). Panel (D): shows the staining of the DAPI, anti-MAGEA1 and anti-TDRD12 (blue, green and red). Not: maximum intensity projection.

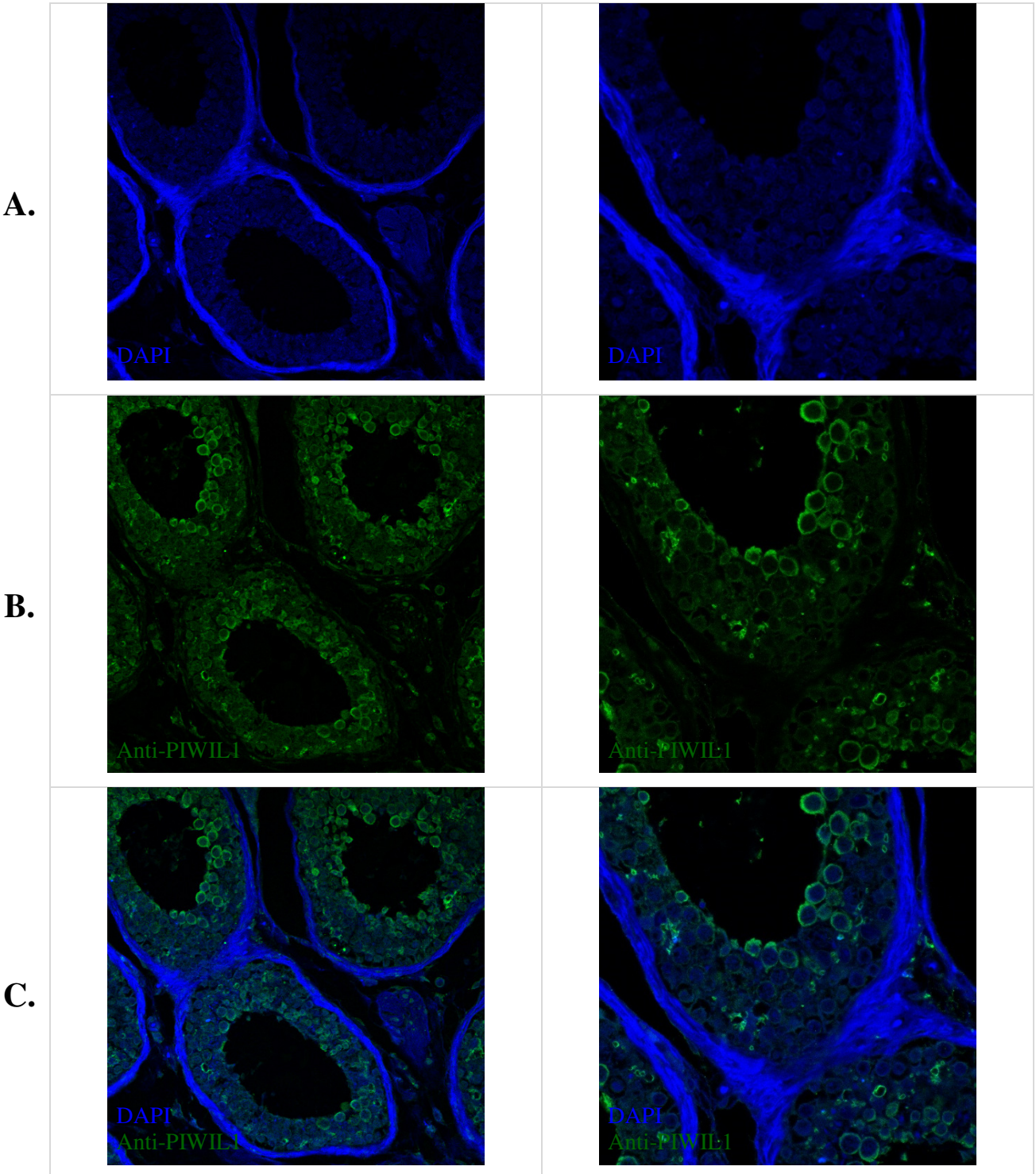

Figure 6.14 IF staining for the PIWIL1 protein in normal testis tissues.
Images for the IF staining for anti-PIWIL1 (SIGMA-ALDRICH; SAB-4200365; 1:100) in normal testis tissues, viewed using a ZEISS LSM 710 confocal microscope. Panel (A): shows the staining of DAPI (blue). Panel (B): shows the staining of the anti-PIWIL1 (green). Panel (C): shows the staining of the DAPI and anti-PIWIL1 (blue and green).

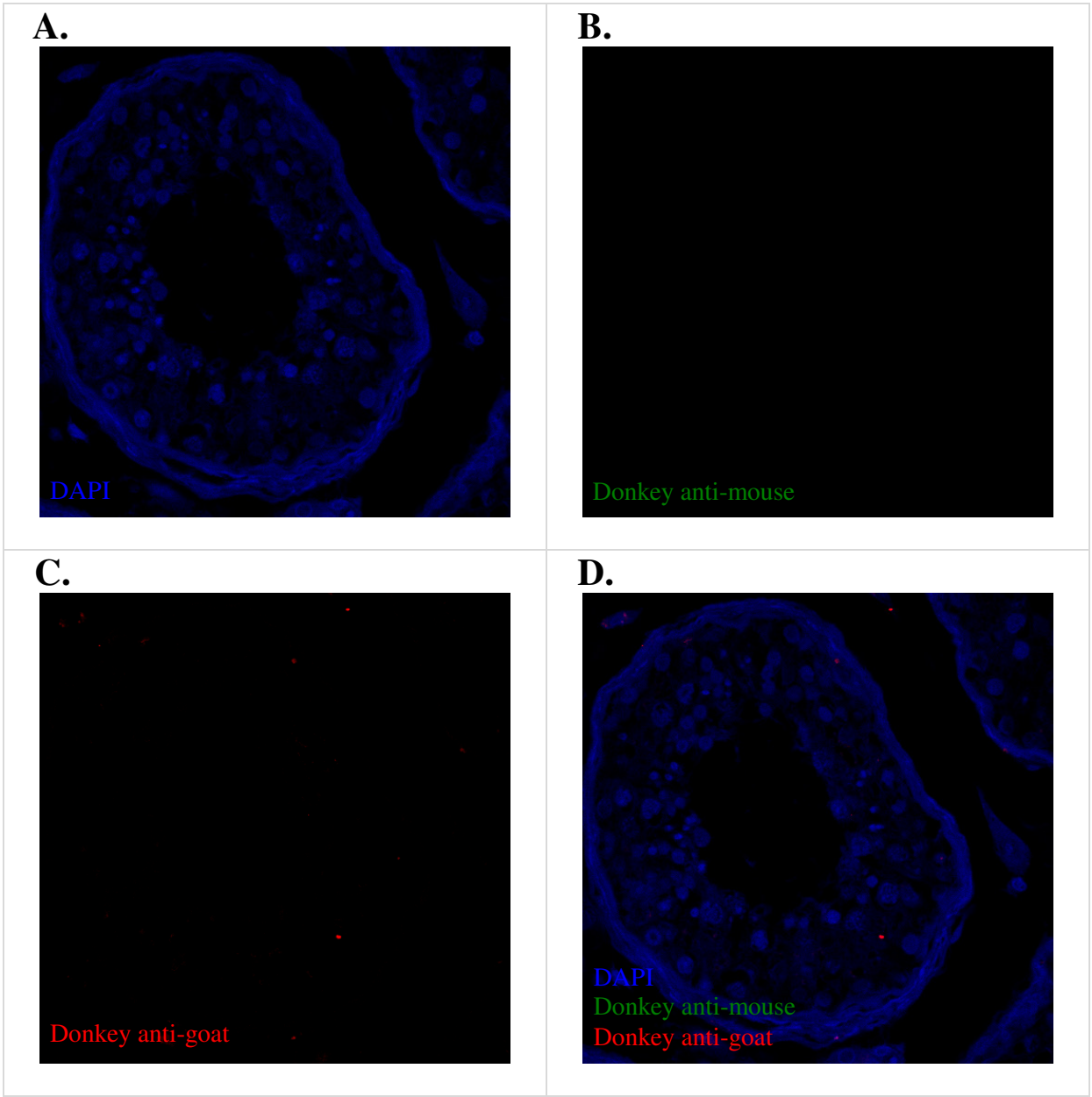

Figure 6.15 IF staining with only secondary antibodies in normal testis tissues (negative controls for Figure 6.16).
Images for the IF staining with only secondary antibodies used as negative controls, viewed using a ZEISS LSM 710 confocal microscope. Panel (A): shows the staining of DAPI (blue). Panel (B): shows donkey anti-mouse secondary antibody (Invitrogen; A31571; green) for the anti-PIWIL1-staining. Panel (C): shows donkey anti-goat secondary antibody (Invitrogen; A11057; red) for the anti-TDRD12-T17-staining. Panel (D): shows the staining of the DAPI, donkey anti-mouse and donkey anti-goat (blue, green and red). Note: Z-Position 4.

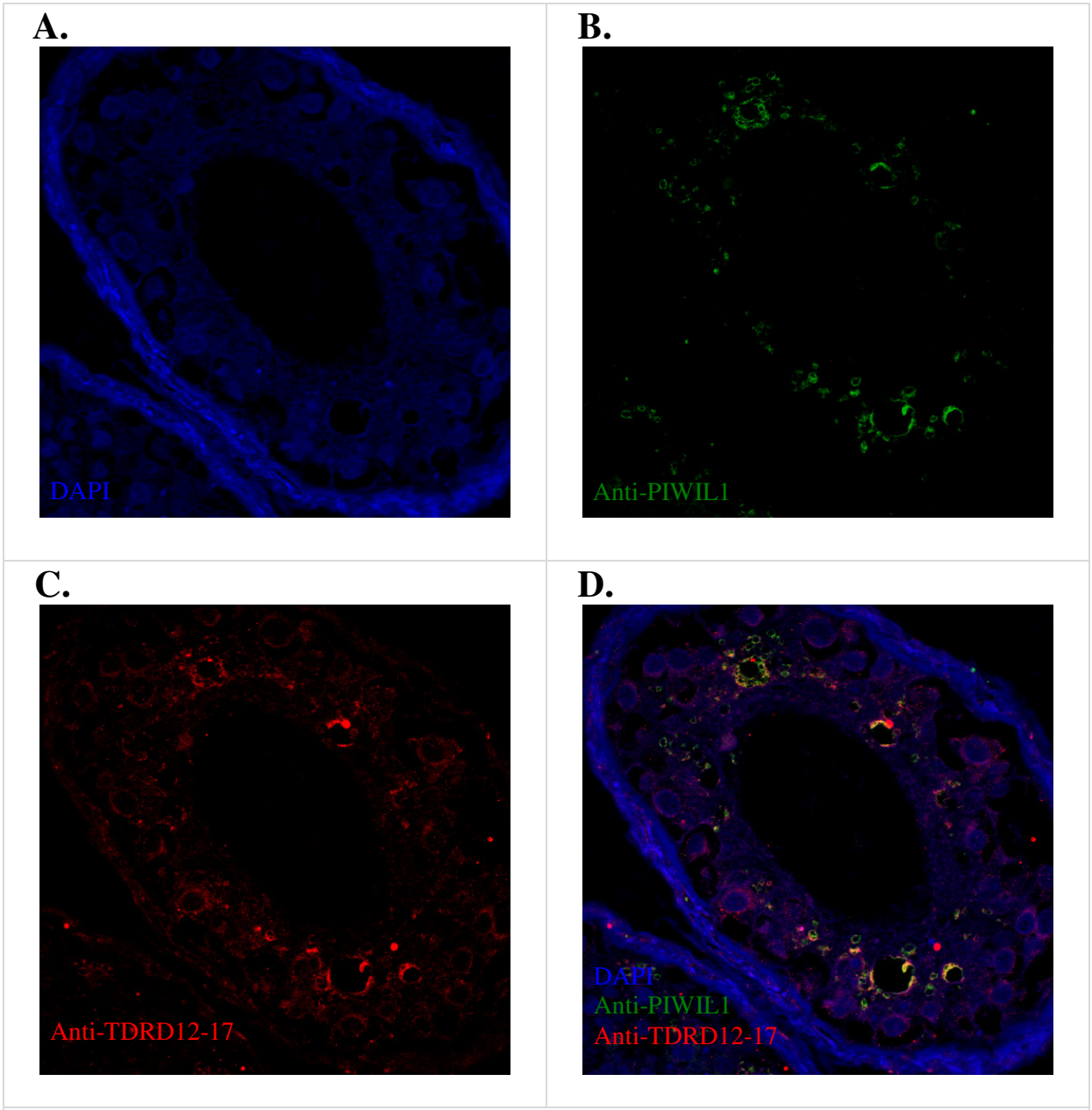

Figure 6.16 IF staining for the TDRD12 (using TDRD12-T17 antibody) and PIWIL1 proteins in normal testis tissues.
Images for the IF staining for anti-PIWIL1 (SIGMA-ALDRICH; SAB-4200365; 1:1500) and anti-TDRD12-T17 (Santa Crus Biotechnology; sc-248802; 1:1000) in normal testis tissues, viewed using a ZEISS LSM 710 confocal microscope. Panel (A): shows the staining of DAPI (blue). Panel (B): shows the staining of the anti-PIWIL1 (green). Panel (C): shows the staining of the anti-TDRD12-T17 (red). Panel (D): shows the staining of the DAPI, anti-PIWIL1 and anti-TDRD12-T17 (blue, green and red). Not: Z-Position 4.

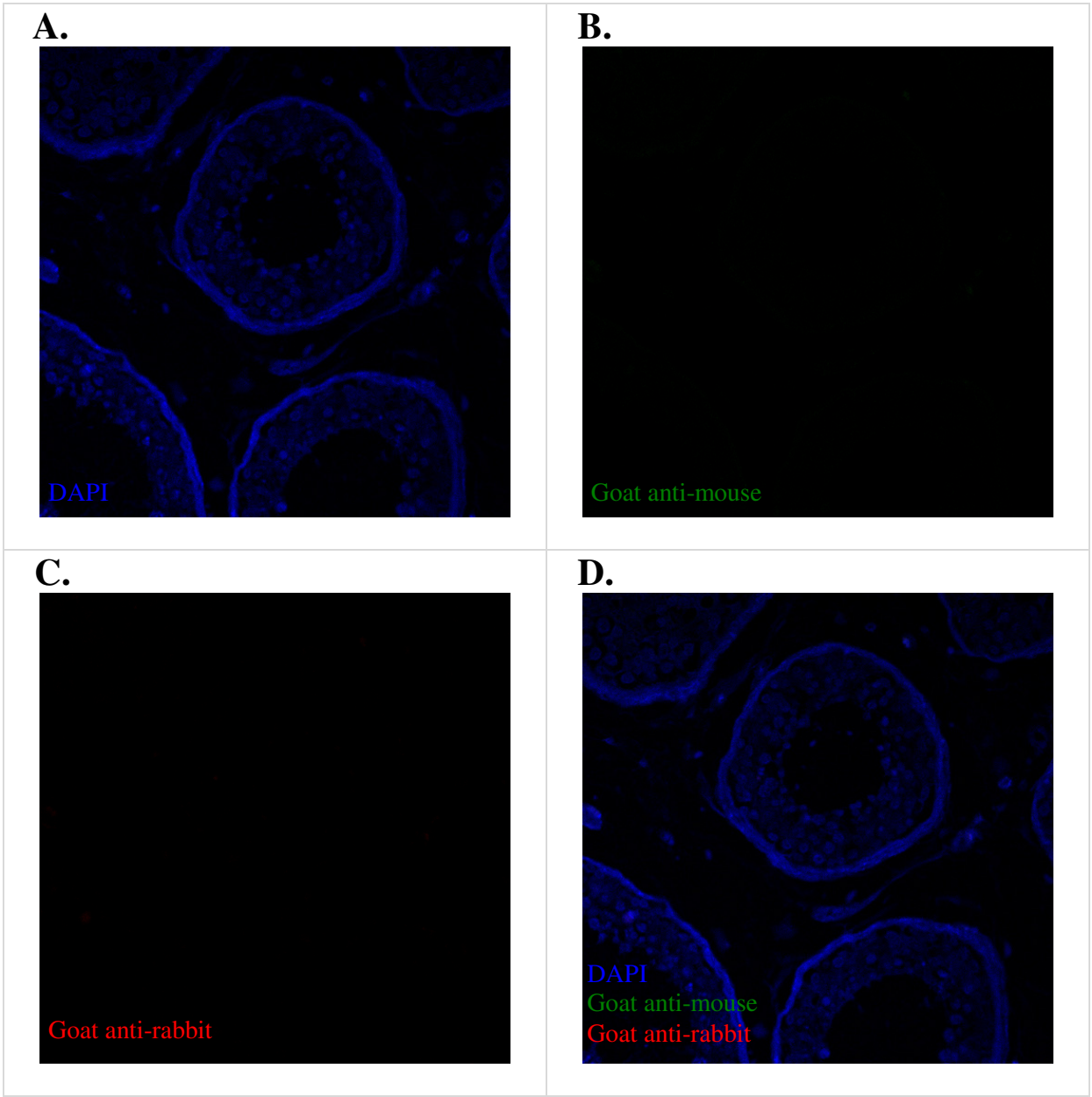

Figure 6.17 IF staining with only secondary antibodies in normal testis tissues (negative controls for Figure 6.18).
Images for the IF staining with only secondary antibodies used as negative controls, viewed using a ZEISS LSM 710 confocal microscope. Panel (A): shows the staining of DAPI (blue). Panel (B): shows goat anti-mouse secondary antibody (Invitrogen; A11029; green) for the anti-PIWIL2-staining. Panel (C): shows goat anti-rabbit secondary antibody (Invitrogen; A11011; red) for the anti-TDRD1-staining. Panel (D): shows the staining of the DAPI, goat anti-mouse and goat anti-rabbit (blue, green and red).

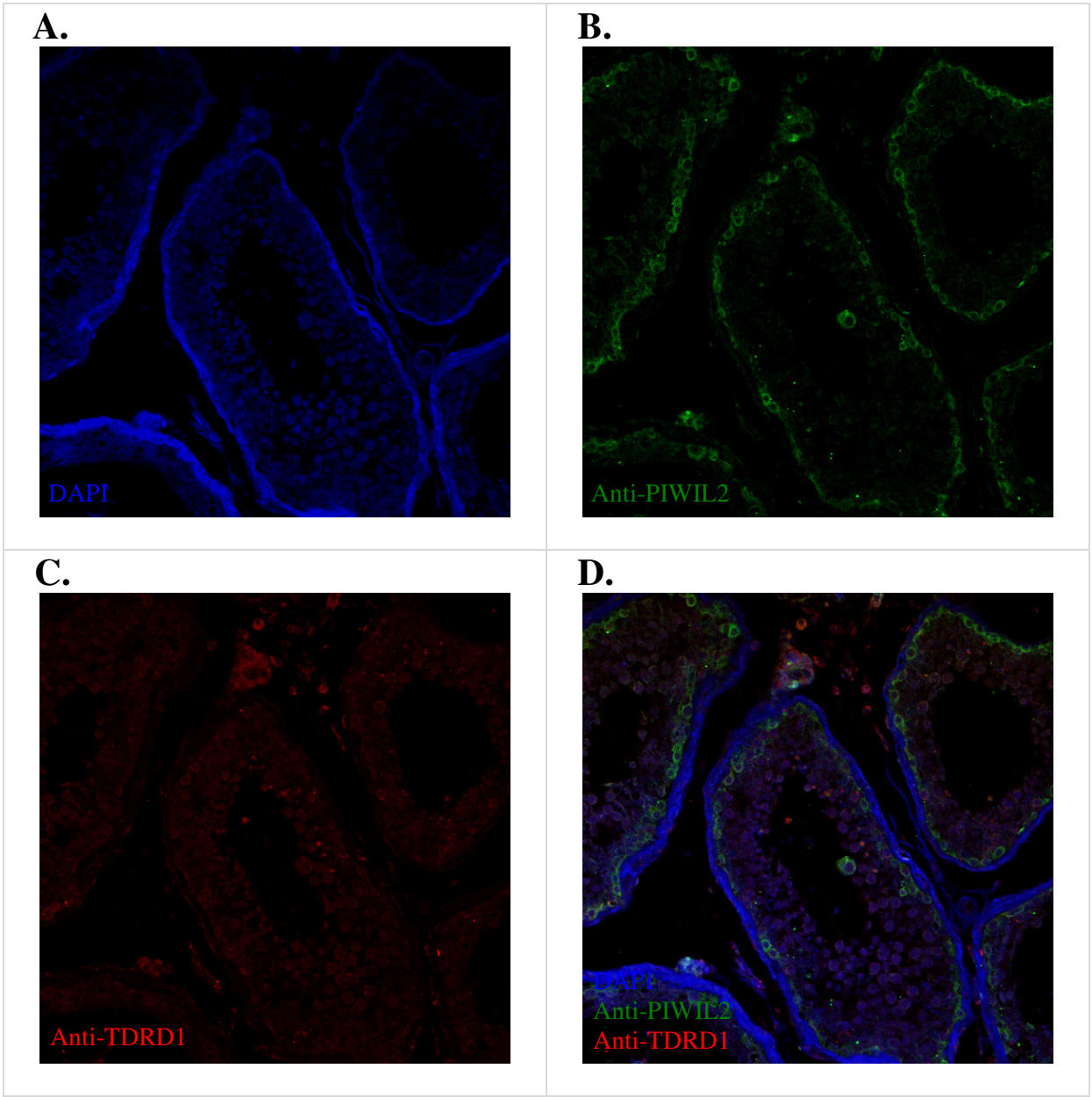

Figure 6.18 IF staining for the PIWIL2 and TDRD1 in normal testis tissues.
Images for the IF staining for anti-PIWIL2 (Abnova; MAB0843; 1:20) and anti-TDRD1 (Abcam; ab107665; 1:20) in normal testis tissues, viewed using a ZEISS LSM 710 confocal microscope. Panel (A): shows the staining of DAPI (blue). Panel (B): shows the staining of the anti-PIWIL2 (green). Panel (C): shows the staining of the anti-TDRD1 (red). Panel (D): shows the staining of the DAPI, anti-PIWIL2 and anti-TDRD1 (blue, green and red). Not: decreased brightness and increased contrast green increased contrast red decreased DAPI; maximum intensity projection.

6.3.3. IF staining analysis of TDRD12, TDRD1, PIWIL1 and PIWIL2 in cancerous cells

Because the *TDRD12* gene was expressed in NT2 and SW480 cells (see the previous Chapters), an analysis was carried out using IF for the sub-cellular localisation of TDRD12, TDRD1, PIWIL1 and PIWIL2 proteins in NT2 and SW480 cells. IF images show TDRD12, TDRD1, PIWIL1 and PIWIL2 fixed and stained with DAPI (shown in blue). The anti-β-actin antibody was used as a positive control. As can be seen from the results, in NT2 cells, TDRD12 (T17 antibody), PIWIL1 and PIWIL2 localisation was detected in both the nucleus and cytoplasm. TDRD12 (ATLAS antibody), TDRD12 (PEP99 antibody) and TDRD1 localisation was detected in the nucleus and cytoplasm, but they seemed mostly to be located in the nucleus. As can also be seen from the results, in SW480 cells, TDRD12 (T17 antibody) and PIWIL1 localisation was detected in both the nucleus and cytoplasm. TDRD12 (ATLAS antibody) and TDRD1 localisation was detected in the nucleus and cytoplasm, but they seemed to be located mostly in the nucleus. Meanwhile, the PIWIL2 seemed mostly cytoplasmic. Finally, TDRD12 (PEP99 antibody) localisation was detected only in the cytoplasm. Figure 6.19 IF staining with only secondary antibodies in NT2 cells (negative controls for Figures 6.20-6.22). Figure 6.20 IF staining for the TDRD1 protein in NT2 cells. Figure 6.21 IF staining for the TDRD12 protein using TDRD12-ATLAS antibody in NT2 cells. Figure 6.22 IF staining for the TDRD12 protein using TDRD12-PEP99 antibody in NT2 cells. Figure 6.23 IF staining with only secondary antibodies in NT2 cells (negative controls for Figure 6.24). Figure 6.24 IF staining for the TDRD12 protein using TDRD12-T17 antibody in NT2 cells. Figure 6.25 IF staining for the PIWIL1 protein in NT2 cells. Figure 6.26 IF staining for the PIWIL2 protein in NT2 cells. Figure 6.27 IF staining with only secondary antibodies in SW480 cells (negative controls for Figure 6.28). Figure 6.28 IF staining for the TDRD1 protein in SW480 cells. Figure 6.29 IF staining with only secondary antibodies in SW480 cells (negative controls for Figure 6.30). Figure 6.30 IF staining for the TDRD12 using TDRD12-ATLAS antibody in SW480 cells. Figure 6.31 IF Staining with only secondary antibodies in SW480 cells (negative controls for Figure 6.32). Figure 6.32 IF staining for the TDRD12 protein using TDRD12-PEP99 antibody in SW480 cells. Figure 6.33 IF staining with only secondary antibodies in SW480 cells (negative controls for Figure 6.34). Figure 6.34 IF staining for the TDRD12 protein using TDRD12-T17 antibody in SW480 cells. Figure 6.35 IF staining for the PIWIL1 protein in SW480 cells. Figure 6.36 IF staining with only secondary antibodies in SW480 cells (negative controls for Figure 6.37). Figure 6.37 IF staining for the PIWIL2 and TDRD12 (ATLAS antibody) in SW480 cells. The images were viewed using a ZEISS LSM 710 confocal microscope.

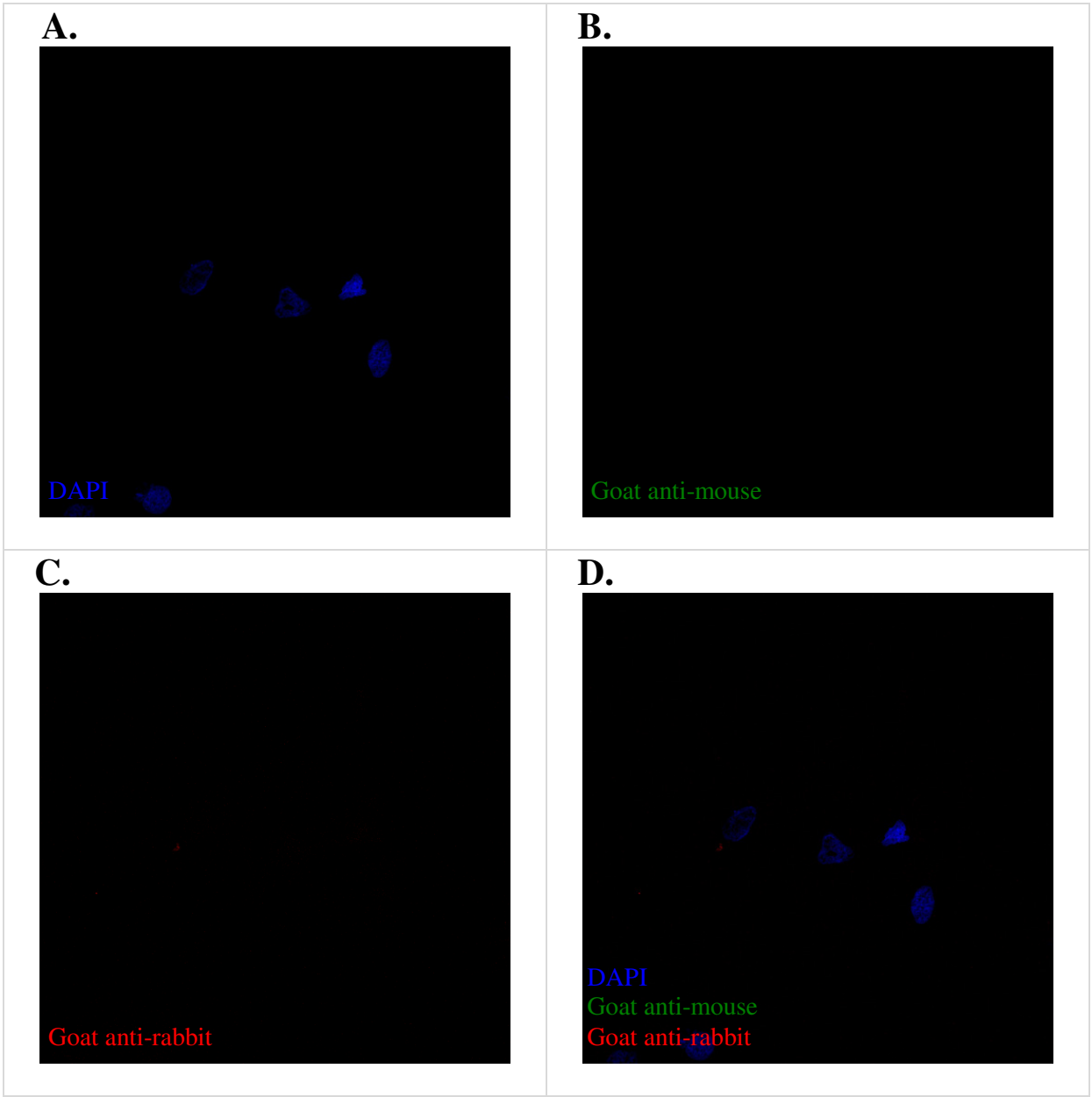

Figure 6.19 IF staining with only secondary antibodies in NT2 cells (negative controls for Figures 6.20-6.22).
Images for the IF staining with only secondary antibodies used as negative controls, viewed using a ZEISS LSM 710 confocal microscope. Panel (A): shows the staining of DAPI (blue). Panel (B): shows goat anti-mouse secondary antibody (Invitrogen; A11029; green) for the anti-β-actin-staining. Panel (C): shows goat anti-rabbit secondary antibody (Invitrogen; A11011; red) for the anti-TDRD1 and anti-TDRD12-staining. Panel (D): shows the staining of the DAPI, goat anti-mouse and goat anti-rabbit. Note: maximum intensity projection.

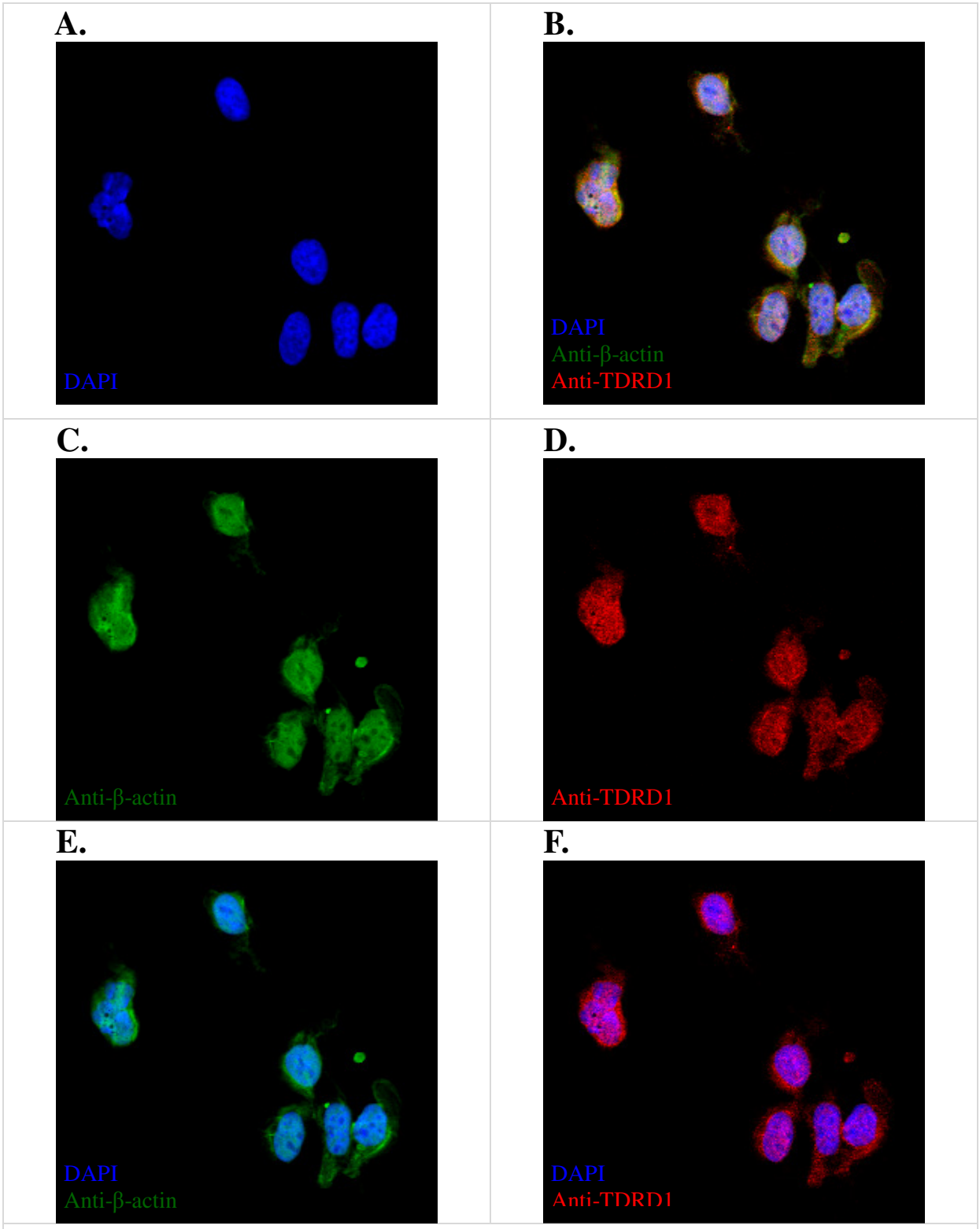

Figure 6.20 IF staining for the TDRD1 protein in NT2 cells.
Images for the IF staining for anti-β-actin (abcam; ab6277; 1:100) and anti-TDRD1 (abcam; ab107665; 1:20) in NT2 cells, viewed using a ZEISS LSM 710 confocal microscope. Panel (A): shows the staining of DAPI (blue). Panel (B): shows the staining of the DAPI, anti-β-actin and anti-TDRD1 (blue, green and red). Panel (C): shows the staining of the anti-β-actin (green). Panel (D): shows the staining of the anti-TDRD1 (red). Panel (E): shows the staining of the DAPI and anti-β-actin (blue and green). Panel (F): shows the staining of the DAPI and anti-TDRD1 (blue and red). Note: maximum intensity projection.

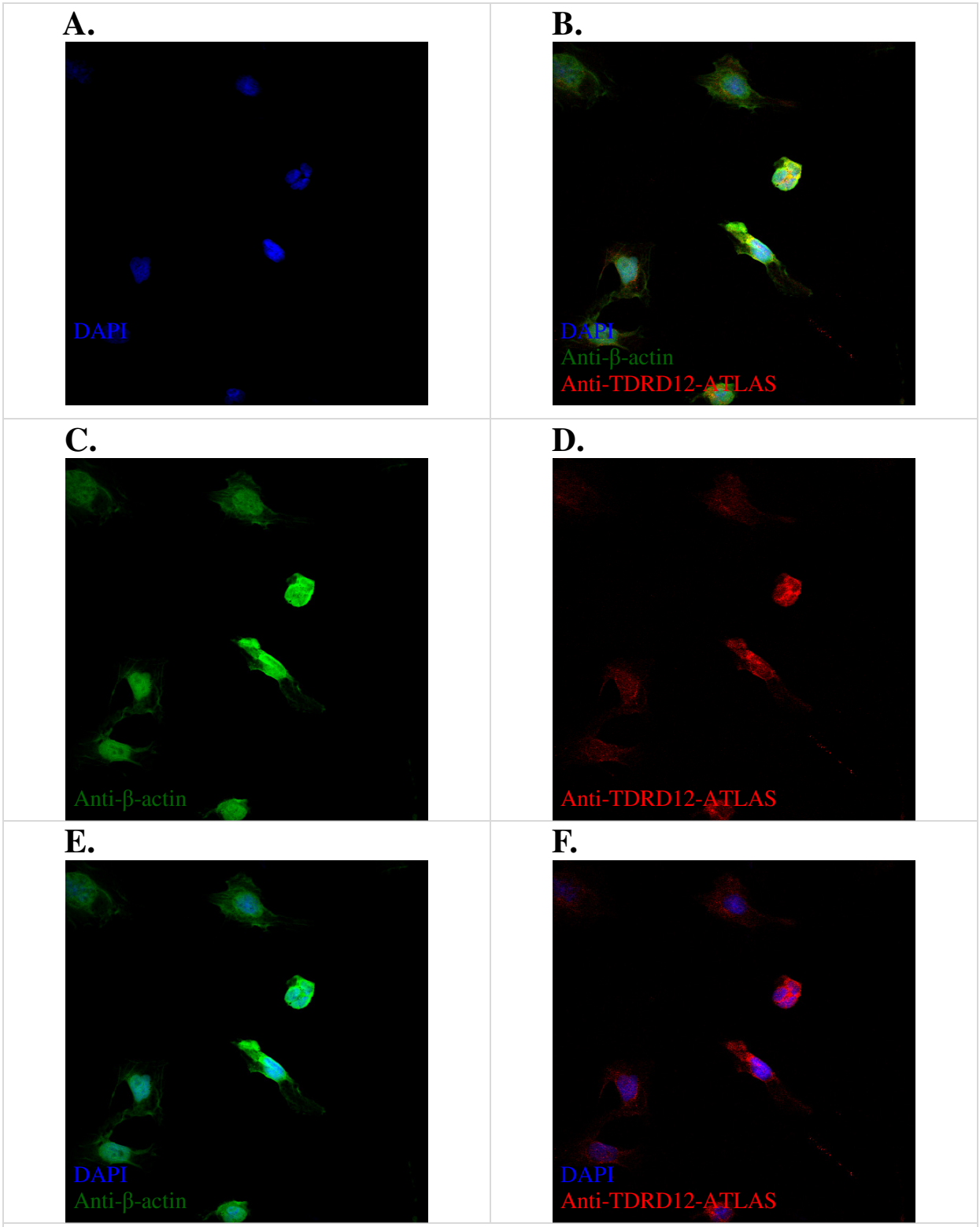

Figure 6.21 IF staining for the TDRD12 protein using TDRD12-ATLAS antibody in NT2 cells. Images for the IF staining for anti-β-actin (abcam; ab6277; 1:100) and anti-TDRD12 (ATLAS ANTIBODIES; HPA-042684; 1:20) in NT2 cells, viewed using a ZEISS LSM 710 confocal microscope. Panel (A): shows the staining of DAPI (blue). Panel (B): shows the staining of the DAPI, anti-β-actin and anti-TDRD12 (blue, green and red). Panel (C): shows the staining of the anti-β-actin (green). Panel (D): shows the staining of the anti-TDRD12 (red). Panel (E): shows the staining of the DAPI and anti-β-actin (blue and green). Panel (F): shows the staining of the DAPI and anti-TDRD12 (blue and red). Note: maximum intensity projection.

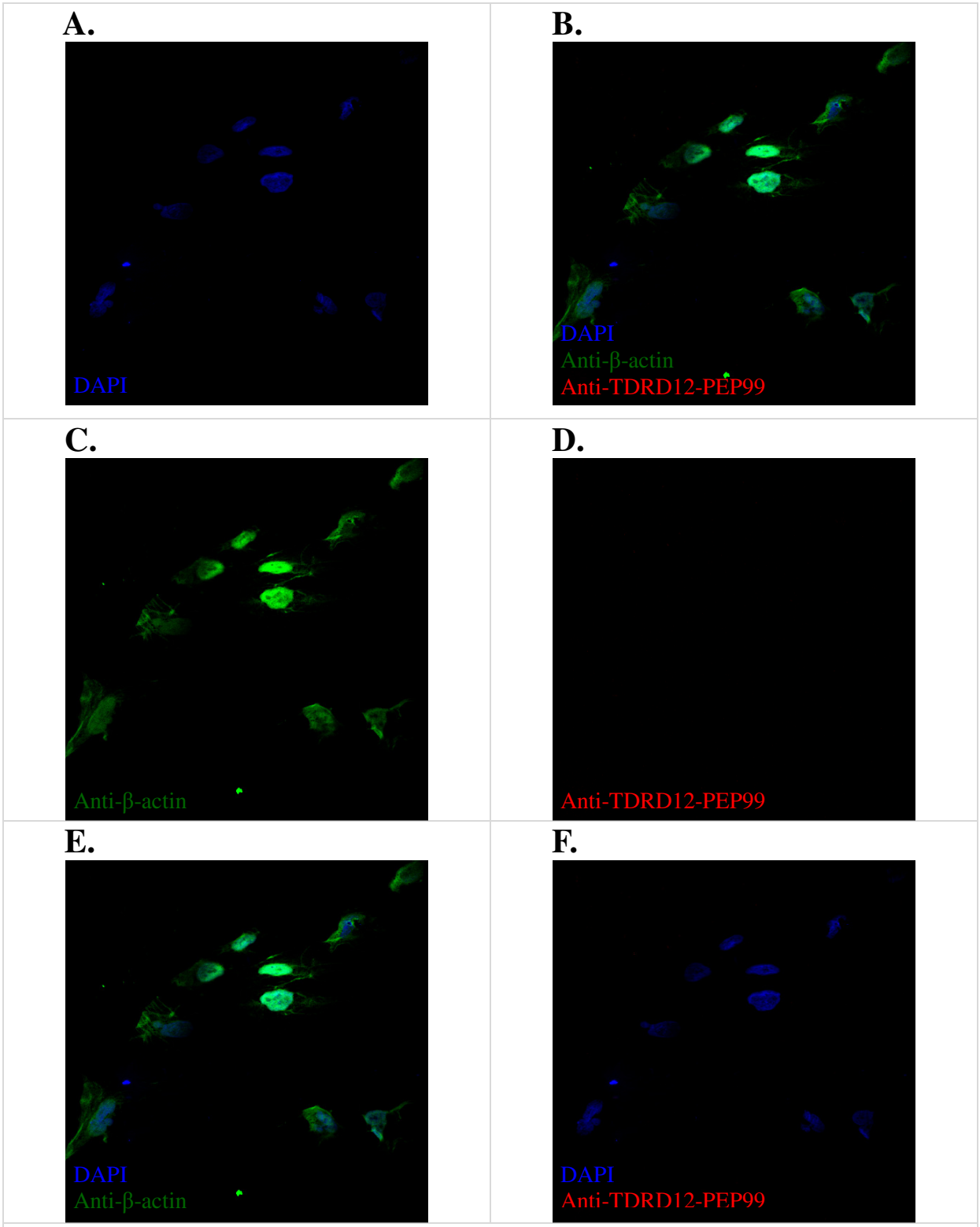

Figure 6.22 IF staining for the TDRD12 protein using TDRD12-PEP99 antibody in NT2 cells. Images for the IF staining for anti-β-actin (abcam; ab6277; 1:100) and anti-TDRD12 (Eurogentec; PEP-1310599; 1:20) in NT2 cells, viewed using a ZEISS LSM 710 confocal microscope. Panel (A): shows the staining of DAPI (blue). Panel (B): shows the staining of the DAPI, anti-β-actin and anti-TDRD12 (blue, green and red). Panel (C): shows the staining of the anti-β-actin (green). Panel (D): shows the staining of the anti-TDRD12 (red). Panel (E): shows the staining of the DAPI and anti-β-actin (blue and green). Panel (F): shows the staining of the DAPI and anti-TDRD12 (blue and red). Note: maximum intensity projection.

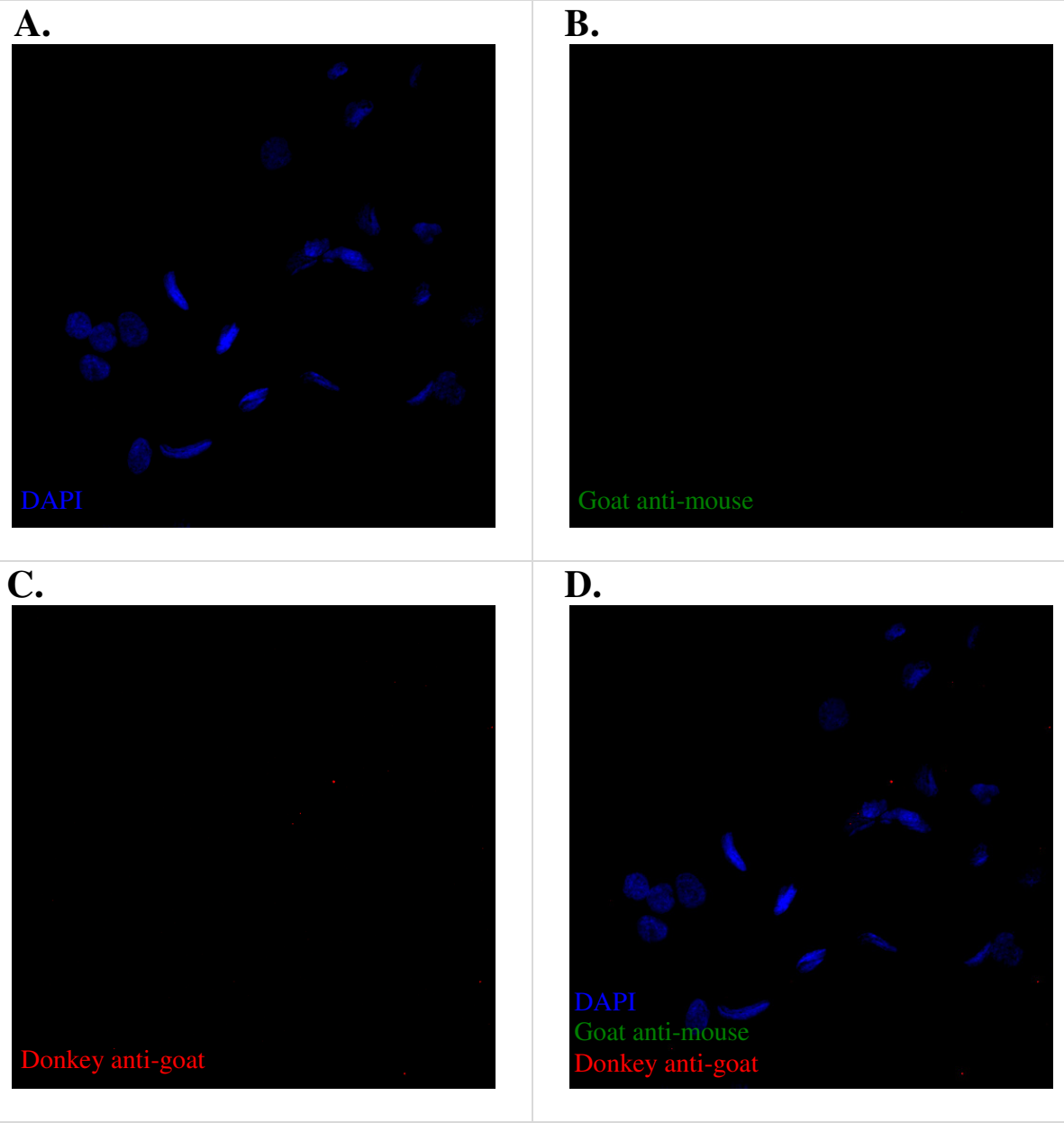

Figure 6.23 IF staining with only secondary antibodies in NT2 cells (negative controls for Figure 6.24).
Images for the IF staining with only secondary antibodies used as negative controls, viewed using a ZEISS LSM 710 confocal microscope. Panel (A): shows the staining of DAPI (blue). Panel (B): shows goat anti-mouse secondary antibody (Invitrogen; A11029; green) for the anti-β-actin and anti-PIWIL1-staining. Panel (C): shows donkey anti-goat secondary antibody (Invitrogen; A11057; red) for the anti-TDRD12-T17-staining. Panel (D): shows the staining of the DAPI, goat anti-mouse and donkey anti-goat. Note: maximum intensity projection.

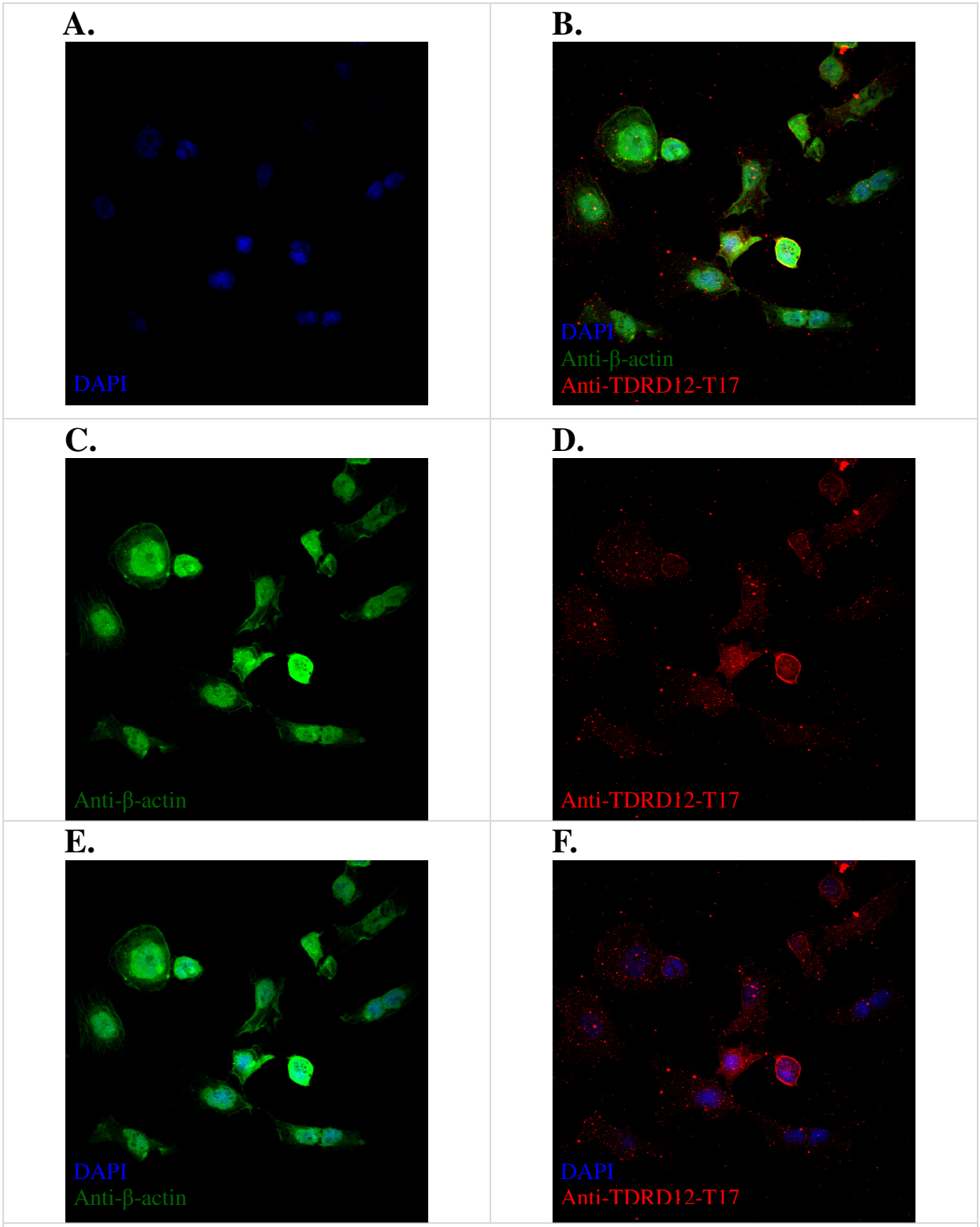

Figure 6.24 IF staining for the TDRD12 protein using TDRD12-T17 antibody in NT2 cells. Images for the IF staining for anti-β-actin (abcam; ab6277; 1:100) and anti-TDRD12-T17 (Santa Crus Biotechnology; sc-248802; 1:500) in NT2 cells, viewed using a ZEISS LSM 710 confocal microscope. Panel (A): shows the staining of DAPI (blue). Panel (B): shows the staining of the DAPI, anti-β-actin and anti-TDRD12-T17 (blue, green and red). Panel (C): shows the staining of the anti-β-actin (green). Panel (D): shows the staining of the anti-TDRD12-T17 (red). Panel (E): shows the staining of the DAPI and anti-β-actin (blue and green). Panel (F): shows the staining of the DAPI and anti-TDRD12-T17 (blue and red). Note: maximum intensity projection.

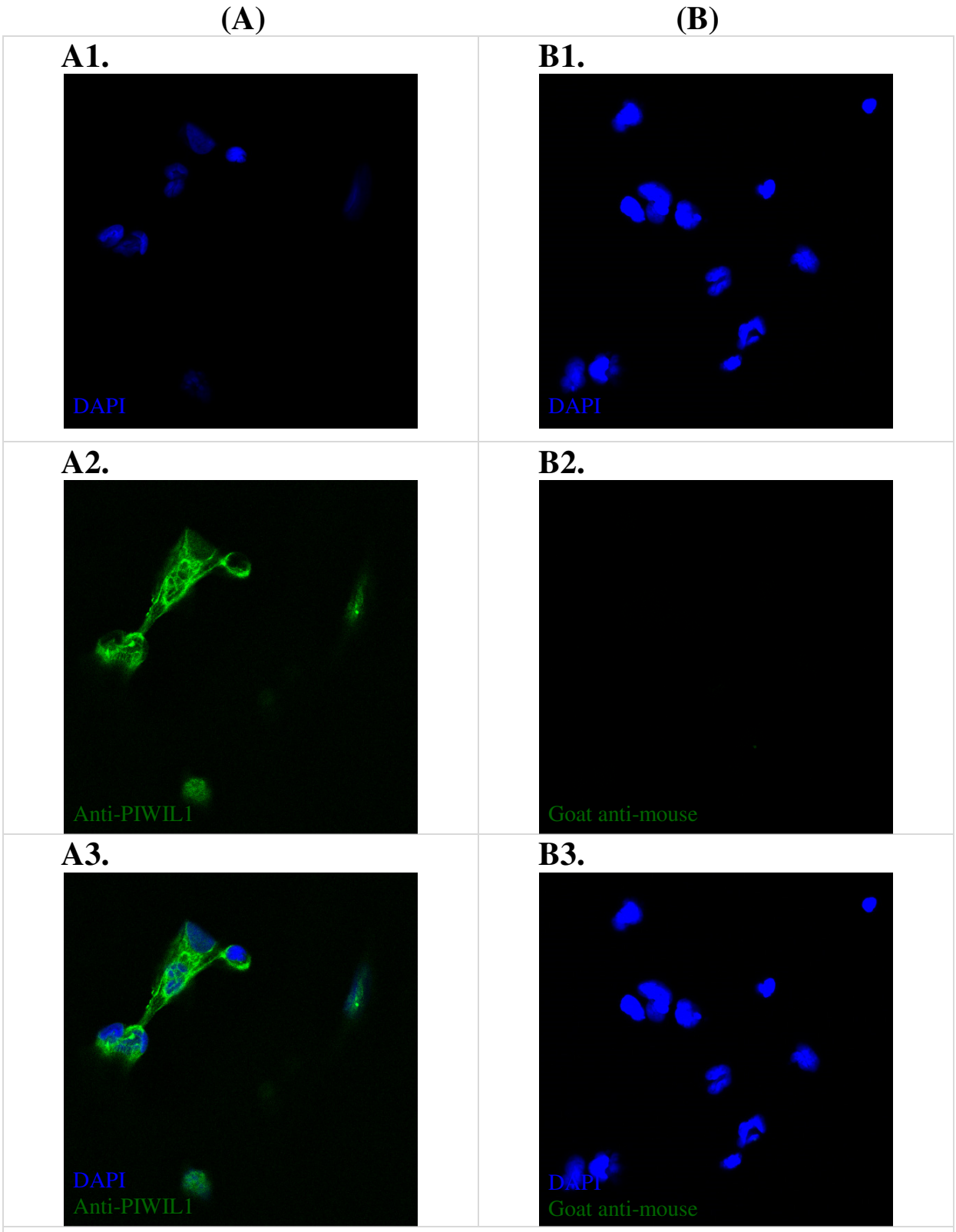

Figure 6.25 IF staining for the PIWIL1 protein in NT2 cells.
Column (A): shows images for the IF staining for anti-PIWIL1 (SIGMA-ALDRICH; SAB-4200365; 1:20) in NT2 cells. Column (B): shows images for the IF staining with only secondary antibody used as a negative control. Panel (A1 and B1): show the staining of DAPI (blue). Panel (A2 and B2): show the staining of the anti-PIWIL1 (green) and goat anti-mouse secondary antibody (Invitrogen; A11029; green). Panel (A3 and B3): show the staining of the DAPI, anti-PIWIL1 and goat anti-mouse (blue and green). Viewed using a ZEISS LSM 710 confocal microscope; Z-Position 9.

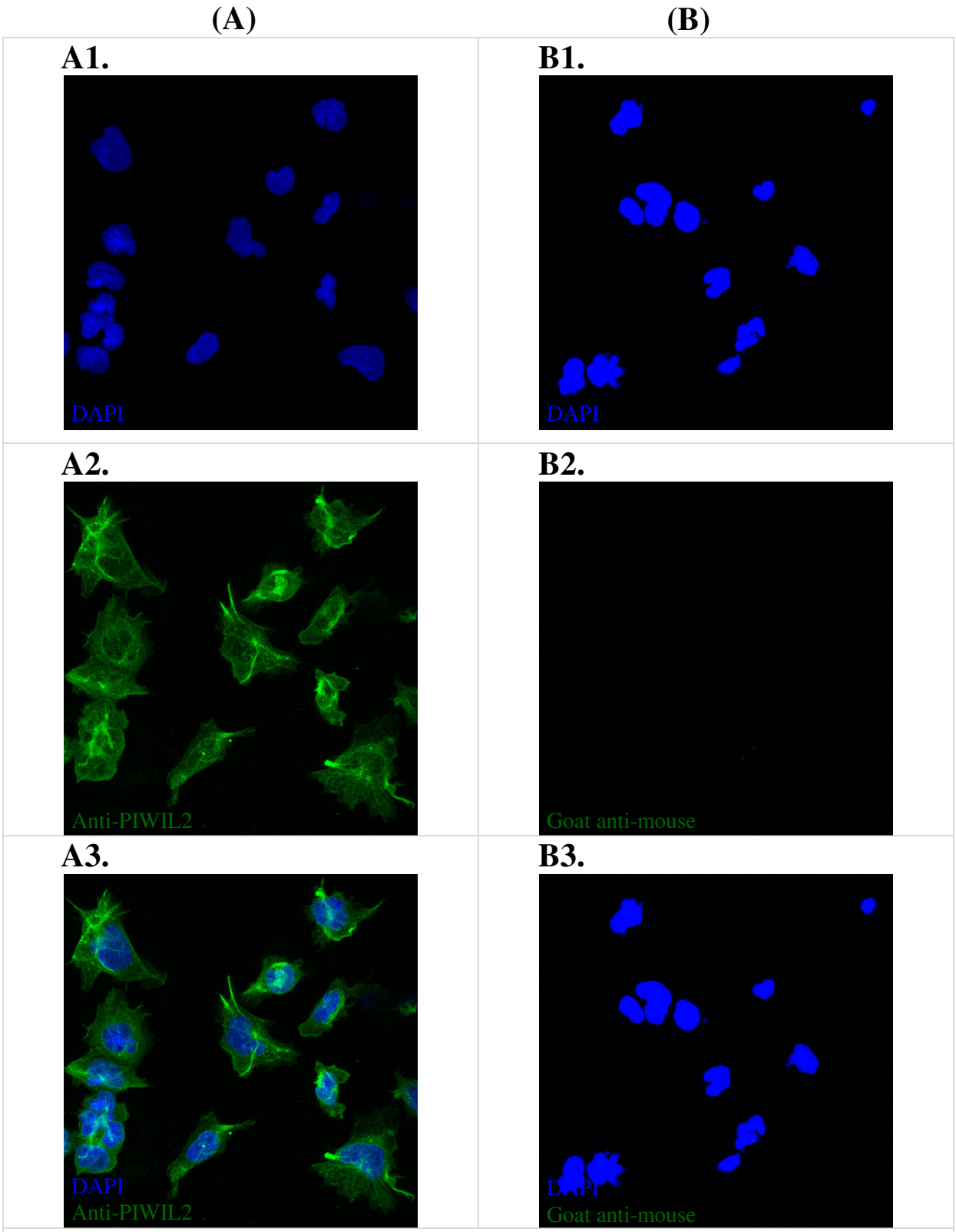

Figure 6.26 IF staining for the PIWIL2 protein in NT2 cells.
Column (A): shows images for the IF staining for anti-PIWIL2 (Abnova; MAB0843; 1:20) in NT2 cells. Column (B): shows images for the IF staining with only secondary antibody used as a negative control. Panel (A1 and B1): show the staining of DAPI (blue). Panel (A2 and B2): show the staining of the anti-PIWIL2 (green) and goat anti-mouse secondary antibody (Invitrogen; A11029; green). Panel (A3 and B3): show the staining of the DAPI, anti-PIWIL2 and goat anti-mouse (blue and green). Viewed using a ZEISS LSM 710 confocal microscope. Note: maximum intensity projection.

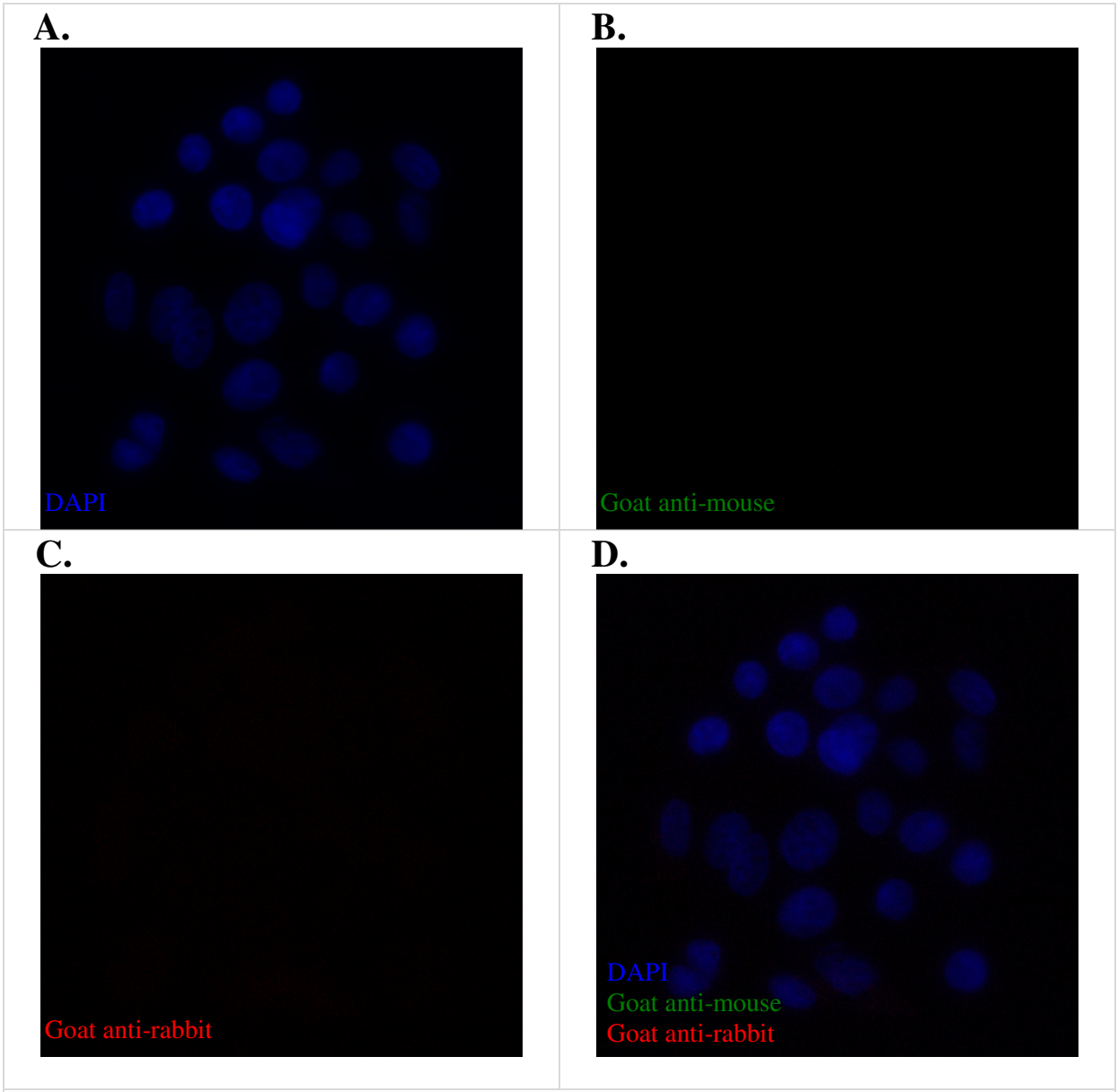

Figure 6.27 IF staining with only secondary antibodies in SW480 cells (negative controls for Figure 6.28).
Images for the IF staining with only secondary antibodies used as negative controls, viewed using a ZEISS LSM 710 confocal microscope. Panel (A): shows the staining of DAPI (blue). Panel (B): shows goat anti-mouse secondary antibody (Invitrogen; A11029; green) for the anti-β-actin-staining. Panel (C): shows goat anti-rabbit secondary antibody (Invitrogen; A11011; red) for the anti-TDRD1-staining Panel (D): shows the staining of the DAPI, goat anti-mouse and goat anti-rabbit (blue, green and red). Note: maximum intensity projection.

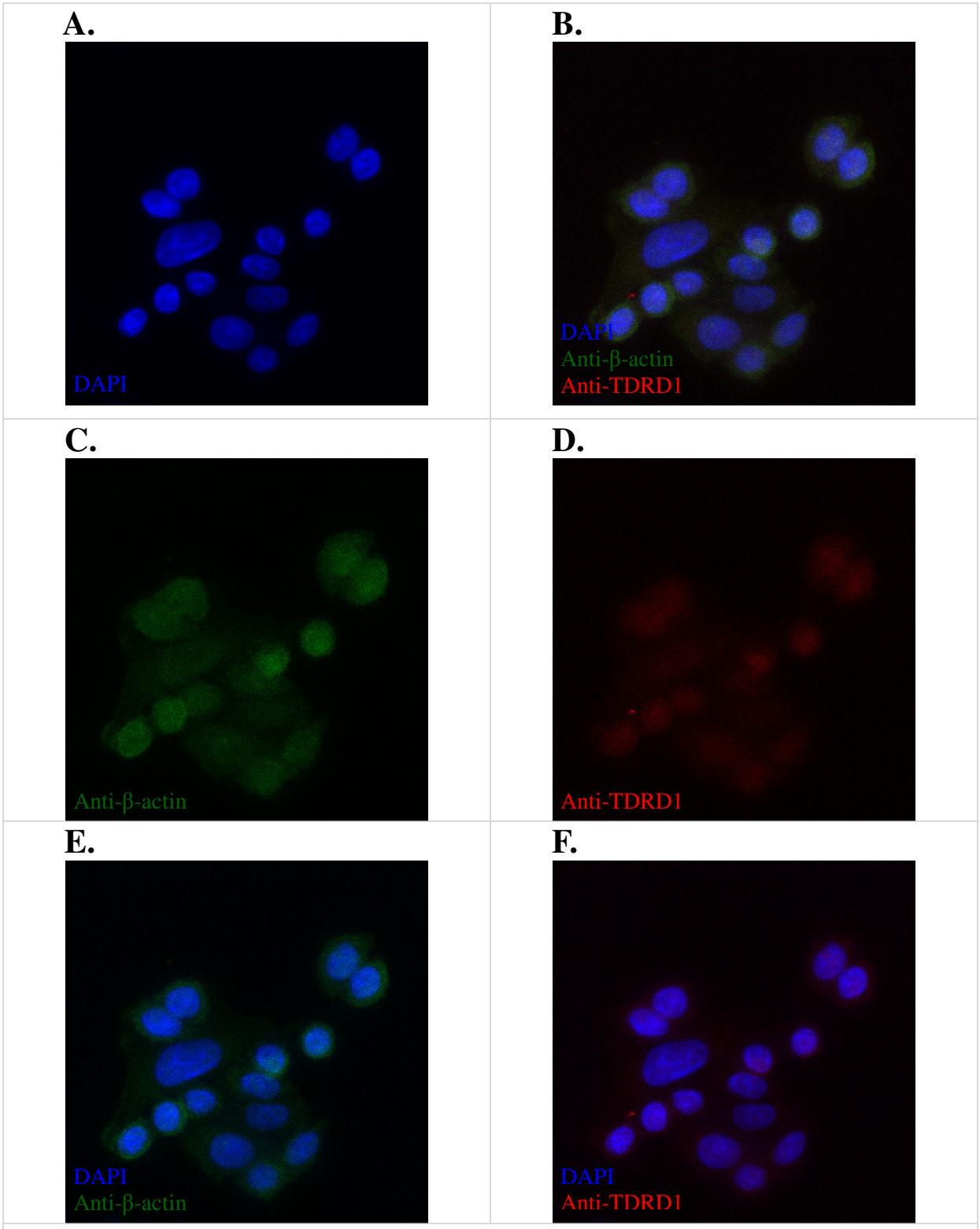

Figure 6.28 IF staining for the TDRD1 protein in SW480 cells.
Images for the IF staining for anti-β-actin (abcam; ab6277; 1:100) and anti-TDRD1 (abcam; ab107665; 1:20) in SW480 cells, viewed using a ZEISS LSM 710 confocal microscope. Panel (A): shows the staining of DAPI (blue). Panel (B): shows the staining of the DAPI, anti-β-actin and anti-TDRD1 (blue, green and red). Panel (C): shows the staining of the anti-β-actin (green). Panel (D): shows the staining of the anti-TDRD1 (red). Panel (E): shows the staining of the DAPI and anti-β-actin (blue and green). Panel (F): shows the staining of the DAPI and anti-TDRD1 (blue and red). Note: maximum intensity projection.

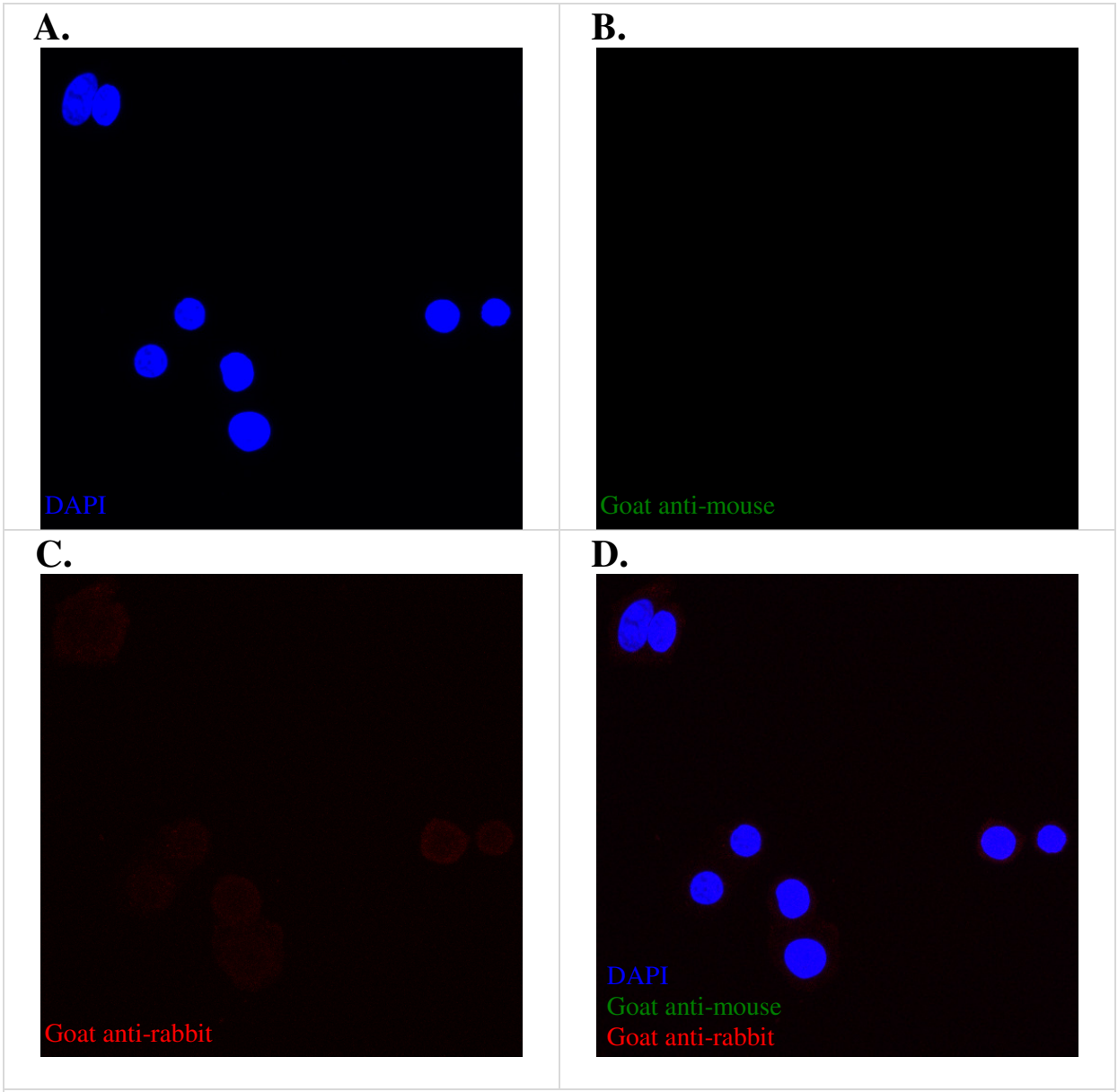

Figure 6.29 IF staining with only secondary antibodies in SW480 cells (negative controls for Figure 6.30).
Images for the IF staining with only secondary antibodies used as negative controls, viewed using a ZEISS LSM 710 confocal microscope. Panel (A): shows the staining of DAPI (blue). Panel (B): shows goat anti-mouse secondary antibody (Invitrogen; A11029; green) for the anti-β-actin-staining. Panel (C): shows goat anti-rabbit secondary antibody (Invitrogen; A11011; red) for the anti-TDRD12-ATLAS-staining Panel (D): shows the staining of the DAPI, goat anti-mouse and goat anti-rabbit (blue, green and red). Note: maximum intensity projection.

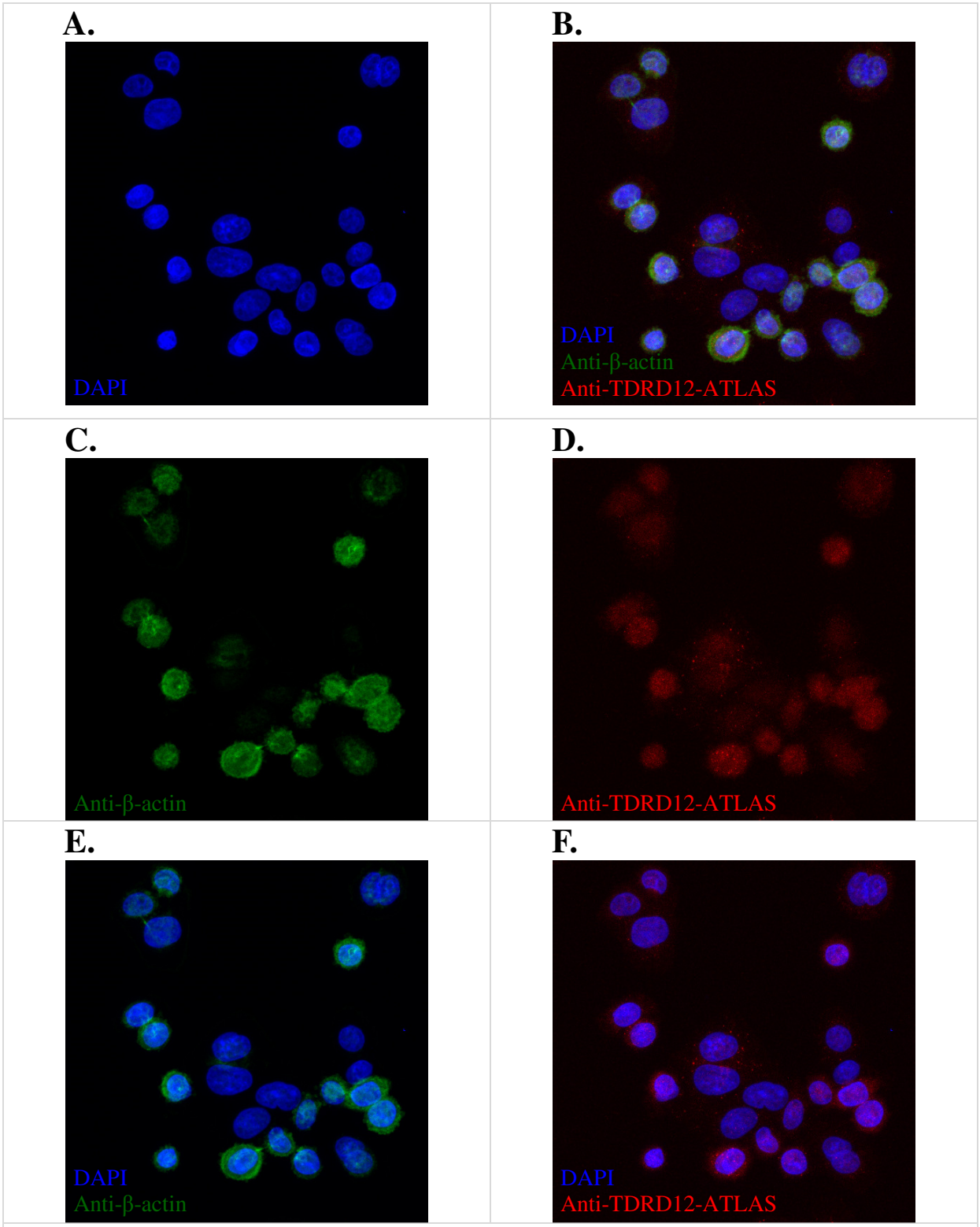

Figure 6.30 IF staining for the TDRD12 using TDRD12-ATLAS antibody in SW480 cells.
Images for the IF staining for anti-β-actin (abcam; ab6277; 1:100) and anti-TDRD12 (ATLAS ANTIBODIES; HPA-042684; 1:20) in SW480 cells, viewed using a ZEISS LSM 710 confocal microscope. Panel (A): shows the staining of DAPI (blue). Panel (B): shows the staining of the DAPI, anti-β-actin and anti-TDRD12 (blue, green and red). Panel (C): shows the staining of the anti-β-actin (green). Panel (D): shows the staining of the anti-TDRD12 (red). Panel (E): shows the staining of the DAPI and anti-β-actin (blue and green). Panel (F): shows the staining of the DAPI and anti-TDRD12 (blue and red). Note: maximum intensity projection.

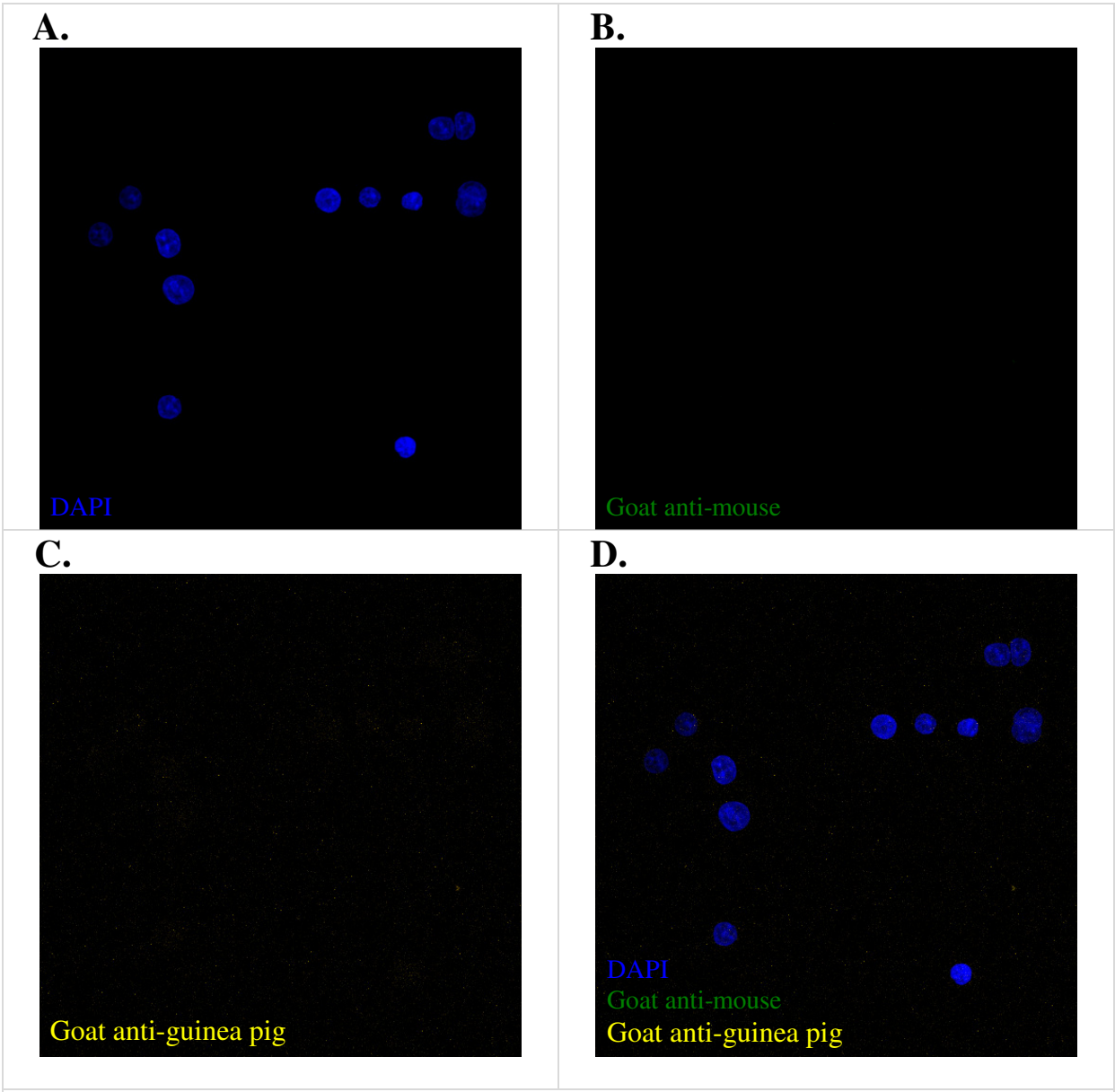

Figure 6.31 IF Staining with only secondary antibodies in SW480 cells (negative controls for Figure 6.32).
Images for the IF staining with only secondary antibodies used as negative controls, viewed using a ZEISS LSM 710 confocal microscope. Panel (A): shows the staining of DAPI (blue). Panel (B): shows goat anti-mouse secondary antibody (Invitrogen; A11029; green) for the anti-β-actin-staining. Panel (C): shows goat anti-guinea pig secondary antibody (Invitrogen; A21450; yellow) for the anti-TDRD12-PEP99-staining. Panel (D): shows the staining of the DAPI, goat anti-mouse and goat anti-guinea pig (blue, green and yellow). Note: maximum intensity projection.

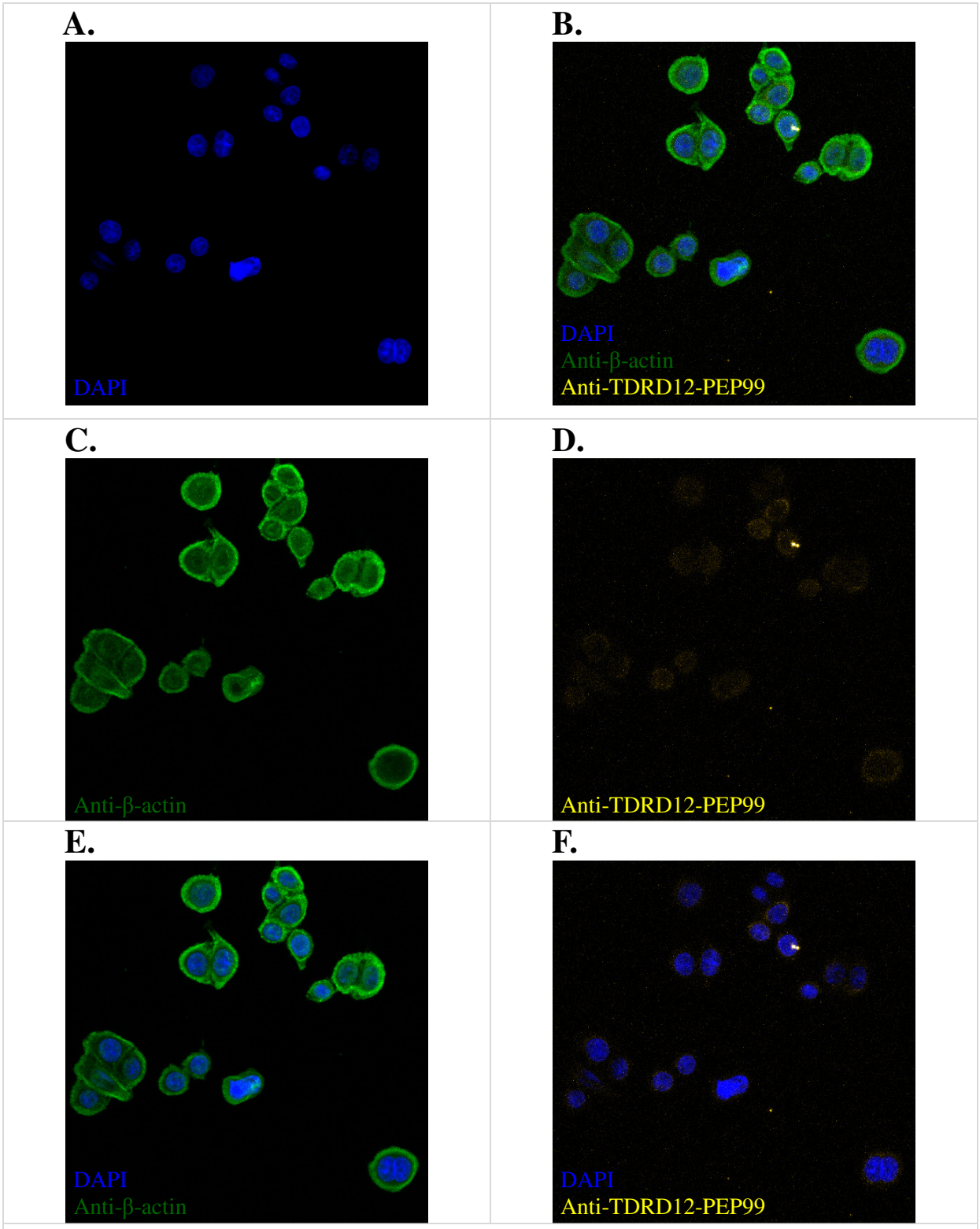

Figure 6.32 IF staining for the TDRD12 protein using TDRD12-PEP99 antibody in SW480 cells. Images for the IF staining for anti-β-actin (abcam; ab6277; 1:100) and anti-TDRD12 (Eurogentec; PEP-1310599; 1:20) in SW480 cells, viewed using a ZEISS LSM 710 confocal microscope. Panel (A): shows the staining of DAPI (blue). Panel (B): shows the staining of the DAPI, anti-β-actin and anti-TDRD12 (blue, green and yellow). Panel (C): shows the staining of the anti-β-actin (green). Panel (D): shows the staining of the anti-TDRD12 (yellow). Panel (E): shows the staining of the DAPI and anti-β-actin (blue and green). Panel (F): shows the staining of the DAPI and anti-TDRD12 (blue and yellow). Note: maximum intensity projection.

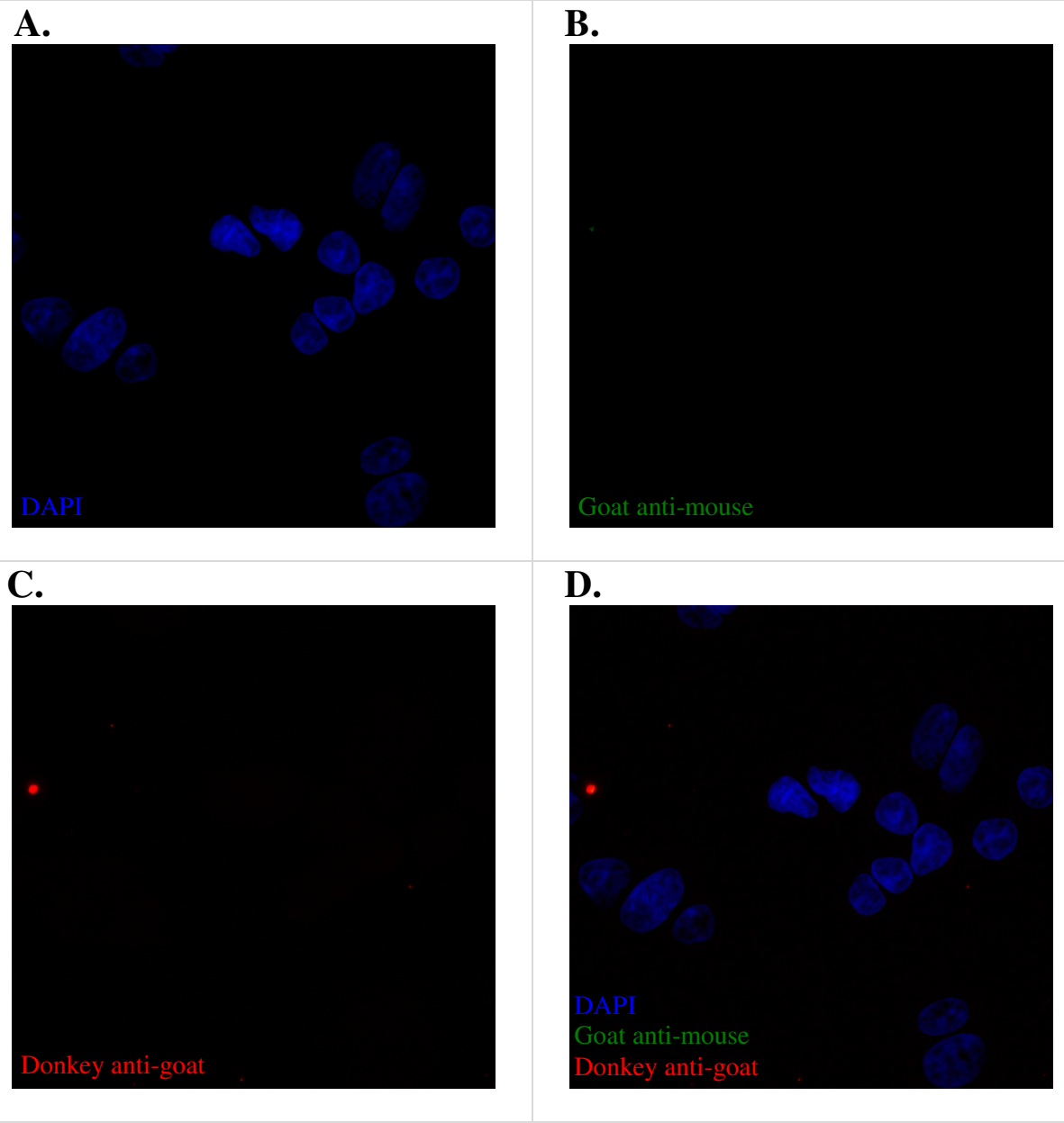

Figure 6.33 IF staining with only secondary antibodies in SW480 cells (negative controls for Figure 6.34).
Images for the IF staining with only secondary antibodies used as negative controls, viewed using a ZEISS LSM 710 confocal microscope. Panel (A): shows the staining of DAPI (blue). Panel (B): shows goat anti-mouse secondary antibody (Invitrogen; A11029; green) for the anti-β-actin-staining. Panel (C): shows donkey anti-goat secondary antibody (Invitrogen; A11057; red) for the anti-TDRD12-T17-staining. Panel (D): shows the staining of the DAPI, goat anti-mouse and donkey anti-goat (blue, green and red). Note: maximum intensity projection.

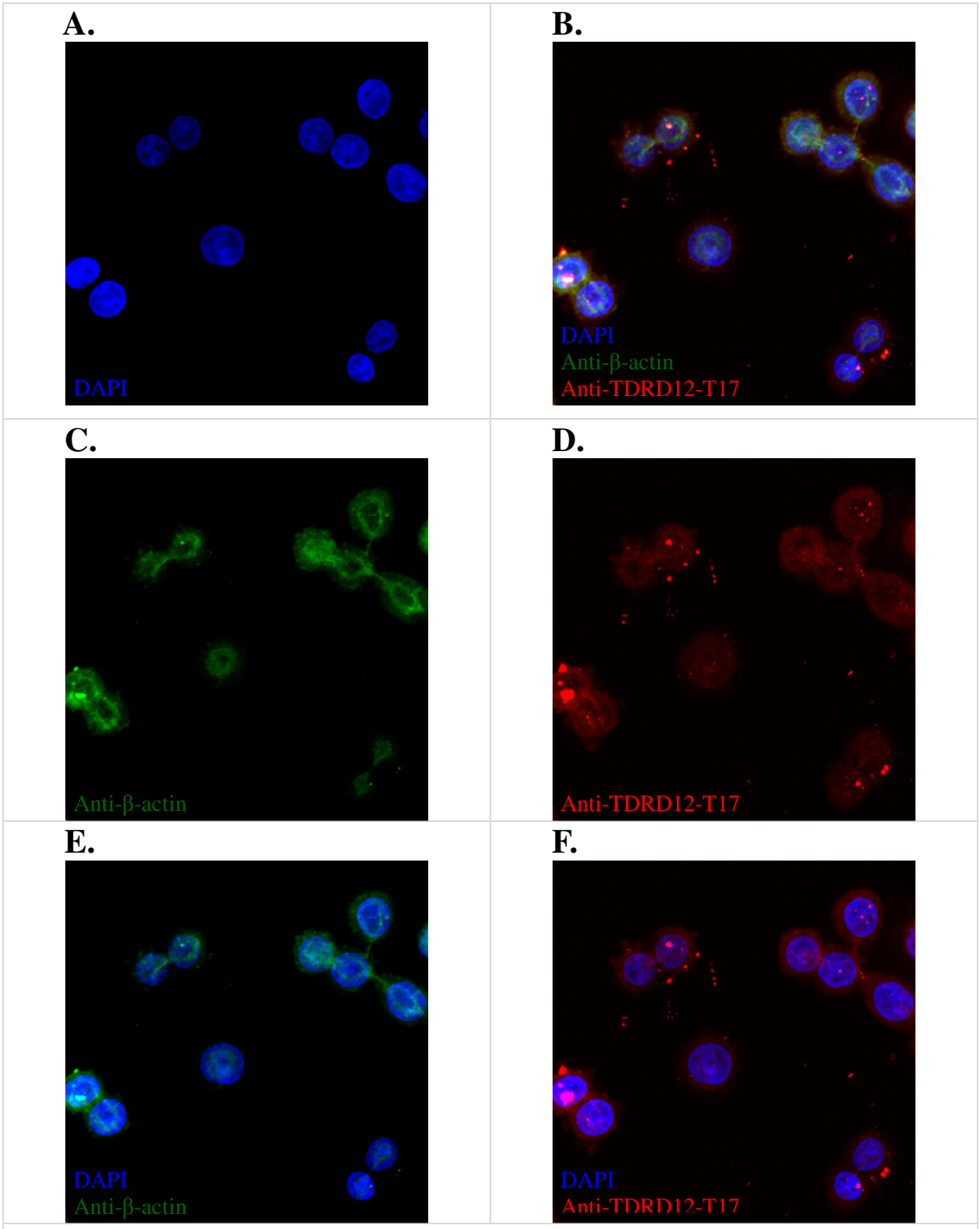

Figure 6.34 IF staining for the TDRD12 protein using TDRD12-T17 antibody in SW480 cells. Images for the IF staining for anti-β-actin (abcam; ab6277; 1:100) and anti-TDRD12-T17 (Santa Crus Biotechnology; sc-248802; 1:500) in SW480 cells, viewed using a ZEISS LSM 710 confocal microscope. Panel (A): shows the staining of DAPI (blue). Panel (B): shows the staining of the DAPI, anti-β-actin and anti-TDRD12-T17 (blue, green and red). Panel (C): shows the staining of the anti-β-actin (green). Panel (D): shows the staining of the anti-TDRD12-T17 (red). Panel (E): shows the staining of the DAPI and anti-β-actin (blue and green). Panel (F): shows the staining of the DAPI and anti-TDRD12-T17 (blue and red). Note: maximum intensity projection.

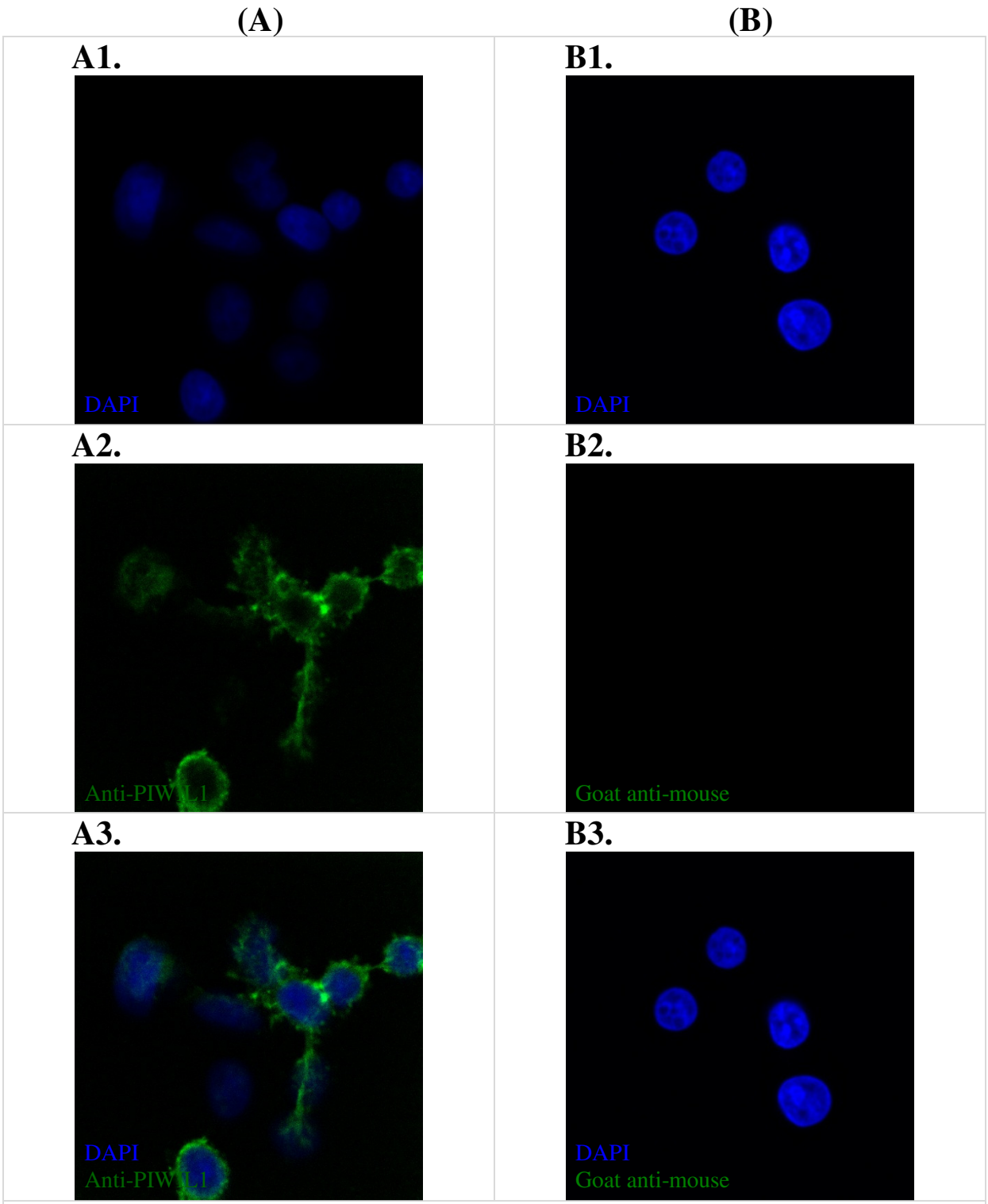

Figure 6.35 IF staining for the PIWIL1 protein in SW480 cells.
Column (A): shows images for the IF staining for anti-PIWIL1 (SIGMA-ALDRICH; SAB-4200365; 1:20) in SW480 cells (Z-Position 18). Column (B): shows images for the IF staining with only secondary antibody used as a negative control (Z-Position 1). Panel (A1 and B1): show the staining of DAPI (blue). Panel (A2 and B2): show the staining of the anti-PIWIL1 (green) and goat anti-mouse secondary antibody (Invitrogen; A11029; green). Panel (A3 and B3): show the staining of the DAPI, anti-PIWIL1 and goat anti-mouse (blue and green). Viewed using a ZEISS LSM 710 confocal microscope.

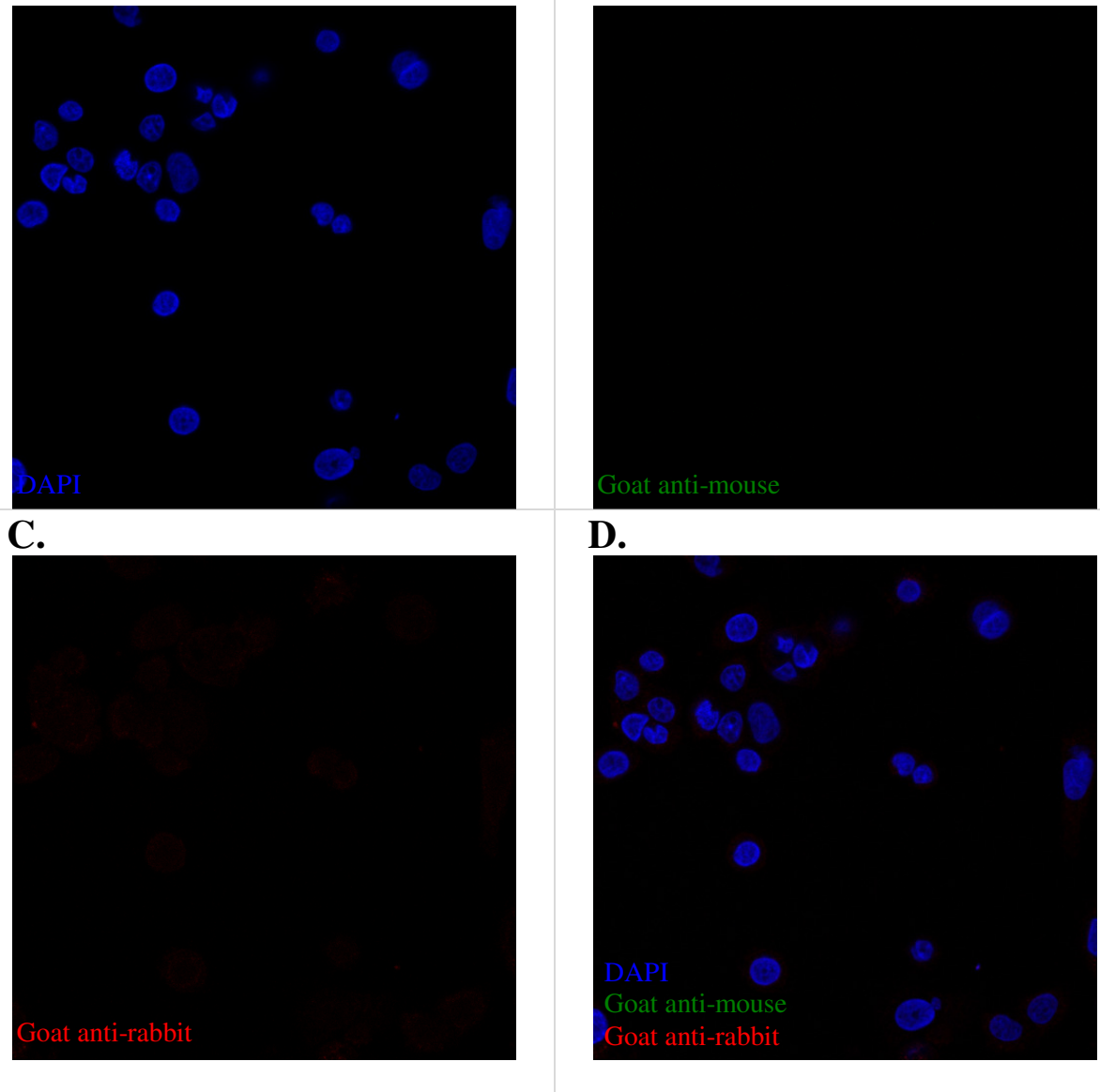

Figure 6.36 IF staining with only secondary antibodies in SW480 cells (negative controls for Figure 6.37).
Images for the IF staining with only secondary antibodies used as negative controls, viewed using a ZEISS LSM 710 confocal microscope. Panel (A): shows the staining of DAPI (blue). Panel (B): shows goat anti-mouse secondary antibody (Invitrogen; A11029; green) for the anti-PIWIL2-staining. Panel (C): shows goat anti-rabbit secondary antibody (Invitrogen; A11011; red) for the anti-TDRD12-ATLAS-staining Panel (D): shows the staining of the DAPI, goat anti-mouse and goat anti-rabbit (blue, green and red). Note: Z-Position 7 (slice 7).

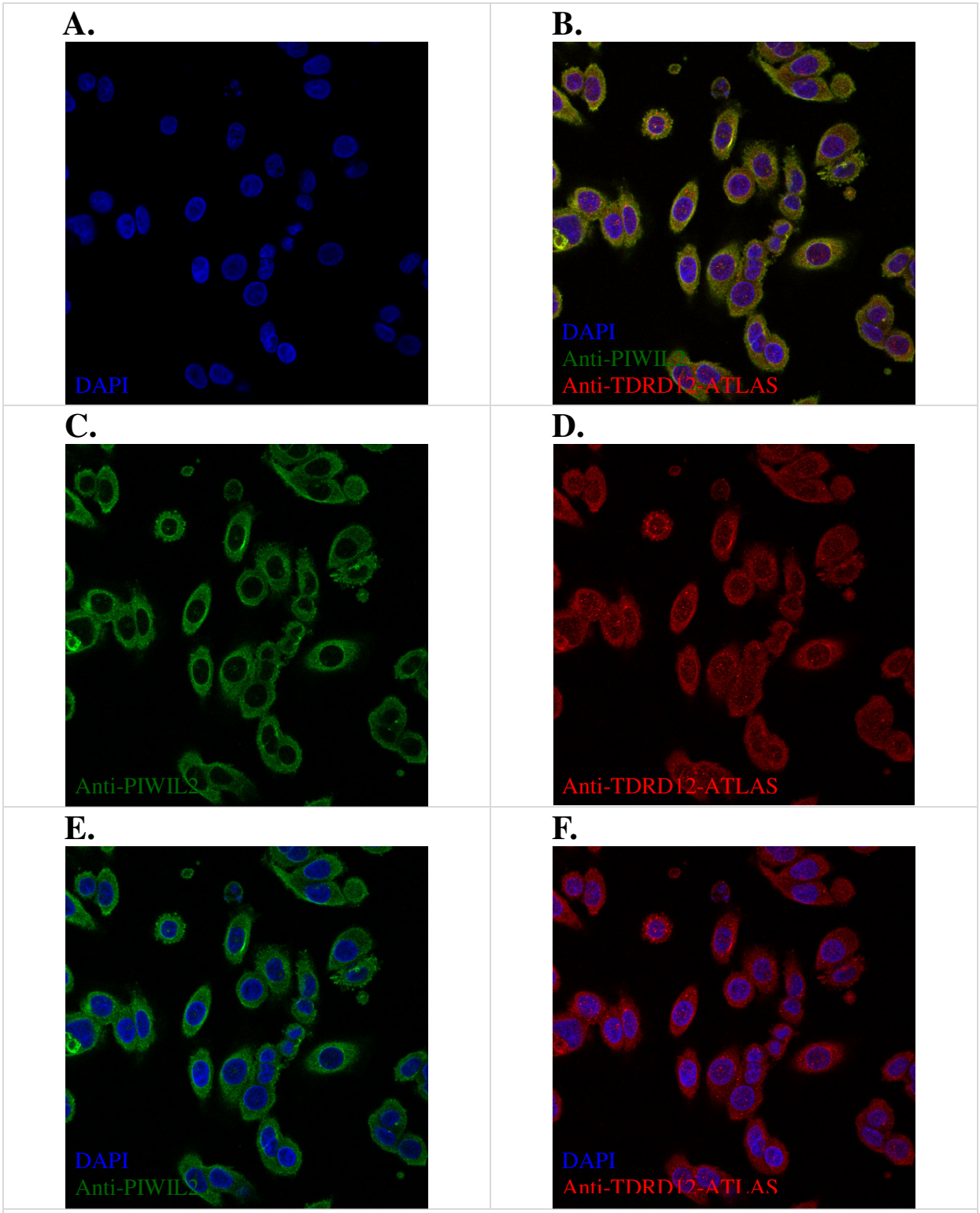

Figure 6.37 IF staining for the PIWIL2 and TDRD12 (ATLAS antibody) in SW480 cells.
Images for the IF staining for anti-PIWIL2 (Abnova; MAB0843; 1:20) and anti-TDRD12 (ATLAS ANTIBODIES; HPA-042684; 1:20) in SW480 cells, viewed using a ZEISS LSM 710 confocal microscope. Panel (A): shows the staining of DAPI (blue). Panel (B): shows the staining of the DAPI, anti-PIWIL2 and anti-TDRD12 (blue, green and red). Panel (C): shows the staining of the anti-PIWIL2 (green). Panel (D): shows the staining of the anti-TDRD12 (red). Panel (E): shows the staining of the DAPI and anti-PIWIL2 (blue and green). Panel (F): shows the staining of the DAPI and anti-TDRD12 (blue and red). Note: Z-Position 7 (slice 7).

6.4. Discussion

The process of identifying suitable target antigens is the initial and most significant step in successfully advancing the development of new antigen-specific immunotherapy or biomarker development in cancer. The discovery of CT antigens has made it possible to recognise the group of target antigens, a technique that can be utilised in several types of prevalent cancers. At present, CT antigens could be considered cancer vaccine targets, and recent research has indicated that they are potentially useful in adoptive T-cell transfer strategies and in an immunotherapeutic strategy designed to carry out CTLA-4 checkpoint blockade (Caballero and Chen, 2009). Human TDRD proteins interact with PIWIL proteins (Ishizu *et al.,* 2012; Iwasaki *et al.,* 2015; Qiao *et al.,* 2002; Ross *et al.,* 2014; Suzuki *et al.,* 2012). The *TDRD12* gene shows high levels of expression in the germ-line, this suggests it is involved in the process of gametogenesis (Chen *et al.,* 2011; Zhou *et al.,* 2014). The TDRD12 protein plays a vital role in interacting with the PIWIL2 and TDRD1 protein orthologues and the *TDRD12* gene is necessary for the process of spermatogenesis in mice (Lim *et al.,* 2014; Pandey *et al.,* 2013; Zhou *et al.,* 2014). Here we demonstrate that human PIWIL2 becomes depleted upon siRNA reduction of TDRD12, suggesting a functional regulatory relationship (refer to Chapter 5).

The work described in this Chapter sought to analyse the sub-cellular localisation of human TDRD12, TDRD1, PIWIL1 and PIWIL2 proteins in normal tissues and cancerous cells, thus ascertaining their cancer marker potential and to explore any functional relationship. The analysis also served as a primary validation for the TDRD12, TDRD1, PIWIL1 and PIWIL2 antibodies. It can be concluded that these antibodies might be useful, they must be analysed further for confirmation. *TDRD12*, *TDRD1*, *PIWIL1* and *PIWIL2* are particular germ-line expressed genes that appear to be up-regulated during the incidence of some cancer types. The CT antigens encoded by these genes are possible immunogenic biomarkers functioning as potential targets that can be utilised for immune-based therapy against cancerous cells. Drawing from the work of Pandey *et al.* (2013), we hypothesise that human TDRD12, TDRD1, PIWIL1 and PIWIL2 proteins are present in a complex. Therefore, we should analyse these four proteins in humans because they appear to function together in other organisms. We explored the idea that they might localise in the same cells and reside in the same sub-cellular position. However, as can be seen from the obtained data, there are some differences (see Table 6.1 below).

Table 6.1 Summary of IHC and IF staining analyses of antibodies in different cell types.

Antibody	Adluminal compartment	Spermatogonial layer	Adluminal compartment	Spermatogonial layer	NT2	SW480
TDRD12-T17						
TDRD12-ATLAS			X	X		
TDRD12-PEP99	X	X	X	X		
TDRD1	X		X	X		
PIWIL1		X		X		
PIWIL2	X		X			
Analysis methods	IHC	IHC	IF	IF	IF	IF

	Nuclear and cytoplasmic
	Nuclear
	Cytoplasmic
X	No signal

From Table 6.1, we can see that most of the used antibodies do not give a co-localisation signal. Localisation patterns in testis suggests that TDRD12, TDRD1 and PIWIL2 proteins are testis-specific and functioning in spermatogenesis; however, they appear to be functioning differentially as there is only limited cellular/sub-cellular localisation. Extending this we looked for commonalities between cancerous cells and sub-cellular localisation in normal tissues using IHC and IF.

PIWIL1 localisation was detected in the adluminal compartment of the seminiferous tubules. MAGEA1 localisation is a marker for the spermatogonial layer of the seminiferous tubules, indicating that PIWIL1 is not functioning in the spermatogonial cells (Figure 6.13 and Figure 6.14). However, we have not used antibody markers for adluminal compartment cells. Thus, to compare them, we would use antibody markers. Notably, we do not have those available for comparison, but they are clearly not spermatogonial cells. PIWIL1 and TDRD12-T17 antibodies represent a co-localisation that is consistent; however, in some of the cells, TDRD12-T17 seems to stain independently in the cytoplasm, without PIWIL1. When PIWIL1 is present, it seems to co-localise to TDRD12-T17 in specific areas, suggesting a potential functional compartment region (see Figure 6.16). However, other large cells seem to be TDRD12-T17 antibody staining independently, suggesting that TDRD12-T17 might act both independently and with PIWIL1. In this case, it appears that TDRD12-T17 and PIWIL1 do co-localise in the cytoplasm, suggesting that they can work together. None of these interactions seems to stain on the spermatogonial cells.

Based on the above results, I would like to now co-stain cancer cells to determine whether or not the pattern observed in the testis, which informs the link between cancer and testis functions of these proteins. It can be seen that all the antibodies give cytoplasmic staining and, in some cases, nuclear staining in cancer cells. This suggest that they are functioning in a similar manner as in the testis, Although this is little more than a suggestive observation and further work is required to explore the interplay between these proteins in both the cancer cells and testis.

6.5. Concluding remarks

This chapter focussed on analysing the sub-cellular localisation of human TDRD12, TDRD1, PIWIL1 and PIWIL2 proteins in normal tissues and cancerous cells in order to determine their cancer marker potential and any potential functional links. This procedure was carried out because the TDRD12 protein presents in complexes with the PIWIL2 and TDRD1 proteins, a complex linked to primary piRNA processing in mice (Pandey *et al.,* 2013). Additionally, the *TDRD12* gene is necessary for the process of spermatogenesis in mice (Pandey *et al.,* 2013). TDRD12, TDRD1, PIWIL1 and PIWIL2 antigens could be utilised for immunotherapy, cancer diagnosis, biomarkers and the creation of cancer drugs; in addition, they may be oncogenic (Gjerstorff *et al.,* 2015; Krishnadas *et al.,* 2013; Whitehurst, 2014). Therefore, this study primarily aimed to explore the potential of these proteins as cancer biomarkers while analysing their antibodies. The IHC and IF analysis techniques were used with a variety of primary antibodies. The results suggested that these antibodies might be useful, but further analysis is required. Moreover, these proteins might be potential biomarkers in the progression of NT2 and SW480 cancerous cells. PIWIL1 and TDRD12-T17 antibodies might have consistent co-localisation, and they appear to have similar sub-cellular localisation patterns; these two antibodies localise in the same cells in the testis, which suggests a co-function of these proteins.

7. General discussion and final concluding remarks

The areas of cancer immunotherapy and diagnosis are rapidly changing due to the continual discoveries of new genes related to cancerous cells and to the enhancements in laboratory methods used for identifying the disease's underlying causes. Additionally, the re-emergence of immunotherapy as a real therapeutic option is fuelling the need for more cancer-specific markers (Mellman *et al.,* 2011). Many of these advances have assisted in identifying novel biomarkers. The recent discovery of several new CTA genes has minimised the effect of metastasis and tumourigenesis. New molecular targets, together with companion diagnostics, are altering the manner in which we view the causes, diagnoses and therapeutic regimes of human cancer (Vockley and Niederhuber, 2015). The knowledge provided by the molecular processes and mechanisms used by CTA genes to control the process of spermatogenesis will be very useful in designing future chemotherapeutic drugs for treatment of cancerous tumours in humans. Despite the collection of molecular evidence that points to potential implications of CTA gene expression in cancer development, we are in the early stages of this new horizon in oncology (Cheng *et al.,* 2011).

The human PIWIL and TDRD proteins, as well as the piRNAs, play fundamental roles in controlling the development of germ-lines. These proteins also protect the genome against disruption by mobile genetic elements (e.g., transposons), and many questions relating to their function remain. For instance, how do the molecular mechanisms of the piRNA biogenesis pathway contribute in the development of germ-lines such as differentiation and germ cell proliferation? What are the functions in cancerous cells? If these questions were addressed, this knowledge could be applied in designing anti-cancer therapies (Ku and Lin, 2014; Rajan and Ramasamy, 2014). The TDRD proteins engage with PIWIL proteins via symmetrical dimethyl arginines (sDMAs). Although Tudor domains from the Tudor family of proteins have been confirmed to perform as sDMA-binding modules, the association of the Tudor family in molecular-level functions in the piRNA pathway remains poorly understood (Gayatri and Bedford, 2014; Iwasaki *et al.,* 2015; Siomi *et al.,* 2010).

Tudor domains have been identified as methyl arginine binders, yet not much is known regarding how they attain maximum specificity for natural ligands. Further research is necessary to ascertain if the multiple tandem domains of proteins in the TDRD family possess any methyl arginine-binding ability. Not much is known about their preference in methylation motifs amongst PIWI proteins and other targets or their function in multivalent interactions (Chen *et al.,* 2011; Gayatri and Bedford, 2014; Iwasaki *et al.,* 2015). Recent advances in molecular biology techniques (e.g., mass spectrometry) will make the genome-wide arginine methylation proteomics possible to study. These technologies will increase our knowledge of the arginine methylation sites and the methylated proteins database, which will be extremely helpful for proposing new physiological functions for methyl arginine-binding domains (Chen *et al.,* 2011; Cheng *et al.,* 2011; Fratta *et al.,* 2011; Hofmann *et al.,* 2008). The role, if any, TDRD12 plays in PIWIL1 via sDMAs may provide a mechanistic target for therapies.

CTAs have been linked to stemness (Yang *et al.,* 2015). Stem cells (SCs) are characterised by their ability to self-renew and their capacity to differentiate and divide into various specialised cell categories (Goodell *et al.,* 2015; Simara *et al.,* 2013; Wong *et al.,* 2013). SCs have the potential to be used in a number of therapeutic applications, particularly in the field of tissue regeneration and engineering (Diekman *et al.,* 2012; Fox and Duncan, 2013; Matsa *et al.,* 2014; Wong *et al.,* 2013). Cancer stem cells (CSCs) are promising targets for new human cancer therapies; CSCs are also important and powerful tools in molecular cancer research. Specific cellular and novel biomarkers are promising targets for the development of drugs and the early diagnosis of cancers. Therefore, more research and investigation is required in the molecular biology of CSCs (García Martinez and Nogués, 2014; Rajendran and Dalerba, 2014). Isolating and identifying CSCs is relevant and vital to the translational work being done in cancer molecular research. CSCs are essential in the development of cancer metastases and, therefore, in cancer relapses. In addition, they have a direct contribution in resistance development to the present approaches in cancer treatment. From a clinical point of view, new clinical trials that explore the effectiveness of targeting and therapy of CSCs are of considerable importance. Insights into the CSCs' mechanisms during cancer pathogenesis and targeting therapies specific to CSCs will enhance the prognosis, as well as the quality of life, for cancer patients (Islam *et al.,* 2015).

The research done here has placed emphasise on germ-line-related genes. A novel group of potential CTA genes (*TDRD1-TDRD12* and *PIWIL1-PIWIL4*) were investigated, and the cancer pipeline dataset's (CancerMA [http://www.cancerma.org.uk/index.html]; Feichtinger *et al.,* 2012b) online tool confirmed some of the above-mentioned genes were significantly up-regulated during the development of some cancer types. This is indicative of the fact that they may have relevant markers for other types of cancers. Examining the complex nature of tumour types is a continuing challenge in the area of oncology and precision medical practice (Blagden, 2015; Jamal-Hanjani *et al.,* 2015; Seoane and Mattos-Arruda, 2014). There is growing evidence that meiotic and germ-line factors play a functional part in the biology of cancer. Janic *et al.* (2010) were the first to find that germ-line genes serve as oncogenic factors in *D. melanogaster*. Specified proteins have been found to serve significant functions in meiosis and to also contain a cancer phenotype-promoting impact when they exist in malignant cancer cells. Indeed, the *D. melanogaster* germ-line genes identified by Janic *et al.* (2010) are also up-regulated in human cancer and include PIWI genes (Feichtinger *et al.,* 2014). This germ-line/meiotic gene cancer hypothesis (McFarlane *et al.,* 2014) is supported by the fact the meiotic factors Mnd1 and Hop2 are required for telomere maintenance in some cancers (Cho *et al.,* 2014; Janic *et al.,* 2010; Watkins *et al.,* 2015). Additionally, Rousseaux *et al.* (2013) demonstrated expression of a sub-group of germ-line genes is an accurate indicator of a poor prognosis in lung cancers.

A new germ-line gene, *TDRD12*, has been analysed in detail here, and TDRD12 protein might serve as a possible immunological target for human cancer cell therapies. The functional role of this protein in normal physiology and/or in cancer must be further analysed. Precision and personalised medicine is usually done based on the predictive nature and power of existing biomarkers, as well as on the stratification methods. Gene expression is the most essential aspect on which stratification efforts are focused, and germ-line factors are emerging as useful facts in this context. The functional roles of several germ-line and CTA genes are not properly characterised in spite of the high degree of interest in CTAs as targets for human immunotherapy. A few of these CTAs have already been served as targets (Hunder *et al.,* 2008; Simpson *et al.,* 2005; Whitehurst, 2014). Therefore, characterising and identifying new cancer-specific biomarkers together with targets is an important challenge in the successful development of diagnoses and immunotherapy treatments for malignant tumour rejection (Feichtinger *et al.,* 2012; Krishnadas *et al.,* 2013).

Such factors are relevant due to the fact that cancer is usually diagnosed and treated in its later stages, and by then cancerous cells have already proliferated in all areas of the body and become metastatic (Aly, 2012; Brown *et al.,* 2015; Islam *et al.,* 2015; Suri, 2006). This research study was mainly focused on the medical biomarker and oncogenic potential of the human cancer- and stem/germ cell-specific gene *TDRD12*, as well as on identifying new CTA genes that could be potentially useful biomarkers/targets in early diagnostic and immunotherapeutic approaches aimed at treating cancer. Seven CTA genes (*TDRD1*, *TDRD4*, *TDRD5*, *TDRD6*, *TDRD12*, *PIWIL1* and *PIWIL2*) were identified to be potential targets or biomarkers for future therapeutic strategies. Further research is required to recognise their roles in developing cancerous cells.

The research study was also focused on the *TDRD12* gene in regulating the HERV and RE gene expression levels in human germ-line tumour cells. Many germ-line-specific genes show high levels of expression profiles in cancerous cells and malignant tumours. The results obtained suggested that the *TDRD12* gene might play a role in conferring stemness to cancerous cells, and this gene might also requires for the germ-line/stem cell regulation of REs and HERVs in human germ-line tumour cells. A large number of the RE, HERV and germ-line genes were up-regulated during the knockdown of the *TDRD12* gene. Consequently, the group of up-regulated genes shows that *TDRD12* might be repressing the REs. Therefore, further analysis of genome wide transcription upon *TDRD12-001* depletion should reveal how extensive the role of *TDRD12* is in controlling stem-line gene and REs expression.

8. References

Ajani, J.A., Song, S., Hochster, H.S. & Steinberg, I.B. 2015, "Cancer stem cells: the promise and the potential", *Seminars in oncology*Elsevier, , pp. S3.

Ajiro, M. & Zheng, Z. 2014, "Oncogenes and RNA splicing of human tumor viruses", *Emerging Microbes & Infections,* vol. 3, no. 9, pp. e63.

Akiyama, Y., Komiyama, M., Miyata, H., Yagoto, M., Ashizawa, T., Iizuka, A., Oshita, C., Kume, A., Nogami, M. & Ito, I. 2014, "Novel cancer-testis antigen expression on glioma cell lines derived from high-grade glioma patients", *Oncology reports,* vol. 31, no. 4, pp. 1683-1690.

Almatrafi, A., Feichtinger, J., Vernon, E.G., Escobar, N.G., Wakeman, J.A., Larcombe, L.D. & McFarlane, R.J. 2014, "Identification of a class of human cancer germline genes with transcriptional silencing refractory to the hypomethylating drug 5-aza-2′-deoxycytidine.", *Oncoscience,* vol. 1, no. 11, pp. 745.

Aloni-Grinstein, R., Shetzer, Y., Kaufman, T. & Rotter, V. 2014, "p53: the barrier to cancer stem cell formation", *FEBS letters,* vol. 588, no. 16, pp. 2580-2589.

Aly, H.A. 2012, "Cancer therapy and vaccination", *Journal of immunological methods,* vol. 382, no. 1-2, pp. 1-23.

Anand, P., Kunnumakkara, A.B., Sundaram, C., Harikumar, K.B., Tharakan, S.T., Lai, O.S., Sung, B. & Aggarwal, B.B. 2008, "Cancer is a preventable disease that requires major lifestyle changes", *Pharmaceutical research,* vol. 25, no. 9, pp. 2097-2116.

Andrews, P.W. 1984, "Retinoic acid induces neuronal differentiation of a cloned human embryonal carcinoma cell line in vitro", *Developmental biology,* vol. 103, no. 2, pp. 285-293.

Andrews, P.W., Casper, J., Damjanov, I., Duggan□Keen, M., Giwercman, A., Hata, J., von Keitz, A., Looijenga, L.H., Millan, J.L. & Oosterhuis, J.W. 1996, "Comparative analysis of cell surface antigens expressed by cell lines derived from human germ cell tumours", *International journal of cancer,* vol. 66, no. 6, pp. 806-816.

Andrews, P.W., Damjanov, I., Simon, D. & Dignazio, M. 1985, "A pluripotent human stem□cell clone isolated from the TERA□2 teratocarcinoma line lacks antigens SSEA□3 and SSEA□4 in vitro, but expresses these antigens when grown as a xenograft tumor", *Differentiation,* vol. 29, no. 2, pp. 127-135.

Andrews, P., Matin, M., Bahrami, A., Damjanov, I., Gokhale, P. & Draper, J. 2005, "Embryonic stem (ES) cells and embryonal carcinoma (EC) cells: opposite sides of the same coin", *Biochemical Society transactions,* vol. 33, no. 6, pp. 1526-1530.

Andrews, P.W. 2002, "From teratocarcinomas to embryonic stem cells", *Philosophical Transactions of the Royal Society B: Biological Sciences,* vol. 357, no. 1420, pp. 405-417.

Antequera, F. & Bird, A. 1999, "CpG islands as genomic footprints of promoters that are associated with replication origins", *Current biology : CB,* vol. 9, no. 17, pp. R661-7.

Apostolopoulos, V., Stojanovska, L. & Gargosky, S.E. 2015, "MUC1 (CD227): a multi-tasked molecule", *Cellular and Molecular Life Sciences,* vol. 72, no. 23, pp. 4475-4500.

Aravin, A.A., Sachidanandam, R., Bourc'his, D., Schaefer, C., Pezic, D., Toth, K.F., Bestor, T. & Hannon, G.J. 2008, "A piRNA pathway primed by individual transposons is linked to de novo DNA methylation in mice", *Molecular cell,* vol. 31, no. 6, pp. 785-799.

Aravin, A.A., Sachidanandam, R., Girard, A., Fejes-Toth, K. & Hannon, G.J. 2007, "Developmentally regulated piRNA clusters implicate MILI in transposon control", *Science (New York, N.Y.),* vol. 316, no. 5825, pp. 744-747.

Bacac, M. & Stamenkovic, I. 2008, "Metastatic cancer cell", *Annual review of pathology,* vol. 3, pp. 221-247.

Bagci, O. & Kurtgöz, S. 2015, "Amplification of cellular oncogenes in solid tumors", *North American journal of medical sciences,* vol. 7, no. 8, pp. 341.

Baker, L.A., Allis, C.D. & Wang, G.G. 2008, "PHD fingers in human diseases: disorders arising from misinterpreting epigenetic marks", *Mutation Research/Fundamental and Molecular Mechanisms of Mutagenesis,* vol. 647, no. 1, pp. 3-12.

Bao, J., Wang, L., Lei, J., Hu, Y., Liu, Y., Shen, H., Yan, W. & Xu, C. 2012, "STK31 (TDRD8) is dynamically regulated throughout mouse spermatogenesis and interacts with MIWI protein", *Histochemistry and cell biology,* vol. 137, no. 3, pp. 377-389.

Barrio, M.M., Abes, R., Colombo, M., Pizzurro, G., Boix, C., Roberti, M.P., Gelize, E., Rodriguez-Zubieta, M., Mordoh, J. & Teillaud, J. 2012, "Human macrophages and dendritic cells can equally present MART-1 antigen to CD8 T cells after phagocytosis of gamma-irradiated melanoma cells", *PloS one,* vol. 7, no. 7, pp. e40311.

Bart, J., Groen, H.J., van der Graaf, W.T., Hollema, H., Hendrikse, N.H., Vaalburg, W., Sleijfer, D.T. & de Vries, E.G. 2002, "An oncological view on the blood-testis barrier", *The lancet oncology,* vol. 3, no. 6, pp. 357-363.

Baulande, S., Criqui, A. & Duthieuw, M. 2014, "Circulating miRNAs as a new class of biomedical markers", *Medecine sciences : M/S,* vol. 30, no. 3, pp. 289-296.

Baylin, S.B. 2005, "DNA methylation and gene silencing in cancer", *Nature clinical practice Oncology,* vol. 2, pp. S4-S11.

Beattie, G.M., Lopez, A.D., Bucay, N., Hinton, A., Firpo, M.T., King, C.C. & Hayek, A. 2005, "Activin A maintains pluripotency of human embryonic stem cells in the absence of feeder layers", *Stem cells,* vol. 23, no. 4, pp. 489-495.

Berry, W.L. & Janknecht, R. 2013, "KDM4/JMJD2 histone demethylases: epigenetic regulators in cancer cells", *Cancer research,* vol. 73, no. 10, pp. 2936-2942.

Blagden, S.P. 2015, "Harnessing Pandemonium: The Clinical Implications of Tumor Heterogeneity in Ovarian Cancer", *Frontiers in oncology,* vol. 5, pp. 149.

Blasco, M.A. 2005, "Telomeres and human disease: ageing, cancer and beyond", *Nature reviews.Genetics,* vol. 6, no. 8, pp. 611-622.

Boer, B., Cox, J.L., Claassen, D., Mallanna, S.K., Desler, M. & Rizzino, A. 2009, "Regulation of the Nanog gene by both positive and negative cis□regulatory elements in embryonal carcinoma cells and embryonic stem cells", *Molecular reproduction and development,* vol. 76, no. 2, pp. 173-182.

Bonnet, D. & Dick, J.E. 1997, "Human acute myeloid leukemia is organized as a hierarchy that originates from a primitive hematopoietic cell", *Nature medicine,* vol. 3, no. 7, pp. 730-737.

Boyer, L.A., Lee, T.I., Cole, M.F., Johnstone, S.E., Levine, S.S., Zucker, J.P., Guenther, M.G., Kumar, R.M., Murray, H.L. & Jenner, R.G. 2005, "Core transcriptional regulatory circuitry in human embryonic stem cells", *Cell,* vol. 122, no. 6, pp. 947-956.

Bredholt, G., Mannelqvist, M., Stefansson, I.M., Birkeland, E., Hellem Bo, T., Oyan, A.M., Trovik, J., Kalland, K.H., Jonassen, I., Salvesen, H.B., Wik, E. & Akslen, L.A. 2015, "Tumor necrosis is an important hallmark of aggressive endometrial cancer and associates with hypoxia, angiogenesis and inflammation responses", *Oncotarget,* .

Brown, S., Kirkbride, P. & Marshall, E. 2015, "Radiotherapy in the acute medical setting", *Clinical medicine (London, England),* vol. 15, no. 4, pp. 382-387.

Butterfield, L.H. 2015, "Cancer vaccines", *BMJ (Clinical research ed.),* vol. 350, pp. h988.

Caballero, O.L. & Chen, Y. 2009a, "Cancer/testis (CT) antigens: potential targets for immunotherapy", *Cancer science,* vol. 100, no. 11, pp. 2014-2021.

Caballero, O.L. & Chen, Y.T. 2009b, "Cancer/testis (CT) antigens: potential targets for immunotherapy", *Cancer science,* vol. 100, no. 11, pp. 2014-2021.

Cairns, R.A., Harris, I.S. & Mak, T.W. 2011, "Regulation of cancer cell metabolism", *Nature reviews.Cancer,* vol. 11, no. 2, pp. 85-95.

Calabro, L., Fonsatti, E., Altomonte, M., Pezzani, L., Colizzi, F., Nanni, P., Gattei, V., Sigalotti, L. & Maio, M. 2005, "Methylation-regulated expression of cancer testis antigens in primary effusion lymphoma: immunotherapeutic implications", *Journal of cellular physiology,* vol. 202, no. 2, pp. 474-477.

Callinan, P.A. & Batzer, M.A. 2006, "Retrotransposable elements and human disease", *Genome dynamics,* vol. 1, pp. 104-115.

Carelle, N., Piotto, E., Bellanger, A., Germanaud, J., Thuillier, A. & Khayat, D. 2002, "Changing patient perceptions of the side effects of cancer chemotherapy", *Cancer,* vol. 95, no. 1, pp. 155-163.

Carmell, M.A., Xuan, Z., Zhang, M.Q. & Hannon, G.J. 2002, "The Argonaute family: tentacles that reach into RNAi, developmental control, stem cell maintenance, and tumorigenesis", *Genes & development,* vol. 16, no. 21, pp. 2733-2742.

Carr, A.C., Vissers, M.C. & Cook, J. 2014, "Relief from cancer chemotherapy side effects with pharmacologic vitamin C", *The New Zealand medical journal,* vol. 127, no. 1388, pp. 66-70.

Ceci, C., Barbaccia, M.L. & Pistritto, G. 2015, "A not cytotoxic nickel concentration alters the expression of neuronal differentiation markers in NT2 cells", *Neurotoxicology,* vol. 47, pp. 47-53.

Cedar, H. & Bergman, Y. 2009, "Linking DNA methylation and histone modification: patterns and paradigms", *Nature reviews.Genetics,* vol. 10, no. 5, pp. 295-304.

Chalmel, F., Rolland, A.D., Niederhauser-Wiederkehr, C., Chung, S.S., Demougin, P., Gattiker, A., Moore, J., Patard, J.J., Wolgemuth, D.J., Jegou, B. & Primig, M. 2007, "The conserved

transcriptome in human and rodent male gametogenesis", *Proceedings of the National Academy of Sciences of the United States of America,* vol. 104, no. 20, pp. 8346-8351.

Chambers, I., Colby, D., Robertson, M., Nichols, J., Lee, S., Tweedie, S. & Smith, A. 2003, "Functional expression cloning of Nanog, a pluripotency sustaining factor in embryonic stem cells", *Cell,* vol. 113, no. 5, pp. 643-655.

Chambers, I. & Smith, A. 2004, "Self-renewal of teratocarcinoma and embryonic stem cells", *Oncogene,* vol. 23, no. 43, pp. 7150-7160.

Chanmee, T., Ontong, P., Kimata, K. & Itano, N. 2015, "Key roles of hyaluronan and its CD44 receptor in the stemness and survival of cancer stem cells", *Frontiers in oncology,* vol. 5.

Checler, F. & da Costa, C.A. 2014, "p53 in neurodegenerative diseases and brain cancers", *Pharmacology & therapeutics,* vol. 142, no. 1, pp. 99-113.

Chen, H., Tsai, S. & Leone, G. 2009, "Emerging roles of E2Fs in cancer: an exit from cell cycle control", *Nature Reviews Cancer,* vol. 9, no. 11, pp. 785-797.

Chen, K., Pan, F., Jiang, H., Chen, J., Pei, L., Xie, F. & Liang, H. 2011a, "Highly enriched CD133 CD44 stem-like cells with CD133 CD44high metastatic subset in HCT116 colon cancer cells", *Clinical & experimental metastasis,* vol. 28, no. 8, pp. 751-763.

Chen, Z., Trotman, L.C., Shaffer, D., Lin, H., Dotan, Z.A., Niki, M., Koutcher, J.A., Scher, H.I., Ludwig, T. & Gerald, W. 2005, "Crucial role of p53-dependent cellular senescence in suppression of Pten-deficient tumorigenesis", *Nature,* vol. 436, no. 7051, pp. 725-730.

Chen, Z., Che, Q., Jiang, F., Wang, H., Wang, F., Liao, Y. & Wan, X. 2015, "Piwil1 causes epigenetic alteration of PTEN gene via upregulation of DNA methyltransferase in type I endometrial cancer", *Biochemical and biophysical research communications,* vol. 463, no. 4, pp. 876-880.

Chen, C., Nott, T.J., Jin, J. & Pawson, T. 2011b, "Deciphering arginine methylation: Tudor tells the tale", *Nature reviews.Molecular cell biology,* vol. 12, no. 10, pp. 629-642.

Chen, S.R. & Liu, Y.X. 2015, "Regulation of spermatogonial stem cell self-renewal and spermatocyte meiosis by Sertoli cell signaling", *Reproduction (Cambridge, England),* vol. 149, no. 4, pp. R159-67.

Chen, Y., Xu, J., Borowicz, S., Collins, C., Huo, D. & Olopade, O.I. 2011c, "c-Myc activates BRCA1 gene expression through distal promoter elements in breast cancer cells", *BMC cancer,* vol. 11, pp. 246-2407-11-246.

Chénais, B. 2015, "Transposable Elements in Cancer and Other Human Diseases", *Current cancer drug targets,* vol. 15, no. 3, pp. 227-242.

Cheng, Y.H., Wong, E.W. & Cheng, C.Y. 2011, "Cancer/testis (CT) antigens, carcinogenesis and spermatogenesis", *Spermatogenesis,* vol. 1, no. 3, pp. 209-220.

Chew, J.L., Loh, Y.H., Zhang, W., Chen, X., Tam, W.L., Yeap, L.S., Li, P., Ang, Y.S., Lim, B., Robson, P. & Ng, H.H. 2005, "Reciprocal transcriptional regulation of Pou5f1 and Sox2 via the Oct4/Sox2 complex in embryonic stem cells", *Molecular and cellular biology,* vol. 25, no. 14, pp. 6031-6046.

Chi, P., Allis, C.D. & Wang, G.G. 2010, "Covalent histone modifications—miswritten, misinterpreted and mis-erased in human cancers", *Nature reviews cancer,* vol. 10, no. 7, pp. 457-469.

Cho, H., Noh, K.H., Chung, J., Takikita, M., Chung, E.J., Kim, B.W., Hewitt, S.M., Kim, T.W. & Kim, J. 2014a, "Synaptonemal complex protein 3 is a prognostic marker in cervical cancer", .

Cho, N.W., Dilley, R.L., Lampson, M.A. & Greenberg, R.A. 2014b, "Interchromosomal homology searches drive directional ALT telomere movement and synapsis", *Cell,* vol. 159, no. 1, pp. 108-121.

Choi, J. & Chang, H. 2012, "The expression of MAGE and SSX, and correlation of COX2, VEGF, and survivin in colorectal cancer", *Anticancer Research,* vol. 32, no. 2, pp. 559-564.

Chung, Y., Or, R.C., Lu, C., Ouyang, W., Yang, S. & Chang, C. 2015, "Sulforaphane down-regulates SKP2 to stabilize p27 KIP1 for inducing antiproliferation in human colon adenocarcinoma cells", *Journal of bioscience and bioengineering,* vol. 119, no. 1, pp. 35-42.

Clevers, H. 2011, "The cancer stem cell: premises, promises and challenges", *Nature medicine,* , pp. 313-319.

Cohen, J. & Sznol, M. 2015, "Therapeutic Combinations of Immune-Modulating Antibodies in Melanoma and Beyond", *Seminars in oncology*Elsevier, , pp. 488.

Contreras-Galindo, R., Kaplan, M.H., Dube, D., Gonzalez-Hernandez, M.J., Chan, S., Meng, F., Dai, M., Omenn, G.S., Gitlin, S.D. & Markovitz, D.M. 2015, "Human Endogenous Retrovirus Type K (HERV-K) Particles Package and Transmit HERV-K-Related Sequences", *Journal of virology,* vol. 89, no. 14, pp. 7187-7201.

Costa, F.F., Le Blanc, K. & Brodin, B. 2007, "Concise review: cancer/testis antigens, stem cells, and cancer", *Stem cells,* vol. 25, no. 3, pp. 707-711.

Courtaut, F., Derangere, V., Chevriaux, A., Ladoire, S., Cotte, A.K., Arnould, L., Boidot, R., Rialland, M., Ghiringhelli, F. & Rebe, C. 2015, "Liver X receptor ligand cytotoxicity in colon cancer cells and not in normal colon epithelial cells depends on LXRbeta subcellular localization", *Oncotarget,* vol. 6, no. 29, pp. 26651-26662.

Coyle, D.E., Li, J. & Baccei, M. 2011, "Regional differentiation of retinoic acid-induced human pluripotent embryonic carcinoma stem cell neurons", *PLoS One,* vol. 6, no. 1, pp. e16174.

Croce, C.M. 2008, "Oncogenes and cancer", *New England Journal of Medicine,* vol. 358, no. 5, pp. 502-511.

Dang-Nguyen, T.Q. & Torres-Padilla, M. 2015, "How cells build totipotency and pluripotency: nuclear, chromatin and transcriptional architecture", *Current opinion in cell biology,* vol. 34, pp. 9-15.

Dankort, D., Filenova, E., Collado, M., Serrano, M., Jones, K. & McMahon, M. 2007, "A new mouse model to explore the initiation, progression, and therapy of BRAFV600E-induced lung tumors", *Genes & development,* vol. 21, no. 4, pp. 379-384.

Dashyan, G.A., Semiglazov, V.F., Donskikh, R.V., Semiglazova, T.Y., Vorotnikov, V.V. & Apollonova, V.S. 2015, "The role of breast cancer stem cells in metastasis", *Voprosy onkologii,* vol. 61, no. 2, pp. 169-173.

Davidson, K.C., Adams, A.M., Goodson, J.M., McDonald, C.E., Potter, J.C., Berndt, J.D., Biechele, T.L., Taylor, R.J. & Moon, R.T. 2012, "Wnt/beta-catenin signaling promotes differentiation, not self-renewal, of human embryonic stem cells and is repressed by Oct4", *Proceedings of the National Academy of Sciences of the United States of America,* vol. 109, no. 12, pp. 4485-4490.

de Araújo Farias, V., O'Valle, F., Lerma, B.A., de Almodóvar, C.R., López-Peñalver, J.J., Nieto, A., Santos, A., Fernández, B.I., Guerra-Librero, A. & Ruiz-Ruiz, M.C. 2015, "Human mesenchymal stem cells enhance the systemic effects of radiotherapy", *Oncotarget,* vol. 6, no. 31, pp. 31164-31180.

De Fazio, S., Bartonicek, N., Di Giacomo, M., Abreu-Goodger, C., Sankar, A., Funaya, C., Antony, C., Moreira, P.N., Enright, A.J. & O'Carroll, D. 2011, "The endonuclease activity of Mili fuels piRNA amplification that silences LINE1 elements", *Nature,* vol. 480, no. 7376, pp. 259-263.

De Los Angeles, A., Ferrari, F., Xi, R., Fujiwara, Y., Benvenisty, N., Deng, H., Hochedlinger, K., Jaenisch, R., Lee, S. & Leitch, H.G. 2015, "Hallmarks of pluripotency", *Nature,* vol. 525, no. 7570, pp. 469-478.

Devine, M.J., Ryten, M., Vodicka, P., Thomson, A.J., Burdon, T., Houlden, H., Cavaleri, F., Nagano, M., Drummond, N.J., Taanman, J.W., Schapira, A.H., Gwinn, K., Hardy, J., Lewis, P.A. & Kunath, T. 2011, "Parkinson's disease induced pluripotent stem cells with triplication of the alpha-synuclein locus", *Nature communications,* vol. 2, pp. 440.

Diekman, B.O., Christoforou, N., Willard, V.P., Sun, H., Sanchez-Adams, J., Leong, K.W. & Guilak, F. 2012, "Cartilage tissue engineering using differentiated and purified induced pluripotent stem cells", *Proceedings of the National Academy of Sciences of the United States of America,* vol. 109, no. 47, pp. 19172-19177.

Ding, V., Lew, Q.J., Chu, K.L., Natarajan, S., Rajasegaran, V., Gurumurthy, M., Choo, A.B. & Chao, S. 2013, "HEXIM1 Induces Differentiation of Human Pluripotent Stem Cells", *PloS one,* vol. 8, no. 8, pp. e72823.

Djamgoz, M.B., Coombes, R.C. & Schwab, A. 2014, "Ion transport and cancer: from initiation to metastasis", *Philosophical transactions of the Royal Society of London.Series B, Biological sciences,* vol. 369, no. 1638, pp. 20130092.

Do, J.T. & Schöler, H.R. 2009, "Regulatory circuits underlying pluripotency and reprogramming", *Trends in pharmacological sciences,* vol. 30, no. 6, pp. 296-302.

Domae, S., Ono, T. & Sasaki, A. 2014, "Cancer/testis antigens: A prospective reagent as diagnostic and immunotherapeutic targets for squamous cell carcinoma of the head and neck", *Japanese Dental Science Review,* vol. 50, no. 4, pp. 91-99.

Domingues, D., Turner, A., Silva, M.D., Marques, D.S., Mellidez, J.C., Wannesson, L., Mountzios, G. & de Mello, R.A. 2014, "Immunotherapy and lung cancer: current developments and novel targeted therapies", *Immunotherapy,* vol. 6, no. 11, pp. 1221-1235.

Donepudi, M.S., Kondapalli, K., Amos, S.J. & Venkanteshan, P. 2014, "Breast cancer statistics and markers", *Journal of cancer research and therapeutics,* vol. 10, no. 3, pp. 506-511.

Dong, L., Yu, D., Wu, N., Wang, H., Niu, J., Wang, Y. & Zou, Z. 2015, "Echinacoside Induces Apoptosis in Human SW480 Colorectal Cancer Cells by Induction of Oxidative DNA Damages", *International journal of molecular sciences,* vol. 16, no. 7, pp. 14655-14668.

Dong, W., Tan, F. & Yang, W. 2015, "Wnt signaling in testis development: Unnecessary or essential?", *Gene,* vol. 565, no. 2, pp. 155-165.

Dotse, E. & Bian, Y. 2014, "Isolation of colorectal cancer stem-like cells", *Cytotechnology,* , pp. 1-11.

Dreesen, O. & Brivanlou, A.H. 2007, "Signaling pathways in cancer and embryonic stem cells", *Stem cell reviews,* vol. 3, no. 1, pp. 7-17.

Du, J., Johnson, L.M., Jacobsen, S.E. & Patel, D.J. 2015a, "DNA methylation pathways and their crosstalk with histone methylation", *Nature Reviews Molecular Cell Biology,* vol. 16, no. 9, pp. 519-532.

Du, W., Cao, Z., Wang, Y., Zhou, F., Pang, W., Chen, X., Tian, Y. & Liang, Y. 2015b, "Specific Biomarkers: Detection of Cancer Biomarkers Through High-Throughput Transcriptomics Data", *Cognitive Computation,* , pp. 1-15.

Duffy, M.J. 2014, "PSA in screening for prostate cancer: more good than harm or more harm than good?", *Adv Clin Chem,* vol. 66, pp. 1-23.

Duffy, M. 2001, "Clinical uses of tumor markers: a critical review", *Critical reviews in clinical laboratory sciences,* vol. 38, no. 3, pp. 225-262.

Duffy, M., Lamerz, R., Haglund, C., Nicolini, A., Kalousová, M., Holubec, L. & Sturgeon, C. 2014, "Tumor markers in colorectal cancer, gastric cancer and gastrointestinal stromal cancers: European group on tumor markers 2014 guidelines update", *International Journal of Cancer,* vol. 134, no. 11, pp. 2513-2522.

Durairajanayagam, D., Rengan, A.K., Sharma, R.K. & Agarwal, A. 2015, "Introduction to the Male Reproductive System", *Unexplained Infertility: Pathophysiology, Evaluation and Treatment,* , pp. 29.

Dyawanapelly, S., Ghodke, S.B., Vishwanathan, R., Dandekar, P. & Jain, R. 2015, "RNA Interference-Based Therapeutics: Molecular Platforms for Infectious Diseases", *Journal of biomedical nanotechnology,* vol. 10, no. 9, pp. 1998-2037.

Ebben, J.D., Treisman, D.M., Zorniak, M., Kutty, R.G., Clark, P.A. & Kuo, J.S. 2010, "The cancer stem cell paradigm: a new understanding of tumor development and treatment", *Expert opinion on therapeutic targets,* vol. 14, no. 6, pp. 621-632.

Eichler, A.F. & Plotkin, S.R. 2008, "Brain metastases", *Current treatment options in neurology,* vol. 10, no. 4, pp. 308-314.

Elizalde, C., Campa, V.M., Caro, M., Schlangen, K., María Aransay, A., dM Vivanco, M. & Kypta, R.M. 2011, "Distinct Roles for Wnt-4 and Wnt-11 During Retinoic Acid-Induced Neuronal Differentiation", *Stem cells,* vol. 29, no. 1, pp. 141-153.

Emens, L.A. & Romero, P. 2015, "Introducing the clinical trials monitor: a new section of the journal for immunotherapy of cancer", *Journal for immunotherapy of cancer,* vol. 3, no. 1, pp. 49.

Ensembl Genome Browser. (2012). *Gene: TDRD12 ENSG00000173809*. [Available from] http://www.ensembl.org/Homo_sapiens/Gene/Splice?g=ENSG00000173809;r=19:33210659-33320483 [Accessed 17 June 12].

Eskenazi, B., Wyrobek, A.J., Sloter, E., Kidd, S.A., Moore, L., Young, S. & Moore, D. 2003, "The association of age and semen quality in healthy men", *Human reproduction (Oxford, England),* vol. 18, no. 2, pp. 447-454.

Esteller, M. 2011, "Non-coding RNAs in human disease", *Nature Reviews Genetics,* vol. 12, no. 12, pp. 861-874.

Evans, M.J. & Kaufman, M.H. 1981, "Establishment in culture of pluripotential cells from mouse embryos", *Nature,* vol. 292, no. 5819, pp. 154-156.

Even-Desrumeaux, K., Baty, D. & Chames, P. 2011, "State of the art in tumor antigen and biomarker discovery", *Cancers,* vol. 3, no. 2, pp. 2554-2596.

Fanali, C., Lucchetti, D., Farina, M., Corbi, M., Cufino, V., Cittadini, A. & Sgambato, A. 2014, "Cancer stem cells in colorectal cancer from pathogenesis to therapy: controversies and perspectives", *World journal of gastroenterology: WJG,* vol. 20, no. 4, pp. 923.

Farazi, T.A., Juranek, S.A. & Tuschl, T. 2008, "The growing catalog of small RNAs and their association with distinct Argonaute/Piwi family members", *Development (Cambridge, England),* vol. 135, no. 7, pp. 1201-1214.

Feichtinger, J., Aldeailej, I., Anderson, R., Almutairi, M., Almatrafi, A., Alsiwiehri, N., Griffiths, K., Stuart, N., Wakeman, J.A., Larcombe, L. & McFarlane, R.J. 2012, "Meta-analysis of clinical data using human meiotic genes identifies a novel cohort of highly restricted cancer-specific marker genes", *Oncotarget,* vol. 3, no. 8, pp. 843-853.

Feichtinger, J., McFarlane, R.J. & Larcombe, L.D. 2014, "CancerEST: a web-based tool for automatic meta-analysis of public EST data", *Database : the journal of biological databases and curation,* vol. 2014, no. 0, pp. bau024.

Feichtinger, J., McFarlane, R.J. & Larcombe, L.D. 2012, "CancerMA: a web-based tool for automatic meta-analysis of public cancer microarray data", *Database : the journal of biological databases and curation,* vol. 2012, pp. bas055.

Fernandez, A., Huggins, I.J., Perna, L., Brafman, D., Lu, D., Yao, S., Gaasterland, T., Carson, D.A. & Willert, K. 2014, "The WNT receptor FZD7 is required for maintenance of the pluripotent state in human embryonic stem cells", *Proceedings of the National Academy of Sciences of the United States of America,* vol. 111, no. 4, pp. 1409-1414.

Fiszer, D. & Kurpisz, M. 1998, "Major histocompatibility complex expression on human, male germ cells: a review", *American journal of reproductive immunology (New York, N.Y.: 1989),* vol. 40, no. 3, pp. 172-176.

Flippot, R., Kone, M., Magné, N. & Vignot, S. 2015, "La signalisation FGF/FGFR: implication dans l'oncogenèse et perspectives thérapeutiques", *Bulletin du cancer, .*

Fox, I.J. & Duncan, S.A. 2013, "Engineering liver tissue from induced pluripotent stem cells: a first step in generating new organs for transplantation?", *Hepatology (Baltimore, Md.),* vol. 58, no. 6, pp. 2198-2201.

Frank, N.Y., Schatton, T. & Frank, M.H. 2010, "The therapeutic promise of the cancer stem cell concept", *The Journal of clinical investigation,* vol. 120, no. 1, pp. 41-50.

Fratta, E., Coral, S., Covre, A., Parisi, G., Colizzi, F., Danielli, R., Marie Nicolay, H.J., Sigalotti, L. & Maio, M. 2011, "The biology of cancer testis antigens: putative function, regulation and therapeutic potential", *Molecular oncology,* vol. 5, no. 2, pp. 164-182.

Freidlin, B. & Korn, E.L. 2014, "Biomarker enrichment strategies: matching trial design to biomarker credentials", *Nature Reviews Clinical Oncology,* vol. 11, no. 2, pp. 81-90.

Fridman, W.H., Remark, R., Goc, J., Giraldo, N.A., Becht, E., Hammond, S.A., Damotte, D., Dieu-Nosjean, M.C. & Sautes-Fridman, C. 2014, "The immune microenvironment: a major player in human cancers", *International archives of allergy and immunology,* vol. 164, no. 1, pp. 13-26.

Friedmann-Morvinski, D. & Verma, I.M. 2014, "Dedifferentiation and reprogramming: origins of cancer stem cells", *EMBO reports,* vol. 15, no. 3, pp. 244-253.

Fujiwara, H. 2014, "Adoptive T-cell therapy for hematological malignancies using T cells gene-modified to express tumor antigen-specific receptors", *International journal of hematology,* vol. 99, no. 2, pp. 123-131.

Füllgrabe, J., Heldring, N., Hermanson, O. & Joseph, B. 2014, "Cracking the survival code: Autophagy-related histone modifications", *Autophagy,* vol. 10, no. 4, pp. 556-561.

Gagliardi, A., Mullin, N.P., Ying Tan, Z., Colby, D., Kousa, A.I., Halbritter, F., Weiss, J.T., Felker, A., Bezstarosti, K. & Favaro, R. 2013, "A direct physical interaction between Nanog and Sox2 regulates embryonic stem cell self-renewal", *The EMBO journal,* vol. 32, no. 16, pp. 2231-2247.

García Martinez, L. & Nogués, C. 2014, "Cancer stem cells", .

Gattei, V., Fonsatti, E., Sigalotti, L., Degan, M., Di Giacomo, A.M., Altomonte, M., Calabro, L. & Maio, M. 2005, "Epigenetic immunomodulation of hematopoietic malignancies", *Seminars in oncology,* vol. 32, no. 5, pp. 503-510.

Gayatri, S. & Bedford, M.T. 2014, "Readers of histone methylarginine marks", *Biochimica et Biophysica Acta (BBA)-Gene Regulatory Mechanisms,* vol. 1839, no. 8, pp. 702-710.

Gerber, J., Heinrich, J. & Brehm, R. 2015, "Blood-testis barrier and Sertoli cell function: Lessons from SCCx43KO mice", *Reproduction (Cambridge, England),* .

Ghildiyal, M. & Zamore, P.D. 2009, "Small silencing RNAs: an expanding universe", *Nature Reviews Genetics,* vol. 10, no. 2, pp. 94-108.

Gjerstorff, M.F., Andersen, M.H. & Ditzel, H.J. 2015, "Oncogenic cancer/testis antigens: prime candidates for immunotherapy", *Oncotarget,* vol. 6, no. 18, pp. 15772-15787.

Goh, S., Olsen, P. & Banerjee, I. 2013, "Correction: Extracellular Matrix Aggregates from Differentiating Embryoid Bodies as a Scaffold to Support ESC Proliferation and Differentiation.", *PloS one,* vol. 8, no. 10, pp. 10.1371.

Gong, S., Li, Q., Jeter, C.R., Fan, Q., Tang, D.G. & Liu, B. 2015, "Regulation of NANOG in cancer cells", *Molecular carcinogenesis,* .

Gonzalez, M.A. & Bernad, A. 2012, "Characteristics of adult stem cells", *Advances in Experimental Medicine and Biology,* vol. 741, pp. 103-120.

Gonzalez-Hernandez, M.J., Cavalcoli, J.D., Sartor, M.A., Contreras-Galindo, R., Meng, F., Dai, M., Dube, D., Saha, A.K., Gitlin, S.D., Omenn, G.S., Kaplan, M.H. & Markovitz, D.M. 2014, "Regulation of the human endogenous retrovirus K (HML-2) transcriptome by the HIV-1 Tat protein", *Journal of virology,* vol. 88, no. 16, pp. 8924-8935.

Goodell, M.A., Nguyen, H. & Shroyer, N. 2015, "Somatic stem cell heterogeneity: diversity in the blood, skin and intestinal stem cell compartments", *Nature Reviews Molecular Cell Biology,* vol. 16, no. 5, pp. 299-309.

Goulet, I., Boisvenue, S., Mokas, S., Mazroui, R. & Cote, J. 2008, "TDRD3, a novel Tudor domain-containing protein, localizes to cytoplasmic stress granules", *Human molecular genetics,* vol. 17, no. 19, pp. 3055-3074.

Greber, B., Coulon, P., Zhang, M., Moritz, S., Frank, S., Müller-Molina, A.J., Araúzo-Bravo, M.J., Han, D.W., Pape, H. & Schöler, H.R. 2011, "FGF signalling inhibits neural induction in human embryonic stem cells", *The EMBO journal,* vol. 30, no. 24, pp. 4874-4884.

Grivna, S.T., Beyret, E., Wang, Z. & Lin, H. 2006, "A novel class of small RNAs in mouse spermatogenic cells", *Genes & development,* vol. 20, no. 13, pp. 1709-1714.

Grivna, S.T., Pyhtila, B. & Lin, H. 2006, "MIWI associates with translational machinery and PIWI-interacting RNAs (piRNAs) in regulating spermatogenesis", *Proceedings of the National Academy of Sciences of the United States of America,* vol. 103, no. 36, pp. 13415-13420.

Grizzi, F., Mirandola, L., Qehajaj, D., Cobos, E., Figueroa, J. & Chiriva-Internati, M. 2015, "Cancer-Testis Antigens and Immunotherapy in the Light of Cancer Complexity", *International reviews of immunology,* vol. 34, no. 2, pp. 143-153.

Guidez, F. 2014, "Retrotransposons: selfish DNA or active epigenetic players in somatic cells?", *Medecine sciences : M/S,* vol. 30, no. 6-7, pp. 659-664.

Guillaudeux, T., Gomez, E., Onno, M., Drenou, B., Segretain, D., Alberti, S., Lejeune, H., Fauchet, R., Jegou, B. & Le Bouteiller, P. 1996, "Expression of HLA class I genes in meiotic and post-meiotic human spermatogenic cells", *Biology of reproduction,* vol. 55, no. 1, pp. 99-110.

Guo, Y., Costa, R., Ramsey, H., Starnes, T., Vance, G., Robertson, K., Kelley, M., Reinbold, R., Scholer, H. & Hromas, R. 2002, "The embryonic stem cell transcription factors Oct-4 and FoxD3 interact to regulate endodermal-specific promoter expression", *Proceedings of the National Academy of Sciences of the United States of America,* vol. 99, no. 6, pp. 3663-3667.

Gupta, S., Termini, J.M., Rivas, Y., Otero, M., Raffa, F.N., Bhat, V., Farooq, A. & Stone, G.W. 2015, "A multi-trimeric fusion of CD40L and gp100 tumor antigen activates dendritic cells and enhances survival in a B16-F10 melanoma DNA vaccine model", *Vaccine,* vol. 33, no. 38, pp. 4798-4806.

Hadziselimovic, F., Hadziselimovic, N.O., Demougin, P., Krey, G. & Oakeley, E. 2015, "Piwi-Pathway Alteration Induces LINE-1 Transposon Derepression and Infertility Development in Cryptorchidism", *Sexual Development,* vol. 9, no. 2, pp. 98-104.

Hanahan, D. & Weinberg, R.A. 2011, "Hallmarks of cancer: the next generation", *Cell,* vol. 144, no. 5, pp. 646-674.

Hanahan, D. & Weinberg, R.A. 2000, "The hallmarks of cancer", *Cell,* vol. 100, no. 1, pp. 57-70.

Harris, T.J. & Drake, C.G. 2013, "Primer on tumor immunology and cancer immunotherapy", *Journal for immunotherapy of cancer,* vol. 1, pp. 12-1426-1-12. eCollection 2013.

Hashim, A., Rizzo, F., Marchese, G., Ravo, M., Tarallo, R., Nassa, G., Giurato, G., Santamaria, G., Cordella, A., Cantarella, C. & Weisz, A. 2014, "RNA sequencing identifies specific PIWI-interacting small non-coding RNA expression patterns in breast cancer", *Oncotarget,* vol. 5, no. 20, pp. 9901-9910.

Hembruff, S.L., Jokar, I., Yang, L. & Cheng, N. 2010, "Loss of transforming growth factor-beta signaling in mammary fibroblasts enhances CCL2 secretion to promote mammary tumor progression through macrophage-dependent and -independent mechanisms", *Neoplasia (New York, N.Y.),* vol. 12, no. 5, pp. 425-433.

Hinrichs, C.S. & Rosenberg, S.A. 2014, "Exploiting the curative potential of adoptive T-cell therapy for cancer", *Immunological reviews,* vol. 257, no. 1, pp. 56-71.

Hirakata, S. & Siomi, M.C. 2015, "piRNA biogenesis in the germline: From transcription of piRNA genomic sources to piRNA maturation", *Biochimica et Biophysica Acta (BBA)-Gene Regulatory Mechanisms,* .

Hirschey, M.D., DeBerardinis, R.J., Diehl, A.M.E., Drew, J.E., Frezza, C., Green, M.F., Jones, L.W., Ko, Y.H., Le, A. & Lea, M.A. 2015, "Dysregulated metabolism contributes to oncogenesis", *Seminars in cancer biology*Elsevier, .

Hochedlinger, K. & Plath, K. 2009, "Epigenetic reprogramming and induced pluripotency", *Development (Cambridge, England),* vol. 136, no. 4, pp. 509-523.

Hofmann, O., Caballero, O.L., Stevenson, B.J., Chen, Y.T., Cohen, T., Chua, R., Maher, C.A., Panji, S., Schaefer, U., Kruger, A., Lehvaslaiho, M., Carninci, P., Hayashizaki, Y., Jongeneel, C.V., Simpson, A.J., Old, L.J. & Hide, W. 2008, "Genome-wide analysis of cancer/testis gene expression", *Proceedings of the National Academy of Sciences of the United States of America,* vol. 105, no. 51, pp. 20422-20427.

Hogarth, C.A. & Griswold, M.D. 2013, "Retinoic acid regulation of male meiosis", *Current opinion in endocrinology, diabetes, and obesity,* vol. 20, no. 3, pp. 217-223.

Holzapfel, B.M., Wagner, F., Thibaudeau, L., Levesque, J. & Hutmacher, D.W. 2015, "Concise Review: Humanized Models of Tumor Immunology in the 21st Century: Convergence of Cancer Research and Tissue Engineering", *Stem cells,* vol. 33, no. 6, pp. 1696-1704.

Honecker, F., Rohlfing, T., Harder, S., Braig, M., Gillis, A.J., Glaesener, S., Barett, C., Bokemeyer, C., Buck, F. & Brümmendorf, T.H. 2014, "Proteome analysis of the effects of all-trans retinoic acid on human germ cell tumor cell lines", *Journal of proteomics,* vol. 96, pp. 300-313.

Hoos, A., Ibrahim, R., Korman, A., Abdallah, K., Berman, D., Shahabi, V., Chin, K., Canetta, R. & Humphrey, R. 2010, "Development of ipilimumab: contribution to a new paradigm for cancer immunotherapy", *Seminars in oncology*Elsevier, , pp. 533.

Hou, M., Lai, Y., He, S., He, W., Shen, H. & Ke, Z. 2015, "SGK3 (CISK) may induce tumor angiogenesis (Hypothesis)", *Oncology Letters,* vol. 10, no. 1, pp. 23-26.

Hu, W., Feng, Z. & Levine, A.J. 2012, "The regulation of multiple p53 stress responses is mediated through MDM2", *Genes & cancer,* vol. 3, no. 3-4, pp. 199-208.

Hu, Z., Brooks, S.A., Dormoy, V., Hsu, C.W., Hsu, H.Y., Lin, L.T., Massfelder, T., Rathmell, W.K., Xia, M., Al-Mulla, F., Al-Temaimi, R., Amedei, A., Brown, D.G., Prudhomme, K.R., Colacci, A., Hamid, R.A., Mondello, C., Raju, J., Ryan, E.P., Woodrick, J., Scovassi, A.I., Singh, N., Vaccari, M., Roy, R., Forte, S., Memeo, L., Salem, H.K., Lowe, L., Jensen, L., Bisson, W.H. & Kleinstreuer, N. 2015, "Assessing the carcinogenic potential of low-dose exposures to chemical mixtures in the environment: focus on the cancer hallmark of tumor angiogenesis", *Carcinogenesis,* vol. 36 Suppl 1, pp. S184-202.

Huang, G., Ye, S., Zhou, X., Liu, D. & Ying, Q. 2015, "Molecular basis of embryonic stem cell self-renewal: from signaling pathways to pluripotency network", *Cellular and Molecular Life Sciences,* vol. 72, no. 9, pp. 1741-1757.

Huang, V. & Li, L. 2014, "Demystifying the nuclear function of Argonaute proteins", *RNA biology,* vol. 11, no. 1, pp. 18-24.

Huang, Y., Bai, J.Y. & Ren, H.T. 2014, "piRNA biogenesis and its functions", *Russian Journal of Bioorganic Chemistry,* vol. 40, no. 3, pp. 293-299.

Hunder, N.N., Wallen, H., Cao, J., Hendricks, D.W., Reilly, J.Z., Rodmyre, R., Jungbluth, A., Gnjatic, S., Thompson, J.A. & Yee, C. 2008, "Treatment of metastatic melanoma with autologous CD4 T cells against NY-ESO-1", *New England Journal of Medicine,* vol. 358, no. 25, pp. 2698-2703.

Hüttemann, M., Jaradat, S. & Grossman, L.I. 2003, "Cytochrome c oxidase of mammals contains a testes-specific isoform of subunit VIb—the counterpart to testes-specific cytochrome c?", *Molecular reproduction and development,* vol. 66, no. 1, pp. 8-16.

Iclozan, C. & Gabrilovich, D.I. 2012, "Recent Advances in Immunotherapy of Lung Cancer", *J Lung Cancer,* vol. 11, no. 1, pp. 1-11.

Iizuka, M. & Smith, M.M. 2003, "Functional consequences of histone modifications", *Current opinion in genetics & development,* vol. 13, no. 2, pp. 154-160.

Ilhan-Mutlu, A., Siehs, C., Berghoff, A.S., Ricken, G., Widhalm, G., Wagner, L. & Preusser, M. 2015, "Expression profiling of angiogenesis-related genes in brain metastases of lung cancer and melanoma", *Tumor Biology,* , pp. 1-10.

Irie, N., Weinberger, L., Tang, W.W., Kobayashi, T., Viukov, S., Manor, Y.S., Dietmann, S., Hanna, J.H. & Surani, M.A. 2014, "SOX17 is a critical specifier of human primordial germ cell fate", *Cell,* .

Ishizu, H., Siomi, H. & Siomi, M.C. 2012, "Biology of PIWI-interacting RNAs: new insights into biogenesis and function inside and outside of germlines", *Genes & development,* vol. 26, no. 21, pp. 2361-2373.

Islam, F., Gopalan, V., Smith, R.A. & Lam, A.K. 2015, "Translational potential of cancer stem cells: A review of the detection of cancer stem cells and their roles in cancer recurrence and cancer treatment", *Experimental cell research,* .

Itou, D., Shiromoto, Y., Shin-ya, Y., Ishii, C., Nishimura, T., Ogonuki, N., Ogura, A., Hasuwa, H., Fujihara, Y. & Kuramochi-Miyagawa, S. 2015, "Induction of DNA methylation by artificial piRNA production in male germ cells", *Current Biology,* vol. 25, no. 7, pp. 901-906.

Iwasaki, Y.W., Siomi, M.C. & Siomi, H. 2015, "PIWI-Interacting RNA: Its Biogenesis and Functions", *Annual Review of Biochemistry,* , no. 0.

Jamal-Hanjani, M., Quezada, S.A., Larkin, J. & Swanton, C. 2015, "Translational Implications of Tumor Heterogeneity", *Clinical Cancer Research,* vol. 21, no. 6, pp. 1258-1266.

James, L.I., Barsyte-Lovejoy, D., Zhong, N., Krichevsky, L., Korboukh, V.K., Herold, J.M., MacNevin, C.J., Norris, J.L., Sagum, C.A. & Tempel, W. 2013, "Discovery of a chemical probe for the L3MBTL3 methyllysine reader domain", *Nature chemical biology,* vol. 9, no. 3, pp. 184-191.

James, D., Levine, A.J., Besser, D. & Hemmati-Brivanlou, A. 2005, "TGFbeta/activin/nodal signaling is necessary for the maintenance of pluripotency in human embryonic stem cells", *Development (Cambridge, England),* vol. 132, no. 6, pp. 1273-1282.

Janic, A., Mendizabal, L., Llamazares, S., Rossell, D. & Gonzalez, C. 2010, "Ectopic expression of germline genes drives malignant brain tumor growth in Drosophila", *Science (New York, N.Y.),* vol. 330, no. 6012, pp. 1824-1827.

Jayashree, B., Nigam, S., Pai, A., Patel, H.K., Reddy, N., Kumar, N. & Rao, C. 2015, "Targets in anticancer research--A review.", *Indian journal of experimental biology,* vol. 53, pp. 489-507.

Jeter, C.R., Yang, T., Wang, J., Chao, H. & Tang, D.G. 2015, "Concise Review: NANOG in Cancer Stem Cells and Tumor Development: An Update and Outstanding Questions", *Stem cells,* .

Jones, M.F., Hara, T., Francis, P., Li, X.L., Bilke, S., Zhu, Y., Pineda, M., Subramanian, M., Bodmer, W.F. & Lal, A. 2015, "The CDX1-microRNA-215 axis regulates colorectal cancer stem cell differentiation", *Proceedings of the National Academy of Sciences of the United States of America,* vol. 112, no. 13, pp. E1550-8.

Jones, R.G. & Thompson, C.B. 2009, "Tumor suppressors and cell metabolism: a recipe for cancer growth", *Genes & development,* vol. 23, no. 5, pp. 537-548.

Jordan, C.T. 2004, "Cancer stem cell biology: from leukemia to solid tumors", *Current opinion in cell biology,* vol. 16, no. 6, pp. 708-712.

Joseph, N.M., Mosher, J.T., Buchstaller, J., Snider, P., McKeever, P.E., Lim, M., Conway, S.J., Parada, L.F., Zhu, Y. & Morrison, S.J. 2008, "The loss of Nf1 transiently promotes self-renewal but not tumorigenesis by neural crest stem cells", *Cancer cell,* vol. 13, no. 2, pp. 129-140.

Jr, H.A.A. & Partridge, A.H. 2014, "Biology of breast cancer in young women", .

Jung, M., Peterson, H., Chavez, L., Kahlem, P., Lehrach, H., Vilo, J. & Adjaye, J. 2010, "A data integration approach to mapping OCT4 gene regulatory networks operative in embryonic stem cells and embryonal carcinoma cells", *PLoS One,* vol. 5, no. 5, pp. e10709.

Jungbluth, A.A., Stockert, E., Chen, Y.T., Kolb, D., Iversen, K., Coplan, K., Williamson, B., Altorki, N., Busam, K.J. & Old, L.J. 2000, "Monoclonal antibody MA454 reveals a heterogeneous expression pattern of MAGE-1 antigen in formalin-fixed paraffin embedded lung tumours", *British journal of cancer,* vol. 83, no. 4, pp. 493-497.

Kaer, K. & Speek, M. 2013, "Retroelements in human disease", *Gene,* vol. 518, no. 2, pp. 231-241.

Kalejs, M. & Erenpreisa, J. 2005, "Cancer/testis antigens and gametogenesis: a review and "brain-storming" session", *Cancer cell international,* vol. 5, no. 1, pp. 4.

Kanda, M., Sugimoto, H. & Kodera, Y. 2015, "Genetic and epigenetic aspects of initiation and progression of hepatocellular", .

Kanwar, S.S., Yu, Y., Nautiyal, J., Patel, B.B. & Majumdar, A.P. 2010, "The Wnt/beta-catenin pathway regulates growth and maintenance of colonospheres", *Molecular cancer,* vol. 9, pp. 212-4598-9-212.

Kar, S., Parbin, S., Deb, M., Shilpi, A., Sengupta, D., Rath, S.K., Rakshit, M., Patra, A. & Patra, S.K. 2014, "Epigenetic choreography of stem cells: the DNA demethylation episode of development", *Cellular and Molecular Life Sciences,* vol. 71, no. 6, pp. 1017-1032.

Karpf, A.R. 2006, "A potential role for epigenetic modulatory drugs in the enhancement of cancer/germ-line antigen vaccine efficacy", *Epigenetics : official journal of the DNA Methylation Society,* vol. 1, no. 3, pp. 116-120.

Karpf, A.R. & Jones, D.A. 2002, "Reactivating the expression of methylation silenced genes in human cancer", *Oncogene,* vol. 21, no. 35, pp. 5496-5503.

Kaur, G., Thompson, L.A. & Dufour, J.M. 2014, "Sertoli cells–Immunological sentinels of spermatogenesis", *Seminars in cell & developmental biology*Elsevier, , pp. 36.

Kaur, S., Momi, N., Chakraborty, S., Wagner, D.G., Horn, A.J., Lele, S.M., Theodorescu, D. & Batra, S.K. 2014, "Altered expression of transmembrane mucins, MUC1 and MUC4, in bladder cancer: pathological implications in diagnosis", *PloS one,* vol. 9, no. 3, pp. e92742.

Ke, X., Zhang, D., Zhu, S., Xia, Q., Xiang, Z. & Cui, H. 2014, "Inhibition of H3K9 methyltransferase G9a repressed cell proliferation and induced autophagy in neuroblastoma cells", .

Kesanakurti, D., Maddirela, D.R., Chittivelu, S., Rao, J.S. & Chetty, C. 2013, "Suppression of tumor cell invasiveness and in vivo tumor growth by microRNA-874 in non-small cell lung cancer", *Biochemical and biophysical research communications,* vol. 434, no. 3, pp. 627-633.

Kim, S. 2015, "New and emerging factors in tumorigenesis: an overview", *Cancer management and research,* vol. 7, pp. 225.

Kim, T., Fuchs, J.R., Schwartz, E., Abdelhamid, D., Etter, J., Berry, W.L., Li, C., Ihnat, M.A., Li, P. & Janknecht, R. 2014, "Pro-growth role of the JMJD2C histone demethylase in HCT-116 colon cancer cells and identification of curcuminoids as JMJD2 inhibitors", *American journal of translational research,* vol. 6, no. 3, pp. 236.

Kim, V.N., Han, J. & Siomi, M.C. 2009, "Biogenesis of small RNAs in animals", *Nature reviews Molecular cell biology,* vol. 10, no. 2, pp. 126-139.

Kim, H.S. 2012, "Genomic impact, chromosomal distribution and transcriptional regulation of HERV elements", *Molecules and cells,* vol. 33, no. 6, pp. 539-544.

Klose, R.J. & Bird, A.P. 2006, "Genomic DNA methylation: the mark and its mediators", *Trends in biochemical sciences,* vol. 31, no. 2, pp. 89-97.

Knisbacher, B.A. & Levanon, E.Y. 2015, "DNA editing of LTR retrotransposons reveals the impact of APOBECs on vertebrate genomes", *Molecular biology and evolution,* , pp. msv239.

Koslowski, M., Tureci, O., Bell, C., Krause, P., Lehr, H.A., Brunner, J., Seitz, G., Nestle, F.O., Huber, C. & Sahin, U. 2002, "Multiple splice variants of lactate dehydrogenase C selectively expressed in human cancer", *Cancer research,* vol. 62, no. 22, pp. 6750-6755.

Kowalczykiewic, D. & Wrzesinski, J. 2011, "The role of piRNA and Piwi proteins in regulation of germline development", *Postepy biochemii,* vol. 57, no. 3, pp. 249-256.

Kozłowska, A., Mackiewicz, J. & Mackiewicz, A. 2013, "Therapeutic gene modified cell based cancer vaccines", *Gene,* vol. 525, no. 2, pp. 200-207.

Kreamer, K.M. 2014, "Immune Checkpoint Blockade: A New Paradigm in Treating Advanced Cancer", *Journal of the advanced practitioner in oncology,* vol. 5, no. 6, pp. 418.

Krishnadas, D.K., Bai, F. & Lucas, K.G. 2013, "Cancer testis antigen and immunotherapy", *ImmunoTargets and Therapy,* vol. 2, pp. 11-19.

Ku, H. & Lin, H. 2014, "PIWI proteins and their interactors in piRNA biogenesis, germline development and gene expression", *National science review,* vol. 1, no. 2, pp. 205-218.

Kuo, Y., Wu, H., Hung, J., Chou, T., Teng, S. & Wu, K. 2015, "Nijmegen breakage syndrome protein 1 (NBS1) modulates hypoxia inducible factor-1α (HIF-1α) stability and promotes in vitro migration and invasion under ionizing radiation", *The international journal of biochemistry & cell biology,* vol. 64, pp. 229-238.

Kuramochi-Miyagawa, S., Kimura, T., Ijiri, T.W., Isobe, T., Asada, N., Fujita, Y., Ikawa, M., Iwai, N., Okabe, M., Deng, W., Lin, H., Matsuda, Y. & Nakano, T. 2004, "Mili, a mammalian member of piwi family gene, is essential for spermatogenesis", *Development (Cambridge, England),* vol. 131, no. 4, pp. 839-849.

Kuramochi-Miyagawa, S., Watanabe, T., Gotoh, K., Totoki, Y., Toyoda, A., Ikawa, M., Asada, N., Kojima, K., Yamaguchi, Y., Ijiri, T.W., Hata, K., Li, E., Matsuda, Y., Kimura, T., Okabe, M., Sakaki, Y., Sasaki, H. & Nakano, T. 2008, "DNA methylation of retrotransposon genes is regulated by Piwi family members MILI and MIWI2 in murine fetal testes", *Genes & development,* vol. 22, no. 7, pp. 908-917.

Kuruma, H., Kamata, Y., Takahashi, H., Igarashi, K., Kimura, T., Miki, K., Miki, J., Sasaki, H., Hayashi, N. & Egawa, S. 2009, "Staphylococcal nuclease domain-containing protein 1 as a potential tissue marker for prostate cancer", *The American journal of pathology,* vol. 174, no. 6, pp. 2044-2050.

Lam, I. & Keeney, S. 2014, "Mechanism and regulation of meiotic recombination initiation", *Cold Spring Harbor perspectives in biology,* vol. 7, no. 1, pp. a016634.

Langer, C.J. 2014, "Emerging Immunotherapies in the Treatment of Non–Small Cell Lung Cancer (NSCLC)", *pathways,* vol. 15, pp. 19.

Langie, S.A., Koppen, G., Desaulniers, D., Al-Mulla, F., Al-Temaimi, R., Amedei, A., Azqueta, A., Bisson, W.H., Brown, D.G., Brunborg, G., Charles, A.K., Chen, T., Colacci, A., Darroudi, F., Forte, S., Gonzalez, L., Hamid, R.A., Knudsen, L.E., Leyns, L., Lopez de Cerain Salsamendi, A., Memeo, L., Mondello, C., Mothersill, C., Olsen, A.K., Pavanello, S., Raju, J., Rojas, E., Roy, R.,

Ryan, E.P., Ostrosky-Wegman, P., Salem, H.K., Scovassi, A.I., Singh, N., Vaccari, M., Van Schooten, F.J., Valverde, M., Woodrick, J., Zhang, L., van Larebeke, N., Kirsch-Volders, M. & Collins, A.R. 2015, "Causes of genome instability: the effect of low dose chemical exposures in modern society", *Carcinogenesis,* vol. 36 Suppl 1, pp. S61-88.

Larkin, J., Chiarion-Sileni, V., Gonzalez, R., Grob, J.J., Cowey, C.L., Lao, C.D., Schadendorf, D., Dummer, R., Smylie, M. & Rutkowski, P. 2015, "Combined nivolumab and ipilimumab or monotherapy in untreated melanoma", *New England Journal of Medicine,* vol. 373, no. 1, pp. 23-34.

Lech, G., Slotwinski, R. & Krasnodebski, I.W. 2014, "The role of tumor markers and biomarkers in colorectal cancer", *Neoplasma,* vol. 61, no. 1, pp. 1-8.

Leyssens, C., Marien, E., Verlinden, L., Derua, R., Waelkens, E., Swinnen, J.V. & Verstuyf, A. 2015, "Remodeling of phospholipid composition in colon cancer cells by 1α, 25 (OH) 2 D 3 and its analogs", *The Journal of steroid biochemistry and molecular biology,* vol. 148, pp. 172-178.

Li, X.Z., Roy, C.K., Dong, X., Bolcun-Filas, E., Wang, J., Han, B.W., Xu, J., Moore, M.J., Schimenti, J.C. & Weng, Z. 2013, "An ancient transcription factor initiates the burst of piRNA production during early meiosis in mouse testes", *Molecular cell,* vol. 50, no. 1, pp. 67-81.

Li, X. & Wang, X. 2015, "The role of human cervical cancer oncogene in cancer progression", *International journal of clinical and experimental medicine,* vol. 8, no. 6, pp. 8363.

Lie, P.P., Cheng, C.Y. & Mruk, D.D. 2013, "Signalling pathways regulating the blood–testis barrier", *The international journal of biochemistry & cell biology,* vol. 45, no. 3, pp. 621-625.

Lim, S.L., Ricciardelli, C., Oehler, M.K., Tan, Izza MD De Arao, Russell, D. & Grützner, F. 2014, "Overexpression of piRNA pathway genes in epithelial ovarian cancer", .

Lim, S.H., Zhang, Y. & Zhang, J. 2012, "Cancer-testis antigens: the current status on antigen regulation and potential clinical use", *American journal of blood research,* vol. 2, no. 1, pp. 29-35.

Lin, J., Chen, Q., Yang, J., Qian, J., Deng, Z., Qian, W., Chen, X., Ma, J., Xiong, D. & Ma, Y. 2014, "DDX43 promoter is frequently hypomethylated and may predict a favorable outcome in acute myeloid leukemia", *Leukemia research,* vol. 38, no. 5, pp. 601-607.

Lin, L., Liu, Y., Li, H., Li, P., Fuchs, J., Shibata, H., Iwabuchi, Y. & Lin, J. 2011, "Targeting colon cancer stem cells using a new curcumin analogue, GO-Y030", *British journal of cancer,* vol. 105, no. 2, pp. 212-220.

Lin, Y., Yang, Y., Li, W., Chen, Q., Li, J., Pan, X., Zhou, L., Liu, C., Chen, C. & He, J. 2012, "Reciprocal regulation of Akt and Oct4 promotes the self-renewal and survival of embryonal carcinoma cells", *Molecular cell,* vol. 48, no. 4, pp. 627-640.

Lindblom, A. & Liljegren, A. 2000, "Regular review: tumour markers in malignancies", *BMJ (Clinical research ed.),* vol. 320, no. 7232, pp. 424-427.

Link, P.A., Gangisetty, O., James, S.R., Woloszynska-Read, A., Tachibana, M., Shinkai, Y. & Karpf, A.R. 2009, "Distinct roles for histone methyltransferases G9a and GLP in cancer germ-line antigen gene regulation in human cancer cells and murine embryonic stem cells", *Molecular cancer research : MCR,* vol. 7, no. 6, pp. 851-862.

Liu, L., Lu, L., Zhong, H., He, B., Kwong, D.W., Ma, D. & Leung, C. 2015, "An iridium (III) complex inhibits JMJD2 activities and acts as a potential epigenetic modulator", *Journal of medicinal chemistry,* vol. 58, no. 16, pp. 6697-6703.

Loriot, A., Boon, T. & De Smet, C. 2003, "Five new human cancer-germline genes identified among 12 genes expressed in spermatogonia", *International journal of cancer.Journal international du cancer,* vol. 105, no. 3, pp. 371-376.

Lu, R. & Wang, G.G. 2013, "Tudor: a versatile family of histone methylation 'readers'", *Trends in biochemical sciences,* vol. 38, no. 11, pp. 546-555.

Lu, Y., Zhang, K., Li, C., Yao, Y., Tao, D., Liu, Y., Zhang, S. & Ma, Y. 2012, "Piwil2 suppresses p53 by inducing phosphorylation of signal transducer and activator of transcription 3 in tumor cells", *PLoS One,* vol. 7, no. 1, pp. e30999.

Lui, W.Y. & Cheng, C.Y. 2012, "Transcriptional regulation of cell adhesion at the blood-testis barrier and spermatogenesis in the testis", *Advances in Experimental Medicine and Biology,* vol. 763, pp. 281-294.

Luo, L.Y. & Hahn, W.C. 2015, "Oncogenic Signaling Adaptor Proteins", *Journal of Genetics and Genomics, .*

Luo, B., Yun, X., Fan, R., Lin, Y.D., He, S.J., Zhang, Q.M., Mo, F.R., Chen, F., Xiao, S.W. & Xie, X.X. 2013, "Cancer testis antigen OY-TES-1 expression and serum immunogenicity in colorectal cancer: its relationship to clinicopathological parameters", *International journal of clinical and experimental pathology,* vol. 6, no. 12, pp. 2835-2845.

Ma, Z. & Vosseller, K. 2014, "Cancer metabolism and elevated O-GlcNAc in oncogenic signaling", *The Journal of biological chemistry,* vol. 289, no. 50, pp. 34457-34465.

Mäbert, K., Cojoc, M., Peitzsch, C., Kurth, I., Souchelnytskyi, S. & Dubrovska, A. 2014, "Cancer biomarker discovery: current status and future perspectives", *International journal of radiation biology,* vol. 90, no. 8, pp. 659-677.

Macheret, M. & Halazonetis, T.D. 2015, "DNA replication stress as a hallmark of cancer", *Annual review of pathology,* vol. 10, pp. 425-448.

Mae, S. & Osafune, K. 2015, "Kidney regeneration from human induced pluripotent stem cells", *Current opinion in organ transplantation,* vol. 20, no. 2, pp. 171-177.

Magee, J.A., Piskounova, E. & Morrison, S.J. 2012, "Cancer stem cells: impact, heterogeneity, and uncertainty", *Cancer cell,* vol. 21, no. 3, pp. 283-296.

Malfavon-Borja, R. & Feschotte, C. 2015, "Fighting fire with fire: endogenous retrovirus envelopes as restriction factors", *Journal of virology,* vol. 89, no. 8, pp. 4047-4050.

Malone, C.D. & Hannon, G.J. 2009, "Small RNAs as guardians of the genome", *Cell,* vol. 136, no. 4, pp. 656-668.

Maluszek, M. 2015, "Multifunctionality of MDM2 protein and its role in genomic instability of cancer cells", *Postepy biochemii,* vol. 61, no. 1, pp. 42-51.

Marcar, L., Ihrig, B., Hourihan, J., Bray, S.E., Quinlan, P.R., Jordan, L.B., Thompson, A.M., Hupp, T.R. & Meek, D.W. 2015, "MAGE-A Cancer/Testis Antigens Inhibit MDM2 Ubiquitylation Function and Promote Increased Levels of MDM4", .

Marchand, M., Punt, C.J., Aamdal, S., Escudier, B., Kruit, W.H., Keilholz, U., Hakansson, L., van Baren, N., Humblet, Y., Mulders, P., Avril, M.F., Eggermont, A.M., Scheibenbogen, C., Uiters, J., Wanders, J., Delire, M., Boon, T. & Stoter, G. 2003, "Immunisation of metastatic cancer patients with MAGE-3 protein combined with adjuvant SBAS-2: a clinical report", *European journal of cancer (Oxford, England : 1990),* vol. 39, no. 1, pp. 70-77.

Marchand, M., van Baren, N., Weynants, P., Brichard, V., Dreno, B., Tessier, M.H., Rankin, E., Parmiani, G., Arienti, F., Humblet, Y., Bourlond, A., Vanwijck, R., Lienard, D., Beauduin, M., Dietrich, P.Y., Russo, V., Kerger, J., Masucci, G., Jager, E., De Greve, J., Atzpodien, J., Brasseur, F., Coulie, P.G., van der Bruggen, P. & Boon, T. 1999, "Tumor regressions observed in patients with metastatic melanoma treated with an antigenic peptide encoded by gene MAGE-3 and presented by HLA-A1", *International journal of cancer.Journal international du cancer,* vol. 80, no. 2, pp. 219-230.

Martello, G. & Smith, A. 2014, "The nature of embryonic stem cells", *Annual Review of Cell and Developmental Biology,* vol. 30, pp. 647-675.

Martin, G.R. 1981, "Isolation of a pluripotent cell line from early mouse embryos cultured in medium conditioned by teratocarcinoma stem cells", *Proceedings of the National Academy of Sciences of the United States of America,* vol. 78, no. 12, pp. 7634-7638.

Mateo, J., Carreira, S., Sandhu, S., Miranda, S., Mossop, H., Perez-Lopez, R., Nava Rodrigues, D., Robinson, D., Omlin, A. & Tunariu, N. 2015, "DNA-Repair Defects and Olaparib in Metastatic Prostate Cancer", *New England Journal of Medicine,* vol. 373, no. 18, pp. 1697-1708.

Mathews, L.A., Cabarcas, S.M. & Hurt, E.M. 2013, *DNA repair of cancer stem cells,* Springer.

Matin, M.M., Walsh, J.R., Gokhale, P.J., Draper, J.S., Bahrami, A.R., Morton, I., Moore, H.D. & Andrews, P.W. 2004, "Specific Knockdown of Oct4 and β2-microglobulin Expression by RNA Interference in Human Embryonic Stem Cells and Embryonic Carcinoma Cells", *Stem cells,* vol. 22, no. 5, pp. 659-668.

Matsa, E., Burridge, P.W. & Wu, J.C. 2014, "Human stem cells for modeling heart disease and for drug discovery", *Science translational medicine,* vol. 6, no. 239, pp. 239ps6.

McFarlane, R.J., Feichtinger, J. & Larcombe, L. 2015, "Germline/meiotic genes in cancer: new dimensions", *Cell Cycle,* vol. 14, no. 6, pp. 791-792.

McFarlane, R.J., Feichtinger, J. & Larcombe, L. 2014, "Cancer germline gene activation: Friend or foe?", *Cell Cycle,* vol. 13, no. 14, pp. 2151-2152.

Meacham, C.E. & Morrison, S.J. 2013, "Tumour heterogeneity and cancer cell plasticity", *Nature,* vol. 501, no. 7467, pp. 328-337.

Meccariello, R., Chianese, R., Ciaramella, V., Fasano, S. & Pierantoni, R. 2014, "Molecular Chaperones, Cochaperones, and Ubiquitination/Deubiquitination System: Involvement in the Production of High Quality Spermatozoa", *BioMed research international,* vol. 2014.

Meek, D.W. 2015, "Regulation of the p53 response and its relationship to cancer", *The Biochemical journal,* vol. 469, no. 3, pp. 325-346.

Mellman, I., Coukos, G. & Dranoff, G. 2011, "Cancer immunotherapy comes of age", *Nature,* vol. 480, no. 7378, pp. 480-489.

Menasche, P., Vanneaux, V., Hagege, A., Bel, A., Cholley, B., Cacciapuoti, I., Parouchev, A., Benhamouda, N., Tachdjian, G., Tosca, L., Trouvin, J.H., Fabreguettes, J.R., Bellamy, V., Guillemain, R., Suberbielle Boissel, C., Tartour, E., Desnos, M. & Larghero, J. 2015, "Human embryonic stem cell-derived cardiac progenitors for severe heart failure treatment: first clinical case report", *European heart journal,* vol. 36, no. 30, pp. 2011-2017.

Michor, F., Iwasa, Y., Vogelstein, B., Lengauer, C. & Nowak, M.A. 2005, "Can chromosomal instability initiate tumorigenesis?", *Seminars in cancer biology*Elsevier, , pp. 43.

Min, J., Liu, L., Li, X., Jiang, J., Wang, J., Zhang, B., Cao, D., Yu, D., Tao, D. & Hu, J. 2015, "Absence of DAB2IP promotes cancer stem cell like signatures and indicates poor survival outcome in colorectal cancer", *Scientific Reports,* vol. 5, pp. 16578.

Mirkovic, J., Howitt, B.E., Roncarati, P., Demoulin, S., Suarez-Carmona, M., Hubert, P., McKeon, F.D., Xian, W., Li, A. & Delvenne, P. 2015, "Carcinogenic HPV infection in the cervical squamo-columnar junction", *The Journal of pathology,* .

Mital, P., Hinton, B.T. & Dufour, J.M. 2011, "The blood-testis and blood-epididymis barriers are more than just their tight junctions", *Biology of reproduction,* vol. 84, no. 5, pp. 851-858.

Mitsui, K., Tokuzawa, Y., Itoh, H., Segawa, K., Murakami, M., Takahashi, K., Maruyama, M., Maeda, M. & Yamanaka, S. 2003, "The homeoprotein Nanog is required for maintenance of pluripotency in mouse epiblast and ES cells", *Cell,* vol. 113, no. 5, pp. 631-642.

Modarressi, M.H., Fard SGModarressi, M. & Fard, S. 2011, "Potential of cancer-testis antigens as targets for cancer immunotherapy", *Bridging cell biology and genetics to the cancer clinic2011.Kerala, India83–98.Back to cited text,* , no. 19.

Molinari, C., Matteucci, F., Caroli, P. & Passardi, A. 2015, "Biomarkers and Molecular Imaging as Predictors of Response to Neoadjuvant Chemoradiotherapy in Patients With Locally Advanced Rectal Cancer", *Clinical colorectal cancer,* .

Morris, L.G. & Chan, T.A. 2015, "Therapeutic targeting of tumor suppressor genes", *Cancer,* vol. 121, no. 9, pp. 1357-1368.

Muller, P.A., Vousden, K.H. & Norman, J.C. 2011, "P53 and its Mutants in Tumor Cell Migration and Invasion", *The Journal of cell biology,* vol. 192, no. 2, pp. 209-218.

Muñoz Descalzo, S., RuÉ, P., Garcia-Ojalvo, J. & Arias, A.M. 2012, "Correlations between the levels of oct4 and nanog as a signature for naive pluripotency in mouse embryonic stem cells", *Stem cells,* vol. 30, no. 12, pp. 2683-2691.

Musselman, C.A., Lalonde, M., Côté, J. & Kutateladze, T.G. 2012, "Perceiving the epigenetic landscape through histone readers", *Nature structural & molecular biology,* vol. 19, no. 12, pp. 1218-1227.

Nagle, J.W. 1992, "Sequence identification of 2,375 human brain genes", *Nature,* vol. 355.

Negrini, S., Gorgoulis, V.G. & Halazonetis, T.D. 2010, "Genomic instability--an evolving hallmark of cancer", *Nature reviews.Molecular cell biology,* vol. 11, no. 3, pp. 220-228.

Nirschl, C.J. & Drake, C.G. 2013, "Molecular pathways: coexpression of immune checkpoint molecules: signaling pathways and implications for cancer immunotherapy", *Clinical cancer research : an official journal of the American Association for Cancer Research,* vol. 19, no. 18, pp. 4917-4924.

Niwa, H., Miyazaki, J. & Smith, A.G. 2000, "Quantitative expression of Oct-3/4 defines differentiation, dedifferentiation or self-renewal of ES cells", *Nature genetics,* vol. 24, no. 4, pp. 372-376.

Noggle, S.A., James, D. & Brivanlou, A.H. 2005, "A molecular basis for human embryonic stem cell pluripotency", *Stem cell reviews,* vol. 1, no. 2, pp. 111-118.

Okamoto, K., Okazawa, H., Okuda, A., Sakai, M., Muramatsu, M. & Hamada, H. 1990, "A novel octamer binding transcription factor is differentially expressed in mouse embryonic cells", *Cell,* vol. 60, no. 3, pp. 461-472.

Omenn, G.S., Guan, Y. & Menon, R. 2014, "A new class of protein cancer biomarker candidates: differentially expressed splice variants of ERBB2 (HER2/neu) and ERBB1 (EGFR) in breast cancer cell lines", *Journal of proteomics,* vol. 107, pp. 103-112.

Osaki, M., Okada, F. & Ochiya, T. 2015, "miRNA therapy targeting cancer stem cells: a new paradigm for cancer treatment and prevention of tumor recurrence", .

Öz, S., Maercker, C. & Breiling, A. 2013, "Embryonic carcinoma cells show specific dielectric resistance profiles during induced differentiation", *PloS one,* vol. 8, no. 3, pp. e59895.

Pal, R. & Ravindran, G. 2006, "Assessment of pluripotency and multilineage differentiation potential of NTERA-2 cells as a model for studying human embryonic stem cells", *Cell proliferation,* vol. 39, no. 6, pp. 585-598.

Palucka, K., Banchereau, J. & Mellman, I. 2010, "Designing vaccines based on biology of human dendritic cell subsets", *Immunity,* vol. 33, no. 4, pp. 464-478.

Pan, G.J., Chang, Z.Y., Schöler, H.R. & Duanqing, P. 2002, "Stem cell pluripotency and transcription factor Oct4", *Cell research,* vol. 12, no. 5, pp. 321-329.

Pan, G., Li, J., Zhou, Y., Zheng, H. & Pei, D. 2006, "A negative feedback loop of transcription factors that controls stem cell pluripotency and self-renewal", *FASEB journal : official publication of the Federation of American Societies for Experimental Biology,* vol. 20, no. 10, pp. 1730-1732.

Pan, J., Goodheart, M., Chuma, S., Nakatsuji, N., Page, D.C. & Wang, P.J. 2005, "RNF17, a component of the mammalian germ cell nuage, is essential for spermiogenesis", *Development (Cambridge, England),* vol. 132, no. 18, pp. 4029-4039.

Pandey, R.R., Tokuzawa, Y., Yang, Z., Hayashi, E., Ichisaka, T., Kajita, S., Asano, Y., Kunieda, T., Sachidanandam, R., Chuma, S., Yamanaka, S. & Pillai, R.S. 2013, "Tudor domain containing 12 (TDRD12) is essential for secondary PIWI interacting RNA biogenesis in mice", *Proceedings of the National Academy of Sciences of the United States of America,* vol. 110, no. 41, pp. 16492-16497.

Panjarian, S.B., Slater, C., Madzo, J., Jelinek, J., Chen, X. & Issa, J. 2015, "Age-dependent DNA methylation in normal breast epithelium and breast cancer", *Cancer research,* vol. 75, no. 15 Supplement, pp. 1071-1071.

Paoletti, C. & Hayes, D.F. 2014, "Molecular testing in breast cancer", *Annual Review of Medicine,* vol. 65, pp. 95-110.

Pardoll, D. 2003, "Does the immune system see tumors as foreign or self?", *Annual Review of Immunology,* vol. 21, no. 1, pp. 807-839.

Pardoll, D.M. 2012, "The blockade of immune checkpoints in cancer immunotherapy", *Nature Reviews Cancer,* vol. 12, no. 4, pp. 252-264.

Parker, J.S. & Barford, D. 2006, "Argonaute: a scaffold for the function of short regulatory RNAs", *Trends in biochemical sciences,* vol. 31, no. 11, pp. 622-630.

Patanè, S. 2014, "ERBB1/EGFR and ERBB2 (HER2/neu)—targeted therapies in cancer and cardiovascular system with cardiovascular drugs", *International journal of cardiology,* vol. 3, no. 176, pp. 1301-1303.

Pek, J.W., Anand, A. & Kai, T. 2012, "Tudor domain proteins in development", *Development (Cambridge, England),* vol. 139, no. 13, pp. 2255-2266.

Pesce, M. & Schöler, H.R. 2001, "Oct-4: gatekeeper in the beginnings of mammalian development", *Stem cells,* vol. 19, no. 4, pp. 271-278.

Plaks, V., Kong, N. & Werb, Z. 2015, "The cancer stem cell niche: how essential is the niche in regulating stemness of tumor cells?", *Cell stem cell,* vol. 16, no. 3, pp. 225-238.

Popat, K., McQueen, K. & Feeley, T.W. 2013, "The global burden of cancer", *Best Practice & Research Clinical Anaesthesiology,* vol. 27, no. 4, pp. 399-408.

Postow, M.A., Callahan, M.K. & Wolchok, J.D. 2015, "Immune Checkpoint Blockade in Cancer Therapy", *Journal of clinical oncology : official journal of the American Society of Clinical Oncology,* vol. 33, no. 17, pp. 1974-1982.

Puglisi, M.A., Tesori, V., Lattanzi, W., Gasbarrini, G.B. & Gasbarrini, A. 2013, "Colon cancer stem cells: controversies and perspectives", *World journal of gastroenterology: WJG,* vol. 19, no. 20, pp. 2997.

Qiao, D., Zeeman, A.M., Deng, W., Looijenga, L.H. & Lin, H. 2002, "Molecular characterization of hiwi, a human member of the piwi gene family whose overexpression is correlated to seminomas", *Oncogene,* vol. 21, no. 25, pp. 3988-3999.

Qiu, H., Fang, X., Luo, Q. & Ouyang, G. 2015, "Cancer stem cells: a potential target for cancer therapy", *Cellular and Molecular Life Sciences,* , pp. 1-14.

Raica, M., Cimpean, A.M. & Ribatti, D. 2009, "Angiogenesis in pre-malignant conditions", *European journal of cancer (Oxford, England : 1990),* vol. 45, no. 11, pp. 1924-1934.

Rajan, K.S. & Ramasamy, S. 2014, "Retrotransposons and piRNA: The missing link in central nervous system", *Neurochemistry international,* vol. 77, pp. 94-102.

Rajendran, P.S. & Dalerba, P. 2014, "Theoretical and Experimental Foundations of the “Cancer Stem Cell” Model", *Cancer Stem Cells,* , pp. 1-16.

Ramachandran, S., Ient, J., Göttgens, E., Krieg, A.J. & Hammond, E.M. 2015, "Epigenetic Therapy for Solid Tumors: Highlighting the Impact of Tumor Hypoxia", *Genes,* vol. 6, no. 4, pp. 935-956.

Ranzani, M., Annunziato, S., Adams, D.J. & Montini, E. 2013, "Cancer gene discovery: exploiting insertional mutagenesis", *Molecular cancer research : MCR,* vol. 11, no. 10, pp. 1141-1158.

Ren, X., Zhang, Y., Li, C., Wang, H., Jiang, Z., Zhang, Z., Guo, Q., Song, G., Bi, K. & Jiang, G. 2013, "Enhancement of baicalin by hexamethylene bisacetamide on the induction of apoptosis contributes to simultaneous activation of the intrinsic and extrinsic apoptotic pathways in human leukemia cells", *Oncology reports,* vol. 30, no. 5, pp. 2071-2080.

Restifo, N.P., Dudley, M.E. & Rosenberg, S.A. 2012, "Adoptive immunotherapy for cancer: harnessing the T cell response", *Nature Reviews Immunology,* vol. 12, no. 4, pp. 269-281.

Reuter, M., Chuma, S., Tanaka, T., Franz, T., Stark, A. & Pillai, R.S. 2009, "Loss of the Mili-interacting Tudor domain–containing protein-1 activates transposons and alters the Mili-associated small RNA profile", *Nature structural & molecular biology,* vol. 16, no. 6, pp. 639-646.

Reya, T., Morrison, S.J., Clarke, M.F. & Weissman, I.L. 2001, "Stem cells, cancer, and cancer stem cells", *Nature,* vol. 414, no. 6859, pp. 105-111.

Reyes, M., Rojas-Alcayaga, G., Pennacchiotti, G., Carrillo, D., Muñoz, J.P., Peña, N., Montes, R., Lobos, N. & Aguayo, F. 2015, "Human papillomavirus infection in oral squamous cell carcinomas from Chilean patients", *Experimental and molecular pathology,* vol. 99, no. 1, pp. 95-99.

Rhinn, M. & Dolle, P. 2012, "Retinoic acid signalling during development", *Development (Cambridge, England),* vol. 139, no. 5, pp. 843-858.

Rivera, E. & Gomez, H. 2010, "Chemotherapy resistance in metastatic breast cancer: the evolving role of ixabepilone", *Breast cancer research : BCR,* vol. 12 Suppl 2, pp. S2.

Rizzo, F., Hashim, A., Marchese, G., Ravo, M., Tarallo, R., Nassa, G., Giurato, G., Rinaldi, A., Cordella, A. & Persico, M. 2014, "Timed regulation of P-element-induced wimpy testis–interacting RNA expression during rat liver regeneration", *Hepatology,* vol. 60, no. 3, pp. 798-806.

Roberts, C., Green, T., Hess, E., Matys, K., Brown, M.J., Haupt, R.M., Luxembourg, A., Vuocolo, S., Saah, A. & Antonello, J. 2014, "Development of a human papillomavirus competitive luminex immunoassay for 9 HPV types", *Human vaccines & immunotherapeutics,* vol. 10, no. 8, pp. 2174-2103.

Romito, A. & Cobellis, G. 2015, "Pluripotent Stem Cells: Current Understanding and Future Directions", *Stem Cells International,* vol. 2015.

Rosenberg, S.A. & Restifo, N.P. 2015, "Adoptive cell transfer as personalized immunotherapy for human cancer", *Science (New York, N.Y.),* vol. 348, no. 6230, pp. 62-68.

Rosner, M.H., Vigano, M.A., Ozato, K., Timmons, P.M., Poirie, F., Rigby, P.W. & Staudt, L.M. 1990, "A POU-domain transcription factor in early stem cells and germ cells of the mammalian embryo", *Nature,* vol. 345, no. 6277, pp. 686-692.

Ross, R.J., Weiner, M.M. & Lin, H. 2014, "PIWI proteins and PIWI-interacting RNAs in the soma", *Nature,* vol. 505, no. 7483, pp. 353-359.

Rousseaux, S., Debernardi, A., Jacquiau, B., Vitte, A.L., Vesin, A., Nagy-Mignotte, H., Moro-Sibilot, D., Brichon, P.Y., Lantuejoul, S., Hainaut, P., Laffaire, J., de Reynies, A., Beer, D.G., Timsit, J.F., Brambilla, C., Brambilla, E. & Khochbin, S. 2013, "Ectopic activation of germline and placental genes identifies aggressive metastasis-prone lung cancers", *Science translational medicine,* vol. 5, no. 186, pp. 186ra66.

Roy, S., K Narang, B., K Rastogi, S. & K Rawal, R. 2015, "A Novel Multiple Tyrosine-kinase Targeted Agent to Explore the Future Perspectives of Anti-Angiogenic Therapy for the Treatment of Multiple Solid Tumors: Cabozantinib", *Anti-Cancer Agents in Medicinal Chemistry (Formerly Current Medicinal Chemistry-Anti-Cancer Agents),* vol. 15, no. 1, pp. 37-47.

Rozen, S. and Skaletsky, H.J. (2000) Primer3 on the WWW for general users and for biologist programmers. In: Krawetz, S. and Misener, S., eds. Bioinformatics Methods and Protocols: Methods in Molecular Biology. Totowa, NJ: Humana Press, pp. 365-386.

Sadri-Ardekani, H. & Atala, A. 2014, "Testicular tissue cryopreservation and spermatogonial stem cell transplantation to restore fertility: from bench to bedside", *Stem cell research & therapy,* vol. 5, no. 3, pp. 1-10.

Saito, K. 2014, "RNAi and Overexpression of Genes in Ovarian Somatic Cells" in *PIWI-Interacting RNAs* Springer, , pp. 25-33.

Saito, Y., Nakaoka, T. & Saito, H. 2015, "microRNA-34a as a Therapeutic Agent against Human Cancer", *Journal of clinical medicine,* vol. 4, no. 11, pp. 1951-1959.

Sakaki-Yumoto, M., Liu, J., Ramalho-Santos, M., Yoshida, N. & Derynck, R. 2013, "Smad2 is essential for maintenance of the human and mouse primed pluripotent stem cell state", *The Journal of biological chemistry,* vol. 288, no. 25, pp. 18546-18560.

Saleem, M., Abbas, K., Manan, M., Ijaz, H., Ahmed, B., Ali, M., Hanif, M., Farooqi, A.A. & Qadir, M.I. 2015, "Review-Epigenetic therapy for cancer", *Pakistan journal of pharmaceutical sciences,* vol. 28, no. 3, pp. 1023-1032.

Sammut, S.J., Feichtinger, J., Stuart, N., Wakeman, J.A., Larcombe, L. & McFarlane, R.J. 2014, "A novel cohort of cancer-testis biomarker genes revealed through meta-analysis of clinical data sets", *Oncoscience,* vol. 1, no. 5, pp. 349.

Santos-Rosa, H. & Caldas, C. 2005, "Chromatin modifier enzymes, the histone code and cancer", *European journal of cancer (Oxford, England : 1990),* vol. 41, no. 16, pp. 2381-2402.

Sasaki, T., Shiohama, A., Minoshima, S. & Shimizu, N. 2003, "Identification of eight members of the Argonaute family in the human genome☆", *Genomics,* vol. 82, no. 3, pp. 323-330.

Sathyanarayanan, V. & Neelapu, S.S. 2015, "Cancer immunotherapy: Strategies for personalization and combinatorial approaches", *Molecular Oncology,* .

Sato, K. & Siomi, M.C. 2013, "Piwi-interacting RNAs: biological functions and biogenesis", *Essays in biochemistry,* vol. 54, no. 1, pp. 39-52.

Sato, N., Meijer, L., Skaltsounis, L., Greengard, P. & Brivanlou, A.H. 2004, "Maintenance of pluripotency in human and mouse embryonic stem cells through activation of Wnt signaling by a pharmacological GSK-3-specific inhibitor", *Nature medicine,* vol. 10, no. 1, pp. 55-63.

Saxe, J.P., Chen, M., Zhao, H. & Lin, H. 2013, "Tdrkh is essential for spermatogenesis and participates in primary piRNA biogenesis in the germline", *The EMBO journal,* vol. 32, no. 13, pp. 1869-1885.

Scanlan, M.J., Gure, A.O., Jungbluth, A.A., Old, L.J. & Chen, Y.T. 2002a, "Cancer/testis antigens: an expanding family of targets for cancer immunotherapy", *Immunological reviews,* vol. 188, pp. 22-32.

Scanlan, M.J., Simpson, A.J. & Old, L.J. 2004, "The cancer/testis genes: review, standardization, and commentary", *Cancer immunity,* vol. 4, pp. 1.

Scanlan, M.J., Welt, S., Gordon, C.M., Chen, Y.T., Gure, A.O., Stockert, E., Jungbluth, A.A., Ritter, G., Jager, D., Jager, E., Knuth, A. & Old, L.J. 2002b, "Cancer-related serological recognition of human colon cancer: identification of potential diagnostic and immunotherapeutic targets", *Cancer research,* vol. 62, no. 14, pp. 4041-4047.

Scholer, H.R., Hatzopoulos, A.K., Balling, R., Suzuki, N. & Gruss, P. 1989, "A family of octamer-specific proteins present during mouse embryogenesis: evidence for germline-specific expression of an Oct factor", *The EMBO journal,* vol. 8, no. 9, pp. 2543-2550.

Schröder, F.H., Hugosson, J., Roobol, M.J., Tammela, T.L., Ciatto, S., Nelen, V., Kwiatkowski, M., Lujan, M., Lilja, H. & Zappa, M. 2009, "Screening and prostate-cancer mortality in a randomized European study", *New England Journal of Medicine,* vol. 360, no. 13, pp. 1320-1328.

Schwartz, C.M., Spivak, C.E., Baker, S.C., McDaniel, T.K., Loring, J.F., Nguyen, C., Chrest, F.J., Wersto, R., Arenas, E. & Zeng, X. 2005, "NTera2: a model system to study dopaminergic differentiation of human embryonic stem cells", *Stem cells and development,* vol. 14, no. 5, pp. 517-534.

Seoane, J. & Mattos-Arruda, D. 2014, "The challenge of intratumour heterogeneity in precision medicine", *Journal of internal medicine,* vol. 276, no. 1, pp. 41-51.

Serra, M., Brito, C., Costa, E.M., Sousa, M.F. & Alves, P.M. 2009, "Integrating human stem cell expansion and neuronal differentiation in bioreactors", *BMC biotechnology,* vol. 9, pp. 82-6750-9-82.

Seymour, T., Twigger, A. & Kakulas, F. 2015, "Pluripotency Genes and Their Functions in the Normal and Aberrant Breast and Brain", *International Journal of Molecular Sciences,* vol. 16, no. 11, pp. 27288-27301.

Shah, P.A. & Goldberg, J. 2015, "Novel Approaches to Pediatric Cancer: Immunotherapy", .

Shi, Y. & Whetstine, J.R. 2007, "Dynamic regulation of histone lysine methylation by demethylases", *Molecular cell,* vol. 25, no. 1, pp. 1-14.

Shoji, M., Tanaka, T., Hosokawa, M., Reuter, M., Stark, A., Kato, Y., Kondoh, G., Okawa, K., Chujo, T. & Suzuki, T. 2009, "The TDRD9-MIWI2 complex is essential for piRNA-mediated retrotransposon silencing in the mouse male germline", *Developmental cell,* vol. 17, no. 6, pp. 775-787.

Siegel, R., Naishadham, D. & Jemal, A. 2012, "Cancer statistics, 2012", *CA: a cancer journal for clinicians,* vol. 62, no. 1, pp. 10-29.

Sigalotti, L., Covre, A., Zabierowski, S., Himes, B., Colizzi, F., Natali, P.G., Herlyn, M. & Maio, M. 2008, "Cancer testis antigens in human melanoma stem cells: expression, distribution, and methylation status", *Journal of cellular physiology,* vol. 215, no. 2, pp. 287-291.

Sigalotti, L., Fratta, E., Coral, S., Cortini, E., Covre, A., Nicolay, H.J., Anzalone, L., Pezzani, L., Di Giacomo, A.M., Fonsatti, E., Colizzi, F., Altomonte, M., Calabro, L. & Maio, M. 2007, "Epigenetic drugs as pleiotropic agents in cancer treatment: biomolecular aspects and clinical applications", *Journal of cellular physiology,* vol. 212, no. 2, pp. 330-344.

Simara, P., Motl, J.A. & Kaufman, D.S. 2013, "Pluripotent stem cells and gene therapy", *Translational research,* vol. 161, no. 4, pp. 284-292.

Simerman, A.A., Dumesic, D.A. & Chazenbalk, G.D. 2014, "Pluripotent muse cells derived from human adipose tissue: a new perspective on regenerative medicine and cell therapy", *Clinical and translational medicine,* vol. 3, pp. 12-1326-3-12. eCollection 2014.

Simoes, P.D. & Ramos, T. 2007, "Human pluripotent embryonal carcinoma NTERA2 cl.D1 cells maintain their typical morphology in an angiomyogenic medium", *Journal of negative results in biomedicine,* vol. 6, pp. 5.

Simpson, A.J., Caballero, O.L., Jungbluth, A., Chen, Y.T. & Old, L.J. 2005, "Cancer/testis antigens, gametogenesis and cancer", *Nature reviews.Cancer,* vol. 5, no. 8, pp. 615-625.

Singh, A.P., Chauhan, S.C., Bafna, S., Johansson, S.L., Smith, L.M., Moniaux, N., Lin, M. & Batra, S.K. 2006, "Aberrant expression of transmembrane mucins, MUC1 and MUC4, in human prostate carcinomas", *The Prostate,* vol. 66, no. 4, pp. 421-429.

Siomi, M.C., Mannen, T. & Siomi, H. 2010, "How does the royal family of Tudor rule the PIWI-interacting RNA pathway?", *Genes & development,* vol. 24, no. 7, pp. 636-646.

Sivasubramaniyan, K., Harichandan, A., Schilbach, K., Mack, A.F., Bedke, J., Stenzl, A., Kanz, L., Niederfellner, G. & Buhring, H.J. 2015, "Expression of stage-specific embryonic antigen-4 (SSEA-4) defines spontaneous loss of epithelial phenotype in human solid tumor cells", *Glycobiology,* vol. 25, no. 8, pp. 902-917.

Soltysova, A., Altanerova, V. & Altaner, C. 2005, "Cancer stem cells", *Neoplasma,* vol. 52, no. 6, pp. 435-440.

Sowa, Y. & Sakai, T. 2015, "Development of novel epigenetic molecular-targeting agents", *Nihon rinsho.Japanese journal of clinical medicine,* vol. 73, no. 8, pp. 1263-1267.

Srivastava, P., Paluch, B.E., Matsuzaki, J., James, S.R., Collamat-Lai, G., Karbach, J., Nemeth, M.J., Taverna, P., Karpf, A.R. & Griffiths, E.A. 2014, "Immunomodulatory action of SGI-110, a hypomethylating agent, in acute myeloid leukemia cells and xenografts", *Leukemia research,* vol. 38, no. 11, pp. 1332-1341.

Stratton, M.R., Campbell, P.J. & Futreal, P.A. 2009, "The cancer genome", *Nature,* vol. 458, no. 7239, pp. 719-724.

Sukach, A. & Ivanov, E. 2007, "Formation of spherical colonies as a property of stem cells", *Cell and Tissue Biology,* vol. 1, no. 6, pp. 476-481.

Suntsova, M., Garazha, A., Ivanova, A., Kaminsky, D., Zhavoronkov, A. & Buzdin, A. 2015, "Molecular functions of human endogenous retroviruses in health and disease", *Cellular and Molecular Life Sciences,* vol. 72, no. 19, pp. 3653-3675.

Suri, A. 2006, "Cancer testis antigens--their importance in immunotherapy and in the early detection of cancer", *Expert opinion on biological therapy,* vol. 6, no. 4, pp. 379-389.

Suzuki, R., Honda, S. & Kirino, Y. 2012, "PIWI Expression and Function in Cancer", *Frontiers in genetics,* vol. 3, pp. 204.

Swarts, D.C., Makarova, K., Wang, Y., Nakanishi, K., Ketting, R.F., Koonin, E.V., Patel, D.J. & van der Oost, J. 2014, "The evolutionary journey of Argonaute proteins", *Nature structural & molecular biology,* vol. 21, no. 9, pp. 743-753.

Tachibana, M., Sugimoto, K., Nozaki, M., Ueda, J., Ohta, T., Ohki, M., Fukuda, M., Takeda, N., Niida, H., Kato, H. & Shinkai, Y. 2002, "G9a histone methyltransferase plays a dominant role in euchromatic histone H3 lysine 9 methylation and is essential for early embryogenesis", *Genes & development,* vol. 16, no. 14, pp. 1779-1791.

Tachibana, M., Ueda, J., Fukuda, M., Takeda, N., Ohta, T., Iwanari, H., Sakihama, T., Kodama, T., Hamakubo, T. & Shinkai, Y. 2005, "Histone methyltransferases G9a and GLP form heteromeric complexes and are both crucial for methylation of euchromatin at H3-K9", *Genes & development,* vol. 19, no. 7, pp. 815-826.

Tagliamonte, M., Petrizzo, A., Tornesello, M.L., Buonaguro, F.M. & Buonaguro, L. 2014, "Antigen-specific vaccines for cancer treatment", *Human vaccines & immunotherapeutics,* vol. 10, no. 11, pp. 3332-3346.

Taguchi, A., Taylor, A.D., Rodriguez, J., Celiktas, M., Liu, H., Ma, X., Zhang, Q., Wong, C., Chin, A. & Girard, L. 2014, "Abstract B24: A systematic search for cancer/testis antigens in lung cancer identifies VCX/Y genes expanding the repertoire of potential immunotherapeutic targets.", *Clinical Cancer Research,* vol. 20, no. 2 Supplement, pp. B24-B24.

Takahashi, K. & Yamanaka, S. 2013, "Induced pluripotent stem cells in medicine and biology", *Development (Cambridge, England),* vol. 140, no. 12, pp. 2457-2461.

Tanaka, T., Hosokawa, M., Vagin, V.V., Reuter, M., Hayashi, E., Mochizuki, A.L., Kitamura, K., Yamanaka, H., Kondoh, G., Okawa, K., Kuramochi-Miyagawa, S., Nakano, T., Sachidanandam, R., Hannon, G.J., Pillai, R.S., Nakatsuji, N. & Chuma, S. 2011, "Tudor domain containing 7 (Tdrd7) is essential for dynamic ribonucleoprotein (RNP) remodeling of chromatoid bodies during spermatogenesis", *Proceedings of the National Academy of Sciences of the United States of America,* vol. 108, no. 26, pp. 10579-10584.

Taverna, S.D., Li, H., Ruthenburg, A.J., Allis, C.D. & Patel, D.J. 2007, "How chromatin-binding modules interpret histone modifications: lessons from professional pocket pickers", *Nature structural & molecular biology,* vol. 14, no. 11, pp. 1025-1040.

Terrasso, A.P., Pinto, C., Serra, M., Filipe, A., Almeida, S., Ferreira, A.L., Pedroso, P., Brito, C. & Alves, P.M. 2015, "Novel scalable 3D cell based model for in vitro neurotoxicity testing: Combining human differentiated neurospheres with gene expression and functional endpoints", *Journal of Biotechnology,* vol. 205, pp. 82-92.

Tertipis, N., Hammar, U., Näsman, A., Vlastos, A., Nordfors, C., Grün, N., Ährlund-Richter, A., Sivars, L., Haeggblom, L. & Marklund, L. 2015, "A model for predicting clinical outcome in patients with human papillomavirus-positive tonsillar and base of tongue cancer", *European journal of cancer, .*

Thoma, C.R., Toso, A., Meraldi, P. & Krek, W. 2011, "Mechanisms of aneuploidy and its suppression by tumour suppressor proteins", *Swiss medical weekly,* vol. 141, pp. w13170.

Thomas, C.M. & Sweep, C.G. 2001, "Serum tumor markers: past, state of the art, and future", *The International journal of biological markers,* vol. 16, no. 2, pp. 73-86.

Thomson, J.A., Itskovitz-Eldor, J., Shapiro, S.S., Waknitz, M.A., Swiergiel, J.J., Marshall, V.S. & Jones, J.M. 1998, "Embryonic stem cell lines derived from human blastocysts", *Science (New York, N.Y.),* vol. 282, no. 5391, pp. 1145-1147.

Thomson, T. & Lin, H. 2009, "The biogenesis and function of PIWI proteins and piRNAs: progress and prospect", *Annual Review of Cell and Developmental Biology,* vol. 25, pp. 355-376.

The National Institutes of Health resource for stem cell research, 2015, *Are Stem Cells Involved in Cancer?* [Online]. Available at:

http://stemcells.nih.gov/info/Regenerative_Medicine/pages/2006chapter9.aspx. Accessed 8 February 2015.

The University of Leicester, Virtual Genetics Education Centre. 2015. *The Cell Cycle, Mitosis and Meiosis*. [Online]. Available at: http://www2.le.ac.uk/departments/genetics/vgec/schoolscolleges/topics/cellcycle-mitosis-meiosis. Accessed 8 September 2015.

Tomasetti, C. & Vogelstein, B. 2015, "Variation in cancer risk among tissues can be explained by the number of stem cell divisions", *Science,* vol. 347, no. 6217, pp. 78-81.

Tomasetti, C., Vogelstein, B. & Parmigiani, G. 2013, "Half or more of the somatic mutations in cancers of self-renewing tissues originate prior to tumor initiation", *Proceedings of the National Academy of Sciences of the United States of America,* vol. 110, no. 6, pp. 1999-2004.

Tonge, P.D. & Andrews, P.W. 2010, "Retinoic acid directs neuronal differentiation of human pluripotent stem cell lines in a non-cell-autonomous manner", *Differentiation,* vol. 80, no. 1, pp. 20-30.

Topalian, S.L., Drake, C.G. & Pardoll, D.M. 2015, "Immune Checkpoint Blockade: A Common Denominator Approach to Cancer Therapy", *Cancer cell,* vol. 27, no. 4, pp. 450-461.

Tselis, A. & Booss, J. 2014, "Human endogenous retroviruses and the nervous system", *Neurovirology: Handbook of Clinical Neurology Series (Series Editors: Aminoff, Boller, Swaab),* vol. 123, pp. 465.

Tsuchiya, N., Ochiai, M., Nakashima, K., Ubagai, T., Sugimura, T. & Nakagama, H. 2007, "SND1, a component of RNA-induced silencing complex, is up-regulated in human colon cancers and implicated in early stage colon carcinogenesis", *Cancer research,* vol. 67, no. 19, pp. 9568-9576.

Turner, J.M. 2007, "Meiotic sex chromosome inactivation", *Development (Cambridge, England),* vol. 134, no. 10, pp. 1823-1831.

Valadez-Vega, C., Alvarez-Manilla, G., Riverón-Negrete, L., García-Carrancá, A., Morales-González, J.A., Zuñiga-Pérez, C., Madrigal-Santillán, E., Esquivel-Soto, J., Esquivel-Chirino, C. & Villagómez-Ibarra, R. 2011, "Detection of cytotoxic activity of lectin on human colon adenocarcinoma (Sw480) and epithelial cervical carcinoma (C33-A)", *Molecules,* vol. 16, no. 3, pp. 2107-2118.

Vallier, L., Alexander, M. & Pedersen, R.A. 2005, "Activin/Nodal and FGF pathways cooperate to maintain pluripotency of human embryonic stem cells", *Journal of cell science,* vol. 118, no. Pt 19, pp. 4495-4509.

Van Cutsem, E., Köhne, C., Hitre, E., Zaluski, J., Chang Chien, C., Makhson, A., D'Haens, G., Pintér, T., Lim, R. & Bodoky, G. 2009, "Cetuximab and chemotherapy as initial treatment for metastatic colorectal cancer", *New England Journal of Medicine,* vol. 360, no. 14, pp. 1408-1417.

Vasileva, A., Tiedau, D., Firooznia, A., Müller-Reichert, T. & Jessberger, R. 2009, "Tdrd6 is required for spermiogenesis, chromatoid body architecture, and regulation of miRNA expression", *Current Biology,* vol. 19, no. 8, pp. 630-639.

Videtic Paska, A. & Hudler, P. 2015, "Aberrant methylation patterns in cancer: a clinical view", *Biochemia medica,* vol. 25, no. 2, pp. 161-176.

Vincent, A. & Van Seuningen, I. 2012, "On the epigenetic origin of cancer stem cells", *Biochimica et Biophysica Acta (BBA)-Reviews on Cancer,* vol. 1826, no. 1, pp. 83-88.

Vishnoi, K., Tyagi, A., Singh, S.M., Das, B.C. & Bharti, A.C. 2015, "Cervical Cancer Stem Cells and Their Association with Human Papillomavirus: Are They Ready as Anticancer Targets?" in *Multi-Targeted Approach to Treatment of Cancer* Springer, , pp. 377-399.

Visvader, J.E. 2011, "Cells of origin in cancer", *Nature,* vol. 469, no. 7330, pp. 314-322.

Vockley, J.G. & Niederhuber, J.E. 2015, "Diagnosis and treatment of cancer using genomics", *BMJ,* vol. 350, pp. h1832.

Vogelstein, B. & Kinzler, K.W. 2004, "Cancer genes and the pathways they control", *Nature medicine,* vol. 10, no. 8, pp. 789-799.

Vogt, P.K. 2012, "Retroviral oncogenes: a historical primer", *Nature Reviews Cancer,* vol. 12, no. 9, pp. 639-648.

Wagers, A.J. 2012, "The stem cell niche in regenerative medicine", *Cell Stem Cell,* vol. 10, no. 4, pp. 362-369.

Walenkamp, A., Crespo, G., Maya, F.F., Fossmark, R., Igaz, P., Rinke, A., Tamagno, G., Vitale, G., Öberg, K. & Meyer, T. 2014, "Hallmarks of gastrointestinal neuroendocrine tumours: implications for treatment", *Endocrine-related cancer,* vol. 21, no. 6, pp. R445-R460.

Wang, G.G., Allis, C.D. & Chi, P. 2007, "Chromatin remodeling and cancer, Part I: Covalent histone modifications", *Trends in molecular medicine,* vol. 13, no. 9, pp. 363-372.

Wang, G.G., Song, J., Wang, Z., Dormann, H.L., Casadio, F., Li, H., Luo, J., Patel, D.J. & Allis, C.D. 2009a, "Haematopoietic malignancies caused by dysregulation of a chromatin-binding PHD finger", *Nature,* vol. 459, no. 7248, pp. 847-851.

Wang, J., Saxe, J.P., Tanaka, T., Chuma, S. & Lin, H. 2009b, "Mili interacts with tudor domain-containing protein 1 in regulating spermatogenesis", *Current Biology,* vol. 19, no. 8, pp. 640-644.

Wang, J. & Mu, X. 2015, "The clinical significances of the abnormal expressions of Piwil1 and Piwil2 in colonic adenoma and adenocarcinoma", *OncoTargets and Therapy,* vol. 8, pp. 1259-1264.

Wang, L.Q. & Chim, C.S. 2015, "DNA methylation of tumor-suppressor miRNA genes in chronic lymphocytic leukemia", *Epigenomics,* , no. 0, pp. 1-13.

Wang, T., Wang, G., Hao, D., Liu, X., Wang, D., Ning, N. & Li, X. 2015a, "Aberrant regulation of the LIN28A/LIN28B and let-7 loop in human malignant tumors and its effects on the hallmarks of cancer", *Molecular cancer,* vol. 14, no. 1, pp. 1.

Wang, X., Xu, J., Wang, H., Wu, L., Yuan, W., Du, J. & Cai, S. 2015b, "Trichostatin A, a histone deacetylase inhibitor, reverses epithelial–mesenchymal transition in colorectal cancer SW480 and prostate cancer PC3 cells", *Biochemical and biophysical research communications,* vol. 456, no. 1, pp. 320-326.

Watkins, J., Weekes, D., Shah, V., Gazinska, P., Joshi, S., Sidhu, B., Gillett, C., Pinder, S., Vanoli, F., Jasin, M., Mayrhofer, M., Isaksson, A., Cheang, M.C., Mirza, H., Frankum, J., Lord, C.J., Ashworth, A., Vinayak, S., Ford, J.M., Telli, M.L., Grigoriadis, A. & Tutt, A.N. 2015, "Genomic Complexity Profiling Reveals That HORMAD1 Overexpression Contributes to Homologous Recombination Deficiency in Triple-Negative Breast Cancers", *Cancer discovery,* vol. 5, no. 5, pp. 488-505.

Watt, F.M. 1998, "Epidermal stem cells: markers, patterning and the control of stem cell fate", *Philosophical transactions of the Royal Society of London.Series B, Biological sciences,* vol. 353, no. 1370, pp. 831-837.

Weiner, G.J. 2015, "Building better monoclonal antibody-based therapeutics", *Nature Reviews Cancer,* vol. 15, no. 6, pp. 361-370.

Weiner, L.M., Surana, R. & Wang, S. 2010, "Monoclonal antibodies: versatile platforms for cancer immunotherapy", *Nature Reviews Immunology,* vol. 10, no. 5, pp. 317-327.

Weissman, I.L. 2015, "Stem cells are units of natural selection for tissue formation, for germline development, and in cancer development", *Proceedings of the National Academy of Sciences of the United States of America,* vol. 112, no. 29, pp. 8922-8928.

Whitehurst, A.W. 2014, "Cause and consequence of cancer/testis antigen activation in cancer", *Annual Review of Pharmacology and Toxicology,* vol. 54, pp. 251-272.

Wischnewski, F., Pantel, K. & Schwarzenbach, H. 2006, "Promoter demethylation and histone acetylation mediate gene expression of MAGE-A1, -A2, -A3, and -A12 in human cancer cells", *Molecular cancer research : MCR,* vol. 4, no. 5, pp. 339-349.

Wodarz, D. & Zauber, A.G. 2015, "Cancer: Risk factors and random chances", *Nature,* vol. 517, no. 7536, pp. 563-564.

Wong, V.W., Sorkin, M. & Gurtner, G.C. 2013, "Enabling stem cell therapies for tissue repair: current and future challenges", *Biotechnology Advances,* vol. 31, no. 5, pp. 744-751.

Wu, G. & Schöler, H.R. 2014, "Role of Oct4 in the early embryo development", *Cell Regeneration,* vol. 3, no. 1, pp. 7.

Wu, S.M. & Hochedlinger, K. 2011, "Harnessing the potential of induced pluripotent stem cells for regenerative medicine", *Nature cell biology,* vol. 13, no. 5, pp. 497-505.

Xiang, D.F., Zhu, J.Q., Hou, C.C. & Yang, W.X. 2014, "Identification and expression pattern analysis of Piwi genes during the spermiogenesis of Portunus trituberculatus", *Gene,* vol. 534, no. 2, pp. 240-248.

Xu, R., Chen, X., Li, D.S., Li, R., Addicks, G.C., Glennon, C., Zwaka, T.P. & Thomson, J.A. 2002, "BMP4 initiates human embryonic stem cell differentiation to trophoblast", *Nature biotechnology,* vol. 20, no. 12, pp. 1261-1264.

Xu, R.H., Sampsell-Barron, T.L., Gu, F., Root, S., Peck, R.M., Pan, G., Yu, J., Antosiewicz-Bourget, J., Tian, S., Stewart, R. & Thomson, J.A. 2008, "NANOG is a direct target of TGFbeta/activin-mediated SMAD signaling in human ESCs", *Cell stem cell,* vol. 3, no. 2, pp. 196-206.

Yabuta, Y., Ohta, H., Abe, T., Kurimoto, K., Chuma, S. & Saitou, M. 2011, "TDRD5 is required for retrotransposon silencing, chromatoid body assembly, and spermiogenesis in mice", *The Journal of cell biology,* vol. 192, no. 5, pp. 781-795.

Yadav, R.P. & Kotaja, N. 2014, "Small RNAs in spermatogenesis", *Molecular and cellular endocrinology,* vol. 382, no. 1, pp. 498-508.

Yakirevich, E., Sabo, E., Lavie, O., Mazareb, S., Spagnoli, G.C. & Resnick, M.B. 2003, "Expression of the MAGE-A4 and NY-ESO-1 cancer-testis antigens in serous ovarian neoplasms", *Clinical cancer research : an official journal of the American Association for Cancer Research,* vol. 9, no. 17, pp. 6453-6460.

Yalak, G. & Vogel, V. 2015, "Ectokinases as novel cancer markers and drug targets in cancer therapy", *Cancer medicine,* vol. 4, no. 3, pp. 404-414.

Yan, H.H., Mruk, D.D., Lee, W.M. & Cheng, C.Y. 2008, "Blood-testis barrier dynamics are regulated by testosterone and cytokines via their differential effects on the kinetics of protein endocytosis and recycling in Sertoli cells", *FASEB journal : official publication of the Federation of American Societies for Experimental Biology,* vol. 22, no. 6, pp. 1945-1959.

Yang, P., Huo, Z., Liao, H. & Zhou, Q. 2015, "Cancer/testis antigens trigger epithelial-mesenchymal transition and genesis of cancer stem-like cells", *Current pharmaceutical design,* vol. 21, no. 10, pp. 1292-1300.

Yang, S., Lin, G., Deng, L. & Lu, G. 2012, "Tumourigenic characteristics of embryonal carcinoma cells as a model for studying tumour progression of human embryonic stem cells", *Cell proliferation,* vol. 45, no. 4, pp. 299-310.

Ye, F., Zhou, C., Cheng, Q., Shen, J. & Chen, H. 2008, "Stem-cell-abundant proteins Nanog, Nucleostemin and Musashi1 are highly expressed in malignant cervical epithelial cells", *BMC cancer,* vol. 8, pp. 108.

Ying, M. & Chen, D. 2012, "Tudor domain-containing proteins of Drosophila melanogaster", *Development, growth & differentiation,* vol. 54, no. 1, pp. 32-43.

Yoon, H., Lee, H., Kim, H.J., You, K.T., Park, Y.N., Kim, H. & Kim, H. 2011, "Tudor domain-containing protein 4 as a potential cancer/testis antigen in liver cancer", *The Tohoku journal of experimental medicine,* vol. 224, no. 1, pp. 41-46.

Young, S., Bansal, P., Vella, E.T., Finelli, A., Levitt, C. & Loblaw, A. 2015, "Systematic review of clinical features of suspected prostate cancer in primary care", *Canadian Family Physician,* vol. 61, no. 1, pp. e26-e35.

Yu, Z., Pestell, T.G., Lisanti, M.P. & Pestell, R.G. 2012, "Cancer stem cells", *The international journal of biochemistry & cell biology,* vol. 44, no. 12, pp. 2144-2151.

Zavala, V.A. & Kalergis, A.M. 2015, "New clinical advances in immunotherapy for the treatment of solid tumours", *Immunology,* vol. 145, no. 2, pp. 182-201.

Zendman, A.J., Ruiter, D.J. & Van Muijen, G.N. 2003, "Cancer/testis-associated genes: identification, expression profile, and putative function", *Journal of cellular physiology,* vol. 194, no. 3, pp. 272-288.

Zhang, L., Kim, S.B., Jia, G., Buhemeida, A., Dallol, A., Wright, W.E., Fornace, A.J., Al-Qahtani, M. & Shay, J.W. 2015, "Exome Sequencing of Normal and Isogenic Transformed Human Colonic Epithelial Cells (HCECs) Reveals Novel Genes Potentially Involved in the Early Stages of Colorectal Tumorigenesis", *BMC genomics,* vol. 16, no. Suppl 1, pp. S8.

Zhang, C. & Wu, J. 2015, "Retinoid acid: the trigger for the cycle of the seminiferous epithelium in the adult testis?", *Biology of reproduction,* vol. 92, no. 5, pp. 115.

Zheng, H., Chang, L., Patel, N., Yang, J., Lowe, L., Burns, D.K. & Zhu, Y. 2008, "Induction of abnormal proliferation by nonmyelinating schwann cells triggers neurofibroma formation", *Cancer cell,* vol. 13, no. 2, pp. 117-128.

Zhong, Y., Guan, K., Guo, S., Zhou, C., Wang, D., Ma, W., Zhang, Y., Li, C. & Zhang, S. 2010, "Spheres derived from the human SK-RC-42 renal cell carcinoma cell line are enriched in cancer stem cells", *Cancer letters,* vol. 299, no. 2, pp. 150-160.

Zhou, J., Leu, N.A., Eckardt, S., McLaughlin, K.J. & Wang, P.J. 2014, "STK31/TDRD8, a germ cell-specific factor, is dispensable for reproduction in mice", *PloS one,* vol. 9, no. 2.

Zhou, J., Yue, W. & Pei, X. 2013, "Advances in cell lineage reprogramming", *Science China.Life sciences,* vol. 56, no. 3, pp. 228-233.

Zhu, Z. & Huangfu, D. 2013, "Human pluripotent stem cells: an emerging model in developmental biology", *Development (Cambridge, England),* vol. 140, no. 4, pp. 705-717.

Zou, W. & Chen, L. 2008, "Inhibitory B7-family molecules in the tumour microenvironment", *Nature Reviews Immunology,* vol. 8, no. 6, pp. 467-477.